

MASARYK UNIVERSITY
FACULTY OF SCIENCE

DEPARTMENT OF
EXPERIMENTAL BIOLOGY

NATURAL PHENOLICS IN ALLEVIATION
OF SYMPTOMS AND COMPLICATIONS OF
TYPE 2 DIABETES MELLITUS

HABILITATION THESIS

JAKUB TREML

BRNO 2025

MY CHOICE OF LEARNING PHARMACY WAS DRIVEN BY MY
INTERESTS, CURIOSITY, AND A DESIRE TO SEEK NEW
MEDICINES FOR PATIENTS.

TU YOUYOU

ABSTRACT

This habilitation thesis is a selection with comments of my 12 peer-reviewed papers that are focused on the determination of the biological activity of plant phenolic compounds. The aim was to find compounds with antioxidant, anti-inflammatory, and antidiabetic effects that could help in the treatment of hyperglycemia in patients with type 2 diabetes mellitus (T2DM) and alleviate its long-term complications. In the introduction I briefly describe my field “molecular pharmacy” and all my other publications. The second part focuses on the pathophysiology of T2DM. The third part concentrates on various natural phenolics and their antioxidant, anti-inflammatory, and antidiabetic effects, and a comparison of the different methods that are used to determine these. The last subchapter deals with the encapsulation of natural phenolics to improve their solubility. The concept of “one compound with a combination of effects” is shown on a model compound – the geranylated flavanone diplacone.

ACKNOWLEDGEMENT

First, I would like to express my gratitude to my wife Miriam and my son Šimon for their support, understanding, and patience.

I would like to especially express my gratitude to Prof. Karel Šmejkal, who has supported me during my career and inspired me to pursue science.

Thanks also go to my great colleagues, former and current students. Namely, Honza Hošek, Daniela Nykodýmová, Ondra Smišťík, Milan Malaník, and Lenka Molčanová.

Especially, I would like to thank Dr. Frank Thomas Campbell for editing the language of the manuscript.

Finally, my thanks go to my family and friends.

ABBREVIATIONS

AAPH	2,2'-Azobis(2-amidinopropane) dihydrochloride
ABTS ^{•+}	2,2' -Azino-bis(3-ethylbenzothiazoline-6-sulfonic acid radical cation
AGEs	Advanced glycation end-products
AP-1	Activator protein 1
ARE	Antioxidant responsive element
CAA	Cellular antioxidant assay
CAT	Catalase
CDs	Cyclodextrins
COX	Cyclooxygenase
Cul3	Cullin 3
DCF	Dichlorodihydrofluorescein
DCFH-DA	2',7'-Dichlorodihydrofluorescein diacetate
DM	Diabetes mellitus
DMP	Department of Molecular Pharmacy
DPP-4	Dipeptidylpeptidase 4
DPPH [•]	2,2-Diphenyl-1-picrylhydrazyl radical
ERK	Extracellular signal-regulated kinase
FRAP	Ferric reducing antioxidant power
GLP-1	Glucagone-like peptide-1
GLUT4	Glucose transporter 4
GOSP	Glucose oxidative stress protection
GP	Glucan particles
HET-CAM	Hen's egg test-chorioallantoic membrane
HP- β -CDs	Hydroxypropyl- β -cyclodextrins
IDF	International Diabetes Federation
IL-1 β	Interleukin 1 β
IR	Insulin receptor

IRS	Insulin receptor substrate
JNK	c-Jun terminal kinase
Keap1	Kelch-like ECH-associated protein
LOX	Lipoxygenase
LPS	Lipopolysaccharide
MAPK	Mitogen-activated protein kinase
MDA	Malondialdehyde
MΦ	Macrophages
MMP2	Matrix metalloproteinase-2
NADH	Nicotinamide adenine dinucleotide
NF-κB	Nuclear factor κB
Nrf2	Nuclear factor erythroid 2-related factor 2
PDO	Protected Designation of Origin
PI3K	Phosphatidylinositol 3-kinase
PKB	Protein kinase B
PPARγ	Peroxisome proliferator-activated receptor γ
PRDX2	Peroxiredoxin-2
PTP1B	Protein tyrosine phosphatase 1B
ROS	Reactive oxygen species
SEAP	Secreted embryonic alkaline phosphatase
SGLT2	Sodium/glucose cotransporter 2
SOD	Superoxidase dismutase
T2DM	Type 2 diabetes mellitus
TBARS	Thiobarbituric acid reactive substances
TLR	Toll-like receptor
TNF-α	Tumor necrosis factor α
TIRF	Total internal reflection fluorescence

CONTENT

1. Introduction	8
1.1. Structure of the thesis	9
1.2. Molecular pharmacy	11
2. T2DM complications and treatment.....	13
3. Natural phenolics.....	17
3.1. Antioxidant activity	20
3.2. Anti-inflammatory activity.....	26
3.3. Antidiabetic activity.....	32
3.4. Encapsulation of natural products	36
4. Conclusion.....	37
5. References	38
6. Articles.....	45
6.1. Article 1	45
6.2. Article 2.....	65
6.3. Article 3.....	81
6.4. Article 4.....	88
6.5. Article 5.....	105
6.6. Article 6.....	121
6.7. Article 7.....	129
6.8. Article 8.....	144
6.9. Article 9.....	176
6.10. Article 10.....	190
6.11. Article 11.....	195
6.12. Article 12.....	205

1. INTRODUCTION

Diabetes mellitus (DM) is a chronic metabolic disease with high morbidity and mortality. Its symptoms are increased thirst, frequent urination, and slow-healing sores. On the biochemical level, the main characteristic of DM is hyperglycemia. There are two basic types of DM: type 1 (T1DM), caused by an absolute deficiency of the hormone insulin, and type 2 (T2DM), in which the blood level of insulin is normal, but its effect is suppressed by insulin resistance. According to the International Diabetes Federation (IDF), 537 million adults were living with DM in 2021, and the number is projected to rise to 783 million by 2045*.

DM has accompanied humankind since time immemorial. The first reference is attributed to Ancient Egyptian medicine, specifically to the Ebers Papyrus from c. 1550 BCE. What was probably DM was described as “*an excessive urination disease*” for which the following treatment mixture was prescribed: “*A measuring glass filled with water from the bird pond, elderberry, fibres of the asit plant, fresh milk, beer-swill, flower of the cucumber, and green dates[#].*”

As can be seen in the example of DM – humans have used plants for treatment for centuries and thus herbal medicine (phytomedicine or phytotherapy) has been part of every medical system in history: the Eber Papyrus in Ancient Egypt, Ayurvedic medicine in India, Shennong Ben Cao Jing – a book of prescriptions in traditional Chinese medicine, and the Hippocratic Corpus in Greece. The traditional drugs were used in different formulations and extracts, whereas the first active compounds were isolated from natural sources during the nineteenth century and entered medical practice, starting with morphine, isolated in 1805 by the German pharmacist Friedrich Sertürner.

The importance of natural products for medicine can be highlighted using two recent events. Based on estimates by Newman and Cragg⁺, more than half of the medicinal compounds used in current practice are directly of natural origin or semi-synthetically modified. Moreover, the Nobel Prize for Physiology or Medicine in 2015 was awarded to the Chinese pharmaceutical chemist Tu Youyou for the discovery of artemisinin, an effective antimalarial natural product

* <https://diabetesatlas.org/>

[#] Sanders LJ. *Diabetes Spectr* 2002; 15(1): 56–60. <https://doi.org/10.2337/diaspect.15.1.56>.

⁺ Newman DJ, Cragg GM. *J Nat Prod* 2020;83(3):770-803. <http://doi.org/10.1021/acs.jnatprod.9b01285>.

(hence her quote). Therefore, there is renewed interest in finding new medicines in nature nowadays.

This work aims at determining the antidiabetic activity of natural phenolic compounds together with their antioxidant and anti-inflammatory activity. This approach might not only decrease hyperglycemia but also alleviate long-term complications associated with this disease.

1.1. STRUCTURE OF THE THESIS

This thesis is a collection of 12 peer-reviewed papers published between 2010 and 2025. All the papers concentrate on the effects of natural phenolics on alleviating the symptoms or complications of T2DM. The first 5 papers describe their antioxidant effects¹⁻⁵, the following 2 papers focus on their anti-inflammatory potential^{6,7}, 2 papers concentrate on the antidiabetic effects^{8,9}, and finally, 3 papers describe the encapsulation of natural phenolics¹⁰⁻¹² to enhance their solubility and biological activity.

The key question of my research is: *“Are there any natural phenolic compounds that are effective as antioxidant, anti-inflammatory, and antidiabetic agents?”* As proof of this concept, the geranylated flavanone diplacone will be highlighted throughout the thesis.

My contribution to the 12 peer-reviewed articles is summarized in the following tables:

1) **Treml, J.**; Smejkal, K. Comprehensive Reviews in Food Science and Food Safety 2016, 15, 720-738 (IF = 5.974).

Experimental work (%)	Supervision (%)	Manuscript (%)	Research direction (%)
-	-	75	50

2) Zima, A.; Hosek, J.; **Treml, J.**; Suchy, P.; Prazanova, G.; Lopes, A.; Zemlicka, M. Molecules 2010, 15, 6035-6049 (IF=1.988).

Experimental work (%)	Supervision (%)	Manuscript (%)	Research direction (%)
35	-	25	25

3) **Treml, J.**; Smejkal, K.; Hosek, J.; Zemlicka, M. Chemical Papers 2013, 67, 484-489 (IF=1.193).

Experimental work (%)	Supervision (%)	Manuscript (%)	Research direction (%)
100	-	80	50

4) **Treml, J.**; Lelakova, V.; Smejkal, K.; Paulickova, T.; Labuda, S.; Granica, S.; Havlik, D.; Padrtova, T.; Hosek, J. *Biomolecules* 2019, 9, 468 (IF=4.082).

Experimental work (%)	Supervision (%)	Manuscript (%)	Research direction (%)
25	50	75	50

5) **Treml, J.**; Vecerova, P.; Herczogova, P.; Smejkal, K. *Molecules* 2021, 26, 2534 (IF=4.927).

Experimental work (%)	Supervision (%)	Manuscript (%)	Research direction (%)
75	50	100	75

6) Malanik, M.; **Treml, J.**; Lelakova, V.; Nykodymova, D.; Oravec, M.; Marek, J.; Smejkal, K. *Bioorganic Chemistry* 2020, 104, 104298 (IF=5.275).

Experimental work (%)	Supervision (%)	Manuscript (%)	Research direction (%)
-	50	25	25

7) Molcanova, L.; **Treml, J.**; Brezani, V.; Marsik, P.; Kurhan, S.; Travnicek, Z.; Uhrin, P.; Smejkal, K. *Journal of Ethnopharmacology* 2022, 296, 115509 (IF=5.400).

Experimental work (%)	Supervision (%)	Manuscript (%)	Research direction (%)
30	-	25	25

8) **Treml, J.**; Nykodýmová, D.; Kubatka, P. *Phytochemistry Reviews* 2025, doi: 10.1007/s11101-025-10121-w (IF=7.300).

Experimental work (%)	Supervision (%)	Manuscript (%)	Research direction (%)
-	25	90	100

9) **Treml, J.**; Václavík, J.; Molčanová, L.; Čulenová, M.; Hummelbrunner, S.; Neuhauser, C.; Dirsch, V. M.; Weghuber, J.; Šmejkal, K. *Journal of Agricultural and Food Chemistry* 2025, doi: 10.1021/acs.jafc.4c11398 (IF=5.700)

Experimental work (%)	Supervision (%)	Manuscript (%)	Research direction (%)
40	-	90	100

10) **Treml, J.**; Salamunova, P.; Hanus, J.; Hosek, J. Food & Function 2021, 12, 1954-1957 (IF=6.317).

Experimental work (%)	Supervision (%)	Manuscript (%)	Research direction (%)
75	-	80	25

11) Salamunova, P.; Cupalova, L.; Majerska, M.; **Treml, J.**; Ruphuy, G.; Smejkal, K.; Stepanek, F.; Hanus, J.; Hosek, J. International Journal of Biological Macromolecules 2021, 169, 443-451 (IF=8.025).

Experimental work (%)	Supervision (%)	Manuscript (%)	Research direction (%)
-	50	25	25

12) Nykodýmová, D.; Molčanová, L.; Kotouček, J.; Mašek, J.; **Treml, J.** ChemistryOpen 2025, doi: 10.1002/open.202500209 (IF=3.100).

Experimental work (%)	Supervision (%)	Manuscript (%)	Research direction (%)
-	75	25	50

1.2. MOLECULAR PHARMACY

I am currently the Head of the Department of Molecular Pharmacy (DMP). The term “molecular pharmacy” is a neologism reflecting the connection between pharmacy, medicinal compounds, and their effects and cellular and molecular biology. This is visible not only in the repertoire of the subjects taught by the DMP, but also in the research areas of its staff.

The designation of DMF was coined by me in 2020, when the Faculty of Pharmacy rejoined Masaryk University and there was an interest to shorten the former name “Department of Molecular Biology and Pharmaceutical Biotechnology”. There were two sources of inspiration: The Molecular Pharmacy research group of Prof. Dr. Daniel Ricklin from the University of Basel, Switzerland, which aims at “drug discovery and screening of therapeutic concepts”¹³, and the Molecular Pharmacy laboratory of Univ.-Prof. Dr.rer.nat. Valery Bochkov from the University of Graz, Austria aiming at “the development of cellular models for screening of natural products as well as synthetic substances”¹⁴.

My peer-reviewed publications include 33 peer-reviewed scientific articles – 12 of them have already been presented in the previous section and the remaining 21 will be briefly introduced

here. The first group of articles concentrates on the determination of biological activity on cell culture and *in vitro* assays. Most of the research was done with plant or mushroom extracts or isolated natural products. The publications are summarized in Table 1.

Publication	The main outcome
Kuczmánová et al. ¹⁵	<i>Agrimonia eupatoria</i> water extract – increases expression of antioxidant enzymes, protects plasmid DNA from oxidative stress, <i>in vivo</i> wound healing.
Stastny et al. ¹⁶	<i>Pleurotus flabellatus</i> methanolic extract – radical scavenging activity; chloroform extract – inhibition of cyclooxygenase 2. <i>P. ostreatus</i> – anti-inflammatory activity = inhibition of nuclear factor κ B (NF- κ B).
Rybníkář et al. ¹⁷	<i>Schisandra chinensis</i> – dibenzocyclooctadiene lignan (–)-gomisin J showed both antioxidant (cellular antioxidant assay, CAA) and anti-inflammatory (NF- κ B) activity.
Peron et al. ¹⁸	<i>Citrus sinensis</i> PDO “Orange of Ribera” peel extract showed significant antioxidant (CAA) and anti-inflammatory (NF- κ B) activity.
Vasilev et al. ¹⁹	<i>Astragalus thracicus</i> – quercetin-3- <i>O</i> - β -D-apiofuranosyl-(1 \rightarrow 2)- β -D-galactopyranoside showed the greatest inhibitory effect on collagenase and elastase.
Dvorska et al. ²⁰	<i>Aronia melanocarpa</i> fruit peel extract – <i>in vitro</i> and <i>in vivo</i> antitumor activity in the 4T1 mouse adenocarcinoma model.
Malaník et al. ²¹	<i>Ziziphora clinopodioides</i> subsp. <i>bungeana</i> – isolated triterpenes were able to inhibit α -glucosidase, and pomolic acid increased translocation of GLUT4 = antidiabetic activity.
Dvorska et al. ²²	<i>Hippophae rhamnoides</i> fruit peel extract – <i>in vitro</i> and <i>in vivo</i> antitumor activity in the 4T1 mouse breast carcinoma model.

Table 1 – Summary of my publications on the topic of biological activity of natural products in cellular and *in vitro* assays.

I have also co-authored a review article summarizing the available ethnobotanical, phytochemical, and pharmacological information about the traditional Amazonian medicinal tree *Maytenus macrocarpa*²³. Moreover, in other three publications I have concentrated on the determination of antiproliferative effects of synthetic compounds, which were tested also in other assays: *N*-phenylpiperazine derivatives with potential antibacterial and antifungal effects²⁴, silicon-based carbamate derivative with potential inhibitory effect on acetyl- and butyrylcholinesterase²⁵, and (4-oxo-2-thioxothiazolidin-3-yl)acetic acids as potential aldose reductase inhibitors²⁶. The compounds were screened to confirm whether the concentrations determined in other assays are safe and non-toxic for human cell culture, and thus whether their future development makes sense.

The second group of articles deals with microbiological topics. Škovranová et al. determined antimicrobial activity, synergism with antibiotics, and membrane disruption of prenylated phenolics isolated from *Morus alba*²⁷ and *Paulownia tomentosa*²⁸ against *Staphylococcus aureus*. Helcman et al., on the other hand, concentrated on the inhibition of a bacterial process called quorum sensing by cannabinoids and other plant phenolics. Quorum sensing is a cell-to-cell communication that allows bacteria to share information about population density²⁹. The other four articles were based on cooperation with the Department of Plant Origin Food Sciences, Veterinary University. The antimicrobial effect was determined for edible films from carrageenan/orange essential oil/trehalose³⁰, soaps from reused plant fried oil³¹, chitosan edible films with plant extracts³², and chitosan films with nanometals³³. I have also co-authored two review articles – one dealing with natural products possessing antiviral effect against herpes simplex virus 1 and 2³⁴, and the other about sulfate reducing bacteria in gut microbiota and their involvement in inflammatory bowel diseases³⁵.

2. T2DM COMPLICATIONS AND TREATMENT

Hyperglycemia is the basis of the pathophysiology of T2DM and can be defined as a blood glucose concentration above 6.9 mM when measured after 8 hours of fasting (or above 10 mM two hours after eating). Persistent or uncompensated hyperglycemia may lead to chronic complications of DM, which manifest throughout the whole vascular system. In the retina, for example, a high glucose concentration causes alterations in microcirculation, capillary closures,

and edema. Diabetic retinopathy affects 30% of patients suffering from DM for 20 years or longer, and its result is blindness. A similar deterioration appears in the kidney, where increased glomerular pressure and hyperfiltration may end in a need for renal dialysis. Moreover, hyperglycemia increases the risk of cardiovascular disease and damages nerves, causing diabetic peripheral neuropathy with symptoms such as numbness, tingling, or pain. In terms of prevalence, the most common complication in patients with T2DM is chronic kidney disease (27.8%), followed by foot problems (pain, loss of sensitivity; 22.9%) and eye damage (18.9%)³⁶.

The pathophysiology of chronic diabetic complications is complex. One of the key factors in its progression is oxidative stress, also defined as an imbalance between the production of reactive oxygen species (ROS) and the antioxidant capacity of the cellular metabolism. A high concentration of glucose fully saturates the hexokinase enzymatic capacity, and the surplus is metabolized through the polyol pathway. As a result, nicotinamide adenine dinucleotide (NADH) accumulates and subsequently serves as a substrate for NADH oxidase to generate ROS, damaging cells. The final product of the polyol pathway, sorbitol, accumulates in the retina, leading to retinopathy (Figure 1)³⁷.

Moreover, glucose spontaneously reacts with free amino groups in proteins forming Schiff bases. Advanced glycation end-products (AGEs) are formed by the following complex reactions. The AGEs participate in tissue damage and macrophage (MΦ) activation leading to inflammation and oxidative stress. The production of ROS then activates certain pro-inflammatory factors and their pathways, such as nuclear factor κB (NF-κB). These factors further activate innate immunity cells and lead to the formation of more ROS, thus creating a “vicious cycle” of positive feedback between ROS production and inflammation (Figure 1)³⁷.

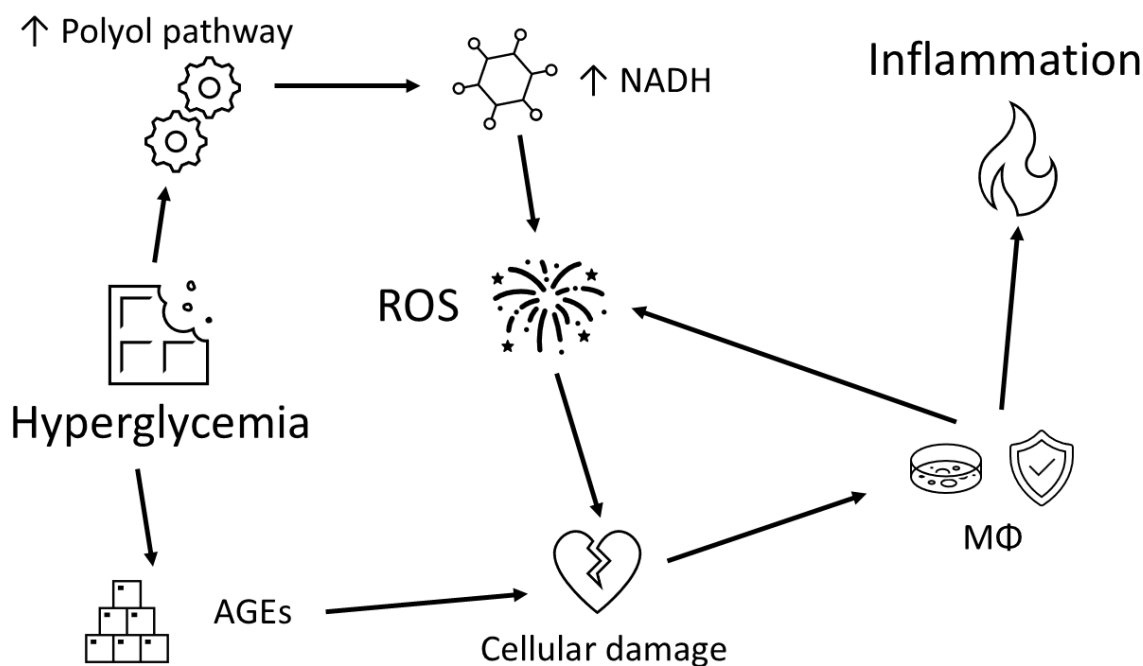


Figure 1 – The complications of T2DM – involvement of oxidative stress and inflammation.

An important part of managing T2DM is changing one's lifestyle and diet. The dietary measures include: choosing drinks without added sugar, eating wholegrain cereals, reducing red meat and instead eating more fruit and vegetables, being sensible with alcohol, adding healthier fats into the diet (unsalted nuts, seeds, avocados, olive oil), reducing amount of salt and getting the vitamins and minerals from food instead from tablets³⁸.

Subsequent pharmacotherapy is usually initiated with metformin³⁹. This biguanide antidiabetic enhances the utilization of glucose in skeletal muscles and adipose tissue and decreases gluconeogenesis in the liver. Structurally the biguanides originate from natural products isolated from the plant *Galega officinalis* L. (Fabaceae)⁴⁰. Treatment with metformin can be accompanied by gastrointestinal problems, such as flatulence and cramps. Another serious complication is lactate acidosis.

For patients with cardiovascular disease and metformin contraindication, gliflozines (or sodium/glucose cotransporter 2 (SGLT2) inhibitors) are the drugs of choice. Gliflozines inhibit the SGLT2 proteins responsible for the reabsorption of glucose in the kidneys and thus decrease glycaemia. Other patients with T2DM might be given gliptins (dipeptidylpeptidase 4 (DPP-4)

inhibitors), pioglitazone from the group of thiazolidinediones, or a sulfonylurea derivative. If combinations of first-line drugs are not effective in reducing hyperglycemia, agonists of the glucagon-like peptide-1 (GLP-1) receptor might be offered. These drugs are administered as subcutaneous injections and lead to significant weight loss. This aspect is very important since obesity accompanies T2DM in most cases. For example, from this group, the medicinal compound semaglutide marketed by Novo Nordisk under the brand name Ozempic has caused a “revolution” in the treatment of obesity³⁹. Another option is inhibitors of α -glucosidase, such as acarbose. Upon their effect, less glucose is absorbed from the gastrointestinal tract. Insulinotherapy is added when the patient suffers from complicated T2DM⁴¹.

Recently, researchers started to focus on describing the changes in the composition of microorganisms in the gastrointestinal tract of T2DM patients, also called gut microbiota. This very complex ecosystem is composed of bacteria, archaea, fungi, viruses, and protozoa. So far, the studies have shown gut microbiota dysbiosis and loss of microbial diversity in T2DM patients – mainly decreased abundance of *Akkermansia muciniphila*, *Faecalibacterium prausnitzii*, and others. It was hypothesized (and shown in animal models) that application of these bacteria in in form of probiotics might improve inflammation and insulin resistance^{42–44}.

Although the topic of T2DM and its pharmacotherapy has been very well described, there is a great need to improve treatment strategies and to investigate novel drug targets⁴⁵. As will be described in the following chapter, natural products offer great potential in terms of the hypoglycemic effect and also alleviate the long-term effects of hyperglycemia⁴⁶.

3. NATURAL PHENOLICS

Natural phenolic compounds (or plant phenolics) are defined as natural products with at least one phenolic functional group. They are widely distributed in the plant kingdom, which makes them the most abundant secondary metabolites of plants, with more than 8,000 structures currently known. As secondary metabolites, natural phenolics are not essential for the basic growth and reproduction of plants but play important roles in their ecological interactions. Quideau et al. have proposed that the term “plant phenolics” should be only used for secondary metabolites arising biogenetically from the shikimate/phenylpropanoid pathway, the “polyketide” acetate/malonate pathway or both of them (Figure 2)^{47,48}.

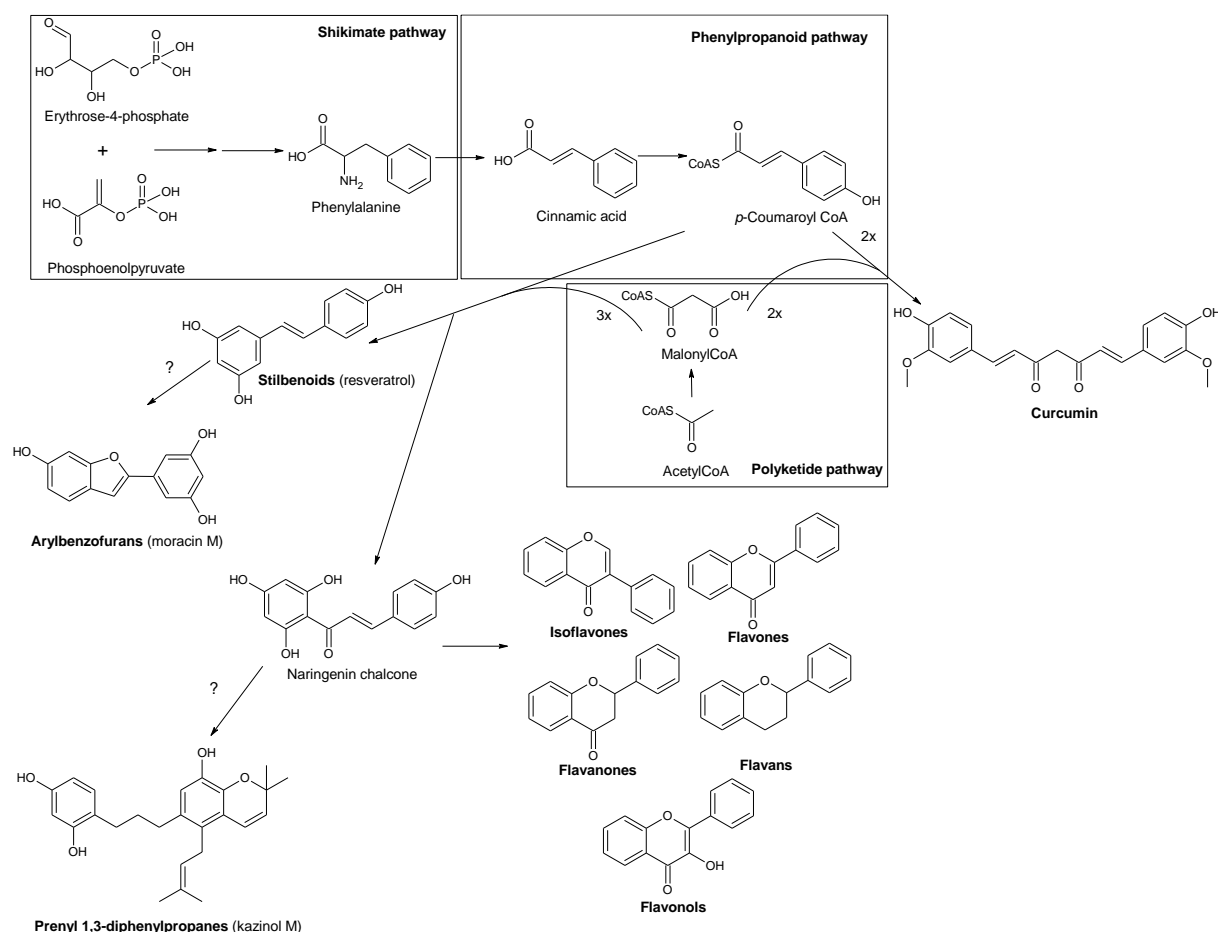


Figure 2 – The biosynthetic origin of natural phenolics throughout this thesis: flavonoids, stilbenoids, prenyl 1,3-diphenylpropanes, arylbenzofurans, and curcumin.

The capacity of plants to synthesize natural phenolics probably evolved due to their terrestrialization in the mid-Palaeozoic era between 480 and 360 million years ago. During the adaptation of life on dry land, plants had to survive solar UV irradiation and thus evolved pathways for the biosynthesis of phenolics. Moreover, plant phenolics exhibiting color attract pollinators to flowers. Since similar relations apply to other secondary metabolites as well, one can suggest that the basis of pharmacotherapy in human medicine started as a by-product of co-evolution between plants and insects⁴⁹.

Throughout this thesis, one natural product will be mentioned more than once and will serve as an illustration of the main topic: a combined antioxidant, anti-inflammatory, and antidiabetic effect. This natural product is the geranylated flavanone **diplocone** (also known as propoline C or nymphaeol A). Diplocone was isolated and identified for the first time by David E. Lincoln in 1980 from the leaf resin of *Diplacus aurantiacus* (Curtis) Jeps. Phrymaceae. It was proposed that diplocone and its derivatives grant protection from herbivorous lepidopteran larvae⁵⁰. The compound was later isolated from other plants: *Paulownia tomentosa* (Thunb.) Steud. Paulowniaceae⁵¹, *Macaranga tanarius* (L.) Muell. Arg. Euphorbiaceae⁵², *Macaranga alnifolia* Baker Euphorbiaceae⁵³, *Schizolaena hystrix* Capuron Sarcolaenaceae⁵⁴, and *Diplacus clevelandii* (Brandeg.) Greene Phrymaceae⁵⁵ and it has also been found in some kinds of propolis⁵⁶.

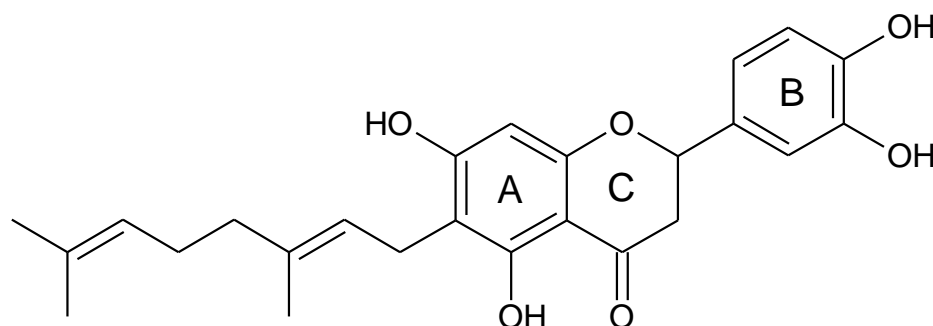


Figure 3 – The structure of diplocone with marked rings A, B, and C.

Diplocone (Figure 3) belongs to the flavonoids, which are very common plant phenolics. The basic structure of a flavone is 2-phenyl-1,4-benzopyrone (C6-C3-C6). According to the arrangement of the structure, we can distinguish isoflavones, flavones, flavans, flavanones, and flavonols⁸. The prenyl or geranyl moiety attached to the structure increases lipophilicity and thus enhances affinity for biological membranes, leading to a stronger biological effect.

Stilbenoids are hydroxylated derivatives of stilbenes with the basic structure C6-C2-C6. They act as phytoalexins and are therefore produced to protect the plants in case of fungal infection. The best-known stilbenoid, *trans*-resveratrol (*trans*-3,5,4'-trihydroxystilbene), is found in species of the genus *Vitis* (grapes), red wine, and other plant species⁵⁷. Prenyl 1,3-diphenylpropanes are probably biosynthesized from chalcones. Their occurrence in nature is rather rare. Arylbenzofurans are uncommon plant phenolics and can be found in substantial amounts in *Morus* spp. Their structure is based on a benzofuran ring substituted with a phenyl group⁵⁸. Curcumin is a bright yellow polyphenol isolated from rhizomes of *Curcuma longa* L. It belongs among curcuminoids, or linear diarylheptanoids (Figure 2).

According to a recent study, the average consumption of polyphenolic compounds in the Czech population is 1.673 g per day per person, and this value might still be underestimated. The most frequent sources are beverages such as coffee, tea, and juices, followed by fruits, cereals, and vegetables, respectively⁵⁹.

Approximately 5-10% of total phenolic compounds are absorbed in the small intestine after ingestion. Based on the molecular weight (and other physical-chemical properties), the phenolics are absorbed through passive diffusion (low molecular weight compounds, such as gallic acid and isoflavones, and lipophilic compounds, such as flavonoid aglycones). Other compounds are actively transported via P-glycoprotein or sodium-glucose cotransporters, such as quercetin glycosides⁶⁰.

The remaining plant phenolics are then transported to the colon, where they are subjected to microbiota. The transformation of phenolic compounds depends on gut microbial composition and also on chemical structure and the type of food ingested. Usually, the polymeric phenolics are depolymerized, flavonols are decomposed into hydroxyphenylacetic acids, flavones and flavanones are broken down into hydroxyphenylpropionic acids, etc. The products of metabolism are then absorbed⁶⁰.

From the colon, the compounds are transported to the liver via the portal vein. The metabolism in the liver follows a similar pattern as that of other xenobiotics. During phase I, the structures of plant phenolics or their metabolites are modified – thiolated, hydroxylated, aminated, or carboxylated. The phase II is then characterized by conjugation reactions when glucuronides, sulphates, or methyl groups are added to enhance water solubilization and thus elimination from the body⁶⁰.

3.1. ANTIOXIDANT ACTIVITY

All aerobic organisms suffer from oxidative stress, but on the other hand they gain much more energy from oxidative phosphorylation than from anaerobic processes. ROS are small molecules that are commonly produced in radical reactions and have the capacity to quickly interact with cellular structures. They include various chemicals: oxygen radicals (such as hydroxyl radical $\cdot\text{OH}$) or nonradical substances (such as hydrogen peroxide H_2O_2). ROS are usually very reactive and damage the nearest biomolecules, impairing the function of the biological system. The antioxidant cellular capacity is represented by antioxidant enzymes, such as superoxide dismutase (SOD; converting superoxide radical to hydrogen peroxide) or catalase (CAT; converting hydrogen peroxide to water)¹.

The cellular response to oxidative stress is regulated by the transcription master regulator nuclear factor erythroid 2-related factor 2 (Nrf2) and under normal conditions remains in cytosol bound to Kelch-like ECH-associated protein (Keap1) (Figure 4). Keap1 facilitates the polyubiquitination of Nrf2 by the Cullin 3 (Cul3) E3 ubiquitin ligase for proteasomal degradation, thus allowing low basal activation. During oxidative stress, certain cysteine residues in Keap1 are modified and subsequent conformational change prevents Keap1 from mediating the ubiquitination of Nrf2 by Cul3. As a result, Nrf2 is stabilized, accumulated, and translocated into the nucleus where it heterodimerizes with sMaf proteins. The heterodimer then binds to the antioxidant responsive element (ARE) for the induction of cytoprotective genes for enzymes involved in the detoxication of ROS (Figure 4)⁶¹.

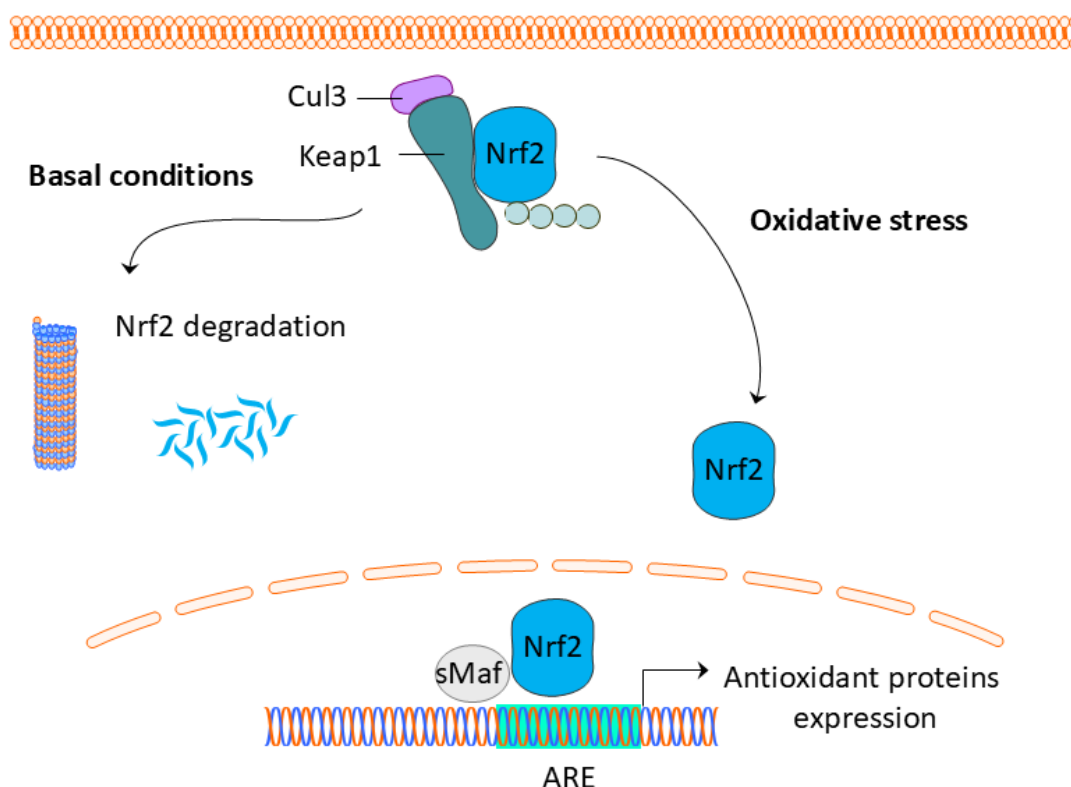


Figure 4 – The Nrf2-ARE pathway (created using Motifolio toolkit).

The exact mechanism by which oxidative stress promotes inflammation and vice versa is not clear. A possible link was proposed by Salzano et al. The oxidative stress in cells leads, among other things, to protein oxidation and oxidative coupling of glutathione to cysteine residues of proteins. One such example is a ubiquitous redox-active intracellular enzyme peroxiredoxin-2 (PRDX2), which is released from macrophages in oxidized form upon oxidative stress or pro-inflammatory activation by lipopolysaccharide (LPS). The released PRDX2 then triggers other macrophages to produce tumor necrosis factor α (TNF- α)⁶².

Compounds that can regulate oxidative stress and enhance the defensive capacities of cells are called antioxidants. Several different assays and methodological approaches are used to measure antioxidant activity⁵:

1. **Direct antioxidant** assays are based on redox reactions and the fast scavenging of ROS:
 - a. **Chemical-based** assays are essentially based on electron-transfer redox reactions. The reaction usually involves chemical radicals, such as 2,2-diphenyl-1-picrylhydrazyl

radical (DPPH[•]), 2,2'-azino-bis(3-ethylbenzothiazoline-6-sulfonic acid radical cation (ABTS^{•+}). Or ferric (Fe³⁺) ions, as in the case of ferric reducing antioxidant power (FRAP) assay. Upon reaction with an antioxidant, the radical or ion undergoes a redox reaction (i.e. electron transfer) that leads to a change in structure and thus in the absorption spectrum, which can be measured and quantified. These assays are very popular among phytochemists because they are rapid, easy-to-do, and relatively cheap. On the other hand, they are very far from the natural conditions in cells, and a positive result does not confirm their effectiveness in cellular systems. One of the other options in this group is an assay based on the protection of plasmid DNA from hydroxyl radical produced by the Fenton reaction or protection from the lipid peroxidation of linoleic acid.

- b. **Cell-based** assays are rather time-consuming and require certain skills from the researcher, however their results are more relevant for *in vivo* conditions. Positive effects in such assays might also give us information about the ability of the antioxidant to enter the cells. An example of this approach is the cellular antioxidant assay (CAA). Cells are first incubated with 2',7'-dichlorodihydrofluorescein diacetate (DCFH-DA), which is then deacetylated to DCFH in cell cytosol. After the addition of 2,2'-azobis(2-amidinopropane) dihydrochloride (AAPH), peroxy radicals are produced and DCFH is converted to fluorescent dichlorofluorescein (DCF).

Antioxidants can counteract this reaction and thus decrease the fluorescence signal.

2. **Indirect antioxidant** assays, which may involve redox activity, concern mainly the enhancement of the antioxidant capacity of cells, for example, the increased expression of antioxidant enzymes through activation of the Nrf2-ARE pathway. These methods can also be divided on a principle similar to the previous one – the influence on enzyme activity can be measured on isolated enzymes or using a cell-based approach, which obviously has greater informative value. Another example is a modified CAA assay, in which the oxidative stress is caused by a high glucose concentration in the medium (thus approximating the conditions of hyperglycemia) and is called the glucose oxidative stress protection (GOSP) assay.

The discrepancies between the results of the chemical-based and cell-based antioxidant activity of the model compound **diplacone** are shown in Table 2. All the cell-based experiments were

done in non-toxic concentrations (verified using a WST-1 kit). Based on the results, diplacone can be described as a direct scavenger of radicals in chemical-based assays, but this effect was not confirmed in the cell-based CAA assay. On the other hand, after a longer incubation in a GOSP assay, a statistically significant effect was observed, probably due to the increased activation of catalase.

Type	Assay	Result	Source
1a	ABTS	3.2× more active than positive control (Trolox)	Zima et al. ²
	DPPH	1.1× more active than positive control (Trolox)	
	FRAP	0.5× more active than positive control (Trolox)	
	Plasmid DNA protection	at conc. of 100 µM, plasmid DNA protected from Fenton reaction	Treml et al. ³
1b	CAA	no activity at conc. of 5 µM after 1h	Treml et al. ⁵
2	GOSP	1.4× more active than positive control (quercetin) at conc. of 5 µM after 48h	
	CAT activity	5× more active than negative control (DMSO as solvent) after 5h at conc. of 5 µM	
	Nrf2-ARE activation	no activity after 24h at conc. of 5 µM	

Table 2 – Results for the chemical-based and cell-based antioxidant activities of diplacone.

A similar pattern of discrepancies was also observed in experiments with stilbenoids described by Treml et al. The compounds were first tested using a chemical-based methodology – the thiobarbituric acid reactive substances (TBARS) assay. In principle, the TBARS assay should show the ability of a compound to protect linoleic acid against lipid peroxidation using AAPH during a 24h incubation. Upon oxidation, linoleic acid forms malondialdehyde (MDA), which reacts with TBA in acidic conditions. The TBA-MDA adduct is then extracted using butanol and its concentration is determined by absorbance measurement. The stilbenoids were

subsequently tested in a cell-based assay, wherein oxidative stress was caused by pyocyanin, a secondary metabolite obtained from the Gram-negative bacteria *Pseudomonas aeruginosa* that is able to generate ROS⁴.

Among the stilbenoids (Figure 5), *trans*-stilbene was the most potent in the TBARS assay, reducing the lipid peroxidation by almost 50%. On the other hand, the most pro-oxidant were *trans*-resveratrol, piceatannol, and piceatannol-3'-O- β -glucopyranoside. Surprisingly, in the cell-based assay, piceatannol and piceatannol-3'-O- β -glucopyranoside were able to reduce the oxidative stress caused by pyocyanin by c. 50% after 1h at a non-toxic concentration of 2 μ M, and *trans*-stilbene was inactive. Only isorhapontigenin was able to activate the Nrf2-ARE pathway, but without increasing the expression of any antioxidant enzymes⁴.

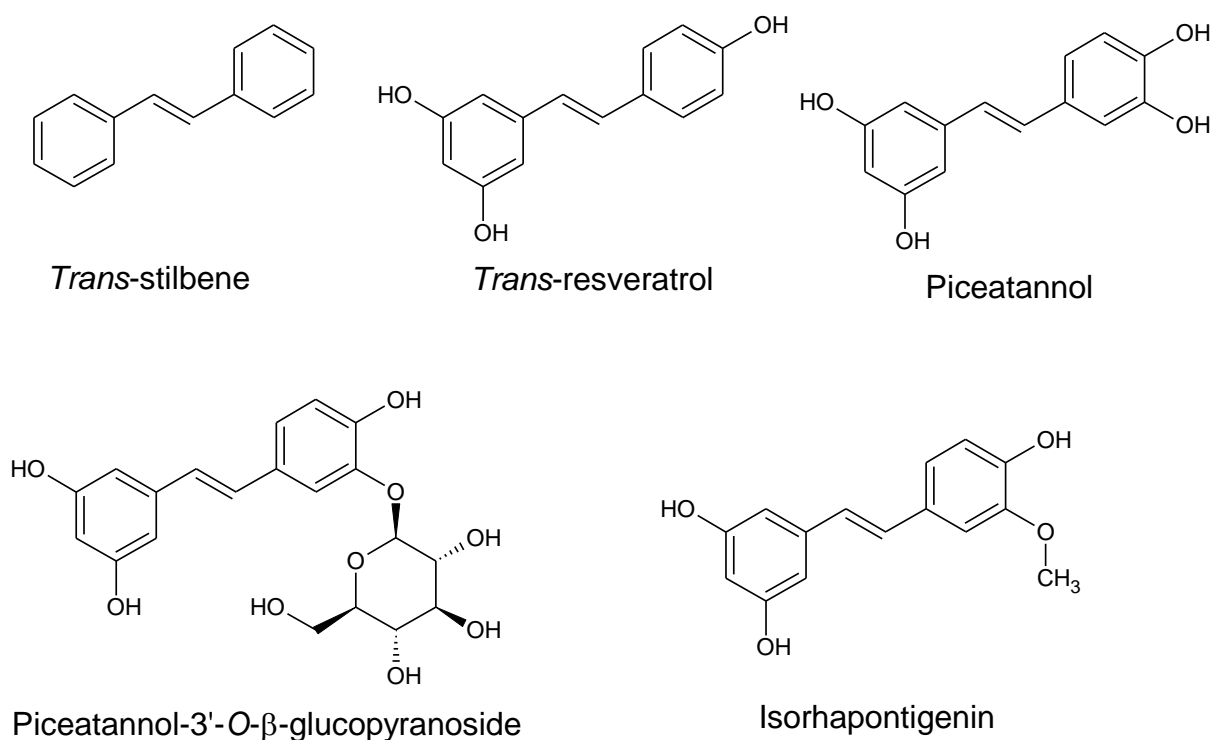


Figure 5 – The structures and effects of stilbenoids.

Overall, both studies show diverse results, with one compound effective in one assay but ineffective in the other. As I have argued, from the point of relevance to biological systems, cellular antioxidant assays surpass those that are chemical-based. Thus, to designate a compound as an antioxidant, one should depend on results from cellular or *in vivo* assays.

Wolfe and Liu used the CAA assay to assess the structure-activity relations study for flavonoids. The structural elements conferring the most active flavonoids were: a 3',4'-dihydroxyl group in the B-ring, a 2,3-double bond combined with a 4-keto group in the C-ring, and a 3-hydroxyl group. Isoflavones showed no cellular antioxidant activity. Flavanols with a galloyl moiety had higher antioxidant activity than those without, and a B-ring 3',4',5'-trihydroxyl group further improved their efficacy. Thus, the most active group of flavonoids are flavonols, such as quercetin⁶³. These results agree with our own results – quercetin was used as a positive control in CAA, and diplacon (as the flavanone) lacks key parts in its structure: 2,3-double bond and a 3-hydroxyl group.

Esatbeyoglu et al. studied *Vitis vinifera* root extract and identified several stilbenoids in it, including resveratrol and piceatannol. In their experiments, they found the extract to protect against hydrogen peroxide-induced DNA damage and induce Nrf2 and its target genes heme oxygenase-1 and γ -glutamylcysteine synthetase⁶⁴. The effects of the extract are better than those observed in our experiments for the compounds alone.

3.2. ANTI-INFLAMMATORY ACTIVITY

Inflammation is a reaction of body tissues to various harmful stimuli, such as pathogens, damaged cells, or chemical irritants. It is a complex defensive response of the innate immune system accompanied by five cardinal signs: *calor* (heat), *dolor* (pain), *rubor* (redness), *tumor* (swelling), and *functio laesa* (loss of function). The function of inflammation is to eliminate the causal agent, clear out damaged cells and tissue and start the reparatory processes. Such processes of acute inflammation usually take a few days. However, inflammation can lead to a harmful dysregulated response and produce systemic damage that results in chronic inflammatory disorders, such as obesity, insulin resistance, and T2DM.

There are several ways in which cells react to stimuli and inflammation develops on a biochemical level. One common mechanism is connected to the NF- κ B pathway (Figure 6). The canonical form of this pathway starts with various membrane receptors, such as toll-like receptors (TLR) activated by LPS from the cell wall of Gram-negative bacteria. Once activated, the pathway leads to phosphorylation of I κ B kinase and subsequently of I κ B. In the normal state, I κ B resides in cytosol and inhibits NF- κ B (a heterodimer complex of p50 and RelA) through a bond. Upon phosphorylation, I κ B is degraded, releasing NF- κ B to enter the cell nucleus, bind to a specific responsive element on DNA and thus orchestrate the production of proinflammatory cytokines, such as TNF- α and interleukin 1 β (IL-1 β)⁶⁵.

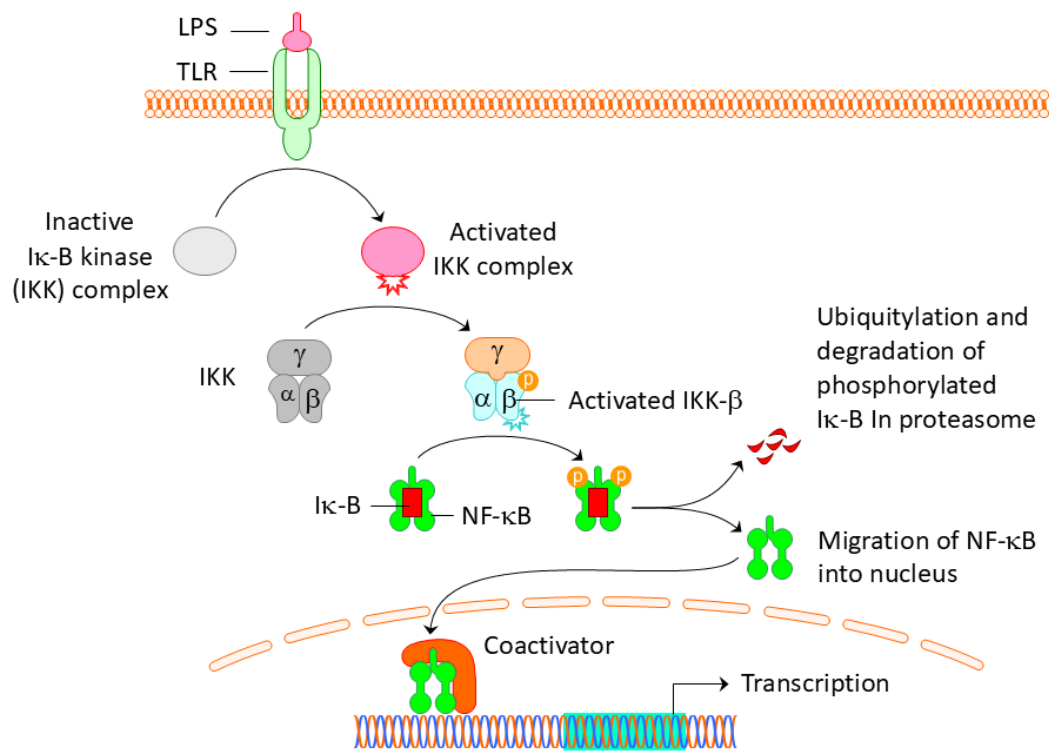


Figure 6 – The canonical NF-κB pathway (created using Motifolio toolkit).

Another mode of cellular response might be mediated via mitogen-activated protein kinases (MAPK). There are several subfamilies of MAPK, such as extracellular signal-regulated kinases (ERK), c-Jun terminal kinases (JNK), and p38. Activated MAPKs translocate to the nucleus and phosphorylate transcription factors such as activator protein 1 (AP-1) and c-Myc, which coordinate the expression of several pro-inflammatory downstream target genes.

Moreover, both NF-κB, JNK and ERK pathways are activated by the insulin receptor pathway. The insulin pathway leads to increased uptake of glucose into cells by translocation of GLUT4 transporters on the cellular surface. Insulin mediates its action via phosphatidylinositol 3-kinase (PI3K) and protein kinase B (PKB or Akt). This leads to an amplification loop connecting inflammation and insulin resistance in T2DM⁶⁶.

The anti-inflammatory activity *in vitro* can be determined with several different methods⁶⁷:

1. **Cell-free** assays are based on the inhibition of certain pro-inflammatory enzymes, usually determined using kits. Examples of enzymes used in such assays are lipoxygenase (LOX) and cyclooxygenase (COX). Both are involved in the conversion of arachidonic acid into eicosanoids.
2. **Cell-based** assays involve inducing inflammation in a monocytic or macrophage cell line (e.g. by LPS) and then determining the outcomes:
 - a. **Griess reaction** is used to detect the production of NO (involved in inflammation) by means of measuring its oxidation products, nitrites, following their diazotation reaction with sulfonamides.
 - b. **Reporter assays** require genetically modified cell lines, in which the activation of the NF- κ B pathway is connected to the production of a certain reporter gene, such as secreted embryonic alkaline phosphatase (SEAP) that can be quantified upon its reaction with the specific substrate QUANTI-Blue™.
 - c. **ELISA** assays are used to measure the inhibition of the production of pro-inflammatory cytokines after activation of the NF- κ B pathway.

Molčanová et al. reported the anti-inflammatory effect of geranylated flavonoids isolated from *P. tomentosa* and among these was the model compound – **diplacone**. Diplacone, at a non-toxic concentration of 1 μ M, was able to reduce the activation of NF- κ B/AP-1 in the LPS-activated THP-1-XBlue™-MD2-CD14 cell line to 80% of the negative control, which was comparable to the positive control prednisone. The anti-inflammatory effect of diplacone was further established in an *in vivo* model of colitis in rats, where this compound ameliorated the symptoms (diarrhea, presence of blood in the stool) and delayed their onset. One of the mechanisms was decreasing the levels of COX-2 and increasing the ratio of the pro-matrix metalloproteinase-2 (pro-MMP2)/MMP-2 activity^{7,68}.

Several other compounds were even more active than diplacone, as shown in Figure 7: diplacol (reduced to 55%; the difference from diplacone highlighted in red in Figure 7), mimulol, paulodiplacone A, paulodiplacol A (60%), tomentoflavone A (65%), tomentone B (70%), 3'-O-methyl-5'-methoxydiplacol, 3'-O-methyl-5'-hydroxydiplacol (75%).

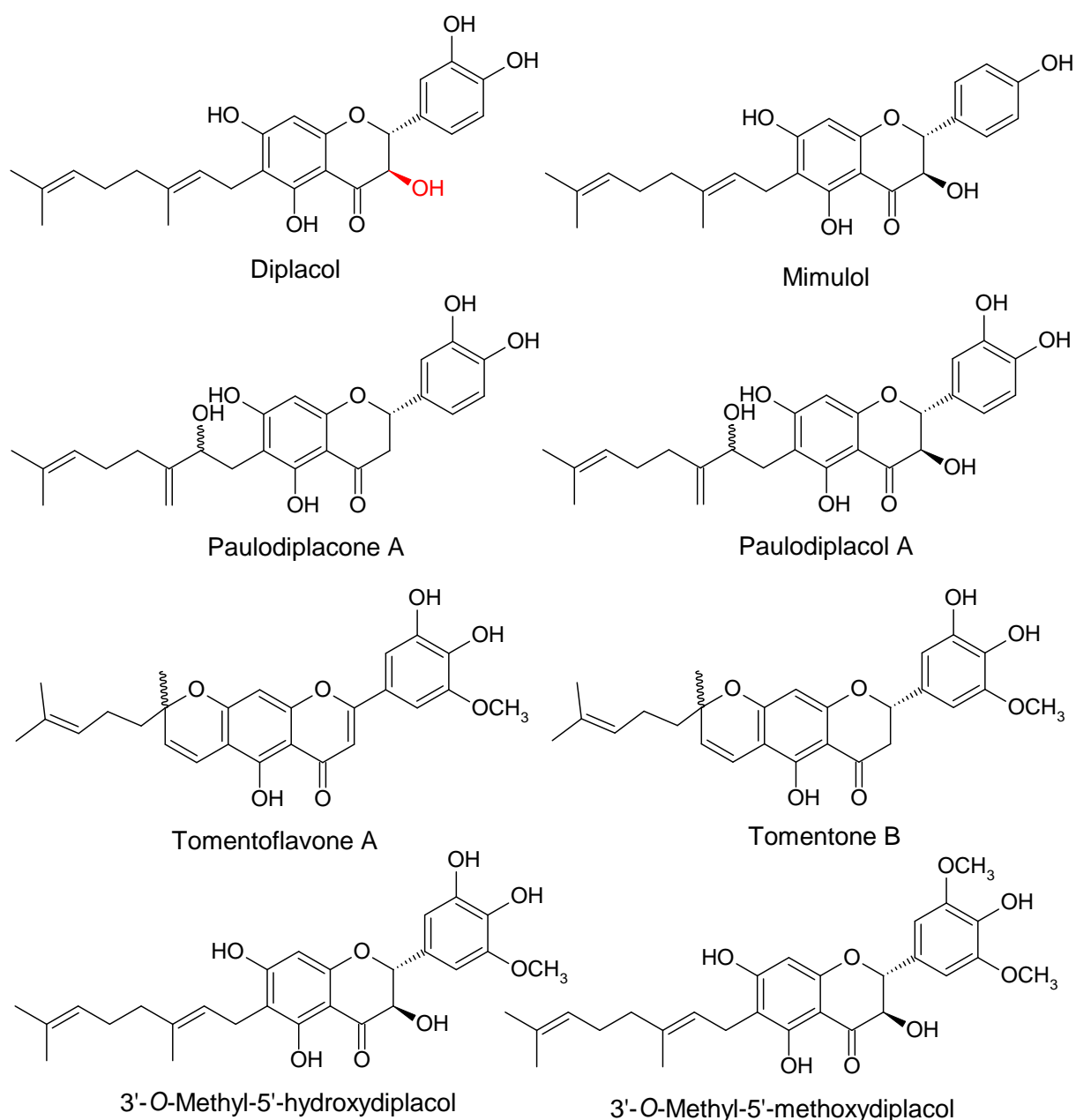


Figure 7 – The anti-inflammatory compounds isolated from *P. tomentosa*.

Results published by Malaník et al. describe the antioxidant and anti-inflammatory effects of natural phenolics isolated from the CHCl_3 -soluble part of an ethanolic extract of branches and twigs of *Broussonetia papyrifera* L. L'Hér. ex Vent. (Moraceae). Among these, prenylated 1,3-diphenylpropane kazinol M and the prenylated flavonols broussoflavonol A and broussoflavonol B (Figure 8) showed inhibitory effects on the activation of NF- κ B/AP-1 in the LPS-activated THP-1-XBlue™-MD2-CD14 cell line. At a non-toxic concentration of 1 μM the

activation was reduced to 75%; prednisone showed a similar effect. These compounds subsequently suppressed the secretion of both IL-1 β and TNF- α (reduction to 50% of the negative control, whereas prednisone was not active) in LPS-stimulated THP-1 cells more significantly than prednisone. Another compound, 5,7,3',4'-tetrahydroxy-3-methoxy-8,5'-diprenylflavone, showed the greatest antioxidant effect in a CAA assay (1.4 \times more active than quercetin, both at 5 μ M) and significantly inhibited NF- κ B/AP-1 activation (reduced to 75%, at 1 μ M). But because the compound did not decrease the secretion of IL-1 β or TNF- α , it probably primarily inhibits AP-1 transcription factor and not NF- κ B⁶.

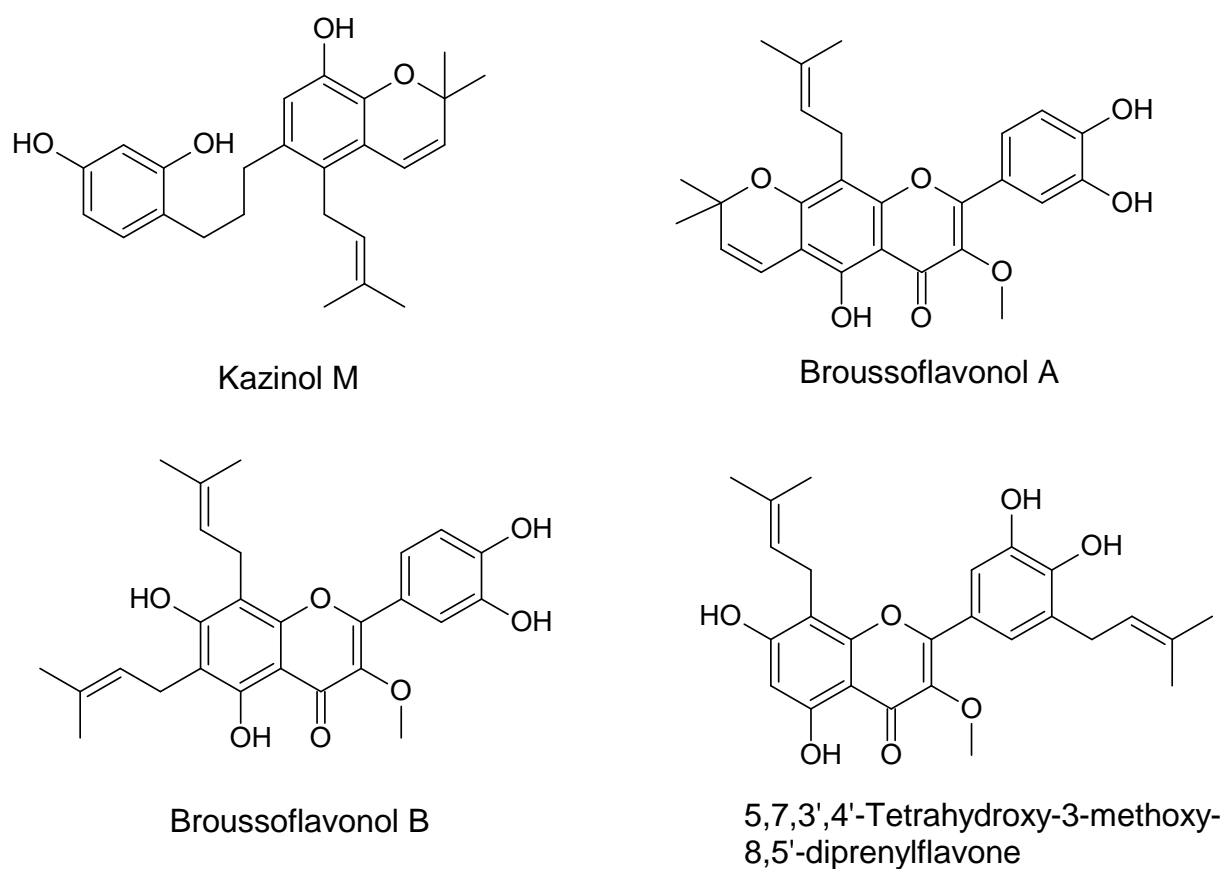


Figure 8 – The structures of kazinol M, brousoflavonol A, B and 5,7,3',4'-tetrahydroxy-3-methoxy-8,5'-diprenylflavone.

From the two publications it can be assumed that the most active anti-inflammatory structure among the prenylated and geranylated flavonoids are flavanonols, followed by flavanones,

flavonols, and flavones. The most active compound was diplacol and its effects should be further elucidated.

Jin et al. performed activity-guided fractionation of the methanolic extract of the flower of *Paulownia coreana* and determined inhibitory activities against LPS-induced nitric oxide production in murine macrophage RAW264.7 cells. In their study, the most active compound was 3'-*O*-methyl-5'-hydroxydiplacone with $IC_{50} = 1.48 \mu M$. This compound was also among those tested in the study by Molčanová et al.⁷, but was not that active – it was able to reduce the NF- κ B activation to approximately 80%, but without statistical significance. Diplacol and diplacone were found very active by Jin et al., with $IC_{50} = 4.53$ and $5.02 \mu M$, respectively⁶⁹.

Moreover, Shahinozzaman et al. tested the anti-inflammatory activity of prenylated flavonoids from Okinawa propolis. The effect was tested as an inhibition of LPS-induced nitric oxide production in murine macrophage RAW264.7 cells. Diplacone (named as nymphaeol A in this study) was the second most active compound, with $IC_{50} = 3.2 \mu M$. The most active compound was nymphaeol C ($IC_{50} = 2.4 \mu M$) or 5'-geranyl-6-prenyl-5,7,3',4'-tetrahydroxyflavanone⁷⁰.

3.3. ANTIDIABETIC ACTIVITY

Insulin is a peptide hormone produced by β -cells in the pancreas. It regulates the anabolic metabolism in the body by absorbing glucose into adipose tissue, skeletal muscles, and liver. The hypoglycemic effect of insulin is counterbalanced by glucagon. This fragile equilibrium tilts towards hyperglycemia in T2DM usually because of insulin resistance, in which insulin does not function properly, likely because of defects throughout the insulin signaling pathway.

Simply put, the effect of insulin starts with binding to an insulin receptor (IR) at the membrane of the target cell. The IR possesses tyrosine kinase activity and phosphorylates itself. This results in recruitment of IR substrate (IRS), PI3K, Akt, and its substrate AS160. Based on that, GLUT4 transporter is translocated from cytosolic vesicles to the membrane to enhance the uptake of glucose. The whole pathway is strictly regulated, for example, the autophosphorylation of IR and its substrates is inhibited by the protein tyrosine phosphatase 1B (PTP1B) (Figure 9)⁷¹.

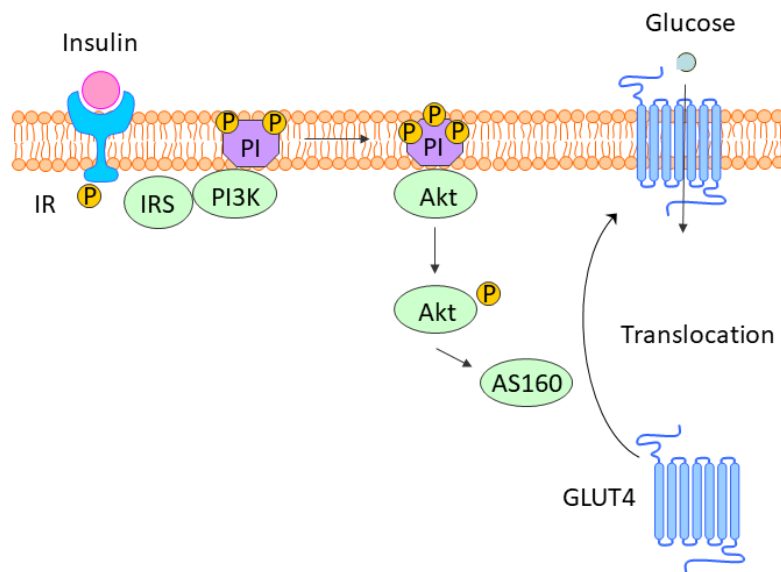


Figure 9 – The insulin transduction pathway (created using Motifolio toolkit).

The antidiabetic activity of natural products can be determined in several ways. Zhang et al. have proposed a classification for *in vitro* assays⁷²:

1. **Phenotypic** assays do not rely on a specific target but determine an overall antidiabetic effect. We can describe them as high-throughput cellular methods and therefore useful as a preliminary initial check:
 - a. **Signaling pathway** assays assess the effect of a test compound on one or multiple pathways related to T2DM.
 - b. The **glucose uptake** assay is based on the accumulation of glucose analogs, either radiolabeled or non-radiolabeled, in cells and its quantification.
 - c. **Insulin secretion** assays concentrate on measurements of intracellular calcium, insulin, cAMP, and ATP.
2. **Target-based** assays, on the other hand, have a great advantage in that the precise mode of action is determined:
 - a. **α -Amylase** and **α -glucosidase** assays are based on the inhibition of these two enzymes that normally digest saccharides in intestines.
 - b. **GLP-1** receptor and peroxisome proliferator-activated receptor γ (**PPAR γ**) **agonist** assays. GLP-1 agonism stimulates the release of insulin from the pancreas and decreases food intake, whereas PPAR γ agonism enhances glucose metabolism and its uptake by cells.
 - c. **PTP1B** and dipeptidyl peptidase-4 (**DPP-4**) **inhibition** assay. Inhibition of PTP1B leads to enhanced signal transduction from the IR and thus a better effect of insulin. DPP-4 inhibitors stop the degradation of incretins and thus enhance their effects. An example of an incretin is GLP-1.
 - d. **GLUT4 translocation** assay can be done using traditional methods, such as western blotting or immunofluorescence. However, there are more sophisticated methods, such as total internal reflection fluorescence (TIRF) microscopy.

Treml et al. concentrated on identifying the geranylated flavonoids and arylbenzofurans isolated from *Paulownia tomentosa* and *Morus alba* as novel PPAR γ partial agonists and hypoglycemic agents. The project workflow started with 36 different natural phenolics that were preselected using molecular docking to a PPAR γ receptor. As a result, 8 (and in next step of selection only 4) positive hits were assayed using *in vitro* cell culture assays, specifically PPAR γ luciferase

reporter gene assay and PPAR γ protein expression by Western blot analysis. Moreover, their ability to induce GLUT4 translocation in cell culture and lower glycemia in chicken embryos was determined⁹.

The selected methods in this project consisted mainly of target-based assays. However, the hen's egg test-chorioallantoic membrane (HET-CAM) assay is a special category on the border between *in vitro* and *in vivo* animal experiments. The HET-CAM assay uses chicken embryos at day 11 of development and therefore is not considered to be an animal experiment and does not require ethical approval. The model has the advantage of mimicking *in vivo* conditions⁷³. Another example of such an approach are experiments on the fruit fly *Drosophila melanogaster* with measurements of the glucose levels in hemolymph. The advantage is that the genetic similarity between humans and fruit flies reaches 60% and as the latter is an invertebrate do not require ethical approvals⁷⁴.

The results of Tremblé et al.⁹ (Figure 10) showed that the concept of using PPAR γ agonism as preselection for further assays of GLUT4 and hypoglycemic activity is not an optimal solution, because the only positive case was **diplacone**, the model compound. Diplacone showed partial agonist activity on PPAR γ (40% of the effect of rosiglitazone, the positive control, at a concentration of 3 μ M), a low effect on GLUT4 translocation (23% of the effect of insulin, the positive control, at a concentration of 10 μ M), and a hypoglycemic effect in the HET-CAM assay (15% of the effect of insulin, at a concentration of 40 μ M, after 120 min.). Mainly the last result contradicts the results reported by Zima et. al. where diplacone did not compellingly reduce blood glucose levels in alloxan-induced diabetic mice. The only exception was a significant reduction of glycemia on day 1 ($p \leq 0.05$). On the other hand, diplacone showed a cytoprotective effect on pancreatic cells. Since alloxan induces diabetes via oxidative damage to the pancreas, this effect might be explained by its antioxidant effect². Therefore further *in vivo* experiments with diplacone are necessary.

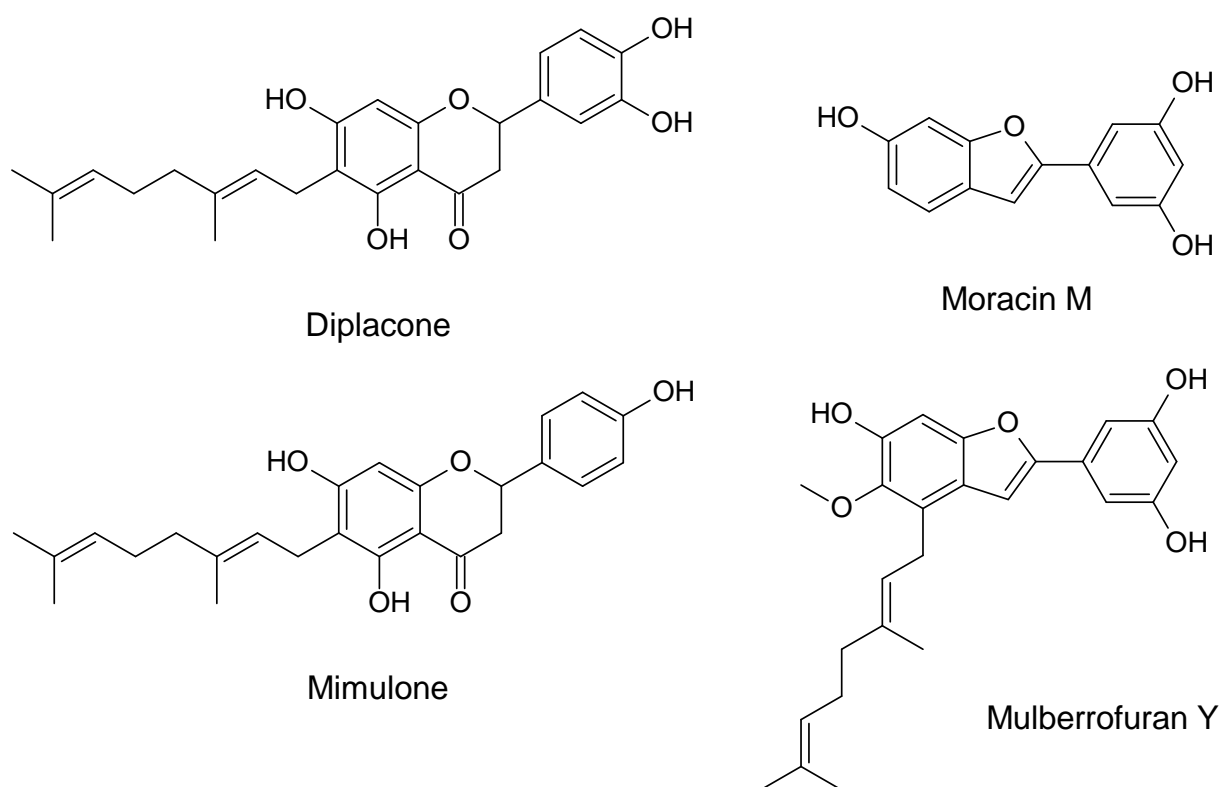


Figure 10 – Structures of diplacone, mimulone, moracin M, and mulberrofuran Y.

Moracin M, an arylbenzofuran obtained from *M. alba*, showed no PPAR γ agonism or enhancement of GLUT4 translocation. But it did show a hypoglycemic effect in the HET-CAM assay (29% of the effect of insulin, at a concentration of 40 μ M, after 120 min.). This result is in accordance with Zhang et al. who observed decreased fasting blood glucose levels in alloxan-diabetic mice after the administration of moracin M⁷⁵. The proposed mechanisms of action include inhibition of PTP1B⁷⁶, induced phosphorylation of PI3K and Akt⁷⁷, and inhibition of DPP-4⁷⁸.

The relationship between the structure of flavonoids and PPAR γ agonism was described by Treml et al. in their review article.⁸ Among all the flavonoid structures, isoflavones were the most promising, namely 4'-fluoro-7-hydroxyisoflavone (recalculated percentage of positive control; %_{PC} = 710.3%). Flavanones, the group to which the model compound diplacone belongs, were the 4th most active when the distribution of %_{PC} values among different classes of flavonoids was compared⁸.

To conclude, two compounds emerged with potential for future experiments. Diplacone with broader effect encompassing PPAR γ agonism, GLUT4 translocation and hypoglycemic effect.

And moracin M with stronger hypoglycemic activity, but a different mechanism than GLUT4 translocation.

3.4. ENCAPSULATION OF NATURAL PRODUCTS

Finally, a well-known fact is that natural phenolics despite their promising biological effects, suffer from poor water solubility, low bioavailability and metabolic instability. One of the ways to overcome such obstacles is the application of novel delivery systems and encapsulation into nanoparticles⁷⁹.

For the purpose of solubilization, Treml et al. used glucan particles (GPs) prepared from baker's yeast *Saccharomyces cerevisiae* Meyen ex E.C. Hansen (Saccharomycetaceae). Their study tested the effect of curcumin encapsulated in GP on the expression of antioxidant enzymes. The study compared the effects of encapsulated curcumin, a mixture of curcumin and GPs (but not encapsulated), curcumin alone, and GPs alone. The results showed that only the mixture was able to increase the expression of the Nrf2 protein and increase the activation of the Nrf2–ARE system significantly after 24h of incubation¹⁰.

Similarly, Šalamúnová et al. incorporated artemisinin, ellagic acid, (-)-epigallocatechin gallate, morusin, and *trans*-resveratrol into GPs and tested their anti-inflammatory and antioxidant effects. The compounds were encapsulated using two different methods – rotary evaporation and spray drying – with the latter more effective in terms of biological activity. No antioxidant activity was detected for the encapsulated compounds. *Trans*-resveratrol encapsulated in GPs was the most active in significantly decreasing the secretion of TNF- α *in vitro* in THP-1 cells stimulated with LPS. Encapsulated *trans*-resveratrol was more effective than the mixture or GPs alone. In inhibition of the NF- κ B pathway, none of the encapsulated compounds was more effective than GPs alone. GPs reduced the activation of NF- κ B down to 15%, which was 5 \times as effective as the positive control, prednisone¹¹.

Both studies showed that GPs are not suitable for the solubilization of natural phenolics because they possess anti-inflammatory effect themselves. On the other hand, Brezani et al. used other type of nanoparticles, such as cationic, anionic, and pegylated liposomes to improve the bioavailability of the poorly soluble lipophilic compound macasiamenene F. The formulation

of neutral liposomes showed high cellular uptake on various cell lines while keeping its anti-inflammatory properties⁸⁰.

Another approach might be encapsulation in cyclodextrins (CDs), which are cyclic oligosaccharides produced from starch, consisting of a hydrophobic interior cavity and hydrophilic exterior⁸¹. For example, Zhang et al. complexed the flavonoid taxifolin with β -CD, which resulted in enhanced *in vitro* cytostatic activity against a hepatocellular carcinoma HepG2 cell line⁸².

Based on this, Nykodýmová et al. encapsulated the geranylated flavanone mimulone into hydroxypropyl- β -cyclodextrins (HP- β -CDs) and anionic, cationic, and neutral liposomes and evaluated their PPAR γ agonistic activity. The encapsulation was effective only for HP- β -CDs, since in this case up to 91.5% of mimulone's activity was preserved¹². Therefore, HP- β -CDs might provide seems to be the best option for natural products encapsulation.

4 . CONCLUSION

This thesis aimed to explore the antioxidant, anti-inflammatory, and antidiabetic effects of plant phenolic compounds. The combinatory effect could be beneficial for a patient with T2DM because not only the main symptom, hyperglycemia, would be treated, but also the oxidative stress and inflammation that worsen the complications of T2DM.

Diplacone was presented as a model compound, and throughout the thesis it was proved that it is the proof-of-concept. Diplacol also showed promising anti-inflammatory activity, whereas moracin M showed hypoglycemic activity.

Several steps need to be taken to successfully follow up on the experiments presented in this thesis:

- ✓ **Efficient and feasible chemical synthesis.** Further *in vivo* experiments will be very demanding in terms of the amounts of the test compounds, which cannot be secured from plant sources.
- ✓ **Further *in vivo* experiments.** The effects have to be confirmed in animal models, such as mice, rats, or pigs. Experiments can even be done on *Drosophila* diabetes models.
- ✓ **Elucidation of the mechanism of action.** It is important to map which proteins are upregulated and which pathways are activated.

- ✓ **Determination of pharmacokinetics, metabolism in the liver, and by fecal microbiota.** For future *in vivo* experiments, knowledge of how the compounds are metabolized is crucial.

5. REFERENCES

- (1) Treml, J.; Šmejkal, K. Flavonoids as Potent Scavengers of Hydroxyl Radicals. *Comprehensive Reviews in Food Science and Food Safety* **2016**, *15* (4), 720–738. <https://doi.org/10.1111/1541-4337.12204>.
- (2) Zima, A.; Hošek, J.; Treml, J.; Muselík, J.; Suchý, P.; Pražanová, G.; Lopes, A.; Žemlička, M. Antiradical and Cytoprotective Activities of Several C-Geranyl-Substituted Flavanones from *Paulownia Tomentosa* Fruit. *Molecules* **2010**, *15* (9), 6035–6049. <https://doi.org/10.3390/molecules15096035>.
- (3) Treml, J.; Šmejkal, K.; Hošek, J.; Žemlička, M. Determination of Antioxidant Activity Using Oxidative Damage to Plasmid DNA — Pursuit of Solvent Optimization. *Chemical Papers* **2013**, *67* (5), 484–489. <https://doi.org/10.2478/s11696-013-0334-8>.
- (4) Treml, J.; Lelakova, V.; Smejkal, K.; Paulickova, T.; Labuda, S.; Granica, S.; Havlik, J.; Jankovska, D.; Padrtova, T.; Hosek, J. Antioxidant Activity of Selected Stilbenoid Derivatives in a Cellular Model System. *Biomolecules* **2019**, *9* (9), 468. <https://doi.org/10.3390/biom9090468>.
- (5) Treml, J.; Večeřová, P.; Herczogová, P.; Šmejkal, K. Direct and Indirect Antioxidant Effects of Selected Plant Phenolics in Cell-Based Assays. *Molecules* **2021**, *26* (9), 2534. <https://doi.org/10.3390/molecules26092534>.
- (6) Malaník, M.; Treml, J.; Leláková, V.; Nykodýmová, D.; Oravec, M.; Marek, J.; Šmejkal, K. Anti-Inflammatory and Antioxidant Properties of Chemical Constituents of *Broussonetia Papyrifera*. *Bioorganic Chemistry* **2020**, *104*, 104298. <https://doi.org/10.1016/j.bioorg.2020.104298>.
- (7) Molčanová, L.; Treml, J.; Brežani, V.; Maršík, P.; Kurhan, S.; Trávníček, Z.; Uhrin, P.; Šmejkal, K. C-Geranylated Flavonoids from *Paulownia Tomentosa* Steud. Fruit as Potential Anti-Inflammatory Agents. *Journal of Ethnopharmacology* **2022**, *296*, 115509. <https://doi.org/10.1016/j.jep.2022.115509>.
- (8) Treml, J.; Nykodýmová, D.; Kubatka, P. Structure Activity Relationship of Flavonoids as PPAR γ Agonists. *Phytochem Rev* **2025**. <https://doi.org/10.1007/s11101-025-10121-w>.
- (9) Treml, J.; Václavík, J.; Molčanová, L.; Čulenová, M.; Hummelbrunner, S.; Neuhauser, C.; Dirsch, V. M.; Weghuber, J.; Šmejkal, K. Identification of Plant Phenolics from *Paulownia Tomentosa* and *Morus Alba* as Novel PPAR γ Partial Agonists and Hypoglycemic Agents. *J. Agric. Food Chem.* **2025**, *73* (22), 13960–13972. <https://doi.org/10.1021/acs.jafc.4c11398>.
- (10) Treml, J.; Salamunova, P.; Hanus, J.; Hosek, J. The Effect of Curcumin Encapsulation into Yeast Glucan Particles on Antioxidant Enzyme Expression *In Vitro*. *Food Funct.* **2021**, *12* (5), 1954–1957. <https://doi.org/10.1039/d0fo03237a>.
- (11) Šalamúnová, P.; Cupalová, L.; Majerská, M.; Treml, J.; Ruphuy, G.; Šmejkal, K.; Štěpánek, F.; Hanuš, J.; Hošek, J. Incorporating Natural Anti-Inflammatory Compounds into Yeast Glucan Particles Increases Their Bioactivity *In Vitro*. *International Journal of Biological Macromolecules* **2021**, *169*, 443–451. <https://doi.org/10.1016/j.ijbiomac.2020.12.107>.

- (12) Nykodýmová, D.; Molčanová, L.; Kotouček, J.; Mašek, J.; Treml, J. PPAR γ Agonistic Activity of Mimulone and Diplacone Encapsulated in Liposomes and Cyclodextrin Complexes. *ChemistryOpen* *n/a* (n/a), 202500209. <https://doi.org/10.1002/open.202500209>.
- (13) *Molecular Pharmacy | Departement Pharmazeutische Wissenschaften | Universität Basel*. <https://pharma.unibas.ch/de/research/research-groups/molecular-pharmacy-2145/> (accessed 2025-08-15).
- (14) *Institute Pharmaceutical Sciences*. <https://pharmazie.uni-graz.at/en/about-the-institute/> (accessed 2025-08-15).
- (15) Kuczmánová, A.; Gál, P.; Varinská, L.; Treml, J.; Kováč, I.; Novotný, M.; Vasilenko, T.; Dall'Acqua, S.; Nagy, M.; Mučaji, P. Agrimonia Eupatoria L. and Cynara Cardunculus L. Water Infusions: Phenolic Profile and Comparison of Antioxidant Activities. *Molecules* **2015**, *20* (11), 20538–20550. <https://doi.org/10.3390/molecules201119715>.
- (16) Stastny, J.; Marsik, P.; Tauchen, J.; Bozik, M.; Mascellani, A.; Havlik, J.; Landa, P.; Jablonsky, I.; Treml, J.; Herczogova, P.; Bleha, R.; Synytsya, A.; Kloucek, P. Antioxidant and Anti-Inflammatory Activity of Five Medicinal Mushrooms of the Genus Pleurotus. *Antioxidants* **2022**, *11* (8), 1569. <https://doi.org/10.3390/antiox11081569>.
- (17) Rybníkář, M.; Malaník, M.; Šmejkal, K.; Švajdlenka, E.; Shpet, P.; Babica, P.; Dall'Acqua, S.; Smitík, O.; Jurček, O.; Treml, J. Dibenzocyclooctadiene Lignans from Schisandra Chinensis with Anti-Inflammatory Effects. *International Journal of Molecular Sciences* **2024**, *25* (6), 3465. <https://doi.org/10.3390/ijms25063465>.
- (18) Peron, G.; Bernabé, G.; Marcheluzzo, S.; Zengin, G.; Ibrahim Sinan, K.; Hošek, J.; Treml, J.; Kaja, I.; Paccagnella, M.; Brun, P.; Castagliuolo, I.; Zancato, M.; Dall'Acqua, S. Orange Fruit Peels from PDO Varieties of Ribera (Sicily, Italy): An Insight into the Chemistry and Bioactivity of Volatile and Non-Volatile Secondary Metabolites Extracted Using a Microwave-Assisted Method. *Journal of Functional Foods* **2024**, *116*, 106147. <https://doi.org/10.1016/j.jff.2024.106147>.
- (19) Vasilev, H.; Šmejkal, K.; Jusková, S.; Vaclavik, J.; Treml, J. Five New Tamarixetin Glycosides from Astragalus Thracicus Griseb. Including Some Substituted with the Rare 3-Hydroxy-3-Methylglutaric Acid and Their Collagenase Inhibitory Effects In Vitro. *ACS Omega* **2024**, *9* (16), 18023–18031. <https://doi.org/10.1021/acsomega.3c09677>.
- (20) Dvorska, D.; Mazurakova, A.; Lackova, L.; Sebova, D.; Kajo, K.; Samec, M.; Brany, D.; Svajdlenka, E.; Treml, J.; Mersakova, S.; Strnadel, J.; Adamkov, M.; Lasabova, Z.; Biringer, K.; Mojzis, J.; Büsselberg, D.; Smejkal, K.; Kello, M.; Kubatka, P. Aronia Melanocarpa L. Fruit Peels Show Anti-Cancer Effects in Preclinical Models of Breast Carcinoma: The Perspectives in the Chemoprevention and Therapy Modulation. *Front. Oncol.* **2024**, *14*. <https://doi.org/10.3389/fonc.2024.1463656>.
- (21) Malaník, M.; Treml, J.; Kubínová, R.; Vávrová, G.; Oravec, M.; Marek, J.; Zhaparkulova, K.; Ibragimova, L.; Bekezhanova, T.; Karaubayeva, A.; Sakipova, Z.; Šmejkal, K. Isolation of a Unique Monoterpene Diperoxy Dimer From Ziziphora Clinopodioides Subsp. Bungeana Together With Triterpenes With Antidiabetic Properties. *Phytochemical Analysis* **2025**, *36* (4), 1223–1230. <https://doi.org/10.1002/pca.3505>.
- (22) Dvorska, D.; Sebova, D.; Kajo, K.; Kapinova, A.; Svajdlenka, E.; Goga, M.; Frenak, R.; Treml, J.; Mersakova, S.; Strnadel, J.; Mazurakova, A.; Baranova, I.; Halasova, E.; Brozmanova, M.; Biringer, K.; Kassayova, M.; Dankova, Z.; Smejkal, K.; Hornak, S.; Mojzis, J.; Sadlonova, V.; Brany, D.; Kello, M.; Kubatka, P. Chemopreventive and Therapeutic Effects of Hippophae Rhamnoides L. Fruit Peels Evaluated in Preclinical Models of Breast Carcinoma. *Front. Pharmacol.* **2025**, *16*. <https://doi.org/10.3389/fphar.2025.1561436>.

- (23) Malanik, M.; Tremel, J.; Rjaskova, V.; Tizkova, K.; Kaucka, P.; Kokoska, L.; Kubatka, P.; Smejkal, K. Maytenus Macrocarpa (Ruiz & Pav.) Briq.: Phytochemistry and Pharmacological Activity. *Molecules* **2019**, *24* (12), 2288. <https://doi.org/10.3390/molecules24122288>.
- (24) Pospisilova, S.; Marvanova, P.; Tremel, J.; Moricz, A. M.; Ott, P. G.; Mokry, P.; Odehnalova, K.; Sedo, O.; Cizek, A.; Jampilek, J. Activity of N-Phenylpiperazine Derivatives Against Bacterial and Fungal Pathogens. *Curr Protein Pept Sci* **2019**, *20* (11), 1119–1129. <https://doi.org/10.2174/1389203720666190913114041>.
- (25) Bak, A.; Pizova, H.; Kozik, V.; Vorcakova, K.; Kos, J.; Tremel, J.; Odehnalova, K.; Oravec, M.; Imramovsky, A.; Bobal, P.; Smolinski, A.; Trávníček, Z.; Jampilek, J. SAR-Mediated Similarity Assessment of the Property Profile for New, Silicon-Based AChE/BChE Inhibitors. *Int J Mol Sci* **2019**, *20* (21), 5385. <https://doi.org/10.3390/ijms20215385>.
- (26) Kucerova-Chlupacova, M.; Halakova, D.; Majekova, M.; Tremel, J.; Stefek, M.; Soltesova Prnova, M. (4-Oxo-2-Thioxothiazolidin-3-Yl)Acetic Acids as Potent and Selective Aldose Reductase Inhibitors. *Chem. Biol. Interact.* **2020**, *332*, 109286. <https://doi.org/10.1016/j.cbi.2020.109286>.
- (27) Škovranová, G.; Čulenová, M.; Tremel, J.; Dzurická, L.; Marova, I.; Sychrová, A. Prenylated Phenolics from Morus Alba against MRSA Infections as a Strategy for Wound Healing. *Front. Pharmacol.* **2022**, *13*. <https://doi.org/10.3389/fphar.2022.1068371>.
- (28) Škovranová, G.; Molčanová, L.; Jug, B.; Jug, D.; Klančnik, A.; Smole-Možina, S.; Tremel, J.; Tušek Žnidarič, M.; Sychrová, A. Perspectives on Antimicrobial Properties of *Paulownia Tomentosa* Steud. Fruit Products in the Control of *Staphylococcus Aureus* Infections. *Journal of Ethnopharmacology* **2024**, *321*, 117461. <https://doi.org/10.1016/j.jep.2023.117461>.
- (29) Helcman, M.; Šmejkal, K.; Čulenová, M.; Béres, T.; Tremel, J. Natural Phenolics Disrupt Microbial Communication by Inhibiting Quorum Sensing. *Microorganisms* **2025**, *13* (2), 287. <https://doi.org/10.3390/microorganisms13020287>.
- (30) Simona, J.; Dani, D.; Petr, S.; Marcela, N.; Jakub, T.; Bohuslava, T. Edible Films from Carrageenan/Orange Essential Oil/Trehalose—Structure, Optical Properties, and Antimicrobial Activity. *Polymers* **2021**, *13* (3), 332. <https://doi.org/10.3390/polym13030332>.
- (31) Antonic, B.; Dordevic, D.; Jancikova, S.; Tremlova, B.; Nejezchlebova, M.; Goldová, K.; Tremel, J. Reused Plant Fried Oil: A Case Study with Home-Made Soaps. *Processes* **2021**, *9* (3), 529. <https://doi.org/10.3390/pr9030529>.
- (32) Dordevic, S.; Dordevic, D.; Sedlacek, P.; Kalina, M.; Tesikova, K.; Antonic, B.; Tremlova, B.; Tremel, J.; Nejezchlebova, M.; Vapenka, L.; Rajchl, A.; Bulakova, M. Incorporation of Natural Blueberry, Red Grapes and Parsley Extract By-Products into the Production of Chitosan Edible Films. *Polymers* **2021**, *13* (19), 3388. <https://doi.org/10.3390/polym13193388>.
- (33) Dordevic, S.; Dordevic, D.; Tesikova, K.; Sedlacek, P.; Kalina, M.; Vapenka, L.; Nejezchlebova, M.; Tremel, J.; Tremlova, B.; Mikulášková, H. K. Nanometals Incorporation into Active and Biodegradable Chitosan Films. *Heliyon* **2024**, *10* (7). <https://doi.org/10.1016/j.heliyon.2024.e28430>.
- (34) Tremel, J.; Gazdová, M.; Šmejkal, K.; Šudomová, M.; Kubatka, P.; Hassan, S. T. S. Natural Products-Derived Chemicals: Breaking Barriers to Novel Anti-HSV Drug Development. *Viruses* **2020**, *12* (2), 154. <https://doi.org/10.3390/v12020154>.

- (35) Kushkevych, I.; Cejnar, J.; Treml, J.; Dordević, D.; Kollar, P.; Vítězová, M. Recent Advances in Metabolic Pathways of Sulfate Reduction in Intestinal Bacteria. *Cells* **2020**, *9* (3), 698. <https://doi.org/10.3390/cells9030698>.
- (36) Deshpande, A. D.; Harris-Hayes, M.; Schootman, M. Epidemiology of Diabetes and Diabetes-Related Complications. *Phys Ther* **2008**, *88* (11), 1254–1264. <https://doi.org/10.2522/ptj.20080020>.
- (37) Oguntibeju, O. O. Type 2 Diabetes Mellitus, Oxidative Stress and Inflammation: Examining the Links. *Int J Physiol Pathophysiol Pharmacol* **2019**, *11* (3), 45–63.
- (38) *10 tips for healthy eating if you are at risk of type 2 diabetes*. Diabetes UK. <https://www.diabetes.org.uk/about-diabetes/type-2-diabetes/preventing/ten-tips-for-healthy-eating> (accessed 2025-08-18).
- (39) *Overview | Type 2 diabetes in adults: management | Guidance | NICE*. <https://www.nice.org.uk/guidance/ng28> (accessed 2025-07-10).
- (40) Witters, L. A. The Blooming of the French Lilac. *J Clin Invest* **2001**, *108* (8), 1105–1107. <https://doi.org/10.1172/JCI14178>.
- (41) Skyler, J. S. Diabetes Mellitus: Pathogenesis and Treatment Strategies. *J. Med. Chem.* **2004**, *47* (17), 4113–4117. <https://doi.org/10.1021/jm0306273>.
- (42) Zhou, Z.; Sun, B.; Yu, D.; Zhu, C. Gut Microbiota: An Important Player in Type 2 Diabetes Mellitus. *Front. Cell. Infect. Microbiol.* **2022**, *12*. <https://doi.org/10.3389/fcimb.2022.834485>.
- (43) Qin, L.; Fan, B.; Zhou, Y.; Zheng, J.; Diao, R.; Wang, F.; Liu, J. Targeted Gut Microbiome Therapy: Applications and Prospects of Probiotics, Fecal Microbiota Transplantation and Natural Products in the Management of Type 2 Diabetes. *Pharmacological Research* **2025**, *213*, 107625. <https://doi.org/10.1016/j.phrs.2025.107625>.
- (44) Deli, C. K.; Fatouros, I. G.; Poullos, A.; Liakou, C. A.; Draganidis, D.; Papanikolaou, K.; Rosvoglou, A.; Gatsas, A.; Georgakouli, K.; Tsimeas, P.; Jamurtas, A. Z. Gut Microbiota in the Progression of Type 2 Diabetes and the Potential Role of Exercise: A Critical Review. *Life* **2024**, *14* (8), 1016. <https://doi.org/10.3390/life14081016>.
- (45) Dahlén, A. D.; Dashi, G.; Maslov, I.; Attwood, M. M.; Jonsson, J.; Trukhan, V.; Schiöth, H. B. Trends in Antidiabetic Drug Discovery: FDA Approved Drugs, New Drugs in Clinical Trials and Global Sales. *Front. Pharmacol.* **2022**, *12*. <https://doi.org/10.3389/fphar.2021.807548>.
- (46) Rodríguez, I. A.; Serafini, M.; Alves, I. A.; Lang, K. L.; Silva, F. R. M. B.; Aragón, D. M. Natural Products as Outstanding Alternatives in Diabetes Mellitus: A Patent Review. *Pharmaceutics* **2023**, *15* (1), 85. <https://doi.org/10.3390/pharmaceutics15010085>.
- (47) Dai, J.; Mumper, R. J. Plant Phenolics: Extraction, Analysis and Their Antioxidant and Anticancer Properties. *Molecules* **2010**, *15* (10), 7313–7352. <https://doi.org/10.3390/molecules15107313>.
- (48) Quideau, S.; Deffieux, D.; Douat-Casassus, C.; Pouységu, L. Plant Polyphenols: Chemical Properties, Biological Activities, and Synthesis. *Angew Chem Int Ed Engl* **2011**, *50* (3), 586–621. <https://doi.org/10.1002/anie.201000044>.
- (49) Kunz, C. F.; de Vries, S.; de Vries, J. Plant Terrestrialization: An Environmental Pull on the Evolution of Multi-Sourced Streptophyte Phenolics. *Philosophical Transactions of the Royal Society B: Biological Sciences* **2024**, *379* (1914), 20230358. <https://doi.org/10.1098/rstb.2023.0358>.
- (50) Lincoln, D. E. Leaf Resin Flavonoids of *Diplacus Aurantiacus*. *Biochemical Systematics and Ecology* **1980**, *8* (4), 397–400. [https://doi.org/10.1016/0305-1978\(80\)90043-5](https://doi.org/10.1016/0305-1978(80)90043-5).

- (51) Smejkal, K.; Grycová, L.; Marek, R.; Lemièrre, F.; Jankovská, D.; Forejtníková, H.; Vanco, J.; Suchý, V. C-Geranyl Compounds from *Paulownia Tomentosa* Fruits. *J Nat Prod* **2007**, *70* (8), 1244–1248. <https://doi.org/10.1021/np070063w>.
- (52) Phommart, S.; Sutthivaiyakit, P.; Chimnoi, N.; Ruchirawat, S.; Sutthivaiyakit, S. Constituents of the Leaves of *Macaranga Tanarius*. *J Nat Prod* **2005**, *68* (6), 927–930. <https://doi.org/10.1021/np0500272>.
- (53) Yoder, B. J.; Cao, S.; Norris, A.; Miller, J. S.; Ratovoson, F.; Razafitsalama, J.; Andriantsiferana, R.; Rasamison, V. E.; Kingston, D. G. I. Antiproliferative Prenylated Stilbenes and Flavonoids from *Macaranga Alnifolia* from the Madagascar Rainforest, 1. *J. Nat. Prod.* **2007**, *70* (3), 342–346. <https://doi.org/10.1021/np060484y>.
- (54) Murphy, B. T.; Cao, S.; Norris, A.; Miller, J. S.; Ratovoson, F.; Andriantsiferana, R.; Rasamison, V. E.; Kingston, D. G. I. Cytotoxic Flavanones of *Schizolaena Hystrix* from the Madagascar Rainforest. *J Nat Prod* **2005**, *68* (3), 417–419. <https://doi.org/10.1021/np049639x>.
- (55) Phillips, W. R.; Baj, N. J.; Gunatilaka, A. A.; Kingston, D. G. C-Geranyl Compounds from *Mimulus Clevelandii*. *J Nat Prod* **1996**, *59* (5), 495–497. <https://doi.org/10.1021/np960240l>.
- (56) Chen, C.-N.; Wu, C.-L.; Lin, J.-K. Propolis C from Propolis Induces Apoptosis through Activating Caspases, Bid and Cytochrome c Release in Human Melanoma Cells. *Biochem Pharmacol* **2004**, *67* (1), 53–66. <https://doi.org/10.1016/j.bcp.2003.07.020>.
- (57) Akinwumi, B. C.; Bordun, K.-A. M.; Anderson, H. D. Biological Activities of Stilbenoids. *Int J Mol Sci* **2018**, *19* (3), 792. <https://doi.org/10.3390/ijms19030792>.
- (58) Vesely, O.; Marsik, P.; Jarosova, V.; Doskocil, I.; Smejkal, K.; Kloucek, P.; Havlik, J. Metabolism of Selected 2-Arylbenzofurans in a Colon In Vitro Model System. *Foods* **2021**, *10* (11), 2754. <https://doi.org/10.3390/foods10112754>.
- (59) Sedláček, P.; Bludovská, M.; Plavinová, I.; Zavadáková, A.; Müller, L.; Müllerová, D. Dietary Intake of Plant Polyphenols: Exploring Trend in the Czech Population. *Cent Eur J Public Health* **2024**, *32* (2), 101–107. <https://doi.org/10.21101/cejph.a7994>.
- (60) Cosme, P.; Rodríguez, A. B.; Espino, J.; Garrido, M. Plant Phenolics: Bioavailability as a Key Determinant of Their Potential Health-Promoting Applications. *Antioxidants* **2020**, *9* (12), 1263. <https://doi.org/10.3390/antiox9121263>.
- (61) Ngo, V.; Duennwald, M. L. Nrf2 and Oxidative Stress: A General Overview of Mechanisms and Implications in Human Disease. *Antioxidants (Basel)* **2022**, *11* (12), 2345. <https://doi.org/10.3390/antiox11122345>.
- (62) Salzano, S.; Checconi, P.; Hanschmann, E.-M.; Lillig, C. H.; Bowler, L. D.; Chan, P.; Vaudry, D.; Mengozzi, M.; Coppo, L.; Sacre, S.; Atkuri, K. R.; Sahaf, B.; Herzenberg, L. A.; Herzenberg, L. A.; Mullen, L.; Ghezzi, P. Linkage of Inflammation and Oxidative Stress via Release of Glutathionylated Peroxiredoxin-2, Which Acts as a Danger Signal. *Proc Natl Acad Sci U S A* **2014**, *111* (33), 12157–12162. <https://doi.org/10.1073/pnas.1401712111>.
- (63) Wolfe, K. L.; Liu, R. H. Structure–Activity Relationships of Flavonoids in the Cellular Antioxidant Activity Assay. *J. Agric. Food Chem.* **2008**, *56* (18), 8404–8411. <https://doi.org/10.1021/jf8013074>.
- (64) Esatbeyoglu, T.; Ewald, P.; Yasui, Y.; Yokokawa, H.; Wagner, A. E.; Matsugo, S.; Winterhalter, P.; Rimbach, G. Chemical Characterization, Free Radical Scavenging, and Cellular Antioxidant and Anti-Inflammatory Properties of a Stilbenoid-Rich Root Extract of *Vitis Vinifera*. *Oxid Med Cell Longev* **2016**, *2016*, 8591286. <https://doi.org/10.1155/2016/8591286>.

- (65) Guo, Q.; Jin, Y.; Chen, X.; Ye, X.; Shen, X.; Lin, M.; Zeng, C.; Zhou, T.; Zhang, J. NF- κ B in Biology and Targeted Therapy: New Insights and Translational Implications. *Sig Transduct Target Ther* **2024**, *9* (1), 53. <https://doi.org/10.1038/s41392-024-01757-9>.
- (66) Cruz, N. G.; Sousa, L. P.; Sousa, M. O.; Pietrani, N. T.; Fernandes, A. P.; Gomes, K. B. The Linkage between Inflammation and Type 2 Diabetes Mellitus. *Diabetes Research and Clinical Practice* **2013**, *99* (2), 85–92. <https://doi.org/10.1016/j.diabres.2012.09.003>.
- (67) Huang, X.; Li, Y.; Sabier, M.; Si, J.; Wang, P.; Shen, Y.; Zhang, X.; Liu, J. Guidelines for the in Vitro Determination of Anti-Inflammatory Activity. *eFood* **2024**, *5* (3), e160. <https://doi.org/10.1002/efd2.160>.
- (68) Vochyánová, Z.; Bartošová, L.; Bujdáková, V.; Fictum, P.; Husník, R.; Suchý, P.; Šmejkal, K.; Hošek, J. Diplacone and Mimulone Ameliorate Dextran Sulfate Sodium-Induced Colitis in Rats. *Fitoterapia* **2015**, *101*, 201–207. <https://doi.org/10.1016/j.fitote.2015.01.012>.
- (69) Jin, Q.; Lee, C.; Lee, J. W.; Lee, D.; Kim, Y.; Hong, J. T.; Kim, J. S.; Kim, J.-H.; Lee, M. K.; Hwang, B. Y. Geranylated Flavanones from Paulownia Coreana and Their Inhibitory Effects on Nitric Oxide Production. *Chem Pharm Bull (Tokyo)* **2015**, *63* (5), 384–387. <https://doi.org/10.1248/cpb.c14-00839>.
- (70) Shahinozzaman, M.; Taira, N.; Ishii, T.; Halim, M. A.; Hossain, M. A.; Tawata, S. Anti-Inflammatory, Anti-Diabetic, and Anti-Alzheimer's Effects of Prenylated Flavonoids from Okinawa Propolis: An Investigation by Experimental and Computational Studies. *Molecules* **2018**, *23* (10), 2479. <https://doi.org/10.3390/molecules23102479>.
- (71) Le, T. K. C.; Dao, X. D.; Nguyen, D. V.; Luu, D. H.; Bui, T. M. H.; Le, T. H.; Nguyen, H. T.; Le, T. N.; Hosaka, T.; Nguyen, T. T. T. Insulin Signaling and Its Application. *Front. Endocrinol.* **2023**, *14*. <https://doi.org/10.3389/fendo.2023.1226655>.
- (72) Zhang, X.; Kupczyk, E.; Schmitt-Kopplin, P.; Mueller, C. Current and Future Approaches for *in Vitro* Hit Discovery in Diabetes Mellitus. *Drug Discovery Today* **2022**, *27* (10), 103331. <https://doi.org/10.1016/j.drudis.2022.07.016>.
- (73) Haselgrübler, R.; Stübl, F.; Essl, K.; Iken, M.; Schröder, K.; Weghuber, J. Gluc-HET, a Complementary Chick Embryo Model for the Characterization of Antidiabetic Compounds. *PLoS One* **2017**, *12* (8), e0182788. <https://doi.org/10.1371/journal.pone.0182788>.
- (74) Miao, Y.; Chen, R.; Wang, X.; Zhang, J.; Tang, W.; Zhang, Z.; Liu, Y.; Xu, Q. Drosophila Melanogaster Diabetes Models and Its Usage in the Research of Anti-Diabetes Management with Traditional Chinese Medicines. *Front Med (Lausanne)* **2022**, *9*, 953490. <https://doi.org/10.3389/fmed.2022.953490>.
- (75) Zhang, M.; Chen, M.; Zhang, H.-Q.; Sun, S.; Xia, B.; Wu, F.-H. In Vivo Hypoglycemic Effects of Phenolics from the Root Bark of Morus Alba. *Fitoterapia* **2009**, *80* (8), 475–477. <https://doi.org/10.1016/j.fitote.2009.06.009>.
- (76) Kwon, R.-H.; Thaku, N.; Timalisina, B.; Park, S.-E.; Choi, J.-S.; Jung, H.-A. Inhibition Mechanism of Components Isolated from Morus Alba Branches on Diabetes and Diabetic Complications via Experimental and Molecular Docking Analyses. *Antioxidants* **2022**, *11* (2), 383. <https://doi.org/10.3390/antiox11020383>.
- (77) Kwak, H. J.; Kim, J.; Kim, S.-Y.; Park, S.; Choi, J.; Kim, S. H. Moracin E and M Isolated from Morus Alba Linné Induced the Skeletal Muscle Cell Proliferation via PI3K-Akt-mTOR Signaling Pathway. *Sci Rep* **2023**, *13* (1), 20570. <https://doi.org/10.1038/s41598-023-47411-2>.
- (78) Olufolabo, K. O.; Lüersen, K.; Oguntimehin, S. A.; Nchiozem-Ngnitedem, V.-A.; Agbebi, E. A.; Faloye, K. O.; Nyamboki, D. K.; Rimbach, G.; Matasyoh, J. C.; Schmidt, B.; Moody, J. O. In Vitro and in Silico Studies Reveal Antidiabetic Properties of

- Arylbenzofurans from the Root Bark of *Morus Mesozygia* Stapf. *Front. Pharmacol.* **2024**, *15*. <https://doi.org/10.3389/fphar.2024.1338333>.
- (79) Ranjbar, S.; Emamjomeh, A.; Sharifi, F.; Zarepour, A.; Aghaabbasi, K.; Dehshahri, A.; Sepahvand, A. M.; Zarrabi, A.; Beyzaei, H.; Zahedi, M. M.; Mohammadinejad, R. Lipid-Based Delivery Systems for Flavonoids and Flavonolignans: Liposomes, Nanoemulsions, and Solid Lipid Nanoparticles. *Pharmaceutics* **2023**, *15* (7), 1944. <https://doi.org/10.3390/pharmaceutics15071944>.
- (80) Brezani, V.; Blondeau, N.; Kotouček, J.; Klásková, E.; Šmejkal, K.; Hošek, J.; Mašková, E.; Kulich, P.; Prachyawarakorn, V.; Heurteaux, C.; Mašek, J. Enhancing Solubility and Bioefficacy of Stilbenes by Liposomal Encapsulation—The Case of Macasiamenene F. *ACS Omega* **2024**, *9* (8), 9027–9039. <https://doi.org/10.1021/acsomega.3c07380>.
- (81) Christaki, S.; Spanidi, E.; Panagiotidou, E.; Athanasopoulou, S.; Kyriakoudi, A.; Mourtzinis, I.; Gardikis, K. Cyclodextrins for the Delivery of Bioactive Compounds from Natural Sources: Medicinal, Food and Cosmetics Applications. *Pharmaceutics* **2023**, *16* (9), 1274. <https://doi.org/10.3390/ph16091274>.
- (82) Zhang, Y.; Yu, J.; Dong, X.-D.; Ji, H.-Y. Research on Characteristics, Antioxidant and Antitumor Activities of Dihydroquercetin and Its Complexes. *Molecules* **2018**, *23* (1), 20. <https://doi.org/10.3390/molecules23010020>.

6. ARTICLES

6.1. ARTICLE 1

Treml, J.; Smejkal, K. Comprehensive Reviews in Food Science and Food Safety 2016, 15, 720-738 (IF = 5.974).

Flavonoids as Potent Scavengers of Hydroxyl Radicals

Jakub Tremł and Karel Šmejkal

Abstract: Oxidative stress is a fundamental principle in the pathophysiology of many diseases. It occurs when the production of reactive oxygen species exceeds the capacity of the cell defense system. The hydroxyl radical is a reactive oxygen species that is commonly formed *in vivo* and can cause serious damage to biomolecules, such as lipids, proteins, and nucleic acids. It plays a role in inflammation-related diseases, like chronic inflammation, neurodegeneration, and cancer. To overcome excessive oxidative stress and thus to prevent or stop the progression of diseases connected to it, scientists try to combat oxidative stress and to find antioxidant molecules, including those that scavenge hydroxyl radical or diminish its production in inflamed tissues.

This article reviews various methods of hydroxyl radical production and scavenging. Further, flavonoids, as natural plant antioxidants and essential component of the human diet, are reviewed as compounds interacting with the production of hydroxyl radicals. The relationship between hydroxyl radical scavenging and the structure of the flavonoids is discussed. The structural elements of the flavonoid molecule most important for hydroxyl radical scavenging are hydroxylation of ring B and a C2–C3 double bond connected with a C-3 hydroxyl group and a C-4 carbonyl group. Hydroxylation of ring A also enhances the activity, as does the presence of gallate and galactouronate moieties as substituents on the flavonoid skeleton.

Keywords: Fenton reaction, flavonoids, hydroxyl radical, scavenging, structure–activity relationship

Introduction

Oxidative stress is a state present in all aerobic organisms. It occurs when the production of reactive oxygen species (ROS) exceeds the limited capacity of the cellular antioxidant system. Aerobic organisms have the advantage of gaining more energy from oxidative phosphorylation than anaerobic organisms get from anaerobic glycolysis. However, a serious disadvantage of oxidative phosphorylation is the possibility of producing ROS. ROS are small molecules, commonly produced in radical reactions, with the capacity to quickly interact with cellular structures. They are represented by various chemical entities: oxygen radicals (such as hydroxyl radical $\cdot\text{OH}$) or nonradical substances (such as hydrogen peroxide H_2O_2) (Ma 2010).

ROS are usually very reactive; they do not have long lifetimes and cannot be transported for long distances in an organism. They therefore damage the cell structures that are closest to the site of their formation. They readily attack nucleic acids, proteins, and lipids. The molecule that is attacked is either damaged, destroyed, or has its function altered. Oxidative stress plays a key role in the origin and development of many diseases connected with inflammation, such as neurodegeneration, cardiovascular diseases, and

cancer. On the other hand, the balanced formation of many ROS plays an essential role in some physiological processes. For example, phagocytes produce large amounts of ROS *via* the NADPH oxidase system as part of their defensive mechanism against pathogens (Valko and others 2007).

Free radicals are molecules containing unpaired electrons, which makes them very reactive. This reactivity leads to donating or accepting electrons from surrounding molecules to achieve a more stable state. The reaction of such a radical with a nonradical causes a radical chain reaction and creates new radicals, which, in turn, react with other molecules. This process is called propagation. The reaction is terminated when 2 radicals react with each other to form a nonradical (Betteridge 2000).

H_2O_2 is a nonradical that belongs among the ROS. Several enzymes generate H_2O_2 , for example, superoxide dismutase. Perhaps fortunately, given its widespread presence *in vivo*, H_2O_2 is only a weak oxidizing or reducing agent and is poorly reactive. H_2O_2 causes some damage directly, but the oxidation of biomolecules is usually mediated by the formation of $\cdot\text{OH}$ (Halliwell and Gutteridge 2007).

Hydroxyl radical—chemistry and biological consequences

Hydroxyl radical ($\cdot\text{OH}$) is the most potent oxidant and one of the most reactive natural free radicals known. It has a very short half-life and thus reacts with molecules at the site of its formation (Betteridge 2000). The reaction rate with other molecules is high, approximately 10^9 to $10^{10} \text{ M}^{-1} \times \text{s}^{-1}$. $\cdot\text{OH}$ recombination

MS 20152113 Submitted 22/12/2015, Accepted 1/3/2016. Authors are with Faculty of Pharmacy, Dept. of Molecular Biology and Pharmaceutical Biotechnology, Univ. of Veterinary and Pharmaceutical Sciences Brno, Palackého tř. 1, 612 42, Brno, Czech Republic. Direct inquiries to author Tremł (E-mail: jakub.tremł@gmail.com).

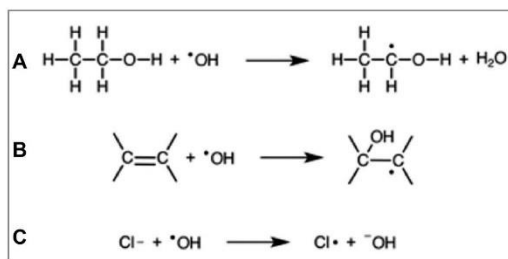
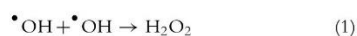


Figure 1—Three main types of reactions of $\cdot\text{OH}$: (A) hydrogen abstraction; (B) addition to double bond; (C) electron transfer.

(Eq. 1) is also very fast (with $k = 5 \times 10^9 \text{ M}^{-1} \times \text{s}^{-1}$) and the steady-state concentration of $\cdot\text{OH}$ in solution is therefore practically zero (Tirzitis and Bartosz 2010). The absorbance peak of $\cdot\text{OH}$ in aqueous solutions occurs at 230 nm, but in general the spectrum is nondescriptive (Halliwell and Gutteridge 2007):



The production of $\cdot\text{OH}$ will be discussed later in the paper. Here, it is necessary to point out that $\cdot\text{OH}$ occurs naturally in organisms, as well as in the atmosphere. $\cdot\text{OH}$ is formed in biological systems by oxidative metabolism, in which (predominantly in mitochondria) superoxide radicals ($\text{O}_2^{\cdot-}$) are formed as an unwanted by-product. The superoxide radical can be removed by the superoxide dismutase enzyme. The product, H_2O_2 , can be removed by another enzyme called catalase, or it can undergo a Fenton reaction in the presence of transition metal ions to generate $\cdot\text{OH}$ (Carocho and Ferreira 2013).

$\cdot\text{OH}$ is also a major oxidizing agent in the Earth's atmosphere, destroying about 3.7 Gt of trace gases, including methane and different fluorocarbons, each year (Ehhalt 1999). In the atmosphere, $\cdot\text{OH}$ is formed primarily *via* the reaction of water vapor with singlet oxygen that had previously resulted from the UV photolysis of ozone (Bahm and Khalil 2004).

There are 3 main types of reactions of $\cdot\text{OH}$: hydrogen abstraction, addition, and electron transfer. All of these reactions predict the nature of the damage caused by $\cdot\text{OH}$. Basically, all of the reactions lead to the formation of new radicals and thus propagate chain reactions. One example of abstraction is the reaction of $\cdot\text{OH}$ with alcohols. The $\cdot\text{OH}$ abstracts H \cdot and forms water, leaving an unpaired electron on the carbon atom of the alcohol (Figure 1A). The reaction of $\cdot\text{OH}$ with an aromatic compound often leads to addition. In this way, $\cdot\text{OH}$ can be added to double bonds to form a hydroxy derivative (Figure 1B). $\cdot\text{OH}$ can also take part in electron-transfer reactions (Figure 1C) (Halliwell and Gutteridge 2007).

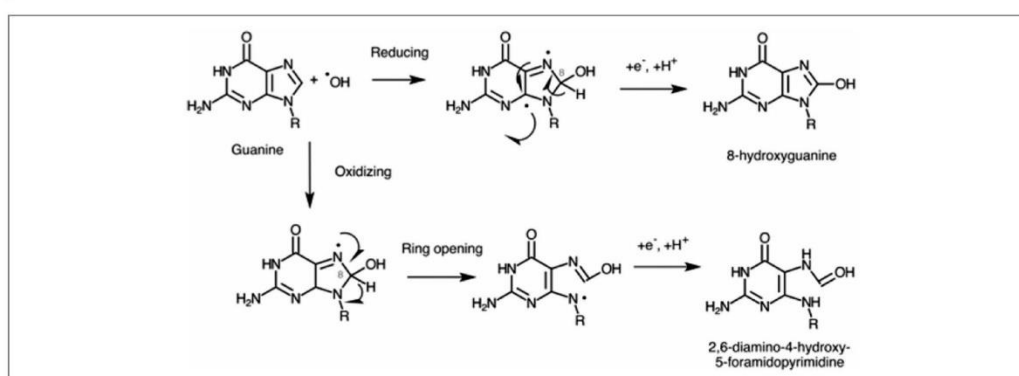
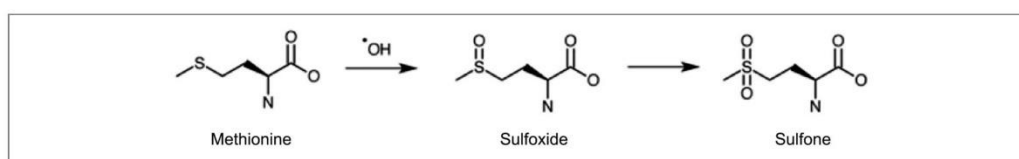
As can be expected from the enormous reactivity of $\cdot\text{OH}$, the exposure of DNA (or RNA) to it yields a large number of products. The distribution of an $\cdot\text{OH}$ attack depends on the electron density at the site of the molecule attacked. Because of its electrophilic nature, $\cdot\text{OH}$ preferentially adds to the site with the greatest electron density. For example, $\cdot\text{OH}$ attacks a molecule of guanine preferentially at C-8 to produce a C-8 OH-adduct radical that can be reduced to 8-hydroxyguanine or undergo ring opening to give 2,6-diamino-4-hydroxy-5-formamidopyrimidine (Figure 2). Similarly, other purines and pyrimidines suffer from the addition of $\cdot\text{OH}$ to the ring and the abstraction of H \cdot . In the case

of cytosine, 87 % of the addition occurs at the C-5. The product distribution will also vary depending on whether the $\cdot\text{OH}$ is generated by radiation or by a Fenton reaction. For example, copper ions bind to GC-rich sequences in DNA and subsequent reaction with H_2O_2 favors the formation of modified guanine products, whereas $\cdot\text{OH}$ produced by radiation impairs all bases to a similar extent. The consequences of DNA damage are mutations. 8-Hydroxyguanine leads to a GC \rightarrow TA transversion mutation because it can bond to adenine, although most 8-hydroxyguanine pairs correctly with cytosine. Deoxyribose and ribose are targets of $\cdot\text{OH}$ attack as well. The formation of one of the products, malondialdehyde (MDA), forms the basis of the deoxyribose assay. Damage to the sugar parts of the DNA structure can lead to breaks in the strands of DNA, because these constitute the phosphate-deoxyribose backbone. Attack at C-1 of the deoxyribose structure can cause the release of a base from the DNA molecule, leaving an abasic site in the DNA (Evans and others 2004).

The most vulnerable molecular components of lipids are the polyunsaturated fatty acids (PUFAs) that are present in large amounts and form parts of cell membranes. The process by which $\cdot\text{OH}$ causes oxidative damage to lipids is called lipid peroxidation. Lipid peroxidation is initiated by the addition of $\cdot\text{OH}$ to a double bond or by the abstraction of a hydrogen atom from a methylene group of a PUFA by $\cdot\text{OH}$ (Figure 1B and A, respectively). In both cases, the result is the formation of a lipid radical ($\text{L}\cdot$). This carbon radical reacts with oxygen to form a lipid peroxy radical ($\text{LOO}\cdot$). The $\text{LOO}\cdot$ can abstract a hydrogen from an adjacent fatty acid to produce a lipid hydroperoxide (LOOH) and a second lipid radical. The LOOH formed can react with metal ions, such as Fe^{2+} , producing lipid alkoxyl radical ($\text{LO}\cdot$). Both alkoxyl and peroxy radicals stimulate the chain reaction of lipid peroxidation by abstracting additional hydrogen atoms, not only from the surrounding lipids, but also from other biomolecules (Buettnner 1993; Catalá 2010).

A great diversity of aldehydes is formed when lipid hydroperoxides break down in biological systems. Some of these aldehydes are highly reactive and may be considered as secondary toxic messengers, which disseminate and augment the initial free radical events. 4-Hydroxy-2-nonenal (4-HNE) is known to be the main aldehyde formed during the lipid peroxidation of n-6 PUFAs, such as linoleic acid and arachidonic acid. Another abundantly formed aldehyde is malondialdehyde (MDA). Its reaction with thiobarbituric acid is the basis of lipid peroxidation detection by the TBARS assay (thiobarbituric acid-reactive substances). Lipid peroxidation reduces membrane fluidity, increasing the "leakiness" of the membrane to substances that do not normally cross it and a further loss of membrane integrity (Grune and others 1993; Catalá 2010).

$\cdot\text{OH}$ can also interact with different proteins. Oxidative damage to proteins also matters, because it can impair the functioning of receptors, antibodies, signal transduction, transport proteins, and enzymes. The chemistry of protein damage is even more complex than that of DNA; the 20 and more amino acids generate a multitude of possible oxidation end products. Methionine, for example, can be attacked by $\cdot\text{OH}$ to form methionine sulfoxide, which can undergo further oxidation to form a sulfone (Figure 3). Even the polypeptide chain of proteins can be attacked by $\cdot\text{OH}$. This leads to hydrogen abstraction, the formation of a carbon radical, and the subsequent cleavage of the peptide bond. This process can be amplified by the metal-catalyzed oxidation of proteins. A metal ion, such as Fe^{2+} , binds to the polypeptide chain and reacts with H_2O_2 to form $\cdot\text{OH}$. The result is oxidative damage to the amino acids nearby or the cleavage of the peptide bond. Moreover, the

Figure 2—Oxidative damage to guanine caused by $\cdot\text{OH}$.Figure 3—Oxidative damage to methionine caused by $\cdot\text{OH}$.

lysine residues of proteins can react with the products of lipid peroxidation (4-HNE and MDA) or with the oxidation products of sugars (Levine and others 1996; Berlett and Stadtman 1997; Cabiscot and others 2000).

The exposure of an organism to an unbalanced oxidative stress has many biological consequences. Some level of stress can be beneficial, as a mild stress may provoke cell proliferation and the adaptation of the defense system. However, uncontrolled proliferation can lead to the development of cancer. Severe stress involves damage to some or all of the molecular targets: DNA, proteins, and lipids. The affected tissue or cell may recover from the oxidative damage after injury by repairing or replacing the damaged cells or molecules; the cell may also survive with persistent oxidative damage and no longer divide. Especially when the DNA is damaged, the result is cell death *via* apoptosis or necrosis, or the cell can mutate into cancer (Dalle-Donne and others 2006; Ma 2010).

Oxidative stress has been implicated in various pathological conditions involving cardiovascular diseases, cancer, neurological disorders, diabetes, or aging. These diseases fall into 2 groups: (i) the first group is characterized by the pro-oxidant shifting of the glutathione redox system and impairment of glucose tolerance—the so-called “mitochondrial oxidative stress” conditions (cancer and diabetes mellitus); (ii) the second group involves diseases characterized by “inflammatory oxidative conditions” and the enhanced activity of NAD(P)H oxidase (atherosclerosis and chronic inflammation) (Harman 1956; Valko and others 2007).

To prevent or overcome the damage to biomolecules and prevent the development of the diseases previously mentioned, the cells take advantage of various ways and enzymatic systems. Sometimes, the capacity of the endogenous enzymes and antioxidants is overwhelmed. For these cases human cells may use exogenous antioxidants supplied in the diet, such as vitamins, carotenoids, and flavonoids. It is the task of scientists to develop suitable meth-

ods for determining the antioxidant activity and to search for new antioxidants in natural sources. Antioxidants are compounds capable of delaying, preventing, or removing oxidative damage to the substrate molecule. Antioxidants can be either small molecules or protein enzymes (Khlebnikov and others 2006; Carochio and Ferreira 2013).

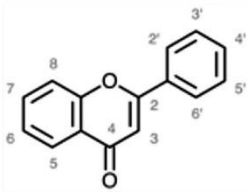
So-called preventive antioxidants are the first line of the defense system. These compounds suppress the formation of ROS, for example, by sequestering metal ions or by reducing H_2O_2 and lipid hydroperoxides to water and lipid hydroxides. The second line of defense consists of scavenging antioxidants, which rapidly remove the active ROS before they can attack biologically essential molecules. Superoxide dismutase (SOD) converts superoxide to H_2O_2 , while carotenoids scavenge singlet oxygen. Many phenolic compounds and flavonoids are scavengers too. Various enzymes function as a third line defense by repairing damage, clearing wastes, and reconstituting the lost function (Scalzo and others 2008; Niki 2010).

Flavonoids

The flavonoids are a large group of plant secondary metabolites. Their name is derived from the Latin word “*flavus*,” meaning yellow, showing their natural pigmentation. Flavonoids are widely distributed in the leaves, seeds, bark, and flowers of plants; over 8000 compounds have been identified. They function in plants mainly to protect against ultraviolet radiation, pathogens, and herbivores; together with the anthocyanin copigments in flowers, they are responsible for attracting pollinating insects, showing characteristic colors in ultraviolet light (Winkel-Shirley 2001; Heim and others 2002; Procházková and others 2011).

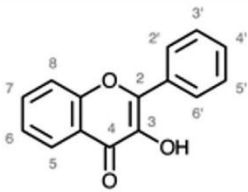
The basic structure of flavonoids is that of the flavone (Table 1) that is chemically 2-phenyl-1,4-benzopyrone. Ring A of the flavonoid skeleton arises biosynthetically from acetate metabolism,

Table 1–Flavones.



Compound	Name	Substitution					
		5	6	7	8	3'	4'
17	Baicalein	OH	OH	OH	H	H	H
18	Baicalin	OH	OH	Glucuronide	H	H	H
42	Wogonine Glucuronide	OH	H	Glucuronide	OMe	H	H
20	Chrysin	OH	H	OH	H	H	H
35	Apigenin	OH	H	OH	H	H	OH
19	Luteolin	OH	H	OH	H	OH	OH

Table 2–Flavanols.



Compound	Name	Substitution					
		3	5	7	2'	3'	4'
12	Kaempferol	OH	OH	OH	H	H	OH
11	Quercetin	OH	OH	OH	H	OH	H
48	Morin	OH	OH	OH	OH	H	H
10	Myricetin	OH	OH	OH	H	OH	OH
38	Hyperoside	Galactoside	OH	OH	H	OH	OH
36	Quercetin-3-galacturonide	Galacturonide	OH	OH	H	OH	H
8	Quercetin-3-glucoside	Glucoside	OH	OH	H	OH	H
37	Miquelianin	Glucuronide	OH	OH	H	OH	H
9	Rutoside	-Rha-Glc	OH	OH	H	OH	H
41	Trihydroxyethylrutoside	-Rha-Glc	OH		7; 3'; 4' = OC ₂ H ₅ OH		
40	Tetrahydroxyethylrutoside	-Rha-Glc			5; 7; 3'; 4' = OC ₂ H ₅ OH		

whereas ring B is derived from a shikimic acid pathway. Ring C is a product of the condensation of intermediates coming from both of these pathways. Flavonoids can be divided into several groups based on the structure of the skeleton and the substitution: flavones (Table 1), flavonols (Table 2), flavanol derivatives of quercitrin and myricitrin (Table 3), flavanones (Table 4), prenylated and geranylated flavanones (Table 5), flavanonols (Table 6), flavanols (Table 7), and anthocyanidins (Table 8). Table 9 then shows some flavonoid metabolites of possible importance for their effect after ingestion.

Flavonoids are an integral part of both human and animal diets. Being phytochemicals, flavonoids cannot be synthesized by humans or animals. Flavonols are the most abundant flavonoids in foods. Flavanones can be mainly found in citrus fruits and flavones in celery. Catechins are present in large amounts in green and black teas, and in red wine, whereas anthocyanins are found in strawberries and other berries (Peterson and Dwyer 1998; Heim and others 2002; Yao and others 2004).

The flavonoid family of plant compounds comprises the most widely distributed group of secondary plant metabolites ingested

by humans. Exact estimation of the average dietary intake of flavonoids is difficult, because of the wide diversity of available flavonoids and the extensive distribution in various plants, and also the differing consumption of humans. Thus, the measurement of dietary intake of flavonoids depends entirely on the criteria of survey, the method used, and the reference compounds selected for analysis. Bearing this in mind, the dietary intake of flavonoids has been estimated to vary from 100 to 1000 mg/d. Flavonoids are relatively heat-stable, but easily lost due to cooking and frying (Hertog and others 1993; Yao and others 2004).

The ability of flavonoids to possess antioxidant or any other desired activity in the human body is highly dependent on absorption and metabolism of that particular flavonoid. Sesink and others (2001) proved that quercetin glycosides are not absorbed intact in humans or, more precisely, are not able to reach the blood circulation, because quercetin glucuronides and not glucosides were present in human plasma after consumption of quercetin glucosides (Walle 2004). Hollman and others (1995) have performed a study to quantify absorption of various forms of quercetin (11).

Table 3–Flavonol derivatives of quercitrin and myricitrin.

Compound	Name	Substitution		
		5'	2''	3''
30	Quercitrin	H	H	H
26	Myricitrin	OH	H	H
34	Quercitrin 2''-O-gallate	H	Galloyl	H
32	Myricitrin 2''-O-gallate	OH	Galloyl	H
33	Myricitrin 3''-O-gallate	OH	H	Galloyl
31	Myricitrin 2'',3''-di-O-gallate	OH	Galloyl	Galloyl

Table 4–Flavanones.

Compound	Name	Substitution						
		5	7	8	2'	3'	4'	5'
7	Naringenin	OH	OH	H	H	H	OH	H
46	Eriodictyol	OH	OH	H	H	OH	OH	H
43	Lysionotin	OH	OH	OMe	OMe	H	OMe	H
6	Hesperetin	OH	OH	H	H	OH	OMe	H
44	Dihydrotricin	OH	OH	H	H	OMe	OH	OMe
5	Naringin	OH	-Rha-Glc	H	H	H	OH	H
49	Hesperidin	OH	-Rha-Glc	H	H	OH	OMe	H

Their conclusion is that humans absorb quercetin (11) conjugated with glucose rather than conjugated with rutinose or quercitrin (11) alone. The authors also concluded that the quercetin glucosides were absorbed intact using a sodium-dependent glucose transporter (SGLT1). On the other hand, it was later found out that some flavonoid glucosides are hydrolyzed by enzymes in small intestine, namely by lactase phloridzin hydrolase in the brush border of the small intestine epithelial cells. The more lipophilic aglycones that are released (or in general more lipophilic flavonoids) then enter epithelial cells by passive diffusion facilitated by the proximity of the cell membrane. An alternative route of hydrolysis is mediated by cytosolic β -glucosidase (CBG), present in epithelial cells. But, CBG hydrolysis requires that polar glycosides to be transported into cells, possible by above mentioned SGLT1. Therefore, the glycosylation of a flavonoid skeleton and its hydrophilic/hydrophobic character strongly affect its absorption, which can be very fast or very slow (Crozier and others 2010).

Some flavonoid metabolites are returned to the lumen of the small intestine in a process mediated by members of the

adenosine triphosphate (ATP)-binding cassette (ABC) family of transporters, including multidrug resistance protein (MRP) and P-glycoprotein (P-gp). On the other hand, flavonoids have been shown to inhibit the activity of these transporters (Crozier and others 2010). After metabolites are absorbed from small intestine into the portal blood, they rapidly reach the liver, where they can again undergo several Phase I and II metabolic conversions and, in some cases, enter the enterohepatic circulation by way of the bile and are returned to the small intestine. To determine how flavonoids are metabolized in the human body, Otake and others (2002) studied metabolism of a flavonoid galangin in freshly plated human hepatocytes. The main products were 2 isomeric glucuronic acid conjugates and a sulfate conjugate, with only a minor portion of the oxidation product kaempferol (12). The conjugation reactions of flavonoids are catalyzed by enzymes UDP-glucuronosyltransferase or sulfotransferase, whereas the oxidation processes are bound to cytochrome P450 enzymes in microsomes. In humans, the metabolizing enzymes sulfotransferases (SULT) and UDP-glucuronosyltransferases (UDPG) are classified

Table 5--Prenylated and geranylated flavanones.

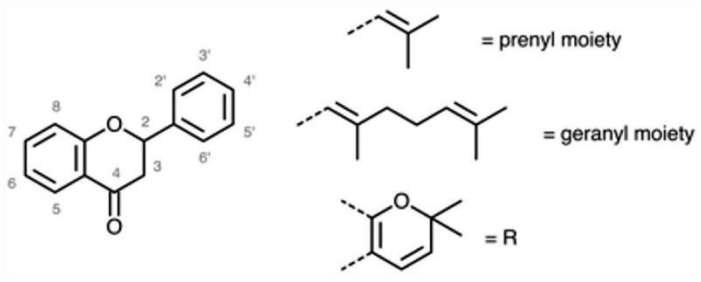
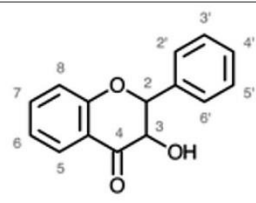
								
Compound	Name	Substitution					4', 5'	
		5	7	8	2'			
22	–	OH	OH	CH ₂ CH ₂ C(CH ₃) ₂ OH	OH		R	
Compound	Name	Substitution						
		5	6	7	2'	3'	4'	5'
21	Euchrestaflavanone B	OH	Prenyl	OH	OH	H	OH	Prenyl
52	Mimulone	OH	Geranyl	OH	H	H	OH	H
51	Diplacone	OH	Geranyl	OH	H	OH	OH	H
50	3'-O-methyl-5'-hydroxydiplacone	OH	Geranyl	OH	H	OMe	OH	H

Table 6--Flavanonols.



		Substitution					
Compound	Name	3	5	7	3'	4'	5'
45	Fustin	OH	H	OH	OH	OH	H
47	Taxifolin	OH	OH	OH	OH	OH	H
29	Amelopsin	OH	OH	OH	OH	OH	OH

into several subfamilies that are expressed differently in the liver. The sulfation process is regioselective under the control of different isoforms of SULT. Moreover, some flavonoid structures, like quercetin (11) and tea flavonoids are prone to *O*-methylation by the enzyme catechol-*O*-methyltransferase (COMT). This reaction has been studied for quercetin by Zhu and others (1994). After intraperitoneal administration of quercetin (11) to hamsters, a urinary extract contained 2 % quercetin (11) and 97 % 3'-*O*-methylquercetin (Walle 2004).

Gut microflora is responsible for further metabolism of flavonoids. It possesses the ability to cleave conjugates and glycosides, and release aglycones. Moreover, the rings of flavonoid skeleton can also undergo cleavage to form smaller molecules, which, together with unchanged aglycones can be reabsorbed, metabolized in Phase I and II in the liver, and enter the enterohepatic circulation or (and this is predominant) be excreted in the urine (Urpi-Sarda and others 2009). Colonic bacteria decompose flavonoids into simple phenolic acids that can be absorbed into the circulating blood. The key point of this process is the scission of the C ring and the loss of carbons C5–C8 as oxaloacetate, which

is eventually metabolized to carbon dioxide. The interaction of flavonoids with colonic bacteria affects their bioavailability and could further change their biological effects, including the antioxidant activity. Some examples of flavonoid metabolites produced by the microflora in the gut are shown in Table 9. Proanthocyanidins are metabolized to phenylacetic acid (53), mono- and dihydroxyphenylacetic acids, mono- and 3,4-dihydroxyphenylpropionic acids (54), or 4-hydroxybenzoic acid (55). Anthocyanins are converted mainly into protocatechuic acid (56), gallic acid (57), syringic acid (58), vanillic acid (59), and phloroglucinol (60) (Crozier and others 2010; De Pascual-Teresa and others 2010; Heinrich and others 2013). The similar metabolites were described also for simple organic acid (like chlorogenic acid derivatives) (Yang and others 2013; Breynaert and others 2015).

In general, antioxidant activity of flavonoids is decreased following the metabolic reactions. However, from the results of several experiments, one can deduce that metabolites of flavonoids are still able to scavenge radicals and participate in antioxidant reactions. The antioxidant activity of metabolites is frequently not negligible though. Dueñas and others (2010) studied antioxidant

Table 7–Flavanols.

(+)-catechin (2*R*,3*S*) (-)-epicatechin (2*R*,3*R*)

Compound	Name	Substitution	
		3	5'
13	(+)-Catechin	OH	H
28	(+)-Gallocatechin	OH	OH
27	(+)-Gallocatechin-3- <i>O</i> -gallate	Galloyl	OH
1	(-)-Epicatechin	OH	H
2	(-)-Epicatechin gallate	Galloyl	H
3	(-)-Epigallocatechin	OH	OH
4	(-)-Epigallocatechin gallate	Galloyl	OH
25	Procyanidin B2	Dimer of (-)-epicatechin	
23	Procyanidin C1	Trimer of (-)-epicatechin	
24	Tetrameric proanthocyanidin	Tetramer of (-)-epicatechin	
39	Procyanidin B4	(+)Catechin-(4 <i>α</i> -8)-(-)epicatechin	

Table 8–Anthocyanidins.

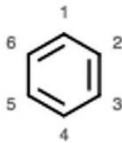
Compound	Name	Substitution					
		3	5	7	3'	4'	5'
14	Pelargonidin	OH	OH	OH	H	OH	H
15	Cyanidin	OH	OH	OH	OH	OH	H
16	Delphinidin	OH	OH	OH	OH	OH	OH

activity of 3'- and 4'-methylethers of catechin (13) and epicatechin (1) using the ferric reducing power (FRAP) assay and a method based on ability to scavenge ABTS^{•+} radical. *O*-methylation of hydroxyls of ring B led to decrease of activity. However, these metabolites still retain significant radical scavenging activity at pH 7.4, indicating that they could function as potential antioxidants in human body. Lotito and others (2011) used FRAP assay to determine radical scavenging activity. They found out that 3'-*O*-methylquercetin and quercetin-3'-*O*-sulfate showed lower activity than quercetin itself, but their activity was still 2 times as high as the Trolox used as a standard. In contrast, activity of 4',4''-di-*O*-methyl(-)-epigallocatechin-3-*O*-gallate was 5 times lower than that of its parental compound. Loke and others (2008) examined inhibition of lipoprotein oxidation by quercetin and its metabolites. The oxidation was caused by 2,2'-azobis(2-methylpropionamidine) dihydrochloride (AAPH) and measured using ferrous oxidation-xynlenol orange (FOX) assay. The data have shown that quercetin (11) was very effective at inhibiting LDL oxidation at 10 mM. Metabolites 3'-*O*-methylquercetin and quercetin-3-*O*-glucuronide showed slightly lower activity. On the other hand, quercetin-3'-*O*-sulfate and 3'-*O*-methylquercetin-

3-*O*-glucuronide were only partially efficient in inhibiting LDL oxidation at this concentration.

Plants contain almost always mixtures of flavonoids. Therefore, when discussing antioxidant activity of flavonoids, we must bear in mind their interactions in those mixtures. Many studies have tried to predetermine the antioxidant capacity of a given food on the basis of its flavonoid content and have, in most cases, failed due to differences between the theoretical and the calculated antioxidant activity of that given product. Hidalgo and others (2010) measured the antioxidant activity of various flavonoids by 2 different *in vitro* tests: DPPH[•] radical scavenging activity and FRAP assay. In order to evaluate the effect of flavonoid interactions on their antioxidant activity they compared the activity of individual flavonoids with that obtained by mixing them with another flavonoid. The majority of DPPH[•] scavenging activities in these combinations showed antagonism, except for some synergistic interactions such as kaempferol (12) paired with myricetin (10). In the FRAP assay, the combination of epicatechin (1) and quercetin-3-*O*-glucoside (8) showed the highest synergistic effect, whereas myricetin (10) with quercetin (11) resulted in an antagonistic effect. Iacopini and others (2008) studied antioxidant activity of various flavonoids in

Table 9—Selected simple flavonoid metabolites.



Compound	Name	Substitution			
		1	3	4	5
53	Phenylacetic acid	Acetyl	H	H	H
54	3,4-Dihydroxyphenylpropionic acid	Propionyl	OH	OH	H
55	4-Hydroxybenzoic acid	COOH	H	OH	H
56	Protocatechuic acid	COOH	OH	OH	H
57	Gallic acid	COOH	OH	OH	OH
58	Syringic acid	COOH	OMe	OH	OMe
59	Vanillic acid	COOH	OMe	OH	H
60	Phloroglucinol	OH	OH	H	OH

red grape. They also studied potential interactive effects among them. The results indicated possible synergy between quercetin (11), rutoside (9) and resveratrol towards ONOO[•]. The effect was additive for catechin (13) and epicatechin (1).

In addition to their antioxidant activity, flavonoids reduce the incidence of cardiovascular diseases in spite of a parallel high intake of fat in the diet. This phenomenon is also known as the French paradox and is associated with moderate and prolonged consumption of red wine containing polyphenols. One of the causes of the phenomenon is the inhibition of the thrombin receptor-activating peptide (TRAP) accompanied by ADP-induced platelet aggregation. De Lange and others (2007) have confirmed this by measuring the effects of polyphenolic grape extract on platelet aggregation. Borradaile and others (1999) described another mechanism by which flavonoids help to reduce the incidence of cardiovascular diseases. When rabbits fed a casein-containing diet drank orange or grapefruit juice instead of water, the concentrations of low-density lipoprotein cholesterol and hepatic cholesteryl ester in their serum were reduced. The exact mechanism of action of the flavonoids hesperetin (6) and naringenin (7) on liver HepG2 cells and on the net apolipoprotein B (apoB) secretion has been studied. The flavonoids dose-dependently reduced the net apoB secretion by as much as 81% after a 24-h incubation. Furthermore, ¹⁴C-acetate-labeling studies showed a 50% reduction in cholesteryl ester synthesis in the presence of either flavonoid, which could explain the reduction of the net apoB secretion caused by incubation with these compounds. The expression and secretion of apoB in liver cells is known to be one of the control mechanisms of low-density lipoprotein (LDL). The overproduction of LDL may cause the hyperlipidemia responsible for an increased risk of coronary heart disease.

In recent years, flavonoids have been investigated intensely as part of the treatment of various types of cancer. When tested on a molecular level, flavonoids exert this anticancer activity, for example, by inhibiting protein kinases (PKs). Under pathological conditions, the expression and activity of PKs can be deregulated, leading to alterations in phosphorylation that result in uncontrolled cell division, inhibition of apoptosis, and other abnormalities. The deregulation of phosphorylation has been closely linked to cancer and other diseases, such as diabetes. Moreover, flavonoids inhibit cyclooxygenase and lipoxygenases, which are also involved in cancer and inflammatory pathologies (Cushman and others 1991; Hashemi and others 2012; Ravishankar and others 2013).

A further important mechanism of activity of flavonoids is their chemopreventive effect *via* inhibition of certain Phase I and II metabolizing enzymes (such as cytochrome P450 or glutathione S-transferase) which metabolically activate a large number of pro-carcinogens triggering carcinogenesis. The chemopreventive effects of flavonoids are closely linked to their anticancer properties that involve the scavenging of ROS and growth-promoting oxidants (Tsyrolov and others 1994; Ravishankar and others 2013).

Flavonoids, especially in oxidized forms (phenoxyl radicals or quinone intermediates) and in greater concentrations, can behave as pro-oxidants. This is sometimes also regarded as an anticancer effect, because it may lead to the apoptosis of tumor cells; however, the pro-oxidant mechanisms involve DNA fragmentation, usually in the presence of transition metals, which can lead to mutation or cell death. Other effects of flavonoids *via* pro-oxidation include mitochondrial dysfunction and the induction of apoptosis in tumor cells (Rahman and others 1990; Galati and O'Brien 2004).

How do we measure the scavenging activity of the hydroxyl radical?

There are various ways of measuring the scavenging activity of [•]OH. The choice of method substantially influences and determines the results. Obviously, we cannot expect the same results for all of the different methods used to measure [•]OH scavenging in antioxidant activity assays of flavonoids. Basically, there are 2 main steps in the procedure of [•]OH-scavenging methods: (i) production of [•]OH: this includes the employment of various physical processes, such as pulse radiolysis, γ -irradiation, or UV photolysis of H₂O₂, and also different chemical reactions, among which the most widely used is the Fenton reaction; (ii) reaction of [•]OH with a suitable probe and the consequent detection of a reaction product or corresponding change in some physical parameter. Because [•]OH is a very reactive substance, it is not possible to measure its presence and concentration directly; but the first reaction of [•]OH with another molecule, a probe or trap, followed by the detection of a reaction product is crucial.

It is also critical to point out that there is a difference between [•]OH scavengers and antioxidants. The mechanism of action of [•]OH scavengers is the direct scavenging, or quenching, of the [•]OH, whereas antioxidants include [•]OH scavengers as well as compounds that counteract oxidizing precursors (such as H₂O₂), chelate metal ions and boost the antioxidant enzyme activity and production. This review focuses primarily on [•]OH scavengers and

the specific methods used to detect their activity. Physical methods of producing $\cdot\text{OH}$ are preferred to measure specifically the $\cdot\text{OH}$ -scavenging activity, because when the Fenton reaction is used to produce $\cdot\text{OH}$, the measured antioxidant exerts the $\cdot\text{OH}$ scavenging and metal-chelating activity in the experiment.

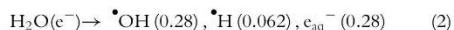
One further requirement is necessary for both approaches. The scavenger or antioxidant should not interfere with the detection mechanism. For example, the compound tested should not alter or diminish the spectra in the measurement of DMPO- $\cdot\text{OH}$. Similarly, the compound should not form a false chromogen in the deoxyribose method.

Production of hydroxyl radical. The foremost place among all the methods of producing the hydroxyl radical is held by pulse radiolysis because of the selectiveness of production and the later scavenging of the $\cdot\text{OH}$. It is also the definitive technique for investigating reactions between antioxidants and $\cdot\text{OH}$ and for measuring their reaction rates (Butler and others 1988; Halliwell 1995). The disadvantages are the need for sophisticated instrumentation and the cost.

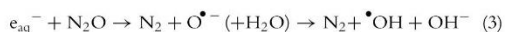
The radicals are usually formed in a reaction cell by a rapid pulse of high-energy electrons coming from a linear accelerator. Many radicals absorb or emit light at wavelengths different from the parent molecule, so the progress of the reaction can be followed by the changes in the spectra (Halliwell and Gutteridge 2007). One advantage of the pulse radiolysis method is that it does not use a probe to detect $\cdot\text{OH}$ and is therefore exempted from the rule mentioned above.

Various chemical species are formed during the radiolysis of water. The rapid pulses of high-energy electrons are readily absorbed by molecules of water and ionization and excitation occur. Molecules of water in an excited state undergo rapid homolytic fission to form $\cdot\text{H}$ and $\cdot\text{OH}$ in 10^{-14} to 10^{-13} s (Eq. 2). Apart from this, clusters of molecules of water surround electrons to produce hydrated electrons. Hydrated electrons are extra electrons solvated in liquid water; they owe their existence to the electron-dipole interactions in water. They are symbolized as e_{aq}^- , where "aq" means "aqueous." The species formed are initially concentrated in microregions called spurs, but in about 10^{-8} s the solution becomes homogeneous (Halliwell and Gutteridge 2007).

The process of radiolysis of water can be summarized by this reaction (Houée-Levin and Bobrowski 2013):



The numbers in parentheses are the radiation chemical yields of the primary products (G-values) in $\mu\text{mol/J}$. About half of the radicals produced are $\cdot\text{OH}$. To achieve nearly selective formation of $\cdot\text{OH}$ the solution must be saturated with N_2O (Eq. 3) (Houée-Levin and Bobrowski 2013).



Ionizing radiation is a form of electromagnetic radiation consisting mainly of γ -rays and X-rays. Gamma-rays (γ -rays) have frequencies above 10^{19} Hz and wavelengths less than 10 pm. The $\cdot\text{OH}$ is usually generated by applying γ -irradiation to molecules of water, resulting in the homolytic fission of the water molecule to form hydroxyl radicals. The γ -rays are usually produced by the radioactive decay of ^{60}Co , which is a continuous source, as compared to pulse radiolysis (Halliwell and Gutteridge 2007; Houée-Levin and Bobrowski 2013). Another way to achieve the homolytic fission of water that is used to generate $\cdot\text{OH}$ is the UV

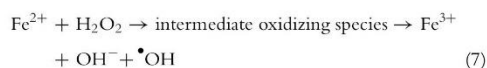
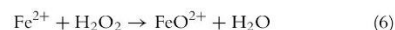
photolysis of H_2O_2 (Eq. 4) (Halliwell and Gutteridge 2007).



The Fenton reaction is the most important of the chemical reactions used to produce $\cdot\text{OH}$ for measuring antioxidant activity (Eq. 5). In 1894, Fenton (1894) published an article describing the oxidation of tartaric acid in the presence of ferrous ions and hydrogen peroxide. The reaction was named after Fenton, although he never wrote it. Haber and Willstätter proposed the classical radical mechanism in 1931 (Barbusiński 2009).

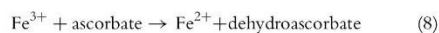


Since the time of publication there has been an ongoing discussion and controversy concerning the reaction mechanism. Bray and Gorin (1932) presented a nonradical mechanism resulting in ferryl species (FeO^{2+}), where iron is in the oxidation state +IV (Eq. 6). This ion is very reactive and readily oxidizes other compounds. Halliwell and Gutteridge reported that the majority of the evidence favors $\cdot\text{OH}$ as the primary damaging species, but other ROS may be generated along the pathway to the formation of $\cdot\text{OH}$. Thus they extended the classical Fenton reaction (Eq. 7) (Halliwell and Gutteridge 2007).

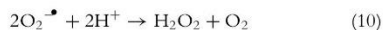


Minero and others (2013) confirmed this hypothesis using stopped-flow spectrophotometry and methyl yellow as the substrate for the reaction. According to their findings both $\cdot\text{OH}$ and some other oxidizing species are formed in the Fenton reaction. The exact ratio of the products depends on the reaction pH. Yamazaki and Piette (1991) obtained similar results. They used 5,5-dimethyl-1-pyrroline *N*-oxide (DMPO) as a spin-trapping probe for the $\cdot\text{OH}$ generated by the Fenton reaction and UV photolysis. After the Fenton reaction the $\cdot\text{OH}$ was not totally free in solution as compared to the photolysis experiment. Ferryl species were also detected in the reaction, depending on the type of chelator used.

Various reactants can be utilized in the methods used to determine the $\cdot\text{OH}$ -scavenging activity. For example, Benherhal and Arumugham (2008) used FeCl_2 and H_2O_2 as reactants, thus performing the classical Fenton reaction (Eq. 5). The reaction can be modified by the presence of a chelator, for example, ethylenediaminetetraacetic acid (EDTA) (Tai and others 2002) or diethylenetriaminepentaacetic acid (DTPA) (Tsuda and others 1996). EDTA has also been employed as the chelator in the deoxyribose damage assay used to determine the $\cdot\text{OH}$ -scavenging activity. When Arouma and others (1987) omitted EDTA, the reaction became "site-specific," because iron was bound to the deoxyribose molecule causing damage "on-spot." This modification was later used to identify the ability of different compounds to chelate metals and, thus, to reduce the production of $\cdot\text{OH}$. In addition to ferrous ions, ferric ions can be used to generate $\cdot\text{OH}$. Ferric ion must first be reduced and can then undergo the Fenton reaction (Eq. 8) (Halliwell and others 1987). Using ascorbate these reactions form a cycle.

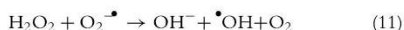


Arimboor and Arumugan (2012) omitted H_2O_2 from the reaction mixture, but $\cdot\text{OH}$ was still generated by a process called "iron-autooxidation." The mechanism of reaction proposed by Genaro-Mattos and others (2009) is shown in reactions 9 and 10. The H_2O_2 formed in reaction 10 subsequently undergoes the Fenton reaction (Eq. 5).



It has also been found that other metal ions, such as copper or cobalt, can undergo the Fenton reaction (Ou and others 2002; Trembl and others 2013). When copper is added to a Fenton reaction mixture as cupric ion (Cu^{2+}), it must be reduced in a way similar to the ferric ion in reaction described by Eq. 8, because the Fenton reaction always starts with the lower oxidation state (Cu^+) (Trembl and others 2013).

There are various methods that use cell cultures to determine the $\cdot\text{OH}$ -scavenging activity. Chen and others (2002) generated $\cdot\text{OH}$ via the reaction of ascorbate, H_2O_2 , and CuSO_4 in a yeast culture. Harris and others (2006) used the RAW 264.7 macrophage-like cell line, which was activated by lipopolysaccharide (LPS) and produced the superoxide radical ($\text{O}_2^{\cdot-}$) and H_2O_2 . These 2 subsequently formed $\cdot\text{OH}$ (Eq. 11). This reaction is often called "the superoxide-assisted (or -driven) Fenton reaction" and is catalyzed by iron (Halliwell and Gutteridge 2007).



Ozgová and others (2003) used rat liver microsomes and examined the influence of antioxidants on the lipid peroxidation induced by $\cdot\text{OH}$. An NADPH-generating system was used to produce $\cdot\text{OH}$: NADP, glucose-6-phosphate, MgCl_2 , and glucose-6-phosphate dehydrogenase. NADPH then participated in the reaction with the cytochrome P-450 obtained from the microsomes. Albano and others (1987) suggested that various ROS are formed in the liver microsomes and, among these, H_2O_2 is involved in the Fenton reaction and the production of $\cdot\text{OH}$.

Reaction of hydroxyl radical with a probe and detection. The $\cdot\text{OH}$ formed in step (i) must be detected in step (ii) via reaction with a probe. The only exception is the method of pulse-radiolysis, which does not use a probe and directly measures the production of radicals. The probe can also be called a trap. $\cdot\text{OH}$ reacts with the trap molecule to form 1 or more stable products that are then detected. Another approach used to evaluate the hydroxyl radical scavenging is called "fingerprinting." The principle of fingerprinting is to measure the damage caused by $\cdot\text{OH}$ rather than detecting the species itself. The chemical attack on a biomolecule leaves a unique "fingerprint" (Halliwell and Gutteridge 2007).

Reactions of antioxidants with $\cdot\text{OH}$ can be measured by electron spin resonance (ESR), sometimes called electron paramagnetic resonance (EPR). ESR is a spectroscopic method that detects the presence of unpaired electrons; it is therefore specific for free radicals. The technique is not sufficiently sensitive to detect the presence of $\cdot\text{OH}$ directly, and thus an adequate spin-trapping compound is needed (Halliwell and Gutteridge 2007). One of the frequently used spin-traps is 5,5-dimethyl-1-pyrroline *N*-oxide (DMPO), which reacts very specifically with $\cdot\text{OH}$ at a high rate (Figure 4). Thus, this technique can be considered to be the second-best option after pulse-radiolysis (Halliwell 1995). The

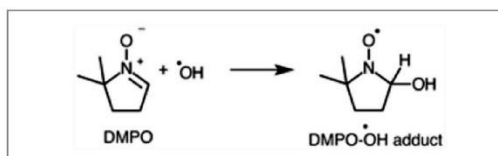


Figure 4—Reaction of 5,5-dimethyl-1-pyrroline *N*-oxide (DMPO) with $\cdot\text{OH}$.

DMPO- $\cdot\text{OH}$ adduct can also be detected by HPLC using electrochemical detection (Husain and others 1987). Other spin-traps are also utilized to detect $\cdot\text{OH}$, for example, phenyl-*t*-butylnitron (PBN) (Harbour and others 1974).

Although pulse-radiolysis is by far the best method for determining the $\cdot\text{OH}$ -scavenging activity, it is quite expensive and requires instrumentation. Therefore, Halliwell and others (1987) developed a new, simple "test-tube" deoxyribose method. The mixture producing $\cdot\text{OH}$ was incubated with the deoxyribose probe for 1 h at 37 °C. The reaction was stopped by adding trichloroacetic acid. The mixture was again incubated for 1 h at 80 °C with thiobarbituric acid (TBA). In this process, the deoxyribose molecule is attacked by $\cdot\text{OH}$ (Kaur and others 2010). The products of the damage are mainly malondialdehyde (MDA) and other MDA-like products. The reaction of MDA and MDA-like products results in the formation of a pink MDA-TBA₂ adduct (Figure 5) that could be detected either spectrophotometrically (at 532 nm) or fluorimetrically (with excitation at 532 nm and emission at 553 nm) (Biaglow and others 1997; Kaur and others 2010).

Separating the MDA-TBA₂ adduct by HPLC and detecting and quantifying it with a fluorescence detector can improve this procedure (Genaro-Mattos and others 2009). Another approach is to separate the free MDA with HPLC and detect it directly with UV at 270 nm (Cheeseman and others 1988). However, there has been some criticism of methods using MDA as a mediator for the determination of $\cdot\text{OH}$, mainly because they are rather unspecific. For instance, it is also used for testing lipid peroxidation. Another doubtful point is that only a small percentage of the deoxyribose is converted to TBA-reactive substances and we cannot properly assay the $\cdot\text{OH}$ scavenging activity of phenolic compounds, which can show pro-oxidant activity in the Fenton reaction (Bektaşoğlu and others 2006).

There is another group of compounds used as probes for $\cdot\text{OH}$ scavenging. Their common structural feature is an aromatic skeleton. The principle of their reaction with $\cdot\text{OH}$ is aromatic hydroxylation (Figure 6). Diez and others (2001) reported that the most specific probe is salicylic acid because of its high reaction rate with $\cdot\text{OH}$ ($5 \times 10^9 \text{ M}^{-1} \times \text{s}^{-1}$) and the relative stability of the resulting products, which can be separated and measured by HPLC-ECD. Another method of separating and measuring the products of hydroxylation of salicylic acid was used by Paulová and others (2000)—HPLC with UV detection at 270 nm. Contrary to the previous conclusion, Singh and Hider (1988) have suggested that salicylic acid suffers from several disadvantages as a probe for $\cdot\text{OH}$. According to their findings, the hydroxylation of salicylic acid leads to the formation of catechol, which forms complexes with iron ions and as feedback can interfere with the Fenton reaction. Therefore, they designed a new probe with trisubstitution at the C-1, C-3, and C-5 positions of the aromatic ring to prevent the formation of catechol. Hydroxylation of this new probe, *N,N'*-(5-nitro-1,3-phenylene)bisglutaramide, increased the absorbance measured at 430 nm. The amino acid phenylalanine is

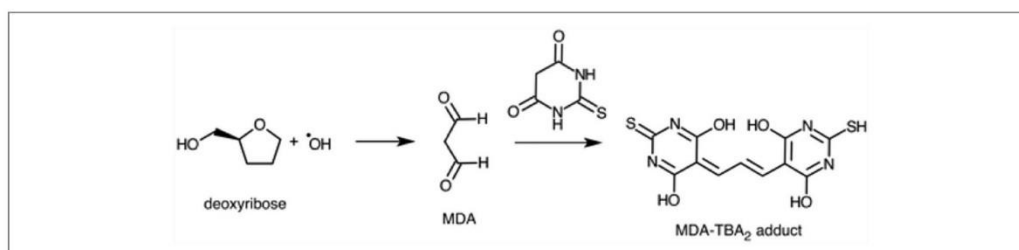


Figure 5—Principle of deoxyribose assay.

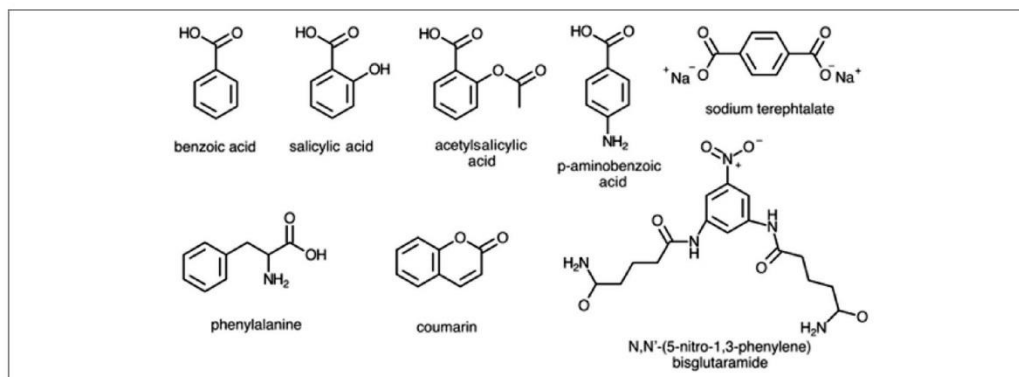


Figure 6—Probes for aromatic hydroxylation.

the next probe commonly used to determine the hydroxyl radical *via* aromatic hydroxylation. Puppo (1992) used phenylalanine in a method determining the $\cdot\text{OH}$ -scavenging activity. The separation and measurement of the tyrosine hydroxy derivatives produced in the reaction were carried out by HPLC-ECD. Various other aromatic compounds can be used in a similar way: benzoic acid (Gutteridge 1987), acetylsalicylic acid (Diez and others 2001), and also probes for fluorescence detection, such as sodium terephthalate and coumarin (Gomes and others 2005). According to Bektaşoğlu and others (2006), the methods for $\cdot\text{OH}$ determination using the principle of aromatic hydroxylation are specific, but require relatively sophisticated instrumentation, such as HPLC-ECD. Therefore, Bektaşoğlu and others (2006) decided to develop a new “test tube” method to determine $\cdot\text{OH}$ -scavenging activity using a modified CUPRAC (cupric ion reducing antioxidant capacity) method. This method utilizes $\cdot\text{OH}$ attacks on the probes used (*p*-aminobenzoate; 2,4- and 3,5-dimethoxybenzoate) and also on the water-soluble antioxidants present. The probes that were hydroxylated in reactions with $\cdot\text{OH}$ are later able to reduce Cu(II)-neocuproine reagent to the chromogen Cu(I)-neocuproine, which strongly absorbs at 450 nm. The scavenging activity of the test substance is compared with the activity of the probe.

Various methods of determining the $\cdot\text{OH}$ -scavenging activity use principles of chemoluminescence, in which light is emitted from a chemical reaction. Parejo and others (2000) used luminol (Figure 7) as a probe for detecting $\cdot\text{OH}$. Luminol reacts with $\cdot\text{OH}$ and emits light at a wavelength of 430 nm. Tsai and others (2001) developed a specific and rapid method using the specific probe indoxyl- β -glucuronide (I β G; Figure 7), which is a low-

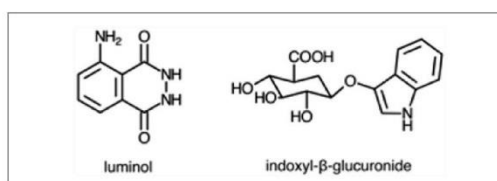


Figure 7—Probes for chemoluminescence.

level chemoluminescence emitter. One great advantage is that it is insensitive to superoxide radical and H_2O_2 . On the contrary, Yoshiki and others (1995) and Chen and others (2002) observed chemoluminescence of flavonoids themselves, probably after the degradation of the hydroperoxide, which was an intermediate resulting from the reaction of $\cdot\text{OH}$ with flavonoids.

Apart from methods that use chemoluminescence, fluorescence is also utilized in determining the $\cdot\text{OH}$ -scavenging activity. Fluorescence is the light emitted by a compound after absorbing light or other electromagnetic radiation. In addition to the products of the aromatic hydroxylation of sodium terephthalate and coumarin, there are other compounds used as fluorescent probes. Cao and others (1997) introduced a method called “hydroxyl radical absorbing capacity” (ORAC- OH), wherein the probe was β -phycoerythrin, a protein pigment from the phycobiliprotein family isolated from *Porphyridium cereum*. The fluorescence of β -phycoerythrin decreased after the attack of a radical, with emission at 540 nm and excitation at 565 nm (Fernández-Pachón and

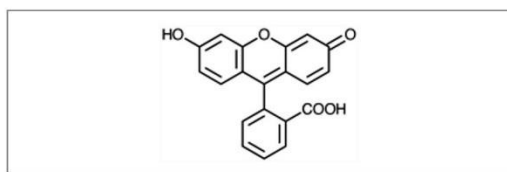


Figure 8—Probe for fluorescence – fluorescein.

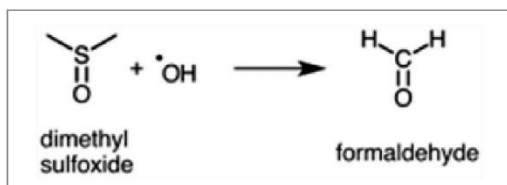


Figure 9—Production of formaldehyde from dimethyl sulfoxide.

others 2005). As a modification of the original ORAC- OH , Kim and Jang (2011) used fluorescein as a probe (Figure 8). Again, the fluorescence decreased after the attack, with emission at 485 nm and excitation at 528 nm.

Dimethyl sulfoxide (DMSO) is another possible probe molecule used to trap OH (Figure 9). DMSO is known to be a good OH scavenger; when attacked by OH , it produces formaldehyde (Klein and others 1981). One of the ways of detecting and quantifying formaldehyde is the spectrophotometric method presented by Nash. Briefly, after the reaction of OH with DMSO the formation of formaldehyde is stopped by ice-cold trichloroacetic acid. Formaldehyde then reacts with acetylacetone in the presence of an ammonium salt and acetic acid. The product is a yellow compound, 3,5-diacyetyl-1,4-dihydrolutidine, which can be measured at 415 nm (Nash 1953; Klein and others 1981). Tai and others (2002) developed a different method of detecting OH and subsequently formed formaldehyde (again from DMSO). Formaldehyde reacts with ammonia and 1,3-cyclohexanedione at pH 4.5. The product has a specific fluorescence with excitation at 404.4 nm and emission at 452.3 nm.

There are also fingerprinting methods other than trapping methods, as mentioned in the introduction to this section. Basically, these methods approach the determination of the OH -scavenging activity by analyzing the damage that OH causes to biomolecules. The most commonly used biomolecule is DNA. An advantage of using DNA is that potential antioxidants protecting the DNA are more likely to do so *in vivo*, and thus the method more nearly resembles real conditions. One possibility is to use lambda DNA, which is a double-stranded and linear molecule, isolated from bacteriophage λ (Benheral and Arumugan 2008), or a plasmid DNA that is also double-stranded but circular and is isolated from an *Escherichia coli* bacterial culture containing the plasmid DNA (Londhe and others 2008). In both cases, the DNA is subjected to OH attack, which causes fragmentation (single- or double-strand breaks) or cross-linking (intra- or inter-strand). The fragmented DNA is then separated by agarose gel electrophoresis and visualized by using ethidium bromide (Trembl and others 2013).

The relationship between flavonoid structure and hydroxyl radical-scavenging activity

The aim of the previous chapter was to summarize the methods used to determine antioxidant activity *via* OH scavenging. Various methods can be used and each method mentioned possesses some specific mechanism of measurement. Therefore, the results of assays also differ according to the method used, and many times they are not fully comparable. The main aim of this short review is to recapitulate the progress made in elucidating the relationship between the structure of flavonoids and their OH -scavenging activity—the structure activity relationship (SAR). The results obtained by using the different methods will be organized in the same order as the methods are listed in the previous chapter.

Pulse radiolysis. Bors and Michel (1999) measured the antioxidant capacities of various flavanols and gallate ester groups. They used pulse radiolysis combined with kinetic spectroscopy. The test compounds were: (–)-epicatechin (1), (–)-epicatechin gallate (2), (–)-epigallocatechin (3) and (–)-epigallocatechin gallate (4). After reaction with OH , the transient spectra of all of the test compounds showed a major absorption peak at 270 to 300 nm, which reflects the semiquinone structure formed at ring B of the flavonoid. Additional absorption bands around 400 nm (for compounds 2, 3, and 4), which correspond to gallate esters, were observed in the spectra obtained. The results showed a clear correlation between the total number of *o*-di- and/or *o*-tri-hydroxyl groups in flavonoid structures with the rate constants of their reaction with OH . Compound 4, with 6 “reactive” hydroxyl groups, showed the highest rate constant, followed by compound 2 with 5; compound 3 with 3. Compound 1, with 2 “reactive” hydroxyl groups, had the lowest rate constant.

Fu and others (2011) used pulse radiolysis to evaluate the OH -scavenging activity of 3 flavanones: naringin (5), hesperetin (6), and naringenin (7). The rate constants and thus the OH -scavenging activity trended downward in the same order. Compound 5 showed the greatest activity, probably due to the presence of a sugar moiety with several hydroxyl groups. Fu and others (2011) also performed a theoretical elucidation of the SAR. They calculated the O–H bond dissociation energies (BDE) of the hydroxyl groups in the flavanones. If the BDE is low, the particular O–H bond is weak and is more involved in the scavenging. The lowest BDE was calculated for both compounds 5 and 7. They both have the free hydroxyl group on C-4', which confirms the essential involvement of ring B in the OH -scavenging activity.

Londhe and others (2009) measured the absorption spectra of OH to determine the scavenging activity of quercetin-3-glucoside (8) and rutoside (9). The ability of these compounds to scavenge OH radicals was measured by comparing it with a standard scavenger such as potassium thiocyanate (KSCN) using a competition technique. The results showed higher activity for compound 8, indicating that the presence of the monosaccharide moiety in quercetin-3-glucoside is more favorable than the disaccharide in rutoside (9).

DMPO trap. Husain and others (1987) determined the OH -scavenging activity of various flavonoids at 1 mM concentration using DMPO as the OH spin trap. OH was produced by UV photolysis of H_2O_2 . The formed adduct, DMPO- OH , was not detected by EPR, but was separated and detected by HPLC with ECD detection. The most active flavonoid was myricetin (10), which scavenged 50% of the OH . Second-most active was quercetin (11) with 48% scavenging activity. The most important feature appears to be the hydroxylation of ring B, because kaempferol (12) has only 1 hydroxyl group at ring B compared to

myricetin (10) or quercetin (11), and possesses a scavenging activity of only 20%. Another structural moiety important for scavenging is the carbonyl group at C-4, as (+)-catechin (13), without this moiety; it displays activity of 31% compared to quercetin (11) with a C-4 carbonyl group.

Tsuda and others (1996) performed similar experiments, but they detected the adduct DMPO- $\cdot\text{OH}$ by EPR and produced $\cdot\text{OH}$ via the Fenton reaction. The compounds tested were the anthocyanidins pelargonidin (14), cyanidin (15), and delphinidin (16). The anthocyanidins tested may act by different mechanisms than other flavonoids, because the results differed diametrically from those obtained by Husain and others (1987). The most active was compound 14 with IC_{50} of 8.5 μM and 1 hydroxyl on ring B, followed by compound 15 with IC_{50} of 36.7 μM and 2 hydroxyl groups on ring B; the last was compound 16, with $\text{IC}_{50} > 100 \mu\text{M}$ and 3 hydroxyl groups. Therefore, the activity of anthocyanidins increases as the number of hydroxyls at ring B declines.

Chang and others (2007) also used EPR to detect of DMPO- $\cdot\text{OH}$. All measurements were done with flavonoids at a concentration of 200 μM . The greatest $\cdot\text{OH}$ -scavenging activity was the 56% shown by baicalein (17), which does not possess a hydroxyl group on ring B but has a carbonyl group at C-4 and 3 hydroxyls on ring A. In view of the results of Husain and others (1987), one would not expect such great activity. For example, compound 13 with hydroxyl groups at ring B, but without a carbonyl at C-4, showed much lower activity (only 31%), and baicalin (18; the 7-O-glucuronide derivative of compound 17), showed only 15% activity. These results lead to the conclusion that the hydroxylation of ring A and the carbonyl group at C-4 are necessary for the enhancement in activity observed for compound 17. This effect may be caused by the chelation of iron, because the $\cdot\text{OH}$ was produced via the Fenton reaction.

Gao and others (2000) obtained similar results. Compound 17 showed much greater activity compared to compound 11, which was used as a positive control and had previously shown high scavenging activity against other radicals. The $\cdot\text{OH}$ was formed via the Fenton reaction and thus iron chelation was a possible mechanism of action for compound 17.

Harris and others (2006) reported that luteolin (19) was more active than chrysin (20) in inhibiting the LPS-dependent production of $\cdot\text{OH}$ in the RAW 264.7 macrophage-like cell line, but compound 20 also showed some degree of activity. This means that hydroxyl groups on ring B may not be essential for this activity. The effect of compound 20 can be explained by its involvement in LPS-induced cell signaling or in interference with the formation of $\cdot\text{OH}$ from $\text{O}_2^{\cdot-}$ and H_2O_2 .

Lee and others (2006) analyzed the $\cdot\text{OH}$ -scavenging activity of prenylated flavonoids obtained from the root bark of *Cudrania tricuspidata* (Carr.) Bureau ex Lavallée (Moraceae), using DMPO as a trap and detection by ESR. Euchrestaflavone B (21) showed the most activity, 1.4 times as high as the Trolox used as a standard. Compound (22), a new flavanone isolated from *C. tricuspidata*, showed 0.6 times as much activity as Trolox. The decrease in activity was caused by the reduction in the number of hydroxyl groups on ring B, as one of the hydroxyl groups at ring B of compound 22 is involved in cyclization with the prenyl moiety.

Shahat and others (2002) tested the scavenging activity of flavonoids and proanthocyanidins obtained from *Crataegus sinaica* Boiss. (Rosaceae). The greatest scavenging activity (57 %) was shown by procyanidin C1 (23), consisting of 3 monomers derived from (–)-epicatechin (1), connected with 4 β -8 bonds. The tetrameric proanthocyanidin (24) surprisingly scavenged only 48%

of the $\cdot\text{OH}$, almost the same amount as the dimeric procyanidin B2 (25). (–)-Epicatechin (1) itself showed activity of only 18%. So the theoretical assumption that an increase in the number of hydroxyl groups would improve the $\cdot\text{OH}$ -scavenging activity did not prove to be fully true. The tetrameric compound 24 probably underwent some disruptive or remodeling reaction with $\cdot\text{OH}$ that diminished the $\cdot\text{OH}$ -scavenging activity.

Deoxyribose assay. Puppo (1992) tested the antioxidant activity of selected flavonoids using the deoxyribose method. $\cdot\text{OH}$ was produced by the Fenton reaction. According to his results, the most active flavonoid was myricetin (10), followed by quercetin (11) and kaempferol (12). This supports the importance of the role of hydroxylation on ring B in the scavenging activity.

Hsu and others (2012) isolated compounds from fresh pods of *Caesalpinia pulcherrima* (L.) Sw. (Fabaceae) and determined their $\cdot\text{OH}$ -scavenging activity. The most active flavonoid compound was myricitrin (26); further results suggest important roles for the galloyl group and hydroxylation on ring B, based mainly on the pattern of decreasing activity: (+)-galloocatechin-3-O-gallate (27), (+)-galloocatechin (28), and (+)-catechin (13). The greater activity of myricitrin (26) in comparison with (+)-galloocatechin (28), followed by amelopsin (29) and (+)-catechin (13) reveals the necessity of the C2–C3 double bond, the C-4 carbonyl group, and the coplanarity of rings B and C.

Moharram and others (2006) isolated compounds from the leaves and stem of *Calliandra haematocephala* Hassk. (Fabaceae) and tested their antioxidant activity in the same way as the scavenging of the $\cdot\text{OH}$. The test compounds were acylated derivatives of myricitrin (26) and quercitrin (30). The most active was myricitrin 2'',3''-di-O-gallate (31). In descending order, lower activity was shown by myricitrin 2''-O-gallate (32), myricitrin 3''-O-gallate (33), quercitrin 2''-O-gallate (34), quercetin (11), myricitrin (26), and quercitrin (30). The greatest scavenging activity is thus shown to be connected with acylation by gallate and the pattern of the hydroxylation on ring B. The arrangement at ring C (the C2–C3 double bond, C-4 carbonyl group, and C-3 hydroxyl group) also appears to be important, because this allows conjugation of the π -bonds of rings A and B.

The assumption that the hydroxylation on the ring B is vital for $\cdot\text{OH}$ scavenging in the deoxyribose method has been confirmed by Si and others (2011). Their measurements revealed that luteolin (19) exhibits twice as much activity as apigenin (35), although it differs by only 1 more hydroxyl group on ring B.

For flavonoids with 1 hydroxyl group on B ring, the crucial structural element appears to be the presence of hydroxyl groups on ring A. Cavia-Saiz and others (2010) have demonstrated this by comparing the activities of naringenin (7) and naringin (5). Compound 5 possesses a C-7 hydroxyl group substituted with rhamnogalactose, and has lower activity. The aglycone, compound 7, which shows a greater effect, is better at stabilizing the radical and can better chelate iron ions.

Marzouk and others (2006) demonstrated that substitution at C-3 does not necessarily reduce the scavenging activity in the deoxyribose method. Quercetin-3-galactouronide (36) shows more activity than quercetin (11). The presence of a galactouronopyranoside moiety increases the activity as compared to substitution with glucuronide (in miquelianin; 37) or galactoside (in hyperoside; 38).

Zhao and others (2006) identified major flavonoids from the pericarp of *Litchi chinensis* Sonn. (Sapindaceae) and determined their antioxidant activity using the deoxyribose method, working mainly with procyanidin B2 (25) and procyanidin B4 (39).

Procyanidin B2 (25) is a dimer of (–)-epicatechin (1), whereas procyanidin B4 (39) consists of (+)-catechin (13) bound with (–)-epicatechin (1). Among the compounds tested with the deoxyribose method, compound 25 showed the greatest activity, because at a concentration of 400 µg/mL it scavenged nearly 97% of the $\cdot\text{OH}$. Compound 39 scavenged only 56% of the $\cdot\text{OH}$ and compound 1 scavenged 52% of the $\cdot\text{OH}$ in this assay. These results suggest that the spatial orientation of ring B and the C-3 hydroxyl group is crucial for the activity. Compound 1 has 2*R*,3*R*-orientation and it allows the structure to scavenge much more $\cdot\text{OH}$ than compound 13 with 2*R*,3*S*-orientation. Thus compound 25 shows the highest activity, because it is a dimer of compound 1. The difference is also seen in the fact that compound 39 has almost the same activity as compound 1.

Van den Berg and others (2000) tested the $\cdot\text{OH}$ -scavenging activity of semisynthetic derivatives of rutoside (9). The introduction of hydroxyethyl groups into the structure of compound 9 increases the activity, and the corresponding tetrahydroxyethylrutoside (40) is the most active compound. On the contrary, Kessler and others (2003) found no difference between the activities of tetrahydroxyethyl- and trihydroxyethylrutoside (40 and 41).

Aromatic hydroxylation. Apart from the deoxyribose method, Puppo (1992) also used HPLC-ECD to determine the $\cdot\text{OH}$ -scavenging activity of flavonoids by determining the inhibition of the hydroxylation of phenylalanine. $\cdot\text{OH}$ was produced by the Fenton reaction. The results are fairly similar to the results of the deoxyribose method. The most active flavonoid was myricetin (10), followed by quercetin (11) and kaempferol (12), which suggests that the hydroxylation of ring B plays an important role in the scavenging activity. Özyürek and others (2008) determined the $\cdot\text{OH}$ -scavenging activity using a modified CUPRAC method. Contrary to the results of Puppo (1992), the highest rate constant for the reaction with $\cdot\text{OH}$ was calculated for compound 11, followed by compounds 10 and 12. In accordance with the results of Zhao and others (2006), compound 1 showed a higher rate constant than compound 13 (Özyürek and others 2008).

Bochořáková and others (2003) determined the $\cdot\text{OH}$ -scavenging activity of selected flavonoids *via* hydroxylation of salicylic acid with $\cdot\text{OH}$ generated by the UV photolysis of H_2O_2 . Rutoside (9) showed the most activity, wogonin glucuronide (42) and baicalin (18) were less effective in scavenging $\cdot\text{OH}$. The hydroxylation of ring B again appears to be a determining factor in the antioxidant activity.

Chemoluminescence. Chen and others (2002) determined the $\cdot\text{OH}$ -scavenging activity of flavonoids by measuring the chemoluminescence produced during the reaction of $\cdot\text{OH}$ with a probe. The presence of an *o*-dihydroxyl group on ring A appears to be an important part of the flavonoid molecule contributing to the scavenging effect. This was discovered when the activity of baicalin (18; IC_{50} 34.6 mg/mL) was compared with the activity of lysiononotin (43; IC_{50} 187 mg/mL). However, the presence of an *o*-dihydroxyl group on ring B was found to be more important, because quercetin (11) showed the highest activity (IC_{50} 12.1 mg/mL). The hydroxyl group substituted at C-3 also proved to be a key feature of the flavonoid structure, as was shown on comparing the activity of the aglycone (quercetin; 11) with its corresponding glycoside (hyperoside, 38; IC_{50} 19.5 mg/mL). The study of Yoshiki and others (1995) described the utilization of a very similar method. However, according to their results, compound 9 showed the greatest activity, which is the opposite of the results obtained by Chen and others (2002), who found that the activity was greater when the C-3 hydroxyl group was not sub-

stituted. The importance of the hydroxylation at ring B was also supported by Yoshiki and others (1995). Compound 10 was more active than compounds 11 and 12.

Chang and others (2010) used another chemoluminescence method developed by Tsai and others (2001) and employing IβG as a probe to measure the $\cdot\text{OH}$ -scavenging activity of flavonoids and flavolignans obtained from *Calamus quiquetnerius* Burret (Arecaceae). The most active flavonoid was dihydrotricin (44), which was more potent than naringenin (7), possibly because of the presence of *ortho* methoxyl groups on ring B, which may help to stabilize the phenoxy radical and thus terminate the chain reaction.

Hydroxyl radical-absorbing capacity—fluorescence. The results of the ORAC_{OH} method performed by Kim and Jang (2011) showed the potent antioxidant activity of compounds 11, 8, and 9. However, the statistical significance of the differences in their activity is low, and from these results it can be suggested that the presence of a C-3 hydroxyl group is not necessary for the scavenging activity. Cao and others (1997) used a different probe for the ORAC_{OH} method. The results of these experiments showed the greatest activity for fustin (45), followed by eriodictol (46) and taxifolin (47). These compounds, a flavanone and 2 flavanols, possess activities twice as great as that of flavonols (such as compounds 10 or 11). The flavonols showed rather pro-oxidant activity in this particular method.

DMSO trap. Arimboor and Arumughan (2012) used the classical Nash method to determine the $\cdot\text{OH}$ -scavenging capacity of flavonoids found in the seeds of *Hippophae rhamnoides* L. (Elaeagnaceae). The most potent was compound 11. Less activity was observed for compounds 12 and 9, which clearly showed a link between the scavenging effect, the hydroxylation on ring B, and the C-3 hydroxyl group. Using the same method, Benherhal and Arumughan (2007) also proved the significant importance of the C2–C3 double bond by showing that compound 11 has more activity than compound 13.

Furthermore, Özgová and others (2003) used the Nash method to examine the influence of flavonoids on the $\cdot\text{OH}$ scavenging. An NADPH-generating system was used in connection with cytochrome P-450 obtained from microsomes and a reaction mixture of iron ions and ascorbate to produce $\cdot\text{OH}$. The results of both methods were compared. None of the tested flavonoids scavenged the $\cdot\text{OH}$ formed in the mixture of iron ions and ascorbate. On the other hand, the $\cdot\text{OH}$ produced in the NADPH-generating system was readily scavenged by compound 10 and less readily by compound 11. The major reason for this discrepancy is probably the different means of producing $\cdot\text{OH}$ in the 2 methods. The first way of producing $\cdot\text{OH}$, the NADPH-generating system, uses various enzymatic systems that leave opportunities for compound 10 to interfere, whereas the reaction mixture of iron ions and ascorbate probably creates $\cdot\text{OH}$ *via* the autooxidation of iron and the test flavonoids exhibited rather pro-oxidant activity.

Tai and others (2002) also detected $\cdot\text{OH}$ -scavenging activity using DMSO as a probe, but they developed a new fluorescence method. Quercetin (11) showed the most activity. Morin (48) was less active, which means that the *o*-dihydroxyl group on ring B is vital for activity. Hesperidin (49) was also less active, and thus the C2–C3 double bond and the C-3 and C-7 hydroxyl groups are also important.

Fingerprinting. The last chapter touching on the results of the structure–activity relationship of flavonoids scavenging $\cdot\text{OH}$ is dedicated to the use of fingerprinting. Benherhal and Arumughan (2008) detected activity of naringenin (7) and naringin (5) that

protects against oxidative damage to DNA. The results showed a clear connection between the protective activity of compound 5 and its ability to chelate iron. Compound 5 showed more activity than its aglycone, so the disaccharide moiety probably enhances iron chelation. Londhe and others (2008) have reported similar conclusions, but in their study quercetin-3-*O*-glucoside (8) protected DNA better than rutoside (9). When both of the substances were glycosides of quercetin (11), the flavonoid with a monosaccharide moiety was more active. Zima and others (2010) determined the antioxidant activity of several geranylated flavanones obtained from *Paulownia tomentosa* (Thunb.) Steud. (Paulowniaceae). The greatest activity found by the DNA protection method was exhibited by 3'-*O*-methyl-5'-hydroxydiplocone (50), followed by diplocone (51) and mimulone (52). This shows the importance of the hydroxylation of ring B in protecting DNA against $\cdot\text{OH}$.

The importance of flavonoid metabolites for their antioxidant effect

To take into account the relatively large metabolism of flavonoids after their dietary intake, we tried to summarize also the activity of simple phenolics obtained after their degradation by gut microflora against the hydroxyl radical. The majority of these metabolites belong to the group of aromatic acids or phloroglucinols. The antioxidant activity of these substances *in vivo* could be based on their direct ability to scavenge radicals, or on the ability to decrease its production through the inhibition of producing enzymes or suppression of their expression in cells. However, the information about the real contribution of these metabolites to ability of flavonoids to act as antioxidant (and to scavenge hydroxyl radical) in living organisms is relatively unclear, and it is difficult to get information only from *in vitro* comparisons. For example, the review of Rice-Evans and others (1996) compares the simple phenols and flavonoids in TEAC assays and shows lower activity of simple phenols than flavonoids. This led some authors to the opinion that dietary phenols have lower importance and antioxidant effect *in vivo* than is generally thought (Olthof and others 2003). On the other hand, there is evidence of antioxidant and/or antimutagenic activity of plant extracts or herbal infusions connected with high concentration of phenolics including hydroxyphenylacetic and dihydroxyphenylacetic acid (Kogianou and others 2013; Kaliora and others 2014), but they do not show the contribution of these simple phenolics on the total effect. Antiradical activity of dihydroxyphenylacetic acid was further proved using DPPH $^+$ and peroxy scavenging activity (LeBlanc and others 2012) and also some other methods (Rubio-Senent and others 2012). The antioxidant power of dihydroxy and trihydroxy phenolic acids was analyzed *via* ABTS $^{+}$, DPPH $^+$ and inhibition liposomal oxidation, together with the inhibition of 2'-deoxyguanosine oxidation produced by $\cdot\text{OH}$ formed in Fenton reaction. ABTS $^{+}$ and DPPH $^+$ assays showed greater effect of trihydroxylated phenols in comparison with dihydroxy-substituted compounds. The type of spacer between the carboxylic acid and the aromatic ring also influences the antioxidant activity, when highest effect was observed for substances with methylenic and ethylenic group, with the lower activity of compounds with unsaturated spacer. For the lipoperoxidation, the *ortho*-dihydroxylated compounds presented a greater antioxidant activity than the trihydroxylated, because of their greater lipophilicity. Oppositely, the pro-oxidant activity was observed in 2'-deoxyguanosine oxidation assay, probably due to the ability of compounds with catechol and pyrogallol moieties to mediate Fe(II)/Fe(III) redox cycle playing

a role in generation of $\cdot\text{OH}$ by the Fenton reaction (Siquet and others 2006).

ORAC testing was used also for assaying of metabolites of ellagitannin, geraniin, chlorogenic acid, and (–)-epigallocatechin gallate, and metabolites like protocatechuic acid (56), dihydrocaffeic acid or dihydroxyphenylacetic acid showed greater antioxidative activity than their respective original compounds (Ishimoto and others 2012). ORAC and FRAP methods were used for proving the effect of several flavonoid metabolites (protocatechuic acid, 3,4-dihydroxyphenylacetic acid, 3,4-dihydroxyphenylpropionic acid (54) and 3-hydroxyphenylacetic acid), and besides the strong antioxidant power, synergic effect of 3,4-dihydroxyphenylacetic acid and ascorbic acid was observed (Noguer and others 2014). Dihydroxyphenylpropionic acid (syn. dihydrocaffeic acid) and similar aromatic acids observed during metabolism of flavonoids or in general phenolics showed relatively strong antiradical activity (ABTS $^{+}$ and DPPH $^+$) and were able to reach the retina in rats where they protected cells against degeneration (Jang and others 2015). Antioxidative effect of flavonoid metabolites was observed also on rat hepatocytes (Miyake and others 2000; Minato and Miyake 2014). The well-organized study tested antioxidative effect of administration of anthocyanin-rich rich *Lonicera caerulea* fruits in healthy human volunteers, and from the metabolic profiling it could be concluded that the activity is connected with the simple aromatic acids shown as metabolites (Heinrich and others 2013). Similar conclusions can be deduced also from study carried on human volunteers consuming chocolate which is rich in phenolic substances (Rios and others 2003).

Summary

To sum up the results, pulse radiolysis studies showed these crucial elements of the flavonoid structure: *o*-hydroxylation on ring B, a gallate moiety at C-3, and glycosylation with a monosaccharide.

The results obtained with methods using DMPO as a trap to detect $\cdot\text{OH}$ have shown the importance of various structural patterns, depending on the way $\cdot\text{OH}$ is produced. The results of Husain and others (1987) showed clearly the importance of the hydroxylation of ring B and the presence of a C-4 carbonyl group. The results of Lee and others (2006) are in accord with this, although they used the Fenton reaction to produce $\cdot\text{OH}$. On the contrary, Chang and others (2007) and Gao and others (2000) proved that for iron chelation the optimal structural parameters are represented by trihydroxylation on ring A. Harris and others (2006) reported that the absence of hydroxylation on ring B does not diminish the scavenging activity when the $\cdot\text{OH}$ is produced by LPS-activated macrophages. According to Tsuda and others (1996), anthocyanidins have a different mode of action than other flavonoids, because they show the opposite effect: less hydroxylation of ring B leads to more activity. Finally, Shahat and others (2002) proved that an increase in the number of units of (–)-epicatechin (1) in oligomeric compounds does not increase the scavenging activity, and the ideal scavenger is trimeric procyanidin C1 (23).

The results of the $\cdot\text{OH}$ -scavenging activity of flavonoids, as determined by the deoxyribose method, showed these structural elements to be vital for this activity: hydroxylation of ring B, a C2–C3 double bond, a C-4 carbonyl group and a C-3 hydroxyl group. Active compounds can possess gallate and galactouronate substituted for the hydroxyl at C-3. Moreover, the spatial conformation of (–)-epicatechin (1) is more active than that of (+)-catechin (13), and the substitution of rutoside (9) with hydroxyethyl groups enhances the scavenging activity.

Experiments that determine the $\cdot\text{OH}$ -scavenging activity of flavonoids by evaluating the effect of aromatic hydroxylation have shown that hydroxylation of ring B is indispensable. Only the measurements done by Özyürek and others (2008) did not prove this assumption.

The $\cdot\text{OH}$ -scavenging activity of flavonoids as determined by chemoluminescence methods shows that the most important feature for the activity is the hydroxylation of ring B. Some results also suggest that additional methoxyl groups on ring B can help to improve the antioxidant activity. If there are no hydroxyl groups on ring B, hydroxylation of ring A becomes important. The role of the C-3 hydroxyl group is questionable.

The results of both ORAC- OH methods contrast with the results of other methods of determining the $\cdot\text{OH}$ -scavenging activity. Quercetin (11) was not more active than its glycosides, and flavanones and flavanonols were more active than flavonols.

Methods using DMSO as the probe revealed again that the hydroxylation of ring B is vital for the $\cdot\text{OH}$ -scavenging activity. Furthermore, a C2–C3 double bond and C-3 and C-7 hydroxyl groups also enhance the antioxidant effect. The results of Ozgova and others (2003) showed differences between the 2 ways of producing $\cdot\text{OH}$. Whereas myricetin (10) successfully scavenged the $\cdot\text{OH}$ produced in a NADPH-generating system, the $\cdot\text{OH}$ produced in a mixture of iron ions and ascorbate was resistant to the activity of any flavonoid tested.

Studies using DNA protection showed that the hydroxylation of ring B and glycosylation with either a mono- or disaccharide to be the most preferential. This effect is probably caused by the enhanced possibility of chelating the iron ions.

According to Procházková and others (2011) the importance of the hydroxylation of ring B also applies to other ROS-scavenging methods. The reaction of ROS with a flavonoid having hydroxyl groups on ring B produces a fairly stable *ortho*-semiquinone by enabling electron delocalization (Heim and others 2002). The advantage of an *ortho* rather than *meta* orientation of the hydroxyl groups was shown by Rice-Evans and others (1996). Methylation of the hydroxyl groups on ring B usually diminishes the scavenging activity (Heim and others 2002). But, according to the results of Chang and others (2010), in some cases it can increase the stability of the radical formed at ring B. The next most important parts of the flavonoid structure are the C2–C3 double bond, the C-3 hydroxyl group, and the C-4 carbonyl group. Heim and others (2002) reported that these structural elements strengthen the conjugation of the A and B rings, increase electron delocalization, and in the end facilitate the stabilization of the radical. There are some results that indicate that a C-3 hydroxyl group has only a slight influence on antioxidant activity (Yoshiki and others 1995; Kim and Jang 2011). The other hydroxyl groups, namely at C-5 and C-7, are also involved in the activity (Heim and others 2002).

Apart from the ROS-scavenging activity, many structural elements can be involved in the chelation of metal ions, such as copper or iron (Procházková and others 2011). In particular, the neighboring hydroxyl and carbonyl groups are involved. This could explain the fact that in some pulse-radiolysis studies (methods using deoxyribose and methods that prevent DNA damage), glycosylation actually increased the antioxidant activity (Marzouk and others 2006; Benherlal and Arumughan 2008; Londhe and others 2009). The hydroxyl groups of the saccharide moieties probably augment the antioxidant activity, although normally this does not apply (Heim and others 2002).

The antioxidant potential of gallic acid (57) is known and thus it is no surprise that gallate esters of catechins have high scav-

enging capacity for ROS (Rice-Evans and others 1996; Bors and Michel 1999). Rice-Evans and others (1996) also reported that that scavenging activity of anthocyanins increases with the number of hydroxyl groups, in contrast to the findings of Tsuda and others (1996). In a similar way, the antioxidant activity of proanthocyanins does not precisely increase with the degree of polymerization (Rice-Evans and others 1996; Shahat and others 2002).

As can be seen, a relatively large number of studies have been carried out to elucidate the potential of flavonoids for interaction with the hydroxyl radical. However, the majority of these experiments, although they showed some basic structural parameters necessary for such activity, were performed *in vitro* using purely chemical methods. This is because the hydroxyl radical is unstable and forms at an extremely high reaction rate. Nevertheless, *in vivo* techniques should be developed and used, so as to involve reaction conditions that are actually present in cellular systems.

The results summarized in this review also emphasize the importance of natural flavonoids in the human diet. Flavonoids of certain structures are potent scavengers of hydroxyl radicals and also other ROS and thus can help the human body to overcome oxidative stress. However, it should be noted that extensive *in vivo* clinical trials must be performed to evaluate the positive effect of flavonoid intake on the development of diseases associated with oxidative stress. Moreover, several studies on human volunteers and animals showed the possible importance of contribution of flavonoid metabolites to overall antioxidant activity.

Conclusions

The structural elements of the flavonoids most vital for hydroxyl radical-scavenging are hydroxylation of ring B and a C2–C3 double bond connected with a C-3 hydroxyl group and a C-4 carbonyl group. Hydroxylation of ring A also enhances the activity, as does the presence of gallate and galactouronate moieties as substituents on the flavonoid skeleton. A similar hydroxylation pattern is valid for simple aromatic acids observed as flavonoid metabolites.

Acknowledgments

This project was supported by the Internal Grant Agency of the Univ. of Veterinary and Pharmaceutical Sciences Brno (grant number 90/2013/FaF). The authors declare that there are no conflicts of interest.

Author Contributions

Jakub Tremil researched the literature, interpreted the results, and prepared the manuscript. Karel Šmejkal revised the manuscript and participated in preparation and drafting the summary and conclusions.

References

- Albano E, Tomasi A, Gorla-Gatti L, Poli G, Vannini V, Dianzani M. 1987. Free radical metabolism of alcohols by rat liver microsomes. *Free Rad Res* 3:243–9. doi: 10.3109/10715768709069789.
- Arimboor R, Arumughan C. 2012. HPLC-DAD-MS/MS profiling of antioxidant flavonoid glycosides in sea buckthorn (*Hippophae rhamnoides* L.) seeds. *Int J Food Sci Nutr* 63:730–8. doi: 10.3109/09637486.2011.652075.
- Arouma OI, Grootveld M, Halliwell B. 1987. The role of iron in ascorbate-dependent deoxyribose degradation. Evidence consistent with a site-specific hydroxyl radical generation caused by deoxyribose molecule. *J Inorg Biochem* 29:289–99. doi:10.1016/0162-0134(87)80035-1.
- Bahm K, Khalil MAK. 2004. A new model of tropospheric hydroxyl radical concentrations. *Chemosphere* 54:143–66. doi: 10.1016/j.chemosphere.2003.08.006.

- Barbusiński K. 2009. Fenton reaction—controversy concerning the chemistry. *Ecol Chem Eng S* 16:347–56.
- Bektaşoğlu B, Çelik SE, Özyürek M, Güçlü K, Apak R. 2006. Novel hydroxyl radical scavenging antioxidant assay for water-soluble antioxidants using a modified CUPRAC method. *Biochem Biophys Res Commun* 345:1194–200. doi:10.1016/j.bbrc.2006.05.038.
- Berlett BS, Stadtman ER. 1997. Protein oxidation in aging, disease and oxidative stress. *J Biol Chem* 272:20313–6. doi:10.1074/jbc.272.33.20313.
- Benherhal PS, Arumughan C. 2007. Chemical composition and in vitro antioxidant studies on *Syzgium cumini* fruit. *J Sci Food Agric* 87:2560–9. doi:10.1002/jsfa.2957.
- Benherhal PS, Arumughan C. 2008. Studies on modulation of DNA integrity in Fenton's system by phytochemicals. *Mutat Res, Fundam Mol Mech Mutagen* 648:1–8. doi:10.1016/j.mrfmm.2008.09.001.
- Betteridge DJ. 2000. What is oxidative stress? *Metabolism* 49:3–8. doi:10.1016/S0026-0495(00)80077-3.
- Biaglow JE, Manevich Y, Uckun F, Held KD. 1997. Quantitation of hydroxyl radicals produced by radiation and copper-linked oxidation of ascorbate by 2-deoxy-D-ribose method. *Free Rad Biol Med* 22:1129–38. doi:10.1016/S0891-5849(96)00527-8.
- Bochořáková H, Paulová H, Slanina J, Musil P, Táborská E. 2003. Main flavonoids in the root of *Scutellaria baicalensis* cultivated in Europe and their comparative antiradical properties. *Phytother Res* 17:640–4. doi:10.1002/ptr.1216.
- Borradaile NM, Carroll KK, Kurowska EM. 1999. Regulation of HepG2 cell apolipoprotein B metabolism by citrus flavonones hesperetin and naringenin. *Lipids* 34:591–8. doi:10.1007/s11745-999-0403-7.
- Bors W, Michel C. 1999. Antioxidant capacity of flavanols and gallate esters: pulse radiolysis studies. *Free Rad Biol Med* 27:1413–26. doi:10.1016/S0891-5849(99)00187-2.
- Bray WC, Gorin MH. 1932. Ferryl ion, a compound of tetravalent iron. *J Am Chem Soc* 54:2124–5. doi:10.1021/ja01344a505.
- Breynaert A, Bosscher D, Kahnt A, Claeys M, Cos P, Pieters L, Hermans Nina. 2015. Development and validation of an *in vitro* experimental gastrointestinal dialysis model with colon phase to study the availability and colonic metabolism of polyphenolic compounds. *Planta Med* 81(12/13):1075–83.
- Buettner GR. 1993. The pecking order of free radicals and antioxidants lipid peroxidation alpha-tocopherol and ascorbate. *Arch Biochem Biophys* 300:535–43. doi:10.1006/abbi.1993.1074.
- Butler J, Hoey BM, Lea JS. 1988. The measurement of radicals by pulse radiolysis. In: Rice-Evans C and Halliwell B, editors. *Free radicals, methodology and concepts*. London: Richelieu Press. p 457–79.
- Cabiscol E, Tamarit J, Ros J. 2000. Oxidative damage to bacteria and protein damage by reactive oxygen species. *Intl Microbiol* 3:3–8.
- Cao G, Sofic E, Prior RL. 1997. Antioxidant and prooxidant behavior of flavonoids: structure-activity relationship. *Free Rad Biol Med* 22:749–60. doi:10.1016/S0891-5849(96)00351-6.
- Carocho M, Ferreira ICFR. 2013. A review on antioxidants, prooxidants and related controversy: natural and synthetic compounds, screening and analysis methodologies and future perspectives. *Food Chemical Toxicol* 51:15–25. doi:10.1016/j.fct.2012.09.021.
- Catalá A. 2010. A synopsis of the process of lipid peroxidation since the discovery of essential fatty acids. *Biochem Biophys Res Commun* 399:318–23. doi:10.1016/j.bbrc.2010.07.087.
- Cavia-Saiz M, Busto MD, Pilar-Izquierdo MC, Ortega N, Perez-Mateos M, Muñoz P. 2010. Antioxidant properties, radical scavenging activity and biomolecule protection capacity of flavonoid naringenin and its glycoside naringin: a comparative study. *J Sci Food Agric* 90:1238–44. doi:10.1002/jsfa.3959.
- Chang W-T, Shao Z-H, Yin J-J, Mehendale S, Wang C-Z, Qin Y, Li J, Chen W-J, Chien C-T, Becker LB, Vanden Hoek TL, Yuan C-S. 2007. Comparative effects of flavonoids on oxidant scavenging and ischemia-reperfusion injury in cardiomyocytes. *Eur J Pharmacol* 566:58–66. doi:10.1016/j.ejphar.2007.03.037.
- Chang C-L, Wang G-J, Zhang L-J, Tsai W-J, Chen R-Y, Wu Y-C, Kuo Y-H. 2010. Cardiovascular protective flavolignans and flavonoids from *Calamus quiquiescens*. *Phytochemistry* 71:271–9. doi:10.1016/j.phytochem.2009.09.025.
- Chen J-W, Zhu Z-Q, Hu T-X, Zhu D-Y. 2002. Structure-activity relationship of natural flavonoids in hydroxyl radical-scavenging effects. *Acta Pharmacol Sin* 23:667–72.
- Cheeseman KH, Beavis A, Esterbauer H. 1988. Hydroxyl-radical-induced iron-catalyzed degradation of 2-deoxyribose. *Biochem J* 252:649–53.
- Crozier A, Del Rio D, Clifford MN. 2010. Bioavailability of dietary flavonoids and phenolic compounds. *Mol Aspects Med* 31:446–67. doi:10.1016/j.mam.2010.09.007.
- Cushman M, Nagarathnam D, Gahlen RL. 1991. Synthesis and evaluation of hydroxylated flavones and related compounds as potential inhibitors of the protein-tyrosine kinase p56lck. *J Natl Prod* 54:1345–52. doi:10.1021/np50077a018.
- Dalle-Donne I, Rossi R, Colombo R, Giustarini D, Milzani A. 2006. Biomarkers of oxidative damage in human disease. *Clin Chem* 52:601–23. doi:10.1373/clinchem.2005.061408.
- De Lange DW, Verhoef S, Gorter G, Kraaijenhagen RJ, van de Wiet A, Akkerman J-WN. 2007. Polyphenolic grape extract inhibits platelet activation through PECAM-1: an explanation for the French paradox. *Alcohol Clin Exp Res* 31:1308–14. doi:10.1111/j.1530-0277.2007.00439.x.
- De Pascual-Teresa S, Moreno D A, García-Viguera C. 2010. Flavanols and anthocyanins in cardiovascular health: a review of current evidence. *Intl J Mol Sci* 11:1679–703. doi:10.3390/ijms11041679.
- Diez L, Livertoux M-H, Stark A-A, Wellman-Rousseau M, Leroy P. 2001. High-performance liquid chromatographic assay of hydroxyl free radical using salicylic acid hydroxylation during in vitro experiments involving thiols. *J Chromatogr B* 763:185–93. doi:10.1016/S0378-4347(01)00396-6.
- Dueñas M, González-Manzano S, González-Paramás A, Santos-Buelga C. 2010. Antioxidant evaluation of O-methylated metabolites of catechin, epicatechin and quercetin. *J Pharm Biomed Anal* 51:443–9. doi:10.1016/j.jpba.2009.04.007.
- Ehrlalt DH. 1999. Gas phase chemistry of the troposphere. In: Baumgärtel H, Grünbein W, Hensel F, and Zellner R, editors. *Global aspects of atmospheric chemistry*. Darmstadt: Springer Verlag. p 21–110.
- Evans MD, Dizdaroğlu M, Cooke MS. 2004. Oxidative DNA damage and disease: induction, repair and significance. *Mutat Res* 567:1–61. doi:10.1016/j.mrrev.2003.11.001.
- Fenton HJH. 1894. Oxidation of tartaric acid in presence of iron. *J Chem Soc Trans* 65:899–910. doi:10.1039/CT89465FP001.
- Fernández-Pachón MS, Villano D, Troncoso AM, García-Parilla MC. 2005. Antioxidant capacity of plasma after red wine intake in human volunteers. *J Agric Food Chem* 53:5024–9. doi:10.1021/jf0501995.
- Fu H, Lin M, Katsumura Y, Muroya Y. 2011. Free-radical scavenging activities of silybin and its analogues: a pulse radiolysis study. *Intl J Chem Kinet* 43:590–7. doi:10.1002/kin.20589.
- Galati G, O'Brien PJ. 2004. Potential toxicity of flavonoids and other dietary phenolics: significance for their chemopreventive and anticancer properties. *Free Rad Biol Med* 37:287–303. doi:10.1016/j.freeradbiomed.2004.04.034.
- Gao Z, Yang X, Huang K, Xu H. 2000. Free-radical scavenging and mechanism study of flavonoids extracted from the radix of *Scutellaria baicalensis* Georgi. *Appl Magnet Reson* 19:35–44. doi:10.1007/BF03162259.
- Genaro-Mattos TC, Dalvi LT, Oliveira RG, Ginani JS, Hermes-Lima M. 2009. Reevaluation of the 2-deoxyribose assay for determination of free radical formation. *Biochim Biophys Acta* 1790:1636–42. doi:10.1016/j.bbagen.2009.09.003.
- Gomes A, Fernandes E, Lima JLF. 2005. Fluorescence probes used for detection of reactive oxygen species. *J Biochem Biophys Meth* 65:45–80. doi:10.1016/j.jbbm.2005.10.003.
- Grune T, Siems WG, Schneider W. 1993. Accumulation of aldehydic lipid peroxidation products during postanoxic reoxygenation of isolated rat hepatocytes. *Free Rad Biol Med* 15:125–31. doi:10.1016/0891-5849(93)90051-U.
- Gutteridge JMC. 1987. Ferrous-salt-promoted damage to deoxyribose and benzoate. *Biochem J* 243:709–14.
- Halliwell B. 1995. Antioxidant characterization: methodology and mechanism. *Biochem Pharmacol* 49:1341–8. doi:10.1016/0006-2952(95)00088-H.
- Halliwell B, Gutteridge JMC. 2007. *Free radicals in biology and medicine*. 4th ed. Oxford: Oxford Univ. Press.
- Halliwell B, Gutteridge JMC, Arouma OI. 1987 The deoxyribose method: a simple "test-tube" assay for determination of rate constants for reactions of hydroxyl radicals. *Anal Biochem* 165:215–9. doi:10.1016/0003-2697(87)90222-3.

- Harbour JR, Chow V, Bolton JR. 1974. An electron spin resonance study of the spin adducts of OH and HO₂ radicals with nitrones in the ultraviolet photolysis of aqueous hydrogen peroxide solutions. *Can J Chem* 52:3549–53. doi:10.1139/v74-527.
- Harman D. 1956. Aging: a theory based on free radical and radiation chemistry. *J Gerontol* 11:298–300. doi:10.1093/geronj/11.3.298.
- Harris GK, Qian Y, Leonard SS, Sbarra DC, Shi X. 2006. Luteolin and chrysin differentially inhibit cyclooxygenase-2 expression and scavenge reactive oxygen species but similarly inhibit prostaglandin-E₂ formation in RAW 264.7 cells. *J Nutr* 136:1517–21.
- Hashemi M, Behrangi N, Borna H, Entezari M. 2012. Protein tyrosine kinase (PTK) as a novel target for some natural anti-cancer molecules extracted from plants. *J Med Plants Res* 6:64375–8. doi:10.5897/JMPR11.1005.
- Heim KE, Tagliaferro AR, Bobilya DJ. 2002. Flavonoid antioxidants: chemistry, metabolism and structure-activity relationship. *J Nutr Biochem* 13:572–84. doi:10.1016/S0955-2863(02)00208-5.
- Heinrich J, Valentova K, Vacek J, Palikova I, Zatloukalova M, Kosina P, Ulrichova J, Vrbkova J, Simanek V. 2013. Metabolic profiling of phenolic acids and oxidative stress markers after consumption of *Lonicera caerulea* L. Fruit. *J Agric Food Chem* 61(19):4526–32.
- Hertog MG, Hollman PCH, Katan MB. 1993. Intake of potentially anticarcinogenic flavonoids and their determinants in adults in the Netherlands. *Nutr Cancer* 20:21–29.
- Hidalgo M, Sánchez-Moreno C, De Pascual-Teresa S. 2010. Flavonoid-flavonoid interaction and its effect on their antioxidant activity. *Food Chem* 121:691–6. doi:10.1016/j.foodchem.2009.12.097.
- Hollman PC, De Vries JH, Van Leeuwen SD, Mengelers SD, Katan MB. 1995. Absorption of dietary quercetin glycosides and quercetin in healthy ileostomy volunteers. *Am J Clin Nutr* 62:1276–82.
- Houčevá-Levin C, Bobrowski K. 2013. The use of methods of radiolysis to explore the mechanisms of free radical modifications in proteins. *J Proteomics* 92:51–62. doi:10.1016/j.jpro.2013.02.014.
- Hsu F-L, Huang W-J, Wu T-H, Lee M-H, Chen L-C, Lu H-J, Hou W-C, Lin M-H. 2012. Evaluation of antioxidant and free radical scavenging capacities of polyphenols from pods of *Caesalpinia pulcherrima*. *Int J Mol Sci* 13:6073–88. doi:10.3390/ijms13056073.
- Husain SR, Cillard J, Cillard P. 1987. Hydroxyl radical scavenging activity of flavonoids. *Photochemistry* 26:2489–91. doi:10.1016/S0031-9422(00)83860-1.
- Iacopini P, Baldi M, Storch P, Sebastiani L. 2008. Catechin, epicatechin, quercetin, rutin and resveratrol in red grape: content, *in vitro* antioxidant activity and interactions. *J Food Compos Anal* 21:589–98. doi:10.1016/j.jfca.2008.03.011.
- Ishimoto H, Tai A, Yoshimura M, Amakura Y, Yoshida T, Hatano T, Ito H. 2012. Antioxidative properties of functional polyphenols and their metabolites assessed by an ORAC assay. *Biosci Biotechnol Biochem* 76(2):395–9.
- Jang H, Choi Y, Ahn HR, Jung SH, Lee CY. 2015. Effects of phenolic acid metabolites formed after chlorogenic acid consumption on retinal degeneration *in vivo*. *Mol Nutr Food Res* 59(10):1918–29.
- Kaliora AC, Kogiannou DAA, Kefalas P, Papassideri IS, Kalogeropoulou N. 2014. Phenolic profiles and antioxidant and anticarcinogenic activities of Greek herbal infusions; balancing delight and chemoprevention? *Food Chem* 142:233–41.
- Kaur R, Thukral AK, Arora S. 2010. Attenuation of free radical by an aqueous extract of peels of safed musli tubes (*Chlorophytum borivilianum* Sant et Fernand). *J Chin Clin Med* 5:7–11.
- Kessler M, Ubeaud G, Jung L. 2003. Anti- and pro-oxidant activity of rutin and quercetin derivatives. *J Pharm Pharmacol* 55:131–42. doi:10.1211/002235702559.
- Khlebnikov AI, Schepetkin IA, Domina NG, Kirpotina LN, Quinn MT. 2006. Improved quantitative structure-activity relationship models to predict antioxidant activity of flavonoids in chemical, enzymatic, and cellular systems. *Bioorg Med Chem* 15:1749–70. doi:10.1016/j.bmc.2006.11.037.
- Kim G-N, Jang H-D. 2011. Flavonol content in water extract of mulberry (*Morus alba* L.) leaf and their antioxidant capacities. *J Food Sci* 76:869–73. doi:10.1111/j.1750-3841.2011.02262.x.
- Klein SM, Cohen G, Cederbaum AI. 1981. Production of formaldehyde during metabolism of dimethyl sulfoxide by hydroxyl radical generating systems. *Biochemistry* 20:6006–12. doi:10.1021/bi00524a013.
- Kogiannou DAA, Kalogeropoulou N, Kefalas P, Polissiou MG, Kaliora AC. 2013. Herbal infusions; their phenolic profile, antioxidant and anti-inflammatory effects in HT29 and PC3 cells. *Food Chem Toxicol* 61:152–9.
- LeBlanc LM, Pare AF, Jean-Francois J, Hebert MJG, Surette ME, Touaibia M. 2012. Synthesis and antiradical/antioxidant activities of caffeic acid phenethyl ester and its related propionic, acetic and benzoic acid analogs. *Molecules* 17:14637–50.
- Lee BW, Lee JH, Gal SW, Moon YH, Park KH. 2006. Selective ABTS radical-scavenging activity of prenylated flavonoids from *Cudrania tricuspidata*. *Biosci Biotechnol Biochem* 70:427–32. doi:10.1271/bbb.70.427.
- Levine RL, Mosoni L, Berlett BS, Stadtman ER. 1996. Methionine residues as endogenous antioxidants in proteins. *Proc Natl Acad Sci USA* 93:15036–40.
- Loke WM, Proudfoot JM, Stewart S, McKinley AJ, Needs PW, Kroon PA, Hodgson JM, Croft KD. 2008. Metabolic transformation has a profound effect on anti-inflammatory activity of flavonoids such as quercetin: lack of association between antioxidant and lipoxygenase inhibitory activity. *Biochem Pharmacol* 75:1045–53. doi:10.1016/j.bcp.2007.11.002.
- Londhe JS, Devasagayam TPA, Foo LY, Ghaskadbi SS. 2008. Antioxidant activity of the medicinal plant *Phyllanthus amarus* Linn. *Redox Rep* 13:199–207. doi:10.1179/135100008x308984.
- Londhe JS, Devasagayam TPA, Foo LY, Ghaskadbi SS. 2009. Radioprotective properties of polyphenols from *Phyllanthus amarus* Linn. *J Rad Res* 50:303–9. doi:10.1269/jrr.08096.
- Lotito SB, Zhang W-J, Yang CS, Crozier A, Frei B. 2011. Metabolic conversion of dietary flavonoids alters their anti-inflammatory and antioxidant properties. *Free Rad Biol Med* 51:454–63. doi:10.1016/j.freeradbiomed.2011.04.032.
- Ma Q. 2010. Transcriptional responses to oxidative stress: pathological and toxicological implications. *Pharmacol Ther* 125:376–93. doi:10.1016/j.pharmthera.2009.11.004.
- Marzouk MS, Moharram FA, Haggag EG, Ibrahim MT, Badary OA. 2006. Antioxidant flavonol glycosides from *Schinus molle*. *Phytother Res* 20:200–5. doi:10.1002/ptr.1834.
- Minato K-I, Miyake Y. 2014. Hexanoyl-lysine as an oxidative-injured marker—application of development of functional food. *Subcell Biochem* 77:163–74.
- Minero C, Lucchiari M, Maurino V, Vione D. 2013. A quantitative assessment of the production of •OH and additional oxidants in the dark Fenton reaction: Fenton degradation of aromatic amines. *RSC Adv* 3:26443–50. doi:10.1039/C3RA44585B.
- Miyake Y, Shimoi K, Kumazawa S, Yamamoto K, Kinai N, Osawa T. 2000. Identification and antioxidant activity of flavonoid metabolites in plasma and urine of eriocitrin-treated rats. *J Agric Food Chem* 48(8):3217–24.
- Moharram FA, Marzouk MSA, Ibrahim MT, Mabry TJ. 2006. Antioxidant galloylated flavonol glycosides from *Calliandra haematocephala*. *Natl Prod Res* 20:927–34. doi:10.1080/14786410500378494.
- Nash T. 1953. The colorimetric estimation of formaldehyde by means of the Hantzsch reaction. *Biochem J* 55:416–21.
- Niki E. 2010. Assessment of antioxidant capacity *in vitro* and *in vivo*. *Free Rad Biol Med* 49:503–15. doi:10.1016/j.freeradbiomed.2010.04.016.
- Noguer M, Cerezo AB, Moya ML, Troncoso AM, Garcia-Parrilla M. 2014. Synergism effect between phenolic metabolites and endogenous antioxidants in terms of antioxidant activity. *Adv Chem Eng Sci* 4(2):258–65.
- Olthof MR, Hollman PCH, Buijsman MNCP, van Amelsvoort JMM, Katan MB. 2003. Chlorogenic acid, quercetin-3-rutinoside and black tea phenols are extensively metabolized in humans. *J Nutr* 133(6):1806–14.
- Otake Y, Hsieh F, Walle T. 2002. Glucuronidation versus oxidation of the flavonoid galangin by human liver microsomes and hepatocytes. *Drug Metab Dispos* 30:576–81. doi:10.1124/dmd.30.5.576.
- Ou B, Hampsch-Woodill M, Flanagan J, Deemer EK, Prior RL, Huang D. 2002. Novel fluorometric assay for hydroxyl radical prevention capacity using fluorescein as the probe. *J Agric Food Chem* 50:2772–7. doi:10.1021/jf011480w.
- Ozgová Š, Heřmánek J, Gut I. 2003. Different antioxidant effects of polyphenols on lipid peroxidation and hydroxyl radicals in the NADPH-, Fe-ascorbate- and Fe-microsomal systems. *Biochem Pharmacol* 66:1127–37. doi:10.1016/S0006-2952(03)00425-8.
- Özyürek M, Bektaşoğlu B, Güçlü K, Apak R. 2008. Hydroxyl radical scavenging assay of phenolics and flavonoids with a modified cupric reducing antioxidant capacity (CUPRAC) method using catalase for hydrogen peroxide degradation. *Anal Chim Acta* 616:196–206. doi:10.1016/j.aca.2008.04.033.
- Parejo I, Codina C, Petrakis C, Kefalas P. 2000. Evaluation of scavenging by Co(II)/EDTA-induced luminol chemoluminescence and DPPH•

- (2,2-diphenyl-1-picrylhydrazyl) free radical assay. *J Pharmacol Toxicol Methods* 44:507–12. doi:10.1016/S1056-8719(01)00110-1.
- Paulová H, Bochořáková H, Slanina J, Táborská E. 2000. Evaluation of hydroxyl radical-scavenging activity of baicalin using HPLC method. *Pharm Pharmacol Lett* 10:27–30.
- Peterson J, Dwyer J. 1998. Flavonoids: dietary occurrence and biochemical activity. *Nutr Res* 18:1995–2018. doi: [http://dx.doi.org/10.1016/S0271-5317\(98\)00169-9](http://dx.doi.org/10.1016/S0271-5317(98)00169-9).
- Procházková D, Boušová I, Wilhelmová N. 2011. Antioxidant and prooxidant properties of flavonoids. *Fitoterapia* 82:513–23. doi: 10.1016/j.fitote.2011.01.018.
- Puppo A. 1992. Effect of flavonoids on hydroxyl radical formation by Fenton-type reactions; influence of the iron chelator. *Phytochemistry* 31:85–8. doi:10.1016/0031-9422(91)83011-9.
- Rahman A, Shahabuddin A, Hadi SM, Parish JH. 1990. Complexes involving quercetin, DNA and Cu(II). *Carcinogenesis* 11:2001–3. doi: 10.1093/carcin/11.11.2001.
- Ravishanker D, Rajora AK, Greco F, Osborn HML. 2013. Flavonoids as prospective compounds for anti-cancer therapy. *Int J Biochem Cell Biol* 45:2821–31. doi:10.1016/j.biocel.2013.10.004.
- Rice-Evans CA, Miller NJ, Paganga G. 1996. Structure-antioxidant activity of flavonoids and phenolic acids. *Free Rad Biol Med* 20:933–56. doi:10.1016/0891-5849(95)02227-9.
- Rios LY, Gonthier M-P, Remesy C, Mila I, Lapiere C, Lazarus SA, Williamson G, Scalbert A. 2003. Chocolate intake increases urinary excretion of polyphenol-derived phenolic acids in healthy human subjects. *Am J Clin Nutr* 77(4):912–8.
- Rubio-Senent F, Rodriguez-Gutierrez G, Lama-Munoz A, Fernandez-Bolanos J. 2012. New phenolic compounds hydrothermally extracted from the olive oil byproduct alperujo and their antioxidative activities. *J Agric Food Chem* 60(5):1175–86.
- Scalzo J, Mezzetti B, Battino M. 2008. Total antioxidant capacity evaluation: critical steps for assaying berry antioxidant features. *BioFactors* 23:221–7. doi:10.1002/biof.5520230407.
- Sesnik ALA, O'Leary KA, Hollman PCH. 2001. Quercetin glucuronides but not glucosides are present in human plasma after consumption of quercetin-3-glucoside or quercetin-4'-glucoside. *J Nutr* 131:1938–41.
- Shahat AA, Cos P, De Bruyne T, Apers S, Hammouda FM, Ismail SI, Azzam S, Claeys M, Goovaerts E, Pieters L, Vanden Berghe D, Vlietinck AJ. 2002. Antiviral and antioxidant activity of flavonoids and proanthocyanidins from *Cnataegis sinica*. *Planta Med* 68:539–41. doi:10.1055/s-2002-32547.
- Si C-L, Lu Y-Y, Zhang Y, Xu J, Qin P-P, Sun R-C, Ni Y-H. 2011. Antioxidative low molecular weight extracts from triploid *Populus tomentosa* xylem. *Bioresources* 6:232–42.
- Singh S, Hider RC. 1988. Colorimetric detection of the hydroxyl radical: comparison of the hydroxyl-radical-generating ability of various iron complexes. *Anal Biochem* 171:47–54. doi:10.1016/0003-2697(88)90123-6.
- Siquet C, Paiva-Martins F, Lima JLFC, Reis S, Borges F. 2006. Antioxidant profile of dihydroxy- and trihydroxyphenolic acids—a structure-activity relationship study. *Free Rad Res* 40(4):433–42.
- Tai C, Gu X, Zou H, Guo Q. 2002. A new simple and sensitive fluorimetric method for the determination of hydroxyl radical and its application. *Talanta* 58:661–7. doi:10.1016/S0039-9140(02)00370-3.
- Tirzitis G, Bartosz G. 2010. Determination of antiradical and antioxidant activity: basic principles and new insights. *Acta Biochim Pol* 57:139–42.
- Tremel J, Šmejkal K, Hošek J, Žemlička M. 2013. Determination of antioxidant activity using oxidative damage to plasmid DNA—pursuit of solvent optimization. *Chem Pap* 67:484–9. doi:10.2478/s11696-013-0334-8.
- Tsai C-H, Stern A, Chiou J-F, Chern C-L, Liu T-Z. 2001. Rapid and specific detection of hydroxyl radical using an ultraweak chemoluminescence analyzer and a low-level chemoluminescence emitter: application to hydroxyl radical-scavenging ability of aqueous extracts of food constituents. *J Agric Food Chem* 49:2137–41. doi: 10.1021/jf001071k.
- Tsuda T, Shiga K, Ohshima K, Kawakishi S, Osawa T. 1996. Inhibition of lipid peroxidation and active oxygen radical scavenging effect of anthocyanin pigments isolated from *Phaseolus vulgaris* L. *Biochem Pharmacol* 52:1033–9. doi:10.1016/0006-2952(96)00421-2.
- Tsyrllov IB, Mikhailenko VM, Gelboin HV. 1994. Isozyme- and species-specific susceptibility of cDNA-expressed CYP1A P-450s to different flavonoids. *Biochim Biophys Acta* 205:325–35. doi:10.1016/0167-4838(94)90252-6.
- Urpi-Sarda M, Monagas M, Khan N, Llorach R, Lamuela-Raventos RM, Jauregui O, Estruch R, Izquierdo-Pulido M, Andres-Lacueva C. 2009. Targeted metabolic profiling of phenolics in urine and plasma after regular consumption of cocoa by liquid chromatography-tandem mass spectrometry. *J Chromatogr A* 1216(43):7258–67.
- Valko M, Leibfritz D, Moncol J, Cronin MTD, Mazur M, Telser J. 2007. Free radicals and antioxidants in normal physiological functions and human disease. *Int J Biochem Cell Biol* 39:44–84. doi:10.1016/j.biocel.2006.07.001.
- Van den Berg R, Haenen GRMM, van den Berg H, van der Vijgh W, Bast A. 2000. The predictive value of the antioxidant capacity of structurally related flavonoids using the Trolox equivalent antioxidant capacity (TEAC) assay. *Food Chem* 70:391–5. doi:10.1016/S0308-8146(00)00092-3.
- Walle T. 2004. Absorption and metabolism of flavonoids. *Free Rad Biol Med* 36:829–37. doi:10.1016/j.freeradbiomed.2004.01.002.
- Winkel-Shirley B. 2001. Flavonoid biosynthesis. A colorful model for genetics, biochemistry, cell biology, and biotechnology. *Plant Physiol* 126:485–93. doi: <http://dx.doi.org/10.1104/pp.126.2.485>.
- Yamazaki I, Piette LH. 1991. EPR spin-trapping study on the oxidizing species formed in the reaction of the ferrous ion with hydrogen peroxide. *J Am Chem Soc* 113:7588–93. doi:10.1021/ja00020a021.
- Yang X-W, Wang N, Li W, Xu W, Wu S. 2013. Biotransformation of 4,5-O-dicaffeoylquinic acid methyl ester by human intestinal flora and evaluation on their inhibition of NO production and antioxidant activity of the products. *Food Chem Toxicol* 55:297–303.
- Yao LH, Jiang YM, Shi J, Tomás-Barberán FA, Datta N, Singanusong R, Chen SS. 2004. Flavonoids in food and their health benefits. *Plant Food Hum Nutr* 59:113–22. doi:10.1007/s11130-004-0049-7.
- Yoshiki Y, Okubo K, Onuma M, Igarashi K. 1995. Chemiluminescence of benzoic and cinnamic acids, and flavonoids in the presence of aldehyde and hydrogen peroxide or hydroxyl radical by Fenton reaction. *Phytochemistry* 39:225–9. doi:10.1016/0031-9422(94)00896-2.
- Zhao M, Yang B, Wang J, Li B, Jiang Y. 2006. Identification of the major flavonoids from pericarp tissues of lychee fruit in relation to their antioxidant activities. *Food Chem* 98:539–44. doi: 10.1016/j.foodchem.2005.06.028.
- Zhu BT, Ezell EL, Liehr JG. 1994. Catechol-O-methyltransferase-catalyzed rapid O-methylation of mutagenic flavonoids. Metabolic inactivation as a possible reason for their lack of carcinogenicity in vivo. *J Biol Chem* 269:292–9.
- Zima A, Hošek J, Tremel J, Muselík J, Suchý P, Pražanová G, Lopes A, Žemlička M. 2010. Antiradical and cytoprotective activities of several C-geranyl-substituted flavanones from *Paulownia tomentosa* fruit. *Molecules* 15:6035–49. doi:10.3390/molecules15096035.

6.2. ARTICLE 2

Zima, A.; Hosek, J.; **Treml, J.**; Suchy, P.; Prazanova, G.; Lopes, A.; Zemlicka, M. *Molecules* 2010, 15, 6035-6049 (IF=1.988).

Article

Antiradical and Cytoprotective Activities of Several C-Geranyl-substituted Flavanones from *Paulownia tomentosa* Fruit

Aleš Zima^{1,*}, Jan Hošek¹, Jakub Tremel¹, Jan Muselík², Pavel Suchý³, Gabriela Pražanová³, Ana Lopes⁴ and Milan Žemlička¹

¹ Department of Natural Drugs, Faculty of Pharmacy, University of Veterinary and Pharmaceutical Sciences Brno, Brno, Czech Republic

² Department of Pharmaceutics, Faculty of Pharmacy, University of Veterinary and Pharmaceutical Sciences Brno, Brno, Czech Republic

³ Department of Human Pharmacology and Toxicology, Faculty of Pharmacy, University of Veterinary and Pharmaceutical Sciences Brno, Brno, Czech Republic

⁴ Faculty of Pharmacy, University of Lisbon, Lisbon, Portugal

* Author to whom correspondence should be addressed; E-Mail: zimaa@vfu.cz;
Tel.: +420541562839.

Received: 17 July 2010; in revised form: 12 August 2010 / Accepted: 27 August 2010 /

Published: 31 August 2010

Abstract: Antiradical and cytoprotective activities of several flavanones isolated from *Paulownia tomentosa* (Thunb.) Steud. (Scrophulariaceae) have been evaluated using different *in vitro* and *in vivo* methods. The capacity of flavanones to scavenge radicals was measured *in vitro* by means of DPPH and ABTS assays, the inhibition of hydroxyl radicals produced in Fenton reactions, FRAP, scavenging superoxide radicals using enzymatic and nonenzymatic assays and the inhibition of peroxynitrite-induced nitration of tyrosine. The *in vivo* testing involved measuring the cytoprotective effect of chosen flavanones against alloxan-induced diabetes in mice. The activity of tested compounds was expressed either as a Trolox[®] equivalent or was compared with rutin or morine as known antioxidant compounds. The highest activity in most tests was observed for diplacone and 3'-O-methyl-5'-hydroxydiplocone, and the structure vs. the antioxidant activity relationship of geranyl or prenyl-substituted flavonoids with different substitutions at the B and C ring was discussed.

Keywords: *Paulownia tomentosa*; prenyl; flavanone; antiradical; cytoprotective

1. Introduction

The so-called civilization diseases are, especially in the Western world, complex illnesses resulting from bad and unhealthy life styled as well as impaired environmental conditions. The incidence of civilization disease is also connected to the increase of the World's population and extended life-times. Such diseases are, for example, neurodegenerative disorders (senile dementia, Alzheimer's disease), cardiovascular illnesses, diabetes mellitus type 2, and cancer. It is now common knowledge that the formation of reactive oxygen species (ROS) and/or nitric species (RNS) is highly implicated in the pathogenesis of such diseases [1,2]. ROS/RNS can be both harmful and beneficial in humans. The beneficial effects of ROS involve, for instance, the defense against infectious agents and several cellular signaling systems. In contrast, when released in high concentration, ROS/RNS can inflict damage to cellular components (lipids, membranes, nucleic acids, etc.). This situation can lead to oxidative stress. Oxidative stress has been defined as "a disturbance in the pro-oxidant and antioxidant balance in favor of the former, leading to potential damage" [2]. To counterbalance the harmful effects of ROS/RNS, organisms are protected by different antioxidants systems, which inhibit or retard the oxidation damage of cells and/or physiological processes [3,4].

Flavonoids are a structurally variable group of polyphenolic compounds that are ubiquitous in Nature. Up until the present, over 8,000 flavonoids have been identified [5]. The beneficial health effects of flavonoids are especially attributed to their antioxidant activity. Attempts to establish the relationship between structure and their radical-scavenging capacity have been successful [5-7]. The activity of flavonoids depends on the position of hydroxy, methoxy, geranyl or other group substitutions. The ability to act as an efficient antioxidant does not depend solely on the availability of phenolic hydrogens but also on the possible stabilization of the resulting radical [7,8].

Paulownia tomentosa (Thunb.) Steud. (Srophulariaceae) is a potent source of biologically active C-geranyl flavanones. According to scientific literature, these compounds have shown cytotoxic, antibacterial and antiradical properties [9-11]. In this present work, flavonoids with a geranyl and prenyl substitution isolated from *P. tomentosa* were evaluated *in vitro* in antiradical assays (DPPH, ABTS, the inhibition of Fenton reaction, inhibition of peroxynitrite induced nitration of tyrosine, FRAP, and the inhibition of superoxide) and *in vivo* for their cytoprotective effects against alloxan-induced diabetes.

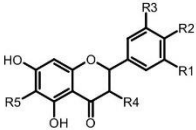
2. Results and Discussion

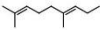
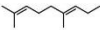
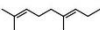
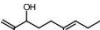
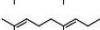
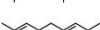
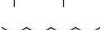
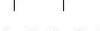

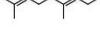
The ability of variously substituted flavonoids from *P. tomentosa*, with a geranyl or prenyl chain at position 6, to act as potential antioxidants was tested. The tested flavanones showed different degrees of activity in all of the assays that were used. The activity of these compounds was expressed as TEAC (Trolox Equivalent Antioxidant Capacity) for ABTS, DPPH, FRAP, and the inhibition of peroxynitrite induced tyrosine nitration. The TEAC value is based on the ability of an antioxidant to scavenge radicals relative to the radical scavenging ability of the water-soluble vitamin E analogue, Trolox® [12], and is expressed as multiples of the activity of Trolox®. Rutin was used as the standard of activity

for comparing the effects in assays based on the inhibition of superoxide radical and inhibition of Fenton reaction. Morine was used as a reference compound in the alloxan-induced pancreatic damage test.

The evaluated compounds all had a flavanone skeleton except **5** and **10** (flavanonol structures). Compounds **1–9** were substituted with a geranyl side chain at the position 6 (hydroxylated geranyl present at **4** and **8**), **10** was substituted by a prenyl chain at the same position. The compounds had different substitution at the B and C ring (Table 1).

Table 1. Structures of compounds tested.



Compound / substituent	R1	R2	R3	R4	R5
Diplacone (1)	OH	OH	H	H	
Mimulone (2)	H	OH	H	H	
3'-O-methyldiplacone (3)	OMe	OH	H	H	
Tomentodiplacone (4)	OMe	OH	H	H	
3'-O-methyldiplacol (5)	OMe	OH	H	OH	
3'-O-methyl-5'-OH-diplacone (6)	OMe	OH	OH	H	
3'-O-methyl-5'-O-methyldiplacone (7)	OMe	OH	OMe	H	
Tomentodiplacone B (8)	OMe	OH	H	H	
Schizolaenone C (9)	OH	H	OH	H	
6-isopentenyl-3'-O-methyltaxifolin (10)	OMe	OH	H	OH	

2.1. ABTS, DPPH, FRAP, the inhibition of peroxynitrite induced tyrosine nitration

Both the ABTS and DPPH tests identified the promising activity of compound **1** (TEAC_{ABTS} 3.2 and TEAC_{DPPH} 1.06) and compound **6** (TEAC_{ABTS} 1.66 and TEAC_{DPPH} 0.98). The reducing potential of the compounds (**4**, **8** and **9** were excluded because of insufficient material), was evaluated in the FRAP assay, where compounds **7** (1.189) and **6** (0.741) showed the highest activity. The ability of the tested compounds to decrease peroxynitrite-induced nitration of tyrosine was investigated as well. The tested compounds showed similar results of activity. The highest ability to prevent against tyrosine nitration showed **9**. The results of the above-mentioned experiments are summarized in Table 2.

The structure and antioxidant activity relationships of flavonoids is determined by a) the *ortho* 3',4'-dihydroxy substitution in the B ring, b) the *meta* 5,7-dihydroxy substitution in the A ring, c) the 2,3-double bond in C ring, d) the 4-keto substitution in C ring, e) the 3-hydroxyl group in the C ring. The spatial arrangement of the substitution is perhaps a greater determinant of antioxidant activity than the flavan skeleton [13,14]. Another substitution influencing antioxidant activity is *O*-methylation, which may decrease antioxidant activity [15]. Steric effects may also induce the suppression of

antioxidant activity; the B ring is particularly sensitive to the position of the methoxy group and 2'-*O*-methyl, 4'-hydroxy substitution at the flavonoid B ring abolishes antioxidant activity, whereas 2'-hydroxy, 4'-*O*-methyl derivatives show activity. The methylation of the 3',4' *ortho* dihydroxy group leads to the decrease of scavenging [16]. Similar structure–activity relationships can also be deduced from the results presented here. Compounds with an *ortho*-dihydroxy substitution of the flavanone B-ring showed the highest activity, but the activity of methoxylated compounds (**3**, **4**, **5**, **7**, **8**) or compound with *para* located hydroxyl (**2**) was much lower. The 3-OH substitution of **5** did not affect activity, similar to the hydroxy substitution of the geranyl side chain (**3** in comparison with **4** and **8**).

These basic rules were established based on the DPPH, ABTS and similar antioxidant assays and may differ slightly from the results obtained from other tests. Different influence of *O*-methylation on activity is described for FRAP and the inhibition of peroxynitrite induced nitration of tyrosine. The increase of reduction ability in FRAP may be evoked by partial *O*-methylation of the B ring. The presence of an electron-donating moiety on the B ring as the methoxy group confers the higher reducing capability, but total number of hydroxy groups and other mentioned structural properties are necessary and enhance the antioxidant activity of the flavonoids [17].

Previously published studies also show the low effect of *O*-methylation on peroxynitrite induced nitration of tyrosine, when the different position of the *O*-methoxy substitution of antocyanins did not influence their activity [18]. It corresponds with results presented here, which show only a low influence of *O*-methylation on peroxynitrite induced nitration of tyrosine (compare diplacone (**1**) and 3'-*O*-methyl diplacone (**3**)). Results also showed that compounds with *O*-methyl group at similar position on the B-ring (**3**–**8**) have similar antiperoxynitrite activity, while the activity of mimulone (**2**), compound with *p*-OH substituted B-ring is low. Also, the changes on the geranyl side chain did not affect the ability of the compounds tested to prevent tyrosine nitration (**4**, **8**, **10**).

Table 2. Antioxidant activities of compounds **1**–**9** determined by using ABTS, DPPH, FRAP, the inhibition of tyrosine nitration (activity expressed as TEAC - ability of the sample to scavenge the radical relative to the radical scavenging ability of Trolox[®]. Value are multiples of activity of Trolox[®]) and superoxide scavenging activity (expressed as % of inhibition at 50 μ M concentration).

	ABTS	DPPH	FRAP	Inhibition of. peroxynitrite induced tyrosine nitration	Superoxide scavenging activity	
					Enzymatic	Non- enzymatic
1	3.2 \pm 0.01	1.06 \pm 0.04	0.522 \pm 0.01	0.84 \pm 0.01	45.2	25.9
2	1.7 \pm 0.01	0.02 \pm 0.01	0.051 \pm 0.00	0.09 \pm 0.01	^a	^a
3	1.4 \pm 0.00	0.12 \pm 0.02	0.118 \pm 0.00	0.80 \pm 0.03	^a	^a
4	1.61 \pm 0.01	0.14 \pm 0.04	^a	0.82 \pm 0.01	^a	^a
5	1.62 \pm 0.01	0.10 \pm 0.00	0.127 \pm 0.01	0.74 \pm 0.01	^a	^a
6	1.66 \pm 0.01	0.98 \pm 0.03	0.741 \pm 0.01	0.84 \pm 0.01	71.2	29.5
7	1.60 \pm 0.01	0.29 \pm 0.02	1.189 \pm 0.06	0.83 \pm 0.02	^a	^a
8	0.97 \pm 0.03	0.12 \pm 0.00	^a	0.82 \pm 0.02	^a	^a
9	^a	^a	^a	0.93 \pm 0.02	^a	^a
Rutin	^a	^a	^a	^a	50.2	43.6

^a Not determined.

2.2. Superoxide scavenging activity assay

Both flavonoids **1** and **6** showed a promising scavenging of radicals. According to the scientific literature, there are some requirements in the arrangement of substituents for superoxide scavenging and the inhibition of xanthinoxidase (XO). Searching the literature led however to conflicting conclusions about superoxide scavenging activity and the inhibition of XO by flavanones. Tested samples met the structural conditions for superoxide scavenging: 5,7-dihydroxy substitution, 3',4'-dihydroxy substitution, and 4-oxo group [19,20]. These conditions are stated for the direct scavenging of superoxide, but not for the inhibition of XO. Some authors state that flavanones are not able to inhibit XO because they lack the C-2 - C-3 double bond. This double bond causes planarity of the A, C and B rings group due to the conjugation effect and is an important factor for XO inhibition [19]. On the other hand, according to some authors, flavanones might inhibit XO due to the fact that their chemical structure is closely related to hypoxanthine, xanthine, and uric acid, and may act as XO substrate analogs [21].

Based on the results of the ABTS and DPPH assays, the activity of compound **1** and compound **6** was measured using a superoxide-scavenging assay. Two systems for generating superoxide radical were used: enzymatic and non-enzymatic. Both assays, as described in past literature, were primary for the proper evaluation of hydrophilic compound activity because of the aqueous character of the reaction mixture [22]. In this work, the optimization of these assays for hydrophobic compounds (C-6 lipophilic substituent) was carried out, and the activity of the compounds tested was compared with rutin at equimolar concentrations of 50 μ M.

Some differences between the results of enzymatic and non-enzymatic assays were found (Table 2). In the non-enzymatic test, the activities of the compounds tested were similar (**1** 25.9%, **6** 29.5%), but lower than the activity of rutin (43.6%). The results of the enzymatic assay showed higher activities of **1**, **6** and rutin, in comparison with the non-enzymatic assay. Compound **6** showed the highest activity (71.2%), significantly higher than rutin (50.2%). From these results it can be concluded, that geranylated flavanones can also act as XO inhibitors and, if needed, serve as compounds for the modeling of more potent structures.

2.3. Inhibition of Fenton reaction assay

Different methods can be used for the measurement of hydroxyl radical scavenging activity [23]. In this study, the Fenton reaction system generating a hydroxyl radical with plasmid DNA as a detection system was used to bring the assay closer to *in vivo* conditions. Plasmid DNA was used as a target for the attack of OH \cdot radicals. Plasmid DNA is constituted from a circular double strand of nucleic acids in its native supercoiled conformation, also known as CCC (covalently closed circle). The attack of OH \cdot degrades the DNA into series of degradation products. The open circle (OC) conformation is the first step of degradation and it is characterized by having only one strand cut, therefore remaining in its circular conformation. The linear (L) form is the result of a cut in both DNA strands. All these forms are visible by electrophoretic separation.

Oxidative damage of biomacromolecules, including DNA, is considered one of the most dangerous actions of ROS. Plasmid DNA as a model of oxidative disruption was successfully used in several

studies [24,25]. The activity of the compounds tested was expressed as a “compounds ratio/ rutin ratio”. Compounds ratio and rutin ratio means ratio of area under curve (AUC), which demonstrates concentration of DNA (see section 3.6), of CCC form /AUC of OC form plus AUC of L form [*i.e.* CCC/(OC+L)]. The higher value means a higher content of CCC-form, thus a lower degradation of plasmid DNA. AUCs of individual plasmid forms were obtained from the densitometric evaluation of electrophoretograms. Among the compounds tested, the highest activity was found for compound **6** (ratio 2,565) and compound **1** (ratio 0,892). The compounds tested can be ordered in decreasing activity: 3'-*O*-methyl-5'-hydroxydiplocone (**6**) > diplocone (**1**) > mimulone (**2**) > 3'-*O*-methyl-diplocone (**3**) > 3'-*O*-methyl-diploacol (**5**) > 3'-*O*-methyl-5'-*O*-methyl-diplocone (**7**) > 6-isopentenyl-3'-*O*-methyltaxifolin (**10**). Table 3 displays the results of this assay in detail. Among the compounds examined for their antioxidant effect, only the two compounds with the *ortho*-dihydroxy substitution at ring B diplocone (**1**) and 3'-*O*-methyl-5'-hydroxydiplocone (**6**), were significantly active. This may imply that the *ortho* hydroxy substitution is important for the antioxidant activity of such compounds, similarly in the results shown in the DPPH test and FRAP (with exception of compound **7**). 6-isopentenyl-3'-*O*-methyltaxifolin (**10**) showed virtually no antioxidant activity in the Fenton reaction inhibition assay, being the only flavanone tested that lacks the geranyl group (compare **5** and **10**).

Table 3. Results of Fenton reaction inhibition assay. Rutin at the molar excess of 50:1 or 10:1 to DNA base pair was compared with the tested compounds at the same molar excess. AUC – area under curve; CCC – covalent closed circle (superhelical form of plasmid); L – linear form of plasmid; OC – open circle (circular form of plasmid).

Compound	AUC			Ratio CCC/ (OC+L)	Compound ratio/ Rutin ratio
	CCC	OC	L		
1 (50:1)	569	1618	98	0.332	0.892
1 (10:1)	453	3272	458	0.121	0.135
3 (50:1)	708	3271	231	0.202	0.543
3 (10:1)	229	3170	294	0.066	0.073
7 (50:1)	514	2854	193	0.169	0.454
7 (10:1)	564	2173	73	0.251	0.279
Rutin (50:1)	1288	3207	254	0.372	1
Rutin (10:1)	1942	1955	207	0.898	1
Natural plasmid	2790	386	193	4.819	-
2 (50:1)	439	634	-	0.692	0.553
2 (10:1)	152	1502	-	0.101	0.199
6 (50:1)	1289	402	-	3.206	2.565
6 (10:1)	656	1406	-	0.467	0.921
10 (50:1)	194	1556	96	0.117	0.094
10 (10:1)	189	1915	122	0.093	0.183
Rutin (50:1)	1055	843	-	1.251	1
Rutin (10:1)	806	1591	-	0.507	1
Natural plasmid	1507	-	-	-	-
5 (50:1)	505	1379	-	0.366	0.491
5 (10:1)	-	1373	-	-	-
Rutin (50:1)	1155	1493	57	0.745	1
Rutin (10:1)	535	1788	47	0.292	1
Natural plasmid	2166	258	-	8.395	-

2.4. Cytoprotective effect against alloxan-induced diabetes

The single *in vivo* test was based on monitoring of cytoprotective effect against alloxan-induced diabetes. Alloxan transported into β -cells of Langerhans islets of mouse pancreas is transformed to dialuric acid, which re-oxidation leads back to alloxan. Several free radicals, such as superoxide, hydroxyl radical or alloxan radical, are formed during this intracellular red/ox process. These free radicals selectively destroy the β -cells, which results in insulin production decrease in treated mice [26]. Flavonoids, as known antioxidants, may prevent the progressive impairment of pancreatic β -cell function due to oxidative stress [27]. Administration of diplacone (**1**) and mimulone (**2**) was not found to reduce the blood glucose levels in alloxan-induced diabetic mice (Figure 1). The only exception was the reduction ($p \leq 0.05$) in blood glucose levels of animals treated with diplacone (**1**) on the first day of the experiment.

Diplacone (**1**) showed significant antioxidant activity in the *in vitro* tests. Whereas the damage of β -cells of Langerhans islets occurs by means of free radicals formed during red/ox reactions (see above), a cytoprotective activity of diplacone (**1**) with consequent decrease of glycemia level was expected in the test focused on cytoprotective effect against alloxan-induced diabetes, as it was described by Soto *et al.* [28]. However, in the present *in vivo* experiment, only minor changes in glycemia level in groups treated with diplacone (**1**) were found. This fact could be caused by low dose of diplacone (**1**) used for experiment [28].

On the other hand, some cytoprotective effect of diplacone (**1**) was proved by histopathological analysis of pancreatic tissue (Figure 2–5). This observation supports fact that flavonoids may act as a cytoprotective substances [29]. Results of cytoprotective activity assay could be correlated with a higher activity of diplacone (**1**) compared with the other tested compounds.

Figure 1. Levels of glycemia mmol/L as determined in alloxan induced diabetes testing of **1** and **2**.

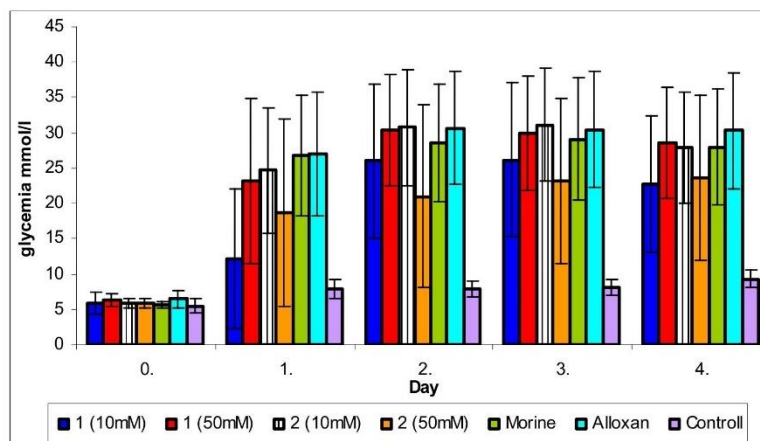


Figure 2. Microphotograph of the pancreas of control mice (HE 400×). Pancreatic islets with distinctly-outlined cell borders (physiological findings).

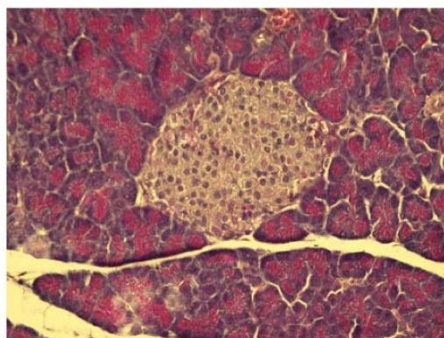


Figure 3. Microphotograph of the pancreas of alloxan-treated mice (HE 600×). Rudimentary reaction to the destroyed pancreatic islet.

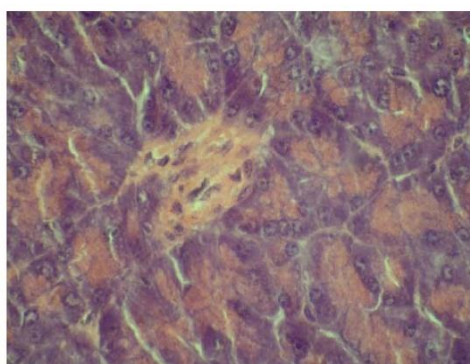


Figure 4. Microphotograph of the pancreas – the effect of mimulone (**2**) on the pancreatic histopathology of diabetic mice (HE 600×). Regressive changes to pancreatic islet cells.

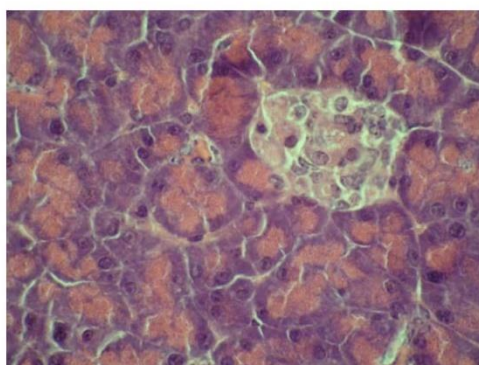
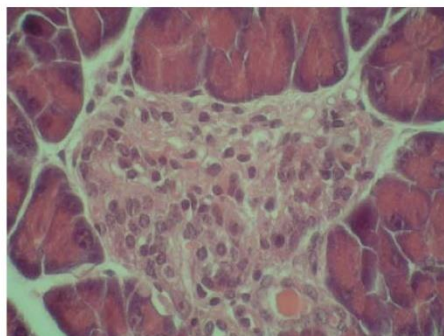


Figure 5. Microphotograph of pancreas – the effect of diplacone (**1**) on the pancreatic histopathology of diabetic mice (HE 600×). Pancreatic islet with an irregular shape; with vacuolised cytoplasm, a pyknotic nucleus and tiny necrosis without a significant inflammatory reaction.



3. Experimental

3.1. Tested compounds

C-6 geranylated flavonoids **1–8** were isolated from *P. tomentosa* fruit [9,10]. Schizolaenone C (**9**) and 6-isopentenyl-3'-O-methyltaxifolin (**10**) were isolated from *P. tomentosa* fruit as well (Table 1) [9,30]. As a standard for comparing the activities of the compounds that rutin (Fluka®), morine (Sigma-Aldrich®) and Trolox® (Sigma-Aldrich®) were used. The purity of all the compounds tested was checked *via* HPLC analysis and exceeded 95%.

3.2. ABTS and DPPH scavenging activity

The antiradical activity of the compounds was determined spectrophotometrically in the Microplate Reader Synergy HT (Bio-Tek Instruments, Inc) in 96 wells plates in kinetic mode. The DPPH and ABTS assay followed modified methods of Brand-Williams *et al.* [31] and Arnao *et al.* [32], respectively. DPPH test: reaction mixture contained DPPH (63.4 µM) and different concentrations of samples in final volume of 300 µL. Detection at 517 nm. All components were dissolved in methanol. ABTS test: the reaction mixture contained ABTS (83.4 µM, in phosphate buffer pH 7.4) and different concentrations of samples in final volume of 350 µL. Detection wavelength was 734 nm. Samples were dissolved in ethanol. All experiments were performed in triplicate. Activity of the tested compounds was expressed as TEAC.

3.3. FRAP

A colorimetric assay, according to Benzie and Strain, was used [33]. Activity was measured spectrophotometrically at 593 nm. The reaction mixture contained TPTZ (0.83 mM), FeCl₃ (1.67 mM) and an acetate buffer (250 mM, pH 3.6). The total volume of the reaction mixture was 3 mL. Samples

were measured in triplicates for 6 min in kinetic mode. The results are presented as the equivalent of the Trolox[®].

3.4. Inhibition of peroxynitrite induced tyrosine nitration

A peroxynitrite solution was prepared and an assay carried out according to the method mentioned previously [34]. The percentage of the inhibition of tyrosine nitration was compared to that of the calibrated Trolox[®] standard. The results are expressed in terms of Trolox[®] equivalent antioxidant capacity.

3.5. Superoxide scavenging activity

Modified enzymatic and non-enzymatic assays described by Valenta^o et al. for the generation of superoxide radical were used [22]. Both methods used spectrophotometric detection at 562 nm, using 96 wells plates and the microplate reader Synergy HT. The assay was performed at room temperature. Samples and standard were measured in equimolar concentrations of 50 μ M and subsequently compared. All experiments were performed in triplicate. Activity of the samples was compared with rutin.

3.5.1. Enzymatic assay

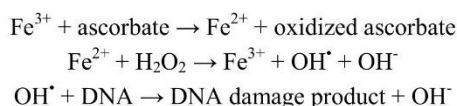
The reaction mixture consisted of xanthine (380 μ M, in 1 μ M NaOH), xanthinoxidase (0.025 U/mL, in 0.1mM EDTA), NBT (42.3 μ M, in a 50mM phosphate buffer with 0.1mM EDTA, pH 7.8) and the tested compounds (in DMSO). The final volume of the reaction mixture was 350 μ L. The reaction was initiated by the addition of XO and proceeded for 2 min. at room temperature.

3.5.2. Non-enzymatic assay

Superoxide was generated in system NADH/PMS. The reaction mixture contained NADH (166 μ M), NBT (43 μ M), PMS (2.7 μ M), the tested compounds in final volume 300 μ L. All components were dissolved in 19 mM phosphate buffer (pH 7.4). Compounds were dissolved in DMSO. The reaction was initiated by the addition of PMS and proceeded for 2 min at room temperature.

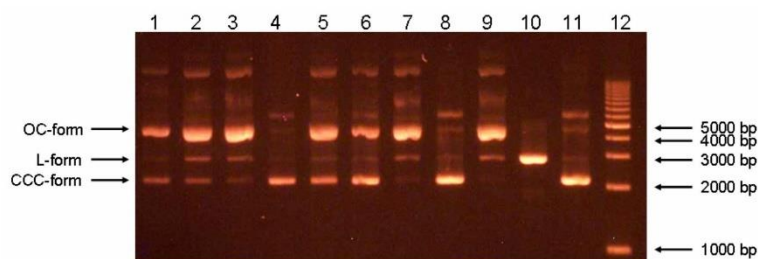
3.6. Inhibition Fenton reaction assay

This assay was proposed in order to evaluate the capacity of compounds to scavenge OH[•] and, consequently, to protect DNA from oxidative degradation. To supply OH[•], a mixture of Fe(III), H₂O₂ and ascorbic acid was used. Ascorbic acid reduces Fe(III) to Fe(II), providing a constant flux of OH[•]. The following equations illustrate the Fenton reaction:



The degradation of plasmid DNA was used as a marker of oxidative damage. Supercoiled plasmid pUC19 was isolated from *Escherichia coli* TOP10F' using a QIAprep Spin Miniprep Kit (QIAGEN, Hilden, Germany). This plasmid (300 ng per reaction) was mixed with compounds dissolved in DMSO and tested in two final ratios of 50:1 and 10:1 (the number of molecules of the tested compound: 1 bp [base pair]), both in the presence or absence of every single intervening agent in the Fenton reaction. Ratio 1:1 was also used, but it was removed from the evaluation because of ambiguous results, which were observed with some compounds. DMSO and rutin were used as negative and positive controls, respectively. A solution of the tested compound was added into a microtube and a TE buffer was used to fill up to the final volume level of 20 μ L. This was followed by the addition of 12 μ L of the established Fenton reaction mixture, with the final concentrations of 0.66 mM H₂O₂, 0.66 mM FeSO₄ and 0.83 mM ascorbic acid. Reaction mixtures were incubated at 37 °C for 1 hour and then analyzed using electrophoresis [0.8% agarose gel, voltage 5 V/cm, visualized by ethidium bromide staining (0.15 mg/mL)] (Figure 6). Visualization was performed on a UV transilluminator (λ 312 nm). The electrophoreogram was captured and analyzed by AlphaEaseFC software, version 4.0.0.34 (Alpha Innotech, USA). The relative percentages of circular (CCC) form, one strand nicked (OC) form and linear (L) form of plasmid DNA were evaluated by measurement of the intensity of individual bands. Afterwards, the quantity of different plasmid forms was expressed as an AUC of peaks obtained on the basis of bands intensity. Any compound tested did not digest plasmid, when it was incubated alone with plasmid (data not shown).

Figure 6. Typical electrophoreogram showing the ability of the individual compound to protect DNA *in vitro*. Lane 1-3: pUC19 + Fenton reaction + **1** (50:1, 10:1, 1:1); Lane 4: pUC19 + **1** 50:1; Lane 5-7: pUC19 + Fenton reaction + rutin (50:1, 10:1, 1:1); Lane 8: pUC19 + rutin 50:1; Lane 9: pUC19 + Fenton reaction + DMSO (vehicle); Lane 10: pUC19 L-form; Lane 11: pUC19 native form; Lane 12: ladder.



3.7. Cytoprotective effect against alloxan-induced diabetes

The *in vivo* test of antioxidant activity studied the protective effect of flavonoid compounds from *P. tomentosa* (**1-8**) in mouse model of alloxan-induced diabetes mellitus. This experiment was divided into two steps. First, as a pre-screening, the cytoprotective activity of compounds **1-8** was evaluated (data not shown). According to the pre-screening results we decided to target on the activity of diplacone (**1**) and mimulone (**2**), both at two concentrations (0.5 mmol/kg and 1 mmol/kg body weight).

Female ICR (imprinting control region) albino mice (30–40 g; Anlab, Czech Republic) were used in the experiment. The animals were placed individually in glass metabolic cages at a temperature of 20–24 °C, fed a standard diet and given water *ad libitum*. The mice were divided into seven groups, each with 10 members: 4 pretreated with the tested compounds in two concentrations, one positive control (only alloxan solution administered), one negative control (isotonic saline solution administered) and one group pretreated with morine known to be a good antioxidant [35].

The tested compounds and alloxan monohydrate were dissolved in a 10% (v/v) DMSO diluted by an *aqua pro injectione*. The solution of the tested compounds was administered to the mice intraperitoneally (at doses of 0.5 mmol/kg and 1 mmol/kg body weight). The alloxan solution (12 mg/mL) was injected into the tail vein (0.1 mL/10 g body weight) 30 min after the application of the tested compounds solution. The experiment was carried out for 5 days, the first day was expressed as day 0. The initial glucose levels were measured in the intact mice. During the next 4 days of the experiment, the glucose levels were measured in the morning after at least 3 h of fasting (Day 2–5). One-drop glucose oxidase test and blood glucose reflective photometer Glucotrend® 2 with Glucotrend® Glucose (max. concentration 33.3 mM; Roche, Germany) test strips were used to determine glucose concentrations (mM) in the venous blood. On the 4th day of the experiment, the animals were destroyed and exsanguinated with pancreas samples taken for histopathological analysis. Samples were fixed in a neutral 10% formol and routinely stained by hematoxyline-eosine. The preparations were examined in an optical microscope, and the observed changes in glucose levels were statistically evaluated using the ANOVA method.

All aspects of animal care complied with the ethical guidelines and technical requirements, and were proven to be consistent with the Animal Scientific Procedures Act 86/609/EC. The state of health of all animals was regularly examined several times a day during both the period of the animal's acclimation and the whole course of the experiment, by the working team whose members are holders of the Certificate on Professional Competence issued by the Central Commission for the Animal Protection pursuant to § 17 of the Act on Protection of Animals against Cruelty (No. 246/1992 Coll.) of the Czech National Council.

4. Conclusions

The antioxidant activities of different flavonoids with a geranyl (compounds **1–9**) or a prenyl substitution (compound **10**) at position 6 and different substitutions at B and C ring were analyzed. Activity was determined using *in vitro* methods - ABTS, DPPH, FRAP, the inhibition of peroxynitrite-induced tyrosine nitration, superoxide scavenging and the inhibition of Fenton reaction assay. A single *in vivo* test was used for the monitoring of cytoprotective effects of compounds **1** and **2** against alloxan-induced diabetes.

Some of the tested compounds showed notable anti-oxidant activity. The compounds were compared with standards Trolox®, rutin, and with morine in the case of the evaluation of cytoprotective effect *in vivo*. Generally, the highest activity was shown to be compounds **1** and **6** with an *ortho* dihydroxy substitution at the B ring of the flavonoid skeleton. The structure vs. antioxidant activity of the evaluated flavonoids was discussed. Studies on the structure-activity relationship have shown and confirmed that the presence of hydroxyl groups and methoxy groups at the A and B rings

appear to be important in the antioxidant and free radical scavenging activities of flavonoid compounds. The conclusions of this study have demonstrated that the fruits of *P. tomentosa* provide an efficacious source of natural antioxidant-active substances.

Acknowledgements

This project was supported by the Internal Grant Agency of the University of Veterinary and Pharmaceutical Sciences Brno, grant number IGA VFU 71/2007 FaF (A.Z.)

References and Notes

1. Cadenas, E. Biochemistry of oxygen toxicity. *Ann. Rev. Biochem.* **1989**, *58*, 79-110.
2. Sies, H. Oxidative stress: Oxidants and antioxidants. *Exp. Physiol.* **1997**, *82*, 291-295.
3. Mates, J.M.; Perez-Gomez, C.; De Castro, I.N. Antioxidant enzymes and human diseases. *Clin. Biochem.* **1999**, *32*, 595-603.
4. McCall, M.R.; Frei, B. Can antioxidant vitamins materially reduce oxidative damage in humans? *Free Radical Biol. Med.* **1999**, *26*, 1034-1053.
5. Pietta, P.G. Flavonoids as antioxidants. *J. Nat. Prod.* **2000**, *63*, 1035-1042.
6. Šmejkal, K.; Holubová, P.; Zima, A.; Muselík, J.; Dvorská, M. Antiradical activity of *Paulownia tomentosa* (Scrophulariaceae) extracts. *Molecules* **2007**, *12*, 1210-1219.
7. Havsteen, B.H. The biochemistry and medical significance of the flavonoids. *Pharmacol. Ther.* **2002**, *96*, 67-202.
8. Rice-Evans, C.A.; Miller, N.J.; Paganga, G. Structure-antioxidant activity relationships of flavonoids and phenolic acids. *Free Radical Biol. Med.* **1996**, *20*, 933-956.
9. Šmejkal, K.; Grycová, L.; Marek, R.; Jankovská, D.; Forejtníková, H.; Vančo, J.; Suchý V. C-geranyl compounds from *Paulownia tomentosa* fruits. *J. Nat. Prod.* **2007**, *70*, 1244-1248.
10. Šmejkal, K.; Chudík, S.; Klouček, P.; Marek, R.; Cvačka, J.; Urbanová, M.; Julínek, O.; Kokoška, L.; Šlapetová, T.; Holubová, P.; Zima, A.; Dvorská, M. Antibacterial C-geranyl flavonoids from *Paulownia tomentosa* fruits. *J. Nat. Prod.* **2008**, *71*, 706-709.
11. Asai, T.; Hara, N.; Kobayashi, S.; Kohshima, S.; Fujimoto, Y. Geranylated flavanones from the secretion on the surface of the immature fruits of *Paulownia tomentosa*. *Phytochemistry* **2008**, *69*, 1234-1241.
12. Van den Berg, R.; Haenen, G.R.M.M.; Van den Berg, H.; Bast, A. Applicability of an improved Trolox equivalent antioxidant capacity (TEAC) assay for evaluation of antioxidant capacity measurements of mixtures. *Food Chem.* **1999**, *66*, 511-517.
13. Cao, G.; Sofic, E.; Prior, R.L. Antioxidant and prooxidant behavior of flavonoids: structure-activity relationships. *Free Radical Biol. Med.* **1997**, *22*, 749-760.
14. Sekher Pannala, A.; Chan, T.S.; O'Brien, P.J.; Rice-Evans, C.A. Flavonoid B-ring chemistry and antioxidant activity: fast reaction kinetics. *Biochem. Biophys. Res. Commun.* **2001**, *282*, 1161-1168.
15. Dugas, A.J., Jr.; Castaneda-Acosta, J.; Bonin, G.C.; Price, K.L.; Fischer, N.H.; Winston, G.W.; Evaluation of the total peroxyl radical scavenging capacity of flavonoids: structure-activity relationships. *J. Nat. Prod.* **2000**, *63*, 327-331.

16. Heim, K.E.; Tagliaferro, A.R.; Bobilya, D.J. Flavonoid antioxidants: chemistry, metabolism and structure activity relationships. *J. Nutr. Biochem.* **2002**, *13*, 572-584.
17. Firuzi, O.; Lacanna, A.; Petrucci, R.; Marrosu, G.; Saso, L. Evaluation of the antioxidant activity of flavonoids by “ferric reducing antioxidant power” assay and cyclic voltammetry. *Biochim. Biophys. Acta* **2005**, *1721*, 174-184.
18. Muselík, J.; García-Alonso, M.; Martín-López, M.P.; Žemlička, M.; Rivas-Gonzalo, J.C. Measurement of antioxidant activity of wine catechins, procyanidins, anthocyanins and pyranoanthocyanins. *Int. J. Mol. Sci.* **2007**, *8*, 797-809.
19. Cos, P.; Li, Y.; Calomme, M.; Jia, P.H.; Cimanga, K.; Van Poel, B.; Pieters, L.; Vlietinck, A.J.; Van den Berghe, D. Structure-Activity Relationship and classification of flavonoids as inhibitors of xanthine oxidase and superoxide scavengers. *J. Nat. Prod.* **1998**, *61*, 71-76.
20. Borges, F.; Fernandes, E. Progress towards the discovery of XO inhibitors. *Curr. Med. Chem.* **2002**, *24*, 195-217.
21. Yao, H.; Liao, Z.X.; Wu, Q.; Lei, G.Q.; Liu, Z.J.; Chen, D.F.; Chen, J.K.; Zhou, T.S. Antioxidative flavanone glycosides from the branches and leaves of *Viscum coloratum*. *Chem. Pharm. Bull.* **2006**, *54*, 133-135.
22. Valentaš, P.; Fernandes, E.; Carvalho, F.; Andrade, P.B.; Seabra, R.M.; Bastos, M.L. Antioxidant activity of *Centaurium erythraea* infusion evidenced by its superoxide radical scavenging and xanthine oxidase inhibitory activity. *J. Agric. Food Chem.* **2001**, *49*, 3476-3479.
23. Gutteridge, J.M.C. Iron promoters of the Fenton reaction and lipid peroxidation can be released from haemoglobin by peroxides. *FEBS Lett.* **1986**, *201*, 291-295.
24. Kang, J.H. Oxidative damage of DNA by the reaction of amino acid with methylglyoxal in the presence of Fe(III). *Int. J. Biol. Macromol.* **2003**, *33*, 43-48.
25. Prakash, D.; Suri, S.; Upadhyay, G.; Singh, B.N. Total phenol, antioxidant and free radical scavenging activities of some medicinal plants. *Int. J. Food Sci. Nutr.* **2007**, *58*, 18-28.
26. Szkudelski, T. The Mechanism of Alloxan and Streptozocin Action in B Cells of the Rat Pancreas. *Physiol. Res.* **2001**, *50*, 536-546.
27. Rahimi, R.; Nikfar, S.; Larijani, B.; Abdollahi, M. A review on the role of antioxidants in the management of diabetes and its complications. *Biomed. Pharmacother.* **2005**, *59*, 365-373.
28. Soto, C.; Recoba, R.; Barron, H.; Alvarez, C.; Favari, L. Silymarin increases antioxidant enzymes in alloxan-induced diabetes in rat pancreas. *Comp. Biochem. Physiol. - Part C Toxicol. Pharmacol.* **2003**, *136*, 205-212.
29. Rice-Evans, C.; Packer, P. *Flavonoids in Health and Disease*, 2nd ed.; CRC Press: New York, NY, USA, 2003; pp. 329-334.
30. Šmejkal, K.; Svačinová, J.; Šlapetová, T.; Schneiderová, K.; Dall'Acqua, S.; Innocenti, G.; Závalová, V.; Kollár, P.; Chudík, S.; Marek, R.; Julínek, O.; Urbanová, M.; Kartal, M.; Csöllei, M.; Doležal, K. Cytotoxic activities of several geranyl-substituted flavanones. *J. Nat. Prod.* **2010**, *73*, 568-572.
31. Brand-Williams, W.; Cuvelier, M.E.; Berset, C. Use of a Free Radical Method to Evaluate Antioxidant Activity. *Food Sci. Technol.* **1995**, *28*, 25-30.
32. Arnao, M.B.; Cano, A.; Acosta, M. The hydrophilic and lipophilic contribution to total antioxidant activity. *Food Chem.* **2001**, *73*, 239-244.

33. Benzie, I.F.F.; Strain, J.J. The ferric reducing ability of plasma (FRAP) as a measure of „antioxidant power“: the FRAP assay. *Anal. Biochem.* **1996**, *239*, 70-76.
34. Vančo, J.; Marek, J.; Trávníček, Z.; Račanská, E.; Muselík, H.; Švajnelová, O. Synthesis, structural characterization, antiradical and antidiabetic activities of copper(II) and zinc(II) Schiff base complexes derived from salicylaldehyde and β -alanine. *J. Inorg. Biochem.* **2008**, *102*, 595-605.
35. Subash, S.; Subramanian, P. Morin a flavonoid exerts antioxidant potential in chronic hyperammonemic rats: a biochemical and histopathological study. *Mol. Cell Biochem.* **2009**, *327*, 153-161.

Sample Availability: Samples of compounds **1-8** are available from the authors.

© 2010 by the authors; licensee MDPI, Basel, Switzerland. This article is an Open Access article distributed under the terms and conditions of the Creative Commons Attribution license (<http://creativecommons.org/licenses/by/3.0/>).

6.3. ARTICLE 3

Treml, J.; Smejkal, K.; Hosek, J.; Zemlicka, M. Chemical Papers 2013, 67, 484-489 (IF=1.193).

ORIGINAL PAPER

Determination of antioxidant activity using oxidative damage to plasmid DNA – pursuit of solvent optimization

Jakub Trembl*, Karel Šmejkal, Jan Hošek, Milan Žemlička

Department of Natural Drugs, Faculty of Pharmacy, University of Veterinary and Pharmaceutical Sciences Brno, Palackého tř. 1/3, 612 42 Brno, Czech Republic

Received 10 October 2012; Revised 1 December 2012; Accepted 2 December 2012

Oxidative stress plays a key role in the pathophysiology of many diseases. Hydroxyl radical is the oxidative species most commonly causing damage to cells. The aim of this work was to optimize the method for antioxidant activity determination on a model lipophilic geranylated flavanone, diplacone. This method uses protection of plasmid DNA from oxidation by a hydroxyl radical generated by the Fenton reaction involving oxidation of metal ions using H_2O_2 and ascorbate. The method was optimized for lipophilic compounds using several solvents and co-solvents. It was found that (2-hydroxypropyl)- β -cyclodextrin (0.1 mass % aq. sol.) is the best co-solvent for our model lipophilic compound to measure the antioxidant activity by the method presented. Other solvents, namely dimethyl sulfoxide, Cremophor EL[®] (0.1 mass % aq. sol.), ethanol, and methanol, were not suitable for the determination of the antioxidant activity by the method described. Tween 80 (0.1 mass % aq. sol.) and a mixture of 10 vol. % ethanol and 9 mass % bovine serum albumin (aq. sol.) significantly decreased the antioxidant activity of the model lipophilic compound and thus were not suitable for this method.

© 2013 Institute of Chemistry, Slovak Academy of Sciences

Keywords: antioxidant activity, plasmid DNA, Fenton reaction, solubility, diplacone

Introduction

Aerobic organisms take advantage of oxidative phosphorylation and therefore gain much more energy from one molecule of glucose compared to anaerobic organisms. The price paid is the production of reactive oxygen species (ROS). ROS consist of various small molecules derived from oxygen, including oxygen radicals (such as hydroxyl radical $\cdot\text{OH}$) and certain non-radicals (such as hydrogen peroxide; H_2O_2). Cells use numerous antioxidant enzymes and defensive molecules to avoid the overproduction of ROS; however, if the production of ROS exceeds the capacity of the cellular antioxidant system, the cell has to face a state called oxidative stress. Oxidative stress plays a key role in the pathophysiology of many diseases such as neurodegeneration, cardiovascular diseases, and cancer (Ma, 2010).

The method presented for antioxidant activity de-

termination is based on the generation of hydroxyl radicals which then cause oxidative damage to plasmid DNA. The hydroxyl radical can be produced by the Fenton reaction Eq. (1). Originally, the metal ion reacting with H_2O_2 was iron but also copper reacts with H_2O_2 (Que et al., 1980). Ascorbate is an excellent antioxidant; however, it also shows a pro oxidant activity due to its reducing character, Eq. (2) (Chiou, 1983). Chiou (1984) reported that H_2O_2 alone (without metal ions) does not show any visible cleavage of DNA, which makes it an important intermediate in the reaction.

There are various ways of DNA damage; it can be fragmented (single- or double-strand breaks) or cross-linked (intra- or inter-strand). The hydroxyl radical also causes base oxidation (e.g., formation of 8-hydroxyguanine or thymine glycol). If not repaired, these DNA alterations lead to mutations or cell death (Cooke et al., 2006). The production and effects of hy-

*Corresponding author, e-mail: jakub.trembl@gmail.com

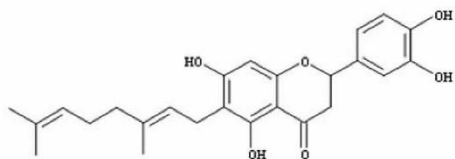
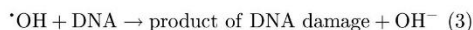
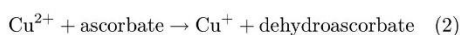
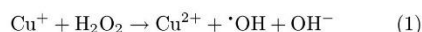


Fig. 1. Structure of diplacone.

hydroxyl radicals used in this method are summarized in the following reactions:



The detection of DNA breakage caused by oxidative damage has been described by Sagripanti and Kraemer (1989). Plasmid DNA consists of a circular double strand in a native supercoiled conformation, also known as covalently closed circular (CCC) conformation. The first step of degradation after the attack by the hydroxyl radical is the formation of an open circular form (OC) with one broken strand. In the second step, both strands are cut resulting in the linear form (L) of plasmid DNA. All forms are made visible by electrophoretic separation (Sagripanti & Kraemer, 1989).

A huge advantage of this method is the use of a naturally occurring hydroxyl radical and DNA to display the oxidative damage and the possible positive protective effect of an antioxidant compound. Compared to other *in vitro* methods used to determine antioxidant activity, this method is one step closer to *in vivo* conditions (Zima et al., 2010). This method was originally designed for aqueous conditions and the testing of water-soluble compounds; therefore, it had to be adopted with some changes and modifications. For lipophilic compounds and extracts, dimethyl sulfoxide (DMSO) was used as a suitable solvent. Furthermore, CuSO_4 was used instead of FeSO_4 , due to its greater stability during storage. To optimize the reaction conditions, various concentrations of H_2O_2 and CuSO_4 were tested.

The aim of this work was to optimize the method for lipophilic water-insoluble compounds testing using several solvents and co-solvents. DMSO, Tween 80 (0.1 mass % aq. sol.), a mixture of 10 vol. % ethanol and 9 mass % bovine serum albumin (BSA) aq. sol., Cremophor EL® (0.1 mass % aq. sol.), (2-hydroxypropyl)- β -cyclodextrin (HP β -CD) (0.1 mass % aq. sol.), ethanol, and methanol were tested. Diplacon, a geranylated flavanone (Fig. 1) obtained from the flowers and fruits of the plant *Paulownia tomentosa*

(Thunb.) Steud. (Scrophulariaceae) (Jiang et al., 2004; Šmejkal et al., 2007), was used as the model lipophilic compound with proven *in vitro* antiradical activity (Šmejkal et al., 2007).

Experimental

General

For the isolation of pUC19 plasmid DNA, *Escherichia coli* TOP 10F' strain transfected with this plasmid was cultivated. The cultivation was performed overnight in Difco™ LB Broth, Miller medium (BD Diagnostics, France). After the cultivation, plasmid DNA was isolated using the isolation kit QIAprep Spin Miniprep (Qiagen, Germany). The concentration and purity of the isolated plasmid DNA were evaluated using a BioPhotometer spectrophotometer (Eppendorf, Germany).

Plasmid DNA was analyzed using gel electrophoresis separation on 0.8 % agarose (voltage 5 V cm^{-1} of gel, 45 min) penetrated by ethidium bromide ($0.15 \mu\text{g mL}^{-1}$) for visualization. After the complete run, pictures of the gel were taken using UV detection ($\lambda = 312 \text{ nm}$; a model Transluminator EBW-20 Ultra-Lum Tech, USA). Intensities of the individual plasmid band conformations were calculated using the AlphaEasy FC 4.0.0 software (Alpha Innotech, USA) for densitometric analysis and described as the area under the curve (AUC).

Material

Agarose (Amresco, USA), ethidium bromide (Sigma-Aldrich, Germany), TE buffer (Amresco), H_2O_2 30 % (Penta, Czech Republic), ascorbate (Lachema, Czech Republic), $\text{CuSO}_4 \cdot 5\text{H}_2\text{O}$ (Lachema) were used in this study.

Diplacon (isolated from *Paulownia tomentosa*, as described by Šmejkal et al. (2007)), DMSO (Sigma-Aldrich), Tween 80 (Lachema), Cremophor EL® (Lachema), HP β -CD (Roquette Pharma, France), ethanol (Amresco), methanol (Penta) were used as solvents and co-solvents.

Determination of antioxidant activity

The reaction was performed in PCR tubes (Axygen, USA). Total volume of the reaction mixture was 20 μL . The reaction was carried out with 300 ng of plasmid DNA in TE buffer. First, diplacon (dissolved in the chosen test solvent and co-solvent to reach the final concentrations of 20 μM and 100 μM) was added. Finally, the Fenton solution consisting of H_2O_2 , ascorbate, and $\text{CuSO}_4 \cdot 5\text{H}_2\text{O}$ was added. The reaction conditions were optimized prior to the antioxidant activity determination. For H_2O_2 , the tested concentrations were: 660 μM , 264 μM , and 52.8 μM ,

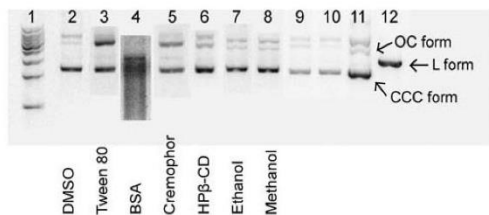


Fig. 2. Gel electrophoresis: dipalcone, 100 μM , dissolved in solvents and co-solvents; 1 – ladder 1 kbp, 2–8 – plasmid DNA + dipalcone + H_2O_2 + CuSO_4 + ascorbate; 9 – plasmid DNA + H_2O_2 + CuSO_4 + ascorbate (positive control); 10 – plasmid DNA + H_2O (negative control); 11 – plasmid DNA; 12 – plasmid DNA (L form only).

and for CuSO_4 : 330 μM , 248 μM , and 165 μM . All experiments carried out to determine the antioxidant activity were performed with a Fenton solution containing H_2O_2 (660 μM), ascorbate (830 μM), and $\text{CuSO}_4 \cdot 5\text{H}_2\text{O}$ (165 μM).

The reaction mixture was incubated at 37°C for 1 h. Then, the samples were analyzed using gel electrophoresis (as described above). Plasmid DNA was separated in the gel as shown in Fig. 2. The OC form is the slowest conformation in the gel and it thus occurs at the top of the gel. The next conformation is the L form, followed by the CCC form. All reactions were carried out in triplicate. The corresponding pure solvents were used instead of the dipalcone solution as positive controls. The negative control contained only water instead of the Fenton solution.

After the run, the gel was analyzed and the intensities of the individual bands were measured. The intensity of each band corresponded to the amount of DNA and was expressed as the percentage of the area under the curve (AUC). A ratio Eq. (4) expressing the amount of intact DNA divided by the total amount of DNA was calculated for each sample. Both strands in the CCC DNA were intact; thus, the percentage was multiplied by 2. To cover the possible influence of solvents and co-solvents on the reaction, the damage index (D_i), dividing the ratio of the sample by the ratio of the positive control (Eq. (5)), was calculated:

$$\text{Ratio}_{\text{sample}} = \frac{\%_{\text{OC}} + (2 \times \%_{\text{CCC}})}{100 \%} \quad (4)$$

$$D_i = \frac{\text{Ratio}_{\text{sample}}}{\text{Ratio}_{\text{positive control}}} \quad (5)$$

Results and discussion

Suitable concentration of CuSO_4 for each solvent and co-solvent was determined. The optimal combination of concentrations should lead to the damage

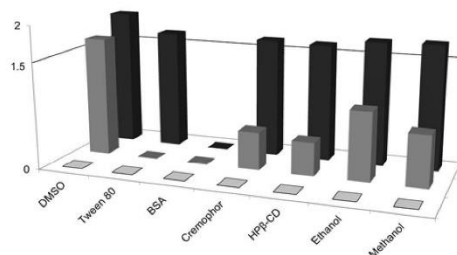


Fig. 3. Optimization of CuSO_4 concentration; □ – 330 μM , ■ – 248 μM , ■ – 165 μM .

of half of the DNA ($\approx 50\%$ of the CCC form). In other words, the optimal ratio Eq. (4) value is approximately 1.5. After the electrophoretic separation and visualization, the ratio representing the amount of intact strands divided by the total amount of DNA in each sample was calculated.

The concentration of H_2O_2 was adjusted from 660 μM to 264 μM and then to 52.8 μM , but this did not lead to the optimal ratio whereas adjusting the concentration of CuSO_4 from 330 μM to 248 μM and 165 μM led to a ratio closer to 1.5. Results of the CuSO_4 concentration optimization are shown in Fig. 3. After the adjustment of the optimal combination of concentrations, 660 μM for H_2O_2 and 165 μM for CuSO_4 , the modified method for antioxidant activity assay was applied for dipalcone dissolved in different solvents and co-solvents at concentrations of 20 μM and 100 μM . Not all pictures of the gels are presented and only the results of dipalcone dissolved in solvents and co-solvents at the concentration of 100 μM are shown in Fig. 2.

D_i was calculated as the ratio of the sample divided by the ratio of the corresponding solvent or co-solvent. This calculation is necessary due to the possible antioxidant or pro-oxidant activity of the solvents. Fig. 4 shows the damage indexes of dipalcone at the concentrations of 20 μM and 100 μM dissolved in all solvents and co-solvents used. ANOVA statistical analysis was performed followed by a post-hoc Tukey's test of damage indexes.

No significant differences were found when the damage index of DMSO was compared with those of Cremophor EL®, HP β -CD, ethanol, and methanol. Thus, these solvents and co-solvents are suitable for the presented method of antioxidant activity determination. However, a significant difference ($p < 0.05$) between the damage indexes of DMSO and Tween 80 was found for dipalcone at the concentration of 100 μM . The latter was lower by 6.8 percentage points. There was also a significant difference between the damage index of BSA when compared with those of other solvents and co-solvents ($p < 0.001$). These differences imply that Tween 80 and BSA are not suitable co-

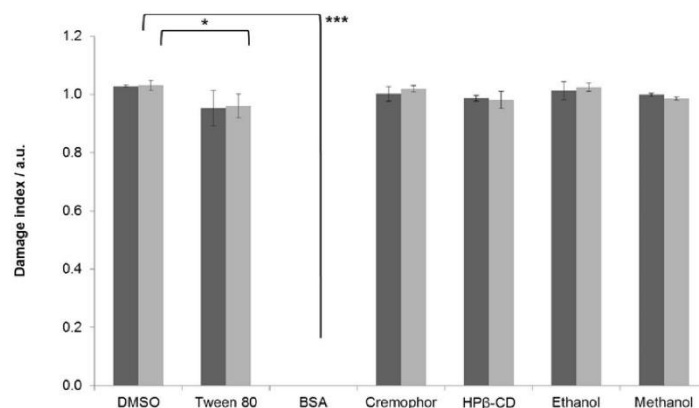


Fig. 4. Damage indexes of 20 μM (■) and 100 μM (▨) diplacone dissolved in solvents and co-solvents (*** – $p < 0.001$, * – $p < 0.05$).

solvents for the presented method of antioxidant activity determination. Another reason for the exclusion of BSA is that it seriously interfered with the electrophoretic detection.

DMSO is known to possess some antioxidant properties. For example, Bektaşoğlu et al. (2006) proved the hydroxyl radical scavenging activity of DMSO using a modified cupric reducing antioxidant capacity (CUPRAC) method. Kishioshka et al. (2007) demonstrated the ability of DMSO to protect liver from acute oxidative hepatitis caused by thioacetamide. In this case, DMSO also functioned as a radical scavenger. DMSO is widely used as a solvent for water-insoluble substances in biological studies. The DMSO molecule contains one highly polar domain and two nonpolar methyl groups which make it a very efficient solvent for water-insoluble compounds.

Santos et al. (2003) described several effects of DMSO on cellular processes and systemic side effects in vivo, e.g., nausea, vomiting, hemolysis, hypertension, and pulmonary edema. Therefore, although it is well known that the dissolving ability of DMSO is excellent and its negative effects on cellular processes do not interfere with the results of the presented method for antioxidant activity determination, we decided to avoid the use of DMSO and to find a less harmful solvent for future testing of lipophilic antioxidants.

Tween 80, a synonym for polysorbate 80, is a nonionic surfactant used in food and pharmaceutical preparations. There is no evidence in literature suggesting that Tween 80 itself has any antioxidant activity. Nevertheless, Tween 80 increases the cytotoxicity of hydrogen peroxide under in vitro conditions and thus may increase the susceptibility of cells to oxidative stress (Tatsuishi et al., 2005).

According to the results of the National Toxicology

Program (1992), toxicity of Tween 80 is low. As mentioned above, when diplacone was dissolved in Tween 80 at the concentration of 100 μM , its antioxidant activity was significantly lower ($p < 0.05$) than when DMSO was the solvent (Fig. 4). The probable reason is that Tween 80 interferes with the chelation of Cu^{2+} caused by diplacone. Thus, Tween 80 was found to be an unsuitable co-solvent for the presented method.

BSA is the most abundant serum protein with the molecular mass of 66 kDa. The role of albumin in ligand binding and free radical-trapping activities has been well described (Roche et al., 2008). Fukuzawa et al. (2005) demonstrated the inhibition of lipid peroxidation by BSA. This effect is caused by the ability of BSA to bind with iron chelates and keep them away from lipid membranes.

Because of the significant difference between the damage index of BSA and those of other solvents and co-solvents ($p < 0.001$), BSA was identified as an unsuitable co-solvent. BSA was not able to dissolve diplacone and thus, nothing prevented the DNA damage.

Cremophor EL[®] (or polyoxyethyleneglycerol tri-*n*-oleate 35) has been used as a co-solvent for hydrophobic drugs in pharmaceutical preparations. Cremophor EL[®] is considered to be relatively non-toxic; however, several reports suggest side effects such as anaphylactoid hypersensitivity, axonal degeneration, and demyelination. Cremophor EL[®] is also known to increase oxidative stress and lipid peroxidation in cells (Gelderblom et al., 2001; Gutiérrez et al., 2006). Similarly, Iwase et al. (2004) provided results suggesting that Cremophor EL[®] increases the susceptibility of thymocytes to oxidative stress caused by hydrogen peroxide.

Cremophor EL[®] showed good ability to dissolve diplacone. There was no significant difference ($p <$

0.05) between the antioxidant activity of dipalacone dissolved in DMSO and that dissolved in Cremophor EL (Fig. 4). Cremophor EL[®] can be used in the method presented, but for future testing of lipophilic antioxidants, the use of Cremophor EL[®] is questionable because of the side effects occurring in vivo, similarly to DMSO.

Cyclodextrins (CD) are cyclic oligosaccharides composed of glucopyranose units which can be presented as truncated cone structures with hydrophobic cavities. The cavities form inclusion complexes with a variety of molecules. Cyclodextrins are widely used in pharmaceutical applications to modify the solubility of poorly water-soluble compounds. Hydroxypropyl- β -CD is now used instead of β -CD because it is more soluble in water and has a relatively low nephrotoxicity (Lu et al., 2009). Calabrò et al. (2004) tested β -CD for antioxidant activity and proved the protective effect of β -CD against lipid peroxidation, probably resulting from the chelation of Fe^{2+} . HP- β -CD showed good ability to dissolve dipalacone. There is no significant difference ($p < 0.05$) between the antioxidant activity of dipalacone dissolved in DMSO and that dissolved in HP- β -CD (Fig. 4). Gould and Scott (2005) proved very low toxicity of HP- β -CD, which makes it a good co-solvent for lipophilic compounds in the method presented and also for further in vivo testing of lipophilic compounds.

Ethanol is widely used as a solvent in laboratory work. Koch et al. (2004) reviewed the factors leading to alcoholic liver disease. Many experiments proved that ethanol increases oxidative stress in hepatocytes. Ethanol-inducible cytochrome P₄₅₀ (CYP2E1), present in microsomes, produces ROS. Electron paramagnetic resonance spectroscopy has also shown free radicals derived from ethanol itself. Moreover, the consumption of ethanol is connected with the dysfunction of the central nervous system. Loureiro et al. (2011) described ROS formation and cytoskeleton disruption in C6 glioma cells after their exposure to ethanol. Ethanol is capable of dissolving dipalacone and it is a suitable solvent for the method presented, as it is evident from the similarity of the damage indexes of dipalacone dissolved in ethanol and that dissolved in DMSO (Fig. 4). However, similarly to DMSO and Cremophor EL[®], its usage is questionable due to its toxic effects on cells.

Methanol is also used as a solvent and cleanser. After ingestion, it causes metabolic acidosis and severe clinical problems such as blindness, serious neurological problems, or even death. Methanol intoxication is associated with mitochondrial damage and microsomal proliferation resulting in higher production of ROS, which, together with the generation of formaldehyde, leads to increased lipid peroxidation increasing the toxic impact of methanol (Parthasarathy et al., 2006). Similarly to ethanol, methanol shows the ability to dissolve dipalacone, but because of its reported

toxicity, its future usage in the lipophilic antioxidants testing is doubtful.

Conclusions

This study shows that HP- β -CD is the best co-solvent of the model lipophilic compound, dipalacone, in the presented method for antioxidant activity determination. Also other solvents and co-solvents tested, namely DMSO, Cremophor EL[®], ethanol, and methanol, do not interfere with the method described but their further usage, especially for in vivo testing, is problematic due to the reported side effects and possible toxicity.

Tween 80 and BSA significantly decreased the antioxidant activity of the model lipophilic compound and were thus found not to be suitable for the dissolving of the lipophilic compounds assayed by the method presented.

Acknowledgements. This project was supported by the Internal Grant Agency of the University of Veterinary and Pharmaceutical Sciences, Brno, grant number 60/2011/FaF.

References

- Bektaşoğlu, B., Çelik, S. E., Özyürek, M., Güçlü, K., & Apak, R. (2006). Novel hydroxyl radical scavenging antioxidant activity assay for water-soluble antioxidants using a modified CUPRAC method. *Biochemical and Biophysical Research Communication*, 345, 1194–1200. DOI: 10.1016/j.bbrc.2006.05.038.
- Calabrò, M. L., Tommasini, S., Donato, P., Raneri, D., Stancanelli, R., Ficarra, P., Ficarra, R., Costa, C., Catania, S., Rustichelli, C., & Gamberini, G. (2004). Effects of α - and β -cyclodextrin complexation on physico-chemical properties and antioxidant activity of some 3-hydroxyflavones. *Journal of Pharmaceutical and Biomedical Analysis*, 35, 365–377. DOI: 10.1016/j.jpba.2003.12.005.
- Chiou, S. H. (1983). DNA- and protein-scission activities of ascorbate in presence of copper ion and a copper-peptide complex. *Journal of Biochemistry*, 94, 1259–1267.
- Chiou, S. H. (1984). DNA-scission activities of ascorbate in presence of metal chelates. *Journal of Biochemistry*, 96, 1307–1310.
- Cooke, M. S., Olinski, R., & Evans, M. D. (2006). Does measurement of oxidative damage to DNA have clinical significance? *Clinica Chimica Acta*, 365, 30–49. DOI: 10.1016/j.cca.2005.09.009.
- Fukuzawa, K., Saitoh, Y., Akai, K., Kogure, K., Ueno, S., Tokumura, A., Otagiri, M., & Shibata, A. (2005). Antioxidant effect of bovine serum albumin on membrane lipid peroxidation induced by iron chelate and superoxide. *Biochimica et Biophysica Acta, Biomembranes*, 1668, 145–155. DOI: 10.1016/j.bbame.2004.12.006.
- Gelderblom, H., Verweij, J., Nooter, A., & Sparreboom, A. (2001). Cremophor EL: the drawbacks and advantages of vehicle selection for drug formulation. *European Journal of Cancer*, 37, 1590–1598. DOI: 10.1016/s0959-8049(01)00171-x.
- Gould, S., & Scott, R. C. (2005). 2-Hydroxypropyl- β -cyclodextrin (HP- β -CD): A toxicology review. *Food and Chemical Toxicology*, 43, 1451–1459. DOI: 10.1016/j.fct.2005.03.007.
- Gutiérrez, M. B., San Miguel, B., Villares, C., González Gallego, J., & Tuñón, M. J. (2006). Oxidative stress induced by

- Cremophor EL in not accompanied by changes in NK- κ B activation of iNOS expression. *Toxicology*, 222, 125–131. DOI: 10.1016/j.tox.2006.02.002.
- Iwase, K., Oyama, Y., Tatsuishi, T., Yamaguchi, J. Y., Nishimura, Y., Kanada, A., Kobayashi, M., Maemura, Y., Ishida, S., & Okano, Y. (2004). Cremophor EL augments the cytotoxicity of hydrogen peroxide in lymphocytes dissociated from rat thymus glands. *Toxicology Letters*, 154, 143–148. DOI: 10.1016/j.toxlet.2004.08.003.
- Jiang, T. F., Du, X., & Shi, Y. P. (2004). Determination of flavonoids from *Paulownia tomentosa* (Thunb) steud by micellar electrokinetic capillary electrophoresis. *Chromatographia*, 59, 255–258. DOI: 10.1365/s10337-003-0154-z.
- Kishioshka, T., Iida, C., Fujii, K., Nagae, R., Onishi, Y., Ichi, I., & Kojo, S. (2007). Effect of dimethyl sulphoxide on oxidative stress, activation of mitogen activated protein kinase and necrosis caused by thioacetamide in the rat liver. *European Journal of Pharmacology*, 564, 190–195. DOI: 10.1016/j.ejphar.2007.03.001.
- Koch, O. R., Pani, G., Borrello, S., Colavitti, R., Cravero, A., Farrò, S., & Galeotti, T. (2004). Oxidative stress and antioxidant defences in ethanol-induced cell injury. *Molecular Aspects of Medicine*, 25, 191–198. DOI: 10.1016/j.mam.2004.02.019.
- Loureiro, S. O., Heimfarth, L., Reis, K., Wild, L., Andrade, C., Guma, F. T. C. R., Gonçalves, C. A., & Pessoa-Pureur, R. (2011). Acute ethanol exposure disrupts actin cytoskeleton and generates reactive oxygen species in c6 cells. *Toxicology in Vitro*, 25, 28–36. DOI: 10.1016/j.tiv.2010.09.003.
- Lu, Z., Cheng, B., Hu, Y., Zhang, Y. H., & Zou, G. L. (2009). Complexation of resveratrol with cyclodextrins: Solubility and antioxidant activity. *Food Chemistry*, 113, 17–20. DOI: 10.1016/j.foodchem.2008.04.042.
- Ma, Q. (2010). Transcriptional responses to oxidative stress: Pathological and toxicological implications. *Pharmacology & Therapeutics*, 125, 376–393. DOI: 10.1016/j.pharmthera.2009.11.004.
- National Toxicology Program (1992). NTP Toxicology and carcinogenesis studies of polysorbate 80 (CAS No. 9005-65-6) in F344/N rats and B6C3F1 mice (Feed studies). *National Toxicological Program, Technical Report Series*, 415, 1–225.
- Parthasarathy, J. S., Kumar, R. S., Manikandan, S., Narayanan, G. S., Kumar, R. V., & Devi, R. S. (2006). Effect of methanol-induced oxidative stress on the neuroimmune system of experimental rats. *Chemico-Biological Interactions*, 161, 14–25. DOI: 10.1016/j.cbi.2006.02.005.
- Que, B. G., Downey, K. M., & So, A. G. (1980). Degradation of deoxyribonucleic acid by 1,10-phenanthroline-copper complex: the role of hydroxyl radicals. *Biochemistry*, 19, 5987–5991. DOI: 10.1021/bi00567a007.
- Roche, M., Rondeau, P., Singh, N. R., Tarnus, E., & Boudon, E. (2008). The antioxidant properties of serum albumin. *FEBS Letters*, 582, 1783–1787. DOI: 10.1016/j.febslet.2008.04.057.
- Sagripanti, J. L., & Kraemer, K. H. (1989). Site-specific oxidative DNA damage at polyguanosines produced by copper plus hydrogen peroxide. *Journal of Biological Chemistry*, 264, 1729–1734.
- Santos, N. C., Figueira-Coelho, J., Martins-Silva, J., & Saldanha, C. (2003). Multidisciplinary utilization of dimethyl sulfoxide: pharmacological, cellular, and molecular aspects. *Biochemical Pharmacology*, 65, 1035–1041. DOI: 10.1016/s0006-2952(03)00002-9.
- Šmejkal, K., Grycová, L., Marek, R., Lemièvre, F., Jankovská, D., Forejtníková, H., Vančo, J., & Suchý, V. (2007). C-Geranyl compounds from *Paulownia tomentosa* fruits. *Journal of Natural Products*, 70, 1244–1248. DOI: 10.1021/np070063w.
- Tatsuishi, T., Oyama, Y., Iwase, K., Yamaguchi, J. Y., Kobayashi, M., Nishimura, Y., Kanada, A., & Hirama, S. (2005). Polysorbate 80 increases the susceptibility to oxidative stress in rat thymocytes. *Toxicology*, 207, 7–14. DOI: 10.1016/j.tox.2004.07.020.
- Zima, A., Hošek, J., Treml, J., Muselík, J., Suchý, P., Pražanová, G., Lopes, A., & Žemlička, M. (2010). Antiradical and cytoprotective activities of several C-geranyl-substituted flavanones from *Paulownia tomentosa* fruit. *Molecules*, 15, 6035–6049. DOI: 10.3390/molecules15096035.

6.4. ARTICLE 4

Treml, J.; Lelakova, V.; Smejkal, K.; Paulickova, T.; Labuda, S.; Granica, S.; Havlik, D.; Padrtova, T.; Hosek, J. *Biomolecules* 2019, 9, 468 (IF=4.082).

Article

Antioxidant Activity of Selected Stilbenoid Derivatives in a Cellular Model System

Jakub Tremel¹, Veronika Leláková¹, Karel Šmejkal^{2,*}, Tereza Paulíčková^{1,2}, Šimon Labuda¹, Sebastian Granica³, Jaroslav Havlík⁴, Dagmar Jankovská², Tereza Padrtová⁵ and Jan Hošek¹

¹ Department of Molecular Biology and Pharmaceutical Biotechnology, Faculty of Pharmacy, University of Veterinary and Pharmaceutical Sciences Brno, 61242 Brno, Czech Republic

² Department of Natural Drugs, Faculty of Pharmacy, University of Veterinary and Pharmaceutical Sciences Brno, 61242 Brno, Czech Republic

³ Department of Pharmacognosy and Molecular Basis of Phytotherapy, Faculty of Pharmacy, Medical University of Warsaw, 02-097 Warsaw, Poland

⁴ Department of Food Science, The Faculty of Agrobiobiology, Food and Natural Resources, The Czech University of Life Sciences Prague, 16500 Prague, Czech Republic

⁵ Department of Chemical Drugs, Faculty of Pharmacy, University of Veterinary and Pharmaceutical Sciences Brno, 61242 Brno, Czech Republic

* Correspondence: karel.mejkal@post.cz; Tel.: +42-072-424-3643

Received: 1 July 2019; Accepted: 3 September 2019; Published: 9 September 2019



Abstract: The stilbenoids, a group of naturally occurring phenolic compounds, are found in a variety of plants, including some berries that are used as food or for medicinal purposes. They are known to be beneficial for human health as anti-inflammatory, chemopreventive, and antioxidative agents. We have investigated a group of 19 stilbenoid substances in vitro using a cellular model of THP-1 macrophage-like cells and pyocyanin-induced oxidative stress to evaluate their antioxidant or pro-oxidant properties. Then we have determined any effects that they might have on the expression of the enzymes catalase, glutathione peroxidase, and heme oxygenase-1, and their effects on the activation of Nrf2. The experimental results showed that these stilbenoids could affect the formation of reactive oxygen species in a cellular model, producing either an antioxidative or pro-oxidative effect, depending on the structure pinostilbene (**2**) worked as a pro-oxidant and also decreased expression of catalase in the cell culture. Piceatannol (**4**) had shown reactive oxygen species (ROS) scavenging activity, whereas isorhapontigenin (**18**) had a mild direct antioxidant effect and activated Nrf2-antioxidant response element (ARE) system and elevated expression of Nrf2 and catalase. Their effects shown on cells in vitro warrant their further study in vivo.

Keywords: stilbenoid; antioxidant; pro-oxidant; pyocyanin; Nrf2; macrophages

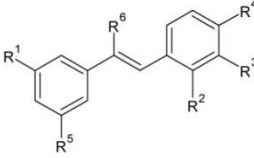
1. Introduction

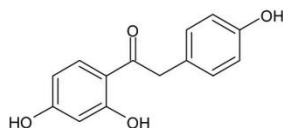
Stilbenoids are a group of secondary plant metabolites belonging to a wide family of plant phenolics. Although stilbenoids share a simple C6-C2-C6 unit, i.e., a 1,2-diphenylethylene structural unit-glycosylation, prenylation (including the formation of Diels-Alder adducts), and the ability to form benzofurans and oligomers make the group structurally large and diverse [1]. Historically, stilbenoids have been studied because of their prominent antibacterial, anticancer, and anti-inflammatory properties, and many studies have also described their antioxidant and chemopreventive properties. Among the stilbenoids chosen for these experiments (see Table 1) and also one of the best known is *trans*-resveratrol (**1**). This stilbenoid has been the focus of thousands of studies in recent years and has been shown to possess a promising potential for interactions with many cellular components.

Its antiaging, anti-inflammatory, antioxidant, and immunomodulatory properties [2,3] have inspired clinical studies and *trans*-resveratrol (1) is currently described as a compound that is beneficial for the treatment of inflammatory diseases, metabolic syndrome, type 2 diabetes, and cardiovascular diseases. However, its relatively low bioavailability and rapid metabolism in vivo make the efficacy of this compound uncertain and reveal the need to investigate stilbenoid derivatives with greater activities [4].

Based on our previous results concerning anti-inflammatory activity (effect of lipopolysaccharide (LPS)-stimulated activation of nuclear factor κ B/activator protein 1 (NF- κ B/AP-1) and also subsequent signaling pathways) [3], we have tested 19 stilbenoid derivatives in the cell model THP-1-XBlue-CD14-MD2. We observed the production of reactive oxygen species (ROS) at the basal level and after stimulation with pyocyanin [5] after short- and long-term exposure to determine any possible antioxidative and pro-oxidative effects, and compare its effects with quercetin [6]. These compounds that showed potential to interact with oxidative processes were further tested for their effects on the expression of enzymes involved in oxidative stress: catalase (CAT), glutathione peroxidase (GPx), heme oxygenase-1 (HO-1), superoxide dismutase 1 (SOD-1) and superoxide dismutase 2 (SOD-2). They were also tested for their effects on nuclear factor erythroid 2-related factor 2 (Nrf2), which controls the basal and induced expression of antioxidant response element-dependent genes to regulate cellular resistance to oxidative stress.

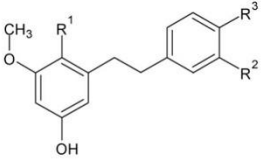
Table 1. Structures of the test stilbenoids.

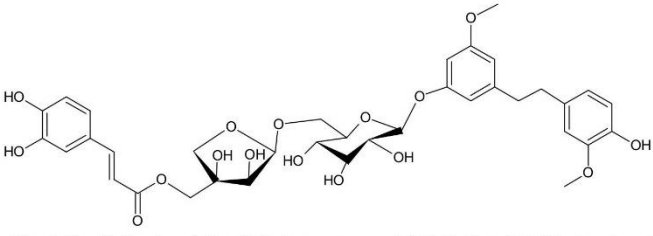
							
		R ¹	R ²	R ³	R ⁴	R ⁵	R ⁶
1	<i>Trans</i> -resveratrol	OH	H	H	OH	OH	H
2	Pinostilbene	OCH ₃	H	H	OH	OH	H
3	Thunallbene	OCH ₃	H	OH	H	OH	H
4	Piceatannol	OH	H	OH	OH	OH	H
5	Piceatannol-3'-O- β -glucopyranoside	OH	H	O-Glc	OH	OH	H
7	Pinostilbenoside	OCH ₃	H	H	O-Glc	OH	H
11	3,5-dimethoxystilbene	OCH ₃	H	H	H	OCH ₃	H
12	<i>Trans</i> -stilbene	H	H	H	H	H	H
13	<i>Cis</i> -stilbene	H	H	H	H	H	H
14	4-Stilbenecarboxylic acid	H	H	H	COOH	H	H
15	Pterostilbene	OCH ₃	H	H	OH	OCH ₃	H
16	<i>Trans</i> - α -methylstilbene	H	H	H	H	H	CH ₃
17	Pinosylvin monomethyl ether	OCH ₃	H	H	H	OH	H
18	Isorhapontigenin	OH	H	OCH ₃	OH	OH	H
19	2,4,3',5'-tetramethoxystilbene	OCH ₃	OCH ₃	H	OCH ₃	OCH ₃	H



1-(2,4-dihydroxyphenyl)-2-(4-hydroxyphenyl)-ethanone (10)

Table 1. Cont.

				
		R ¹	R ²	R ³
6	Batatasin III	H	OH	H
8	2-carboxyl-3-O-methyl-4'-β-D-glucopyranosyl-dihydroresveratrol	COOH	H	O-Glc

				
3-O-caffeoyl-(9→5)-β-apiosyl-(1→6)-β-glucopyranosyl-5,3'-O-dimethyldihdropiceatannol (9)				

2. Materials and Methods

2.1. Test Compounds

The stilbenoid derivatives to be tested (1–19, Table 1) were isolated from natural sources or obtained commercially. The naturally occurring stilbenoids *trans*-resveratrol (1), pinostilbene (2), thunalbene (3), piceatannol (4), piceatannol-3'-O-β-glucopyranoside (5), batatasin III (6), pinostilbenoside (7), 1-(2,4-dihydroxyphenyl)-2-(4-hydroxyphenyl)-ethanone (10), 3,5-dimethoxystilbene (11), pterostilbene (15), pinosylvin monomethyl ether (17), and isorhapontigenin (18) were obtained from Sigma-Aldrich, synthetic compounds *trans*-stilbene (12), *cis*-stilbene (13), 4-stilbenecarboxylic acid (14), *trans*-α-methylstilbene (16), and 2,4,3',5'-tetramethoxystilbene (19) were purchased from Sigma-Aldrich (Steinheim, Germany). The compounds 2-carboxyl-3-O-methyl-4'-β-D-glucopyranosyl-dihydroresveratrol (8) and 3-O-caffeoyl-(9→5)-β-apiosyl-(1→6)-β-glucopyranosyl-5,3'-O-dimethyldihdropiceatannol (9) were kindly provided by Dr. Sebastian Granica (Medical University of Warsaw, Warsaw, Poland) who had isolated them from *Tragopogon tommasinii* Sch.Bip. (Asteraceae, Cichorieae) [7].

2.2. Induction of Lipid Peroxidation

Lipid peroxidation was measured using linoleic acid and 2,2'-azobis(2-amidinopropane)dihydrochloride (AAPH) as has been previously described [8], with some slight modifications. The reaction mixture and also the positive control consisted of 8 mM linoleic acid (Sigma Aldrich, Saint Louis, MO, USA) and 20 mM of AAPH (Sigma Aldrich). Each test compound was added to an experimental tube at a concentration of 15 μM. The negative control contained only the vehicle (DMSO). The reaction mixtures were then incubated for 24 h at 37 °C. Following incubation, the content of malondialdehyde (MDA) formed by lipid peroxidation was measured as described in Section 2.2.1. All of the experiments were performed in triplicate.

2.2.1. Thiobarbituric Acid Reactive Substances Assay

The content of MDA in each reaction mixture was quantified as described by Vasantha Rupasinghe and Yasmin [9], with some modifications. The thiobarbituric acid (TBA) reagent (20% (*w/v*) trichloroacetic acid (Sigma Aldrich) along with 0.375% (*w/v*) TBA in 0.25M HCl (Sigma Aldrich)) was added to each reaction mixture. The mixtures were incubated for 30 min at 95 °C and then cooled to room temperature. The MDA-TBA adduct which formed was extracted from the mixture with an equal volume of butanol (Sigma Aldrich). The extraction was done in two steps: The mixtures were vigorously vortexed for 15 min, and then centrifuged for 5 min at 16,000× *g*. Each butanol fraction was transferred to a 96-well plate, and the absorbance was measured at 532 nm using a FluoStar Omega spectrophotometer (BMG Labtech, Ortenberg, Germany).

2.3. Cell Culturing

THP-1-XBlue-MD2-CD14 cells were supplied by Invivogen (San Diego, CA, USA) and cultured in RPMI 1640 medium containing stabilized 2 mM L-glutamine (Biosera, Nuaille, France), supplemented with antibiotics (100 U/mL penicillin and 100 mg/mL streptomycin (Biosera), and 10% fetal bovine serum (FBS) (HyClone, Logan, UT, USA). The cells were kept in an incubator at 37 °C in a water-saturated atmosphere of air containing 5% CO₂. The suspensions of THP-1-XBlue-MD2-CD14 cells were passaged approximately twice a week.

The HepG2 human hepatoma cell line was purchased from the European Collection of Cell Cultures (Salisbury, UK). Cells were grown in DMEM low glucose medium (Biosera) supplemented with antibiotics (100 U/mL penicillin, 100 mg/mL streptomycin), 10% FBS, and 2 mM L-glutamine. Cultures were kept in an incubator at 37 °C in a water-saturated atmosphere of air containing 5% CO₂. Stabilized cells (12–35th passage) were split into microtitration plates and used for further experiments.

All procedures, such as viability control (each time only cells with viability greater than 95% were used), erythrosine B staining, and light microscopy, were done in standard aseptic conditions. Each experiment for each compound was done three times in an independent triplicate.

2.4. Antioxidant Activity Testing

Antioxidant activity was initiated by triggering the formation of ROS by applying pyocyanin to the cultured cell. In order to measure the fluorescent probe 2',7'-dichlorodihydrofluorescein diacetate (DCFH-DA) was introduced to the cell culture, where it was immediately deesterified to form 2',7'-dichlorodihydrofluorescein, which then causes fluorescence when it was oxidized by ROS [10]. The compounds and standard of quercetin [6] (Koch Light Laboratories, Haverhill, UK) were tested at a final concentration of 2 µM, which previous cytotoxicity tests revealed as non-toxic for all of these compounds [3]. Stock solutions (20 mM) of the test compounds were prepared by dilution with DMSO, and stored frozen at −80 °C. Before each experiment, they were thawed and diluted to achieve the desired final concentration of 2 µM. Pyocyanin was used to trigger oxidative stress in the cells [5]. The stock solution of it at a concentration of 100 mM in DMSO was stored in a freezer. Before each experiment, the stock solution was thawed and diluted to achieve a final concentration of 100 µM per well. The maximum amount of DMSO in solution with cell culture was 0.1% (*v/v*).

2.4.1. Determination of Antioxidant Activity

A suspension of cells in RPMI 1640 serum-free medium at a concentration of 500,000 cells/mL was aliquoted into a 96-well microtiter plate, 100 µL per well. The cells were incubated for 2 h at 37 °C in 5% CO₂ atmosphere to acclimatize, and the test compound of final concentration 2 µM was added. Quercetin was used as the reference compound, along with a negative control—DMSO alone. This procedure was followed by 1 h of incubation (37 °C, an atmosphere of 5% CO₂). Pyocyanin solution (as the positive control) was then added to all wells after that period, and the incubation followed next 30 min. After that DCFH-DA solution was added and after 30 min for the short term

or 24 h for the long-term exposure, the fluorescence (excitation at 485 nm; emission at 538 nm) was measured using a FluoStar Omega spectrophotometer.

2.4.2. Determination of Antioxidant Activity—Pyocyanin Free Model

The testing was carried out under the same conditions as were used to determine the antioxidant activity of the test compounds alone, without pyocyanin added to stimulate the formation of ROS. Pyocyanin served as a positive control for comparison. Both 2 h and 24 h exposures of cells to tested compounds were used.

2.5. Protein Expression of Antioxidant Enzymes

The effect of test compounds on protein expression of antioxidant enzymes was observed in THP-1-XBlue-MD2-CD14 cells. The cells were incubated in the form of floating monocytes (1,000,000 cells/mL) in 3 mL of a serum-free RPMI 1640 medium and seeded into 6-well plates in triplicate at 37 °C. After a 6 h treatment with one of the test compounds at a concentration of 2 μ M dissolved in DMSO, the cells were collected using lysis buffer (50 mM Tris-HCl (pH 7.5), 1 mM EGTA, 1 mM EDTA, 1 mM sodium orthovanadate, 50 mM sodium fluoride, 5 mM sodium pyrophosphate, and 0.27 M sucrose) with protease inhibitors (Roche, Mannheim, Germany). The protein concentration was measured using a Bradford method protein assay kit (Sigma Aldrich) according to the manufacturer's instructions.

To separate the proteins, 20 μ g of the proteins from the cell lysates were loaded onto a 12% SDS-polyacrylamide gel. They were then transferred electrophoretically to polyvinylidene fluoride (PVDF) membranes with 0.2 μ m pores (Bio-Rad, Hercules, USA) that were subsequently blocked using 5% bovine serum albumin (BSA) (SERVA, Heidelberg, Germany) dissolved in TBST buffer (10 mM Tris-HCl (pH 7.5), 150 mM NaCl, and 0.1% (v/v) Tween-20) for 1 h.

The membranes were incubated with the primary antibody (mouse anti-CAT 1:1000 (Sigma-Aldrich; product No. C0979), rabbit anti-SOD1 1:1000 (Sigma-Aldrich; product No. HPA001401), rabbit anti-SOD2 1:1000 (Abcam, Cambridge, UK; product No. ab16956), rabbit anti-NRF2 1:1000 (Abcam; product No. ab137550), rabbit anti-GPx1 (Abcam; product No. ab22604), mouse anti-HO-1 (Abcam; product No. ab13248), or mouse anti- β -actin 1:5000 (Abcam; product No. ab8226)) at 4 °C overnight. After washing, the secondary antibody (anti-mouse IgG (Sigma-Aldrich; product No. A0168) or anti-rabbit IgG (Sigma-Aldrich; product No. A0545) at a dilution of 1:2000), was applied to the membranes, and they were incubated for 1 h at room temperature. Bands were visualized using a chemiluminescent kit (Bio-Rad) and a PXi Syngene Chemiluminescent Imaging System (Syngene, Cambridge, UK) and quantified by optical densitometry (AlphaEaseFC 4.0.0 software, Alpha Innotech, San Leandro, CA, USA).

2.6. Activation of Nrf2-Antioxidant Response Element System

The influence of the test compounds on the activity of Nrf2 was estimated using an antioxidant Response Element (ARE) reporter kit (BPS Bioscience, San Diego, CA, USA). HepG2 cells were transiently transfected for 24 h (35,000 cell/well in 96-well plates) with the ARE luciferase reporter vector (firefly luminescence) plus a constitutively expressing Renilla vector using the TransFast Transfection reagent (Promega, Madison, WI, USA). After serum recovery, the cells were treated for 24 h with each of the test compounds at a concentration of 2 μ M dissolved in DMSO (a non-toxic concentration). As a positive control for this experiment, we have used DL-sulforaphane (Sigma Aldrich) at a concentration of 10 μ M solved in DMSO, as recommended by ARE reporter kit. The luciferase activity from the cell lysates was detected using a Dual luciferase reporter assay system (Promega) and a FluoStar Omega spectrophotometer. Data were normalized to Renilla luminescence.

2.7. Statistical Evaluation

The experimental data were processed in Excel (Microsoft). The results of the blank experiment were subtracted, and the experimental results were normalized to the positive control. Outliers were

removed using the ROUT statistical method ($Q = 5\%$) in GraphPad Prism 6.01 (San Diego, CA, USA). Groups were compared with the help of the one-way ANOVA test followed by Fisher's LSD multiple comparison test. The value $p < 0.05$ was assigned as statistically significant.

3. Results

The antioxidant or pro-oxidant activity of 19 natural and synthetic stilbenoids was determined using various in vitro methods. First of all, the influence of test compounds on lipid peroxidation in a cell-free assay was measured. Lipid peroxidation was studied because lipids are the main components of cellular membranes and often the targets of oxidative stress. The products of this oxidation are lipid peroxides, which can have toxic effects on other cellular components, such as DNA or proteins [11].

Thus, we evaluated the effects of stilbenoids in the peroxidation of lipids in linoleic acid by AAPH. The results are displayed in Figure 1. *Trans*-stilbene (12) with 46.4% inhibition of lipid peroxidation, followed by pterostilbene (15) and 3,5-dimethoxystilbene (11), most effectively diminished lipid peroxidation. On the other hand, quercetin did not inhibit lipid peroxidation. This was rather surprising because quercetin had been chosen as the standard precisely because we did not expect it to show pro-oxidant activity at a concentration of 15 μM [12]. Resveratrol (1) with -49.4% was the most effective pro-oxidant stilbenoid. Pinostilbene (2), piceatannol (4), and piceatannol-3'-O- β -glucopyranoside (5) also showed some statistically significant pro-oxidant effects.

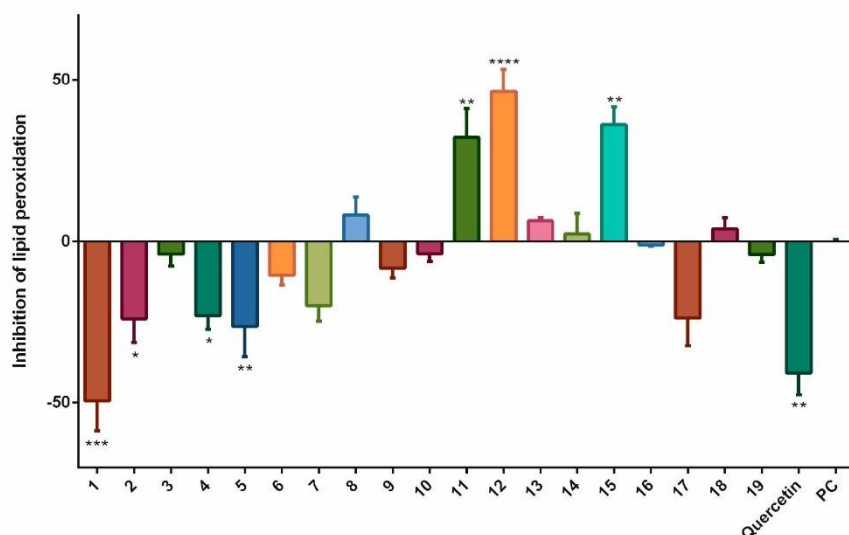


Figure 1. The effects of stilbenoids 1–19 (at a concentration of 15 μM) on the lipid peroxidation of linoleic acid caused by 2,2'-azobis(2-amidinopropane)dihydrochloride (AAPH), and measured as the production of malondialdehyde (MDA) using the thiobarbituric acid reactive substances (TBARS) assay. Quercetin was used as a standard (15 μM) and AAPH alone served as the positive control (PC). The negative control (NC) contained linoleic acid alone, and thus, no lipid peroxidation occurred. The effects of the vehicle were subtracted from that of each stilbenoid. * = $p < 0.05$; ** = $p < 0.01$; *** = $p < 0.001$; and **** = $p < 0.0001$.

To evaluate these results, we have employed an antioxidant method using the THP-1-XBlue-CD14-MD2 cell model. Some stilbenoids showed an effect on the pyocyanin-stimulated formation ROS after 1 h of incubation. A statistically significant decrease in the levels of ROS was observed for piceatannol (4) (53.8%), and piceatannol-3'-O- β -glucopyranoside (5) (41.4%), but neither

compound was as active as the quercetin standard (77.8%). Several other compounds showed some increase in the formation of ROS. For pinostilbene (2) and thunalbene (3), this effect was statistically significant, showing them to act as pro-oxidants in this short-term incubation model (Figure 2).

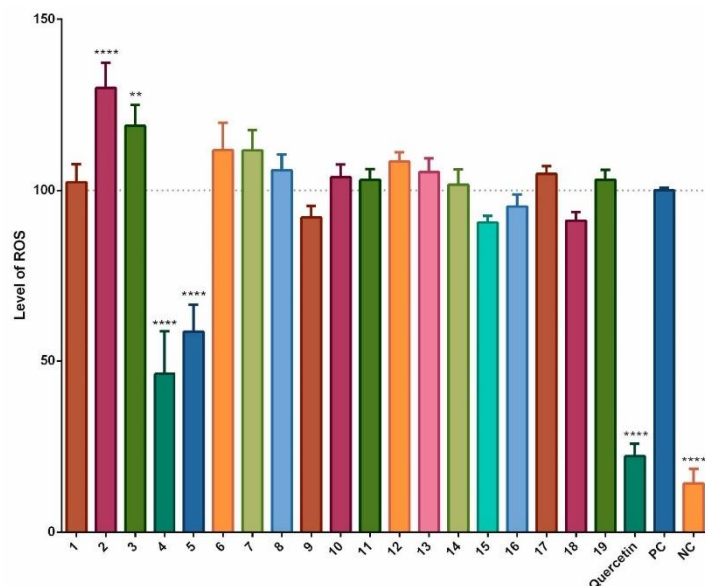


Figure 2. Antioxidant and pro-oxidant effects of stilbenoids 1–19 (at a concentration of 2 μ M) on the formation of ROS after 1 h of incubation. In the THP-1-XBlue-CD14-MD2 cell model, the formation of ROS was triggered by adding 100 μ M pyocyanin; quercetin was used as the standard (2 μ M), pyocyanin alone served as the positive control (PC; 100 μ M) and the vehicle alone was the negative control (NC). ** = $p < 0.01$; **** = $p < 0.0001$.

From the results, we can observe that the stilbenoids which acted as antioxidants in lipid peroxidation assay (e.g., *trans*-stilbene (12)) did not prove to be antioxidants in a cell-based assay. The advantage of assays using cell cultures is that apart from observing the activity, we can also have a clue whether the compound is able to cross the cell membrane or not.

The effects of long-termed incubation of stilbenoids 1–19 on the formation of ROS following simulation with pyocyanin were evaluated using a 24 h period of incubation. Figure 3 shows that, as in the short-termed system, piceatannol (4), and piceatannol-3'-O- β -glucopyranoside (5) as did isorhapontigenin (18) decreased the formation of ROS, but a statistically significant effect was observed only for quercetin, the positive control. In contrast, pinostilbene (2), thunalbene (3), batatasin III (6), pinostilbenoside (7), and 2-carboxyl-3-O-methyl-4'- β -D-glucopyranosyl-dihydroresveratrol (8) increased the formation of ROS to a statistically significant degree.

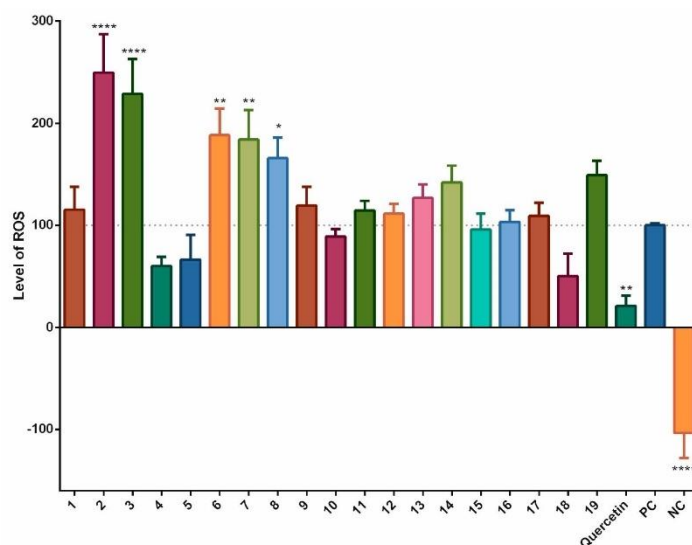


Figure 3. Antioxidant or pro-oxidant effects of stilbenoids 1–19 (at a concentration of 2 μ M) on the formation of ROS after 24 h of incubation. In the THP-1-XBlue-CD14-MD2 cell model, the formation of ROS was triggered by adding 100 μ M pyocyanin; quercetin was used as the standard (2 μ M), pyocyanin alone served as the positive control (PC; 100 μ M) and the vehicle alone was the negative control (NC). * = $p < 0.05$; ** = $p < 0.01$; and **** = $p < 0.0001$.

We also evaluated the effects of the stilbenoids alone in the cell model, without artificially stimulating the production of ROS. Incubation times of 2 h and 24 h were chosen. The results of the 2-h incubation are shown in Figure 4. The pattern was similar to that for the data shown in Figure 1. Statistically significant increases in the levels of ROS were observed for pinostilbene (2) (29.1%), batatasin III (6) (17.4%), pinostilbenoside (7) (26.3%), and pinosylvin monomethyl ether (17) (18.2%) compared to the negative control. Thunalbene (3), 3,5-dimethoxystilbene (11), *trans*-stilbene (12), and *cis*-stilbene (13) were also pro-oxidant, but with less significant increases in production of ROS. On the other hand, piceatannol (4), piceatannol-3'-O- β -glucopyranoside (5), and quercetin standard significantly reduced the levels of ROS.

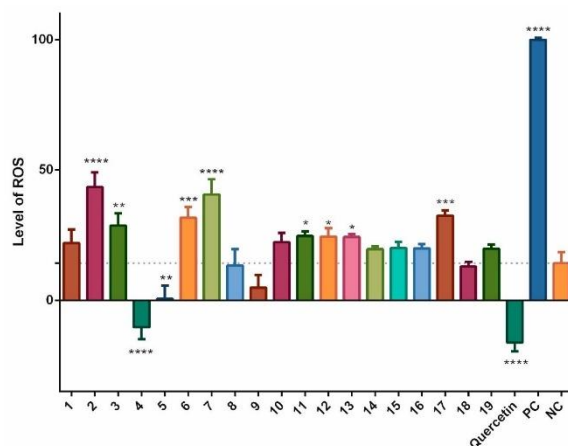


Figure 4. Antioxidant and pro-oxidant effects of stilbenoids 1–19 alone (at a concentration of 2 μ M) on the formation of ROS after 2 h of incubation. In the THP-1-XBlue-CD14-MD2 cell model, the formation of ROS was triggered by stilbenoids alone; quercetin was used as the standard (2 μ M), pyocyanin alone served as the positive control (PC; 100 μ M), and the vehicle alone was the negative control (NC). * = $p < 0.05$; ** = $p < 0.01$; *** = $p < 0.001$; and **** = $p < 0.0001$.

Results of the 24 h incubation are shown in Figure 5. We detected only slightly decreased levels of ROS after incubation with some of the stilbenoids alone, but, a pronounced increase was observed for resveratrol (1) (36.9%) and pinostilbene (2) (60.4%) compared to the negative control.

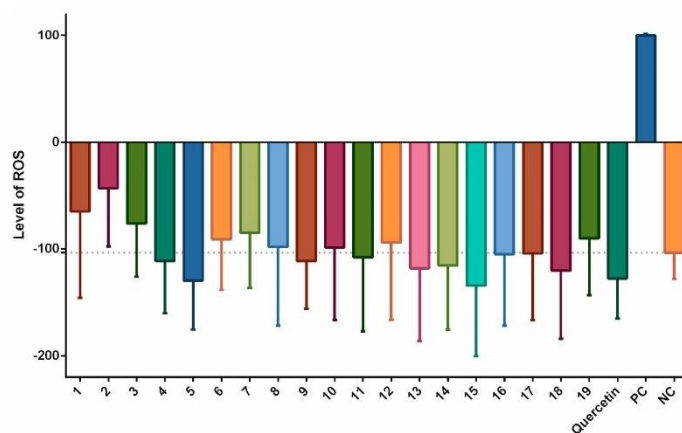


Figure 5. Antioxidant and pro-oxidant effects of stilbenoids 1–19 alone (at a concentration of 2 μ M) on the formation of ROS after 24 h of incubation. In the THP-1-XBlue-CD14-MD2 cell model, the formation of ROS was triggered by stilbenoids alone; quercetin was used as the standard (2 μ M), pyocyanin alone served as the positive control (PC; 100 μ M), and the vehicle alone was the negative control (NC).

Based on the of the results described above, we analyzed the effects of compounds 2, 4, and 18 on the expression of enzymes associated with oxidative stress, because the observed activities might also have been caused by effects of these compounds on endogenous enzymatic antioxidant systems.

We analyzed the effects of compounds **2**, **4**, and **18** at a concentration of 2 μ M after 6 h of incubation with THP-1-XBlue-CD14-MD2 cells on the levels of CAT, GPx, HO-1, SOD-1, and SOD-2. As shown in Figure 6, the test compounds did affect the expression of these enzymes. A 6 h of incubation with compound **2** had decreased the expression of CAT in a statistically significant manner ($p < 0.001$). However, the expression of the same enzyme (CAT) was significantly increased by quercetin ($p < 0.01$). Also, the expression of CAT enzyme was increased by compound **18**, but not in a significant manner. Compound **2** had proven to be pro-oxidant in the previous experiments, so it was not surprising that it downregulated the levels of antioxidant enzymes. On the other hand, quercetin and compound **18** had proven to be antioxidant and upregulated the expression of CAT.

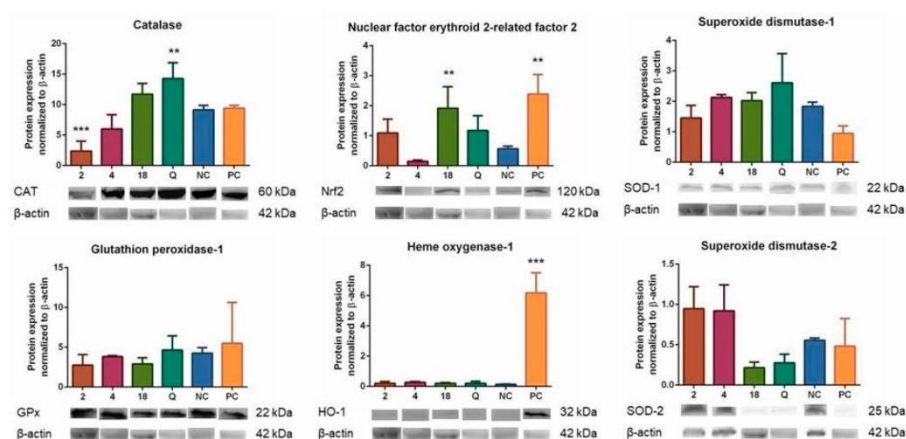


Figure 6. Effects of compounds **2**, **4**, and **18** (at a concentration of 2 μ M) on the levels of selected antioxidant enzymes CAT, GPx, HO-1, and SOD-1 and -2, and on the expression of Nrf2 after 6 h of incubation. The THP-1-XBlue-CD14-MD2 cell model was used with quercetin as the standard (2 μ M), pyocyanin alone (100 μ M) as the positive control (PC), and the vehicle alone as the negative control (NC). ** = $p < 0.01$; *** = $p < 0.001$; and **** = $p < 0.0001$.

For another protein expression, the results were significant when cells were incubated with compound **18** and positive control ($p < 0.01$) for Nrf2 protein. Also, the positive control pyocyanin significantly elevated the expression of HO-1 protein ($p < 0.001$). The changes in the results for other compounds and enzymes were not statistically significant, although expression of SOD-2 was elevated after incubation with compounds **2** and **4**.

The obvious effects of compounds **2**, **4**, **18** and quercetin on the expression of several enzymes associated with antioxidant defense encouraged us to analyze their effects on the upstream regulator Nrf2. To verify the mechanism causing the effects of test compounds, we evaluated their direct effects on the activation of Nrf2-ARE. Figure 7 shows that compound **18**, as well as DL-sulforaphane, the positive control, triggered the activation of the Nrf2-ARE system in a statistically significant manner ($p < 0.001$ and $p < 0.05$, respectively). This might explain the mechanism behind the increased expression of Nrf2 and CAT induced by compound **18**. Surprisingly, quercetin did not activate the Nrf2-ARE pathway, although it was able to increase the expression of CAT.

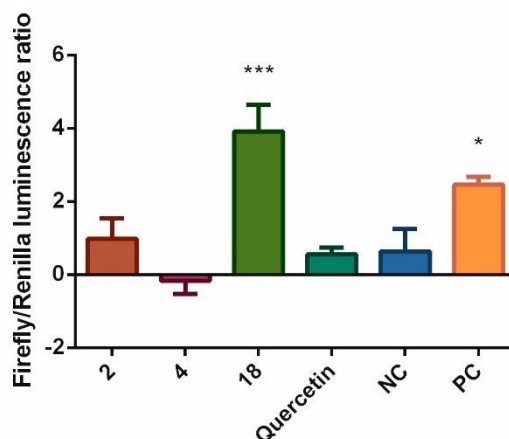


Figure 7. The effects of selected stilbenoids **2**, **4**, and **18** (at a concentration of 2 μ M) on the activation of Nrf2-ARE system. The HepG2 cell model was transiently transfected with the ARE luciferase reporter vector firefly luminescence and a constitutively expressing Renilla vector. The results are expressed as the ratio of firefly to Renilla luminescence. Quercetin was used as the standard (2 μ M), DL-sulforaphane was used as a positive control at a concentration of 10 μ M (PC), and the vehicle alone served as the negative control (NC). * = $p < 0.05$; *** = $p < 0.001$.

4. Discussion

The antioxidant and pro-oxidant activities of natural and synthetic compounds can be tested in different ways. Cell-based methods have an advantage over biochemical screening in that they are more complex, and their results offer a more thorough interpretation of the conditions within the organism. We, therefore, used first the lipoperoxidation cell-free measurement of TBARS and then for verification the THP-1-XBlue-CD14-MD2 cell model and the formation of ROS triggered using pyocyanin (a blue-green phenazine pigment with oxidoreductive properties). It stimulates oxidative metabolism, increasing the formation of ROS via the oxidation of NADPH [5]. The flavonoid quercetin was used for reference because it is a well-known antioxidant, and at greater concentrations shows pro-oxidant properties [6]. Like the flavonoids represented by quercetin, the stilbenoids are phenolics found at high concentrations in medicinal plants, vegetables, walnuts, and edible fruits, such as grapes or berries [1]. The most well-known stilbenoid is resveratrol (**1**). In combination with anthocyanins, this compound is believed to be responsible for the beneficial phenomenon called the French paradox. In addition to its anti-inflammatory and antioxidant activities, it is antiviral, neuroprotective, cardioprotective, and chemoprotective [13].

Stilbenoids affect organisms in different ways, depending on their structural characteristics. Therefore, we studied a large group of synthetic and natural stilbenoids (**1–19**), to find out, if and how their structures affect their antioxidant or pro-oxidant effects in cellular systems. In the cell-free lipoperoxidation inhibition assay, the most active compound was *trans*-stilbene (**12**), followed by pterostilbene (**15**) and 3,5-dimethoxystilbene (**11**). And unexpectedly, quercetin and resveratrol (**1**) acted as pro-oxidants.

The cell-based antioxidant assay showed rather different outcomes. Piceatannol (**4**) and piceatannol-3'-O- β -glucopyranoside (**5**) showed significant antioxidant activities after a short-term incubation with cells stimulated by pyocyanin. 3-O-caffeoyl-(9 \rightarrow 5)- β -apiosyl-(1 \rightarrow 6)- β -glucopyranosyl-5,3'-O-dimethyldihdropiceatannol (**9**), pterostilbene (**15**), *trans*- α -methylstilbene (**16**) and isorhapontigenin (**18**) decreased the formation of ROS, but not significantly. The other compounds did not decrease the formation of ROS as much as

quercetin, the positive control. On the contrary, pinostilbenoside (7) and pinostilbene (2) showed significant pro-oxidant activities. Clearly, the glycosylation of 4 reduced the antioxidant activity, however not significantly.

Long-term exposure of cells to compounds 1–19 with pyocyanin showed no statistically significant antioxidant effects, but isorhapontigenin (18) diminished the formation of ROS by 49.7%, followed by piceatannol (4) and piceatannol-3'-O- β -glucopyranoside (5). Mild activity (10%), greater than in the short-term exposure, was also observed for 1-(2,4-dihydroxyphenyl)-2-(4-hydroxyphenyl)-ethanone (10). Other compounds had little effects on the levels of ROS, or were pro-oxidative, as seen for pinostilbene (2), thunalbene (3), batatasin III (6), pinostilbenoside (7), and 2-carboxyl-3-O-methyl-4'- β -D-glucopyranosyl-dihydroresveratrol (8).

Twelve of the 19 test compounds are hydroxystilbenoids (with a free hydroxyl). These can be divided into two groups according to their structure: Those which can form quinoid systems after two-electron oxidation, and those which cannot [14]. Hydroxystilbenes that contain a catechol or pyrogallol moiety belong to the first group, whereas the ones which possess only phenol or resorcinol arrangements cannot be so oxidized to form quinoids [15]. Compounds in the first group generally display much greater scavenging effects and can increase their overall antioxidant activity, for example, by chelating metal ions [16]. Piceatannol (4) was the only compound with a free catechol moiety. The structurally similar piceatannol-3'-O- β -glucopyranoside (5) has an *ortho* hydroxy group, but the critical is occupied by a glycosidic bond. Compound 4 had a greater antioxidant activity, which confirms previous studies showing the antioxidant potential of highly hydroxylated stilbenoids [14,15]. Piceatannol (4) affects the same molecular targets involved in antioxidant defense (AP-1, Nrf2, HO-1, COX, iNOS, NF- κ B, and IKK) as resveratrol (1), but it showed a much greater direct scavenging effect and also greater inhibition COX-2, NF- κ B and the formation of the pro-inflammatory cytokines TNF- α and IL-1 β [17,18]. Because the antioxidant activity is greater for the short-term exposure of cells than for the long, the direct scavenging effect will likely predominate over stimulation of the antioxidant defense, but possible improvement in the overall antioxidant status cannot be excluded [19,20]. The blocked hydroxy groups of stilbenoids may be responsible for reducing the antioxidant effect not only directly, but also indirectly, by reducing the ability to inhibit enzymes responsible for the formation of ROS, such as xanthinoxidase, monoaminoxidase or, - in case of nitrogen-containing reactive species - iNOS [21,22].

Another compound with antioxidant activity was isorhapontigenin (18), which showed only a small effect after one hour of incubation (8.8%), but much more (49.7%) after 24 h. This result can be attributed to modulation of the antioxidant defense by antioxidant or pro-oxidant enzymes. Studying the same compound, Abbas et al. have found increased levels of glutathione and the antioxidant enzymes SOD and CAT [23], and another study has shown the increased expression and activity of SOD-2 and GPx1 [24], which we also found.

Several test compounds were inactive, showing neither antioxidant nor pro-oxidant effects. Although other studies have reported antioxidant activities for these compounds, possible because greater concentration (5–50 μ M) were tested [1,14,16], we feel concentrations for greater than those likely to be found are not realistic for the *in vivo* evaluation of biological effects.

Several studies have depicted stilbenoids as pro-oxidative compounds [14,16]. Resveratrol (1) and its hydroxylated derivatives can be oxidized either enzymatically or non-enzymatically to form phenoxyl radical, which can, escaping further cellular antioxidant processing, increase levels of ROS. Pro-oxidative effects of hydroxylated stilbenoids have usually been described for much greater concentrations than were used in our study, but we observed pro-oxidant effects for several compounds at a concentration of 2 μ M only for both short-term and long-term incubations. The common structural feature of compounds showing pro-oxidative effects in the short-term incubation was the presence of a methoxy group at position 3, and hydroxyl at position 5, and no other substituents attached to this ring, as seen for pinostilbene (2). Pinostilbene (2) was also the most pro-oxidative substance, increased the level of ROS by 60.4% in comparison to the control in the long-term incubation. Resveratrol (1)

with a 36.9% increase of ROS was next, and pinostilbenoside (7), thunalbene (3) and batatasin III (6) with 3,5-dihydroxy, 2,4-dihydroxy, or 3,5-methoxy arrangements also increased the levels of ROS. The pro-oxidant effect shown by resveratrol (1) after long-term incubation and possibly also by other stilbenoids can be ascribed to H₂O₂ and other ROS formed as they decompose in culture medium [16]. This has not been observed during short-term exposures. Contrary to our results, Chao et al. found resveratrol (1) and pinostilbene (2) protecting neuron SH-SY5Y cells against oxidative stress caused by 6-hydroxydopamine [25].

Enzymatic systems that eliminate excessive ROS, such as CAT, GPx, and SOD, and enzymes that regenerate and produce endogenous antioxidants, such as glutathione reductase, thioredoxin reductase, or glutathione synthetase, make the most important contribution to the antioxidant defense of cells [26]. By increasing the expression of the aforementioned enzymes, natural phenolics exert an indirect antioxidant effect. It is possible that the increased expression of antioxidant enzymes is mediated by activation of the Keap1-Nrf2-ARE (Kelch-like ECH-associated protein 1-nuclear factor erythroid 2-related factor 2 (Nrf2)-antioxidant responsible elements) signalization pathway. Some phenolics are able, via Nrf2, to induce certain enzymes of phase 1 and phase 2 (e.g., glutathione-S-transferase, UDP-glucuronyltransferase) of metabolic elimination to detoxify pro-oxidant xenobiotics. [26,27]. Nrf2 is blocked in the cytoplasm by its inhibitor Keap1. Nrf2, activated by electrophilic stimuli, such as ROS, reactive nitrogen species (RNS), heavy metal ions, or some diseases) is released from the cytoplasmic protein Keap1 and translocated into nucleus, where it binds to the ARE area that regulates the expression of the target genes, for example, of HO-1, NAD(P)H:quinone oxidoreductase (NQO-1), or γ -glutamylcysteine synthetase (γ GCS), which increases the levels of glutathione [28–30].

Enzymes that cause antioxidant effects are activated by an increase in their responsible coding genes mediated by Nrf2. Most compounds that affect Nrf2 is thought to be pro-oxidants acting on Keap1, probably by reacting with sulfhydryl groups of cysteine. Nrf2 is then released [26]. Compared to the direct antioxidant effect of scavenging ROS (commonly observed using concentrations of 10–100 μ M), the activity involving Keap1/Nrf2/ARE is more effective, requiring only 0.5–5 μ M concentrations. It is independent of the stoichiometry and can amplify the initial direct effect of phenolics beyond the timeframe of direct activity, making them effective even after they are no longer present in situ [26].

Armed with this knowledge, we analyzed the effects of compounds 2, 4, and 18 on the expression of enzymes associated with oxidative stress. The effects of compounds 2, 4, and 18 on the levels of CAT, GPx, HO-1, and SOD-1 and -2 were evaluated after 6 h of incubation. The compound 2 decreased expression of CAT enzyme and basically unaffected expression of other proteins. Compound 18 elevated expression of Nrf2 significantly and CAT non-significantly. Standard quercetin significantly increased the expression of CAT and positive control pyocyanin upregulated HO-1. Greater concentrations of test compounds, or a different period of incubation, or both together might increase the effect. The effect of compound 18 on the expression of several enzymes associated with antioxidant defense was clearly visible, and we, therefore, analyzed effects of the test compounds 2, 4 and 18 on the upstream regulation caused by Nrf2. As seen in Figure 7, compound 18 increased the activation of Nrf2-ARE system in a significant manner. This result corresponds to the elevated expression of Nrf2 and CAT.

Our results confirm previous studies showing that the stilbenoids, such as resveratrol (1) significantly affect the activity of Nrf2 and the levels of enzymes under its control. Resveratrol (1) enhances autophagy by increasing the activity of Nrf2. This activity is mediated by the binding of the adaptor protein p62, phosphorylated by kinases in the cytoplasm, to Keap1 in competition with Nrf2. The phosphorylated p62 binds to Keap1, releasing Nrf2, which translocates to the nucleus. [28,30]. Similar effects have been observed for oxyresveratrol [31]. Another stilbenoid able to increase the activity of Nrf2 is pterostilbene (15). A study by Saw et al. has shown, that pterostilbene (15) (and quercetin and kaempferol, two other phenols found in berries) directly scavenged ROS, activated the Nrf2-ARE signal pathway and acted synergistically when used together at some concentrations [19]. The incubation of cells with piceatannol (4) (10–20 μ M) also increased the expression of HO-1. It is expected, that electrophilic quinone formed by the oxidation of piceatannol (4) binds directly to Keap1

and initiates this process [32]. The activity of cajanin stilbene acid may also be due to the effect on Nrf2 [33]. Similar effects were also seen in tests of extracts rich in stilbenoids, such as *Vitis vinifera* root extract which contains resveratrol (1) [29].

5. Conclusions

A group of several stilbenoids was investigated in vitro, using a cellular model of THP-1 macrophage-like cells to evaluate their antioxidant or pro-oxidant properties, to determine any effects that might possibly have on the expression of the enzymes catalase, glutathione peroxidase, and heme oxygenase-1, and their effects on the activation of Nrf2. The experimental results showed that these stilbenoids could affect the formation of reactive oxygen species in a cellular model, producing either an antioxidative or pro-oxidative effect, depending on the structure. Selected stilbenoids also affected the expression of antioxidant enzymes and showed some effects on the activation of Nrf2. Depending upon their structure, stilbenoids can possess either antioxidative or pro-oxidative effects, and they can also affect enzymatic antioxidant defenses. Pinostilbene (2) showed rather pro-oxidant effects and also decreased expression of CAT in cell culture. Piceatannol (4) had antioxidant effect as it directly scavenged ROS and isorhapontigenin (18) had a mild direct antioxidant effect, but on the other hand, activated Nrf2-ARE system and elevated expression of Nrf2 and CAT.

Author Contributions: Conceptualization, J.T., K.Š. and Jaroslav Havlík.; Data curation, J.T., Jan Hošek, V.L., S.G. and T.P.; Funding acquisition, K.Š. and Jaroslav Havlík.; Investigation, D.J., Tereza Paulíčková, Š.L., V.L. and S.G.; Methodology, J.T., K.Š. and Jan Hošek.; Project administration, K.Š. and Jaroslav Havlík.; Visualization, J.T.; Writing—original draft, J.T., K.Š., D.J., Tereza Padrtová, Jaroslav Havlík, and Jan Hošek.; Writing—review and editing, K.Š., Tereza Padrtová, J.T. and Jaroslav Havlík.

Funding: This research was funded by GACR, grant no. 16-07193S and Internal Grant Agency of VFU Brno—The project 302/2018/FaF. CIISB research infrastructure project LM2015043 funded by MEYS CR is gratefully acknowledged for the financial support of the measurements at the CF Proteomics and Josef Dadok National NMR Centre.

Acknowledgments: We thanks to Frank Thomas Campbell for a language editing of the manuscript.

Conflicts of Interest: The authors declare no conflict of interest.

References

1. Dvorakova, M.; Landa, P. Anti-inflammatory activity of natural stilbenoids: A review. *Pharmacol. Res.* **2017**, *124*, 126–145. [\[CrossRef\]](#)
2. Baur, J.A.; Sinclair, D.A. Therapeutic potential of resveratrol: The in vivo evidence. *Nat. Rev. Drug Discov.* **2006**, *5*, 493–506. [\[CrossRef\]](#) [\[PubMed\]](#)
3. Leláková, V.; Šmejkal, K.; Jakubczyk, K.; Veselý, O.; Landa, P.; Václavík, J.; Bobál, P.; Pížová, H.; Temml, V.; Steinacher, T.; et al. Parallel in vitro and in silico investigations into anti-inflammatory effects of non-prenylated stilbenoids. *Food Chem.* **2019**, *285*, 431–440. [\[CrossRef\]](#) [\[PubMed\]](#)
4. Cottart, C.-H.; Nivet-Antoine, V.; Languillier-Morizot, C.; Beaudeau, J.-L. Resveratrol bioavailability and toxicity in humans. *Mol. Nutr. Food Res.* **2010**, *54*, 7–16. [\[CrossRef\]](#) [\[PubMed\]](#)
5. Hall, S.; McDermott, C.; Anoopkumar-Dukie, S.; McFarland, A.J.; Forbes, A.; Perkins, A.V.; Davey, A.K.; Chess-Williams, R.; Kiefel, M.J.; Arora, D.; et al. Cellular Effects of Pyocyanin, a Secreted Virulence Factor of *Pseudomonas aeruginosa*. *Toxins* **2016**, *8*, 236. [\[CrossRef\]](#) [\[PubMed\]](#)
6. D’Andrea, G. Quercetin: A flavonol with multifaceted therapeutic applications? *Fittoterapia* **2015**, *106*, 256–271. [\[CrossRef\]](#) [\[PubMed\]](#)
7. Granica, S.; Piwowarski, J.P.; Randazzo, A.; Schneider, P.; Żyżyńska-Granica, B.; Zidorn, C. Novel stilbenoids, including cannabispipradienone glycosides, from *Tragopogon tommasinii* (Asteraceae, Cichorieae) and their potential anti-inflammatory activity. *Phytochemistry* **2015**, *117*, 254–266. [\[CrossRef\]](#) [\[PubMed\]](#)
8. Peyrat-Maillard, M.N.; Cuvelier, M.E.; Berset, C. Antioxidant activity of phenolic compounds in 2,2′-azobis (2-amidinopropane) dihydrochloride (AAPH)-induced oxidation: Synergistic and antagonistic effects. *J. Am. Oil Chem. Soc.* **2003**, *80*, 1007. [\[CrossRef\]](#)

9. Vasantha Rupasinghe, H.P.; Yasmin, A. Inhibition of oxidation of aqueous emulsions of omega-3 fatty acids and fish oil by phloretin and phloridzin. *Molecules* **2010**, *15*, 251–257. [[CrossRef](#)]
10. Rastogi, R.P.; Singh, S.P.; Häder, D.P.; Sinha, R.P. Detection of reactive oxygen species (ROS) by the oxidant-sensing probe 2',7'-dichlorodihydrofluorescein diacetate in the cyanobacterium *Anabaena variabilis* PCC 7937. *Biochem. Biophys. Res. Commun.* **2010**, *397*, 603–607. [[CrossRef](#)]
11. Gaschler, M.M.; Stockwell, B.R. Lipid peroxidation in cell death. *Biochem. Biophys. Res. Commun.* **2017**, *482*, 419–425. [[CrossRef](#)] [[PubMed](#)]
12. Trembl, J.; Šmejkal, K. Flavonoids as Potent Scavengers of Hydroxyl Radicals. *Comp. Rev. Food Sci. Food Saf.* **2016**, *15*, 720–738. [[CrossRef](#)]
13. Smoliga, J.M.; Baur, J.A.; Hausenblas, H.A. Resveratrol and health—A comprehensive review of human clinical trials. *Mol. Nutr. Food Res.* **2011**, *55*, 1129–1141. [[CrossRef](#)] [[PubMed](#)]
14. Murias, M.; Jäger, W.; Handler, N.; Erker, T.; Horvath, Z.; Szekeres, T.; Nohl, H.; Gille, L. Antioxidant, prooxidant and cytotoxic activity of hydroxylated resveratrol analogues: Structure–activity relationship. *Biochem. Pharmacol.* **2005**, *69*, 903–912. [[CrossRef](#)] [[PubMed](#)]
15. Szekeres, T.; Saiko, P.; Fritzer-Szekeres, M.; Djavan, B.; Jäger, W. Chemopreventive effects of resveratrol and resveratrol derivatives. *Ann. N. Y. Acad. Sci.* **2011**, *1215*, 89–95. [[CrossRef](#)] [[PubMed](#)]
16. Kucinska, M.; Piotrowska, H.; Luczak, M.W.; Mikula-Pietrasik, J.; Ksiazek, K.; Wozniak, M.; Wierzbowski, M.; Dudka, J.; Jäger, W.; Murias, M. Effects of hydroxylated resveratrol analogs on oxidative stress and cancer cells death in human acute T cell leukemia cell line: Prooxidative potential of hydroxylated resveratrol analogs. *Chem.-Biol. Interact.* **2014**, *209*, 96–110. [[CrossRef](#)] [[PubMed](#)]
17. Jeong, S.O.; Son, Y.; Lee, J.H.; Cheong, Y.K.; Park, S.H.; Chung, H.T.; Pae, H.O. Resveratrol analog piceatannol restores the palmitic acid-induced impairment of insulin signaling and production of endothelial nitric oxide via activation of anti-inflammatory and antioxidative heme oxygenase-1 in human endothelial cells. *Mol. Med. Rep.* **2015**, *12*, 937–944. [[CrossRef](#)]
18. Son, Y.; Chung, H.T.; Pae, H.O. Differential effects of resveratrol and its natural analogs, piceatannol and 3,5,4'-trans-trimethoxystilbene, on anti-inflammatory hemeoxygenase-1 expression in RAW264.7 macrophages. *Biofactors* **2014**, *40*, 138–145. [[CrossRef](#)]
19. Saw, C.L.; Guo, Y.; Yang, A.Y.; Paredes-Gonzalez, X.; Ramirez, C.; Pung, D.; Kong, A.N. The berry constituents quercetin, kaempferol, and pterostilbene synergistically attenuate reactive oxygen species: Involvement of the Nrf2-ARE signaling pathway. *Food Chem. Toxicol.* **2014**, *72*, 303–311. [[CrossRef](#)]
20. Pulido, R.; Bravo, L.; Saura-Calixto, F. Antioxidant activity of dietary polyphenols as determined by a modified ferric reducing/antioxidant power assay. *J. Agric. Food Chem.* **2000**, *48*, 3396–3402. [[CrossRef](#)]
21. Halliwell, B. Free radicals and antioxidants: Updating a personal view. *Nutr. Rev.* **2012**, *70*, 257–265. [[CrossRef](#)] [[PubMed](#)]
22. Zhou, C.X.; Kong, L.D.; Ye, W.C.; Cheng, C.H.; Tan, R.X. Inhibition of xanthine and monoamine oxidases by stilbenoids from *Veratrum taliense*. *Planta Med.* **2001**, *67*, 158–161. [[CrossRef](#)] [[PubMed](#)]
23. Abbas, A.M. Cardioprotective effect of resveratrol analogue isorhapontigenin versus omega-3 fatty acids in isoproterenol-induced myocardial infarction in rats. *J. Physiol. Biochem.* **2016**, *72*, 469–484. [[CrossRef](#)] [[PubMed](#)]
24. Wang, H.; Yang, Y.L.; Zhang, H.; Yan, H.; Wu, X.J.; Zhang, C.Z. Administration of the resveratrol analogues isorhapontigenin and heyneanol-A protects mice hematopoietic cells against irradiation injuries. *BioMed Res. Int.* **2014**, *2014*. [[CrossRef](#)] [[PubMed](#)]
25. Chao, J.; Li, H.; Cheng, K.W.; Yu, M.S.; Chang, R.C.; Wang, M. Protective effects of pinostilbene, a resveratrol methylated derivative, against 6-hydroxydopamine-induced neurotoxicity in SH-SY5Y cells. *J. Nutr. Biochem.* **2010**, *21*, 482–489. [[CrossRef](#)] [[PubMed](#)]
26. Sandoval-Acuna, C.; Ferreira, J.; Speisky, H. Polyphenols and mitochondria: An update on their increasingly emerging ROS-scavenging independent actions. *Arch. Biochem. Biophys.* **2014**, *559*, 75–90. [[CrossRef](#)] [[PubMed](#)]
27. Liu, H.; Yang, J.; Huang, S.; Liu, R.; He, Y.; Zheng, D.; Liu, C. Mulberry crude extracts induce Nrf2 activation and expression of detoxifying enzymes in rat liver: Implication for its protection against NP-induced toxic effects. *J. Funct. Foods* **2017**, *32*, 367–374. [[CrossRef](#)]

28. Zhao, Y.; Song, W.; Wang, Z.; Wang, Z.; Jin, X.; Xu, J.; Bai, L.; Li, Y.; Cui, J.; Cai, L. Resveratrol attenuates testicular apoptosis in type 1 diabetic mice: Role of Akt-mediated Nrf2 activation and p62-dependent Keap1 degradation. *Redox Biol.* **2018**, *14*, 609–617. [[CrossRef](#)]
29. Esatbeyoglu, T.; Ewald, P.; Yasui, Y.; Yokokawa, H.; Wagner, A.E.; Matsugo, S.; Winterhalter, P.; Rimbach, G. Chemical characterization, free radical scavenging, and cellular antioxidant and anti-inflammatory properties of a stilbenoid-rich root extract of *Vitis vinifera*. *Oxid. Med. Cell. Longev.* **2016**, *2016*. [[CrossRef](#)]
30. Shen, Z.; Wang, Y.; Su, Z.; Kou, R.; Xie, K.; Song, F. Activation of p62-keap1-Nrf2 antioxidant pathway in the early stage of acetaminophen-induced acute liver injury in mice. *Chem. Biol. Interact.* **2018**, *282*, 22–28. [[CrossRef](#)]
31. Jia, Y.N.; Lu, H.P.; Peng, Y.L.; Zhang, B.S.; Gong, X.B.; Su, J.; Zhou, Y.; Pan, M.H.; Xu, L. Oxyresveratrol prevents lipopolysaccharide/p-galactosamine-induced acute liver injury in mice. *Int. Immunopharmacol.* **2018**, *56*, 105–112. [[CrossRef](#)] [[PubMed](#)]
32. Lee, H.H.; Park, S.A.; Almazari, I.; Kim, E.H.; Na, H.K.; Surh, Y.J. Piceatannol induces heme oxygenase-1 expression in human mammary epithelial cells through activation of ARE-driven Nrf2 signaling. *Arch. Biochem. Biophys.* **2010**, *501*, 142–150. [[CrossRef](#)] [[PubMed](#)]
33. Huang, M.-Y.; Lin, J.; Lu, K.; Xu, H.-G.; Geng, Z.-Z.; Sun, P.-H.; Chen, W.-M. Anti-Inflammatory Effects of Cajaninstilbene Acid and Its Derivatives. *J. Agric. Food Chem.* **2016**, *64*, 2893–2900. [[CrossRef](#)] [[PubMed](#)]



© 2019 by the authors. Licensee MDPI, Basel, Switzerland. This article is an open access article distributed under the terms and conditions of the Creative Commons Attribution (CC BY) license (<http://creativecommons.org/licenses/by/4.0/>).

6.5. ARTICLE 5

Treml, J.; Vecerova, P.; Herczogova, P.; Smejkal, K. *Molecules* 2021, 26, 2534 (IF=4.927).

Article

Direct and Indirect Antioxidant Effects of Selected Plant Phenolics in Cell-Based Assays

Jakub Tremblé ^{1,*}, Petra Večeřová ¹, Petra Herczogová ^{1,2} and Karel Šmejkal ^{2,*}

¹ Department of Molecular Pharmacy, Faculty of Pharmacy, Masaryk University, Palackého tr. 1946/1, 612 00 Brno, Czech Republic; petra.vece@seznam.cz (P.V.); petra.herczogova@gmail.com (P.H.)

² Department of Natural Drugs, Faculty of Pharmacy, Masaryk University, Palackého tr. 1946/1, 612 00 Brno, Czech Republic

* Correspondence: tremblj@pharm.muni.cz (J.T.); smejkalk@pharm.muni.cz (K.Š.)



Citation: Tremblé, J.; Večeřová, P.; Herczogová, P.; Šmejkal, K. Direct and Indirect Antioxidant Effects of Selected Plant Phenolics in Cell-Based Assays. *Molecules* **2021**, *26*, 2534. <https://doi.org/10.3390/molecules26092534>

Academic Editor:
Celestino Santos-Buelga

Received: 25 February 2021
Accepted: 22 April 2021
Published: 26 April 2021

Publisher's Note: MDPI stays neutral with regard to jurisdictional claims in published maps and institutional affiliations.



Copyright: © 2021 by the authors. Licensee MDPI, Basel, Switzerland. This article is an open access article distributed under the terms and conditions of the Creative Commons Attribution (CC BY) license (<https://creativecommons.org/licenses/by/4.0/>).

Abstract: **Background:** Oxidative stress is a key factor in the pathophysiology of many diseases. This study aimed to verify the antioxidant activity of selected plant phenolics in cell-based assays and determine their direct or indirect effects. **Methods:** The cellular antioxidant assay (CAA) assay was employed for direct scavenging assays. In the indirect approach, the influence of each test substance on the gene and protein expression and activity of selected antioxidant enzymes was observed. One assay also dealt with activation of the Nrf2-ARE pathway. The overall effect of each compound was measured using a glucose oxidative stress protection assay. **Results:** Among the test compounds, acteoside showed the highest direct scavenging activity and no effect on the expression of antioxidant enzymes. It increased only the activity of catalase. Diplocone was less active in direct antioxidant assays but positively affected enzyme expression and catalase activity. Morusin showed no antioxidant activity in the CAA assay. Similarly, pomiferin had only mild antioxidant activity and proved rather cytotoxic. **Conclusions:** Of the four selected phenolics, only acteoside and diplocone demonstrated antioxidant effects in cell-based assays.

Keywords: antioxidants; CAA; catalase; glucose toxicity; plant phenolics; superoxide dismutase; Nrf2-ARE

1. Introduction

Oxidative stress is a disturbance of the balance between pro-oxidant and antioxidant states that favors the former. The essence of the pro-oxidant process is the production of reactive oxygen (ROS) and nitrogen species (RNS). ROS include molecules of various structures: for example, oxygen radicals (such as hydroxyl radical $\cdot\text{OH}$ or peroxyl radical $\text{RO}_2\cdot$) and strongly oxidizing non-radical substances (such as hydrogen peroxide, H_2O_2) [1,2]. ROS production, which leads to DNA damage, protein alteration, or lipid peroxidation, is a known factor in developing various pathological conditions, such as cardiovascular diseases, cancer, neurological disorders, diabetes mellitus, and aging [3].

In addition to these deleterious effects, there is also a positive side to producing ROS. For example, they are produced by phagocytic NADPH oxidase (in oxidative burst), and $\text{NO}\cdot$ regulates vascular tone [1,3]. Current understanding uses the concept of “eustress”, a certain level of oxidative stress necessary for cellular life. For example, H_2O_2 at nanomolar concentrations serves as a redox signaling molecule, but at supraphysiological concentrations (>100 nM), it damages biomolecules [4].

Two basic groups of antioxidants are usually recognized as providing cellular protection against harmful oxidative stress: (i) direct antioxidants, which undergo redox reactions and scavenge ROS or RNS, and (ii) indirect antioxidants, which may or may not be redox-active and activate the nuclear factor erythroid 2 (NFE2)-related factor 2 (Nrf2) and antioxidant response element (ARE) pathway resulting in antioxidant enzyme expression [4].

Antioxidant activity assays follow the same division. The direct antioxidant effect can be evaluated using a chemical-based assay, such as the 2,2-diphenyl-1-picrylhydrazyl radical (DPPH•) scavenging assay or the ferric reducing antioxidant power (FRAP) assay. In general, the mechanisms of these in vitro methods depend on scavenging stable free radicals or reducing ferric ions, respectively. Another approach is to establish the antioxidant capacity under more biologically relevant conditions. These assays are cellular-based and focus on direct scavenging. An example of such a method is the cellular antioxidant activity (CAA) assay, which identifies antioxidants able to prevent ROS (obtained from the decomposition of 2,2'-azobis(2-methylpropionamidine) dihydrochloride (AAPH)) from oxidizing dihydrodichlorofluorescein DCFH₂ to fluorescent dichlorofluorescein DCF [5].

The indirect antioxidant activity reflects the removal of ROS by enzymes, such as superoxide dismutase—SOD or catalase—CAT, and small thiol molecules, e.g., glutathione (GSH). SOD converts superoxide anion (O₂^{•−}), a byproduct of normal oxygen metabolism, into H₂O₂, which CAT then decomposes into water and oxygen [6]. The expression of both enzymes is regulated by ARE, which is activated by Nrf2 [7]. A member of the cap 'n' collar (CNC) subfamily of basic region leucine zipper (bZip) transcription factors, Nrf2 is found in an inactive form in the cytosol, bound to Kelch-like ECH-associated protein 1 (Keap1). Upon oxidative stress, Nrf2 dissociates from Keap1 and translocates into the nucleus, activating the ARE [6,8].

The Nrf2 system was, therefore, found to be the target of various indirect antioxidants, and this mode of action has been confirmed for various phenolics, e.g., epigallocatechin-3-gallate [9] or 3-*O*-caffeoyl-1-methylquinic acid [10]. The proposed mechanism of Nrf2 activation is most likely the alteration of the structure of Keap1 because it contains several cysteine thiol residues that function as sensors of cellular redox changes. Thus, oxidation or covalent modification of some of these residues would release Nrf2 and facilitate its accumulation in the nucleus [11].

The main difference between the two approaches is that the direct measurement is quite rapid, whereas the indirect effect requires more time because it entails the biosynthesis of new proteins [5]. A third approach combines direct antioxidant activity and indirect antioxidant effects in a cellular-based assay, with a long incubation time (e.g., 24 h or longer). In these settings, both direct scavenging and indirect activation of Nrf2/ARE may concur to the final effect. An example of this type of method is the glucose oxidative stress protection (GOSP) assay, which creates a condition of hyperglycemia to increase the production of ROS [12,13].

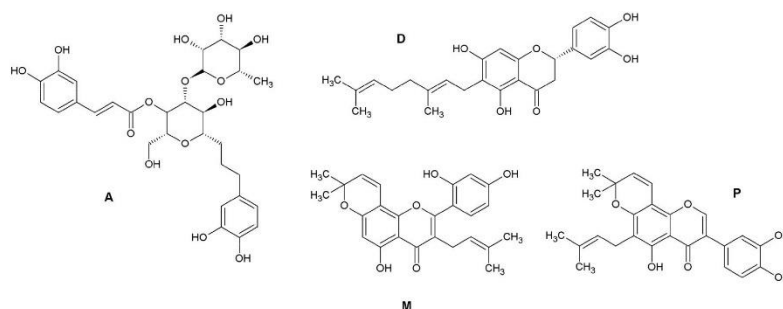


Figure 1. The compounds selected for experiments: acteoside (A), diplacone (D), morusin (M), and pomiferin (P).

Dietary phenolics of polyphenols occupy a special place among the antioxidants that occur in plants [14]. The structures of these compounds contain an aromatic ring with one or more hydroxyl groups. This group of natural products is very widely distributed in the plant kingdom, with more than 8000 phenolic structures currently known [15]. Many of these compounds possess direct or indirect antioxidant activity [6]. We selected four plant

phenols that had shown some degree of in vitro antioxidant activity [16–19] for further testing in cell-based assays (Figure 1). Acteoside (A) is a caffeoyl phenylethanoid glycoside obtained from *Paulownia tomentosa*, as is the geranylated flavanone diplacone (D) [17,20]. Morusin (M) was selected as an example of the prenylated flavones obtained from *Morus alba*, and pomiferin (P), a prenylated isoflavone, comes from *Maclura pomifera* [18,21]. Here, we aimed our study at testing the direct scavenging or indirect modulation of expression of some antioxidant enzymes by these typical representatives of natural phenolics.

2. Results and Discussion

2.1. Antiproliferative Activity

The direct scavenging effect and ability to modulate antiradical defense in a model cellular system of the test compounds were analyzed. Before carrying out antioxidant assays in cellular systems, it was necessary to determine the concentrations above which the test compounds became cytotoxic. A model assay employing THP-1 monocytes was used. Diplacone had previously been shown to be non-toxic at a concentration of 10 μM when incubated with THP-1 cells [22]. It had also been found that the half-maximal inhibitory concentration (IC_{50}) of morusin for the THP-1 cells is 24.3 μM [23,24].

The cytotoxic (antiproliferative) activity of the other two test compounds, acteoside and pomiferin, for the THP-1 cell line could not be found in the literature, and it was, therefore, measured using a WST-1 assay kit. As shown in Figure 2, acteoside influenced the viability of THP-1 cells only slightly, even at the high concentration of 50 μM . The information published about cytotoxic effects observed for acteoside is quite inconsistent. Lee et al. measured the cytotoxicity of this compound using the MTT assay on HL-60 human promyelocytic leukemic cells and found the IC_{50} value after a 24 h incubation to be approximately 30 μM [25]. On the other hand, Sgarbossa et al. claimed to find no cytotoxic effect on the immortalized human keratinocyte cell line HaCaT using the MTT assay at a concentration of 200 μM even after 72 h of incubation [26]. Similarly, Nam et al. and Speranza et al. reported no cytotoxic effect on the THP-1 cell line at concentrations of 16 μM and 100 μM , resp. The only difference from our experiment was using the MTT assay, whereas we employed the WST-1 test [27,28].

Pomiferin greatly reduced the viability of THP-1 cells, with an IC_{50} of 1.0 μM (Figure 2), suggesting that it may possess antitumor activity because THP-1 cells are cancer-derived. Our conclusion is consistent with other results. Son et al. found that pomiferin inhibited histone deacetylase (HDAC), an enzyme involved in cell proliferation, and thus may reduce the proliferation of tumor cells. This was confirmed by further experiments with the MTT assay, in which pomiferin inhibited the growth of several human tumor cell lines with IC_{50} ranging from 1 to 5 μM [29]. Similarly, Yang et al. demonstrated the selective antiproliferative activity of pomiferin against the tumorigenic breast epithelial cell line MCF-7 (IC_{50} = 5.2 μM) [30]. Both articles also compared the antiproliferative activity of pomiferin on normal, non-tumor cells—SON et al. employed primary human hepatocytes that were affected much less (IC_{50} = 123 μM) [29]. Yang et al. proved a limited toxicity toward non-tumorigenic breast epithelial cells (MCF-10A) [30].

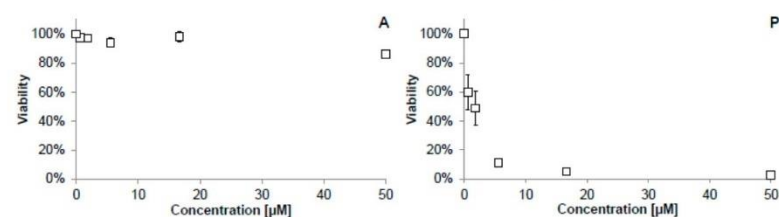


Figure 2. The antiproliferative activity of the test compounds after 24 h of incubation with the THP-1 cell line, measured using a WST-1 kit: (A) acteoside; (P) pomiferin. The viability was calculated as a percentage of the control cells treated only with DMSO.

2.2. Cellular Antioxidant Activity (CAA) Assay

After the cytotoxicity had been evaluated, the overall antioxidant activity of the test compounds was analyzed using the CAA assay. CAA measures the ability of compounds to prevent AAPH-generated peroxy radicals from forming fluorescent DCF in THP-1 cells. AAPH gradually decomposes into carbon-centered radicals that then react rapidly with O_2 to give ROO^\bullet radicals [31]. The compounds were tested at a nontoxic concentration of 5 μ M. The toxicity of pomiferin was not considered problematic because a short incubation time was used for this assay (2 h).

As seen in Figure 3, the most active compound was acteoside, with a CAA value of 85.1 ± 0.7 and activity greater than that of quercetin, the positive control (n.s. difference). The activity of both acteoside and quercetin was significantly higher than that of DMSO, the negative control (NC; Figure 3). The ability of acteoside to scavenge radicals directly has been reported in the literature. Koo et al. showed its DPPH $^\bullet$ and NO^\bullet scavenging activities [16]. Similarly, Siciliano et al. measured the ability of acteoside to scavenge the radical cation 2,2'-azino-bis(3-ethylbenzothiazoline-6-sulfonate) ($ABTS^{\bullet+}$) using the Trolox equivalent antioxidant capacity (TEAC) assay [32]. Further, Li et al. demonstrated the scavenging activity of acteoside in the FRAP and cupric reducing antioxidant capacity (CUPRAC) assays [33]. Moreover, Lee et al. proved the ability of acteoside to scavenge $^\bullet OH$ and $O_2^{\bullet-}$ [34]. The advantage of CAA is that the radical scavenging effect of a compound is measured only inside the cells because after de-esterification DCFH stays inside the cells [35]. It also confirms the ability of acteoside to cross the cell membrane, as shown by Koo et al., who found that acteoside decreased the lipid peroxidation and neurotoxicity of glutamate in cortical cell cultures [16].

Pomiferin showed mild antioxidant activity. It has been reported to be a scavenger of DPPH $^\bullet$ and $O_2^{\bullet-}$ [18,36,37]. Bozkurt et al. also observed that a 300 mg/kg dose of pomiferin administered to rats significantly reduced the lipid peroxidation induced by indomethacin in their stomachs. Lipid peroxidation was measured by determining the levels of malondialdehyde (MDA) [38]. Similarly, Hwang et al. showed the antioxidant activity of the large quantity of pomiferin present in Osage orange extract [39].

Interestingly, neither diplacone nor morusin demonstrated any antioxidant effect in the CAA assay, as seen in Figure 3. Diplacone had previously shown DPPH $^\bullet$ scavenging activity and was the most active of the geranylated flavonoids extracted from *P. tomentosa* [17]. Diplacone has shown activity in other antioxidant methods—scavenging of $ABTS^{\bullet+}$, $O_2^{\bullet-}$, $HClO$, and inhibiting the plasmid DNA oxidative damage caused by the Fenton reaction [36,40,41]. Similarly, Moon et al. showed that incubation cells of the human lymphoblastoid cell line AHH-1 with diplacone and exposing them to γ -radiation protected them from oxidative stress and DNA damage [42]. However, J774A.1 cells incubated for 30 min with diplacone produced almost double the amount of ROS, measured as DCF, as was produced by untreated cells. Although the difference did not appear to be statistically significant, it demonstrated a mild pro-oxidant effect for diplacone [36]. This result is following the conclusion published by Malanik et al. that a crucial structural element for activity in the CAA assay is the 5,7-*m*-dihydroxy arrangement of the flavonoid ring A, with no substituent at C-6. Diplacone has a geranyl moiety at C-6, and its activity in CAA is, therefore, reduced [43].

Hošek et al. have reported that cudraflavone B, a compound structurally similar to morusin, scavenges $HClO$ [36]. On the other hand, incubating this compound with J774A.1 cells alone for 30 min tripled the production of ROS, measured as DCF, compared to untreated cells [36]. However, contradictory results reported in the literature have found morusin reducing the production of ROS in cell cultures. Cheng et al. reported that morusin reduced 12-*O*-tetradecanoylphorbol-13-acetate (TPA)-mediated production of ROS in a mouse epidermal JB6 P $^+$ cell model [19]. Lee et al. reported a decrease in NO^\bullet -induced cell death in neuroblastoma SH-SY5Y cells during incubation with morusin [44]. Similarly, Yang et al. observed that morusin suppresses the production of NO^\bullet in RAW264.7 cells caused by lipopolysaccharide (LPS) and interferon- γ [45]. Moreover, finally, Ko et al.

found that morusin inhibits the formation of $O_2^{\bullet-}$ in rat neutrophils stimulated with phorbol myristate acetate (PMA) [46]. The difference between these findings and our result probably stems from using different cell lines and ROS generators. Morusin was obviously better at counteracting TPA, LPS, NO^{\bullet} , PMA, and radicals formed from them than radicals generated by AAPH.

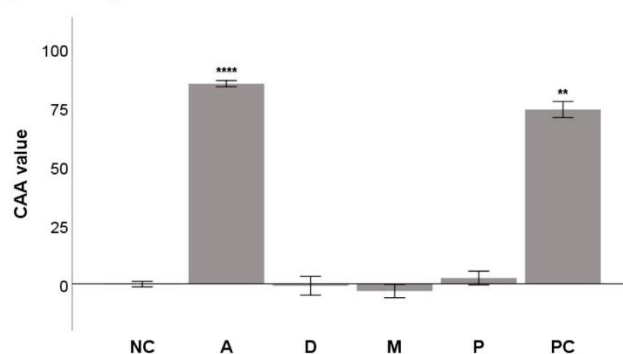


Figure 3. The antioxidant activity of acteoside (A), diplacone (D), morusin (M), and pomiferin (P) at a concentration of 5 μ M in a CAA assay in THP-1 cells. Quercetin at a concentration of 5 μ M was used as a positive control (PC). DMSO, the solvent used for both the test compounds and quercetin, was added as the negative control (NC). The results are expressed as the mean \pm SEM for two independent experiments measured in triplicate and are statistically compared to NC (** $p < 0.01$, and **** $p < 0.0001$).

2.3. Glucose Oxidative Stress Protection (GOSP) Assay

After the CAA assay experiments, acteoside and diplacone were chosen for further evaluation in a GOSP assay. Morusin was not chosen because it showed the lowest values in the CAA assay. Similarly, pomiferin was omitted due to its unfavorable cytotoxicity profile. In the GOSP assay, the cells were exposed to a hyperglycemic condition that increased oxidative stress. The amount of intracellular stress was visualized by the conversion to fluorescent dichlorofluorescein (DCF).

Chronic hyperglycemia is a characteristic condition for diabetes mellitus (DM) that negatively impacts cells and tissues. The toxicity of high levels of glucose manifests itself, especially in the β -cells of the pancreas, where it reduces the secretion of insulin. In other organs, it is responsible for the chronic microvascular complications of DM. The molecular mechanisms of glucose toxicity involve the glycation of proteins via Schiff bases and Amadori compounds that increase ROS production [47]. Overproduction of $O_2^{\bullet-}$ in the mitochondrial electron transport chain (ETC) increased production of ROS as glucose is the main energy source and fuel for ETC [48].

After a 48 h incubation of HepG2 cells in hyperglycemic conditions, both test compounds were able to reduce oxidative stress and the production of DCF to the level of normoglycemia in a statistically significant manner ($p < 0.001$; Figure 4). Both acteoside and diplacone reduced oxidative stress down to 28% of the level of the hyperglycemic condition and were more effective than the quercetin used as a positive control.

El-Marasy et al. have reported that acteoside alleviates oxidative stress in rats with streptozotocin-nicotinamide (STZ-NA)-induced type 2 diabetes [49]. This was observed as reduced levels of malondialdehyde (MDA), a marker of lipid peroxidation. The content of reduced glutathione in the liver was also increased. In addition, acteoside significantly lowered blood glucose levels, glycosylated hemoglobin, and total cholesterol compared to control diabetic rats [49]. Glucose toxicity during hyperglycemia is marked by increased formation of advanced glycation endproducts (AGEs) and greater aldose reductase ac-

tivity. According to the results of Yu et al., both of these parameters were inhibited by acteoside [50].

Zima et al. described the effects of diplacone administered to rats with alloxan-induced diabetes. While the impact of diplacone on glucose levels was minor, the compound showed a cytoprotective effect on β -cells of the islets of Langerhans, which was confirmed by histopathological analysis. The protection of β -cells correlated with the greater antioxidant activity of diplacone than the other compounds examined [41].

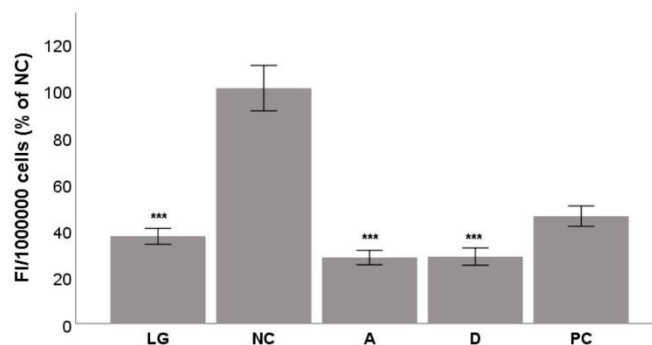


Figure 4. The antioxidant activity of acteoside (A) and diplacone (D) at a nontoxic concentration of 5 μ M in a GOSP assay in HepG2 cells. Quercetin at a concentration of 5 μ M was used as a positive control (PC). DMSO, the solvent used for both the test compounds and quercetin, was added as the negative control (NC). Normoglycemic control was achieved using a low glucose medium (LG). All other samples were incubated in a high-glucose medium. The results are expressed as the mean \pm SEM for two independent experiments measured in triplicate and were statistically compared to NC (*** $p < 0.001$).

2.4. Indirect Antioxidant Activity—Modulation of Antioxidant Enzymes

2.4.1. Protein Expression

Further, it was important to discern whether the test compounds acteoside and diplacone can also protect cells against oxidative stress also by indirect modulation of antioxidant enzymes and not only by the direct scavenging activity shown previously [32,33,36,40,41].

Because the most common representative ROS are $O_2^{\bullet-}$, H_2O_2 , and $\bullet OH$ [51], we chose to evaluate antioxidant enzymes that deal with them, namely CAT, SOD1, and SOD2. We also evaluated the expression of another protein—Nrf2, a transcription factor involved in the antioxidant response of cells. We incubated acteoside and diplacone with THP-1 cells and observed their influence on the level of protein expression.

After incubation periods of 8 and 24 h, acteoside showed almost no influence on the expression of the selected proteins (data not shown). On the other hand, incubation with diplacone increased the level of the CAT enzyme after both 8 h and 24 h. After 8 h of incubation, diplacone treatment increased the level of SOD2 and showed a moderate effect on the expression of Nrf2. After 24 h of incubation, increases were observed in the levels of SOD1 and SOD2. Unfortunately, none of these effects were statistically significant (Figures 5 and 6).

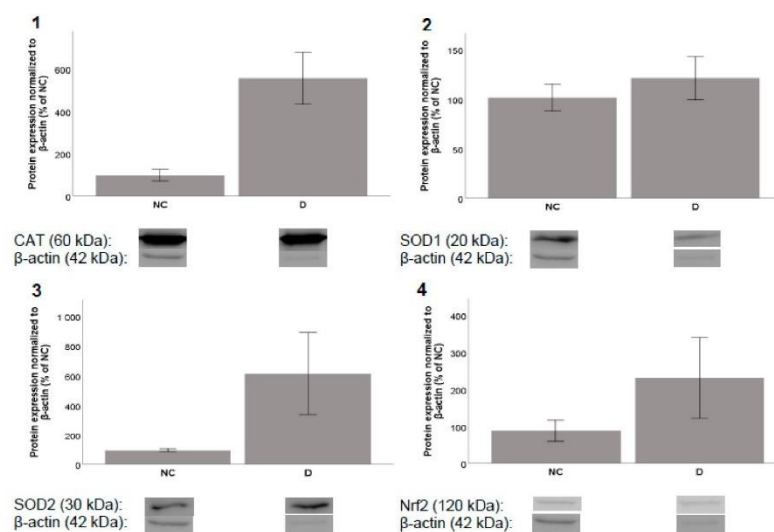


Figure 5. Effects of diplacone (D) at a concentration of 2.5 μ M on the expression of (1) CAT, (2) SOD1, (3) SOD2, and (4) Nrf2 after 8 h incubation with THP-1 cells. DMSO was used as the solvent and was added as the negative control (NC). The results are expressed as the mean \pm SEM and were measured in triplicate.

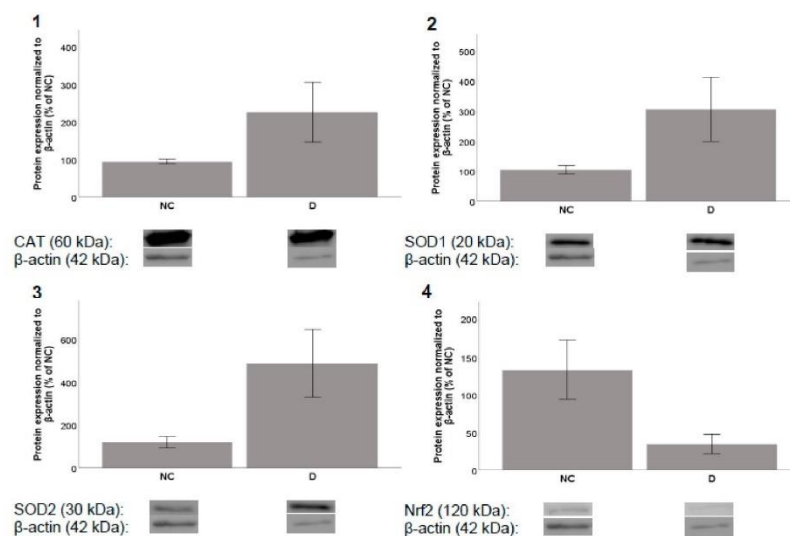


Figure 6. Effects of diplacone (D) at a concentration of 2.5 μ M on the expression of (1) CAT, (2) SOD1, (3) SOD2, and (4) Nrf2 after 24 h incubation with THP-1 cells. DMSO was used as the solvent and was added as the negative control (NC). The results are expressed as the mean \pm SEM and were measured in triplicate.

2.4.2. Gene Expression

To confirm the impact of diplacone, we tried to evaluate it also on the level of mRNA transcription. The results of the experiment are shown in Figure 7. For this experiment, we have chosen genes with elevated protein expression levels after 8 h of incubation. Unfortunately, we did not observe any elevation of the transcription levels of CAT or SOD2 mRNA.

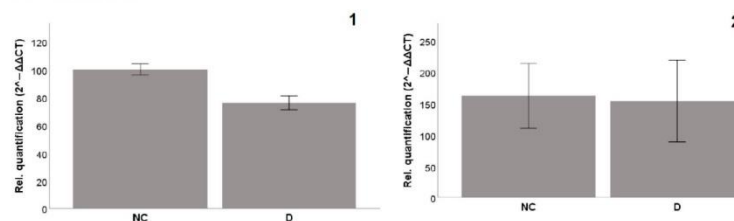


Figure 7. Effects of diplacone (D) at a concentration of 2.5 μ M on the gene expression (mRNA levels) of (1) CAT and (2) SOD2 after 8 h incubation with THP-1 cells. DMSO was used as the solvent and was added as the negative control (NC). The results are expressed as the mean \pm SEM for two independent experiments measured in triplicate.

2.4.3. Activation of the Nrf2-ARE System

Next, we tried to find out if either acteoside or diplacone could support the translocation of Nrf2 to the nucleus and the activation of ARE. Figure 8 shows that the luminescence produced by the ARE luciferase reporter (normalized to Renilla luminescence) did not increase when incubated with acteoside or diplacone. This probably means that neither of these compounds activates the Nrf2-ARE system in HepG2 cells. Both compounds were tested at a nontoxic concentration of 5 μ M.

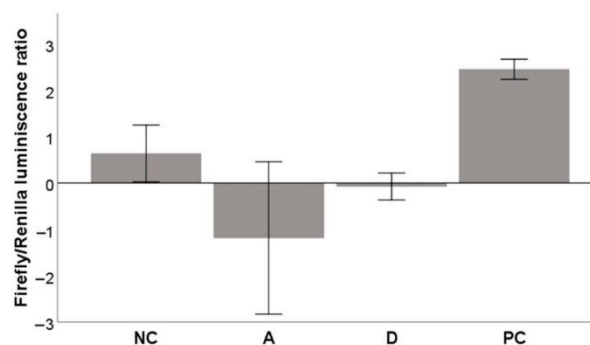


Figure 8. Effects of acteoside (A) and diplacone (D) at a concentration of 5 μ M on the activation of the Nrf2-ARE system. The HepG2 cell model was transiently transfected with the ARE luciferase reporter vector firefly luminescence and a constitutively expressing Renilla vector. The results are expressed as the ratio of firefly to Renilla luminescence. DMSO was used as the solvent and was added as the negative control (NC). DL-sulforaphane at a concentration of 10 μ M was used as a positive control (PC). The results are expressed as the mean \pm SEM for two independent experiments measured in triplicate.

2.4.4. Activity of the Enzyme CAT

Finally, one of the mechanisms contributing to the ability of acteoside and diplacone to help the THP-1 to survive under oxidative stress is an increase in the CAT activity. To discern this possibility, we carried out an experiment with an incubation time of 5 h. The results shown in Figure 9 indicate that both acteoside and diplacone increased CAT

activity with statistical significance ($p < 0.01$ and $p < 0.001$, resp.). The effect of acteoside was slightly greater than that of diplacone.

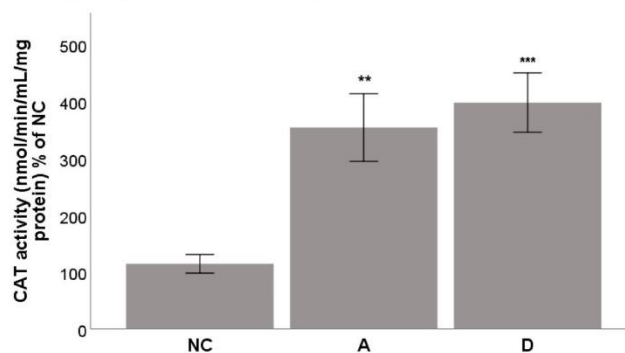


Figure 9. Effects of acteoside (A) and diplacone (D) at a concentration of 5 μ M on the activity of the enzyme CAT. THP-1 cells were incubated with the compounds for 5 h, and then the activity of the enzyme CAT was calculated. DMSO was used as the solvent and was added as the negative control (NC). Results are expressed as the mean \pm SEM for two independent experiments measured in triplicate and were statistically compared to NC (** $p < 0.01$, and *** $p < 0.001$).

Our experiments showed that the antiradical effect of acteoside was expressed more in direct scavenging of ROS in the CAA assay, but it also showed indirectly as an increase in the activity of the CAT enzyme. These two effects also appeared in the GOSP assay. Similarly, Huan et al. have found that acteoside increases the CAT activity in homogenized liver tissue [52]. Our results show that the indirect antiradical effect of acteoside is not related to increased expression of antioxidant enzymes or activation of the Nrf2-ARE system.

In contrast to the results of our experiments, Sgarbossa et al. found acteoside upregulates the expression of heme oxygenase 1 (HO-1) in both mRNA and the protein level in human keratinocyte HaCaT cells. This effect was observed after 24 h of incubation with acteoside at a concentration of 200 μ M. Because the induction of the HO-1 gene is regulated primarily by Nrf2 and BACH1 transcription factors, Sgarbossa et al. also tested the influence of acteoside on the expression of these respective proteins. Whereas the Nrf2 factor activates the ARE sequence, BACH1 plays an inhibitory role. After 24 h of incubation, acteoside increased steady-state nuclear levels of Nrf2 protein and decreased the BACH1 protein levels. According to Sgarbossa et al., the antioxidant effect of acteoside is partially direct (by scavenging) and partially indirect (by activation of enzymes) [26]. We have observed only the direct scavenging effect and the indirect effect on the CAT activity, which can be due to different concentrations and cell cultures. The concentration of acteoside we used in our experiments was 40 \times lower than the one used by Sgarbossa et al. However, their concentration would be obtained in vivo only with difficulty because acteoside is known for its poor bioavailability; its maximum concentration in rat plasma after peroral administration of 200 mg/kg was a mere 0.7 μ M [48].

Surprisingly, diplacone showed no direct antioxidant effect in the CAA assay. On the other hand, its activity in the GOSP assay was comparable to acteoside. Diplacone also induced the expression of antioxidant enzymes, and it increased the activity of catalase in THP-1 cells. Although the results of increased expression are not statistically significant, they show the ability of diplacone to modulate the system of the antiradical defense of cells. Under specific conditions, some antioxidants may behave as pro-oxidants [53]. In the presence of heavy metals and oxygen, even some flavonoids undergo redox cycling and form ROS. A similar thing happens when flavonoids are present at high concentrations in cells [54,55]. These findings could explain why diplacone may act as a weak pro-oxidant in THP-1 cells [36] and thus activate the antioxidant defense system. In our experiment,

we have observed increased Nrf2 protein levels after 8 h incubation. This accords with the overall evaluation of plant polyphenols that generate nanomolar amounts of H_2O_2 and thus act as activators of signaling factors [56]. However, diplacone was not shown to activate the Nrf2-ARE system, which means there may be another mechanism involved.

3. Materials and Methods

3.1. Test Compounds

The test compounds were isolated and characterized at the Faculty of Pharmacy, University of Veterinary and Pharmaceutical Sciences Brno, Brno, Czech Republic [17,18,20,21]. The purity of all compounds tested was confirmed by HPLC analysis to exceed 95% in all cases. All of the test compounds were dissolved in DMSO; the final concentration of DMSO in the cellular assays was 0.1% (v/v).

3.2. Maintenance and Cultivation of the Cell Lines

Both cell lines, THP-1 human monocytic leukemia and HepG2 human hepatoma were purchased from the European Collection of Cell Cultures (Salisbury, UK) and were cultured according to reported procedures [21,57].

3.3. Antiproliferative Activity

The viability of THP-1 cells was measured using the cell proliferation reagent WST-1 (Roche, Basel, Switzerland) according to the manufacturer's manual, as reported previously [58]. The antiproliferative activity of acteoside and pomiferin in THP-1 was screened in five concentrations, ranging from 0.61 to 50 μ M.

3.4. Cellular Antioxidant Activity (CAA) Assay

The antioxidant activity of the test compounds was measured in THP-1 cells using the method of Wolfe and Liu [59] with some modifications, as reported previously [43].

3.5. Glucose Oxidative Stress Protection (GOSP) Assay

The protection against glucose oxidative stress provided by acteoside and diplacone was measured in HepG2 cells using a previously reported assay with some modifications [12,13].

Briefly, the HepG2 cells were incubated in 24-well plates (100,000 cells/well) in a low glucose DMEM growth medium (Biosera, Kansas City, MO, USA; 5 mM glucose) to simulate normoglycemic conditions. High-glucose DMEM growth medium with added glucose (Sigma-Aldrich, Saint Louis, MO, USA) up to 55 mM concentration was used to create hyperglycemic conditions. The cells were incubated with acteoside, diplacone, or quercetin (used as a positive control) in a concentration of 5 μ M. The solvent, DMSO, was used as a negative control (NC).

After 48 h of incubation, the cells were washed with PBS (Biosera) and further incubated for 30 min in a medium containing 10 μ M 2',7'-dichlorodihydrofluorescein-diacetate (DCFH₂-DA; Sigma-Aldrich) dissolved in DMSO (the final concentration of DMSO in the medium was 0.1% (v/v)) at 37 °C. The cells were then washed again with PBS and lysed using trypsin/EDTA 1× (Biosera). The lysates were transferred into a black 96-well plate, and the fluorescence signal of the dichlorofluorescein product was measured using a FLU-Ostar Omega microplate reader (BMG Labtech, Ortenberg, Germany) at the wavelengths λ (ex./em.) = 485/520 nm.

The fluorescence intensity (FI) was recalculated to accord with the number of viable cells obtained from a parallel experiment with the same incubation conditions and measurement of antiproliferative activity using a WST-1 kit. The values of FI/10⁶ viable cells of the NC were assigned as 100%, and other values were referenced to these.

3.6. Indirect Antioxidant Activity—Modulation of Antioxidant Enzymes

3.6.1. Protein Expression

The effects on protein expression of antioxidant enzymes and Nrf2 were observed in the THP-1 cell line using the method reported previously [57,60]. Briefly, the THP-1 cells were incubated in the form of floating monocytes (1×10^6 cells/mL) with diplacone for 8 and 24 h. The cells were collected, and protein lysates were prepared. The lysates were then separated using SDS-PAGE, and the proteins were transferred to polyvinylidene fluoride membranes using Western blotting and visualized using antibodies and a chemiluminescent kit (Bio-Rad, Hercules, CA, USA).

Specific primary antibodies were applied: mouse anti-CAT 1:1000 (Sigma-Aldrich; product No. C0979), rabbit anti-SOD1 1:1000 (Sigma-Aldrich; product No. HPA001401), rabbit anti-SOD2 1:1000 (Sigma-Aldrich; product No. HPA001814), rabbit anti-NRF2 1:1000 (Abcam, Cambridge, UK; product No. ab137550) or mouse anti- β -actin 1:5000 (Abcam; product No. ab8226). After washing, the secondary antibodies were applied: anti-mouse IgG (Sigma-Aldrich; product no. A0168), or anti-rabbit IgG (Sigma-Aldrich; product no. A0545) at a dilution of 1:2000.

3.6.2. Gene Expression

To isolate RNA and evaluate gene expression, the THP-1 cells (floating monocytes, 500,000 cells/mL) were incubated in 100 μ L of a serum-free RPMI 1640 medium and seeded into 96-well plates in triplicate at 37 °C with diplacone at a concentration of 2.5 μ M in DMSO.

After 8 h, the total RNA was isolated from the cells using a RealTime Ready cell lysis kit (Roche, Basel, Switzerland) according to the manufacturer's instructions. The gene expression of CAT, SOD2, or β -actin was quantified by two-step reverse-transcription quantitative (real-time) PCR (RT-qPCR). The reverse transcription step was performed with a Transcriptor Universal cDNA Master (Roche), using cell lysate as the template. The reaction consisted of three steps: (1) primer annealing at 29 °C for 10 min, (2) reverse transcription at 55 °C for 10 min, and (3) transcriptase inactivation at 85 °C for 5 min.

A Fast Start Universal Probe Master (Roche) and gene expression assays (Applied Biosystems, Foster City, CA, USA) were used for qPCR. These assays contain specific primers and TaqMan probes that bind to an exon–exon junction to prevent DNA contamination. The parameters for the qPCR work were adjusted according to the manufacturer's recommendations: 50 °C for 2 min, then 95 °C for 10 min, followed by 40 cycles at 95 °C for 15 s and 60 °C for 1 min. The results were normalized to the amount of ROX reference dye, and the change in gene expression was determined by the $2^{-\Delta\Delta CT}$ method. Transcription of the control cells was set as 100%, and other experimental groups were multiples of this value.

3.6.3. Activation of the Nrf2-ARE System

The activation of the Nrf2-ARE system in HepG2 cells was determined using an ARE reporter kit (BPS Bioscience, San Diego, CA, USA) as described previously [57]. The cells were transiently transfected for 1 h (35,000 cells/well in 96-well plates) with the ARE luciferase reporter vector (firefly luminescence) plus a constitutively expressing Renilla vector using the TransFast transfection reagent (Promega, Madison, WI, USA). After serum recovery, the cells were treated for 24 h with acteoside or diplacone at a concentration of 5 μ M. As a positive control for this experiment, we used DL-sulforaphane (Sigma-Aldrich) at a concentration of 10 μ M dissolved in DMSO, as recommended by ARE reporter kit. Luciferase activity from the cell lysates was detected using a dual-luciferase reporter assay system (Promega, Madison, WI, USA). Data were normalized to the Renilla luminescence.

3.6.4. Activity of the Enzyme CAT

THP-1 cells (floating monocytes, 750,000 cells/mL) were incubated in 2 mL of serum-free RPMI 1640 medium and seeded into 6-well plates in triplicate at 37 °C. The cells

were treated for 5 h with acteoside or diplacone at a concentration of 5 μ M. The cells were then lysed, and the protein concentration was measured using the Bradford method. Then the activity of the CAT enzyme in the cell lysates was measured using a catalase assay kit (Cayman Chemical Company, Ann Arbor, MI, USA) according to the manufacturer's instructions. The activity of CAT was expressed in nmol/min/mL/mg of proteins in the sample.

3.7. Statistical Analysis

Statistical analyses were carried out using IBM SPSS Statistics for Windows, software version 26.0 (Armonk, NY, USA). The data were graphed as the mean \pm SEM. Comparisons between groups were made using a Mann–Whitney U test or Kruskal–Wallis test followed by pair-wise comparison with Bonferroni correction, depending on the number of experiments being compared.

4. Conclusions

We selected four plant phenolics previously determined to have antioxidant activity. Among these compounds, acteoside showed a direct antioxidant effect in a CAA assay. It also showed great activity in a GOSP assay. In both cases, the activity was higher than that of quercetin, the positive control. On the other hand, acteoside did show any effect on the expression of typical antioxidant enzymes or activate the Nrf2-ARE pathway. Instead, it increased only the activity of the enzyme CAT. Diplacone showed an antioxidant effect only in the GOSP assay, not in the CAA assay. This compound showed a positive effect on the expression of the enzymes CAT, SOD1, and SOD2. Again, the activity of enzyme CAT was increased.

Our results show that the antioxidant activity of compounds measured using in vitro chemical assays does not always correspond with an ability to counteract the production of ROS in cell-based systems.

Author Contributions: Conceptualization, J.T. and K.Š.; methodology, J.T.; validation, J.T.; formal analysis, J.T.; investigation, J.T., P.V., and P.H.; resources, J.T. and K.Š.; data curation, J.T.; writing—original draft preparation, J.T.; writing—review and editing, K.Š.; visualization, J.T.; supervision, K.Š.; project administration, J.T.; funding acquisition, K.Š. All authors have read and agreed to the published version of the manuscript.

Funding: This research received no external funding.

Institutional Review Board Statement: Not applicable.

Informed Consent Statement: Not applicable.

Data Availability Statement: Not applicable.

Conflicts of Interest: The authors declare no conflict of interest.

Sample Availability: Samples of the compounds acteoside, diplacone, morusin, and pomiferin are available from the authors.

References

1. Niki, E. Oxidative Stress and Antioxidants: Distress or Eustress? *Arch. Biochem. Biophys.* **2016**, *595*, 19–24. [[CrossRef](#)] [[PubMed](#)]
2. Trembl, J.; Šmejkal, K. Flavonoids as Potent Scavengers of Hydroxyl Radicals. *Compr. Rev. Food Sci. Food Saf.* **2016**, *15*, 720–738. [[CrossRef](#)]
3. Valko, M.; Leibfriz, D.; Moncol, J.; Cronin, M.T.D.; Mazur, M.; Telser, J. Free Radicals and Antioxidants in Normal Physiological Functions and Human Disease. *Int. J. Biochem. Cell Biol.* **2007**, *39*, 44–84. [[CrossRef](#)] [[PubMed](#)]
4. Sies, H. Hydrogen Peroxide as a Central Redox Signaling Molecule in Physiological Oxidative Stress: Oxidative Eustress. *Redox Biol.* **2017**, *11*, 613–619. [[CrossRef](#)] [[PubMed](#)]
5. López-Alarcón, C.; Denicola, A. Evaluating the Antioxidant Capacity of Natural Products: A Review on Chemical and Cellular-Based Assays. *Anal. Chim. Acta* **2013**, *763*, 1–10. [[CrossRef](#)] [[PubMed](#)]
6. Jung, K.-A.; Kwak, M.-K. The Nrf2 System as a Potential Target for the Development of Indirect Antioxidants. *Molecules* **2010**, *15*, 7266–7291. [[CrossRef](#)] [[PubMed](#)]

7. Reisman, S.A.; Yeager, R.L.; Yamamoto, M.; Klaassen, C.D. Increased Nrf2 Activation in Livers from Keap1-Knockdown Mice Increases Expression of Cytoprotective Genes That Detoxify Electrophiles More than Those That Detoxify Reactive Oxygen Species. *Toxicol. Sci.* **2009**, *108*, 35–47. [\[CrossRef\]](#) [\[PubMed\]](#)
8. Ma, Q. Role of Nrf2 in Oxidative Stress and Toxicity. *Annu. Rev. Pharmacol. Toxicol.* **2013**, *53*, 401–426. [\[CrossRef\]](#)
9. Chen, C.; Yu, R.; Owuor, E.D.; Kong, A.N. Activation of Antioxidant-Response Element (ARE), Mitogen-Activated Protein Kinases (MAPKs) and Caspases by Major Green Tea Polyphenol Components during Cell Survival and Death. *Arch. Pharm. Res.* **2000**, *23*, 605–612. [\[CrossRef\]](#)
10. Kweon, M.-H.; In Park, Y.; Sung, H.-C.; Mukhtar, H. The Novel Antioxidant 3-O-Caffeoyl-1-Methylquinic Acid Induces Nrf2-Dependent Phase II Detoxifying Genes and Alters Intracellular Glutathione Redox. *Free Radic. Biol. Med.* **2006**, *40*, 1349–1361. [\[CrossRef\]](#)
11. Surh, Y.-J.; Kundu, J.K.; Na, H.-K. Nrf2 as a Master Redox Switch in Turning on the Cellular Signaling Involved in the Induction of Cytoprotective Genes by Some Chemopreventive Phytochemicals. *Planta Med.* **2008**, *74*, 1526–1539. [\[CrossRef\]](#)
12. Lunder, M.; Roškar, I.; Hošek, J.; Štrukelj, B. Silver Fir (*Abies Alba*) Extracts Inhibit Enzymes Involved in Blood Glucose Management and Protect against Oxidative Stress in High Glucose Environment. *Plant Foods Hum. Nutr.* **2019**, *74*, 47–53. [\[CrossRef\]](#)
13. Chandrasekaran, K.; Swaminathan, K.; Chatterjee, S.; Dey, A. Apoptosis in HepG2 Cells Exposed to High Glucose. *Toxicol. In Vitro* **2010**, *24*, 387–396. [\[CrossRef\]](#)
14. Xu, D.-P.; Li, Y.; Meng, X.; Zhou, T.; Zhou, Y.; Zheng, J.; Zhang, J.-J.; Li, H.-B. Natural Antioxidants in Foods and Medicinal Plants: Extraction, Assessment and Resources. *Int. J. Mol. Sci.* **2017**, *18*, 96. [\[CrossRef\]](#)
15. Tsao, R. Chemistry and Biochemistry of Dietary Polyphenols. *Nutrients* **2010**, *2*, 1231–1246. [\[CrossRef\]](#)
16. Koo, K.A.; Kim, S.H.; Oh, T.H.; Kim, Y.C. Acteoside and Its Aglycones Protect Primary Cultures of Rat Cortical Cells from Glutamate-Induced Excitotoxicity. *Life Sci.* **2006**, *79*, 709–716. [\[CrossRef\]](#)
17. Šmejkal, K.; Grycová, L.; Marek, R.; Lemiére, F.; Jankovská, D.; Forejtníková, H.; Vančo, J.; Suchý, V. C-Geranyl Compounds from *Paulownia tomentosa* Fruits. *J. Nat. Prod.* **2007**, *70*, 1244–1248. [\[CrossRef\]](#)
18. Veselá, D.; Kubínová, R.; Muselík, J.; Žemlička, M.; Suchý, V. Antioxidative and EROD Activities of Osajin and Pomiferin. *Fitoterapia* **2004**, *75*, 209–211. [\[CrossRef\]](#)
19. Cheng, P.-S.; Hu, C.-C.; Wang, C.-J.; Lee, Y.-J.; Chung, W.-C.; Tseng, T.-H. Involvement of the Antioxidative Property of Morusin in Blocking Phorbol Ester-Induced Malignant Transformation of JB6 P+ Mouse Epidermal Cells. *Chem.-Biol. Interact.* **2017**, *264*, 34–42. [\[CrossRef\]](#)
20. Šmejkal, K.; Babula, P.; Šlapetová, T.; Brognara, E.; Dall'Acqua, S.; Žemlička, M.; Innocenti, G.; Cvačka, J. Cytotoxic Activity of C-Geranyl Compounds from *Paulownia tomentosa* Fruits. *Planta Med.* **2008**, *74*, 1488–1491. [\[CrossRef\]](#)
21. Hošek, J.; Bartoš, M.; Chudík, S.; Dall'Acqua, S.; Innocenti, G.; Kartal, M.; Kokoška, L.; Kollár, P.; Kutil, Z.; Landa, P.; et al. Natural Compound Cudraflavone B Shows Promising Anti-Inflammatory Properties In Vitro. *J. Nat. Prod.* **2011**, *74*, 614–619. [\[CrossRef\]](#) [\[PubMed\]](#)
22. Hošek, J.; Závalová, V.; Šmejkal, K.; Bartoš, M. Effect of Dipsacene on LPS-Induced Inflammatory Gene Expression in Macrophages. *Folia Biol. (Praha)* **2010**, *56*, 124–130. [\[PubMed\]](#)
23. Zelová, H.; Hanáková, Z.; Čermáková, Z.; Šmejkal, K.; Dal'Acqua, S.; Babula, P.; Cvačka, J.; Hošek, J. Evaluation of Anti-Inflammatory Activity of Prenylated Substances Isolated from *Morus Alba* and *Morus Nigra*. *J. Nat. Prod.* **2014**, *77*, 1297–1303. [\[CrossRef\]](#) [\[PubMed\]](#)
24. Kollar, P.; Bárta, T.; Hošek, J.; Souček, K.; Závalová, V.M.; Artinian, S.; Talhouk, R.; Šmejkal, K.; Suchý, P.; Hampl, A. Prenylated Flavonoids from *Morus Alba* L. Cause Inhibition of G1/S Transition in THP-1 Human Leukemia Cells and Prevent the Lipopolysaccharide-Induced Inflammatory Response. *Evid.-Based Complement. Altern. Med.* **2013**, *2013*. [\[CrossRef\]](#)
25. Lee, K.-W.; Kim, H.-J.; Lee, Y.S.; Park, H.-J.; Choi, J.-W.; Ha, J.; Lee, K.-T. Acteoside Inhibits Human Promyelocytic HL-60 Leukemia Cell Proliferation via Inducing Cell Cycle Arrest at G0/G1 Phase and Differentiation into Monocyte. *Carcinogenesis* **2007**, *28*, 1928–1936. [\[CrossRef\]](#)
26. Sgarbossa, A.; Dal Bosco, M.; Pressi, G.; Cuzzocrea, S.; Dal Toso, R.; Menegazzi, M. Phenylpropanoid Glycosides from Plant Cell Cultures Induce Heme Oxygenase 1 Gene Expression in a Human Keratinocyte Cell Line by Affecting the Balance of NRF2 and BACH1 Transcription Factors. *Chem.-Biol. Interact.* **2012**, *199*, 87–95. [\[CrossRef\]](#)
27. Nam, S.-Y.; Kim, H.-M.; Jeong, H.-J. Attenuation of IL-32-Induced Caspase-1 and Nuclear Factor- κ B Activations by Acteoside. *Int. Immunopharmacol.* **2015**, *29*, 574–582. [\[CrossRef\]](#)
28. Speranza, L.; Franceschelli, S.; Pesce, M.; Reale, M.; Menghini, L.; Vinciguerra, I.; Lutiis, M.A.D.; Felaco, M.; Grilli, A. Antiinflammatory Effects in THP-1 Cells Treated with Verbascoside. *Phytother. Res.* **2010**, *24*, 1398–1404. [\[CrossRef\]](#)
29. Son, I.H.; Chung, I.-M.; Lee, S.I.; Yang, H.D.; Moon, H.-I. Pomiferin, Histone Deacetylase Inhibitor Isolated from the Fruits of *Maclura Pomifera*. *Bioorg. Med. Chem. Lett.* **2007**, *17*, 4753–4755. [\[CrossRef\]](#)
30. Yang, R.; Hanwell, H.; Zhang, J.; Tsao, R.; Meckling, K.A. Antiproliferative Activity of Pomiferin in Normal (MCF-10A) and Transformed (MCF-7) Breast Epithelial Cells. *J. Agric. Food Chem.* **2011**, *59*, 13328–13336. [\[CrossRef\]](#)
31. Halliwell, B.; Gutteridge, J. *Free Radicals in Biology and Medicine*, 4th ed.; Oxford University Press: Oxford, UK, 2007; ISBN 978-0-19-856869-8.

32. Siciliano, T.; Bader, A.; Vassallo, A.; Braca, A.; Morelli, I.; Pizza, C.; De, T. Secondary Metabolites from *Ballota Undulata* (Lamiaceae). *Biochem. Syst. Ecol.* **2005**, *33*, 341–351. [\[CrossRef\]](#)
33. Li, X.; Xie, Y.; Li, K.; Wu, A.; Xie, H.; Guo, Q.; Xue, P.; Maleshibek, Y.; Zhao, W.; Guo, J.; et al. Antioxidation and Cytoprotection of Acteoside and Its Derivatives: Comparison and Mechanistic Chemistry. *Molecules* **2018**, *23*, 498. [\[CrossRef\]](#)
34. Lee, H.-D.; Kim, J.H.; Pang, Q.Q.; Jung, P.-M.; Cho, E.J.; Lee, S. Antioxidant Activity and Acteoside Analysis of *Abeliophyllum Distichum*. *Antioxidants* **2020**, *9*, 1148. [\[CrossRef\]](#)
35. Kalyanaraman, B.; Darley-Usmar, V.; Davies, K.J.A.; Dennery, P.A.; Forman, H.J.; Grisham, M.B.; Mann, G.E.; Moore, K.; Roberts, L.J.; Ischiropoulos, H. Measuring Reactive Oxygen and Nitrogen Species with Fluorescent Probes: Challenges and Limitations. *Free Radic. Biol. Med.* **2012**, *52*, 1–6. [\[CrossRef\]](#)
36. Hošek, J.; Toniolo, A.; Neuwirth, O.; Bolego, C. Prenylated and Geranylated Flavonoids Increase Production of Reactive Oxygen Species in Mouse Macrophages but Inhibit the Inflammatory Response. *J. Nat. Prod.* **2013**, *76*, 1586–1591. [\[CrossRef\]](#)
37. Orhan, I.E.; Senol, F.S.; Demirci, B.; Dvorska, M.; Smejkal, K.; Zemlicka, M. Antioxidant Potential of Some Natural and Semi-Synthetic Flavonoid Derivatives and the Extracts from *Maclura Pomifera* (Rafin.) Schneider (Osage Orange) and Its Essential Oil Composition. *Turk. J. Chem.* **2016**, *41*, 403–411. [\[CrossRef\]](#)
38. Bozkurt, İ.; Dilek, E.; Erol, H.S.; Çakir, A.; Hamzaoglu, E.; Koç, M.; Keleş, O.N.; Halici, M.B. Investigation on the Effects of Pomiferin from *Maclura Pomifera* on Indomethacin-Induced Gastric Ulcer: An Experimental Study in Rats. *Med. Chem. Res.* **2017**, *26*, 2048–2056. [\[CrossRef\]](#)
39. Hwang, H.-S.; Winkler-Moser, J.K.; Tisserat, B.; Harry-O'kuru, R.E.; Berhow, M.A.; Liu, S.X. Antioxidant Activity of Osage Orange Extract in Soybean Oil and Fish Oil during Storage. *J. Am. Oil Chem. Soc.* **2021**, *98*, 73–87. [\[CrossRef\]](#)
40. Trembl, J.; Šmejkal, K.; Hošek, J.; Žemlička, M. Determination of Antioxidant Activity Using Oxidative Damage to Plasmid DNA—Pursuit of Solvent Optimization. *Chem. Pap.* **2013**, *67*, 484–489. [\[CrossRef\]](#)
41. Zima, A.; Hošek, J.; Trembl, J.; Muselik, J.; Suchý, P.; Pražanová, G.; Lopes, A.; Žemlička, M. Antiradical and Cytoprotective Activities of Several C-Geranyl-Substituted Flavanones from *Paulownia Tomentosa* Fruit. *Molecules* **2010**, *15*, 6035–6049. [\[CrossRef\]](#)
42. Moon, H.-I.; Jeong, M.H.; Jo, W.S. Protective Activity of C-Geranylflavonoid Analogs from *Paulownia Tomentosa* against DNA Damage in 137Cs Irradiated AHH-1 Cells. *Nat. Prod. Comm.* **2014**, *9*. [\[CrossRef\]](#)
43. Malaník, M.; Trembl, J.; Leláková, V.; Nykodýmová, D.; Oravec, M.; Marek, J.; Šmejkal, K. Anti-Inflammatory and Antioxidant Properties of Chemical Constituents of *Broussonetia Papyrifera*. *Bioorg. Chem.* **2020**, *104*, 104298. [\[CrossRef\]](#) [\[PubMed\]](#)
44. Lee, H.J.; Lyu, D.H.; Koo, U.; Nam, K.-W.; Hong, S.S.; Kim, K.O.; Kim, K.H.; Lee, D.; Mar, W. Protection of Prenylated Flavonoids from *Mori Cortex Radicis* (Moraceae) against Nitric Oxide-Induced Cell Death in Neuroblastoma SH-SY5Y Cells. *Arch. Pharm. Res.* **2012**, *35*, 163–170. [\[CrossRef\]](#) [\[PubMed\]](#)
45. Yang, Z.-G.; Matsuzaki, K.; Takamatsu, S.; Kitanaka, S. Inhibitory Effects of Constituents from *Morus Alba* Var. *Multicaulis* on Differentiation of 3T3-L1 Cells and Nitric Oxide Production in RAW264.7 Cells. *Molecules* **2011**, *16*, 6010–6022. [\[CrossRef\]](#) [\[PubMed\]](#)
46. Ko, H.-H.; Wang, J.-J.; Lin, H.-C.; Wang, J.-P.; Lin, C.-N. Chemistry and Biological Activities of Constituents from *Morus Australis*. *Biochim. Biophys. Acta Gen. Subj.* **1999**, *1428*, 293–299. [\[CrossRef\]](#)
47. Kawahito, S.; Kitahata, H.; Oshita, S. Problems Associated with Glucose Toxicity: Role of Hyperglycemia-Induced Oxidative Stress. *World J. Gastroenterol.* **2009**, *15*, 4137–4142. [\[CrossRef\]](#) [\[PubMed\]](#)
48. Burgos-Morón, E.; Abad-Jiménez, Z.; Martínez de Marañón, A.; Iannantuoni, F.; Escribano-López, I.; López-Domènech, S.; Salom, C.; Jover, A.; Mora, V.; Roldan, I.; et al. Relationship between Oxidative Stress, ER Stress, and Inflammation in Type 2 Diabetes: The Battle Continues. *J. Clin. Med.* **2019**, *8*, 1385. [\[CrossRef\]](#)
49. El-Marasy, S.A.; El-Shenawy, S.M.; Moharram, F.A.; El-Sherbeeny, N.A. Antidiabetic and Antioxidant Effects of Acteoside from *Jacaranda Mimosifolia* Family Biognoniaceae in Streptozotocin–Nicotinamide Induced Diabetes in Rats. *Open Access Maced. J. Med. Sci.* **2020**, *8*, 125–133. [\[CrossRef\]](#)
50. Yu, S.Y.; Lee, I.-S.; Jung, S.-H.; Lee, Y.M.; Lee, Y.-R.; Kim, J.-H.; Sun, H.; Kim, J.S. Caffeoylated Phenylpropanoid Glycosides from *Brandisia Hancei* Inhibit Advanced Glycation End Product Formation and Aldose Reductase In Vitro and Vessel Dilation in Larval Zebrafish In Vivo. *Planta Med.* **2013**, *79*, 1705–1709. [\[CrossRef\]](#)
51. Milkovic, L.; Cipak Gasparovic, A.; Cindric, M.; Mouthuy, P.-A.; Zarkovic, N. Short Overview of ROS as Cell Function Regulators and Their Implications in Therapy Concepts. *Cells* **2019**, *8*, 793. [\[CrossRef\]](#)
52. Huan, S.K.-H.; Wang, K.-T.; Lee, C.-J.; Sung, C.-H.; Chien, T.-Y.; Wang, C.-C. Wu-Chia-Pi Solution Attenuates Carbon Tetrachloride-Induced Hepatic Injury through the Antioxidative Abilities of Its Components Acteoside and Quercetin. *Molecules* **2012**, *17*, 14673–14684. [\[CrossRef\]](#)
53. Carrocho, M.; Ferreira, I.C.F.R. A Review on Antioxidants, Prooxidants and Related Controversy: Natural and Synthetic Compounds, Screening and Analysis Methodologies and Future Perspectives. *Food Chem. Toxicol.* **2013**, *51*, 15–25. [\[CrossRef\]](#)
54. Galati, G.; O'Brien, P.J. Potential Toxicity of Flavonoids and Other Dietary Phenolics: Significance for Their Chemopreventive and Anticancer Properties. *Free Radic. Biol. Med.* **2004**, *37*, 287–303. [\[CrossRef\]](#)
55. Procházková, D.; Boušová, I.; Wilhelmová, N. Antioxidant and Prooxidant Properties of Flavonoids. *Fitoterapia* **2011**, *82*, 513–523. [\[CrossRef\]](#)

56. Kanner, J. Polyphenols by Generating H_2O_2 , Affect Cell Redox Signaling, Inhibit PTPs and Activate Nrf2 Axis for Adaptation and Cell Surviving: In Vitro, In Vivo and Human Health. *Antioxidants* **2020**, *9*, 797. [[CrossRef](#)]
57. Trembl, J.; Leláková, V.; Šmejkal, K.; Paulířková, T.; Labuda, Š.; Granica, S.; Havlík, J.; Jankovská, D.; Padrtová, T.; Hošek, J. Antioxidant Activity of Selected Stilbenoid Derivatives in a Cellular Model System. *Biomolecules* **2019**, *9*, 468. [[CrossRef](#)]
58. Hanáková, Z.; Hošek, J.; Babula, P.; Dall'Acqua, S.; Václavík, J.; Šmejkal, K. C-Geranylated Flavanones from Paulownia Tomentosa Fruits as Potential Anti-Inflammatory Compounds Acting via Inhibition of TNF- α Production. *J. Nat. Prod.* **2015**, *78*, 850–863. [[CrossRef](#)]
59. Wolfe, K.L.; Liu, R.H. Cellular Antioxidant Activity (CAA) Assay for Assessing Antioxidants, Foods, and Dietary Supplements. *J. Agric. Food Chem.* **2007**, *55*, 8896–8907. [[CrossRef](#)]
60. Trembl, J.; Šalamúnová, P.; Hanuš, J.; Hošek, J. The Effect of Curcumin Encapsulation into Yeast Glucan Particles on Antioxidant Enzyme Expression In Vitro. *Food Funct.* **2021**. [[CrossRef](#)]

6.6. ARTICLE 6

Malanik, M.; **Treml, J.**; Lelakova, V.; Nykodymova, D.; Oravec, M.; Marek, J.; Smejkal, K. *Bioorganic Chemistry* 2020, 104, 104298 (IF=5.275).



Anti-inflammatory and antioxidant properties of chemical constituents of *Broussonetia papyrifera*

Milan Malaník^{a,*}, Jakub Trembl^b, Veronika Leláková^b, Daniela Nykodýmová^b, Michal Oravec^c, Jaromír Marek^d, Karel Šmejkal^a

^a Department of Natural Drugs, Faculty of Pharmacy, Masaryk University, Palackého třída 1946/1, 61200 Brno, Czech Republic

^b Department of Molecular Pharmacy, Faculty of Pharmacy, Masaryk University, Palackého třída 1946/1, 61200 Brno, Czech Republic

^c Global Change Research Institute of the Czech Academy of Sciences, Bělá 986/4a, 60300 Brno, Czech Republic

^d X-ray Diffraction and Bio-SAXS Core Facility, Central European Institute of Technology, Masaryk University, Kamenice 5, 62500 Brno, Czech Republic

ARTICLE INFO

Keywords:

Broussonetia papyrifera

Anti-inflammatory

Antioxidant

NF-κB

ABSTRACT

Extensive phytochemical analysis of the CHCl₃-soluble part of an ethanolic extract of branches and twigs of *Broussonetia papyrifera* led to the isolation of fourteen compounds, including a novel 5,11-dioxabenzob[fluorene]-10-one derivative named broussonetofluorenone C (12). The isolated compounds 1–14 were characterized based on their NMR and HRMS data, and examined for their anti-inflammatory activities in LPS-stimulated THP-1 cells as well as for their cellular antioxidant effects. Compounds 7–10 and 12 showed inhibitory effects on NF-κB/AP-1 activation and compounds 7–9 were subsequently confirmed to suppress the secretion of both IL-1β and TNF-α in LPS-stimulated THP-1 cells more significantly than the prednisone used as a positive control. In the CAA assay, compound 10 exhibited the greatest antioxidant effect, greater than that of the quercetin used as a positive control. The results show possible beneficial effects and utilization of *B. papyrifera* wood in the treatment of inflammatory diseases as well as oxidative stress.

1. Introduction

Broussonetia papyrifera (L.) L'Hér. ex Vent. (Moraceae), commonly known as paper mulberry, is native to Southeast Asia. It has been introduced to other countries throughout the world to be cultivated as a roadside tree and for paper production. Different parts of *B. papyrifera* are used in both industry and medicine. Its roots, bark, branches, and fruits have traditionally been used in Chinese folk medicine to promote diuresis, arrest bleeding, and suppress edema [1]. Extracts, as well as pure compounds, have exhibited antioxidant, anti-inflammatory, anti-diabetic, antibacterial, and antiproliferative properties [2,3]. Previous phytochemical investigations revealed that *B. papyrifera* is a rich source of bioactive phenolic substances such as coumarins, lignans, 1,3-diphenylpropanes, chalcones, flavans, or flavonols, especially those containing a prenyl group [2,3].

Paper mulberry currently attracts researchers as a source of anti-inflammatory agents. The root bark of *B. papyrifera*, is extensively studied, although Lin et al. [4] observed no significant differences in a comparative study of the anti-inflammatory and antinociceptive activity of its various parts. The root bark extract inhibited both the TNF-α-induced NF-κB transcriptional activity and the expression of pro-

inflammatory genes in 3T3-L1 adipocytes [5]. Another study showed that flavonoids isolated from the root bark of *B. papyrifera* significantly suppressed the production of pro-inflammatory mediators (NO, iNOS, TNF-α, and IL-6) in LPS-stimulated RAW264.7 cells [6], whereas other phenolics did not inhibit IL-6, IL-2 and TNF-α production in Jurkat cells [7]. On the other hand, the only information about the chemical composition and potential biological activity of woody parts of the plant is a report by Xu et al. [8] describing the radical scavenging activity of wood extracts. Therefore, as a part of an ongoing investigation of anti-inflammatory agents obtained from plants of the family Moraceae and in connection with a recently published comprehensive review that summarized the anti-inflammatory effects of prenylated phenolic compounds [9], the branches and twigs of *B. papyrifera* have been subjected to extensive chromatographic separation to isolate analogous compounds as potential lead substances to suppress inflammation. The inflammatory response of cells of the immune system is connected to the “respiratory burst” by which an infecting agent is destroyed. However, in the case of chronic inflammation or autoimmune disease, the inflammatory/oxidative environment can trigger cellular damage [10]. Therefore, this research is aimed at finding natural products that combat inflammation as well as oxidative stress.

* Corresponding author.

E-mail addresses: milan.malanik@seznam.cz (M. Malaník), karel.mejkal@post.cz (K. Šmejkal).

<https://doi.org/10.1016/j.bioorg.2020.104298>

Received 19 June 2020; Received in revised form 20 August 2020; Accepted 16 September 2020

Available online 19 September 2020

0045-2068/ © 2020 Elsevier Inc. All rights reserved.

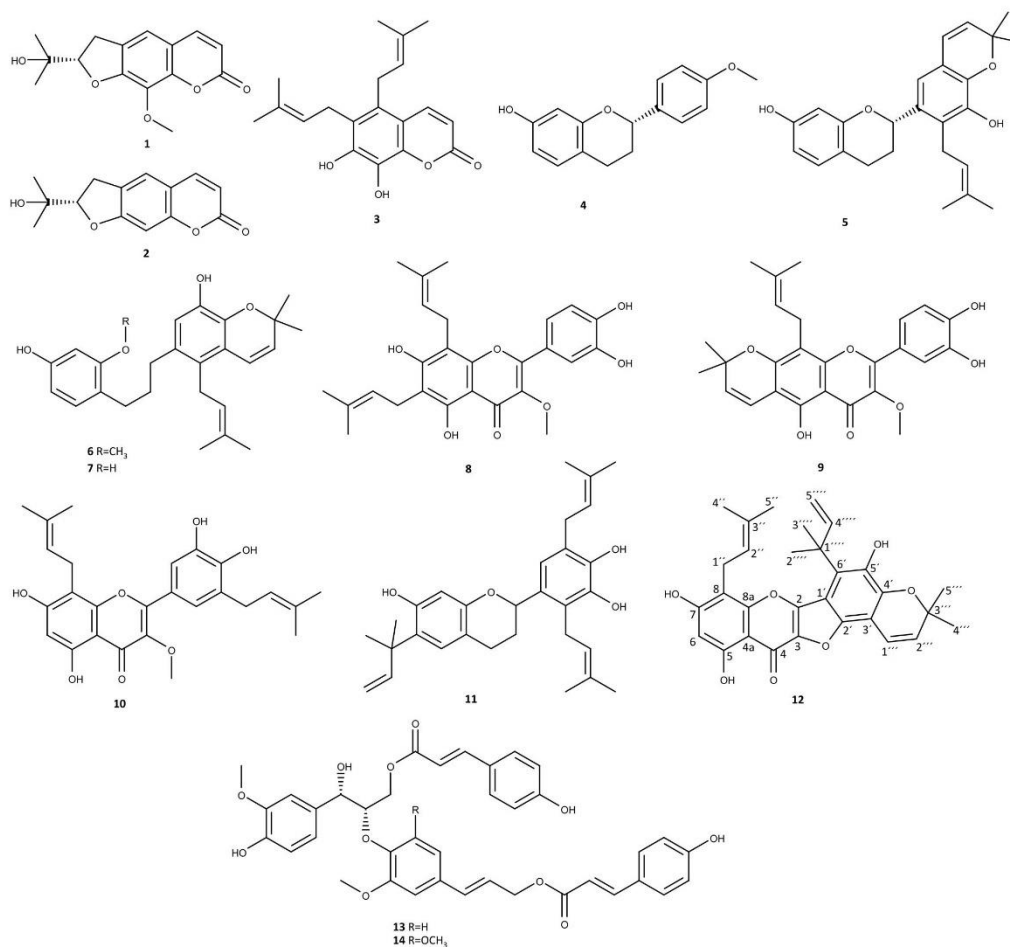


Fig. 1. Structures of the compounds 1–14 isolated from branches and twigs of *B. papyrifera*.

Herein, the isolation and elucidation of the structures of fourteen compounds (Fig. 1) along with the evaluation of their ability to attenuate the activity of NF- κ B/AP-1 in LPS-stimulated THP-1 macrophages and their cellular antioxidant activities are reported.

2. Materials and methods

2.1. General experimental procedures

Optical rotations were measured on an automatic polarimeter AA-5. UV and ECD spectra were recorded on a JASCO J-815 CD spectrometer. IR spectra were determined by the ATR method with a Nicolet Impact 410 FT-IR spectrometer. ^1H NMR and 2D experiments were obtained using a JEOL ECZR 400 MHz spectrometer. ^{13}C NMR spectra were recorded on a Bruker Avance III spectrometer equipped with a broad band fluorine observation SmartProbe TM. The signal of TMS or the residual solvent signals of CD_3OD , CDCl_3 , or $\text{DMSO}-d_6$ were used for reference. HRMS analysis was performed using an LTQ Orbitrap XL-

high resolution mass spectrometer equipped with a HESI II (Heated electrospray ionization) source. Samples were analyzed twice on HPLC-HRMS with the positive and negative polarity of MS-Orbitrap. Column chromatography (CC) was carried out using silica gel with a particle size of 40–63 μm (Merck, USA). Analytical HPLC was measured on an Agilent 1100 instrument equipped with a DAD using an Ascentis Express RP-Amide analytical column (100 mm \times 2.1 mm, particle size 2.7 μm). Dionex UltiMate 3000 liquid chromatograph with an Ascentis RP-Amide column (250 mm \times 10 mm, particle size 5 μm) was used for preparative purposes. HPLC solvents (MeOH and MeCN) were purchased from VWR International, France, and other analytical grade solvents from Lach-Ner, Czech Republic.

2.2. Plant material

The branches and twigs of *B. papyrifera* (L.) L'Hér. ex Vent. were collected during May 2017 in the greenhouse of the Faculty of Pharmacy, Masaryk University (MU), Brno, Czech Republic, and

identified by Assoc. Prof. Karel Šmejkal. A voucher specimen (BP052017) has been deposited in the herbarium of the Department of Natural Drugs, MU.

2.3. Extraction and isolation

The air-dried and chopped branches and twigs of *B. papyrifera* (3.2 kg) were extracted with 96% EtOH (3 × 24 h) at room temperature using ultrasonication to support the extraction process. The solvent was removed using a rotavapor to obtain 143 g of crude extract that was partitioned consecutively with *n*-hexane, CHCl₃, and EtOAc. The CHCl₃-soluble extract (30.9 g) was subjected to silica gel CC (*n*-hexane:CHCl₃:MeOH, 10:80:10, v/v/v) to afford twenty-three fractions (BP-1 to BP-23). Fraction BP-7 was subjected to silica gel CC (CHCl₃:EtOAc, 85:15, v/v) to yield twelve subfractions (BP-7-A to BP-7-L). Subsequently, selected subfractions were purified by means of preparative HPLC with an Ascentis RP-Amide column (250 mm × 10 mm, 5 μm) using a further defined mixture of MeCN and 0.2% HCOOH (5 mL/min). Subfraction BP-7-D was purified using gradient elution (55–80% MeCN, 25 min) to obtain compounds **4** (5 mg, *t_R* = 9.5 min), **5** (20 mg, *t_R* = 19.4 min), and **6** (4 mg, *t_R* = 20.2 min). Subfraction BP-7-H was separated using gradient elution (25–30% MeCN, 25 min) to afford compounds **2** (72 mg, *t_R* = 15.6 min) and **1** (10 mg, *t_R* = 16.7 min). Subfraction BP-7-I was separated with a gradient elution (50–70% MeCN, 20 min) to afford compound **3** (3 mg, *t_R* = 18.5 min). Fraction BP-8 was subjected to silica gel CC (CHCl₃:toluene:MeOH, 80:5:15, v/v/v) to yield nine subfractions (BP-8-A to BP-8-I). Purification of subfraction BP-8-H with a gradient elution (40–100% MeCN, 30 min) afforded compounds **8** (4 mg, *t_R* = 25.5 min) and **9** (12 mg, *t_R* = 28.6 min). Fraction BP-10 was subjected to silica gel CC (*n*-hexane:EtOAc:MeOH, 65:30:5, v/v/v) to afford twelve subfractions (BP-10-A to BP-10-L). Subfraction BP-10-B was purified with a gradient elution (70–100% MeCN, 30 min) to give compounds **11** (5 mg, *t_R* = 17.3 min) and **12** (3 mg, *t_R* = 28.0 min). Purification of subfraction BP-10-D with a gradient elution (30–100% MeCN, 30 min) afforded compound **10** (7 mg, *t_R* = 28.1 min). Fraction BP-12 was subjected to silica gel CC (CHCl₃:EtOAc:MeOH, 90:5:5, v/v/v) to yield fourteen subfractions (BP-12-A to BP-12-N). Subfraction BP-12-E was purified with a gradient elution (50–70% MeCN, 25 min) to give **13** (15 mg, *t_R* = 15.0 min), **14** (8 mg, *t_R* = 16.1 min), and **7** (8 mg, *t_R* = 19.3 min).

2.3.1. Broussoufluorenone C (**12**)

Amorphous yellow powder; UV (MeOH) λ_{max} (log ε) 242 (4.60), 268 (4.62), 302 (4.60) nm, 370 (4.63) nm; IR (ATR) ν_{max} 3354, 2919, 2844, 1651, 1608, 1575, 1456, 1367, 1281, 1230, 1124, 1031 cm⁻¹; ¹H NMR (CDCl₃, 400 MHz) δ 12.76 (1H, s, 5-OH), 6.91 (1H, d, *J* = 10.0 Hz, H-1"), 6.38 (1H, dd, *J* = 10.5, 17.4 Hz, H-4"), 6.37 (1H, s, H-6), 5.96 (1H, s, 7-OH), 5.90 (1H, s, 5'-OH), 5.74 (1H, d, *J* = 10.0 Hz, H-2"), 5.24 (1H, t, *J* = 6.8 Hz, H-2"), 4.89 (1H, d, *J* = 10.5 Hz, H-5a"), 4.67 (1H, d, *J* = 17.4 Hz, H-5b"), 3.66 (2H, d, *J* = 6.8 Hz, H-1'), 1.88 (3H, s, H-5'), 1.78 (3H, s, H-4'), 1.74 (6H, s, H-2"), 1.55 (6H, s, H-4", H-5"); ¹³C NMR (CDCl₃, 125.27 MHz) δ 170.7 (C, C-4), 161.1 (C, C-5), 160.4 (C, C-7), 154.7 (C, C-8a), 149.9 (CH, C-2), 149.8 (CH, C-4"), 146.8 (C, C-2'), 143.2 (C, C-4'), 141.8 (C, C-5'), 138.7 (C, C-3), 135.0 (C, C-3'), 132.1 (C, C-1'), 130.0 (CH, C-2"), 124.5 (C, C-6'), 121.2 (CH, C-2"), 115.1 (CH, C-1"), 111.3 (CH₂, C-5"), 109.8 (C, C-4a), 105.3 (C, C-8), 104.7 (C, C-3'), 99.8 (CH, C-6), 79.7 (C, C-3"), 43.1 (C, C-1"), 31.3 (CH₃, C-2"), 31.3 (CH₃, C-3"), 28.3 (CH₃, C-4"), 28.3 (CH₃, C-5"), 25.8 (CH₃, C-4'), 22.4 (CH₂, C-1'), 18.1 (CH₃, C-5"); HRESIMS [M+H]⁺ *m/z* 503.2065 (calcd for C₃₀H₃₁O₇, 503.2069).

2.4. X-ray crystallographic analysis of compounds **1** and **2**

Single crystals of **1** and **2** were obtained by vapor diffusion of MeOH

at reduced temperature (4–8 °C). X-ray diffraction data were collected at 120(2) K with the Rigaku MicroMax-007 HF DW X-ray generator and the Rigaku Saturn944 + CCD detector using Mo Kα radiation (λ = 0.710 73 Å), and the crystal structure was solved by direct methods and refined by full matrix least-squares methods using SHELXT [11] and SHELXL [12]. Crystallographic data for **1** (CCDC 2002495) have been deposited with the Cambridge Crystallographic Data Centre. Copies of the data can be obtained, free of charge, on application to the Director, CCDC, 12 Union Road, Cambridge CB2 1EZ, UK (fax: +44-(0) 1223-336033 or e-mail: deposit@ccdc.cam.ac.uk).

2.5. Cell culture

The THP-1 human monocytic leukemia cell line was purchased from the European Collection of Authenticated Cell Cultures (Salisbury, UK). The THP-1-XBlue™-MD2-CD14 cell line was purchased from Invivogen (San Diego, CA, USA). Both cell lines were cultured as reported previously [13].

2.6. Cell viability testing

The viability of THP-1 cells was measured using the cell proliferation reagent WST-1 (Roche, Basel, Switzerland) according to the manufacturer's manual as reported previously [14].

2.7. Detection of the activation of NF-κB/AP-1

The activity of transcriptional factors NF-κB/AP-1 was evaluated on the THP-1-XBlue™-MD2-CD14 cell line expressing an NF-κB/AP-1-inducible secreted embryonic alkaline phosphatase (SEAP) reporter gene. The cells were treated with the test compounds dissolved in DMSO at a concentration of 1 μM. After a 1 h incubation, cells were stimulated by LPS 1 μg/mL. The activity of NF-κB/AP-1 was determined after 24 h using Quanti-Blue reagent (Invivogen, San Diego, CA, USA), as reported previously [15].

2.8. Differentiation into macrophages and evaluation of cytokine secretion

THP-1 monocytes (1.5 × 10⁵/well in 24-well plates) were differentiated to macrophages using phorbol myristate acetate (PMA) according to the same protocol described previously [16]. Cells were incubated with the test compounds dissolved in DMSO at a concentration of 1 μM and stimulated by LPS (1 μg/mL) 1 h later. The concentrations of the secreted cytokines IL-1β and TNF-α were measured after 24 h using Human IL-1β and TNF-α ELISA Kit (Dialone, Besançon, France) according to the manufacturer's manual. The experiments were performed in the same manner as reported previously [17].

2.9. Cellular antioxidant activity (CAA) assay

The antioxidant activity of the compounds was measured using the method of Wolfe and Liu [18] with some modifications. THP-1 cells (floating monocytes, 600 000 cells/mL) were pre-incubated for 1 h in serum-free RPMI 1640 medium containing 25 μM 2',7'-dichlorodihydrofluorescein-diacetate (DCFH₂-DA; Sigma-Aldrich) dissolved in DMSO [the final concentration of DMSO in the medium was 0.1% (v/v)] at 37 °C. After the incubation, the cells were centrifuged, washed with PBS, re-suspended in serum-free RPMI 1640 medium and seeded into 96-well plate in triplicate (60 000 cells/well). The cells were then incubated with the test compounds dissolved in DMSO at a concentration of 5 μM for 1 h. The cells were then incubated with 600 μM 2,2'-azobis(2-methylpropionamide) dihydrochloride (AAPH; Sigma Aldrich) to induce the generation of ROS. The plate was immediately placed into a FLUOstar Omega microplate reader (BMG Labtech) at 37 °C. The level of oxidized fluorescent 2',7'-dichlorodihydrofluorescein (DCF) was measured every 5 min for 1 h with excitation at

485 nm and emission at 538 nm. Each plate included triplicate control and blank wells: control wells contained cells treated with DCFH-DA and oxidant; blank wells contained cells treated with the dye and serum-free RPMI 1640 medium but without oxidant. Quercetin was used as a positive control at the same concentration as the test compounds.

After the blank was subtracted from the fluorescence readings, the area under the curve of fluorescence versus time was integrated to calculate the CAA values of the test compounds: CAA unit = $100 \cdot (\int SA / \int CA) \times 100$, where $\int SA$ is the integrated area under the sample fluorescence versus time curve and $\int CA$ is the integrated area obtained from the control curve.

2.10. Statistical analysis

Statistical analyses were carried out using GraphPad Prism 6.01 software (San Diego, CA, USA). The data were graphed as the mean \pm SEM. Comparisons between groups were made using a Kruskal Wallis test followed by Dunn's multiple comparisons test.

3. Results and discussion

3.1. Isolation of compounds and elucidation of structures

In total, fourteen compounds including a novel 5,11-dioxabenzofluoren-10-one, broussoufluorenone C (**12**), were isolated from the CHCl_3 -soluble part of an ethanolic extract of branches and twigs of *B. papyrifera*. The isolated compounds **1–14** were identified by conscientious evaluation of their NMR and MS data. The absolute configurations of compounds containing the chiral center were elucidated by a combination of NMR, optical rotations, electronic circular dichroism (ECD), and comparison with the data in the literature. In addition, the absolute configurations of furanocoumarins **1** and **2** were unambiguously determined by single-crystal X-ray crystallography as obtained ECD data were in contrast with the data published previously [19]. Accordingly, (S)-8-methoxymarmesin (**1**) [20], (S)-marmesin (**2**) [20], fipsovin (**3**) [21], broussin (**4**) [22], kazinol B (**5**) [23], kazinol N (**6**) [24], kazinol M (**7**) [24], broussouflavonol B (**8**) [25], broussouflavonol A (**9**) [25], 5,7,3',4'-tetrahydroxy-3-methoxy-8,5'-diprenylflavone (**10**) [26], kazinol Q (**11**) [27], *threo*-dadahol B (**13**) [28], and *threo*-dadahol A (**14**) [29] were identified and together with broussoufluorenone C (**12**) subsequently evaluated in biological assays.

Compound **12** was obtained as an amorphous yellow powder. Its molecular formula was established as $\text{C}_{30}\text{H}_{30}\text{O}_7$ based on the HRESIMS ion at m/z 503.2065 $[\text{M} + \text{H}]^+$ (calcd for $\text{C}_{30}\text{H}_{31}\text{O}_7$, 503.2069). The ^1H NMR data of **12** exhibited resonances for six methyl groups [δ_{H} 1.55–1.88 (each 3H, s)], a methylene [δ_{H} 3.66 (2H, d, $J = 6.8$ Hz)], four olefinic protons [δ_{H} 4.67 (1H, d, $J = 17.4$ Hz), δ_{H} 4.89 (1H, d, $J = 10.5$ Hz), δ_{H} 5.24 (1H, t, $J = 6.8$ Hz), δ_{H} 5.74 (1H, d, $J = 10.0$ Hz)], and three downfielded protons [δ_{H} 6.37 (1H, s), δ_{H} 6.38 (1H, dd, $J = 10.5, 17.4$ Hz), and δ_{H} 6.91 (1H, d, $J = 10.0$ Hz)]. The remaining three singlets corresponded to three hydroxyl groups [δ_{H} 5.90, 5.96, and 12.76 (each 1H, s)]. A detailed evaluation of the ^1H - ^1H COSY, HSQC, and HMBC data revealed the presence of a flavonoid skeleton and three prenyl groups – one 3,3-dimethylallyl, one 1,1-dimethylallyl, and one prenyl unit that cyclized with hydroxyl to form a 2,2-dimethylpyran ring. The assignment of prenyl groups was deduced based on the HMBC correlations (Fig. 2). H-1'' (δ_{H} 3.66) of the 3,3-dimethylallyl unit as well as H-6 (δ_{H} 6.37) and 7-OH (δ_{H} 5.96) correlated with C-8 (δ_{C} 105.4). Thus, 3,3-dimethylallyl is attached to C-8. The HMBC correlation of H-4''' (δ_{H} 6.38) of 1,1-dimethylallyl and 5'-OH (δ_{H} 5.90) with C-6' (δ_{C} 124.5) indicated the location of the 1,1-dimethylallyl unit. H-1''' (δ_{H} 6.91) of the 2,2-dimethylpyran ring provided HMBC correlations with C-2' (δ_{C} 147.2), C-3' (δ_{C} 104.7), and C-4' (δ_{C} 143.2), together with HMBC correlation of 5'-OH (δ_{H} 5.90) with C-4' (δ_{C} 143.2) suggesting the presence of 4',5'-dihydroxy

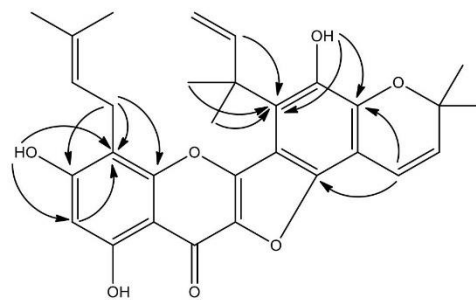


Fig. 2. Key HMBC correlations for compound **12**.

substitution of the flavonoid ring B. As no remaining proton was observed, a comparison with data reported previously [23] was used to deduce that the OH at C-3 must have cyclized with the flavonoid ring B to form a furan ring as part of a 5,11-dioxabenzofluoren-10-one skeleton, which rarely occur in nature. Accordingly, compound **12** was characterized as shown and named broussoufluorenone C.

3.2. Cell viability testing

In the first instance, the effect of isolated compounds **1–14** on the cell viability was determined using a WST-1 assay. Several substances displayed relatively non-toxic profiles with IC_{50} values greater than 10 μM . However, compounds **5**, **7**, **11**, **13**, and **14** affected the viability of THP-1 cells with IC_{50} values < 10 μM . Especially, prenylated flavonoids **7** (IC_{50} 3.6 μM) and **11** (IC_{50} 2.6 μM) as well as 8-O-4'-neolignans **13** (IC_{50} 2.7 μM) and **14** (IC_{50} 5 μM) exhibited cytotoxic properties against THP-1 cells. Therefore, a concentration of 1 μM for the 24 h incubation was used for the evaluation of the anti-inflammatory potential in order to compare the results. This concentration was not toxic (viability > 90%) for most of the compounds, except for compound **11** (viability 64%). For the cellular antioxidant assay, a test concentration of 5 μM was used since the incubation time with the cells was only 2 h.

3.3. Anti-inflammatory potential in cell-based models

To evaluate the anti-inflammatory activity of pure compounds **1–14**, their effect on NF- κB /AP-1 signaling in LPS-stimulated THP-1-XBlueTM-MD2-CD14 cells was investigated. As shown in Fig. 3, most of the test substances showed inhibitory effects on NF- κB /AP-1, except for coumarins **1–3**, flavans **4** and **5**, and 8-O-4'-neolignan **14**. The strongest inhibition was shown by compounds **7** ($p < 0.0001$) and **12** ($p = 0.0002$), and was comparable to that of the prednisone, used as a positive control. Significant inhibitory activity was also observed for compounds **6**, **8–11**, and **13**. Interestingly, compound **7**, which differs from **6** by only one methyl group was found to have much greater inhibitory activity. This suggests that O-methylation of 1,3-dihydroxybenzene ring could lead to reduced NF- κB /AP-1 inhibitory activity. Subsequently, the most effective compounds **7**, **9**, **10**, and **12** (compound **11** was excluded due to its significant cytotoxicity), along with compound **8**, a structural analogue of **9** with a free prenyl group at C-6, were selected for evaluation of their effects on the secretion of pro-inflammatory cytokines IL-1 β and TNF- α . Remarkably, compounds **7–9** suppressed the secretion of both IL-1 β and TNF- α and in both cases, their inhibitory activity was greater than that of prednisone (Fig. 4). On the other hand, compound **10** displayed no inhibitory effect and compound **12** only moderate effect. The results indicate that substitution of the flavonoid ring A has a more significant impact on the anti-inflammatory properties than substitution of ring B. However, it is very difficult to draw even a preliminary conclusion about the

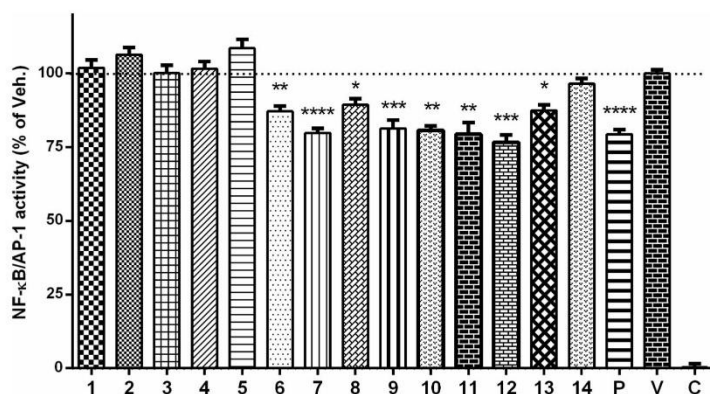


Fig. 3. Inhibitory effects of compounds 1–14 at a concentration of 1 μ M on the NF- κ B/AP-1 activity in THP-1-XBlue™-MD2-CD14 cells stimulated with 1 μ g/mL of LPS. Prednisone at a concentration of 1 μ M was used as a positive control (P). DMSO, the solvent used for both the test compounds and prednisone, was added to the vehicle control (V) and to the non-stimulated cells (C). The results are expressed as the mean \pm SEM for three independent experiments measured in triplicates (* indicates a significant difference in comparison with the vehicle-treated cells (V) $p < 0.05$, ** $p < 0.01$, *** $p < 0.001$, and **** $p < 0.0001$).

structure–activity relationship from the reported data, as the dataset for the comparison is still small. This is the first report of the anti-inflammatory activity of compounds 7, 9, 10, and 12. The anti-inflammatory activity of compound 8 in LPS-stimulated RAW264.7 cells [6] and 3T3-L1 adipocytes [5] has been demonstrated previously. Hence, broussonflavonol B (8) is the most promising candidate to evaluate by using *in vivo* assays to further confirm its anti-inflammatory properties.

3.4. Cellular antioxidant activity (CAA) assay

The antioxidant activity of the test compounds 1–14 was evaluated using the CAA assay, a method more biologically relevant than many simple chemical antioxidant activity assays. The CAA assay is based on using 2,2'-azobis(2-methylpropionamide) dihydrochloride (AAPH) to produce reactive oxygen species (ROS). The level of oxidative stress induced in the cell line is shown by an increase in the fluorescence signal as ROS convert 2',7'-dichlorodihydrofluorescein (DCFH₂) to 2',7'-dichlorofluorescein (DCF). Compound 10 showed the highest value of CAA (25.9; $p < 0.001$), which was greater than that of the quercetin used as a positive control (Fig. 5). Moreover, compounds 7 and 9 also exhibited significant antioxidant activity (CAA values of 6.4 and 5.4, resp.; $p < 0.01$). Obtained results confirmed the general relationship of flavonoid structure and antioxidant activity that catechol motif of the flavonoid ring B is the most important for antioxidant activity as it was observed for compounds 9, 10, and quercetin. Although flavan 11 also contains the 3',4'-dihydroxy substitution of the flavonoid ring B, its

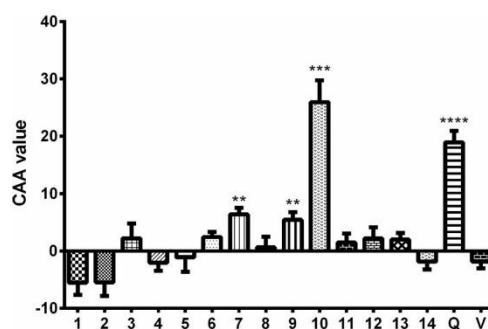


Fig. 5. Antioxidant activity of compounds 1–14 at a concentration of 5 μ M in a CAA assay in THP-1 cells. Quercetin at a concentration of 5 μ M was used as a positive control (Q). DMSO, the solvent used for both the tested compounds and quercetin, was added to the vehicle control (V). The results are expressed as the mean \pm SEM for three independent experiments measured in triplicates (* $p < 0.01$, ** $p < 0.001$, and **** $p < 0.0001$).

activity was very low as it lacks the C-2–C-3 double bond and C-4 carbonyl group that support the conjugation of the rings A and B, increase electron delocalization, and facilitate the stabilization of the radical [30]. Compound 8 meets all these requirements, unfortunately, it was inactive that can be explained by the presence of C-6 prenylation

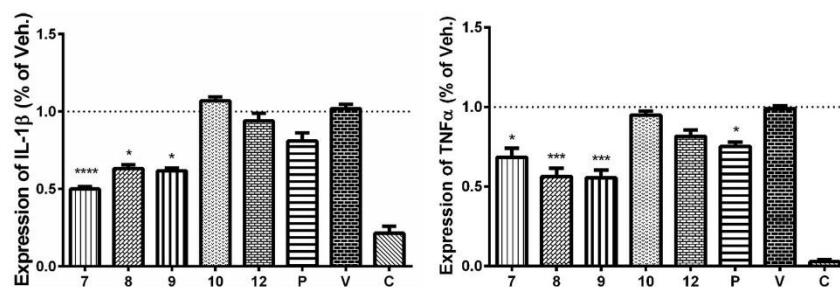


Fig. 4. Inhibitory effects of compounds 7–10 and 12 at a concentration of 1 μ M on the secretion of IL-1 β and TNF- α in THP-1-XBlue™-MD2-CD14 cells stimulated with 1 μ g/mL of LPS. Prednisone at a concentration of 1 μ M was used as a positive control (P). DMSO, the solvent used for both the test compounds and prednisone, was added to the vehicle control (V) and to the non-stimulated cells (C). The results are expressed as the mean \pm SEM for three independent experiments measured in triplicates (* $p < 0.05$, ** $p < 0.001$, and **** $p < 0.0001$).

that decreases antioxidant activity. Therefore, the highest CAA value of compound **10** can also be attributed to a 5,7-*m*-dihydroxy arrangement of the flavonoid ring A with no substituent at C-6. Moreover, C-5'-prenylation significantly increases antioxidant activity that can be related to more efficient pass through the membrane to enter the cell. Similarly, Kumazawa et al. [31] reported that flavanones with C-2' or C-5'-geranyl substitution (nymphaeol B and isonymphaeol B, respectively) inhibited oxidation of β -carotene/linoleic acid emulsion better than those with C-6 geranyl substitution of the flavonoid ring A (nymphaeol A, syn. diplacone). Significant antioxidant activity is also predicted for uralenol (syn. 5'-prenylquercetin) [32]. Thus, 5,7,3',4'-tetrahydroxy-5'-prenylflavones could potentially be leading antioxidant agents.

Unlike flavonoids, furanocoumarins are not expected to possess any antioxidant properties as they lack a phenolic hydroxyl group(s) with an electron-donating potential [33]. However, the furanocoumarins **1** and **2** displayed slightly pro-oxidant properties, what agrees with the results recently published for marmesin glycoside [34]. Furthermore, (S)-marmesin (**2**) had been previously completely inactive in antioxidant activity assays based on simple chemical reactions [33,35], thus demonstrating the differences between the results of a CAA assay and purely chemical assays. Clearly, it is important to use a more biologically relevant model to better predict the antioxidant activity *in vivo*.

4. Conclusions

This study brought new findings about the phytochemical profile and biological activity of industrially and medicinally important plant *B. papyrifera*. In summary, fourteen compounds have been identified, including a novel 5,11-dioxabenzob[fluorene]-10-one derivative (**12**). Subsequently, the anti-inflammatory and antioxidant activities of isolated compounds **1–14** have been investigated as they have not been evaluated previously. Chemical constituents **7–9** and **12** were demonstrated to be potent anti-inflammatory agents with moderate antioxidant activity, while compound **10** exhibited significant antioxidant effect but did not affect the secretion of pro-inflammatory cytokines. Compounds **7–9** showed the ability to inhibit NF- κ B signaling in the THP-1-XBlue™-MD2-CD14 cell line as well as to inhibit the production of the pro-inflammatory cytokines TNF- α and IL-1 β . Among these, compounds **7** and **9** were able to reduce the production of ROS in THP-1 cells. Therefore, subsequent evaluation of compounds **7–9** *in vivo* is surely warranted. Structure-activity relationships indicate that 5,7,3',4'-tetrahydroxy-5'-prenylflavones (with no substituent at C-6) could be more effective antioxidants than non-prenylated flavonoids. Considering the results, *B. papyrifera* deserves more attention in connection with its bioactive constituents and could be cultivated more extensively for both industrial and medicinal purposes.

Declaration of Competing Interest

The authors declare that they have no known competing financial interests or personal relationships that could have appeared to influence the work reported in this paper.

Acknowledgement

This work was supported by the Internal Grant Agency of UVPS Brno, grant numbers 303/2019/FaF (to M.M. and K.Š.) and 309/2019/FaF (to V.L. and J.T.). MS analyses were supported by the SustES project (CZ.02.1.01/0.0/0.0/16.019/0000797; MEYS CR). CIISB research infrastructure project LM2018127 funded by MEYS CR is gratefully acknowledged for the financial support of the measurements at the CF (X-ray Diffraction and Bio-SAXS Core Facility CEITEC). The financial support of K.Š. and V.L. by Czech Science Foundation project no. 16-

07193S is gratefully acknowledged. We thank to Frank Thomas Campbell for a language editing of the manuscript.

Appendix A. Supplementary data

Supplementary data to this article can be found online at <https://doi.org/10.1016/j.bioorg.2020.104298>.

References

- [1] Y. Xinrong, F. Bingyi, S. Fang, Q. Jinlin, L. Quan, W. Shuqian, H. Werner, C. Yinfu, Z. Xinsheng, C. Anmin, M. Yingfu, G. Yuan, G. Zheming (Eds.), *Encyclopedic Reference of Traditional Chinese Medicine*, Springer-Verlag, Berlin Heidelberg, 2003, <https://doi.org/10.1007/978-3-662-05177-1>.
- [2] D. Lee, A. D. Kinghorn, Bioactive Compounds from the Genus *Broussonetia*, in: A. Rahman (Ed.), *Stud. Nat. Prod. Chem.*, Elsevier, 2003: pp. 3–33. [https://doi.org/10.1016/S1572-5995\(03\)80137-0](https://doi.org/10.1016/S1572-5995(03)80137-0).
- [3] G.-W. Wang, B.-K. Huang, L.-P. Qin, The Genus *Broussonetia*: A Review of its Phytochemistry and Pharmacology, *Phytother. Res.* 26 (2012) 1–10, <https://doi.org/10.1002/ptr.3575>.
- [4] L.-W. Lin, H.-Y. Chen, C.-R. Wu, P.-M. Liao, Y.-T. Lin, M.-T. Hsieh, H. Ching, Comparison with Various Parts of *Broussonetia papyrifera* as to the Antinociceptive and Anti-inflammatory Activities in Rodents, *Biosci. Biotechnol. Biochem.* 72 (2008) 2377–2384, <https://doi.org/10.1271/bbb.80276>.
- [5] J.M. Lee, S.S. Choi, M.H. Park, H. Jang, Y.H. Lee, K.W. Kim, S.R. Oh, J. Park, H.W. Ryu, J.H. Choi, *Broussonetia papyrifera* Root Bark Extract Exhibits Anti-inflammatory Effects on Adipose Tissue and Improves Insulin Sensitivity Potentially Via AMPK Activation, *Nutrients*. 12 (2020) 773, <https://doi.org/10.3390/nut12030773>.
- [6] H.W. Ryu, M.H. Park, O.-K. Kwon, D.-Y. Kim, J.-Y. Hwang, Y.H. Jo, K.-S. Ahn, B.Y. Hwang, S.-R. Oh, Anti-inflammatory flavonoids from root bark of *Broussonetia papyrifera* in LPS-stimulated RAW264.7 cells, *Bioorganic Chem.* 92 (2019) 103233, <https://doi.org/10.1016/j.bioorg.2019.103233>.
- [7] J.-L. Tian, T.-L. Liu, J.-J. Xue, W. Hong, Y. Zhang, D.-X. Zhang, C.-C. Cui, M.-C. Liu, S.-L. Niu, Flavonoids derivatives from the root bark of *Broussonetia papyrifera* as a tyrosinase inhibitor, *Ind. Crops Prod.* 138 (2019) 111445, <https://doi.org/10.1016/j.indcrop.2019.06.008>.
- [8] M.-L. Xu, L. Wang, J.-H. Hu, S.K. Lee, M.-H. Wang, Antioxidant activities and related polyphenolic constituents of the methanol extract fractions from *Broussonetia papyrifera* stem bark and wood, *Food Sci. Biotechnol.* 19 (2010) 677–682, <https://doi.org/10.1007/s10068-010-0095-x>.
- [9] V. Brežani, K. Šmejkal, J. Hošek, V. Tomášová, Anti-inflammatory Natural Prenylated Phenolic Compounds - Potential Lead Substances, *Curr. Med. Chem.* 25 (2018) 1094–1159, <https://doi.org/10.2174/0929867324666170810161157>.
- [10] P. Arulseelan, M.T. Fard, W.S. Tan, S. Gothal, S. Fakurazi, M.E. Norhaizan, S.S. Kumar, Role of Antioxidants and Natural Products in Inflammation, *Oxid. Med. Cell. Longev.* 2016 (2016) e5276130, <https://doi.org/10.1155/2016/5276130>.
- [11] G.M. Sheldrick, SHELXT – Integrated space-group and crystal-structure determination, *Acta Crystallogr. Sect. A Found. Adv.* 71 (2015) 3–8, <https://doi.org/10.1107/S2053273314026370>.
- [12] G.M. Sheldrick, Crystal structure refinement with SHELXL, *Acta Crystallogr. Sect. C Struct. Chem.* 71 (2015) 3–8, <https://doi.org/10.1107/S2053229614024218>.
- [13] J. Hošek, M. Bartoš, S. Chudík, S. Dall'Acqua, G. Innocenti, M. Kartal, L. Kokoška, P. Kollár, Z. Kutlí, P. Landa, R. Marek, V. Závalová, M. Ženlíčka, K. Šmejkal, Natural Compound Cudraflavone B Shows Promising Anti-inflammatory Properties *in Vitro*, *J. Nat. Prod.* 74 (2011) 614–619, <https://doi.org/10.1021/np100638h>.
- [14] Z. Hanáková, J. Hošek, P. Babula, S. Dall'Acqua, J. Václavík, K. Šmejkal, C-Geranylated Flavonones from *Paulownia tomentosa* Fruits as Potential Anti-inflammatory Compounds Acting via Inhibition of TNF- α Production, *J. Nat. Prod.* 78 (2015) 850–863, <https://doi.org/10.1021/acs.jnatprod.5b00005>.
- [15] V. Lešáková, K. Šmejkal, K. Jakubczyk, O. Veselý, P. Landa, J. Václavík, P. Bobáľ, H. Pířová, V. Temml, T. Steinacher, D. Schuster, S. Granica, Z. Hanáková, J. Hošek, Parallel *in vitro* and *in silico* investigations into anti-inflammatory effects of non-prenylated stilbenoids, *Food Chem.* 285 (2019) 431–440, <https://doi.org/10.1016/j.foodchem.2019.01.128>.
- [16] V. Brežani, V. Lešáková, S.T.S. Hassan, K. Berchová-Bimová, P. Nový, P. Klouček, P. Maršik, S. Dall'Acqua, J. Hošek, K. Šmejkal, Anti-Infectivity against Herpes Simplex Virus and Selected Microbes and Anti-Inflammatory Activities of Compounds Isolated from *Eucalyptus globulus* Labill, *Viruses*. 10 (2018) 360, <https://doi.org/10.3390/v10070360>.
- [17] J. Hošek, V. Lešáková, P. Bobáľ, H. Pířová, M. Gazdová, M. Malaník, K. Jakubczyk, O. Veselý, P. Landa, V. Temml, D. Schuster, V. Prachyawarakorn, P. Pailee, G. Ren, F. Zpurný, M. Oravec, K. Šmejkal, Prenylated Stilbenoids Affect Inflammation by Inhibiting the NF- κ B/AP-1 Signaling Pathway and Cyclooxygenases and Lipoxygenase, *J. Nat. Prod.* 82 (2019) 1839–1848, <https://doi.org/10.1021/acs.jnatprod.9b00081>.
- [18] K.L. Wolfe, R.H. Liu, Cellular Antioxidant Activity (CAA) Assay for Assessing Antioxidants, Foods, and Dietary Supplements, *J. Agric. Food Chem.* 55 (2007) 8896–8907, <https://doi.org/10.1021/jf0715166>.
- [19] H. Ishii, F. Sekiguchi, T. Ishikawa, Studies on the chemical constituents of rutaceous plants—XII: Absolute configuration of rutaretin methyl ether, *Tetrahedron*. 37 (1981) 285–290, [https://doi.org/10.1016/S0040-4020\(01\)92011-3](https://doi.org/10.1016/S0040-4020(01)92011-3).
- [20] R.F. Luz, I.J.C. Vieira, R. Braz-Filho, V.F. Moreira, ¹³C-NMR Data from Coumarins

- from Moraceae Family, Am. J. Anal. Chem. 06 (2015) 851–866, <https://doi.org/10.4236/ajac.2015.611081>.
- [21] Y. Akihara, E. Ohta, T. Nehira, H. Ōmura, S. Ohta, New Prenylated ortho-Dihydroxycoumarins from the Fruits of *Ficus nipponica*, Chem. Biodivers. 14 (2017) e1700196, <https://doi.org/10.1002/cbdv.201700196>.
- [22] M. Takasugi, Y. Kumagai, S. Nagao, T. Masamune, A. Shirata, K. Takahashi, The co-occurrence of flavan and 1,3-diphenylpropane derivatives in wounded paper mulberry, Chem. Lett. 9 (1980) 1459–1460, <https://doi.org/10.1246/cl.1980.1459>.
- [23] H.W. Ryu, B.W. Lee, M.J. Curtis-Long, S. Jung, Y.B. Ryu, W.S. Lee, K.H. Park, Polyphenols from *Broussonetia papyrifera* Displaying Potent α -Glucosidase Inhibition, J. Agric. Food Chem. 58 (2010) 202–208, <https://doi.org/10.1021/jf903068k>.
- [24] S. Kato, T. Fukai, J.I. Matsumoto, T. Nomura, Components of *Broussonetia kazinoki* SIEB. (2): Structures of Four New Isoprenylated 1, 3-Diphenylpropane Derivatives, Kazinols J, I, M, and N, Chem. Pharm. Bull. (Tokyo). 34 (1986) 2448–2455, <https://doi.org/10.1248/cpb.34.2448>.
- [25] J. Matsumoto, T. Fujimoto, C. Takino, M. Saitoh, Y. Hano, T. Fukai, T. Nomura, Components of *Broussonetia papyrifera* (L.) Vent. I. Structures of Two New Isoprenylated Flavonols and Two Chalcone Derivatives, Chem. Pharm. Bull. (Tokyo). 33 (1985) 3250–3256, <https://doi.org/10.1248/cpb.33.3250>.
- [26] F. Guo, L. Feng, C. Huang, H. Ding, X. Zhang, Z. Wang, Y. Li, Prenylflavone derivatives from *Broussonetia papyrifera*, inhibit the growth of breast cancer cells *in vitro* and *in vivo*, Phytochem. Lett. 6 (2013) 331–336, <https://doi.org/10.1016/j.phytol.2013.03.017>.
- [27] H.-H. Ko, M.-H. Yen, R.-R. Wu, S.-J. Won, C.-N. Lin, Cytotoxic Isoprenylated Flavans of *Broussonetia kazinoki*, J. Nat. Prod. 62 (1999) 164–166, <https://doi.org/10.1021/mp980281c>.
- [28] K.B. Kang, E.J. Park, R.R. da Silva, H.W. Kim, P.C. Dorrestein, S.H. Sung, Targeted Isolation of Neuroprotective Dicomaroyl Neolignans and Lignans from *Sageretia theezans* Using *in Silico* Molecular Network Annotation Propagation-Based Dereplication, J. Nat. Prod. 81 (2018) 1819–1828, <https://doi.org/10.1021/acs.jnatprod.8b00292>.
- [29] B.-N. Su, M. Cuendet, M.E. Hawthorne, L.B.S. Kardono, S. Riswan, H.H.S. Fong, R.G. Mehta, J.M. Pezzuto, A.D. Kinghorn, Constituents of the Bark and Twigs of *Artocarpus dadah* with Cyclooxygenase Inhibitory Activity, J. Nat. Prod. 65 (2002) 163–169, <https://doi.org/10.1021/np010451c>.
- [30] J. Trembl, K. Šmejkal, Flavonoids as Potent Scavengers of Hydroxyl Radicals, Compr. Rev. Food Sci. Food Saf. 15 (2016) 720–738, <https://doi.org/10.1111/1541-4337.12204>.
- [31] S. Kumazawa, R. Ueda, T. Hamasaka, S. Fukumoto, T. Fujimoto, T. Nakayama, Antioxidant Prenylated Flavonoids from Propolis Collected in Okinawa, Japan, J. Agric. Food Chem. 55 (2007) 7722–7725, <https://doi.org/10.1021/jf071187h>.
- [32] A. Wang, Y. Lu, X. Du, P. Shi, H. Zhang, A theoretical study on the antioxidant activity of Uralenol and Neuralenol scavenging two radicals, Struct. Chem. 29 (2018) 1067–1075, <https://doi.org/10.1007/s11224-018-1090-8>.
- [33] P.T. Thuong, T.M. Hung, T.M. Ngoc, D.T. Ha, B.S. Min, S.J. Kwack, T.S. Kang, J.S. Choi, K. Bae, Antioxidant activities of coumarins from Korean medicinal plants and their structure-activity relationships, Phytother. Res. 24 (2010) 101–106, <https://doi.org/10.1002/ptr.2890>.
- [34] N.K. Kassim, P.C. Lim, A. Ismail, K. Awang, Isolation of antioxidative compounds from *Micromelum minutum* guided by preparative thin layer chromatography-2,2-diphenyl-1-picrylhydrazyl (PTLC-DPPH) bioautography method, Food Chem. 272 (2019) 185–191, <https://doi.org/10.1016/j.foodchem.2018.08.045>.
- [35] Y. Bai, D. Li, T. Zhou, N. Qin, Z. Li, Z. Yu, H. Hua, Coumarins from the roots of *Angelica dahurica* with antioxidant and antiproliferative activities, J. Funct. Foods. 20 (2016) 453–462, <https://doi.org/10.1016/j.jff.2015.11.018>.

6.7. ARTICLE 7

Molcanova, L.; **Treml, J.**; Brezani, V.; Marsik, P.; Kurhan, S.; Travnicek, Z.; Uhrin, P.; Smejkal, K. Journal of Ethnopharmacology 2022, 296, 115509 (IF=5.400).



Contents lists available at ScienceDirect

Journal of Ethnopharmacology

journal homepage: www.elsevier.com/locate/jethpharm

C-geranylated flavonoids from *Paulownia tomentosa* Steud. fruit as potential anti-inflammatory agents

Lenka Molčanová^{a,*}, Jakub Tremel^{b,*}, Veronika Brezáni^{b,c}, Petr Maršík^d, Sebnem Kurhan^d, Zdeněk Trávníček^e, Pavel Uhrin^f, Karel Šmejkal^a

^a Department of Natural Drugs, Faculty of Pharmacy, Masaryk University, Palackého tř. 1946/1, CZ-61200, Brno, Czech Republic

^b Department of Molecular Pharmacy, Faculty of Pharmacy, Masaryk University, Palackého tř. 1946/1, CZ-61200, Brno, Czech Republic

^c Veterinary Research Institute, Hudcova 296/70, CZ-62100, Brno, Czech Republic

^d Department of Food Quality and Safety, Czech University of Life Sciences Prague, Kamýčká 129, CZ-16500, Prague 6–Suchbát, Czech Republic

^e Regional Centre of Advanced Technologies and Materials, Czech Advanced Technology and Research Institute, Palacký University, Šlechtitelů 27, CZ-77900, Olomouc, Czech Republic

^f Institute of Vascular Biology and Thrombosis Research, Center for Physiology and Pharmacology, Medical University of Vienna, Vienna, Austria

ARTICLE INFO

Keywords:

Anti-inflammatory
Geranylated flavonoids
NF- κ B
Paulownia tomentosa
THP-1-XBlue™-MD2-CD14

ABSTRACT

Ethnopharmacological relevance: *Paulownia tomentosa* Steud., a traditional Chinese medicinal plant, was used for many centuries in Chinese herbal medicine as a component of remedies for many illnesses, including inflammatory diseases. It is a rich source of phenolic compounds, mainly geranylated flavonoids, which are currently studied for their promising biological activities.

Aim of the study: The study aimed to isolate minor geranylated flavanones and flavones from *P. tomentosa* fruit and evaluate their cytotoxicity and possible anti-inflammatory effects in a cell-based model of inflammation.

Materials and methods: Chromatographic separation of chloroform portion of the ethanolic extract of *P. tomentosa* fruit led to the isolation of twenty-seven flavonoids (1–27), twenty-six of them geranylated with different modifications and one non-geranylated flavanone, and two phenolic compounds. Compounds were identified using UV, IR, HRMS, NMR, and CD spectroscopy. Ten of these compounds (7–10, 12, 21, 22, 24, 25, and 27) were determined to be new flavonoid derivatives obtained from a natural source for the first time. Selected compounds were analyzed for cytotoxicity and anti-inflammatory potential to affect the activation of nuclear factor κ B/activator protein 1 (NF- κ B/AP-1) after lipopolysaccharide (LPS) stimulation.

Results: All the test compounds (1–21 and 23–26) reduced the activation of NF- κ B/AP-1 24 h after the addition of LPS. Eight compounds (5, 14–18, 21, and 26) were more active than prednisone, a widely used anti-inflammatory drug. However, this effect was not seen significantly on the level of TNF- α and IL-1 β , which can be explained by the plurality of possible outcomes of activation of the NF- κ B pathway in cells.

Conclusions: Results of the presented study confirmed that constituents from traditional Chinese medicinal plant *P. tomentosa* Steud. have promising anti-inflammatory activities and can serve as a potential source of inspiration for new anti-inflammatory medications.

1. Introduction

Legends and records say that in ancient times people used *Paulownia* for various purposes. For many centuries, Chinese people have been planting *Paulownia* trees around their dwellings, because they believed it

can bring good luck. According to records, even 2600 years ago people were using *Paulownia* timber. The wood was used for the construction of houses, production of furniture and paper, handicrafts, farm implements, musical instruments, and it was used also for medicinal properties (Zhu et al., 1986).

* Corresponding author.

** Corresponding author.

E-mail addresses: lenka.molcanova1993@gmail.com, molcanova@pharm.muni.cz (L. Molčanová), tremelj@pharm.muni.cz (J. Tremel), veronika.lelakova@gmail.com (V. Brezáni), marsik@af.czu.cz (P. Maršík), kurhan@af.czu.cz (S. Kurhan), zdenek.travnick@upol.cz (Z. Trávníček), Pavel.Uhrin@meduniwien.ac.at (P. Uhrin), smejkal@pharm.muni.cz (K. Šmejkal).

<https://doi.org/10.1016/j.jep.2022.115509>

Received 14 April 2022; Received in revised form 21 June 2022; Accepted 22 June 2022

Available online 24 June 2022

0378-8741/© 2022 Elsevier B.V. All rights reserved.

Paulownia is known as „Princess tree”, „Empress tree”, „Royal *Paulownia*”, or „Foxglove tree” (Kaur et al., 2015), because its flowers resemble flowers of foxglove (Erbar and Gülden, 2011). In China it is commonly known as „Mao pao tong” or „Yuan bian zhong” (Hong et al., 1998), in Korea as „Odong-Namoo”, and in Japan as „Kiri” (Kaur et al., 2015).

Different parts of the plant had been used in Chinese herbal medicine as components of remedies for many diseases. In traditional Chinese medicine, *Paulownia* was reported to have effects on inflammatory diseases, e.g., it can „resolve toxin and disperse swelling”, it can help with „swelling pain due to external injury” or „toxin swelling from hemorrhoids”, and it was used for the treatment of erysipelas (Zhou et al., 2011), enteritis, tonsillitis, and dysentery (Jiang et al., 2004). The injections and tablets made of *Paulownia* fruits, leaves, and wood were used for relieving the cough and reducing the phlegm in the treatment of bronchitis and many other inflammations. Daily application of water solutions prepared from fruit and leaves can promote the healthy growth of hair and turn grey hair darker. The fruit can reduce blood pressure (Zhu et al., 1986).

Paulownia tomentosa Steud. (Paulowniaceae) is a rich source of secondary metabolites, mainly of phenolic character. Flavonoids, lignans, phenolic glycosides, phenolic acids, terpenoids, quinones, glycerides, and other compounds have been isolated from different parts of this plant, with flavonoids being the most numerous group. More than seventy prenylated and geranylated flavonoids (prenylation occurs mostly at position C-6), have been isolated from the leaves, flowers, and fruit of *P. tomentosa* (Jiang et al., 2004; Šmejkal et al. 2007, 2008, 2010, Asai et al., 2008, Kobayashi et al., 2008; Cho et al. 2012, 2013, Navrátilová et al., 2013, Schneiderová et al., 2013, Hanáková et al., 2015, Hanáková et al., 2017, Ryu et al., 2017, Molčanová et al., 2021). The side chain of many of these compounds is further modified by oxidation, reduction, dehydration, or cyclization, and many of the compounds, both with and without modifications to the side chain, have never been isolated from any other plant species. These compounds exhibit potent biological activities, such as antioxidant, anti-inflammatory, cytotoxic, antibacterial, antiparasitic, antiviral, or neuroprotective (Cheng et al., 2019). Most recently, their P-glycoprotein-affecting activity has been described (Marques et al., 2021).

Inflammation is a complex and crucial defensive response of the body that often occurs when infectious microorganisms such as bacteria, viruses, or fungi invade the body and reside in particular tissues or circulate in the blood. It may also be a response to processes such as tissue injury, cell death, cancer, ischemia, or degeneration of tissues or organs. In most cases, it is a specific and self-controlled immune response, that tries to resolve infection or repair tissue or wound. On the other hand, inflammation can produce a harmful dysregulated response, or it can be associated with disruption of the homeostasis of physiological processes that have no direct connection to classical inflammation triggers and can lead to systemic damage that results in chronic inflammatory disorders. Different cells, enzymes, cytokines, chemokines, eicosanoids, and transcription factors are among the inflammatory mediators that drive cellular pathways and have been studied extensively in association with pathological conditions in humans. The inflammatory process includes triggering signaling cascades, activating transcription factors, expressing genes, increasing the levels of inflammatory enzymes, and releasing various oxidants and pro-inflammatory molecules from immune or inflammatory cells, and leads to immune, vascular, and cellular biochemical reactions (Maleki et al., 2019; Azab et al., 2016, Andrade and Valentão, 2018).

Because *P. tomentosa* is an important source of geranylated flavonoids with interesting anti-inflammatory activities (Hanáková et al., 2015, Hanáková et al., 2017; Ryu et al., 2017, Vočhyánová et al., 2015), our continuous research done on this plant is now focused on isolating minor geranylated flavanones and flavones (Chart 1) and testing their anti-inflammatory potential ability to affect the activation of nuclear factor κ B/activator protein 1 (NF- κ B/AP-1) after lipopolysaccharide

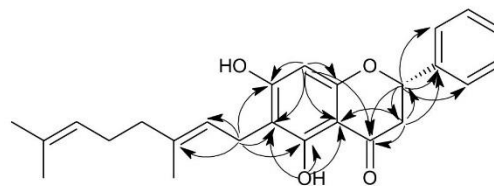


Fig. 1. HMBC correlations typical for flavanone skeleton and assignment of the position of geranyl chain.

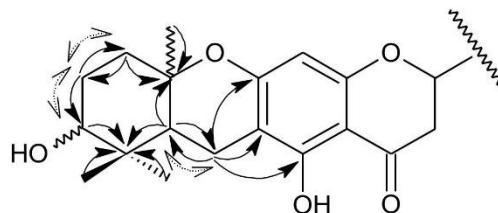


Fig. 2. Key HMBC (→) and COSY (<--->) correlations for assignment of unusual double-cyclized geranyl chain of compound 7.

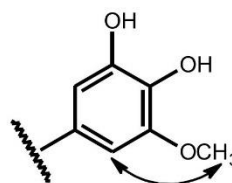


Fig. 3. NOESY correlation typical for assignment of position of methoxy group.

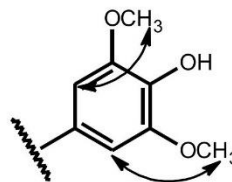


Fig. 4. NOESY correlation typical for assignment of the position of methoxy groups.

(LPS) stimulation. We further present the isolation and identification of nine new geranylated flavonoids and one non-prenylated flavanone, and the anti-inflammatory potentials of selected compounds together with those of several previously isolated substances (Molčanová et al., 2021).

2. Material and methods

2.1. Plant material

The fruits of *P. tomentosa* were collected at the campus of the University of Veterinary and Pharmaceutical Sciences Brno, Brno, Czech Republic, during October 2004 and October and November 2010.

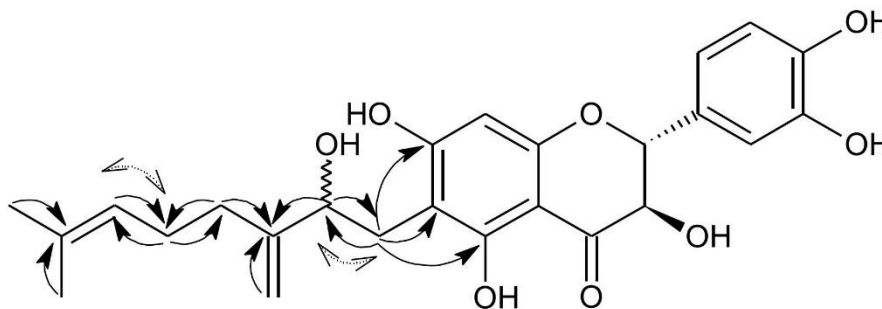


Fig. 5. Key HMBC (→) and COSY (<--->) correlations of geranyl chain of compound 21.

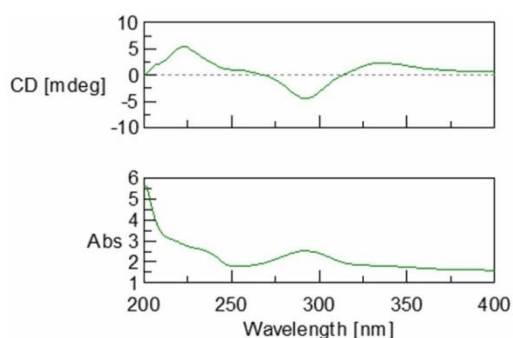


Fig. 6. CD spectrum of 2S-flavanone.

Voucher specimens (PT-040 and PT102010, respectively) have been deposited at the herbarium of the Department of Natural Drugs, Faculty of Pharmacy, Masaryk University, Brno, Czech Republic.

2.2. General experimental procedures

UV spectra were obtained using an Agilent 1100 chromatographic system with an Agilent 1100 Series diode array detector to analyze the apex of the peak corresponding to the compound (Agilent Technologies,

Santa Clara, CA, USA). Circular dichroism spectra were recorded on a JASCO J-815 CD spectrometer (Jasco, Easton, MD, USA), which was also used to calculate $\log \epsilon$ and $\Delta \epsilon$. IR spectra (ATR technique) were measured with a Nicolet Impact 400D FT-IR instrument (Thermo Fischer Scientific, Waltham, MA, USA). 1D and 2D NMR spectra were obtained on a JEOL ECZR 400 MHz NMR spectrometer (JEOL, Tokyo, Japan) with TMS as the internal standard. DMSO- d_6 was purchased from Eurisotop (Cambridge Isotope Laboratories Inc., Tewksbury, MA, USA). HRMS data were recorded using a UPLC-HRAM-MS system consisting of q-TOF mass spectrometer Impact II (Bruker Daltonik, Bremen, Germany) coupled with a UPLC Ultimate 3000 chromatographic system (Thermo Fischer Scientific), in both the positive and negative modes. Analytical HPLC measurements were carried out with an Agilent 1100 chromatographic system (Agilent Technologies). Semi-preparative RP-HPLC was performed using a Dionex UltiMate 3000 HPLC System with fraction collector (Thermo Fischer Scientific) and a YL 9100 HPLC System (Young Lin, Anyang, The Republic of Korea) with a FOXY R2 fraction collector (Teledyne Isco, Lincoln, NE, USA).

The gradient elution for UPLC-HRAM-MS used MeOH and 0.2% formic acid. The gradient of the mobile phase consisted initially of 50% MeOH and reached 100% in the 10th minute (flow rate 0.3 mL/min). An Ascentis Express RP-Amide, 10 cm \times 2.1 mm, particle size 2.7 μ m, analytical HPLC column (Sigma-Aldrich, St. Louis, MO, USA) was used (column temperature 40 °C). Samples were dissolved in MeOH and the injection volume was 5 μ L. A solution of sodium formate clusters was used for the exact calibration of mass in both the positive and the negative ionization modes.

Compounds were separated by column chromatography using silica

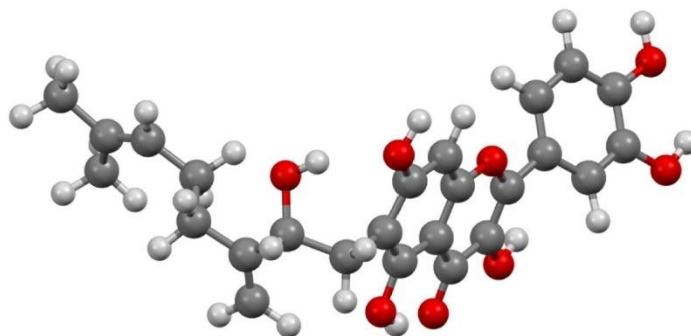


Fig. 7. The geometry of compound 21 optimized at the B3LYP/def2-TZVP level of theory. Carbons = dark grey, hydrogens = light grey, oxygens = red. (For interpretation of the references to color in this figure legend, the reader is referred to the Web version of this article.)

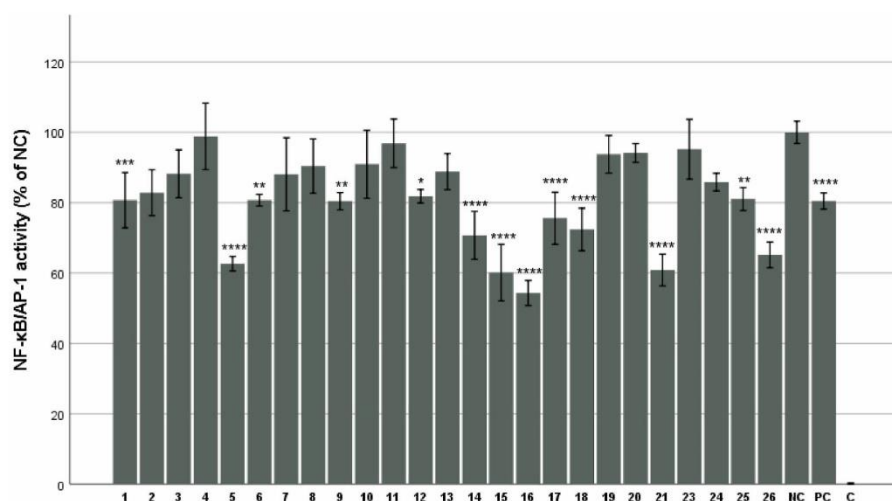


Fig. 8. Inhibitory effects of compounds 1–21 and 23–26 at a concentration of 1 μ M on the NF- κ B/AP-1 activity in THP-1-XBlue™-MD2-CD14 cells stimulated with 1 μ g/mL of LPS. Prednisone at a concentration of 1 μ M was used as a positive control (PC). DMSO, the solvent used for both the test compounds and prednisone, was added to the vehicle control (NC) and to the non-stimulated cells (C). The results are expressed as the mean \pm SEM for three independent experiments measured in hexaplicates (* indicates a significant difference in comparison with the vehicle-treated cells (NC); * p < 0.05, ** p < 0.01, *** p < 0.001, and **** p < 0.0001).

gel with a particle size of 40–63 μ m (Merck, Billerica, MA, USA). Further semi-preparative HPLC separations were performed with an Ascentis RP-Amide, 25 cm \times 10 mm, particle size 5 μ m, semi-preparative HPLC column (Sigma-Aldrich) or an Ascentis C18, 25 cm \times 10 mm, particle size 5 μ m, semi-preparative HPLC column (Sigma-Aldrich). Silica gel 60 F₂₅₄ (20 \times 20 cm, 200 μ m) TLC plates (Merck) and an Ascentis Express RP-Amide, 10 cm \times 2.1 mm, particle size 2.7 μ m, analytical HPLC column (Sigma-Aldrich) were used for analytical purposes. Gradient grade MeCN and MeOH for HPLC were purchased from Sigma-Aldrich or VWR International, France, and other analytical grade solvents from Lach-Ner, Czech Republic.

2.3. Extraction and isolation

The extraction of *P. tomentosa* fruit (2004) and further separation into several portions by liquid-liquid extraction has been described in previous work (Šmejkal et al., 2008). Part of the chloroform portion (365 g) derived from the ethanolic fruit extract was further separated by column chromatography to give 20 fractions labeled A–T (Navrátilová et al., 2013).

Fraction PT30 (19.967 g) was separated on silica gel by column chromatography using a mobile phase consisting of MeOH:CHCl₃ 6:94 (v/v). Subfractions of 125 mL were collected. Based on TLC and HPLC analysis, similar subfractions were combined to give 16 final subfractions and the MeOH wash. Selected subfractions were then subjected to further separation by semi-preparative RP-HPLC using gradient elution with different ratios of MeCN or MeOH and H₂O containing 0.2% HCOOH (5 mL/min), and either an Ascentis RP-Amide or Ascentis C18 semi-preparative HPLC column (see Separation scheme A1, Supplementary data). Subfractions were collected using a fraction collector and based on the UV-detector response (λ 254, 280, and 350 nm).

Subfraction PT30/16 (183 mg) was separated by semi-preparative RP-HPLC using gradient elution (30–70% MeCN, 30 min, RP-Amide column) to obtain methyl ferulate (1.6 mg, t_R 12.0 min) and 12 (4.4 mg, t_R 20.8 min). Compound 20 (10.7 mg, t_R 18.5 min) was obtained by repeated purification of subfraction PT30/29 (182 mg) using gradient elution (45–55% MeCN, 20 min, and subsequently 65–75% MeOH, 20

min, RP-Amide column in both cases). Subfraction PT30/35–39 (857 mg) was subjected to semi-preparative RP-HPLC separation using gradient elution (35–83% MeCN, 30 min, RP-Amide column) to yield 23 (24.3 mg, t_R 27.4 min). Compound 9 (9.8 mg, t_R 19.5 min) was purified using gradient elution (40–70% MeOH, RP-Amide column) from subfraction PT30/35–39/2 (44 mg). Subfractions PT30/35–39/3 (23.4 mg) and PT30/35–39/5 (11.2 mg) were further separated using gradient elution (50–60% MeCN, 15 min and 52–58% MeCN, 20 min, respectively, C18 column in both cases) to obtain 6 (5.6 mg, t_R 21.7 min) and 25 (1.1 mg, t_R 23.5 min), respectively. Compound 27 (2.1 mg, t_R 12.2 min) was obtained by purifying subfraction PT30/40–42 (345 mg) using gradient elution (30–95% MeCN, 25 min, RP-Amide column). Subfraction PT30/35–39/4 was combined with subfractions PT30/40–42/7+8+9 (total amount 90.5 mg) and the aggregate was separated by gradient elution (45–95% MeCN, 20 min, RP-Amide column) to obtain compounds 7 (20.7 mg; t_R 20.5 min), 17 (25.3 mg, t_R 22.9 min), and 23 (2.0 mg). Subfraction PT30/43–48 (1366 mg) was separated using gradient elution (50–80% MeCN, 15 min, RP-Amide column) to obtain three pure compounds, 10 (20.2 mg, t_R 20.2 min), 7 (76.8 mg), and 16 (488.8 mg, t_R 23.4 min). Subfraction PT30/43–48/3+C (24.9 mg) was further purified repeatedly using gradient elution (50–70% MeCN, 20 min, C18) to yield compound 17 (3.5 mg). Subfraction PT30/49–57 (608 mg) yielded 16 (67.7 mg) after separation using gradient elution (50–90% MeOH, 30 min, RP-Amide column). Subfractions PT30/49–57/3 (43.6 mg) and PT30/49–57/4 (41 mg) were further purified repeatedly by gradient elution (50–55% MeCN, 20 min and 45–55% MeCN, 20 min, respectively, RP-Amide column used in both cases) to obtain compounds 21 (7.4 mg, t_R 19.8 min), and 22 (5.9 mg, t_R 19.3 min), respectively. Subfraction PT30/75–76 (76 mg) was separated using gradient elution (40–60% MeCN, 20 min, RP-Amide column) to yield compounds 19 (6.5 mg, t_R 17.3 min) and 24 (0.9 mg, t_R 20.5 min). Subfraction PT30/77–108 (455 mg) was subjected to semi-preparative RP-HPLC separation using gradient elution (20–70% MeCN, 30 min, RP-Amide column) to obtain vanillic acid (2.5 mg, t_R 4.9 min), 19 (117.2 mg), and 24 (6.3 mg).

The extraction of *P. tomentosa* fruit (2010), further fractionation of the extract into several portions by liquid-liquid extraction, and the

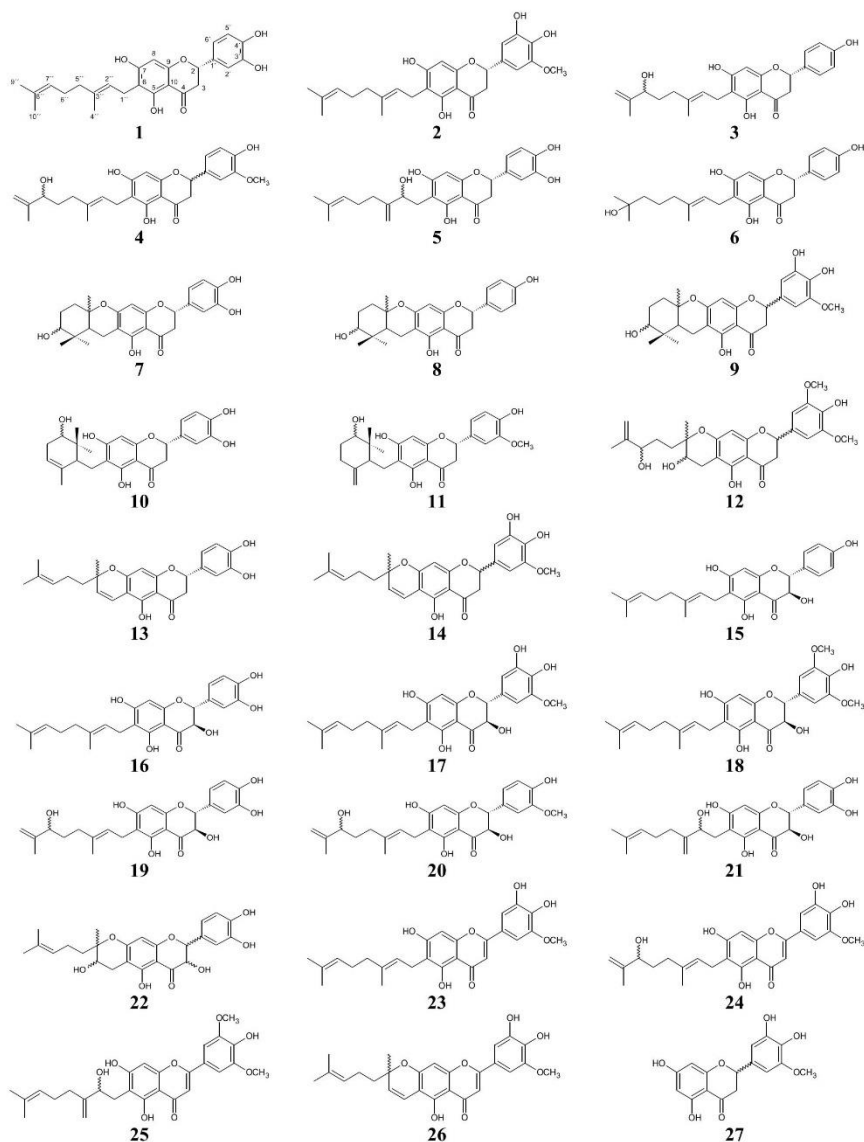


Chart 1. Structures of compounds 1–27 isolated from the fruit of *P. tomentosa*.

basic chromatographic separation of the methanol portion using silica gel have been described previously (Hanáková et al., 2015). Fraction *PT4-18/35-37* was chosen for further separation using column chromatography (silica gel, mobile phase $C_6H_6:CHCl_3:MeOH:HCOOH$ 10:86:4:0.1, v/v/v) to obtain *PT4-18/35-37/11-13* and *14-55*. Subsequent semi-preparative RP-HPLC (50–82.5% MeCN, 22 min, and 60–90% MeCN, 22 min, respectively, both using RP-Amide columns) yielded compounds 2 (216 mg), 4 (6 mg), 8 (18 mg, t_R 22.8 min), 11 (39 mg), and 23 (9 mg).

The isolation and characterization of compounds 1–3, 5, 11, 13–15, 18, and 26 have been described in previous work (Molčanová et al., 2021). The purity of the isolated compounds was evaluated using HPLC-DAD analysis (10–100% MeCN, 36 min, 0.3 mL/min) and exceeded 95% in all cases.

Paulodiplacone C (7): yellowish amorphous substance; UV (c 5.68×10^{-5} M, MeOH) λ_{max} (log ϵ) 292 (4.65), 334 (weak) (4.50) nm; ECD (c 5.68×10^{-5} M, MeOH) λ ($\Delta\epsilon$) 292 (–2.37), 334 (+1.25) nm; IR (ATR) ν_{max} 3233, 2962, 1634, 1601, 1524, 1440, 1333, 1297, 1282, 1262,

1183, 1154, 1110, 1080, 1018, 981, 871, 812, 776 cm^{-1} ; ^1H and ^{13}C NMR data, see Table 1; UPLC-HRAM-MS (positive) m/z 441.1916 $[\text{M}+\text{H}]^+$ (calcd for $\text{C}_{25}\text{H}_{29}\text{O}_7^+$, 441.1913).

Mimulone I (8): yellowish amorphous substance; UV (ϵ 5.89 $\times 10^{-5}$ M, MeOH) λ_{max} (log ϵ) 294 (4.54), 334 (weak) (4.47) nm; ECD (ϵ 5.89 $\times 10^{-5}$ M, MeOH) λ ($\Delta\epsilon$) 290 (−1.85), 334 (+0.75) nm; IR (ATR) ν_{max} 3300, 2921, 1591, 1517, 1450, 1344, 1257, 1156, 1045, 764 cm^{-1} ; ^1H and ^{13}C NMR data, see Table 1; UPLC-HRAM-MS (positive) m/z 425.1956 $[\text{M}+\text{H}]^+$ (calcd for $\text{C}_{25}\text{H}_{29}\text{O}_6^+$, 425.1964).

Tomentone C (9): red-orange amorphous substance; UV (ϵ 5.32 $\times 10^{-5}$ M, MeOH) λ_{max} (log ϵ) 294 (4.67), 336 (weak) (4.53) nm; ECD (ϵ 5.32 $\times 10^{-5}$ M, MeOH) λ ($\Delta\epsilon$) 270–310 (−0), 320–350 (−0) nm; ^1H and ^{13}C NMR data, see Table 1; UPLC-HRAM-MS (positive) m/z 471.2011 $[\text{M}+\text{H}]^+$ (calcd for $\text{C}_{26}\text{H}_{31}\text{O}_8^+$, 471.2019).

Paulodiplacone D (10): red-orange amorphous substance; UV (ϵ 5.68 $\times 10^{-5}$ M, MeOH) λ_{max} (log ϵ) 293 (4.63), 337 (weak) (4.50) nm; ECD (ϵ 5.68 $\times 10^{-5}$ M, MeOH) λ ($\Delta\epsilon$) 293 (−1.94), 337 (+1.08) nm; IR (ATR) ν_{max} 3123, 2965, 2925, 1634, 1608, 1517, 1443, 1337, 1289, 1187, 1157, 1113, 1080, 1047, 1022, 985, 812, 773, 765 cm^{-1} ; ^1H and ^{13}C NMR data, see Table 2; UPLC-HRAM-MS (positive) m/z 441.1910 $[\text{M}+\text{H}]^+$ (calcd for $\text{C}_{25}\text{H}_{29}\text{O}_7^+$, 441.1913).

Paulownione H (12): orange amorphous substance; UV (ϵ 5.00 $\times 10^{-5}$ M, MeOH) λ_{max} (log ϵ) 293 (4.71), 336 (weak) (4.56) nm; ECD (ϵ 5.00 $\times 10^{-5}$ M, MeOH) λ ($\Delta\epsilon$) 270–310 (−0), 320–350 (−0) nm; IR (ATR) ν_{max} 3416, 2967, 2934, 1639, 1614, 1519, 1456, 1430, 1340, 1297, 1215, 1158, 1095, 1025 cm^{-1} ; ^1H and ^{13}C NMR data, see Table 2; UPLC-HRAM-MS (positive) m/z 501.2118 $[\text{M}+\text{H}]^+$ (calcd for $\text{C}_{27}\text{H}_{33}\text{O}_8^+$, 501.2125).

Paulodiplacone A (21): yellowish amorphous substance; UV (ϵ 5.48 $\times 10^{-5}$ M, MeOH) λ_{max} (log ϵ) 293 (4.65), 337 (weak) (4.52) nm; ECD (ϵ 5.48 $\times 10^{-5}$ M, MeOH) λ ($\Delta\epsilon$) 296 (−2.28), 337 (+1.52) nm; IR (ATR)

ν_{max} 3174, 2921, 2848, 1631, 1524, 1495, 1443, 1348, 1271, 1161, 1113, 1084, 1022, 981, 897, 816, 768 cm^{-1} ; ^1H and ^{13}C NMR data, see Table 2; UPLC-HRAM-MS (positive) m/z 457.1864 $[\text{M}+\text{H}]^+$ (calcd for $\text{C}_{25}\text{H}_{29}\text{O}_8^+$, 457.1862).

Paulodiplacone B (22): yellow-brown amorphous substance; UV (ϵ 5.48 $\times 10^{-5}$ M, MeOH) λ_{max} 296, 337 (weak) nm; ^1H and ^{13}C NMR data, see Table 3; UPLC-HRAM-MS (positive) m/z 457.1848 $[\text{M}+\text{H}]^+$ (calcd for $\text{C}_{25}\text{H}_{29}\text{O}_8^+$, 457.1862).

Tomentoflavone B (24): yellow-brown amorphous substance; UV (ϵ 5.34 $\times 10^{-5}$ M, MeOH) λ_{max} (log ϵ) 279 (4.61), 343 (4.59) nm; IR (ATR) ν_{max} 3149, 2929, 2848, 1649, 1601, 1511, 1451, 1436, 1341, 1267, 1177, 1095, 1044, 981, 820, 761 cm^{-1} ; ^1H and ^{13}C NMR data, see Table 3; UPLC-HRAM-MS (positive) m/z 469.1867 $[\text{M}+\text{H}]^+$ (calcd for $\text{C}_{26}\text{H}_{29}\text{O}_8^+$, 469.1862).

Tomentoflavone D (25): brown amorphous substance; UV (ϵ 5.19 $\times 10^{-5}$ M, MeOH) λ_{max} (log ϵ) 275 (4.63), 347 (4.62) nm; ^1H and ^{13}C NMR data, see Table 3; UPLC-HRAM-MS (positive) m/z 483.2011 $[\text{M}+\text{H}]^+$ (calcd for $\text{C}_{27}\text{H}_{31}\text{O}_8^+$, 483.2019).

4',5',5',7-Tetrahydroxy-3'-methoxy flavanone (27): orange amorphous substance; UV (ϵ 7.86 $\times 10^{-5}$ M, MeOH) λ_{max} (log ϵ) 289 (4.53), 334 (weak) (4.38) nm; ECD (ϵ 7.86 $\times 10^{-5}$ M, MeOH) λ ($\Delta\epsilon$) 270–310 (−0), 320–350 (−0) nm; ^1H and ^{13}C NMR data, see Table 4; UPLC-HRAM-MS (positive) m/z 319.0814 $[\text{M}+\text{H}]^+$ (calcd for $\text{C}_{16}\text{H}_{15}\text{O}_7^+$, 319.0818).

2.4. Cell cultures

The human monocytic leukemia cell line THP-1-XBlue™-MD2-CD14 was purchased from Invivogen (San Diego, CA, USA), and the THP-1 human monocytic leukemia cell line from the European Collection of Authenticated Cell Cultures (Salisbury, UK). Both cell lines were

Table 1
NMR spectroscopic data for paulodiplacone C (7), mimulone I (8), and tomentone C (9) (400 MHz, DMSO- d_6).

Paulodiplacone C (7)				Mimulone I (8)				Tomentone C (9)			
Position	δ_{C} , type	δ_{H} (J in Hz)	HMBC	δ_{C} , type	δ_{H} (J in Hz)	HMBC		δ_{C} , type	δ_{H} (J in Hz)	HMBC	
2	79.0, CH	5.29, m	3, 4, 1', 2', 6'	78.7, CH	5.32, m			79.4, CH	5.28, m	3, 4, 1', 2', 6'	
3	42.8, CH ₂	2.59, m	4, 10, 1'	42.6, CH ₂	2.55, m			42.8, CH ₂	2.59, m	4, 10, 1'	
		3.14, m	2, 4, 1'		3.12, m	2			3.19, m	2, 4, 1'	
4	197.0, C			196.1, C				197.0, C			
5	161.2, C			161.6, C				161.5, C			
6	108.1, C			108.3, C				108.3, C			
7	165.5, C			167.2, C				165.8, C			
8	95.0, CH	5.91, s	4, 6, 7, 9, 10	95.6, CH	5.88, s	6, 7, 9, 10		95.0, CH	5.90, s	4, 6, 7, 9, 10	
9	160.9, C			161.1, C				160.8, C			
10	102.0, C			103.4, C				101.9, C			
1'	130.1, C			129.7, C				C			
2'	114.9, CH	6.84, s	2, 1', 3', 4', 6'	128.9, CH	7.26, d (8.4)	2, 4', 6' (ov)		102.8, CH	6.57, s	2, 1', 3', 4', 6'	
3'	146.1, C			115.6, CH	6.74, d (8.4)	1', 4', 5' (ov)		148.7, C			
4'	146.1, C			158.2, C				134.8, C			
5'	115.9, CH	6.70, s	1', 3', 4'	115.6, CH	6.74, d (8.4)	1', 3', 4' (ov)		146.1, C			
6'	118.5, CH	6.70, s	2, 1', 2', 4'	128.9, CH	7.26, d (8.4)	2, 2', 4' (ov)		108.3, CH	6.51, s	2, 1', 2', 4', 5'	
1''	20.5, CH ₂	2.35, m	5, 6, 7, 2'', 3'', 8'', 9''	20.6, CH ₂	2.31, m	5, 6, 7, 2'', 3'', 9''		20.5, CH ₂	2.34, m	5, 6, 7, 2'', 3'', 8'', 9''	
2''	52.6, CH	2.09, t (7.4)	6, 1'', 3'', 4'', 6'', 8'', 9''	52.4, CH	2.11, t (7.4)	3'', 4'', 8''		52.6, CH	2.10, t (7.4)	6, 1'', 3'', 4'', 8'', 9''	
3''	45.7, C			45.8, C				45.8, C			
4''	25.9, CH ₃	0.88, s	2'', 3'', 5'', 6''	25.8, CH ₃	0.88, s	2'', 3'', 5'', 6''		25.8, CH ₃	0.88, s	2'', 3'', 5'', 6''	
5''	24.1, CH ₃	0.92, s	2'', 3'', 4'', 6''	24.2, CH ₃	0.91, s	2'', 3'', 4'', 6''		24.2, CH ₃	0.92, s	2'', 3'', 4'', 6''	
		0.92, s			0.92, s				0.92, s		
6''	85.5, CH	3.59, s	2'', 3'', 5'', 8''	85.3, CH	3.58, s			85.5, CH	3.59, s	2'', 3'', 5'', 8''	
		3.60, s			3.59, s				3.61, s		
7''	26.1, CH ₂	1.48, m	3'', 6'', 8''	26.0, CH ₂	1.48, m			26.1, CH ₂	1.48, m	3'', 6'', 8''	
		1.80, m	3'', 6'', 8'', 9''		1.80, m	6''			1.81, m	3''	
8''	39.5, CH ₂	1.24, m	2'', 7'', 9'', 10''	39.5, CH ₂	1.24, m			39.5, CH ₂	1.25, m	2'', 7'', 9'', 10''	
		1.39, m	2'', 6'', 7''		1.39, m				1.40, m	2'', 6'', 7''	
9''	86.3, C			86.8, C				86.5, C			
10''	18.7, CH ₃	1.18, s	2'', 8'', 9''	18.9, CH ₃	1.18, s	2'', 8'', 9''		18.6, CH ₃	1.18, s	2'', 8'', 9''	
		1.19, s			1.19, s				1.19, s		
OH-5		12.60, s	4, 5, 6, 7, 9, 10		12.65, s			12.61, s			
		12.61, s			12.65, s			12.62, s			
MeO-3'								56.4, CH ₃	3.72, s	3'	

ov – signals overlapped; carbons were assigned based on the HSQC and HMBC data.

Table 2NMR spectroscopic data for paulodiplacone D (10), paulownione H (12), and paulodiplacol A (21) (400 MHz, DMSO-*d*₆).

Paulodiplacone D (10)				Paulownione H (12)				Paulodiplacol A (21)			
Position	δ_C , type	δ_H (J in Hz)	HMBC	δ_C , type	δ_H (J in Hz)	HMBC		δ_C , type	δ_H (J in Hz)	HMBC	
2	78.9, CH	5.28, dd (2.8, 12.7)	3, 4, 1', 2', 6'	79.0, CH	5.26, m	4, 1', 2', 6'		83.5, CH	4.86, d (11.2)	3, 4, 1', 2', 6'	
3	42.8, CH ₂	2.59, dd (2.8, 17.2)	4, 10, 1'	42.8, CH ₂	2.55, m	4, 10		72.0, CH	4.41, dd (4.6, 11.2)	2, 4, 1'	
		3.11 (ov)	2, 4, 1'		3.18 (ov)	2, 4, 1'					
4	196.8, C			194.8, C				198.0, C			
5	161.4, C			161.4, C				161.7, C			
6	109.8, C			107.7, C				106.6, C			
7	165.8, C			170.6, C				166.9, C			
8	95.1, CH	5.91, s	6, 7, 9, 10	96.3, CH	5.73, s	4, 6, 7, 9, 10		95.3, CH	5.82, s	4, 6, 7, 9, 10	
9	160.9, C			161.1, C				160.8, C			
10	101.9, C			100.5, C				100.3, C			
1'	130.2, C			129.8, C				128.8, C			
2'	114.9, CH	6.83, s	2, 1', 3', 4', 6'	104.9, CH	6.73, s	2, 1', 3', 4', 6' (ov)		115.9, CH	6.82, s	2, 1', 3', 4', 6'	
3'	146.2, C			148.4, C				146.4, C			
4'	146.2, C			136.1, C				146.0, C			
5'	115.9, CH	6.70, s	1', 3', 4' (ov)	148.4, C				115.6, CH	6.69, s	1', 3', 4' (ov)	
6'	118.4, CH	6.70, s	2, 1', 2', 4' (ov)	104.9, CH	6.73, s	2, 1', 2', 4', 5' (ov)		119.9, CH	6.69, s	2, 1', 2', 4' (ov)	
1''	22.0, CH ₂	2.56, m	5, 6, 7, 2'', 3'', 8''	25.4, CH ₂	2.39, m	5, 6, 7, 2'', 3''		29.5, CH ₂	2.55, m	5, 6, 7, 2'', 3''	
2''	47.1, CH	2.42, m	6, 1'', 3'', 5'', 8'', 10''	76.4, CH	2.68, m	5, 6, 7, 2'', 3''		2.66, m		5, 6, 7, 2'', 3''	
3''	137.2, C			86.1, C	3.48 (ov)	6, 1'', 3'', 4'', 5''		73.7, CH	4.17, t (6.4)	6, 1'', 3'', 4''	
4''	22.9, CH ₃	1.49, br s	2'', 3'', 5''	22.9, CH ₃	1.12, s	2'', 3'', 5''		152.6, C		2'', 3'', 5''	
5''	119.6, CH	5.14, br s	4'', 6'', 7'', 2''	34.2, CH ₂	1.50, m	4'', 6''		108.7, CH ₂	4.62, br s	2'', 3'', 5''	
6''	32.2, CH ₂	1.83, m	3'', 5'', 7'', 8''	2.00, m	2.00, m	2'', 4'', 6''		31.2, CH ₂	4.77, br s	2'', 3'', 5''	
7''	73.4, CH	2.00, m	3'', 5'', 7'', 8''	31.5, CH ₂	1.63, m	5'', 7'' (ov)		26.5, CH ₂	2.05, br s	3'', 5'', 7'', 8''	
8''	38.6, C		2'', 5'', 6'', 8'', 9'', 10''	1.95, m	1.95, m	5''		5''		5''	
9''	25.6, CH ₃	0.89, s	2'', 7'', 8'', 9''	82.7, CH	4.24, t (7.4)	8'', 9'', 10''		125.2, CH	5.09, br s	5'', 6'', 9'', 10''	
10''	16.1, CH ₃	0.79, s	2'', 7'', 8'', 10''	146.9, C				131.1, C			
OH-5		12.57, s	5, 6, 10	109.9, CH ₂	4.68, s	7'', 8'', 10''		26.0, CH ₃	1.61, s	7'', 8'', 10''	
MeO-3'				4.90, s	4.90, s	7'', 8'', 10''					
MeO-5'				18.2, CH ₃	1.62, s	7'', 8'', 9'' (ov)		18.2, CH ₃	1.54, s	7'', 8'', 9''	
				12.54, s	12.54, s			12.23, s	12.23, s	5, 6, 10	
				12.57, s	12.57, s						
				56.6, CH ₃	3.73, s	3' (ov)					
				56.6, CH ₃	3.73, s	5' (ov)					

ov – signals overlapped; carbons were assigned based on the HSQC and HMBC data.

cultured as reported previously (Hošek et al., 2011; Brežani et al., 2018).

2.5. Cell viability testing

The effect of test compounds on the viability of THP-1-XBlue™-MD2-CD14 cells was measured as described previously (Hanáková et al., 2015; Leláková et al., 2019) using the cell proliferation reagent WST-1 (Roche, Basel, Switzerland). The test compounds (4, 6–10, 12, 16, 17, 19–21, and 23–25) dissolved in DMSO (Sigma-Aldrich) were added at increasing concentrations (0.37, 1.1, 3.3, 10, and 30 μ M). Experiments were run in three independent measurements performed in triplicates. The cytotoxicity of compounds 1–3, 5, 11, 13–15, 18, and 26 has been measured previously (Molčanová et al., 2021).

2.6. Detection of the activation of NF- κ B/AP-1

The activity of transcriptional factors NF- κ B/AP-1 was evaluated on the THP-1-XBlue™-MD2-CD14 cell line expressing an NF- κ B/AP-1-inducible SEAP reporter gene as reported previously (Hošek et al., 2011; Leláková et al., 2019). The test compounds (1–21 and 23–26) dissolved in DMSO at a concentration of 1 μ M were added. These concentrations had no cytotoxic effects. Experiments were carried out in three independent measurements performed in hexaplicates.

2.7. Differentiation into macrophages and evaluation of cytokine secretion

THP-1 monocytes were differentiated into macrophages using phorbol myristate acetate (PMA) and the cytokine production was triggered by adding LPS according to the protocol described previously (Brezani et al., 2018; Hošek et al., 2019). After 24 h, the supernatants (for TNF- α) and cell lysates (for IL-1 β) were collected. The concentrations of the cytokines (in the supernatants for TNF- α and cell lysates for IL-1 β) were measured using a Human TNF- α ELISA Kit (Life Technologies Co., Frederick, MD, USA) and a Human IL-1 β ELISA Kit (Diacclone, Besançon, France), according to the manufacturer's manual (Brezani et al., 2018; Hošek et al., 2019). The experiment was run in a triplicate.

2.8. Statistical analysis

Statistical analyses were carried out using IBM SPSS Statistics for Windows software, version 26.0 (IBM, Armonk, NY, USA). The data were graphed as the mean \pm SEM. Comparisons between groups were made using a Kruskal Wallis test followed by a pairwise comparison with a Bonferroni correction.

2.9. Computational details

Geometry optimization of compound 21 was performed with the

Table 3NMR spectroscopic data for paulodiplacol B (22), tomentoflavone B (24), and tomentoflavone D (25) (400 MHz, DMSO-*d*₆).

Paulodiplacol B (22)				Tomentoflavone B (24)				Tomentoflavone D (25)			
Position	δ_C type	δ_H (J in Hz)	HMBC	δ_C type	δ_H (J in Hz)	HMBC		δ_C type	δ_H (J in Hz)	HMBC	
2	83.7, CH	4.92, m	3, 4, 1', 2', 6'	164.0, C				163.2, C			
3	72.2, CH	4.47, m	2, 4, 1'	103.6, CH	6.75, s	2, 4, 10, 1'		103.3, CH	6.61, s	2, 4, 1'	
4	198.7, C			182.3, C				181.1, C			
5	162.5, C			158.6, C				159.1, C			
6	101.3, C			111.4, C				110.5, C			
7	161.0, C			163.0, C				168.9, C			
8	95.6, CH	5.80, s	6, 7, 9, 10	93.6, CH	6.49, s	6, 7, 9, 10		94.3, CH	6.21, s	6, 7, 9, 10	
9	161.0, C			155.7, C				156.7, C			
10	101.3, C			103.9, C				102.4, C			
1'	128.4, C			120.7, C				129.4, C			
2'	115.9, CH	6.82, s	2, 1', 3', 4', 6'	102.8, CH	7.09, s	2, 1', 3', 4', 6'		102.6, CH	7.05, s	2, 3, 1', 3', 4', 6'	
3'	146.6, C			149.2, C				149.4, C			
4'	145.9, C			139.6, C				139.1, C			
5'	115.6, CH	6.69, s	1', 3', 4' (ov)	146.7, C				149.4, C			
6'	119.9, CH	6.69, s	2, 1', 2', 4' (ov)	107.9, CH	7.09, s	2, 1', 2', 4', 5'		107.6, CH	7.05, s	2, 3, 1', 2', 4', 5'	
1''	25.0, CH ₂	2.36, m	5, 6, 2', 3'	21.5, CH ₂	3.18, d (6.7)	5, 6, 7, 2'', 3''		30.2, CH ₂	2.69, m	5, 6, 2'	
2''	65.7, CH	3.69, t (n. d.)	6, 4'', 5''	122.2, CH	5.14, t (6.7)	6, 1'', 4'', 5''		74.4, CH	4.14, m		
3''	81.2, C			134.8, C				n. o.			
4''	19.2, CH ₃	1.14, s	2'', 3'', 5''	16.5, CH ₃	1.68, s	2'', 3'', 5''		108.3, CH ₂	4.60, s	2'', 5''	
5''	37.8, CH ₂	1.55, m	2'', 3'', 6'', 7''	35.8, CH ₂	1.86, m	2'', 3'', 4'', 6'', 7''		31.5, CH ₂	2.05, s	2'', 5''	
6''	21.5, CH ₂	2.02, m	5'', 7'', 8''	33.8, CH ₂	1.41, m	3'', 5'', 7'', 8'', 10''		26.5, CH ₂	2.05, s	5''	
7''	124.5, CH	5.04, t (6.8)	5'', 6'', 9'', 10''	74.0, CH	3.76, t (6.6)	6'', 8'', 9'', 10''		125.2, CH	5.09, m		
8''	131.4, C			148.9, C				131.3, C			
9''	25.9, CH ₃	1.59, s	7'', 8'', 10''	110.3, CH ₂	4.65, s	7'', 8'', 10''		26.0, CH ₃	1.60, s	7'', 8'', 10''	
10''	17.9, CH ₃	1.52, s	7'', 8'', 9''	18.2, CH ₃	4.76, s	7'', 8'', 10''		18.2, CH ₃	1.53, s	7'', 8'', 9''	
OH-5		12.20, s		13.20, s				13.19, s			
MeO-3'				56.8, CH ₃	3.82, s	3'		56.8, CH ₃	3.81, s	3'	
MeO-5'								56.8, CH ₃	3.81, s	5'	

ov – signals overlapped, n. d. – not determined; carbons were assigned based on the HSQC and HMBC data.

Table 4NMR spectroscopic data for 4',5,5',7-tetrahydroxy-3'-methoxy flavanone (27) (400 MHz, DMSO-*d*₆).

4',5,5',7-Tetrahydroxy-3'-methoxy flavanone (27)			
Position	δ_C type	δ_H (J in Hz)	HMBC
2	79.2, CH	5.30, dd (2.7, 12.7)	4, 1', 2', 6'
3	42.8, CH ₂	2.61, dd (2.7, 17.1)	4, 10
4		3.16, dd (12.7, 17.1)	2, 4, 1'
4	196.4, C		
5	163.3, C		
6	96.6, CH	5.80, s	4, 5, 7, 8, 10
7	168.4, C		
8	95.6, CH	5.81, s	4, 6, 7, 9, 10
9	163.3, C		
10	102.0, C		
1'	129.2, C		
2'	102.9, CH	6.56, s	2, 1', 3', 4', 6'
3'	148.9, C		
4'	134.9, C		
5'	146.3, C		
6'	108.3, CH	6.52, s	2, 1', 2', 4', 5'
OH-5		12.13, s	
MeO-3'	56.4, CH ₃	3.72, s	3'

Carbons were assigned based on the HSQC and HMBC data.

Spartan'20 (ver. 1.0.0) software package (Spartan 20, Wavefunction Inc., Irvine CA, USA, 2020) using the density functional theory (DFT) with the B3LYP functional and def2-TZVP basis set. The calculation was performed in a vacuum.

3. Results and discussion

3.1. Compound isolation and structure elucidation

Selected fractions obtained from the chloroform portion of ethanolic

extracts derived from *P. tomentosa* fruits (Šmejkal et al., 2008; Navrátilová et al., 2013; Hanáková et al., 2015) were separated in several steps using column chromatography on silica gel and reversed-phase semi-preparative HPLC, leading to the isolation of several lipophilic geranylated flavonoids and two other phenolic compounds: flavanones with unmodified geranyl chains diplacone (1) and 3'-O-methyl-5'-hydroxydiplacone (2); flavanones with modified acyclic geranyl chains mimulone B (3), tomentodiplacone (4), paulodiplacone A (5), and (S,E)-5,7-dihydroxy-6-(7-hydroxy-3,7-dimethyl-2-*e*-n-1-yl)-2-(4-hydroxyphenyl)-3,4-dihydro-2H-1-benzopyran-4-one (6); flavanones with cyclic geranyl chains paulodiplacone C (7), mimulone I (8), tomentone C (9), paulodiplacone D (10), tomentodiplacone P (11), and paulownione H (12); pyranoflavonones tomentone II (13) and tomentone B (14); dihydroflavonols with unmodified geranyl chains mimulol (15), diplacol (16), 3'-O-methyl-5'-hydroxydiplacol (17), and 3'-O-methyl-5'-methoxydiplacol (18); dihydroflavonols with modified acyclic geranyl chains 3,3',4',5,7-pentahydroxy-6-[6-hydroxy-3,7-dimethyl-2(E),7-octadienyl]flavanone (19), tomentodiplacol (20), and paulodiplacol A (21); a dihydroflavonol with a cyclic geranyl chain paulodiplacol B (22); a flavone with an unmodified geranyl chain paulocatalinone C (23, syn. tomentoflavone C); flavones with modified acyclic geranyl chains tomentoflavone B (24) and tomentoflavone D (25); a pyranoflavone tomentoflavone A (26); a non-prenylated flavonoid 4',5,5',7-tetrahydroxy-3'-methoxy flavanone (27); and the simple phenolic compounds methyl ferulate and vanillic acid. The NMR and MS spectroscopic data for ten of the compounds (7–10, 12, 21, 22, 24, 25, and 27) did not match those of any compound previously isolated from *P. tomentosa*, and these were determined to be new flavonoid derivatives obtained from a natural source for the first time. Compounds 4, 6, 16, 17, 19, 20, 23, and methyl ferulate were identified by comparing their spectroscopic data with those in the literature (Šmejkal et al. 2007, 2008; Chen and Chi, 2014; Phillips et al., 1996; Jin et al., 2015; Asai et al., 2008; Tang et al., 2017; Phuong et al., 2014).

3'-O-Methyl-5'-hydroxydipicol (17) had been isolated previously from the flowers of *P. coreana* (Jin et al., 2015), and paucatalinone C (23) had been obtained from the fruit of *P. catalpifolia* (Tang et al., 2017), but this is the first report of their isolation (together with methyl ferulate) from *P. tomentosa*. The data supporting the identification of isolated compounds are gathered in Supplementary data (Figures A1–A148). The isolation and characterization of compounds 1–3, 5, 11, 13–15, 18, and 26 have been described in previous work (Molčanová et al., 2021).

The UV spectra of flavanones and dihydroflavonols 4, 6–10, 12, 16, 17, 19–22, and 27 showed maximal values of absorption at ~295 nm, which are mostly affected by the conjugation of ring A and its substitution pattern, and weak absorption bands at ~335 nm, which are probably caused by the absence of conjugation between ring B and the rest of the molecule (Figures A1, A9, A19, A28, A36, A46, A56, A65, A74, A83, A91, A100, A132, Supplementary data) (Vihakas, 2014; Molčanová et al., 2021). Compounds 23–25 exhibited UV spectra with maximum absorptions at ~275 nm (conjugation of ring A) and ~345 nm, which is detected in flavonoids wherein rings B and C are conjugated (via a double bond between carbons C-2 and C-3 in ring C) (Figures A108, A116, A125, Supplementary data), and these were assigned as absorption maxima typical for a flavone skeleton (Vihakas, 2014; Molčanová et al., 2021).

Infrared spectra were measured for selected compounds, all but one newly isolated, which were obtained in sufficient amounts (7, 8, 10, 12, 21, 23, and 24; Figures A10, A20, A37, A47, A92, A109, A117, Supplementary data). These IR spectra displayed broad absorption bands at ν_{\max} 3500–3200 cm^{-1} indicating the presence of hydroxy groups, intensive bands at ν_{\max} 3000–2850 cm^{-1} showing the presence of the methyl and methylene groups of prenylated compounds, an intensive band at ν_{\max} 1650–1580 cm^{-1} indicating the presence of a carbonyl group, and a series of absorption bands at ν_{\max} 1600–1450 cm^{-1} typical for aromatic compounds. Similar absorption bands for C-geranylated flavonoids had been observed previously (Navrátilová et al., 2013; Hanáková et al., 2015; Molčanová et al., 2021).

Analysis of the mass spectra in the positive mode (Figures A2, A11, A21, A29, A38, A48, A57, A66, A75, A84, A93, A101, A110, A118, A126, A133, A142, Supplementary data) showed the molecular ion $[\text{M}+\text{H}]^+$, adduct ions $[\text{M}+\text{Na}]^+$ and $[\text{M}+\text{K}]^+$, and the main fragment ion of the parent flavonoid structure with a methylene resulting from the neutral loss of a C9 unit (–124.1252 u.m.a., when it was not modified) from the C10 geranyl side chain (Cheng et al., 2019). In the negative mode (Figures A12, A39, A49, A58, A67, A76, A119, A134, A143, Supplementary data) the molecular ion peak $[\text{M}-\text{H}]^-$ was observed.

The compositions of all compounds were further elucidated by evaluating the NMR data using the ^1H NMR spectrum together with HSQC, HMBC, COSY, and NOESY experiments. The NMR data of most of the isolated compounds showed generally similar signals which were assigned to the flavonoid skeleton and geranyl side chain. The ^1H NMR spectra of flavanones 4, 6–10, 12, and 27 showed the presence of three doublets of doublets with approximate values of $\delta_{\text{H-2}}$ 5.3 ppm ($J = 3.0, 13.0$ Hz), $\delta_{\text{H-3a}}$ 2.7 ppm ($J = 3.0, 17.0$ Hz), and $\delta_{\text{H-3b}}$ 3.1 ppm ($J = 13.0, 17.0$ Hz) (Hanáková et al., 2015). Dihydroflavonols 16, 17, and 19–22 displayed two doublets at about $\delta_{\text{H-2}}$ 4.9 ppm and $\delta_{\text{H-3}}$ 4.5 ppm; their coupling constants were in the range of 11–12 Hz indicating a *trans* arrangement of H-2 and H-3 (Šmejkal et al., 2007). A proton singlet at about $\delta_{\text{H-3}}$ 6.7 ppm in 23–25 resulted from the presence of a flavone skeleton (Molčanová et al., 2021). The singlet at about δ_{H} 5.95 ppm was assigned to H-8 because of its HMBC correlations to C-6, C-7, C-9, and C-10, and a weaker correlation to C-4 (Fig. 1), as described previously (Hanáková et al., 2015; Molčanová et al., 2021). Carbon C-6 was assigned as the connection of the geranyl chain to the flavonoid skeleton based on the HMBC correlations of H-1'' with C-5 and C-7, and a NOESY correlation mainly with OH-5 (Molčanová et al., 2021). Further analysis of the NMR spectra revealed that the phenolic ring B of the flavonoid skeleton was either 4'-hydroxy- (6 and 8), 3',4'-dihydroxy- (7, 10, 16, 19, 21, and 22), 3'-methoxy-4'-hydroxy- (4 and 20), 3'-methoxy-4',

5'-dihydroxy- (9, 17, 23, 24, and 27), or 3',5'-dimethoxy-4'-hydroxy substituted (12 and 25).

The NMR data obtained for the isolated compounds showed the presence of geranyl (C_{10}) side chains in the compounds analyzed. An unmodified geranyl chain was observed for compounds 16, 17, and 23. Compounds 4, 6, 19–21, 24, and 25 showed acyclic geranyl chains modified by hydroxylation, mostly with the formation of a terminal double bond (except for compound 6). Several compounds showed a geranyl chain modified by cyclization (7–10, 12, and 22). Only compound 27 showed a singlet signal for proton H-6 instead of signals for a geranyl chain.

Compound 7 was obtained as a yellowish amorphous substance. Its molecular formula was determined by UPLC-HRAM-MS to be $\text{C}_{25}\text{H}_{28}\text{O}_7$ based on the presence of the molecular ion $[\text{M}+\text{H}]^+$ at m/z 441.1916 (calcd for $\text{C}_{25}\text{H}_{29}\text{O}_7^+$, 441.1913). The UV spectrum and NMR data (Table 1) revealed a flavanone skeleton. Two aromatic singlets, at $\delta_{\text{H-5,6}}$ 6.70 ppm and $\delta_{\text{H-2'}}$ 6.84 ppm (integrating for two and one hydrogens, respectively), and their HMBC correlations, showed the formation of a 3',4'-dihydroxyphenyl ring B (Molčanová et al., 2021). Further evaluation of the NMR data revealed the signals of two oxygenated carbons, at δ_{C} 85.5 and 86.3 ppm. No double bond signal indicated presence of a geranyl chain. The carbon signal at $\delta_{\text{C-10'}}$ 20.5 ppm was assigned as the connection with the flavanone moiety based on its HMBC correlations with C-5, C-6, and C-7 (Fig. 2). Further correlations with the carbon at $\delta_{\text{C-2'}}$ 52.6 ppm and the oxygenated quaternary carbon at $\delta_{\text{C-9'}}$ 86.3 ppm confirmed cyclization with OH-7. Another quaternary carbon at $\delta_{\text{C-3'}}$ 45.7 ppm (bearing methyl groups at $\delta_{\text{C-4'}}$ 25.9 ppm and at $\delta_{\text{C-5'}}$ 24.1 ppm) was connected to C-2 and further to the carbon at $\delta_{\text{C-6'}}$ 85.5 ppm which bears hydrogen at $\delta_{\text{H-6'}}$ 3.59 and 3.60 ppm (the two signals integrating for only one hydrogen indicated a mixture of stereoisomers at this chiral center). Proton signals for H-7 and H-8 (δ_{H} 1.48, 1.80, 1.24, and 1.39 ppm, respectively) were further assigned using HMBC, COSY, and NOESY correlations. Another ring was formed and terminated with a methyl group at $\delta_{\text{C-10''}}$ 18.7 ppm that was connected to carbon C-9''. This type of double-cyclized geranyl chain has never before been described for any compound isolated from *P. tomentosa*. Based on the data obtained, compound 7 was assigned the composition shown and named paulodiplacone C, in keeping with the previous paulodiplacones with 3',4'-dihydroxy flavanone structures (Molčanová et al., 2021).

Compound 8 was isolated as a yellowish amorphous substance. UPLC-HRAM-MS analysis in the positive mode revealed the presence of the molecular ion $[\text{M}+\text{H}]^+$ at m/z 425.1956 (calcd for $\text{C}_{25}\text{H}_{29}\text{O}_6^+$, 425.1964), corresponding to the molecular formula $\text{C}_{25}\text{H}_{28}\text{O}_6$. The NMR signals (Table 1) were mostly consistent with those of compound 7, a flavanone having an unusual double-cyclized geranyl chain. The only difference was found in the substitution of ring B, where the presence of two aromatic doublets at $\delta_{\text{H-2,6'}}$ 7.26 ppm and $\delta_{\text{H-3,5'}}$ 6.74 ppm ($J = 8.4$ Hz), each integrating for two protons, showed a 4'-hydroxyphenyl arrangement. This new compound was named mimulone I (8), because it has the same substitution of ring B observed in other mimulones (Navrátilová et al., 2013; Hanáková et al., 2015).

Compound 9 was obtained as a red-orange amorphous substance. Its molecular formula determined by UPLC-HRAM-MS was $\text{C}_{26}\text{H}_{30}\text{O}_8$, based on the presence of the molecular ion $[\text{M}+\text{H}]^+$ at m/z 471.2011 (calcd for $\text{C}_{26}\text{H}_{31}\text{O}_8^+$, 471.2019). Flavanone and geranyl chain signals similar to those for compounds 7 and 8 were again present (Table 1), with the only difference being the substitution of ring B. Singlets were observed at $\delta_{\text{H-2'}}$ 6.57 ppm and $\delta_{\text{H-6'}}$ 6.51 ppm, integrating for one proton each. The strong correlation of the methoxy protons (δ_{H} 3.72 ppm, 3H) with H-2' in the NOESY spectrum (Fig. 3) was used with the HMBC correlations to assign the position of the methoxy group and confirm the 3'-methoxy-4',5'-dihydroxy phenyl arrangement of ring B. According to these analyses, the composition of compound 9 was assigned as shown and it was named tomentone C, because the same substitution of ring B has been described for tomentone B (Molčanová et al., 2021).

Compound 10 was obtained as a red-orange amorphous substance.

On the basis of UPLC-HRAM-MS analysis supported by the presence of the molecular ion $[M+H]^+$ at m/z 441.1910 (calcd for $C_{25}H_{29}O_7$, 441.1913), the molecular formula was established as $C_{25}H_{29}O_7$. The UV spectrum and NMR signals (Table 2) corresponded to previously isolated compounds possessing a flavanone skeleton (Hanáková et al., 2015; Molčanová et al., 2021) with 3',4'-dihydroxyphenyl arrangement of ring B. The NMR data of the geranyl chain revealed the presence of methyl groups at δ_H 0.79, 0.89, and 1.49 ppm, one olefinic proton of a double bond at δ_H 5.14 ppm, and a multiplet at δ_H 3.21 ppm indicating the presence of a hydroxy group. The carbon at δ_C 11.2 ppm was established as the connection with the flavanone due to its HMBC correlations with carbons of ring A and it also showed HMBC correlations to δ_C 38.6, 47.1, and 137.2 ppm. The COSY spectrum showed a correlation of δ_H 1.1' 2.56 ppm and δ_H 2.2' 2.42 ppm, and the carbon at δ_C 47.1 ppm was therefore assigned as C-2''. It also provided correlations to δ_C 38.6, 119.6, and 137.2 ppm, which were assigned as C-8'', C-5'', and C-3'', respectively. These data indicated cyclization, but not with OH-7 as in the case of compounds 7, 8, or 9, because the quaternary carbon C-8'' bears two methyl groups, at δ_C 9.1' 25.6 and 16.1 ppm, respectively. The methyl group at δ_C 4.4' 22.9 ppm showed HMBC correlations to C-2'', C-3'', and C-5''. An oxygenated carbon at δ_C 73.4 ppm was assigned as C-7'' and the carbon at δ_C 32.2 ppm as C-6'' using HMBC, COSY, and NOESY correlations. The composition proposed for compound 10 (paulodiplacone D) shows a novel type of geranyl chain modification that has not been observed in compounds from *P. tomentosa* before.

Compound 12 was isolated as an orange amorphous substance. Its molecular formula was determined to be $C_{27}H_{32}O_9$ based on UPLC-HRAM-MS analysis in the positive mode, which showed the presence of the molecular ion $[M+H]^+$ at m/z 501.2118 (calcd for $C_{27}H_{32}O_9$, 501.2125). Analysis of the NMR spectra (Table 2) showed a flavanone structure with a symmetric 3',5'-dimethoxy-4'-hydroxyphenyl ring B with an aromatic singlet at δ_H 2.6' 6.73 ppm integrating for two hydrogens. Based on NOESY correlations (Fig. 4) with H-2' and H-6', two equal singlets for methoxy groups at δ_H 3.73 ppm integrating for six hydrogens were assigned to carbons C-3' and C-5', and the hydroxy group was assigned to C-4'. Further analysis revealed oxygenated carbons at δ_C 76.4, 82.7, and 86.1 ppm, methyl groups at δ_C 18.2 and 22.9 ppm, and signals at δ_C 109.9 and 146.9 ppm that indicated a terminal double bond of the geranyl chain (Hanáková et al., 2015; Molčanová et al., 2021). The carbon at δ_C 11' 25.4 ppm was assigned as the connection with the flavanone skeleton. The carbon at δ_C 2' 76.4 ppm (bearing a hydroxy group) was further connected with the quaternary carbon at δ_C 3' 86.1 ppm, which indicated linkage with oxygen and the creation of a ring. The methyl group at δ_C 22.9 ppm was established as C-4'' due to its HMBC correlations to C-2'', C-3'', and C-5'' (δ_C 34.2 ppm). Another methyl group at δ_C 18.2 ppm was assigned as C-10'', because it showed correlations to the carbons of the terminal double bond (δ_C 8' 146.9 and 109.9 ppm, respectively) and to the carbon at δ_C 82.7 ppm (bearing another hydroxy group) which was assigned as C-7''. The connection with the oxygenated ring through the carbon at δ_C 6' 31.5 ppm was confirmed, and a new type of cyclized and hydroxylated geranyl chain modification was identified. Compound 12 with the proposed composition shown was named paulownione H in keeping with the previous paulowniones A, B, and C with a 3',5'-dimethoxy-4'-hydroxyphenyl ring B (Hanáková et al., 2015; Hanáková et al., 2017).

Compound 21 was obtained as a yellowish amorphous substance. UPLC-HRAM-MS analysis in the positive mode revealed a molecular formula of $C_{25}H_{28}O_8$ based on the presence of the molecular ion $[M+H]^+$ at m/z 457.1864 (calcd for $C_{25}H_{28}O_8$, 457.1862). NMR analysis (Table 2) showed signals for a dihydroflavonol with a doublet at δ_H 2.486 ppm ($J = 11.2$ Hz), a doublet of doublets at δ_H 3.441 ppm ($J = 4.6, 11.2$ Hz), and a 3',4'-dihydroxy arrangement of ring B. The carbon signal at δ_C 73.7 ppm suggested the presence of a geranyl chain modified by oxidation, and diagnostic HMBC correlations of the triplet at δ_H 4.17 ppm with C-1'', C-3'', and C-4'' showed this proton to be H-2''. The signal at δ_C 11' 29.5 ppm was assigned as the connection with the

dihydroflavonol moiety. The presence of a methylene group linked to C-3 was suggested by the observation of broad singlets with chemical shifts at δ_H 4.4' 4.62 and 4.77 ppm connected to the carbon at δ_C 4' 108.7 ppm and their HMBC correlations to the quaternary carbon at δ_C 3' 152.6 ppm. HMBC and COSY correlations of the overlapping singlets at δ_H 2.05 ppm integrating for four hydrogens confirmed that they belong to carbons C-5'' and C-6'' despite the unusual shape of their signals (Fig. 5) (Molčanová et al., 2021). Two methyl singlets, at δ_H 9' 1.61 and 1.54 ppm, respectively, and the olefinic proton at δ_H 7' 5.09 ppm (broad singlet) formed the other part of the geranyl chain. This compound was isolated from a natural source for the first time. Because its composition was similar to that of paulodiplacone A (Molčanová et al., 2021) and considering its dihydroflavonol skeleton it was named paulodiplacol A (21).

Compound 22 was obtained as a yellow-brown amorphous substance. Its molecular formula was established to be $C_{25}H_{28}O_8$ based on the presence of the molecular ion $[M+H]^+$ at m/z 457.1848 (calcd for $C_{25}H_{28}O_8$, 457.1862). NMR data (Table 3) revealed signals for a dihydroflavonol having a 3',4'-dihydroxy substituted ring B similar to compound 21. Analysis of the NMR data for the geranyl moiety showed two oxidized carbons, at δ_C 65.7 and 81.2 ppm, which were assigned as C-2'' and C-3'', respectively, and formed a ring connected to OH-7. The methyl group at δ_H 4.4' 1.14 ppm provided correlation with C-2'', C-3'', and C-5'' (δ_C 37.8 ppm), and the geranyl chain was terminated with two methyl groups, at δ_H 9' 1.59 and 1.52 ppm, respectively. Based on the data obtained, the geranyl chain was found to be cyclized to form a 2H-pyran ring as previously described for tomentodiplacone N (Hanáková et al., 2015). Compound 22, isolated as a new compound, was named paulodiplacol B, and assigned the composition shown.

Compound 24 was obtained as a yellow-brown amorphous substance. The molecular formula was demonstrated by UPLC-HRAM-MS to be $C_{26}H_{28}O_8$, based on the presence of the molecular ion $[M+H]^+$ at m/z 469.1867 (calcd for $C_{26}H_{28}O_8$, 469.1862). The UV spectrum indicated a flavone skeleton, which was confirmed by observation of a proton singlet at δ_H 3.675 ppm and its HMBC correlations (Table 3). The NMR signals of ring B were mostly consistent with those of compound 9, and it was therefore assigned as 3'-methoxy-4',5'-dihydroxyphenyl. Part of the side chain resembled an unmodified geranylated derivative (δ_H 1' 2.4' 3.18, 5.14, and 1.68 ppm, respectively) (Hanáková et al., 2015; Molčanová et al., 2021). The 1H NMR spectrum showed a triplet at δ_H 3.76 ppm, indicating modification with an additional hydroxyl group. The observation of a CH_2 unit with chemical shifts at δ_C 110.3 ppm and δ_H 4.65 and 4.76 ppm, together with the quaternary carbon δ_C 148.9 ppm, suggested the presence of a methylene group (C-9'') linked to C-8''. An oxygenated carbon at δ_C 74.0 ppm was connected to the first part of the geranyl chain by two CH_2 groups (δ_C 5' 35.8 and 33.8 ppm, respectively). This type of modification of the geranyl chain has been described previously for several compounds, e.g., tomentodiplacol (Šmejkal et al., 2007), tomentomimulol (Schneiderová et al., 2013), or mimulone B (Schneiderová et al., 2013). Analysis of all the spectroscopic data for 24 led to the elucidation of its composition for the first time here, and it was named tomentoflavone B. Similarly, C-geranylated flavones and flavonols have previously been isolated from the fruit of *P. tomentosa* (tomentoflavone A) (Molčanová et al., 2021) and from the fruit peel of *P. catalpifolia* (paucatalinones C, D, E, and K) (Wang et al., 2017, 2019).

Compound 25 was obtained as a brown amorphous substance. UPLC-HRAM-MS analysis in the positive mode revealed a molecular formula of $C_{27}H_{30}O_8$ based on the presence of the molecular ion $[M+H]^+$ at m/z 483.2011 (calcd for $C_{27}H_{30}O_8$, 483.2019). The UV spectrum showed a flavone structural moiety, which was confirmed in the 1H NMR spectrum (Table 3) by observation of a singlet at δ_H 3.661 ppm. Geranyl chain signals similar to those for compound 21 were again present (with weaker intensity due to a smaller amount), and the signals of a 3',5'-dimethoxy-4'-hydroxyphenyl ring B corresponded to those of compound 12. The obtained data resulted in the identification of a new geranylated

flavone named tomentoflavone D (**25**), which was assigned with the composition shown.

Compound **27** was isolated as an orange amorphous substance. Its molecular formula was determined to be $C_{16}H_{14}O_7$ based on UPLC-HRAM-MS analysis in the positive mode, which showed the presence of the molecular ion $[M+H]^+$ at m/z 319.0814 (calcd for $C_{16}H_{15}O_7^+$, 319.0818). The UV spectrum together with the NMR signals (Table 4) of the flavonoid nucleus corresponded to a flavanone pattern and the signals for ring B corresponded to those of compounds **9**, **23**, and **24**. The singlet at δ_H 5.81 ppm was assigned to H-8, but unlike the other flavonoids, no signals for a geranyl chain were observed. Instead, the 1H NMR spectrum showed another proton singlet at δ_H 5.80 ppm for H-6, which was assigned based on its HMBC correlations. 4',5,5',7-Tetrahydroxy-3'-methoxy flavanone (**27**) was isolated from a natural source for the first time here.

In addition, the absolute configurations of compounds **6–10**, **12**, **16**, **17**, **19–21**, and **27** at the stereogenic centers C-2 and C-3 were determined by analyzing circular dichroism (CD) spectra. Compounds **6–8** and **10** showed a positive Cotton effect for the $n \rightarrow \pi^*$ electronic transition at 320–350 nm and a negative Cotton effect for the $\pi \rightarrow \pi^*$ electronic transition at 270–310 nm, which led to their assignment as 2S-flavanones (Fig. 6) (Slade et al., 2005; Hanáková et al., 2015). Compounds **9**, **12**, and **27** displayed no discernible Cotton effects (using different concentrations), and they were therefore considered to be racemic mixtures of 2S and 2R enantiomers (Slade et al., 2005; Hanáková et al., 2015). The dihydroflavonols (**16**, **17**, and **19–21**) with *trans* relative configurations of their C-2 and C-3 substituents as shown by the NMR data and a positive $n \rightarrow \pi^*$ Cotton effect at wavelengths 320–350 nm were assigned a 2R,3R-configuration (Slade et al., 2005; Hanáková et al., 2015). Modifications of the geranyl chain in compounds **7–10**, **12**, **19–22**, **24**, and **25** formed other stereogenic centers, but too little material was isolated for their configurations to be determined. In the case of compounds **7**, **8**, and **9** several stereoisomers are likely present concurrently as suggested by the presence of two distinguishable singlets for H-5'', H-6'', H-10'', and OH-5 in their 1H NMR spectra. The absolute configuration for compound **22** could not be determined because the isolated substance was unstable. Later HPLC analysis showed the presence of two peaks in the chromatogram, and because the compound has several chiral centers, it had likely become a mixture of stereoisomers.

Based on the fact that we were not able to obtain suitable single-crystals of any of the studied compounds for single-crystal X-ray analysis, we decided to determine the geometry of the selected compound **21** by mean of quantum chemical calculations at the B3LYP/def2-TZVP level of theory using the Spartan'20 (ver. 1.0.0) software package. The optimized geometry of **21** is shown in Fig. 7, while the atomic coordinates of the molecule in the XYZ format are given in Supplementary data (Table A4).

The calculated bond distances are quite typical for such organic molecules. The molecule consists of three moieties, i.e. the group of ten carbon atoms from the main chain (A) of the geranyl group, the carbon and oxygen atoms forming the 10-membered ring B in the chromone moiety, and the carbon atoms forming the 6-membered phenyl ring (C). The least-squares planes were fitted through the atoms of the individual fragments of **27**, as defined above, to reveal a spatial arrangement of the molecule (Macrae et al., 2020) and the results of this can be seen in Figure A149, where the dihedral angles between the corresponding two least-square planes are as follows: the angle between the chain A (green color) and ring B (blue color) = 85.52° , the angle between the chain A (green color) and ring C (red color) = 83.59° , and the angle between the rings B and C = 39.62° .

3.2. Cell viability testing

Before evaluating the anti-inflammatory potential of the test compounds, their cytotoxicity for cellular systems should be determined.

The assay aimed to determine the safe concentration of each compound which would not affect the cellular viability and could be used for subsequent experiments. A lipophilic geranyl chain can confer on a molecule a strong affinity for biological membranes and greater ability to interact with the environment of the cells, which means a greater potential for cytotoxic activity (Botta et al., 2005; Šmejkal, 2014; Molčanová et al., 2019). Compounds **8** and **25** showed IC_{50} values $> 30 \mu M$, compounds **4**, **7**, **9**, **10**, **12**, and **20** showed IC_{50} values in the range of 10–30 μM , and compounds **6**, **17**, **19**, **21**, **23**, and **24** in the range of 3.3–10 μM . The most cytotoxic compound was determined to be diplacol (**16**), which showed IC_{50} in the range of 1.1–3.3 μM . At a concentration of 1.1 μM the cell viability was around 100%, therefore 1 μM was established as the non-toxic concentration. The antiproliferative and cytotoxic potentials of compounds **1–3**, **5**, **11**, **13–15**, **18**, and **26** have been reported in previous work (Molčanová et al., 2021). Diplacone (**1**) was the most potent antiproliferative and cytotoxic agent in this group with $IC_{50} = 9.31 \pm 0.72 \mu M$ and $LC_{50} = 18.01 \pm 1.19 \mu M$ as tested on the THP-1 cell line using WST-1 and LDH assays, respectively (Molčanová et al., 2021). Based on the cytotoxicity assays, the following anti-inflammatory tests were performed on each of the compounds **1–21** and **23–26** at non-toxic concentrations of 1 μM .

3.3. Anti-inflammatory potential in cell-based models

LPS stimulation of the TLR-4 in the cells induced signaling cascades leading to the activation of NF- κ B/AP-1 and subsequent production of the reporter protein secreted embryonic alkaline phosphatase (SEAP), the activity of which was measured spectrophotometrically using a QUANTI-Blue™ assay (Brezáni et al., 2018). All of the test compounds (**1–21** and **23–26**) reduced the activation of NF- κ B/AP-1 24 h after the addition of LPS (Fig. 8). From this set of 25 geranylated flavonoids, we found thirteen compounds that attenuated the activity of NF- κ B/AP-1 in a statistically significant manner (**5**, **14–18**, **21**, and **26** with $***p < 0.0001$; **1** with $***p < 0.001$; **6**, **9**, **25** with $**p < 0.01$; and **12** with $*p < 0.05$). Eight of these compounds (**5**, **14–18**, **21**, and **26**) were found to be more active than prednisone, a widely used anti-inflammatory drug.

The most active dihydroflavonols diplacol (**16**) and mimulol (**15**) have an unmodified geranyl side chain, as do three other active compounds (**1**, **17**, and **18**). On the other hand, several compounds with modified geranyl chains also showed interesting activity, e.g., hydroxylation and formation of a terminal double bond seemed to favor the effect (**5**, **21**, and **25**), as did the formation of a pyran ring (**14** and **26**). Most of the test compounds were flavanones and dihydroflavonols, but two of the four flavones tested possessed interesting activity. Compounds **14** and **26**, each with a 3'-methoxy-4',5'-dihydroxyphenyl arrangement of ring B and a geranyl chain forming a pyran ring, were both significantly active, even though one is a flavanone and the other a flavone. This shows that both flavanones and flavones can have the potential for anti-inflammatory activity. The substitution of ring B with a methoxy group may also be important for this effect, as shown by the case of flavanones **7–9**. All three have the same unusual double-cyclized geranyl chain, but only compound **9** has a methoxy group on ring B and only it possesses significant activity. A similar observation was made for the case of compounds **13** and **14**. Both are pyranoflavanones, but they differ in the substitution of ring B, with the methoxy group of compound **14** significantly increasing its activity. 3',4'-Dihydroxy (**1**, **5**, **16**, **21**) or 3'-methoxy-4',5'-dihydroxy (**9**, **14**, **17**, and **26**) substitution of ring B was observed in most of the active compounds, but 3',5'-dimethoxy-4'-hydroxy (**12**, **18**, and **25**) and 4'-hydroxy (**6** and **15**) substitutions were also associated with the activity. Combinations of several structural characteristics may be important for the anti-inflammatory effect.

Compounds **5**, **15**, **16**, **21**, and **26** were the most active in the assay of NF- κ B/AP-1 activity. Their effects on the LPS-stimulated secretion of pro-inflammatory cytokines tumor necrosis factor α (TNF- α) and interleukin 1β (IL- 1β) were therefore further evaluated. This assay was carried out on PMA-differentiated THP-1 macrophages using ELISA. The

results are shown in Figures A149 and A150 (Supplementary data). Surprisingly, none of the test compounds reduced the production of either TNF- α or IL-1 β . In the case of IL-1 β , the measurements were performed in the cell lysates. We decided on this because the amount of this cytokine released into the media after 24 h of incubation of the cells with LPS was only in the range of pg/ μ g of total protein, whereas the concentration of IL-1 β in the cell lysate was eight times as much and therefore easier to detect.

The discrepancy between the results shown in Fig. 2 and Figures A149 and A150 (Supplementary data) can be explained by the plurality of possible outcomes of the activation of the NF- κ B pathway in cells (Liu et al., 2017). Another explanation is that the THP-1-XBlue™-MD2-CD14 cell line serves as a gene reporter for another pathway, i.e., the AP-1 transcription factor. AP-1 regulates a broad range of processes in cells, such as proliferation, apoptosis, differentiation, survival, cell migration, and transformation (Ye et al., 2014). Therefore, this possibility needs more clarification in further experiments.

The ability of 23 flavanones or dihydroflavonols isolated from the fruit of *P. tomentosa*, together with the non-prenylated flavanones eriodictol and naringenin, to reduce the production of the pro-inflammatory cytokine TNF- α in THP-1 cells after LPS stimulation has been evaluated (Hanáková et al., 2015). Several compounds affected the production of TNF- α in a statistically significant manner, and the compounds mimulone H, tomentodiplacone B, tomentodiplacol B, tomentodiplacone N, 3'-O-methyldiplacone, 3'-O-methyldiplacol, 3'-O-methyl-5'-methoxydiplacone, and 6-geranyl-5,7-dihydroxy-3',4'-dimethoxyflavanone affected the secretion of TNF- α as much as or more than the prednisone that was used as a positive control for the assay. Non-prenylated compounds showed weaker activity. Selected compounds, namely diplacone (1), mimulone H, tomentodiplacone N, 3'-O-methyldiplacone, and 3',4'-O-dimethyl-5'-hydroxydiplacone, were chosen for further experiments, and it was reported that they reduced both the secretion of TNF- α and the level of its corresponding mRNA and inhibited the nuclear translocation of NF- κ B, which controls the expression of TNF- α , by blocking the degradation of I κ B (Hanáková et al., 2015). The results of the present study confirm the previously published anti-inflammatory potential of *P. tomentosa* flavonoids. Furthermore, nineteen prenylated or geranylated flavanones or dihydroflavonols and 6-geranylchromone obtained from fruit of *P. tomentosa* were assayed for their ability to inhibit cyclooxygenases (COX-1 and COX-2) and 5-lipoxygenase (5-LOX) (Hanáková et al., 2017). The test compounds showed varying degrees of activity, with several of them showing activity comparable to or greater than the standards used in the mentioned assays. However, only the compound tomentodiplacone O showed greater selectivity against COX-2 versus COX-1 when compared with ibuprofen. The ability of the test compounds to interact with the above-mentioned enzymes was supported by molecular docking studies, which revealed the possible incorporation of selected test substances into the active sites of these enzymes. Furthermore, one of the COX/LOX dual inhibitors, diplacone (1), was studied *in vitro* to evaluate its effect on inflammation in LPS-treated THP-1 macrophages, supporting its previously observed anti-inflammatory activity and revealing the mechanism of action (Hanáková et al., 2017). Nineteen geranylated flavanones or dihydroflavonols were isolated from the fruit of *P. tomentosa* in another series and six of these compounds were tested for inhibitory effects on the TNF- α -induced expression of IL-8, which is related to respiratory inflammatory diseases such as chronic obstructive pulmonary disease in human alveolar basal epithelial cells (Ryu et al., 2017). Results showed that the compounds tomentins F, G, H, I, J, and K inhibited the TNF- α -induced IL-8 level significantly. In human neutrophil elastase (HNE) enzyme assays, all of the compounds tested displayed significant HNE inhibition and were compared with the positive controls quercetin, luteolin, and apigenin. The compounds isopaucatalinone B, tomentins A and J, prokinawan, 3'-O-methyldiplacone, and 6-geranyl-5,7,3',5'-tetrahydroxy-4'-methoxyflavanone were the most active. These results suggest that dihydroflavonols and flavanones

from *P. tomentosa* fruits possess potent anti-inflammatory activities and HNE inhibition and may be good lead compounds for certain inflammation-related respiratory diseases (Ryu et al., 2017).

Diplacone (1) and mimulone, two geranylated flavanones obtained from *P. tomentosa*, were previously tested *in vivo* on a model of colitis in rats; they ameliorated the symptoms of colitis, delayed their onset, and reduced the levels of antioxidant enzymes (Vočhyánová et al., 2015). These compounds may provide an option for the alternative or supplementary treatment of patients, and their structures can provide leads or inspiration for the synthesis of new anti-inflammatory agents for the treatment of inflammatory bowel diseases, such as Crohn's disease or ulcerative colitis (Vočhyánová et al., 2015).

Other experiments have confirmed the potential of geranylated flavonoids of *Paulownia* spp. to interact with the biochemical pathways involved in inflammation. Compounds from the flowers of *P. coreana* inhibited the LPS-induced production of NO in RAW264.7 cells, compared with aminoguanidine as a positive control (Jin et al., 2015). Of these, flavanones with a geranyl group at C-6 exhibited significantly greater inhibitory activity than the simple flavanones. These results indicate that the presence of an unmodified geranyl group at the C-6 position of a flavanone derivative is an important factor for the inhibitory activity of NO, and hydroxylation of the geranyl group might be responsible for a loss of activity. NO plays an important role in the inflammatory process, and inhibitors of NO production may be potential anti-inflammatory agents (Jin et al., 2015). Furthermore, the anti-inflammatory effects of C-geranylated flavonoids (paulowninones D, E, F, and G) from the flowers of *P. fortunei* were evaluated on H9c2 cells for LPS-induced inflammation using an MTT assay. Astragale injection® was used as the positive control. The experimental results for all of these four flavonoids showed strong activity and greatly increased cell vitality compared to the positive control, suggesting they may potentially protect cardiomyocytes against LPS-induced inflammation. In addition, all four compounds greatly reduced the levels of serum IL-6 and TNF- α in the same cell model using the ELISA method, showing effects comparable to those observed for the positive control (Zhang et al., 2020). These findings suggest that flavonoid constituents obtained from *Paulownia* spp. may have potential uses in the treatment of inflammation or may be valuable sources of inspiration for the development of new drug candidates.

4. Conclusions

Twenty-seven flavonoids (1–27), twenty-six of them geranylated with different modifications, and one non-geranylated flavanone were isolated from the fruit of *P. tomentosa* and studied for their anti-inflammatory potential using THP-1-XBlue™-MD2-CD14 cells. Ten new compounds (7–10, 12, 21, 22, 24, 25, and 27) were characterized structurally using UV, IR, HRMS, NMR, and CD analyses. Most of the novel compounds showed the presence of a geranyl moiety functionalized by cyclization and/or hydroxylation. The compounds were tested for their anti-inflammatory potential to affect the activation of NF- κ B/AP-1 after LPS stimulation. All of the test compounds (1–21 and 23–26) reduced the activation of NF- κ B/AP-1 24 h after the addition of LPS. From the set of 25 geranylated flavonoids, thirteen compounds attenuated the activities of NF- κ B/AP-1 in a statistically significant manner and eight (5, 14–18, 21, and 26) were found to be more active than prednisone, a widely used anti-inflammatory drug. The most active compounds were dihydroflavonols with an unmodified geranyl side chain. On the other hand, several compounds with geranyl chains modified by, e.g., hydroxylation and the formation of a terminal double bond, or the formation of a pyran ring, also possessed interesting activity. Flavanones and flavones also showed a statistically significant effect, which shows that the combination of several structural characteristics can be important for the anti-inflammatory activity. The five most active compounds (5, 15, 16, 21, and 26) were further studied for their effects on the LPS-stimulated secretion of pro-inflammatory cytokines TNF- α

and IL-1 β using ELISA. None of the compounds showed significant activity, which can be explained by the plurality of possible outcomes of activation of the NF- κ B pathway in cells. The isolated active compounds have to be tested on the animal models to determine their effects on living organisms for their potential usage in the future.

Funding

This work was supported by the Czech Sciences Foundation [grant number CSF Bilateral AT-CZ 21-38204L – Complexes of selected transition metals with plant-derived compounds with anti-NF- κ B and pro-PPAR dual activities] (K.Š.); Masaryk University, Grant Agency of Masaryk University [grant number MUNI/C/0032/2021 – Izolace obsahových látek z různých frakcí získaných z plodů *Paulownia tomentosa* pomocí různých chromatografických metod]; Masaryk University, Specific research – support for student projects [grant numbers MUNI/A/1688/2020 – Izolace sekundárních metabolitů s potenciální biologickou aktivitou z rostlinných zdrojů and MUNI/A/1654/2020 – Testing of biological activity of selected natural substances *in vitro*]; and the Research infrastructure METROFOOD-CZ (Ministry of Education, Youth and Sports of the Czech Republic) [grant number LM2018100] including access to its facilities.

CRediT authorship contribution statement

Lenka Molčanová: Conceptualization, Data curation, Formal analysis, Investigation, Methodology, Validation, Visualization, Roles/ Writing - original draft, Writing - review & editing. **Jakub Tremel:** Conceptualization, Data curation, Formal analysis, Methodology, Project administration, Resources, Supervision, Validation, Writing - review & editing. **Veronika Brežani:** Data curation, Formal analysis, Investigation, Methodology, Writing - review & editing. **Petr Marsík:** Data curation, Formal analysis, Funding acquisition, Investigation, Methodology, Writing - review & editing. **Sebnem Kurhan:** Data curation, Investigation. **Zdeněk Trávníček:** Data curation, Formal analysis, Funding acquisition, Investigation, Methodology, Writing - review & editing. **Pavel Uhrin:** Formal analysis, Funding acquisition, Writing - review & editing. **Karel Šmejkal:** Conceptualization, Data curation, Formal analysis, Funding acquisition, Project administration, Resources, Writing - review & editing. All authors have read and agreed to the published version of the manuscript.

Declaration of competing interest

The authors declare that they have no known competing financial interests or personal relationships that could have appeared to influence the work reported in this paper.

Data availability

The data that has been used is confidential.

Acknowledgments

Special thanks to Dr. Frank Thomas Campbell for the language correction and manuscript editing.

List of abbreviations

IL-1 β : interleukin 1 β , LPS: lipopolysaccharide, NF- κ B/AP-1: nuclear factor κ B/activator protein 1, PMA: phorbol myristate acetate, TNF- α : tumor necrosis factor α .

Appendix A. Supplementary data

Supplementary data to this article can be found online at <https://doi.org/10.1016/j.jep.2022.115509>.

References

- Andrade, P.B., Valentão, P., 2018. Insights into natural products in inflammation. *Int. J. Mol. Sci.* 19, 644. <https://doi.org/10.3390/ijms19030644>.
- Asai, T., Hara, N., Kobayashi, S., Kohshima, S., Fujimoto, Y., 2008. Geranylated flavanones from the secretion on the surface of the immature fruits of *Paulownia tomentosa*. *Phytochemistry* 69, 1234–1241. <https://doi.org/10.1016/j.phytochem.2007.11.011>.
- Azab, A., Nassar, A., Azab, A.N., 2016. Anti-inflammatory activity of natural products. *Molecules* 21, 1321. <https://doi.org/10.3390/molecules21101321>.
- Botta, B., Vitali, A., Menendez, P., Misiti, D., Delle Monache, G., 2005. Prenylated flavonoids: pharmacology and biotechnology. *Curr. Med. Chem.* 12, 713–739. <https://doi.org/10.2174/0929867053202241>.
- Brezani, V., Leláková, V., Hassan, S.T.S., Berchová-Bímová, K., Nový, P., Klouček, P., Marsík, P., Dall'Acqua, S., Hošek, J., Šmejkal, K., 2018. Anti-infectivity against herpes simplex virus and selected microbes and anti-inflammatory activities of compounds isolated from *Bucayptus globulus* labill. *Viruses* 10, 360. <https://doi.org/10.3390/v10070360>.
- Chen, C.-N., Chi, L.-L., 2014. Prenylflavanone Compounds for Modulating Diabetes. Patent EP 2783684 A1.
- Cheng, C.-I., Jia, X.-h., Xiao, C.-m., Tang, W.-z., 2019. Paulownia C-geranylated flavonoids: their structural variety, biological activity and application prospects. *Phytochemistry Rev.* 18, 549–570. <https://doi.org/10.1007/s11101-019-09614-2>.
- Cho, J.K., Ryu, Y.B., Curtis-Long, M.J., Ryu, H.W., Yuk, H.J., Kim, D.W., Kim, H.J., Lee, W.S., Park, K.H., 2012. Cholinesterase inhibitory effects of geranylated flavonoids from *Paulownia tomentosa* fruits. *Bioorg. Med. Chem.* 20, 2595–2602. <https://doi.org/10.1016/j.bmc.2012.02.044>.
- Cho, J.K., Curtis-Long, M.J., Lee, K.H., Kim, D.W., Ryu, H.W., Yuk, H.J., Park, K.H., 2013. Geranylated flavonoids displaying SARS-CoV papain-like protease inhibition from the fruits of *Paulownia tomentosa*. *Bioorg. Med. Chem.* 21, 3051–3057. <https://doi.org/10.1016/j.bmc.2013.03.027>.
- Erbar, C., Gülden, C., 2011. Ontogeny of the flowers in *Paulownia tomentosa* – a contribution to the recognition of the resurrected monogeneric family Paulowniaceae. *Flora* 206, 205–218. <https://doi.org/10.1016/j.flora.2010.05.003>.
- Hanáková, Z., Hošek, J., Babula, P., Dall'Acqua, S., Václavík, J., Šmejkal, K., 2015. C-geranylated flavanones from *Paulownia tomentosa* fruits as potential anti-inflammatory compounds acting via inhibition of TNF- α production. *J. Nat. Prod.* 78, 850–863. <https://doi.org/10.1021/acs.jnatprod.5b00005>.
- Hanáková, Z., Hošek, J., Kutil, Z., Temml, V., Landa, P., Vaněk, T., Schuster, D., Dall'Acqua, S., Cvačka, J., Polanský, O., Šmejkal, K., 2017. Anti-inflammatory activity of natural geranylated flavonoids: cyclooxygenase and lipoxygenase inhibitory properties and proteomic analysis. *J. Nat. Prod.* 80, 999–1006. <https://doi.org/10.1021/acs.jnatprod.6b01011>.
- Hong, D., Yang, H., Jin, C.-L., Holmgren, N.H., 1998. Scrophulariaceae through gesneriaceae. In: Wu, Z.-y., Raven, P.H. (Eds.), *Flora of China*. Missouri Botanical Garden Press, pp. 1–212.
- Hošek, J., Bartos, M., Chudík, S., Dall'Acqua, S., Innocenti, G., Kartal, M., Kokoska, L., Kollár, P., Kutil, Z., Landa, P., Marek, R., Závalová, V., Zemlicka, M., Šmejkal, K., 2011. Natural compound cudraflavone B shows promising anti-inflammatory properties *in vitro*. *J. Nat. Prod.* 74, 614–619. <https://doi.org/10.1021/np100638h>.
- Hošek, J., Leláková, V., Bobál, P., Pížová, H., Gazdová, M., Malaník, M., Jakubczyk, K., Veselý, O., Landa, P., Temml, V., Schuster, D., Prachyavarakorn, V., Pailee, P., Ren, G., Zpurný, F., Oravec, M., Šmejkal, K., 2019. Prenylated stilbenoids affect inflammation by inhibiting the NF- κ B/AP-1 signaling pathway and cyclooxygenases and lipoxygenase. *J. Nat. Prod.* 82, 1839–1848. <https://doi.org/10.1021/acs.jnatprod.9b00081>.
- Jiang, T.-F., Du, X., Shi, Y.-P., 2004. Determination of flavonoids from *Paulownia tomentosa* (thunb) Steud by micellar electrokinetic capillary electrophoresis. *Chromatographia* 59, 255–258.
- Jin, Q., Lee, C., Lee, J.W., Lee, D., Kim, Y., Hong, J.T., Kim, J.S., Kim, J.-H., Lee, M.K., Hwang, B.Y., 2015. Geranylated flavanones from *Paulownia coreana* and their inhibitory effects on nitric oxide production. *Chem. Pharm. Bull.* 63, 384–387. <https://doi.org/10.1248/cpb.c14-00839>.
- Kaur, S., Wong, H.K., Southall, M.D., Mahmood, K., 2015. *Paulownia tomentosa* (princess tree) extract reduces DNA damage and induces DNA repair processes in skin cells. *Advances in DNA Repair Chapter 10*, 315–334. <https://doi.org/10.5772/60005>.
- Kobayashi, S., Asai, T., Fujimoto, Y., Kohshima, S., 2008. Anti-herbivore structures of *Paulownia tomentosa*: morphology, distribution, chemical constituents and changes during shoot and leaf development. *Ann. Bot.* 101, 1035–1047. <https://doi.org/10.1093/aob/mcn033>.
- Leláková, V., Šmejkal, K., Jakubczyk, K., Veselý, O., Landa, P., Václavík, J., Bobál, P., Pížová, H., Temml, V., Steinacher, T., Schuster, D., Granica, S., Hanáková, Z., Hošek, J., 2019. Parallel *in vitro* and *in silico* investigations into anti-inflammatory effects of non-prenylated stilbenoids. *Food Chem.* 285, 431–440. <https://doi.org/10.1016/j.foodchem.2019.01.128>.
- Liu, T., Zhang, L., Joo, D., Sun, S.-C., 2017. NF- κ B signaling in inflammation. *Signal Transduct. Targeted Ther.* 2, 17023. <https://doi.org/10.1038/sigtrans.2017.23>.
- Macrae, C.F., Sovago, I., Cottrell, S.J., Galek, P.T.A., McCabe, P., Pidcock, E., Platings, M., Shields, G.P., Stevens, J.S., Towler, M., Wood, P.A., 2020. Mercury 4.0: from visualization to analysis, design and prediction. *J. Appl. Crystallogr.* 53, 226–235. <https://doi.org/10.1107/S1600576719014092>.
- Maleki, S.J., Crespo, J.F., Cabanillas, B., 2019. Anti-inflammatory effects of flavonoids. *Food Chem.* 299, 125124. <https://doi.org/10.1016/j.foodchem.2019.125124>.

- Marques, S.M., Šupolíková, L., Molčanová, L., Šmejkal, K., Bednář, D., Slaninová, I., 2021. Screening of natural compounds as P-glycoprotein inhibitors against multidrug resistance in cancer. *Biomedicines* 9, 357. <https://doi.org/10.3390/biomedicines9040357>.
- Molčanová, L., Janošková, D., Dall'Acqua, S., Šmejkal, K., 2019. C-prenylated flavonoids with potential cytotoxic activity against solid tumor cell lines. *Phytochemistry Rev.* 18, 1051–1100. <https://doi.org/10.1007/s11101-019-09641-z>.
- Molčanová, L., Kauerová, T., Dall'Acqua, S., Maršik, P., Kollár, P., Šmejkal, K., 2021. Antiproliferative and cytotoxic activities of C-geranylated flavonoids from *Paulownia tomentosa* Steud. *Fruit. Bioorg. Chem.* 111, 104797. <https://doi.org/10.1016/j.bioorg.2021.104797>.
- Navrátilová, A., Schneiderová, K., Veselá, D., Hanáková, Z., Fontana, A., Dall'Acqua, S., Cvačka, J., Innocenti, G., Novotná, J., Urbanová, M., Pelletier, J., Čížek, A., Zemlicková, H., Šmejkal, K., 2013. Minor C-geranylated flavanones from *Paulownia tomentosa* fruits with MRSA antibacterial activity. *Phytochemistry* 89, 104–113. <https://doi.org/10.1016/j.phytochem.2013.01.002>.
- Phillips, W.R., Baj, N.J., Gunatilaka, A.A.L., Kingston, D.G.I., 1996. C-geranyl compounds from *Mimulus clevelandii*. *J. Nat. Prod.* 59, 495–497. <https://doi.org/10.1021/np960240i>.
- Phuong, N.T.M., Cuong, T.T., Quang, D.N., 2014. Anti-inflammatory activity of methyl ferulate isolated from *Stemona tuberosa* Lour. *Asian Pac. J. Trop. Med.* 7 (Suppl. 1), S327–S331. [https://doi.org/10.1016/S1995-7645\(14\)60254-6](https://doi.org/10.1016/S1995-7645(14)60254-6).
- Ryu, H.W., Park, Y.J., Lee, S.U., Lee, S., Yuk, H.J., Seo, K.-H., Kim, Y.-U., Hwang, B.Y., Oh, S.-R., 2017. Potential anti-inflammatory effects of the fruits of *Paulownia tomentosa*. *J. Nat. Prod.* 80, 2659–2665. <https://doi.org/10.1021/acs.jnatprod.7b00325>.
- Schneiderová, K., Šlapetová, T., Hrabal, R., Dvořáková, H., Procházková, P., Novotná, J., Urbanová, M., Cvačka, J., Šmejkal, K., 2013. Tomentomimulol and mimulone B: two new C-geranylated flavonoids from *Paulownia tomentosa* fruits. *Nat. Prod. Res.* 27, 613–618. <https://doi.org/10.1080/14786419.2012.683002>.
- Slade, D., Ferreira, D., Marais, J.P.J., 2005. Circular dichroism, a powerful tool for the assessment of absolute configuration of flavonoids. *Phytochemistry* 66, 2177–2215. <https://doi.org/10.1016/j.phytochem.2005.02.002>.
- Šmejkal, K., Grycová, L., Marek, R., Lemiére, F., Jankovská, D., Forejtníková, H., Vančo, J., Suchý, V., 2007. C-geranyl compounds from *Paulownia tomentosa* fruits. *J. Nat. Prod.* 70, 1244–1248. <https://doi.org/10.1021/np070063w>.
- Šmejkal, K., Chudík, S., Klouček, P., Marek, R., Cvačka, J., Urbanová, M., Julínek, O., Kokoska, L., Šlapetová, T., Holubová, P., Zima, A., Dvorská, M., 2008. Antibacterial C-geranylflavonoids from *Paulownia tomentosa* fruits. *J. Nat. Prod.* 71, 706–709. <https://doi.org/10.1021/np070446u>.
- Šmejkal, K., Svačinová, J., Šlapetová, T., Schneiderová, K., Dall'Acqua, S., Innocenti, G., Závalová, V., Kollár, P., Chudík, S., Marek, R., Julínek, O., Urbanová, M., Kartal, M., Csöllei, M., Doležal, K., 2010. Cytotoxic activities of several geranyl-substituted flavanones. *J. Nat. Prod.* 73, 568–572. <https://doi.org/10.1021/np900681y>.
- Šmejkal, K., 2014. Cytotoxic potential of C-prenylated flavonoids. *Phytochemistry Rev.* 13, 245–275. <https://doi.org/10.1007/s11101-013-9308-2>.
- Spartan 20, 2020. Wavefunction Inc., Irvine CA, USA.
- Tang, W.-Z., Wang, Y.-A., Gao, T.-Y., Wang, X.-J., Zhao, Y.-X., 2017. Identification of C-geranylated flavonoids from *Paulownia catalpifolia* Gong Tong fruits by HPLC-DAD-ESI-MS/MS and their anti-aging effects on 2BS cells induced by H₂O₂. *Chin. J. Nat. Med.* 15. [https://doi.org/10.1016/S1875-5364\(17\)30059-6](https://doi.org/10.1016/S1875-5364(17)30059-6), 0384–0391.
- Vihakas, M., 2014. Flavonoids and Other Phenolic Compounds: Characterization and Interactions with Lepidopteran and Sawfly Larvae. Doctoral thesis, University of Turku, Finland.
- Vochýánová, Z., Bartošová, L., Bujdákova, V., Fictum, P., Husník, R., Suchý, P., Šmejkal, K., Hošek, J., 2015. Dipalacone and mimulone ameliorate dextran sulfate sodium-induced colitis in rats. *Fitoterapia* 101, 201–207. <https://doi.org/10.1016/j.fitote.2015.01.012>.
- Wang, Y.-a., Xue, J., Jia, X.-h., Du, C.-l., Tang, W.-z., Wang, X.-j., 2017. New antioxidant C-geranylated flavonoids from the fruit peels of *Paulownia catalpifolia* T. Gong ex D. Y. Hong. *Phytochem. Lett.* 21, 169–173. <https://doi.org/10.1016/j.phytol.2017.06.025>.
- Wang, Y.-A., Guo, X., Jia, X.-H., Xue, J., Du, H.-F., Du, C.-L., Tang, W.-Z., Wang, X.-J., Zhao, Y.-X., 2019. Undescribed C-geranylflavonoids isolated from the fruit peel of *Paulownia catalpifolia* T. Gong ex D.Y. Hong with their protection on human umbilical vein endothelial cells injury induced by hydrogen peroxide. *Phytochemistry* 158, 126–134. <https://doi.org/10.1016/j.phytochem.2018.11.010>.
- Ye, N., Ding, Y., Wild, C., Shen, Q., Zhou, J., 2014. Small molecule inhibitors targeting activator protein 1 (AP-1). *J. Med. Chem.* 57, 6930–6948. <https://doi.org/10.1021/jm5004733>.
- Zhang, J.-K., Li, M., Li, M., Du, K., Lv, J., Zhang, Z.-G., Zheng, X.-K., Feng, W.-S., 2020. Four C-geranyl flavonoids from the flowers of *Paulownia fortunei* and their anti-inflammatory activity. *Nat. Prod. Res.* 34, 3189–3198. <https://doi.org/10.1080/14786419.2018.1556263>.
- Zhou, J., Xie, G., Yan, X., 2011. Encyclopedia of Traditional Chinese Medicines Molecular Structures, Pharmacological Activities, Natural Sources and Applications, vol. 6. Indexes, Springer-Verlag Berlin Heidelberg. <https://doi.org/10.1007/978-3-642-16744-7>.
- Zhu, Z.-H., Chao, C.-J., Lu, X.-Y., Xiong, Y.G., 1986. *Paulownia* in China: Cultivation and Utilization. Asian Network for Biological Sciences and International Development Research Centre, Chinese Academy of Forestry, Beijing.

6.8. ARTICLE 8

Treml, J.; Nykodýmová, D.; Kubatka, P. *Phytochemistry Reviews* 2025, doi: 10.1007/s11101-025-10121-w (IF=7.300).



Structure activity relationship of flavonoids as PPAR γ agonists

Jakub Tremł · Daniela Nykodýmová · Peter Kubatka



Received: 1 October 2024 / Accepted: 24 March 2025
© The Author(s) 2025

Abstract Peroxisome proliferator-activated receptor γ (PPAR γ) is a transcriptional factor and key regulatory element in glucose and lipid metabolism. We have attempted to determine the structure–activity relationship between flavonoids as PPAR γ agonists through a literature search. To compare results from different studies and methods, we have recalculated them to the percentage of positive control (%_{PC}). We have also described various methods used to determine PPAR γ agonists. The most promising PPAR γ agonists are isoflavones, namely 4'-fluoro-7-hydroxy-isoflavone (**4**; %_{PC} = 710.3%). The results presented in this review could be used for further semisynthetic modifications of flavonoids to enhance their PPAR γ agonistic activity.

Keywords Flavonoids · Isoflavones · Diabetes mellitus · PPAR γ

Introduction

Peroxisome proliferator-activated receptors (PPAR) are transcription factors that are induced by a plethora of ligands. There are three isoforms of PPAR: PPAR α , PPAR β/δ , and PPAR γ . The PPAR are members of the nuclear receptor superfamily and are located predominantly in the nucleus, forming inactive heterodimers with the retinoid X receptor (RXR). Upon ligand binding, the complex undergoes a conformational change. It switches to an active state, in which it binds to specific DNA sequences called peroxisome proliferator response elements (PPRE) and manages gene transcription (Ahmadian et al. 2013).

The isoform PPAR γ is specifically involved in adipogenesis, glucose homeostasis, inflammation, and the uptake and storage of fatty acids. Its natural ligands are unsaturated fatty acids and eicosanoids, with thiazolidinediones (TZDs) serving as synthetic examples. Previous research has established that PPAR γ is implicated in the pathogenesis of several serious diseases, including type 2 diabetes mellitus, chronic inflammation, cardiovascular and neurodegenerative diseases, and cancer. Therefore, it is considered to be an important therapeutic target (Hamblin et al. 2009; Ahmadian et al. 2013; Grygiel-Górniak 2014).

The TZDs are highly effective peroral antidiabetics, but their prescription gradually declined because of concerns about their adverse effects: fluid retention, weight gain, cardiac hypertrophy, increased risk of

J. Tremł (✉) · D. Nykodýmová
Department of Molecular Pharmacy, Faculty of
Pharmacy, Masaryk University, Palackého tř. 1,
612 00 Brno, Czech Republic
e-mail: tremlj@pharm.muni.cz

P. Kubatka
Department of Histology and Embryology, Jessenius
Faculty of Medicine, Comenius University in Bratislava,
Mala Hora 4, 03601 Martin, Slovakia

heart attack, and bladder cancer. The agonistic effect of TZDs on peroxisome proliferator-activated receptor γ (PPAR γ) leads to insulin sensitization, which is their mechanism of action (Matin et al. 2009; Ahmadian et al. 2013; Wang et al. 2014). Therefore, partial PPAR γ agonists retaining glucose-lowering benefits are considered as promising strategy to reduce the risk of adverse effects (Soccio et al. 2014).

Plant natural products have always been a promising pool of structures for drug discovery, and the field of PPAR γ agonists is no exception (Wang et al. 2014). Among them, the flavonoids play a very important role. The name of these polyphenolic structures comes from the Latin word “flavus,” meaning yellow, their natural pigmentation. In nature, flavonoids can be found in many plant parts: leaves, seeds, bark, and flowers. They act as attractants for pollinators, protectors against UV irradiation, and antimicrobials. On the other hand, flavonoids are considered to be indispensable components in a variety of nutraceutical, pharmaceutical, medicinal, and cosmetic applications. More than 10,000 different flavonoids have been isolated and identified (Dixon and Pasinetti 2010; Trembl and Šmejkal 2016; Panche et al. 2016).

Moreover, Matin et al. have hypothesized that the 7-hydroxy-benzopyran-4-one moiety shared by many flavonoids resembles the core structure of TZDs and also of fibrates, known agonists of PPAR α . Since fibrates alleviate weight gain, they might reduce certain side effects induced by PPAR γ activation. Thus, flavonoids sharing the 7-hydroxy-benzopyran-4-one moiety appear to be promising partial dual PPAR γ/α agonists (Matin et al. 2009).

Structurally, flavonoids can be divided into two main groups, the 3-phenylchromans (the isoflavonoids, including isoflavones (Fig. 1), isoflavans and isoflavanones (Fig. 2) and the 2-phenylchromans (the flavonoids, including flavans (Fig. 3), flavones (Fig. 4), flavanones (Fig. 5), flavonols (Fig. 6), anthocyanidins and anthocyanines (Fig. 7), and flavanols (including flavonolignans; Fig. 8)).

Structure–activity relationship study

A literature search for studies of the structure–activity relationship (SAR) of flavonoids and their PPAR γ agonistic effects was performed with databases Google Scholar, Science Direct, and SciFinder® for

the years 2000–2024, using the keywords “flavonoids” (“flavanes”, etc.) and “PPAR γ ” or “PPAR gamma”. Fifty-three scientific studies fitting the abovementioned criteria were found. The outline of the article is presented in the Fig. 9.

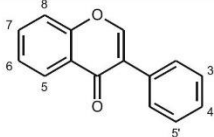
The first part of this chapter deals with the methods used to detect PPAR γ agonism—two groups of methods involve incubation with a cell culture; the other group is cell-free and deals with binding to an isolated PPAR γ protein.

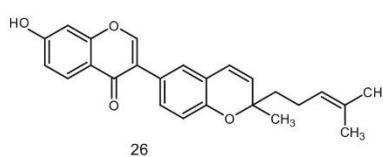
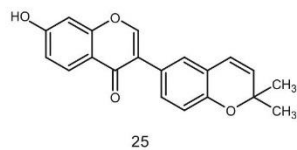
The second part presents scientific articles describing the PPAR γ agonistic activity of more than one class of flavonoids. These studies allow us to directly line up the flavonoid classes according to their effect on PPAR γ agonism. The literature search found 20 such research articles. Because each scientific article used a different methodology, we decided to recalculate the resulting values (fold activation or EC₅₀) relative to the value of a positive control with the percentage of the positive control (%_{PC}) as the mean of comparison. When the recalculation was not possible due to missing result of a positive control, we summarized the results in a table.

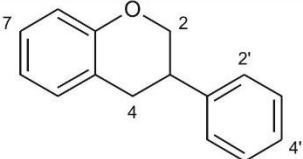
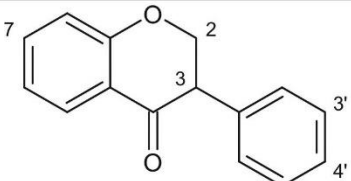
The third part focuses on SARs within individual flavonoid classes and uses the same kind of comparison, using %_{PC} or summarization in tables. All figures showing the %_{PC} values of various flavonoids are visualized as scatter plots using IBM SPSS Statistics for Windows, version 26.0 (Armonk, NY, USA).

Methods used to measure PPAR γ agonism

The first approach involved incubation of the test compounds with cells followed by the preparation of nuclear extracts (Fig. 10). The amount of PPAR γ present in the extract correlated with the rate of PPAR γ activation during the incubation and can be detected using the ELISA method. In principle, the wells are coated with PPRE dsDNA, to which the PPAR γ binds and is later detected with specific antibodies (Salam et al. 2008; Scazzocchio et al. 2011; Ghorbani et al. 2012). Another method uses detection with the electrophoretic mobility shift assay (EMSA). In this case, PPRE dsDNA is labeled with biotin and incubated with nuclear extract. The samples are then separated using nondenaturing polyacrylamide gel, transferred to a nylon membrane, and visualized using streptavidin bound to horseradish peroxidase and chemiluminescence (Ding et al. 2010).

								
No.	Compound	5	6	7	8	3'	4'	5'
1	ψ-Baptigenin	H	H	OH	H	methylenebis(oxy)		H
2	Biochanin A	OH	H	OH	H	H	OCH ₃	H
3	Genistein	OH	H	OH	H	H	OH	H
4	4'-Fluoro-7-hydroxyisoflavone	H	H	OH	H	H	F	H
5	3',5'-Dimethoxy-7-hydroxyisoflavone	H	H	OH	H	OCH ₃	H	OCH ₃
6	3'-Methoxy-7-hydroxyisoflavone	H	H	OH	H	OCH ₃	H	H
7	3',4',5'-Trifluoro-7-hydroxyisoflavone	H	H	OH	H	F	F	F
8	Formononetin	H	H	OH	H	H	OCH ₃	H
9	3',4',7-Trihydroxyisoflavone	H	H	OH	H	OH	OH	H
10	Daidzin	H	H	<i>O</i> -D-Glc ^a	H	H	OH	H
11	Genistin	OH	H	<i>O</i> -D-Glc ^a	H	H	OH	H
12	Prunetin	OH	H	OCH ₃	H	H	OH	H
13	Puerarin	H	H	OH	<i>C</i> -D-Glc ^a	H	OH	H
14	Daidzein	H	H	OH	H	H	OH	H
15	Calycosin	H	H	OH	H	OH	OCH ₃	H
16	6-Hydroxydaidzein	H	OH	OH	H	H	OH	H
17	3'-Hydroxygenistein	OH	H	OH	H	OH	OH	H
18	3'-Chlorodaidzein	H	H	OH	H	Cl	OH	H
19	3',4',6-Trihydroxyisoflavone	H	OH	H	H	OH	OH	H
20	4',6,7-Trihydroxyisoflavone	H	OH	OH	H	H	OH	H
21	Corylifol A	H	H	OH	H	Geranyl	OH	H
22	4',7-Dihydroxy-3',5'-diprenylisoflavone	H	H	OH	H	Prenyl	OH	Prenyl
23	8-Prenyldaidein	H	H	OH	Prenyl	H	OH	H
24	Neobavaisoflavone	H	H	OH	H	Prenyl	OH	H

^a Glc = glucoside**Fig. 1** Structures of isoflavones 1–26. **25** = Corylin; **26** = neocorylin

						
No.	Compound	2	4	7	2'	4'
27	Equol (3 <i>S</i>)	H	H	OH	H	OH
28	(3 <i>R</i> ,4 <i>S</i>)-4,2',4'-Trihydroxy-7-methoxy-4'- <i>O</i> - β -D-glucopyranosylisoflavan	H	OH	OCH ₃	OH	<i>O</i> -D-Glc ^b
29	(3 <i>S</i> ,4 <i>R</i>)-4,2',4'-Trihydroxy)-7-methoxyisoflavan	H	OH	OCH ₃	OH	OH
30	(2 <i>S</i> ,3 <i>R</i> ,4 <i>R</i>)-4,2',4'-Trihydroxy-2,7-dimethoxyisoflavan	OCH ₃	OH	OCH ₃	OH	OH
						
No.	Compound	2	3	7	3'	4'
31	3,4',7-Trihydroxy-2-methoxy-3'-geranyl-isoflavanone	OCH ₃	OH	OH	Geranyl	OH

^b Glc = glucoside

Fig. 2 Structures of isoflavanes **27–30** and isoflavanone **31**

The second approach is a cell-based transactivation or reporter luciferase assay, in which a plasmid DNA is transfected into a cell culture (Fig. 11). Usually, three separate plasmids are transfected to the cells: an expression plasmid containing the sequence of the whole PPAR γ gene or just the ligand-binding domain (LBD) connected to Gal4 transcription factor; a

reporter plasmid containing PPRE sequence or upstream activation sequence (UAS), where Gal4 binds, this reporter plasmid also contains a gene for luciferase, which is produced upon activation by PPAR γ or Gal4; and the last plasmid is a control that usually produces another type of luciferase from *Renilla reniformis*, a species of soft sea coral (Mueller

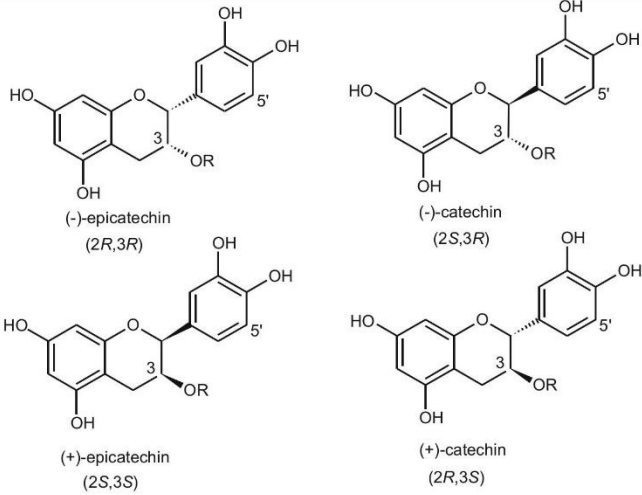
			
No.	Compound	3	5'
32	(-)-Epigallocatechin gallate	Galloyl	OH
33	(-)-Galocatechin gallate	Galloyl	OH
34	(-)-Epicatechin gallate	Galloyl	H
35	(-)-Catechin gallate	Galloyl	H
36	(-)-Epigallocatechin	H	OH
37	(-)-Epicatechin	H	H
38	(-)-Catechin	H	H
39	(+)-Catechin	H	H
40	Procyanidin B2	Dimer of (-)-epicatechin	
41	Epigallocatechin	Mixture of (+) and (-) enantiomers	
42	Galocatechin (mixture of (+) and (-))	H	OH
43	Epigallocatechin gallate	Mixture of (+) and (-) enantiomers	
44	Epicatechin gallate	Mixture of (+) and (-) enantiomers	

Fig. 3 Structures of flavans **32–50**. **45** = Oncoglabrinol A, **46** = onoglabrinol B; **47** = onoglabrinol C; **48** = catechin-7-4'-*O*-digallate; **49** = catechin-7-3'-*O*-digallate; **50** = (+)-catechin-7-*O*-gallate

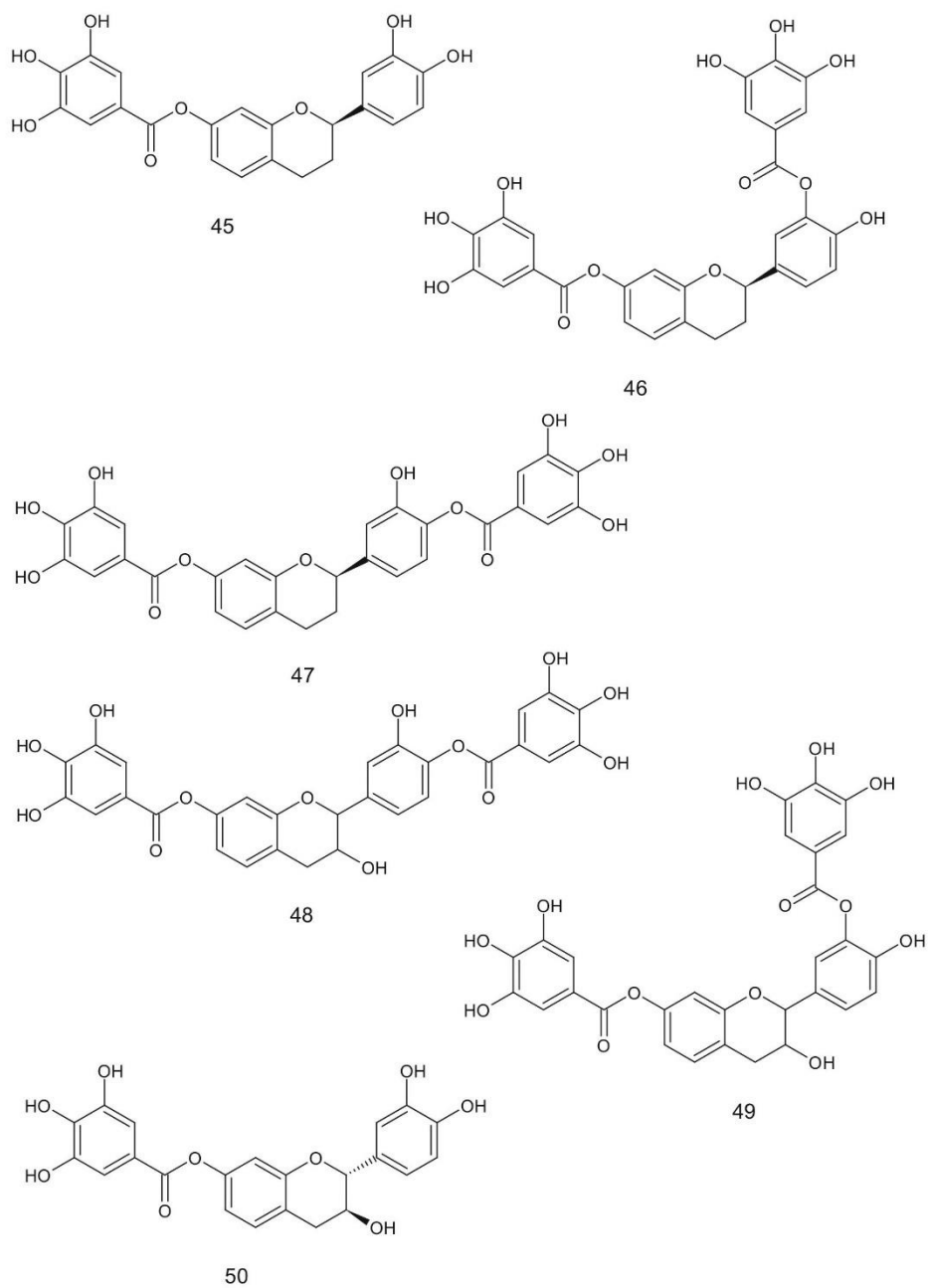
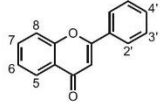


Fig. 3 continued

Fig. 4 Structures of flavones **51**—**107**. **93** = α -Naphthoflavone; **99** = β -naphthoflavone; **104** = cyclomulberrin; **105** = nigrasin I

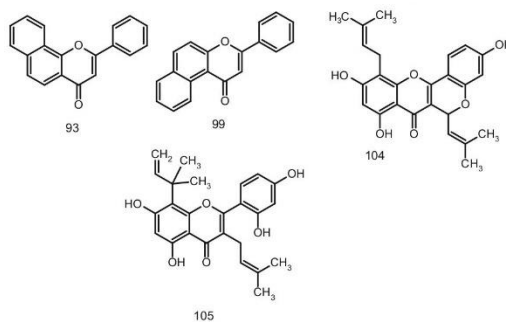


No.	Compound	5	6	7	8	2'	3'	4'
51	Apigenin	OH	H	OH	H	H	H	OH
52	Chrysin	OH	H	OH	H	H	H	H
53	Luteolin	OH	H	OH	H	H	OH	OH
54	Diosmetin	OH	H	OH	H	H	OH	OCH ₃
55	5,4'-Dihydroxyflavone	OH	H	H	H	H	H	OH
56	4'-(4''-Nitrobenzoyloxy)-7-methoxy-6-isopentenylflavone	H	Prenyl	OCH ₃	H	H	H	4''-Nitrobenzoyloxy
57	4'-Acetyloxy-7-methoxy-6-isopentenylflavone	H	Prenyl	OCH ₃	H	H	H	Acetyloxy
58	4'-Hydroxy-7-methoxy-6-isopentenylflavone	H	Prenyl	OCH ₃	H	H	H	OH
59	4'-Hydroxy-7-methoxy-6-isopentenylflavone	H	Isopentyl	OCH ₃	H	H	H	OH
60	Acerosin	OH	OCH ₃	OH	OCH ₃	H	OH	OCH ₃
61	Hispidulin	OH	OCH ₃	OH	H	H	H	OH
62	Scutellarein	OH	OH	OH	H	H	H	OH
63	Homoplantagin	OH	OCH ₃	<i>O</i> -D-Glc ^c	H	H	H	OH
64	Apigenin-8- <i>C</i> - α -L-arabinopyranoside	OH	H	OH	<i>C</i> -L-Ara ^d	H	H	OH
65	Baicalin	OH	OH	<i>O</i> -D-GlcA ^c	H	H	H	H
66	Oroxylin A	OH	OCH ₃	OH	H	H	H	H
67	Chrysin 5,7-diprenyl ether	<i>O</i> -prenyl	H	<i>O</i> -prenyl	H	H	H	H
68	Chrysin 5-prenyl-7-benzyl ether	<i>O</i> -prenyl	H	<i>O</i> -benzyl	H	H	H	H
69	Chrysin 5-benzyl-7-prenyl ether	<i>O</i> -benzyl	H	<i>O</i> -prenyl	H	H	H	H
70	Chrysin 5-benzyl-7-benzyl ether	<i>O</i> -benzyl	H	<i>O</i> -benzyl	H	H	H	H
71	Chrysin 5-benzyl ether	<i>O</i> -benzyl	H	OH	H	H	H	H
72	Chrysin 5-methyl-7-benzyl ether	OCH ₃	H	<i>O</i> -benzyl	H	H	H	H
73	Chrysin 7-benzyl ether	OH	H	<i>O</i> -benzyl	H	H	H	H
74	Chrysin 5-(4''-fluoro)benzyl ether	<i>O</i> -(4''-fluoro)benzyl	H	OH	H	H	H	H
75	Chrysin 5-allyl ether	<i>O</i> -allyl	H	OH	H	H	H	H
76	Chrysin 5-(4''-chloro)benzyl ether	<i>O</i> -(4''-chloro)benzyl	H	OH	H	H	H	H
77	Apigenin-7- <i>O</i> - β -D-glucuronide	OH	H	<i>O</i> -D-GlcA ^c	H	H	H	OH
78	Chrysoeriol	OH	H	OH	H	H	OCH ₃	OH
79	Chrysoeriol-7- <i>O</i> - β -D-glucuronide	OH	H	<i>O</i> -D-GlcA ^c	H	H	OCH ₃	OH
80	Diosmetin-7- <i>O</i> - β -D-glucuronide methyl ester	OH	H	<i>O</i> -D-GlcA ^c	H	H	OH	OCH ₃

Fig. 4 continued

				methyl ester				
81	Apigenin-7- <i>O</i> -β-D-glucuronide methyl ester	OH	H	<i>O</i> -D-GlcA ^c methyl ester	H	H	H	OH
82	Linarin	OH	H	<i>O</i> -L-Rha-D-Glc ^c	H	H	H	OCH ₃
83	Acacetin	OH	H	OH	H	H	H	OCH ₃
84	7-Methoxyflavone	H	H	OCH ₃	H	H	H	H
85	7,8-Dihydroxyflavone	H	H	OH	OH	H	H	H
86	Flavone	H	H	H	H	H	H	H
87	7,4'-Dihydroxyflavone	H	H	OH	H	H	H	OH
88	Wogonin	OH	H	OH	OCH ₃	H	H	H
89	Baicalcin	OH	OH	OH	H	H	H	H
90	Tangeretin	OCH ₃	OCH ₃	OCH ₃	OCH ₃	H	H	OCH ₃
91	4',7,8-Trihydroxyflavone	H	H	OH	OH	H	H	OH
92	3',7,8-Trihydroxyflavone	H	H	OH	OH	H	OH	H
94	Vitexin	OH	H	OH	<i>O</i> -D-Glc ^c	H	H	OH
95	Neodiosmin	OH	H	<i>O</i> -Neohesp ^c	H	H	OH	OCH ₃
96	Diosmin	OH	H	<i>O</i> -L-Rha-D-Glc ^c	H	H	OH	OCH ₃
97	5,6-Dihydroxyflavone	OH	OH	H	H	H	H	H
98	3',4'-Dihydroxyflavone	H	H	H	H	H	OH	OH
100	2',3',6-Trihydroxyflavone	H	OH	H	H	OH	OH	H
101	3',4',6-Trihydroxyflavone	H	OH	H	H	H	OH	OH
102	3',5,6-Trihydroxyflavone	OH	OH	H	H	H	OH	H
103	4',6-Dihydroxyflavone	H	OH	H	H	H	H	OH
106	8-(1''-Hydroxyisoprenyl)-5,6-dihydroxy-7,4'-dimethoxyflavone	OH	OH	OCH ₃	1''-Hydroxyisoprenyl	H	H	OCH ₃
107	Oroxyloside	OH	OCH ₃	<i>O</i> -D-GlcA ^c	H	H	H	H

^c Glc = glucoside; Ara = arabinose; GlcA = glucuronide; Rha = rhamnoside; Neohesp = neohesperidoside (L-rhamnosyl-(1→2)-D-glucose)



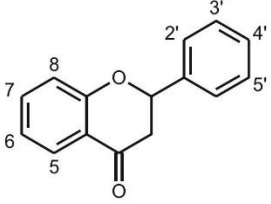
									
No.	Compound	5	6	7	8	2'	3'	4'	5'
108	Hesperidin	OH	H	<i>O</i> -L-Rha-D-Glc ^d	H	H	OH	OCH ₃	H
109	Naringenin	OH	H	OH	H	H	H	OH	H
111	Hesperetin	OH	H	OH	H	H	OH	OCH ₃	H
112	4'-Benzoyloxy-7-methoxy-6-isopentenylflavanone	H	Prenyl	OCH ₃	H	H	H	Benzoyloxy	H
113	3'-Fluoro-4'-hydroxy-7-methoxy-6-isopentenylflavanone	H	Prenyl	OCH ₃	H	H	F	OH	H
114	4'-Hydroxy-7-methoxy-6-isopentenylflavanone	H	Prenyl	OCH ₃	H	H	H	OH	H
115	Naringin	OH	H	<i>O</i> -Neohesp ^d	H	H	H	OH	H
116	Eriodictyol	OH	H	OH	H	H	OH	OH	H
117	Bavachinin	H	Prenyl	OCH ₃	H	H	H	OH	H
118	Bavachin	H	Prenyl	OH	H	H	H	OH	H
120	Isobavachin	H	H	OH	Prenyl	H	H	OH	H
121	3'-Hydroxyisobavachin	H	H	OH	Prenyl	H	OH	OH	H
124	Alpinetin	OCH ₃	H	OH	H	H	H	H	H
125	(2 <i>R</i> ,2 <i>S</i>)-4''-Hydroxybavachinin enantiomers	H	4''-Hydroxyprenyl	OCH ₃	H	H	H	OH	H
126	(2 <i>R</i> ,2 <i>S</i>)-(2 <i>R</i> '',2 <i>S</i> '')-2'',3''-Dihydroxybavachinin epimers	H	2'',3''-Dihydroxyprenyl	OCH ₃	H	H	H	OH	H
127	(2 <i>R</i> ,2 <i>S</i>)-4'',5''-Dihydroxybavachinin enantiomers	H	4'',5''-Dihydroxyprenyl	OCH ₃	H	H	H	OH	H

Fig. 5 Structures of flavanones **108**–**130**. **110** = Norkurarinone; **119** = 2(*R,S*)-4'-hydroxy-6,7-[2-(1-methoxy-1-methylethyl)-furan]-flavanone; **122** = 5-dehydroxyparatocarpin K; **123** = brosimacutin E

128	(2 <i>R</i> ,2 <i>S</i>)-Bavachin 7- <i>O</i> - β -D-glucopyranoside epimers	H	Prenyl	<i>O</i> -D-Glc ^d	H	H	H	OH	H
129	(2 <i>S</i>)-4''-Hydroxybavachin	H	4''-Hydroxyprenyl	OH	H	H	H	OH	H
130	(2 <i>S</i>)-5''-Hydroxybavachin	H	5''-Hydroxyprenyl	OH	H	H	H	OH	H

^d Glc = glucoside; Rha = rhamnoside; Neohesp = neohesperidoside (L-rhamnosyl-(1 \rightarrow 2)-D-glucose)

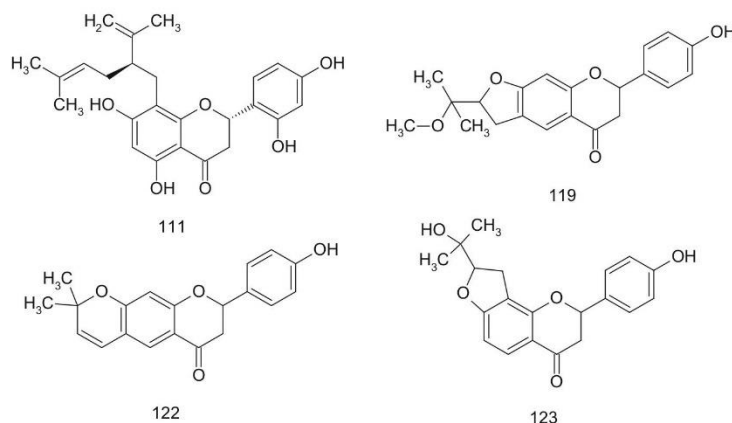


Fig. 5 continued

et al. 2008; Shin et al. 2009; Goldwasser et al. 2010; Christensen et al. 2010; Iio et al. 2012; Puhl et al. 2012; Quang et al. 2013; Feng et al. 2014, 2016; Liu et al. 2014; Ma et al. 2015, 2016; Sakamoto et al. 2016; Pallauf et al. 2017; Du et al. 2017; Xu et al. 2018; Nazreen et al. 2019; Zhou et al. 2021; Yang et al. 2024). The control plasmid can also contain a gene for β -galactosidase (Liang et al. 2001; Dang et al. 2003; Chacko et al. 2007; Liu et al. 2008; Matin et al. 2009; Cho et al. 2010; Ramachandran et al. 2012), or green fluorescent protein (GFP) (Pferschy-Wenzig et al. 2014; Mossine et al. 2022). On the other hand, several studies did not use a control plasmid (Shen et al. 2006; Fang et al. 2008; Lim et al. 2012; Jia et al. 2013; Ahmed et al. 2017; Yue et al. 2018; Shams Eldin et al. 2018; Miao et al. 2022), and two studies used a stably transfected PPAR γ 2 CALUX reporter cell line (Gijsbers et al. 2013; Beekmann et al. 2015). Moreover, Beekman et al. adapted this method to measure the induction of the expression of a reporter gene in pGL4

plasmid DNA using a quantitative polymerase chain reaction (qPCR) (Beekmann et al. 2015).

The third type of method presented in this review is a cell-free competitive ligand-binding assay that has many variants (Fig. 12). One variant is a PPAR γ fluorescence polarization-based assay, in which ligands (the test compounds) compete with a fluorescent probe in binding to the LBD of PPAR γ and thereby reducing the signal (Mueller and Jungbauer 2008, 2009; Shin et al. 2009; Zochling et al. 2011; Hui et al. 2014). Another variant uses a time-resolved fluorescence energy transfer (TR-FRET) approach with a fluorescent probe ligand and terbium-labeled LBD, where ligand binding induces energy transfer from terbium to the fluorophore of the ligand to increase fluorescence emission and the binding of the test compound decreases the signal (Ko et al. 2022, 2023; Wang et al. 2022; An et al. 2023a, b). Dang et al. used radioactive [³H]-rosiglitazone as a competitor in their PPAR γ binding assay (Dang et al.

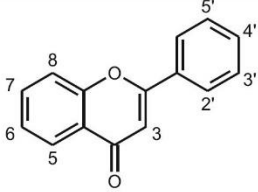
										
No.	Compound	3	5	6	7	8	2'	3'	4'	5'
131	Quercetin	OH	OH	H	OH	H	H	OH	OH	H
132	Syringetin	OH	OH	H	OH	H	H	OCH ₃	OH	OCH ₃
133	Kaempferol	OH	OH	H	OH	H	H	H	OH	H
134	Kaempferol-3-O-rutinoside	<i>O</i> -L-Rha-D-Glc ^c	OH	H	OH	H	H	H	OH	H
135	Rutin	<i>O</i> -L-Rha-D-Glc ^c	OH	H	OH	H	H	OH	OH	H
136	Myricetin	OH	OH	H	OH	H	H	OH	OH	OH
137	Dillenetin 3- <i>O</i> -(6''- <i>O</i> - <i>p</i> -coumaroyl)-β-D-glucopyranoside	<i>O</i> -(6''- <i>O</i> - <i>p</i> -coumaroyl)-β-D-Glc	OH	H	OH	H	H	OCH ₃	OCH ₃	H
138	4'-Methoxyflavonol	OH	H	H	H	H	H	H	OCH ₃	H
139	Quercitrin	<i>O</i> -L-Rha ^c	OH	H	OH	H	H	OH	OH	H
140	Myrcitrin	<i>O</i> -L-Rha ^c	OH	H	OH	H	H	OH	OH	OH
141	4',7,8-Trihydroxyflavonol	OH	H	H	OH	OH	H	H	OH	H
142	Quercetin-3- <i>O</i> -glucuronide	<i>O</i> -D-GlcA ^c	OH	H	OH	H	H	OH	OH	H
143	Kaempferol-3- <i>O</i> -glucuronide	<i>O</i> -D-GlcA ^c	OH	H	OH	H	H	H	OH	H
144	Galangin 3-benzyl-5-methyl ether	<i>O</i> -benzyl	OCH ₃	H	OH	H	H	H	H	H
145	Galangin	OH	OH	H	OH	H	H	H	H	H
146	Morin	OH	OH	H	OH	H	OH	H	OH	H
150	Rhamnetin	OH	OH	H	OCH ₃	H	H	OH	OH	H
151	3-Hydroxyflavone	OH	H	H	H	H	H	H	H	H
152	Quercetin-3,7- <i>O</i> -α-L-dirhamnoside	<i>O</i> -L-Rha ^c	OH	H	<i>O</i> -L-Rha ^c	H	H	OH	OH	H
153	6-Hydroxyflavonol	OH	H	OH	H	H	H	H	H	H
154	5,6-Dihydroxy-7-methoxyflavonol	OH	OH	OH	OCH ₃	H	H	H	H	H
155	Fisetin	OH	H	H	OH	H	H	OH	OH	H
156	Quercetin-3- <i>O</i> -glucoside	<i>O</i> -D-Glc ^c	OH	H	OH	H	H	OH	OH	H

Fig. 6 Structures of flavonols **131**—**159**. **147** = Nigragenon L; **148** = macakurzin C; **149** = macakurzin C 3,5-dimethyl ether

157	Isorhamnetin-3- <i>O</i> -rutinoside	<i>O</i> -L-Rha-D-Glc ^c	OH	H	OH	H	H	OCH ₃	OH	H
158	Isorhamnetin-3- <i>O</i> -glucoside	<i>O</i> -D-Glc ^c	OH	H	OH	H	H	OCH ₃	OH	H
159	Isorhamnetin	OH	OH	H	OH	H	H	OCH ₃	OH	H

^c Glc = glucoside; Rha = rhamnoside; GlcA = glucuronide

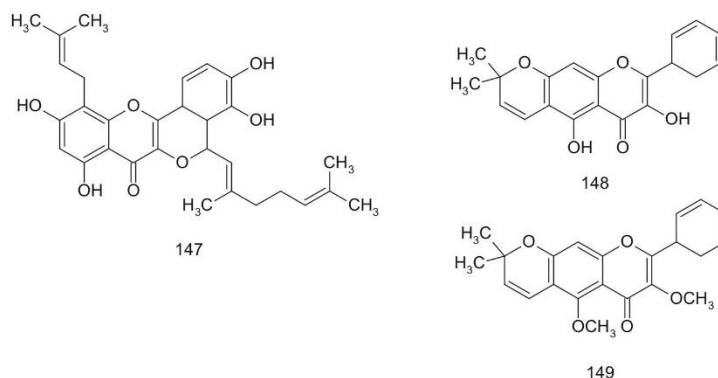


Fig. 6 continued

2003). Hu et al. used a cell-free assay based on the ligand-dependent interaction between PPAR γ and transcriptional mediators/intermediary factor 2 (TIF2) fused to bacterial alkaline phosphatase, the activity of which was detected with a specific substrate and reading of absorbance (Hu et al. 2013). Similarly, Lee et al. used an approach of ELISA 96-well plates precoated with steroid receptor coactivator-1 (SRC-1). The binding of PPAR γ and SRC-1 was augmented by PPAR γ agonists and the amount of bound PPAR γ proteins was detected using primary and secondary antibodies (Lee et al. 2020).

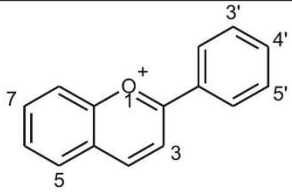
SAR between various classes of flavonoids as PPAR γ agonists

Salam et al. performed a structure-based virtual screening of the PPAR- γ ligand-binding domain using a natural product library of 29 potential agonists. Among these, six flavonoids were found to be active using a transcriptional factor assay. The EC₅₀ activity of rosiglitazone was 0.8 μ M, followed by ψ -baptigenin (**1**; isoflavone; %_{PC} = 27.6%), hesperidin (**108**; flavanone glycoside; %_{PC} = 12.1%), apigenin (**51**; flavone; %_{PC} = 10.1%), biochanin A (**2**; isoflavone; %_{PC} = 8.7%), chrysin (**52**; flavone; %_{PC} = 8.2%), and

genistein (**3**; isoflavone; %_{PC} = 4.3%). The disparity can be explained using the molecular docking data because it had been predicted that compound **1** would bind to the LBD of PPAR γ via the hydroxyl group on C-7 of the A-ring and the 5,7-dihydroxyl arrangement on the A-ring likely diminishes the agonist activity (Salam et al. 2008).

In a study by Mueller et al., PPAR γ was activated by oregano extract (e.g., *Origanum vulgare* L.) and its components were tested. The oregano extract did not transactivate PPAR γ , because the components act differently. The isoflavone **2** showed a %_{PC} of 0.65% when compared with rosiglitazone (EC₅₀ = 0.21 μ M), followed by naringenin (**109**; flavanone; %_{PC} = 0.26%). Others, such as flavones (**51**, luteolin (**53**), diosmetin (**54**)) and a flavonol (quercetin (**131**)) were inactive and thus can be described as PPAR γ antagonists (Mueller et al. 2008).

Another study by Quang et al. concentrated on flavonoids isolated from *Sophora flavescens* Aiton roots. Among the test compounds, the isoflavone formononetin (**8**) showed the greatest effect (%_{PC} = 45.0%) compared to troglitazone (EC₅₀ = 0.72 μ M), a drug from the thiazolidinedione class, similar to rosiglitazone. Other active compounds were: the flavanone norkurarinone (**110**; %_{PC} = 10.9%) and the

								
No.	Compound	1	3	5	7	3'	4'	5'
160	Delphinidin		OH	OH	OH	OH	OH	OH
161	Cyanidin		OH	OH	OH	OH	OH	H
162	Peonidin chloride	Cl ⁻	OH	OH	OH	OCH ₃	OH	H
163	Cyanin		<i>O</i> -D-Glc ^f	<i>O</i> -D-Glc ^f	OH	OH	OH	H
164	Keracyanin		<i>O</i> -L-Rha-D-Glc ^f	OH	OH	OH	OH	H
165	Oenin		<i>O</i> -D-Glc ^f	OH	OH	OCH ₃	OH	OCH ₃
166	Pelargonin		<i>O</i> -D-Glc ^f	<i>O</i> -D-Glc ^f	OH	H	OH	H
167	Cyanidin-3- <i>O</i> -β-glucoside		<i>O</i> -D-Glc ^f	OH	OH	OH	OH	H

^f Glc = glucoside; Rha = rhamnoside

Fig. 7 Structures of anthocyanidins and anthocyanins **160**–**167**

flavanonol (*2R*)-3 α ,7,4'-trihydroxy-5-methoxy-8-(γ , γ -dimethylallyl)-flavanone (**168**; %_{PC} = 6.9%) (Quang et al. 2013).

Moreover, a study by Matin et al. has demonstrated that the 7-hydroxy-benzopyran-4-one structure (present in isoflavones and flavones) is crucial for the PPAR γ agonist effect because it exhibits similarity to the core structure of thiazolidinediones. Seventy-seven compounds were assayed and several were found to be more effective than rosiglitazone (PPAR γ fold activation = 2.9) at a concentration of 5 μ M. The four most active were: 4'-fluoro-7-hydroxyisoflavone (**4**; %_{PC} = 710.3%), compound **1** (%_{PC} = 417.2%), 3',5'-dimethoxy-7-hydroxyisoflavone (**5**; %_{PC} = 410.3%), and 3'-methoxy-7-hydroxyisoflavone (**6**; %_{PC} = 313.8%). Although the isoflavone class was the most effective, this was not universally the case, for example, another isoflavone **3** had much less effect (%_{PC} = 69.0%). Flavones were the second most effective class, with compounds **54** and 5,4'-dihydroxyflavone (**55**; both %_{PC} = 86.2%), followed by the flavonol syringetin (**132**;

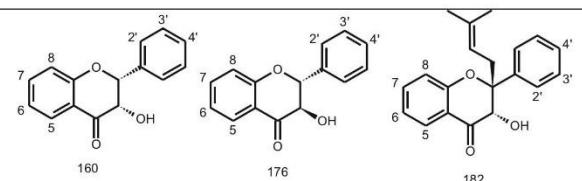
%_{PC} = 65.5%), and the flavanone hesperetin (**111**; %_{PC} = 51.7%). The lack of PPAR γ activity among flavanones and isoflavones is a vital requirement (Matin et al. 2009).

Gijsbers et al. tested the PPAR γ agonism of compounds present in tomato (*Solanum lycopersicum* L.) extracts. Among the test compounds two were active at a concentration of 1 μ M, the flavonol kaempferol (**133**) and the flavanone **109** (both %_{PC} \approx 1.0%). Other flavonols (such as kaempferol-3-*O*-rutinoside (**134**), **131**, and rutin (**135**)) and anthocyanidins (delphinidin (**160**) and cyanidin (**161**)) were inactive (Gijsbers et al. 2013).

Du et al. designed, synthesized and evaluated 30 bavachinin (**117**; flavanone; %_{PC} = 0.4%) analogs as PPAR γ agonists. Among them, seven compounds were more active than the parent compound. The most active were the flavones: 4'-(4''-nitrobenzoyloxy)-7-methoxy-6-isopentenylflavone (**56**; %_{PC} = 18.6%), 4'-acetyloxy-7-methoxy-6-isopentenylflavone (**57**; %_{PC} = 10.3%), 4'-hydroxy-7-methoxy-6-isopentenyl-

Fig. 8 Structures of flavanonols **168**—**185**.

170 = Silybin A;
171 = silybin B;
172 = isosilybin A;
173 = isosilybin B;
174 = silychristin;
175 = silydianin;
178 = nigragenon B;
179 = sanggenol F;
180 = nigragenon D;
181 = nigrasin K;
183 = nigragenon E;
184 = sanggenon A;
185 = sanggenol H

								
No.	Compound	5	6	7	8	2'	3'	4'
168	(2 <i>R</i>)-3 <i>α</i> ,7,4'-Trihydroxy-5-methoxy-8-(γ,γ -dimethylallyl)-flavanone	OCH ₃	H	OH	Prenyl	H	H	OH
169	Silibinin	mixture of two diastereomers, silybin A (170) and silybin B (171)						
176	(+)-Taxifolin (2 <i>R</i> ,3 <i>R</i>)	OH	H	OH	H	H	OH	OH
177	Taxifolin	Mixture of (+) and (-) enantiomers						
182	Nigragenon A	OH	Prenyl	OH	H	OH	H	OH

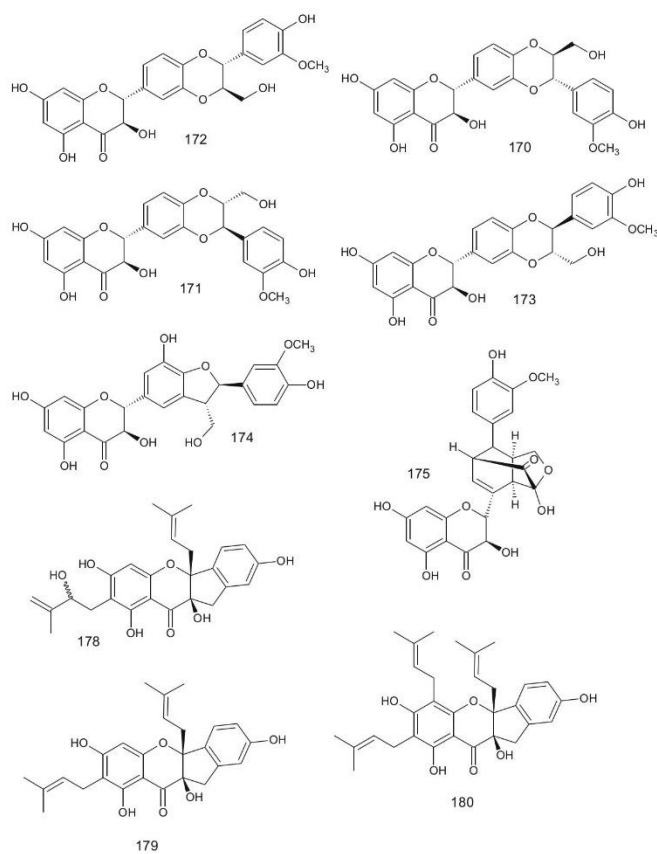
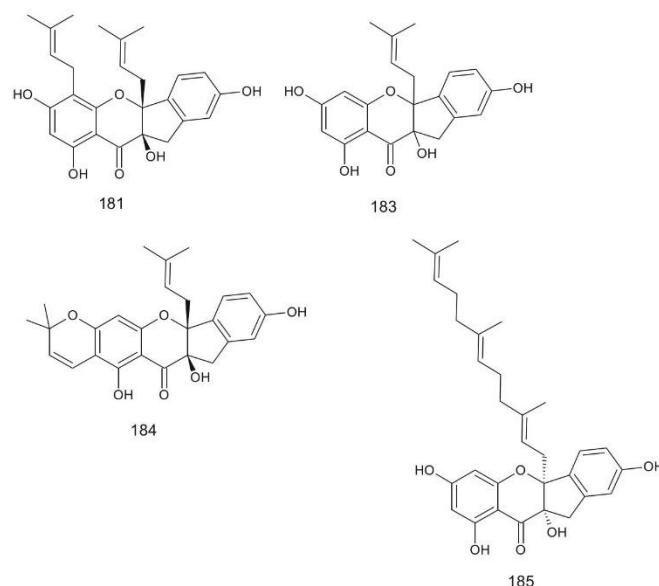


Fig. 8 continued



flavone (**58**; %_{PC} = 7.1%), and 4'-hydroxy-7-methoxy-6-isopentylflavone (**59**; %_{PC} = 2.3%), followed by the flavanones: 4'-benzoyloxy-7-methoxy-6-isopentenylflavanone (**112**; %_{PC} = 3.2%), 3'-fluoro-4'-hydroxy-7-methoxy-6-isopentenylflavanone (**113**; %_{PC} = 2.4%), and 4'-hydroxy-7-methoxy-6-isopentylflavanone (**114**; %_{PC} = 0.6%) (Du et al. 2017).

Zoechling et al. researched the PPAR γ agonism of flavonoids detected in red wine. The most active class of flavonoids were the flavanols: (-)-epigallocatechin gallate (**32**; %_{PC} = 100.0%), (-)-gallocatechin gallate (**33**; %_{PC} = 84.0%), (-)-epicatechin gallate (**34**; %_{PC} = 35.6%), and (-)-catechin gallate (**35**; %_{PC} = 23.1%). On the other hand, (-)-epigallocatechin (**36**), (-)-epicatechin (**37**), and (+)-catechin (**39**) were not active. The second most active class were the anthocyanidins with compound **161** (%_{PC} = 15.0%), followed by the flavonols: myricetin (**136**; %_{PC} = 10.5%), compound **131** (%_{PC} = 3.7%), and **133** (%_{PC} = 0.7%). Flavones were represented only by compound **51** (%_{PC} = 1.3%) and flavanones by compound **109** (%_{PC} = 0.6%) (Zoechling et al. 2011).

Liu et al. studied the PPAR γ agonistic activity of diterpenoids and flavonoids from the aerial parts of *Scoparia dulcis* L. The most active compound was the flavone **53** (%_{PC} = 10%), when compared to

rosiglitazone (EC₅₀ = 0.03 μ M). Other flavones, such as acerosin (**60**; %_{PC} = 0.7%), hispidulin (**61**; %_{PC} = 0.4%), scutellarein (**62**; %_{PC} = 0.2%), and compound **51** (%_{PC} = 0.1%), showed only minor activity. No activity was detected for flavones homoplantagin (b) and apigenin-8-C- α -L-arabinopyranoside (**64**) or the flavonol dillenetin 3-O-(6"-O-p-coumaroyl)- β -D-glucopyranoside (**137**) (Liu et al. 2014).

Mueller and Jungbauer screened extracts from culinary plants, herbs, and spices to find a rich source of PPAR γ ligands. Most active among the flavonoids were the flavonols **136** (%_{PC} = 4.8%) and **131** (%_{PC} = 4.3%), followed by flavone **53** (%_{PC} = 3.0%). Other compounds, such as flavonol **133** (%_{PC} = 0.3%), flavone **51** (%_{PC} = 0.2%), and flavanol (-)-catechin (**38**; %_{PC} = 0.1%), showed very low activity. Moreover, other compounds such as an anthocyanidin peonidin chloride (**162**), flavanol **37**, and the proanthocyanidin (procyanidin B2; **40**) showed no activity (Mueller and Jungbauer 2009).

Yang et al. researched several natural products from *Clerodendrum trichotomum* Thunb. and their α -glucosidase inhibitory and PPAR- γ agonist activities. The most active flavone **53** (%_{PC} = 1.3%) was compared to rosiglitazone (EC₅₀ = 0.03 μ M), followed by flavanol **131** (%_{PC} = 0.62%), and two flavones:

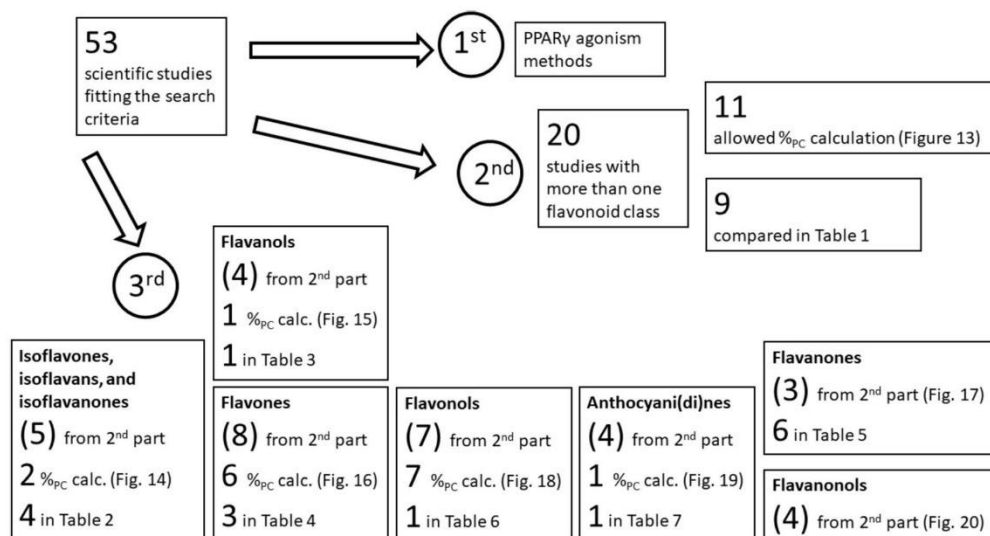
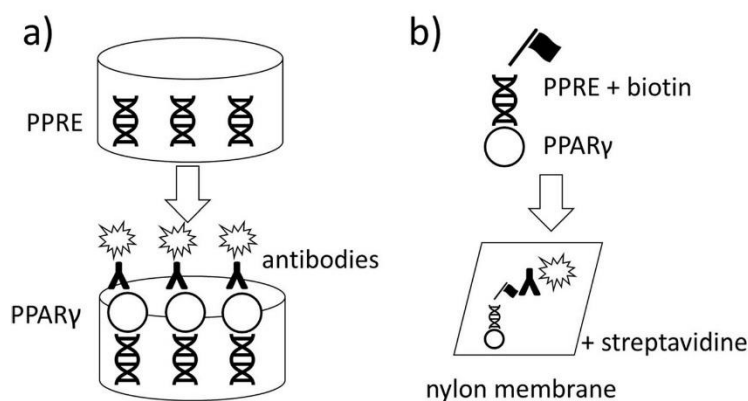


Fig. 9 The outline of the article

Fig. 10 The methods to measure PPAR γ agonism using nuclear extracts from cells: **a** ELISA; **b** EMSA



apigenin 7-*O*- β -D-glucuronide (**77**; %_{PC} = 0.35%) and **51** (%_{PC} = 0.62%). Other flavones were inactive, such as chrysoeriol (**78**), chrysoeriol 7-*O*- β -D-glucuronide (**79**), diosmetin 7-*O*- β -D-glucuronide methyl ester (**80**), apigenin 7-*O*- β -D-glucuronide methyl ester (**81**), and linarin (**82**) (Yang et al. 2024).

Mossine et al. studied response of sixty-four flavonoids to PPAR γ transcriptional factor in relation to neuroinflammation in astrocytes. Rosiglitazone showed 1.743-fold activation at a concentration of

50 μ M. Among the flavonoids, the most active were flavones: **52** (%_{PC} = 245.38%), acacetin (**83**; %_{PC} = 212.11%), and 7-methoxyflavone (**84**; %_{PC} = 169.48%). Followed by galangin (**145**; flavonol; %_{PC} = 166.48%), 7,4'-dihydroxyflavone (**87**; %_{PC} = 151.64%), daidzein (**14**; %_{PC} = 135.51%), flavone **51** (%_{PC} = 135.34%), flavonol **133** (%_{PC} = 132.93%), flavone **86** (%_{PC} = 131.38%), flavanone **111** (%_{PC} = 125.13%), isoflavone **8** (%_{PC} = 113.08%), isoflavone **2** (%_{PC} = 112.51%), 3',4',7-

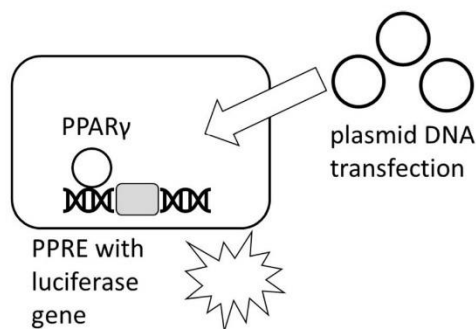


Fig. 11 The methods to measure PPAR γ agonism using cell-based transactivation (reporter luciferase assay)

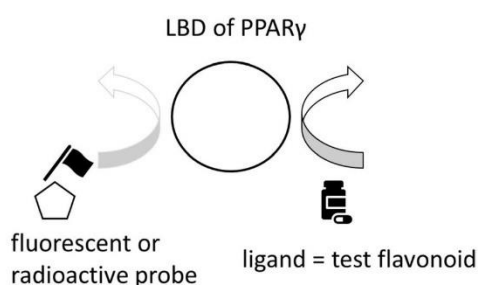


Fig. 12 The methods to measure PPAR γ agonism using cell-free ligand binding assays

trihydroxyisoflavone (**9**; %_{PC} = 98.74%), flavone **55** (%_{PC} = 98.05%), wogonin (**88**; flavone; %_{PC} = 97.30%), flavone **53** (%_{PC} = 93.23%), isoflavone **3** (%_{PC} = 90.94%), flavanone **109** (%_{PC} = 88.18%), 4'-methoxyflavonol (**138**; %_{PC} = 98.74%), 2',3',6-trihydroxyflavone **100** (%_{PC} = 74.81%), baicalein (**89**; flavone; %_{PC} = 71.72%), tangeretin (**90**; flavone; %_{PC} = 65.69%), 4',7,8-trihydroxyflavone (**91**; %_{PC} = 65.40%), flavanone **108** (%_{PC} = 63.51%), 3',7,8-trihydroxyflavone (**92**; %_{PC} = 62.36%), daidzin (**10**; isoflavone; %_{PC} = 62.36%), genistin (**11**; isoflavone; %_{PC} = 61.50%), baicalin (**65**; flavone; %_{PC} = 60.41%), α -naphthoflavone (**93**; %_{PC} = 71.72%), taxifolin (**177**; flavanonol; %_{PC} = 57.77%), morin (**146**; flavonol; %_{PC} = 56.80%), cyanin (**163**; anthocyanin; %_{PC} = 55.82%), keracyanin (**164**; anthocyanin; %_{PC} = 55.25%), fisetin (**155**; flavonol; %_{PC} = 54.79%), quercitrin (**139**; flavonol; %_{PC} = 54.10%), vitexin (**94**; flavone; %_{PC} = 53.13%), naringin (**115**; flavanone; %_{PC} = 50.95%), flavanol **37**

(%_{PC} = 50.37%), flavanol **135** (%_{PC} = 50.32%), neodiosmin (**95**; flavone; %_{PC} = 50.09%), oenin (**165**; anthocyanin; %_{PC} = 50.09%), flavanol **39** (%_{PC} = 48.82%), prunetin (**12**; isoflavone; %_{PC} = 48.36%), pelargonin (**166**; anthocyanin; %_{PC} = 47.68%), puerarin (**13**; isoflavone; %_{PC} = 47.22%), flavanol **136** (%_{PC} = 46.76%), myricitrin (**140**; flavonol; %_{PC} = 48.36%), eriodictyol (**116**; flavanone; %_{PC} = 44.06%), diosmin (**96**; flavone; %_{PC} = 42.97%), 7,8-dihydroxyflavone **85** (%_{PC} = 42.74%), anthocyanidin **161** (%_{PC} = 41.37%), flavanol **131** (%_{PC} = 40.85%), epigallocatechin (**41**; flavanol; %_{PC} = 40.68%), quercetin-3-*O*-glucoside (**156**; flavonol; %_{PC} = 36.55%), gallocatechin (**42**; flavanol; %_{PC} = 34.88%), epigallocatechin gallate (**43**; flavanol; %_{PC} = 34.65%), 4',7,8-trihydroxyflavonol (**141**; %_{PC} = 33.91%), anthocyanidin **160** (%_{PC} = 40.68%), silibinin (**169**; a mixture of two diastereomers, silybin A (**170**) and silybin B (**171**); %_{PC} = 28.34%), 5,6-dihydroxyflavone (**97**; %_{PC} = 26.28%), epicatechin gallate (**44**; flavanol; %_{PC} = 24.50%), 3',4'-dihydroxyflavone (**98**; %_{PC} = 20.65%), rhamnetin (**150**; flavonol; %_{PC} = 14.52%), 3-hydroxyflavone (**151**; flavonol; %_{PC} = 9.87%), and β -naphthoflavone (**99**; %_{PC} = 3.84%) (Mossine et al. 2022).

Based on the results by Liang et al., the most potent PPAR γ agonist was flavone **51** (8.1-fold activation), followed by flavanol **133** (7.7-fold), and flavone **52** (5.6-fold). The positive control in this experiment was indomethacin (13.34-fold), but the value of %_{PC} cannot be calculated, because indomethacin was tested at a concentration of 100 μ M, whereas the flavonoids were at 10 μ M. Other compounds demonstrated some level of PPAR γ agonism, but without statistical significance: flavones **85**, **86**, and **53**, flavonols **145** and **151**, and isoflavones **2** and **3** (Liang et al. 2001).

An et al. measured the binding activity of various flavonoids, but not that of the positive control (rosiglitazone), which makes it impossible to compare their study with others. The most effective was flavanol **38** (97% bind. act.), followed by flavanol **133** (83%), flavone **52** (71%), flavanone **109** (68%), and isoflavone **3** (41%) (An et al. 2023a).

Shams Eldin et al. performed bioactivity-guided isolation of potential antidiabetic and antihyperlipidemic compounds from *Trigonella stellata* Forssk. and reported PPAR γ agonistic activity for (3*R*,4*S*)-4,2',4'-trihydroxy-7-methoxy-4'-*O*- β -d-

glucopyranosylisoflavan (**28**) at a concentration of 12.5 $\mu\text{g/mL}$; this compound led to 1.22-fold activation. Rosiglitazone was much more active, with 3.5-fold activation at a concentration of 1.79 $\mu\text{g/mL}$. Other isolated compounds, such as (3*S*,4*R*)-4,2',4'-trihydroxy-7-methoxyisoflavan (**29**), (2*S*,3*R*,4*R*)-4,2',4'-trihydroxy-2,7-dimethoxyisoflavan (**30**), flavone **87**, or quercetin-3,7-*O*- α -L-dirhamnoside (**152**), did not show any activity (Shams Eldin et al. 2018).

Lee et al. studied the cytotoxic effects of flavonoids on human cervical and prostate cancer cells and linked this effect to PPAR γ agonism. The only active compound among those tested compounds was 6-hydroxyflavonol (**153**), with approximately twofold activation at a concentration of 20 μM , while the positive control, indomethacin had a similar effect at a much higher concentration (320 μM). Other test compounds were not active; among them a flavonol 5,6-dihydroxy-7-methoxyflavonol (**154**), flavones **100**, 3',4',6-trihydroxyflavone (**101**), 3',5,6-trihydroxyflavone (**102**), and 4',6-dihydroxyflavone (**103**), and two isoflavones 3',4',6-trihydroxyisoflavone (**19**) and 4',6,7-trihydroxyisoflavone (**20**) (Lee et al. 2010).

Pallauf et al. screened flavonoids as putative inducers of various transcriptional factors, with PPAR γ among them. The most active were flavones **51** (approx. 14-fold activation), and **53** (ninefold). The second most active class were the isoflavones (**9** and **3**, approx. 4 and 3.5-fold, respectively), followed by flavonols: **133**, **155** (threefold), and **131** (2.5-fold). The least active were flavanones **111** and **109** (2 and 1.5-fold, resp.) (Pallauf et al. 2017).

Ma et al. determined the PPAR γ agonist activity of prenylflavone derivatives isolated from the seeds of *Psoralea corylifolia* L. The most active class of flavonoids were flavanones: **117** (13.12-fold) and bavachin **118** (7.94-fold), followed by the isoflavone corylifol A (**21**; 6.34-fold). All of these compounds were tested at a concentration of 25 μM , whereas rosiglitazone was tested at 5 μM (68.65-fold). Other isolated compounds, such as the flavanones (2*R*,*S*)-4'-hydroxy-6,7-[2-(1-methoxy-1-methylethyl)-furano]-flavanone (**119**), isobavachin (**120**), 3'-hydroxyisobavachin (**121**), 5-dehydroxyparatocarpin K (**122**), and brosimacutin E (**123**)) and the isoflavones and isoflavanones (4',7-dihydroxy-3',5'-diprenylisoflavone

(**22**), 3,4',7-trihydroxy-2-methoxy-3'-geranylisoflavanone (**31**), 8-prenyldaidzein (**23**), neobavaisoflavone (**24**), corylin (**25**), and neocorylin (**26**)) were inactive (Ma et al. 2016).

Christensen et al. identified several bioactive compounds obtained from the flowers of black elder (*Sambucus nigra* L.). Among these, flavanone **109** was able to activate PPAR γ (twofold at a concentration of 40 μM). Rosiglitazone (1 μM) was much more active (100-fold), whereas other flavanols, such as **135**, **156**, **134**, isorhamnetin-3-*O*-rutinoside (**157**), isorhamnetin-3-*O*-glucoside (**158**), **131**, and **133** were unable to activate PPAR γ (Christensen et al. 2010).

Pferschy-Wenzig et al. investigated compounds isolated from milk thistle seeds for their PPAR γ agonistic effect. The only active compound was flavonolignan isosilybin A (**172**; 2.1-fold at 30 μM), and it was less active than pioglitazone (sevenfold at 5 μM). Other silymarin constituents were inactive (flavonolignans: **170**, **171**, isosilybin B (**173**), silychristin (**174**), and silydianin (**175**) and the flavanolol (+)-taxifolin (**176**)) (Pferschy-Wenzig et al. 2014).

Xu et al. investigated the PPAR γ agonistic activity of several isoprenylated flavanols and flavones isolated from twigs of *Morus nigra* L. Their study showed a similar effect for the flavanols nigragenon B (**178**) and sanggenol F (**179**); both approx. twofold at a concentration of 3 μM . Other flavanols, such as nigragenon D (**180**) and nigrasin K (**181**), were active, but only at the higher concentration of 30 μM , and the rest were inactive (flavanols: nigragenon A (**182**) and E (**183**), sanggenon A (**184**), sanggenol H (**185**); and flavones: cyclomulberrin (**104**), and nigrasin I (**105**)). Rosiglitazone showed a greater effect: 12-fold at a concentration of 1 μM . Based on this result, Xu et al. summarized the following SAR of PPAR γ agonistic effects: (a) The presence of a prenyl group at position C-6 or C-8 was crucial. (b) The prenyl group at C-6 (**178** and **179**) was preferable to the one at C-8 (**181**). (c) Cyclization of the prenyl group (**184**) greatly diminished the effect. (Xu et al. 2018).

Of the 20 research articles, eleven allowed the calculation of %_{PC}. For direct comparison, all of the values for compounds in the flavonoid classes were put together and displayed in Fig. 13. We can deduce from Fig. 13 that isoflavones show the highest values

of %_{PC}, which makes them the most promising flavonoid class in terms of PPAR γ agonism. The second highest values were for flavones, followed by flavonols, flavanones, flavanols, flavanonols, and anthocyanidins and anthocyanins.

The SARs arising from the other nine studies are presented in Table 1. The results from Liang et al. agree with the results presented in the Fig. 13 (Liang et al. 2001). On the other hand, other studies, such as An et al., Pallauf et al., and Ma et al., propose that isoflavones are not the most effective among the flavonoids (Ma et al. 2016; Pallauf et al. 2017; An et al. 2023a).

SAR within the classes of flavonoids as PPAR γ agonists

Isoflavones, isoflavans, and isoflavanones

As a conclusion from the five studies (Salam et al. 2008; Matin et al. 2009; Pallauf et al. 2017; Shams Eldin et al. 2018; Mossine et al. 2022) showing results of more than one isoflavone or isoflavan already presented in the previous part, we can formulate several outlines for SAR:

1. The 7-hydroxyisoflavone arrangement on the A-ring is generally more effective than the 5,7-dihydroxyl arrangement (e.g. compound **1** (%_{PC} = 27.6%) vs. **2** (%_{PC} = 8.7%) (Salam et al. 2008)).
2. The most effective structure was **4** (%_{PC} = 710.3%) (Matin et al. 2009).
3. Hydrogen bond acceptors at positions C-3' and C-4' of the B-ring are important for the effect.
4. On the other hand, increased steric bulk of the isoflavone B-ring leads to decreased PPAR γ activity (e.g. 3',4',5'-trifluoro-7-hydroxyisoflavone (**7**; %_{PC} = 51.7%) (Matin et al. 2009)).
5. The crucial function of free hydroxyl group at position C-7 of the A-ring can be seen when we compare activity of compound **14** with its 7-*O*-glucoside derivative **10** (Mossine et al. 2022).
6. Among the isoflavans, the only active compound possessed a β -D-glucopyranosyl moiety at position C-4' of the B-ring (Shams Eldin et al. 2018).

Shen et al. analyzed the antidiabetic effect associated with the PPAR γ activation of isoflavones isolated from herbal extracts: **8** and calycosin (**15**) from *Astragalus membranaceus* Moench, **9** from *Pueraria thomsonii* Benth., and two other common isoflavones, **3** and **2**. The study showed that only **8** (%_{PC} = 138.5%) was more effective than the positive control, pioglitazone (EC₅₀ = 3.6 μ M). The second most effective was **2** (%_{PC} = 97.3%), followed by **3** (%_{PC} = 15.7%), **15** (%_{PC} = 8.0%), and **14** (%_{PC} = 4.9%). These results underscore the importance of the methoxy group attached to C-4' and the absence of a hydroxy group at C-3' of the B-ring (Shen et al. 2006).

Mueller et al. showed that metabolites from red clover can exert higher binding affinities than their precursor molecules. One of the natural products from red clover 6-hydroxydaidzein (**16**; %_{PC} = 3.6%) showed the most potent PPAR γ binding effect when compared with its precursor **14** (%_{PC} = 0.03%) and both were compared with rosiglitazone (IC₅₀ = 0.12 μ M). The second most active compound was 3'-hydroxygenistein (**17**; %_{PC} = 1.0%). Other isoflavones, such as **2** (%_{PC} = 0.6%) and **3** (%_{PC} = 0.5%), were less active. Compound **8** was found to be inactive (Mueller and Jungbauer 2008).

Chacko et al. reported the activation of PPAR γ in endothelial cells (HUVECs) exposed to isoflavones. Rosiglitazone led to a roughly threefold activation at a concentration of 2 μ M. All the test isoflavones and isoflavans were used at a concentration of 1 μ M, which makes it impossible to calculate %_{PC}. Compound **2** caused approximately fourfold activation and thus was more active than rosiglitazone. This compound was followed by **3** with almost 3.8-fold activation, **9** (approx. twofold), and the isoflavan equol (**27**; approx. 1.7-fold). This study also tested various chlorine derivatives and proved the positive effect of 3'-chlorination of the B-ring on the PPAR γ agonism: 3'-chlorodaidzein (**18**) brought about approx. sixfold activation. On the other hand, the addition of chlorine at C-6 or C-8 of the A-ring diminished the activity of **9**. In conclusion, this study proved the necessity of having a 7-hydroxy group on the A-ring for PPAR γ agonism, chlorination at position C-3', but not at C-6

or C-8, and the greater effect of isoflavones over isoflavanes (Chacko et al. 2007).

Dang et al. tested the activation of the PPAR γ receptor by compound **3**. Incubation of the test compound at a concentration of 5 μ M for 48 h led to a roughly 60-fold induction. This effect was compared to rosiglitazone in a binding assay, and it was shown that compound **3** interacts directly with the same LBD as rosiglitazone, although with a lower binding affinity. Unfortunately, the results presented do not allow for direct comparison with a calculation of %_{PC} (Dang et al. 2003).

Cho et al. concentrated on the PPAR γ transcriptional activity of dietary soy isoflavones. Compound **14** and its derivative **27** showed 3.8-fold and 4.1-fold activation, respectively, of the PPAR γ receptor at a concentration of 10 μ M. The difference between these effects is not statistically significant and there was no positive control (Cho et al. 2010).

Finally, Sakamoto et al. tested the PPAR γ agonist activity of **9** and reported its twofold activation at a concentration of 6.25 μ M, but without any reference to the activity of a positive control (Sakamoto et al. 2016).

The overall results of %_{PC} calculations for isoflavones, isoflavans, and isoflavanonones are presented in Fig. 14. The three most effective isoflavones were: **4**, **1**, and **5**. The Table 2 then presents four other studies. According to the results by Chacko et al., isoflavone **14** was more active than isoflavan **27**, but Cho et al. showed opposite result (Chacko et al. 2007; Cho et al. 2010).

Flavanols

The four studies (Mueller and Jungbauer 2009; Zoechling et al. 2011; Mossine et al. 2022; An et al. 2023a) presented in the previous chapter all report flavanols as the most active among other classes of flavonoids (with the exception of Mossine et al.), but the effects of particular compounds contradict each other. Zoechling et al. described the sequence of decreasing activity as follows: **32** > **33** > **34** > **35**. Other compounds, such as **36**, **37**, and **39**, were inactive. According to their study, the most crucial structural features for the PPAR γ agonist activity are (Zoechling et al. 2011):

1. Esterification with gallic acid acting on the hydroxyl group at C-3 is essential.
2. A 3',4',5'-trihydroxy (i.e. = gallo-) arrangement on the B-ring increases the activity.
3. (2*R*,3*R*) stereoisomers on the C-ring (i.e. = epi-) are more active.

Mueller and Jungbauer found very low activity for **38** (%_{PC} = 0.1%). Moreover, another flavanol **37** and a proanthocyanidin (**40**; a dimer of two flavanols: (–)-epicatechin-(4 β → 8)-(–)-epicatechin) showed no activity (Mueller and Jungbauer 2009).

An et al. on the other hand, were able to detect binding activity of **38** to PPAR γ (An et al. 2023a).

Moreover, Mossine et al. reported compound **37** as the most effective, followed by compounds **39**, **41**, **42**, **43**, and **44**. The configuration on C-2 and C-3 of the C-ring is not clear and compounds 41–44 are thus

Fig. 13 Distribution of %_{PC} values among different classes of flavonoids visualized as scatter plot. Asterisks represent individual compounds

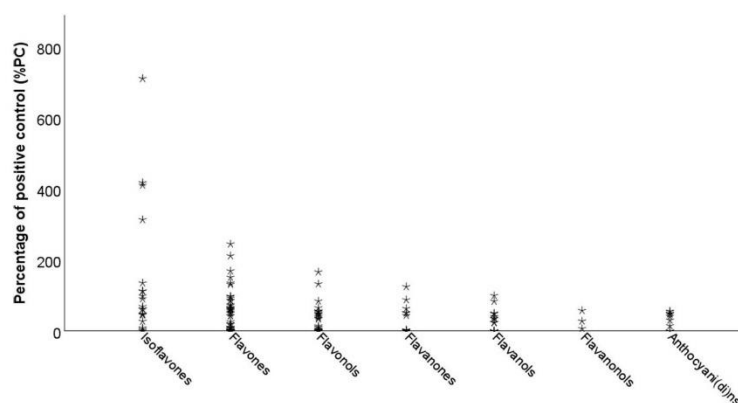


Table 1 Overall SAR results for studies that did not allow the calculation of %_{PC}

Reference	SAR of various classes of flavonoids
Liang et al. (2001)	Flavones > flavonols
An et al. (2023a)	Flavanols > flavonols > flavone > flavanone > isoflavone
Shams Eldin et al. (2018)	Isoflavans
Lee et al. (2010)	Flavonols
Pallauf et al. (2017)	Flavones > isoflavones > flavanols > flavanones
Ma et al. (2016)	Flavanones > isoflavones
Christensen et al. (2010)	Flavanones
Pferschy-Wenzig et al. (2014)	Flavonolignan
Xu et al. (2018)	Flavanonols

considered as mixtures of both (+) and (-) enantiomers. Based on the overall results presented in the Fig. 15, the (-)-enantiomer **32** was more active when compared with its corresponding mixture of (+) and (-), **43** (Mossine et al. 2022).

Shin et al. studied adipocyte differentiation in human bone marrow mesenchymal stem cells. They found that **38** (%_{PC} = 90.5%) promotes this effect via PPAR γ agonism when compared to troglitazone (4.2-fold) at a concentration of 10 μ M, whereas, its stereoisomer **39** (%_{PC} = 47.6%) showed only half as much activity. Shin et al. also determined that **38** bound directly to the active site of PPAR γ when it was used as a competitor for troglitazone in a ligand binding assay (Shin et al. 2009).

Ahmed et al. studied chemical constituents from *Oncocalyx glabratus* (Engl.) M. G. Gilbert and their effect on PPAR γ . Rosiglitazone was tested at a concentration of 10 μ M and showed 2.8-fold induction. Among the test compounds (at a concentration of 50 μ g/mL), only oncoglabrinol A (**45**; 2.7-fold) and a substance (4.3-fold) that, based on NMR data, was described as a mixture of the compounds catechin-7-4'-*O*-digallate (**48**) and catechin-7-3'-*O*-digallate (**49**), were found to be active. Others, such as oncoglabrinol B (**46**), oncoglabrinol C (**47**), **39**, and (+)-catechin-7-*O*-gallate (**50**), were inactive. We cannot be sure, but, based on the available data, it seems that the 7-4'-*O*-digallate arrangement is necessary for the effect (Ahmed et al. 2017).

The overall results in the Fig. 15 show that the three most active flavanols are **32**, **38**, and **33**. The results by Ahmed et al. are summarized in the Table 3 (Ahmed et al. 2017).

Flavones

Using the results of the eight studies (Liang et al. 2001; Salam et al. 2008; Mueller and Jungbauer 2009; Liu et al. 2014; Pallauf et al. 2017; Du et al. 2017; Mossine et al. 2022; Yang et al. 2024) already presented, we can formulate several outlines of SAR for flavones:

1. The most important features are esterification at position C-4' (B-ring) and an isopentenyl group at position C-6 (A-ring) (Du et al. 2017).
2. The PPAR γ agonistic effect generally increases with the number of hydroxyl groups on the B-ring (**53** > **51** > **52**), except for the study by Pallauf et al., where **51** was the most effective (Pallauf et al. 2017), and Mossine et al. where the sequence was: **52** > **51** > **53** (Mossine et al. 2022).

Lim et al. found that compound **65** suppresses NF- κ B-mediated inflammation in aged rat kidneys through PPAR γ activation. At a concentration of 10 μ M, the activity of thiazolidinedione reached 1.5-fold of the control, and **65** (%_{PC} = 86.7%) performed similarly (Lim et al. 2012).

Hui et al. researched the therapeutic potential of oroxylin A (**66**) in acute myelogenous leukemia by dual effects targeting PPAR γ and RXR α . The positive control rosiglitazone showed very high binding activity (IC₅₀ = 2.4 μ M) towards PPAR γ . Compound **66** (%_{PC} = 3.4%) showed much less activity (Hui et al. 2014).

Feng et al. studied how compound **51** reduces obesity-related inflammation using PPAR γ activation and regulation of the macrophage polarization. Rosiglitazone was detected as a PPAR γ agonist at a

concentration of 10 μM with approx. 12-fold activation, whereas compound **51** ($\%_{\text{PC}} = 75\%$) showed a lesser effect (Feng et al. 2016).

Puhl et al. concentrated on the PPAR γ agonist activity of compound **53**. Based on their results, **53** is a partial agonist ($\%_{\text{PC}} = 16.7\%$) when compared to rosiglitazone (12-fold activation at a concentration of 1 μM) (Puhl et al. 2012).

An et al. screened prenylated derivatives of chrysin as potential partial PPAR γ agonists with the ability to induce secretion of adiponectin. In their study, the most active compound was chrysin 5,7-diprenyl ether (**67**; $\%_{\text{PC}} = 93.4\%$) based on its binding activity towards PPAR γ at a concentration of 10 μM and compared with GW1929 (*N*-(2-benzoylphenyl)-*O*-[2-(methyl-2-pyridinylamino)ethyl]-L-tyrosine hydrate). The activity of other compounds was as follows: chrysin 5-prenyl-7-benzyl ether (**68**; $\%_{\text{PC}} = 85.2\%$), chrysin 5-benzyl-7-prenyl ether (**69**; $\%_{\text{PC}} = 75.6\%$), chrysin 5-benzyl-7-benzyl ether (**70**; $\%_{\text{PC}} = 71.5\%$), chrysin 5-benzyl ether (**71**; $\%_{\text{PC}} = 65.3\%$), chrysin 5-methyl-7-benzyl ether (**72**; $\%_{\text{PC}} = 60.1\%$), chrysin 7-benzyl ether (**73**; $\%_{\text{PC}} = 58.4\%$), chrysin 5-(4''-fluoro)benzyl ether (**74**; $\%_{\text{PC}} = 45.7\%$), **52** ($\%_{\text{PC}} = 35.9\%$), chrysin 5-allyl ether (**75**; $\%_{\text{PC}} = 33.7\%$), and chrysin 5-(4''-chloro)benzyl ether (**76**; $\%_{\text{PC}} = 32.2\%$) (An et al. 2023b).

Nazreen et al. investigated PPAR γ agonism of three new constituents isolated from *Callistemon lanceolatus* (Sm.) Sweet and among them 8-(1''-hydroxyisoprenyl)-5,6-dihydroxy-7,4'-dimethoxyflavone (**106**) showed a potent transactivation effect ($\%_{\text{PC}} = 60.3\%$) at a concentration of 10 μM in comparison with rosiglitazone (80.47% transactivation activity) (Nazreen et al. 2019).

Feng et al. (2014) showed that compound **52** suppresses inflammation by regulating the M1/M2 status in macrophages by activating PPAR γ with a 1.4-fold effect at a concentration of 10 μM (Feng et al. 2014).

Ding et al. performed experiments on insulin sensitivity in adipocytes and found that compound **53** enhances it via the activation of PPAR γ transcriptional activity at a concentration of 20 μM after 12 h of incubation (Ding et al. 2010).

Zhou et al. researched effect of oroxyloside (**107**) on PPAR γ agonism and suppression of cell cycle progression by glycolipid metabolism switch-mediated increase of reactive oxygen species levels. Compound **107** showed 1.8-fold activation of PPAR γ at a concentration of 200 μM . A similar effect was achieved by incubation with rosiglitazone, but at a concentration of 50 μM (Zhou et al. 2021).

The overall results in the Fig. 16 show that the three most active flavones are **52**, **83**, and **84**. The other results are summarized in the Table 4.

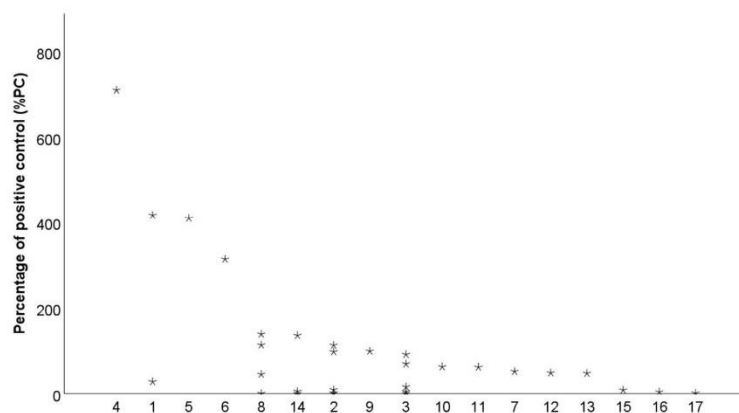
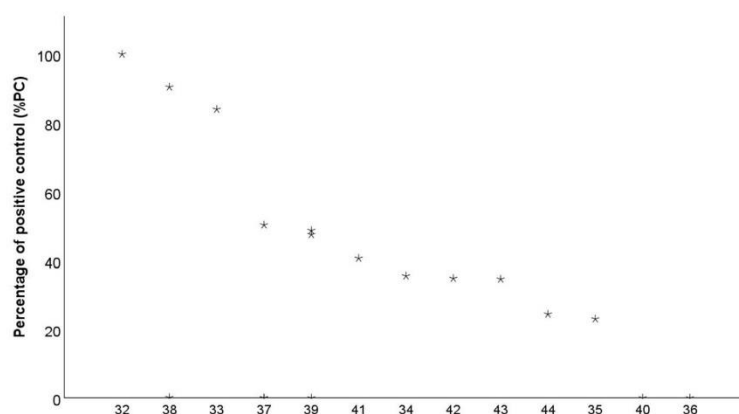


Fig. 14 Distribution of $\%_{\text{PC}}$ values among different isoflavones, isoflavans, and isoflavanones visualized as scatter plot. Asterisks represent individual compounds: **1** = ψ -baptigenin; **2** = biochanin A; **3** = genistein; **4** = 4'-fluoro-7-hydroxyisoflavone; **5** = 3',5'-dimethoxy-7-hydroxyisoflavone; **6** = 3'-

methoxy-7-hydroxyisoflavone; **7** = 3',4',5'-trifluoro-7-hydroxyisoflavone; **8** = formononetin; **9** = 3',4',7-trihydroxyflavone; **10** = daidzin; **11** = genistin; **12** = prunetin; **13** = puerarin; **14** = daidzein; **15** = calycosin; **16** = 6-hydroxydaidzein; **17** = 3'-hydroxygenistein

Table 2 Overall SAR results for isoflavones and isoflavans that did not allow the calculation of %_{PC}

Reference	SAR of isoflavones, isoflavans, and isoflavanones
Chacko et al. (2007)	17 > 2 > 3 > 14 > 27 (isoflavan)
Dang et al. (2003)	3
Cho et al. (2010)	27 (isoflavan) ≥ 14 (n.s.)
Sakamoto et al. (2016)	14

**Fig. 15** Distribution of %_{PC} values among different flavanols visualized as scatter plot. Asterisks represent individual compounds: **32** = (-)-epigallocatechin gallate; **33** = (-)-gallo-catechin gallate; **34** = (-)-epicatechin gallate; **35** = (-)-catechin

gallate; **36** = (-)-epigallocatechin; **37** = (-)-epicatechin; **38** = (-)-catechin; **39** = (+)-catechin; **40** = procyanidin B2; **41** = epi-gallocatechin; **42** = gallocatechin; **43** = epigallocatechin gallate; **44** = epicatechin gallate

Flavanones

As a conclusion from the three studies (Ma et al. 2016; Du et al. 2017; Mossine et al. 2022) that showed results for more than one flavanone already presented in the previous chapter, we can formulate several outlines of SAR:

1. The effect of compound **117** was greatly reduced by replacing the methoxy group at position C-7 with a hydroxyl or moving the prenyl group from position C-6 to C-8 of the A-ring or cyclizing it (Ma et al. 2016).
2. A key factor for the effect was also the replacement of the hydroxyl group at position C-4' with a benzoyloxy group (Du et al. 2017).
3. Other key factor for the effect is a free hydroxyl group at C-7 of the A-ring: **111** versus **108** and **109** versus **115** (Mossine et al. 2022).

Iio et al. studied the effect of compound **111** on the up-regulation of the expression of ATP-binding

cassette transporter A1 (ABCA1) and the promotion of cholesterol efflux from THP-1 macrophages. Compound **111** caused a significant threefold increase in PPAR γ activation at a concentration of 15 μ M, whereas rosiglitazone was much more active (11-fold activation at 2 μ M) (Iio et al. 2012).

Liu et al. screened two flavonoids derived from *Citrus aurantium* L. for their ability to up-regulate the transcription of adiponectin via PPAR γ . Both **109** and **111** showed dose-dependent effects and approx. fourfold activation at a concentration of 40 μ M. On the other hand, rosiglitazone performed much better, with eightfold activation at 10 μ M (Liu et al. 2008).

Ghorbani et al. showed that citrus flavonoid **108** activates PPAR γ and consequently induces p53 and inhibits NF- κ B to trigger apoptosis. The compound **108** activated PPAR γ at a concentration of 25 μ M. No positive control was used (Ghorbani et al. 2012).

Hu et al. found that alpinetin (**124**) has an anti-inflammatory effect on LPS-induced inflammation in macrophages by activating PPAR γ . Compound **124**

Table 3 Overall SAR results for flavanols that did not allow the calculation of %_{PC}

Reference	SAR of flavanols
Ahmed et al. (2017)	45 > mixture of 48 and 49

was less active (1.3-fold at a concentration of 50 µg/mL) than rosiglitazone (1 µM; 1.8-fold) (Hu et al. 2013).

Goldwasser et al. concentrated on grapefruit flavonoid **109** and its effect on the PPAR γ transcriptional activity. The activity of compound **109** reached 17% at a concentration of 150 µM. On the other hand, ciglitazone reached 24% at 10 µM (Goldwasser et al. 2010).

Ma et al. investigated microbial transformation of prenylflavanones **117** and **118** from *Psoralea corylifolia* L. by using two fungal species, *Cunninghamella blakesleeana* and *C. elegans*, and their PPAR γ agonistic effect. Rosiglitazone showed 20.56-fold activation at a concentration of 20 µM, whereas other compounds were tested at 25 µM. The prenylflavanone **117** (11.65-fold) was transformed to (2*R*,2*S*)-4''-hydroxybavachinin enantiomers (**125**; 3.85-fold) and (2*R*,2*S*)-4'',5''-dihydroxybavachinin enantiomers (**126**; 3.52-fold). The other compounds were inactive, such as the other product of **117**: (2*R*,2*S*)-(2*R*'',2*S*'')-2'',3''-dihydroxybavachinin epimers (**127**). And the products of **118**: (2*R*,2*S*)-bavachin-7-*O*- β -D-glucopyranoside epimers (**128**), (2*S*)-4''-hydroxybavachin (**129**), and (2*S*)-5''-hydroxybavachin (**130**). The hydroxylation of the prenyl moiety thus led to decrease of activity (Ma et al. 2015).

The overall results in the Fig. 17 show that the three most active flavones are **111**, **109**, and **108**. The other results are summarized in the Table 5.

Flavonols

We can formulate several outlines of SAR from the seven studies (Liang et al. 2001; Mueller and Jungbauer 2009; Lee et al. 2010; Zoechling et al. 2011; Gijsbers et al. 2013; Pallauf et al. 2017; Mossine et al. 2022) showing results of more than one flavanones already presented in the previous chapter:

- (1) Generally, there is a direct correlation between PPAR γ agonist activity and the number of

hydroxyl groups on the B-ring of the flavonol (**136** > **131** > **133** > **145**), except for the results from Pallauf et al. and Gijsbers et al. where compound **133** was more active than **131** (Gijsbers et al. 2013; Pallauf et al. 2017) and the results from Mossine et al. where the most compound was **145** (Mossine et al. 2022).

- (2) On the other hand, in the study by Lee et al., the only important hydroxyl group was the one at position C-6 of the A-ring (Lee et al. 2010).

Fang et al. investigated a possible mechanism for the antidiabetic activity of compounds **133** and **131** isolated from *Euonymus alatus* (Thunb.) Sieb., including their ability to activate the PPAR γ receptor. Both compounds were less active: **131** (%_{PC} \approx 16.5%) and **133** (%_{PC} \approx 9%) than rosiglitazone (100% activation at 20 µM) (Fang et al. 2008).

Beekman et al. studied the effects of flavonol aglycones and glucuronides on the activation of PPAR γ . Compound **133** was the most active (%_{PC} = 5.2%) followed by **131** (%_{PC} = 4.4%); both were compared to rosiglitazone (EC₉₀ = 0.69 µM). Both corresponding plasma conjugates, quercetin-3-*O*-glucuronide (**142**) and kaempferol-3-*O*-glucuronide (**143**), were inactive (Beekmann et al. 2015).

Ko et al. performed a study with derivatives of **145** and tested their ability to promote the production of adiponectin via PPAR γ partial agonism. The most active compound was galangin 3-benzyl-5-methyl ether (**144**; %_{PC} = 11.8%), whereas **145** was less active (%_{PC} = 3.6%). Both were compared to troglitazone (*Ki* = 0.2 µM) (Ko et al. 2022).

Yue et al. concentrated on the connection between the activation of PPAR γ and consequent anti-arthritis effects by the attenuation of synovial angiogenesis. They found a potent effect for compound **146** (%_{PC} = 84.2%) in comparison to rosiglitazone (380-fold at 10 µM) (Yue et al. 2018).

Wang et al. studied prenylated flavonoids isolated from *Morus nigra* L. and their insulin-sensitizing activity. Among them, nigragenon L (**147**) showed the most potent effect and was confirmed to be the ligand of PPAR γ (%_{PC} = 3.6%) when compared to rosiglitazone (IC₅₀ = 0.1 µM) (Wang et al. 2022).

Ko et al. researched macakurzin C (**148**) and its derivatives as potential novel pharmacophores for the modulation of PPAR γ and other isoforms. Compound **148** (%_{PC} = 18.8%) was only slightly active in

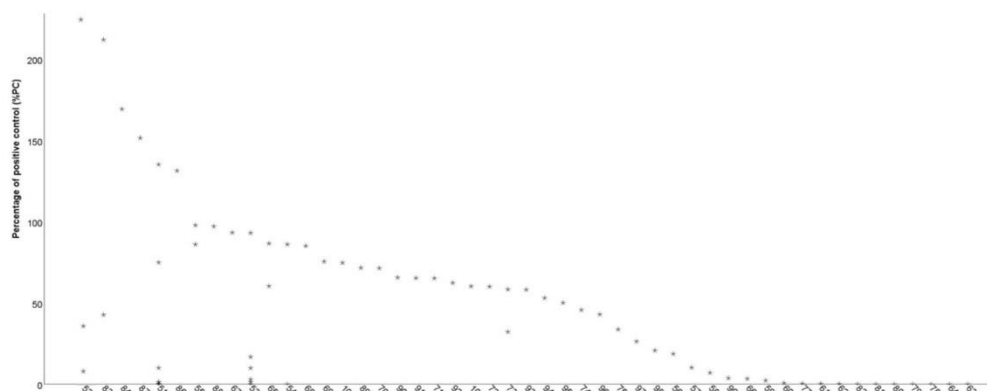


Fig. 16 Distribution of %_{PC} values among different flavones visualized as scatter plot. Asterisks represent individual compounds: **51** = apigenin; **52** = chrysin; **53** = luteolin; **54** = diosmetin; **55** = 5,4'-dihydroxyflavone; **56** = 4'-(4''-nitrobenzoyloxy)-7-methoxy-6-isopentenylflavone; **57** = 4'-acetyloxy-7-methoxy-6-isopentenylflavone; **58** = 4'-hydroxy-7-methoxy-6-isopentenylflavone; **59** = 4'-hydroxy-7-methoxy-6-isopentenylflavone; **60** = acerosin; **61** = hispidulin; **62** = scutellarein; **63** = homoplantagin; **64** = apigenin-8-C- α -L-arabinopyranoside; **65** = baicalin; **66** = oroxylin A; **67** = chrysin 5,7-diprenyl ether; **68** = chrysin 5-prenyl-7-benzyl ether; **69** = chrysin 5-benzyl-7-prenyl ether; **70** = chrysin 5-benzyl-7-benzyl ether; **71** = chrysin 5-benzyl ether; **72** = chrysin 5-methyl-7-benzyl ether; **73** = chrysin 7-benzyl ether;

74 = chrysin 5-(4''-fluoro)benzyl ether; **75** = chrysin 5-allyl ether; **76** = chrysin 5-(4''-chloro)benzyl ether; **77** = apigenin-7-O- β -D-glucuronide; **78** = chrysoeriol; **79** = chrysoeriol-7-O- β -D-glucuronide; **80** = diosmetin-7-O- β -D-glucuronide methyl ester; **81** = apigenin-7-O- β -D-glucuronide methyl ester; **82** = linarin; **83** = acacetin; **84** = 7-methoxyflavone; **86** = flavone; **87** = 7,4'-dihydroflavone; **88** = wogonin; **89** = baicalein; **90** = tangeretin; **91** = 4',7,8-trihydroxyflavone; **92** = 3',7,8-trihydroxyflavone; **93** = α -naphthoflavone; **94** = vitexin; **95** = neodiosmin; **96** = diosmin; **97** = 5,6-dihydroxyflavone; **98** = 3',4'-dihydroxyflavone; **99** = β -naphthoflavone; **100** = 2',3',6-trihydroxyflavone; **106** = 8-(1''-hydroxyisoprenyl)-5,6-dihydroxy-7,4'-dimethoxyflavone

Table 4 Overall SAR results for flavones that did not allow the calculation of %_{PC}

Reference	SAR of flavones
Feng et al. (2014)	51
Ding et al. (2010)	53
Zhou et al. (2021)	107

comparison with its 3,5-dimethyl ether derivative (**149**; %_{PC} = 66.7%), both compared to pioglitazone (K_i = 0.6 μ M) (Ko et al. 2023).

Miao et al. studied inhibitory effect of compound **146** on the transformation of fibroblasts towards myofibroblasts through regulating PPAR γ . Compound **146** showed similar effect (%_{PC} = 100%) in comparison with rosiglitazone (threefold activation at 10 μ M, both) (Miao et al. 2022).

Ramachandran et al. found that isorhamnetin (**159**) modulates PPAR γ activation and thus inhibits proliferation and invasion and induces apoptosis in gastric cancer. At a concentration of 25 μ M, compound **159** induced 3.5-fold activation (Ramachandran et al. 2012).

The overall results in the Fig. 18 show that the three most active flavonols are **145**, **133**, and **146**. The other results are summarized in the Table 6.

Anthocyanidins and anthocyanins

The summary of the results of the four studies (Mueller and Jungbauer 2009; Zoechling et al. 2011; Gijsbers et al. 2013; Mossine et al. 2022) in the previous chapter shows rather conflicting outcomes about SAR of anthocyanidins:

1. Based on the results of Zoechling et al., anthocyanidins, namely compound **161**, are the second

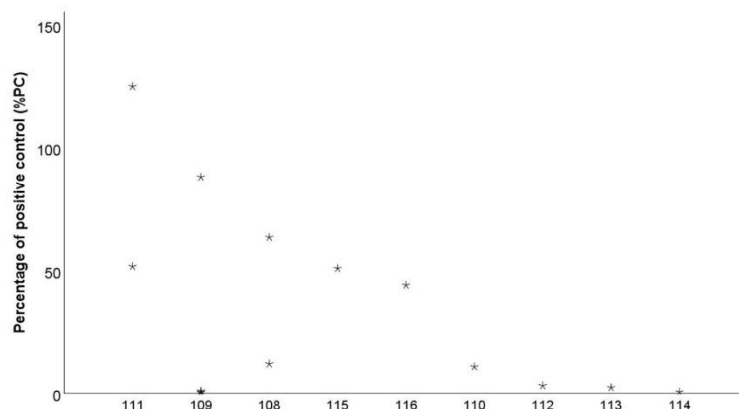


Fig. 17 Distribution of %_{PC} values among different flavanones visualized as scatter plot. Asterisks represent individual compounds: **108** = hesperidin; **109** = naringenin; **110** = norkurarinone; **111** = hesperetin; **112** = 4'-benzoyloxy-7-methoxy-

6-isopentenylflavanone; **113** = 3'-fluoro-4'-hydroxy-7-methoxy-6-isopentenylflavanone; **114** = 4'-hydroxy-7-methoxy-6-isopentenylflavanone; **115** = naringin; **116** = eriodictyol

Table 5 Overall SAR results for flavanones that did not allow the calculation of %_{PC}

Reference	SAR of flavanones
Iio et al. (2012)	111
Liu et al. (2008)	109 ≈ 111
Ghorbani et al. (2012)	108
Hu et al. (2013)	112
Goldwasser et al. (2010)	109
Ma et al. (2015)	117 > 125 > 126

most active class of flavonoids (Zoechling et al. 2011).

- But Gijsbers et al. and Mueller and Jungbauer showed that compounds **160**, **161**, or **162** have no effect (Mueller and Jungbauer 2009; Gijsbers et al. 2013).
- Moreover, Mossine et al. demonstrated that anthocyanins (**163**) are more effective than the corresponding anthocyanidines (**161**) (Mossine et al. 2022).

Jia et al. demonstrated that compound **161** is an agonistic ligand for PPAR α , β/δ , and γ , reducing the amounts of lipids in the liver. In comparison with troglitazone (threefold activation at 10 μ M), **161** (%_{PC} = 83.3%) showed high activity (Jia et al. 2013).

Scazzocchio et al. studied the insulin-like effects of cyanidin-3-*O*- β -glucoside (**167**; eightfold at 10 μ M) via the up-regulation of PPAR γ activity in human omental adipocytes.

The overall results in the Fig. 19 show that the three most active anthocyanidines and anthocyanins are **161**, **163**, and **164**. The other results are summarized in the Table 7.

Flavanonols

It is true also for flavanonols that the summary of the results of the four studies (Quang et al. 2013; Pferschy-Wenzig et al. 2014; Xu et al. 2018; Mossine et al. 2022) in the previous chapter brings conflicting outcomes about SAR:

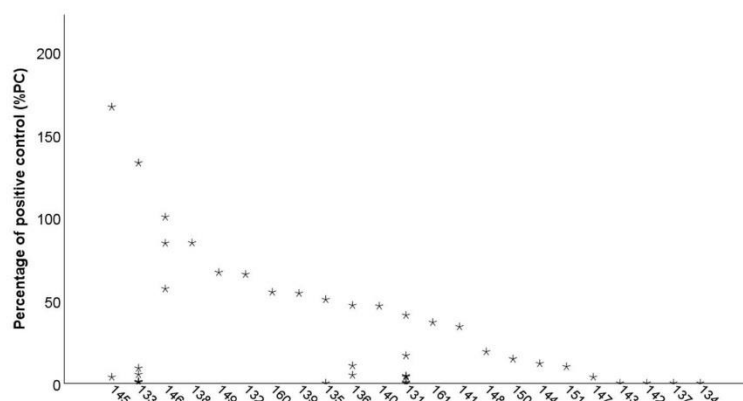


Fig. 18 Distribution of %_{PC} values among different flavonols visualized as scatter plot. Asterisks represent individual compounds: **131** = quercetin; **132** = syringetin; **133** = kaempferol; **134** = kaempferol-3-*O*-rutinoside; **135** = rutin; **136** = myricetin; **137** = dillenetin 3-*O*-(6''-*O*-*p*-coumaroyl)- β -D-glucopyranoside; **138** = 4'-methoxyflavonol; **139** = quercitrin; **140** = myricitrin;

141 = 4',7,8-trihydroxyflavonol; **142** = quercetin-3-*O*-glucuronide; **143** = kaempferol-3-*O*-glucuronide; **144** = galangin 3-benzyl-5-methyl ether; **145** = galangin; **146** = morin; **147** = nigragenon L; **148** = macakurzin C; **149** = macakurzin C 3,5-dimethyl ether

Table 6 Overall SAR results for flavonols that did not allow the calculation of %_{PC}

Reference	SAR of flavonols
Ramachandran et al. (2012)	159

1. The most effective was compound **177** showing the importance of two hydroxyl groups at C-3' and C-4' of the B-ring (Mossine et al. 2022)
2. Among the flavonolignans, the most effective was compound **169** (Mossine et al. 2022). On the other hand, Pferschy-Wenzig et al. proved effect for compound **172** (Pferschy-Wenzig et al. 2014).
3. The results presented by Xu et al. suggest that combination of two prenyl groups at C-2 of the C-ring and C-6 of the A-ring are crucial for effectivity (compounds **178** and **179**) (Xu et al. 2018).

The overall results in the Fig. 20 show that the three most active flavanoneols are **177**, **169**, and **168**. The other results are summarized in the Table 7.

Conclusion

In conclusion, we have demonstrated the highly variable, but also promising effects of different flavonoids on PPAR γ agonism. As far as we are aware, this is the first attempt to recalculate results from different studies, and our results can therefore serve to guide further research in the semisynthetic modification of flavonoids to gain better activity for PPAR γ agonism. Further, the compounds that are active should be tested with other in vitro and in vivo methods.

The most promising results were found for isoflavones, in particular 4'-fluoro-7-hydroxy-isoflavone (**4**; %_{PC} = 710.3%). Among flavones, the most active was chrysin (**52**; %_{PC} = 245.38%), for flavonols it was (-)-epigallocatechin gallate (**32**; %_{PC} = 100.0%), for flavanones hesperetin (**111**; %_{PC} = 125.13%), for flavonols galangin (**145**; %_{PC} = 166.48%), for anthocyanidins and anthocyanins cyanidin (**161**; %_{PC} = 83.3%) and for flavanoneols taxifolin (**177**; %_{PC} = 57.77%).

Fig. 19 Distribution of %_{PC} values among different anthocyanidins and anthocyanins visualized as scatter plot. Asterisks represent individual compounds:
160 = delphinidin;
161 = cyanidin;
162 = peonidin chloride;
163 = cyanin;
164 = keracyanin;
165 = oenin;
166 = pelargonin

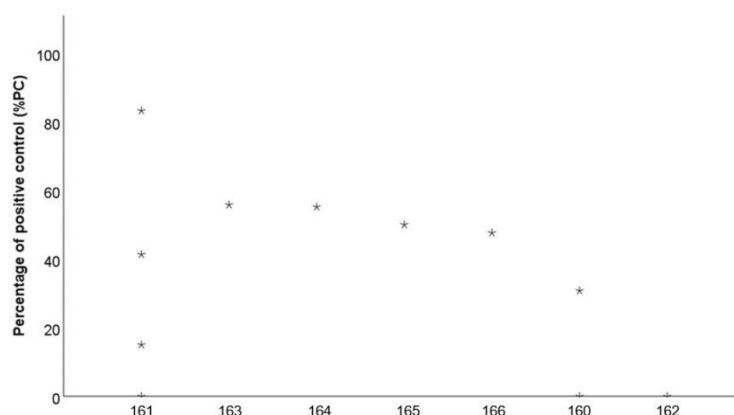
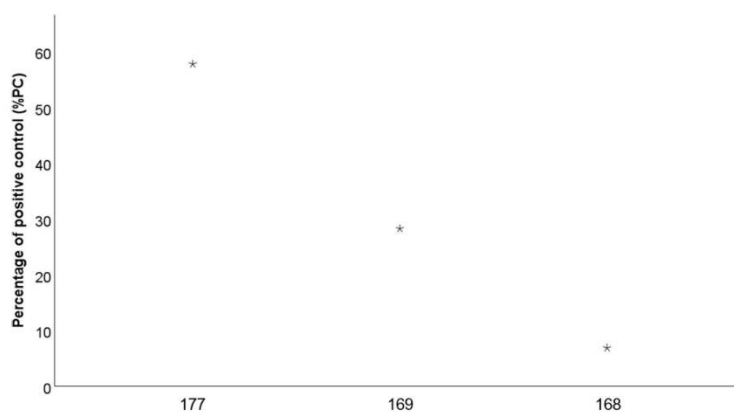


Table 7 Overall SAR results for anthocyanidins and anthocyanins that did not allow the calculation of %_{PC}

Reference	SAR of flavonols
Scazzocchio et al. (2011)	167

flavonoids possessed a hydroxyl group at C-7 of the A-ring, which interacted with the residues Ser289, His323, and Tyr479 of PPAR γ via hydrogen bond interactions. Also, the other side of the molecule, the B-ring, is involved in π - π stacking hydrophobic interaction with residues Phe282, Phe363, and Phe360 (Matin et al. 2009).

Fig. 20 Distribution of %_{PC} values among different flavanoneols visualized as scatter plot. Asterisks represent individual compounds: **168** = (2*R*)-3 α ,7,4'-trihydroxy-5-methoxy-8-(γ , γ -dimethylallyl)-flavanone; **169** = silibinin; **177** = taxifolin



Therefore, the most promising flavonoid structure for PPAR γ agonist is the 7-hydroxyisoflavone. Matin et al. have performed virtual screening of the active compounds on the active site of PPAR γ . All the active

Acknowledgements The authors thank Frank Thomas Campbell for a language editing of the manuscript.

Funding Open access publishing supported by the institutions participating in the CzechELib Transformative Agreement.

Declarations

Conflict of interest The authors declare that the research was conducted without any commercial or financial relationships that could be construed as a potential conflict of interest.

Open Access This article is licensed under a Creative Commons Attribution 4.0 International License, which permits use, sharing, adaptation, distribution and reproduction in any medium or format, as long as you give appropriate credit to the original author(s) and the source, provide a link to the Creative Commons licence, and indicate if changes were made. The images or other third party material in this article are included in the article's Creative Commons licence, unless indicated otherwise in a credit line to the material. If material is not included in the article's Creative Commons licence and your intended use is not permitted by statutory regulation or exceeds the permitted use, you will need to obtain permission directly from the copyright holder. To view a copy of this licence, visit <http://creativecommons.org/licenses/by/4.0/>.

References

- Ahmadian M, Suh JM, Hah N et al (2013) PPAR γ signaling and metabolism: the good, the bad and the future. *Nat Med* 19:557–566. <https://doi.org/10.1038/nm.3159>
- Ahmed S, Al-Rehaily AJ, Ahmad MS et al (2017) Chemical constituents from *Oncocalyx glabratus* and their biological activities. *Phytochem Lett* 20:128–132. <https://doi.org/10.1016/j.phytol.2017.04.016>
- An S, Hwang SY, Gong J et al (2023a) Computational prediction of the phenotypic effect of flavonoids on adiponectin biosynthesis. *J Chem Inf Model* 63:856–869. <https://doi.org/10.1021/acs.jcim.3c00033>
- An S, Ko H, Jang H et al (2023b) Prenylated chrysin derivatives as partial PPAR γ agonists with adiponectin secretion-inducing activity. *ACS Med Chem Lett* 14:425–431. <https://doi.org/10.1021/acsmedchemlett.2c00511>
- Beekmann K, Rubió L, de Haan LHJ et al (2015) The effect of quercetin and kaempferol aglycones and glucuronides on peroxisome proliferator-activated receptor-gamma (PPAR- γ). *Food Funct* 6:1098–1107. <https://doi.org/10.1039/C5FO00076A>
- Chacko BK, Chandler RT, D'Alessandro TL et al (2007) Anti-inflammatory effects of isoflavones are dependent on flow and human endothelial cell PPAR γ 1. *J Nutr* 137:351–356. <https://doi.org/10.1093/jn/137.2.351>
- Cho KW, Lee O-H, Banz WJ et al (2010) Daidzein and the daidzein metabolite, equol, enhance adipocyte differentiation and PPARgamma transcriptional activity. *J Nutr Biochem* 21:841–847. <https://doi.org/10.1016/j.jnutbio.2009.06.012>
- Christensen KB, Petersen RK, Kristiansen K, Christensen LP (2010) Identification of bioactive compounds from flowers of black elder (*Sambucus nigra* L.) that activate the human peroxisome proliferator-activated receptor (PPAR) gamma. *Phytother Res* 24(Suppl 2):129–132. <https://doi.org/10.1002/ptr.3005>
- Dang Z-C, Audinot V, Papapoulos SE et al (2003) Peroxisome proliferator-activated receptor gamma (PPARgamma) as a molecular target for the soy phytoestrogen genistein. *J Biol Chem* 278:962–967. <https://doi.org/10.1074/jbc.M209483200>
- Ding L, Jin D, Chen X (2010) Luteolin enhances insulin sensitivity via activation of PPAR γ transcriptional activity in adipocytes. *J Nutr Biochem* 21:941–947. <https://doi.org/10.1016/j.jnutbio.2009.07.009>
- Dixon RA, Pasinetti GM (2010) Flavonoids and isoflavonoids: from plant biology to agriculture and neuroscience. *Plant Physiol* 154:453–457. <https://doi.org/10.1104/pp.110.161430>
- Du G, Zhao Y, Feng L et al (2017) Design, synthesis, and structure-activity relationships of bavachinin analogues as peroxisome proliferator-activated receptor γ agonists. *ChemMedChem* 12:183–193. <https://doi.org/10.1002/cmdc.201600554>
- Fang X-K, Gao J, Zhu D-N (2008) Kaempferol and quercetin isolated from *Euonymus alatus* improve glucose uptake of 3T3-L1 cells without adipogenesis activity. *Life Sci* 82:615–622. <https://doi.org/10.1016/j.lfs.2007.12.021>
- Feng X, Qin H, Shi Q et al (2014) Chrysin attenuates inflammation by regulating M1/M2 status via activating PPAR γ . *Biochem Pharmacol* 89:503–514. <https://doi.org/10.1016/j.bcp.2014.03.016>
- Feng X, Weng D, Zhou F et al (2016) Activation of PPAR γ by a natural flavonoid modulator, apigenin ameliorates obesity-related inflammation via regulation of macrophage polarization. *EBioMedicine* 9:61–76. <https://doi.org/10.1016/j.ebiom.2016.06.017>
- Ghorbani A, Nazari M, Jeddi-Tehrani M, Zand H (2012) The citrus flavonoid hesperidin induces p53 and inhibits NF- κ B activation in order to trigger apoptosis in NALM-6 cells: involvement of PPAR γ -dependent mechanism. *Eur J Nutr* 51:39–46. <https://doi.org/10.1007/s00394-011-0187-2>
- Gijsbers L, van Eekelen HDLM, de Haan LHJ et al (2013) Induction of peroxisome proliferator-activated receptor γ (PPAR γ)-mediated gene expression by tomato (*Solanum lycopersicum* L.) extracts. *J Agric Food Chem* 61:3419–3427. <https://doi.org/10.1021/jf304790a>
- Goldwasser J, Cohen PY, Yang E et al (2010) Transcriptional regulation of human and rat hepatic lipid metabolism by the grapefruit flavonoid naringenin: role of PPAR α , PPAR γ and LXR α . *PLoS ONE* 5:e12399. <https://doi.org/10.1371/journal.pone.0012399>
- Grygiel-Górniak B (2014) Peroxisome proliferator-activated receptors and their ligands: nutritional and clinical implications: a review. *Nutr J* 13:17. <https://doi.org/10.1186/1475-2891-13-17>
- Hamblin M, Chang L, Fan Y et al (2009) PPARs and the cardiovascular system. *Antioxid Redox Signal* 11:1415–1452. <https://doi.org/10.1089/ars.2008.2280>
- Hu K, Yang Y, Tu Q et al (2013) Alpinetin inhibits LPS-induced inflammatory mediator response by activating PPAR- γ in THP-1-derived macrophages. *Eur J Pharmacol* 721:96–102. <https://doi.org/10.1016/j.ejphar.2013.09.049>
- Hui H, Chen Y, Yang H et al (2014) Oroxylin A has therapeutic potential in acute myelogenous leukemia by dual effects targeting PPAR γ and RXR α . *Int J Cancer* 134:1195–1206. <https://doi.org/10.1002/ijc.28435>

- Iio A, Ohguchi K, Iinuma M et al (2012) Hesperetin upregulates ABCA1 expression and promotes cholesterol efflux from THP-1 macrophages. *J Nat Prod* 75:563–566. <https://doi.org/10.1021/np200696r>
- Jia Y, Kim J-Y, Jun H et al (2013) Cyanidin is an agonistic ligand for peroxisome proliferator-activated receptor- α reducing hepatic lipid. *Biochem Biophys Acta* 1831:698–708. <https://doi.org/10.1016/j.bbailip.2012.11.012>
- Ko H, Jang H, An S et al (2022) Galangin 3-benzyl-5-methylether derivatives function as an adiponectin synthesis-promoting peroxisome proliferator-activated receptor γ partial agonist. *Bioorg Med Chem* 54:116564. <https://doi.org/10.1016/j.bmc.2021.116564>
- Ko H, An S, Jang H et al (2023) Macakurzin C derivatives as a novel pharmacophore for pan-peroxisome proliferator-activated receptor modulator. *Biomol Ther (Seoul)* 31:312–318. <https://doi.org/10.4062/biomolther.2022.097>
- Lee J-Y, Kim J-K, Cho M-C et al (2010) Cytotoxic flavonoids as agonists of peroxisome proliferator-activated receptor γ on human cervical and prostate cancer cells. *J Nat Prod* 73:1261–1265. <https://doi.org/10.1021/np100148m>
- Lee KE, Bharadwaj S, Yadava U, Kang SG (2020) Computational and in vitro investigation of (-)-epicatechin and proanthocyanidin B2 as inhibitors of human matrix metalloproteinase 1. *Biomolecules* 10:1379. <https://doi.org/10.3390/biom10101379>
- Liang Y-C, Tsai S-H, Tsai D-C et al (2001) Suppression of inducible cyclooxygenase and nitric oxide synthase through activation of peroxisome proliferator-activated receptor- γ by flavonoids in mouse macrophages. *FEBS Lett* 496:12–18. [https://doi.org/10.1016/S0014-5793\(01\)02393-6](https://doi.org/10.1016/S0014-5793(01)02393-6)
- Lim HA, Lee EK, Kim JM et al (2012) PPAR γ activation by baicalin suppresses NF- κ B-mediated inflammation in aged rat kidney. *Biogerontology* 13:133–145. <https://doi.org/10.1007/s10522-011-9361-4>
- Liu L, Shan S, Zhang K et al (2008) Naringenin and hesperetin, two flavonoids derived from *Citrus aurantium* up-regulate transcription of adiponectin. *Phytother Res* 22:1400–1403. <https://doi.org/10.1002/ptr.2504>
- Liu Q, Yang Q-M, Hu H-J et al (2014) Bioactive diterpenoids and flavonoids from the aerial parts of *Scoparia dulcis*. *J Nat Prod* 77:1594–1600. <https://doi.org/10.1021/np500150f>
- Ma S, Zheng C, Feng L et al (2015) Microbial transformation of prenylflavonoids from *Psoralea corylifolia* by using *Cunninghamella blakesleeana* and *C. elegans*. *J Mol Catal B Enzym* 118:8–15. <https://doi.org/10.1016/j.molcatb.2015.04.015>
- Ma S, Huang Y, Zhao Y et al (2016) Prenylflavone derivatives from the seeds of *Psoralea corylifolia* exhibited PPAR- γ agonist activity. *Phytochem Lett* 16:213–218. <https://doi.org/10.1016/j.phytol.2016.04.016>
- Matin A, Gavande N, Kim MS et al (2009) 7-Hydroxy-benzopyran-4-one derivatives: a novel pharmacophore of peroxisome proliferator-activated receptor α and - γ (PPAR α and γ) dual agonists. *J Med Chem* 52:6835–6850. <https://doi.org/10.1021/jm900964r>
- Miao Y, Geng Y, Yang L et al (2022) Morin inhibits the transformation of fibroblasts towards myofibroblasts through regulating “PPAR- γ -glutaminolysis-DEPTOR” pathway in pulmonary fibrosis. *J Nutr Biochem* 101:108923. <https://doi.org/10.1016/j.jnutbio.2021.108923>
- Mossine VV, Waters JK, Gu Z et al (2022) Bidirectional responses of eight neuroinflammation-related transcriptional factors to 64 flavonoids in astrocytes with transposable insulated signaling pathway reporters. *ACS Chem Neurosci* 13:613–623. <https://doi.org/10.1021/acscchemneuro.1c00750>
- Mueller M, Jungbauer A (2008) Red clover extract: a putative source for simultaneous treatment of menopausal disorders and the metabolic syndrome. *Menopause* 15:1120–1131. <https://doi.org/10.1097/gme.0b013e31817062ce>
- Mueller M, Jungbauer A (2009) Culinary plants, herbs and spices—a rich source of PPAR γ ligands. *Food Chem* 117:660–667. <https://doi.org/10.1016/j.foodchem.2009.04.063>
- Mueller M, Lukas B, Novak J et al (2008) Oregano: a source for peroxisome proliferator-activated receptor γ antagonists. *J Agric Food Chem* 56:11621–11630. <https://doi.org/10.1021/jf802298w>
- Nazreen S, Alam MS, Hamid H et al (2019) New flavone and phenolic esters from *Callistemon lanceolatus* DC: their molecular docking and antidiabetic activities. *Arab J Chem* 12:1260–1267. <https://doi.org/10.1016/j.arabjc.2014.11.029>
- Pallauf K, Duckstein N, Hasler M et al (2017) Flavonoids as putative inducers of the transcription factors Nrf2, FoxO, and PPAR γ . *Oxid Med Cell Longev* 2017:4397340. <https://doi.org/10.1155/2017/4397340>
- Panche AN, Diwan AD, Chandra SR (2016) Flavonoids: an overview. *J Nutr Sci* 5:e47. <https://doi.org/10.1017/jns.2016.41>
- Pferschy-Wenzig E-M, Atanasov AG, Malainer C et al (2014) Identification of isosilybin A from milk thistle seeds as an agonist of peroxisome proliferator-activated receptor gamma. *J Nat Prod* 77:842–847. <https://doi.org/10.1021/np400943b>
- Puhl AC, Bernardes A, Silveira RL et al (2012) Mode of peroxisome proliferator-activated receptor γ activation by luteolin. *Mol Pharmacol* 81:788–799. <https://doi.org/10.1124/mol.111.076216>
- Quang TH, Ngan NTT, Minh CV et al (2013) Anti-inflammatory and PPAR transactivational properties of flavonoids from the roots of *sophora flavescens*. *Phytother Res* 27:1300–1307. <https://doi.org/10.1002/ptr.4871>
- Ramachandran L, Manu KA, Shanmugam MK et al (2012) Isorhamnetin inhibits proliferation and invasion and induces apoptosis through the modulation of peroxisome proliferator-activated receptor γ activation pathway in gastric cancer. *J Biol Chem* 287:38028–38040. <https://doi.org/10.1074/jbc.M112.388702>
- Sakamoto Y, Kanatsu J, Toh M et al (2016) The Dietary isoflavone daidzein reduces expression of pro-inflammatory genes through PPAR α/γ and JNK pathways in adipocyte and macrophage co-cultures. *PLoS ONE* 11:e0149676. <https://doi.org/10.1371/journal.pone.0149676>
- Salam NK, Huang TH-W, Kota BP et al (2008) Novel PPAR- γ agonists identified from a natural product library: a virtual screening, induced-fit docking and biological assay study. *Chem Biol Drug des* 71:57–70. <https://doi.org/10.1111/j.1747-0285.2007.00606.x>

- Scazzocchio B, Vari R, Filesi C et al (2011) Cyanidin-3-O- β -glucoside and protocatechuic acid exert insulin-like effects by upregulating PPAR γ activity in human omental adipocytes. *Diabetes* 60:2234–2244. <https://doi.org/10.2337/db10-1461>
- Shams Eldin SM, Radwan MM, Wanas AS et al (2018) Bioactivity-guided isolation of potential antidiabetic and anti-hyperlipidemic compounds from *trigonella stellata*. *J Nat Prod* 81:1154–1161. <https://doi.org/10.1021/acs.jnatprod.7b00707>
- Shen P, Liu M, Ng T et al (2006) Differential effects of iso-flavones, from *Astragalus Membranaceus* and *Pueraria Thomsonii*, on the activation of PPAR α Ppar γ , and adipocyte differentiation in vitro. *J Nutr* 136:899–905. <https://doi.org/10.1093/jn/136.4.899>
- Shin DW, Kim SN, Lee SM et al (2009) (–)-Catechin promotes adipocyte differentiation in human bone marrow mesenchymal stem cells through PPAR γ transactivation. *Biochem Pharmacol* 77:125–133. <https://doi.org/10.1016/j.bcp.2008.09.033>
- Soccio RE, Chen ER, Lazar MA (2014) Thazolidinediones and the promise of insulin sensitization in type 2 diabetes. *Cell Metab* 20:573–591. <https://doi.org/10.1016/j.cmet.2014.08.005>
- Treml J, Šmejkal K (2016) Flavonoids as potent scavengers of hydroxyl radicals. *Comprehensive Reviews in Food Science and Food Safety* 15:720–738. <https://doi.org/10.1111/1541-4337.12204>
- Wang L, Waltenberger B, Pferschy-Wenzig E-M et al (2014) Natural product agonists of peroxisome proliferator-activated receptor gamma (PPAR γ): a review. *Biochem Pharmacol* 92:73–89. <https://doi.org/10.1016/j.bcp.2014.07.018>
- Wang L, Wang J, Ma M et al (2022) Prenylated flavonoids from *Morus nigra* and their insulin sensitizing activity. *Phytochemistry* 203:113398. <https://doi.org/10.1016/j.phytochem.2022.113398>
- Xu L-J, Yu M-H, Huang C-Y et al (2018) Isoprenylated flavonoids from *Morus nigra* and their PPAR γ agonistic activities. *Fitoterapia* 127:109–114. <https://doi.org/10.1016/j.fitote.2018.02.004>
- Yang Y, Zhang Q, Wang J et al (2024) Bioactive constituents from *Clerodendrum trichotomum* and their α -glucosidase inhibitory and PPAR- γ agonist activities. *Fitoterapia* 179:106266. <https://doi.org/10.1016/j.fitote.2024.106266>
- Yue M, Zeng N, Xia Y et al (2018) Morin exerts anti-arthritis effects by attenuating synovial angiogenesis via activation of peroxisome proliferator activated receptor- γ . *Mol Nutr Food Res* 62:1800202. <https://doi.org/10.1002/mnfr.201800202>
- Zhou Y, Guo Y, Zhu Y et al (2021) Dual PPAR γ/α agonist oroxyloside suppresses cell cycle progression by glycolipid metabolism switch-mediated increase of reactive oxygen species levels. *Free Radical Biol Med* 167:205–217. <https://doi.org/10.1016/j.freeradbiomed.2021.02.032>
- Zoechling A, Liebner F, Jungbauer A (2011) Red wine: a source of potent ligands for peroxisome proliferator-activated receptor γ . *Food Funct* 2:28–38. <https://doi.org/10.1039/C0FO00086H>

Publisher's Note Springer Nature remains neutral with regard to jurisdictional claims in published maps and institutional affiliations.

6.9. ARTICLE 9

Treml, J.; Václavík, J.; Molčanová, L.; Čulenová, M.; Hummelbrunner, S.; Neuhauser, C.; Dirsch, V. M.; Weghuber, J.; Šmejkal, K. *Journal of Agricultural and Food Chemistry* 2025, doi: 10.1021/acs.jafc.4c11398 (IF=5.700)

Identification of Plant Phenolics from *Paulownia tomentosa* and *Morus alba* as Novel PPAR γ Partial Agonists and Hypoglycemic Agents

Jakub Trembl*, Jiří Václavík, Lenka Molčanová, Marie Čulenová, Scarlet Hummelbrunner, Cathrina Neuhauser, Verena M. Dirsch, Julian Weghuber, and Karel Šmejkal



Cite This: *J. Agric. Food Chem.* 2025, 73, 13960–13972



Read Online

ACCESS |

Metrics & More

Article Recommendations

Supporting Information

ABSTRACT: The aim of our study was to determine the PPAR γ agonism and hypoglycemic activity of natural phenolics isolated from *Paulownia tomentosa* and *Morus alba*. We started with a molecular docking preselection, followed by *in vitro* cell culture assays, such as PPAR γ luciferase reporter gene assay and PPAR γ protein expression by Western blot analysis. The ability of the selected compounds to induce GLUT4 translocation in cell culture and lower blood glucose levels in chicken embryos was also determined. Among the thirty-six plant phenolic compounds, moracin M showed the highest hypoglycemic effect in an *in ovo* experiment ($7.33 \pm 2.37\%$), followed by mulberrofuran Y ($3.84 \pm 1.34\%$) and diplacone ($3.69 \pm 1.37\%$). Neither moracin M nor mulberrofuran Y showed a clear effect on the enhancement of GLUT4 translocation or agonism on PPAR γ , while diplacone succeeded in both ($3.62 \pm 0.16\%$ and $2.4\text{-fold} \pm 0.2$, respectively). Thus, we believe that the compounds moracin M, mulberrofuran Y, and diplacone are suitable for further experiments to elucidate their mechanisms of action.

KEYWORDS: diabetes mellitus, hypoglycemic, natural products, plant phenolics, PPAR γ

INTRODUCTION

Diabetes mellitus (DM) is a group of endocrine disorders characterized by hyperglycemia. According to the International Diabetes Federation, 537 million adults had DM in 2021, and the number is expected to increase by 46% by 2045.¹ There are two major types of DM – type 1, associated with insulin deficiency, and type 2 (T2DM), associated with insulin resistance manifesting as relative insulin insufficiency despite adequate insulin production. Uncontrolled hyperglycemia (usually in undiagnosed or uncooperative patients) leads to long-term complications such as diabetic nephropathy, retinopathy, and neuropathy.² Treatment of T2DM, therefore, includes glucose-lowering medications along with general lifestyle changes to reduce body weight.³

Among oral antidiabetic agents, thiazolidinediones (TZDs) are highly effective and were first approved for treatment by the Food and Drug Administration (FDA) in the 1990s. A major boom in their prescription followed until 2005, but later their prescription gradually declined due to concerns about adverse effects, mainly the increased risk of heart attack and bladder cancer.^{4,5} The mechanism of action of TZDs is an agonistic effect on peroxisome proliferator-activated receptor γ (PPAR γ), which leads to insulin sensitization.^{4,5}

PPAR γ is a member of the nuclear receptor family. Upon ligand binding, PPAR γ transactivates specific target genes, thereby contributing to the regulation of glucose and lipid metabolism. The effects of PPAR γ agonists are tissue-specific; in adipose tissue, they enhance adipogenesis, lipid metabolism, and the expression of the glucose transporter type 4 (GLUT4). The overall beneficial effect on T2DM is complemented by the

production of adiponectin, which also increases glucose uptake in muscle cells.⁵ Today, partial PPAR γ agonists that retain glucose-lowering benefits are considered as promising strategy to reduce the risk of adverse effects.⁶ Natural products from traditionally used medicinal plants have always been a promising pool of structures for drug discovery, and the field of PPAR γ agonists and hypoglycemics is no exception.⁴

Paulownia tomentosa (Thunb.) Steud. (Paulowniaceae) is a deciduous tree and known in China as “Pao tong”.⁷ Its parts are widely used in Traditional Chinese Medicine (TCM) for the treatment of inflammation, which is a known condition associated with the development of T2DM.^{8,9} For example, tablets made from *Paulownia* leaves, fruit, and wood extracts are used to relieve cough and reduce mucus production in bronchitis.¹⁰ *Morus alba* L. (Moraceae) is also a deciduous tree known in TCM as “Sang”.¹¹ Traditionally, an aqueous extract of *M. alba* leaves has been prescribed for the treatment of diabetes mellitus.¹² In addition, mulberry fruit is commonly eaten fresh, dried, or processed as wine or juice. Its extracts have been associated with significant hypoglycemic activity.¹³ Both plants contain large amounts of plant phenolics, which are natural products containing aromatic rings substituted with one or more hydroxyl groups.^{14,15} Foods containing such

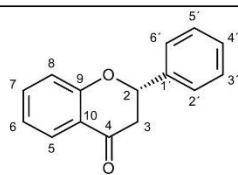
Received: November 19, 2024

Revised: May 5, 2025

Accepted: May 15, 2025

Published: May 20, 2025





Compound	3'	4'	5'	3	5	6	7
1	OH	OH	H	H	OH	H	OH
2	H	OH	H	H	OH	H	OH
3	H	OH	H	H	OH		OH
4	H	OH	H	H	OH		OH
5	H	OH	H	H	OH		OH
6	H	OH	H	H	OH		OH
8	OH	OH	H	H	OH		OH
9	OMe	OH	OH	H	OH		OH
10	OMe	OH	OMe	H	OH		OH
12	OMe	OH	H	H	OH		OH
14	OMe	OH	H	H	OH		OH
18	OMe	OH	H	OH	OH		OH

Figure 1. continued

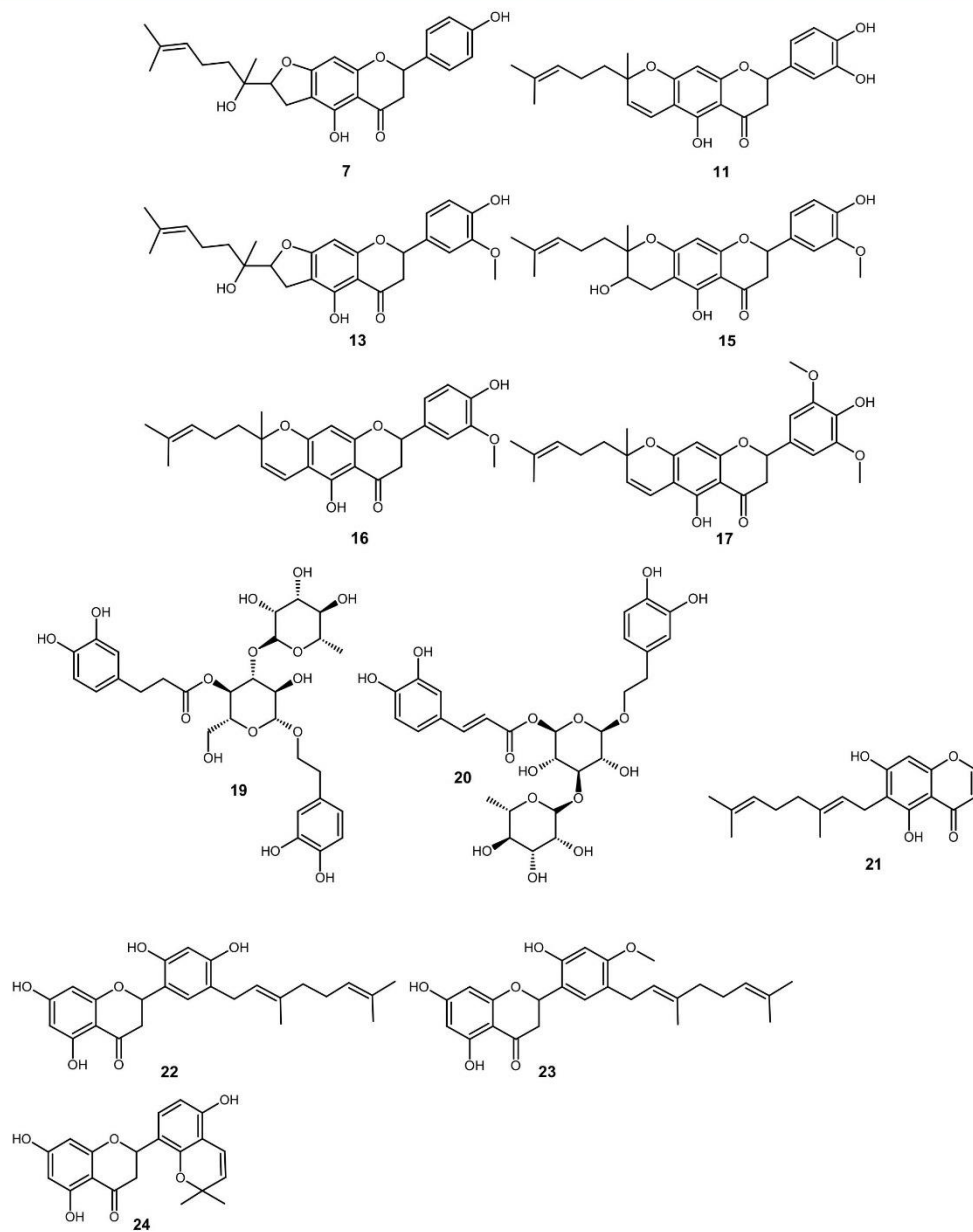


Figure 1. continued

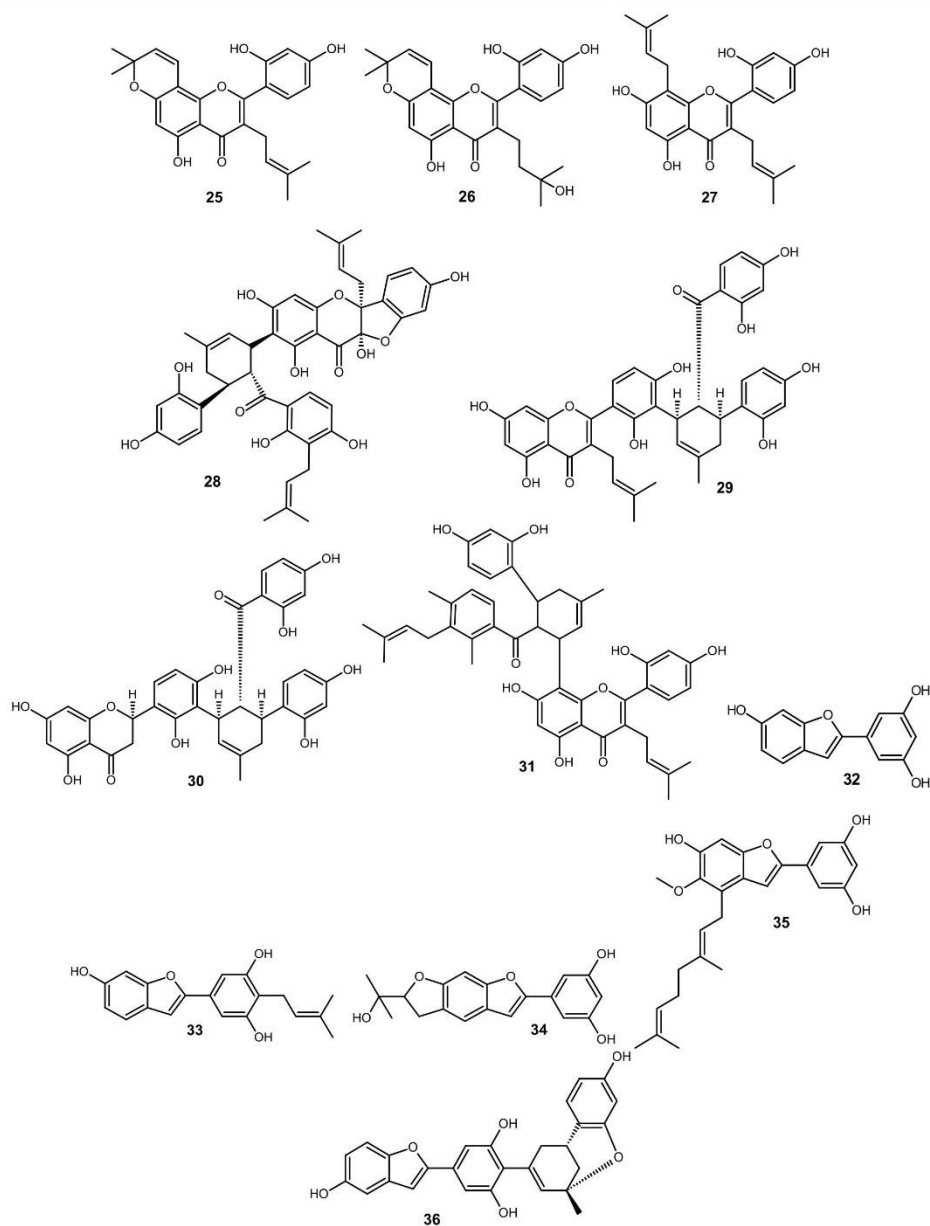


Figure 1. Compounds used for molecular docking: eriodictyol (1), naringenin (2), mimulone (3), mimulone F (4), mimulone G (5), mimulone H (6), bonannione B (7), diplacone (8), 3'-O-methyl-5'-hydroxydipalcone (9), 3'-O-methyl-5'-methyldipalcone (10), tomentone II (11), tomentodipalcone G (12), tomentodipalcone L (13), tomentodipalcone M (14), tomentodipalcone N (15), tomentodipalcone O (16), paulownione C (17), 6-isopentenyl-3'-O-methyltaxifolin (18), acteoside (19), isoacteoside (20), 5,7-dihydroxy-6-geranylchromone (21), kuwanon E (22), kuwanon U (23), sanggenon H (24), morusin (25), morusinol (26), kuwanon C (27), sanggenon E (28), kuwanon K (29), kuwanon L (30), kuwanon H (31), moracin M (32), moracin C (33), moracin O (34), mulberrofuran Y (35), mulberrofuran H (36).

compounds have health-protective functions that are relevant to the control of diet- and lifestyle-related chronic diseases, including T2DM. In addition to their beneficial antioxidant activity, many have been shown to have hypoglycemic effects.^{16–18}

The aim of this study was to screen and determine the PPAR γ agonism and hypoglycemic activity of thirty-six plant phenolic compounds. First, a preselection was performed by molecular docking to PPAR γ , and second, the selected compounds were evaluated by *in vitro* cell culture-based PPAR γ luciferase reporter gene assay and Western blot experiments to detect PPAR γ protein expression. The ability of the selected compounds to induce GLUT4 translocation in cell culture and to lower blood glucose levels in chicken embryos was then determined.

MATERIALS AND METHODS

Test Compounds. Eriodictyol (1) and naringenin (2) were used as nonprenylated flavanones for computational docking analysis together with compounds previously isolated from *Paulownia tomentosa*: 15 geranylated flavanones, mimulone (3),¹⁹ mimulone F (4),²⁰ mimulone G (5),²⁰ mimulone H (6),²⁰ bonannione B (7),²⁰ diplacone (8),¹⁹ 3'-O-methyl-5'-hydroxydiplocone (9),²¹ 3'-O-methyl-5'-O-methyldiplocone (10),²¹ tomentone II (11),²² tomentodiplocone G (12),²³ tomentodiplocone L (13),²⁰ tomentodiplocone M (14),²⁰ tomentodiplocone N (15),²⁰ tomentodiplocone O (16),²⁴ and paulownione C (17).²⁴ Prenylated flavanone 6-isopentenyl-3'-O-methyltaxifolin (18),¹⁹ caffeoyl phenylethanoid glycosides acteoside (19),²⁵ isoacteoside (20),²⁵ and the chromone 5,7-dihydroxy-6-geranylchromone (21)²⁶ (Figure 1). Moreover, computational docking analysis was also performed with the geranylated flavanones kuwanon E (22),²⁷ and kuwanon U (23);²⁷ prenylated flavanone sanggenon H (24),²⁸ three prenylated flavones, morusin (25),²⁹ morusinol (26),²⁸ and kuwanon C (27);²⁸ four Diels–Alder adducts, sanggenon E (28),²⁸ kuwanon K (29),³⁰ kuwanon L (30),³⁰ and kuwanon H (31);³⁰ and five benzofurans, moracin M (32),³⁰ moracin C (33),³⁰ moracin O (34),³⁰ mulberrofuran Y (35),²⁸ and mulberrofuran H (36),²⁸ all previously isolated from *Morus* sp. (Figure 1).

Isolation of Compounds for Bioactivity Assays. Compounds diplocone (8) and tomentone II (11) were obtained by the isolation procedures described in previous works. Briefly, the fruit of *Paulownia tomentosa* (Thunb.) Steud. (Paulowniaceae) was extracted with ethanol and further fractionated by liquid–liquid extraction into several portions. The methanol-soluble portion was subsequently separated by column chromatography using silica gel.²¹ Selected fraction *PT11a* was chosen for further separation using column chromatography and semipreparative RP-HPLC, leading to the isolation of compounds 8 and 11.²²

New plant material, 14.46 kg of the immature fruit of *P. tomentosa*, was collected in October 2021 and identified by Prof. PharmDr. Karel Šmejkal, Ph.D. The fruit was extracted with ethanol and the dried ethanolic extract (373.25 g) was further fractionated by liquid–liquid extraction into several portions. The chloroform portion (80.93 g) was subsequently separated by column chromatography using silica gel. Selected fraction *PT21/CH/A35–39+B31–39* was separated using semipreparative RP-HPLC, leading to the isolation of mimulone (3).

Kuwanon U (23) was obtained as described previously. Briefly, the dried root bark from *Morus alba* L. (Moraceae) was extracted with ethanol. Liquid–liquid extraction of the ethanol extract was carried out with chloroform and ethyl acetate. The chloroform soluble fraction was then separated using silica gel column chromatography and by semipreparative RP-HPLC, leading to the isolation of kuwanon U (23).³⁰ Similarly, moracin C (35) and mulberrofuran Y (33) had been isolated previously from the chloroform-soluble fraction.²⁸ The ethyl acetate-soluble material led to the isolation of moracin M (32) and moracin O (34).³⁰

The test compounds used for the subsequent biological experiments were dissolved in dimethyl sulfoxide (DMSO); the final concentration of DMSO in the cellular assays was 0.1% (v/v). The purity of test compounds 3, 8, 11, 23, and 32–35 was confirmed by HPLC analysis to exceed 95% in all cases (for the methodology and results, see Supporting Information: Figures S1–S8).

Molecular Docking. Molecular docking was done as reported previously.³¹ The crystal structure of the PPAR γ receptor bound to rosiglitazone (Protein Data Bank (PDB) ID: 1FM6) was downloaded from the Collaboratory for Structural Bioinformatics PDB.³²

PyRX was used in conjunction with AutoDock Vina. As a binding site, we used the position of rosiglitazone determined by crystallographic experiment. For the graphical evaluation of the results, PyMOL was used, and the best solution, ranked by binding affinity, was chosen.

Chemicals, Cell Culture Reagents, and Plasmids. Fetal bovine serum (FBS), phosphate saline buffer (PBS), and Dulbecco's modified Eagle's medium (DMEM) were obtained from Lonza (Basel, Switzerland). All other chemicals were from Sigma-Aldrich (Vienna, Austria).

The PPAR luciferase reporter plasmid (tk-PPREx3-luc), pCMX-Gal4-hPPAR γ , and tk(MH1000)-4xLuc were a gift from Prof. Ronald M. Evans (Howard Hughes Medical Institute, La Jolla, CA),³³ the plasmid encoding enhanced green fluorescent protein (pEGFP-N1) was from Clontech (Mountain View, CA), and the plasmid encoding human PPAR γ (pSG5-PL-hPPAR- γ 1) was a gift from Prof. Walter Wahli and Prof. Beatrice Desvergne (Center for Integrative Genomics, University of Lausanne, Switzerland).³⁴

PPAR γ Luciferase Reporter Gene Transactivation. The PPAR γ luciferase reporter gene transactivation experiments were done as reported previously.³⁵ Briefly, human embryonic kidney HEK-293 cells (American Type Culture Collection (ATCC), Manassas, VA) were grown in DMEM supplemented with 2 mM L-glutamine, 100 U/mL benzylpenicillin, 100 μ g/mL streptomycin, and 10% FBS. Cells were seeded in 10 cm dishes at a density of 6×10^6 cells/dish for 18 h, and then transfected by the calcium phosphate precipitation method with 4 μ g of PPAR γ expression plasmid, 4 μ g of reporter plasmid (tk-PPREx3-luc), and 2 μ g of pEGFP-N1 used as internal control. Six hours later, cells were reseeded in 96-well plates (5×10^4 cells/well) in DMEM without phenol red with 5% charcoal-stripped FBS, L-glutamine, and antibiotics. Cells were treated as indicated and incubated for 18 h. After cell lysis, the luminescence of the firefly luciferase and the fluorescence of EGFP were quantified on a GeniosPro plate reader (Tecan, Grödig, Austria). The luminescence signals were normalized to the EGFP-derived fluorescence to account for differences in cell number or transfection efficiency.

One-hybrid luciferase reporter system experiments on the PPAR γ ligand binding domain (PPAR γ -LBD) were done as reported previously.³⁶ HEK-293 cells were transfected using the calcium phosphate method with the following plasmids: 6 μ g of pCMX-Gal4-hPPAR γ and 6 μ g of tk(MH1000)-4xLuc. Additionally, all cells were cotransfected with 3 μ g of pEGFP-N1 to control transfection efficiency.

Protein Expression. The effect of selected test compounds on PPAR γ protein expression was measured on the HepG2 human hepatoma cell line, which was purchased from the European Collection of Cell Cultures (Salisbury, UK) and was cultured as reported previously.³⁷ The HepG2 cells were incubated for 24 h with the selected test compounds.³⁸ After the incubation, the cells were lysed and the lysates were processed using sodium dodecyl sulfate–polyacrylamide gel electrophoresis (SDS–PAGE) and Western blot as reported previously.^{39,40} Specific primary antibodies used for PPAR γ : rabbit anti-PPAR γ 1:1000 (Sigma-Aldrich; product No. SAB4502262).

Total Internal Reflection Fluorescence (TIRF) Microscopy. HeLa cells stably expressing GLUT4-myc-GFP were maintained in RPMI 1640 cell culture medium supplemented with 100 μ g/mL penicillin, 100 μ g/mL streptomycin, 1% G418, and 10% fetal bovine serum (FBS) (M&B Stricker, Bernried, Germany) at 37 °C in a humidified atmosphere with 5% CO₂. As previously reported,^{41–43}

40,000 HeLa GLUT4-myc-GFP cells/well were seeded into 96-well imaging plates (MoBiTec, Goettingen, Germany), grown overnight, washed twice with Hanks' Balanced Salt solution (HBSS, Sigma-Aldrich, Schnellendorf, Germany), and starved for 3 h with HBSS. The cells were imaged using TIRF-Microscopy and stimulated with compounds 3, 8, 32, and 35 (10 μ M) and human insulin (100 nM) dissolved in KRPH buffer (pH = 7.4). Images were recorded at 10 min time intervals, before and after stimulation. TIRF-Microscopy was performed on an epi-fluorescence microscope (Nikon Eclipse Ti2, Tokyo, Japan) using a 60 \times CFI Plan-Apochromat objective. Scanning of multiple stage positions was supported by a motorized x-y stage (CMR-STG-MHIX2, Märzhäuser, Germany). Emission diode lasers (Toptica Photonics, Munich, Germany) were used for excitation of GFP at 488 nm and the fluorescence signal was recorded by an sCMOS camera (Zyla 4.2, Andor, Northern Ireland).

Hen's Egg Test-Chorioallantoic Membrane (HET-CAM). The HET-CAM was used as reported previously.^{49,45} Briefly, eggs were incubated at 38 °C, 40–50% humidity for 11 days in an egg incubator (HEKA Brüteräte, Rietberg, Germany). They were automatically and constantly turned. On the experimental day, the eggs were checked for fertilization via candling, and the air bladder area was marked. The eggshell was lightly pecked with a pointed pair of tweezers in this area and 300 μ L of the Insulin Analog NovoRapid (3U/mL), which served as positive control and the compounds 3, 8, 32, and 35 were applied with a syringe into the air compartment of the egg and incubated for an additional 1 to 2 h in the egg incubator. The compounds were dissolved in DMSO (Sigma-Aldrich) before being diluted in water and tested at a concentration of 40 μ M. DMSO at 0.4% was applied to some eggs as an additional control besides water. After the incubation, the eggshell above the air bladder was carefully removed and the eggshell membrane was equilibrated with PBS (PAN-Biotech, Aidenbach, Germany). Following this, the eggshell membrane was removed and the chorioallantoic membrane was cut with a microscissor. A suitable blood vessel was placed on a plastic pH strip and patted dry using filter paper before being cut, and leaking blood was collected. The blood glucose levels were determined via a blood glucose meter (Accu-Check Performa, Roche Diabetes Care GmbH, Mannheim, Germany). For each time point, at least 10 fertilized eggs were used. The experiment was repeated three times.

Statistical Evaluation. Statistical analyses were carried out using IBM SPSS Statistics for Windows software, version 26.0 (IBM, Armonk, NY). The data were graphed as the mean \pm SEM. Comparisons between groups were made using a Kruskal–Wallis test, followed by a pairwise comparison with a Bonferroni correction or using a Mann–Whitney U test in the case of results of HET-CAM. Moreover, the data were compared using the calculation of Cohen's *d* effect size.

RESULTS

PPAR γ Receptor Molecular Docking Study. The thirty-six test compounds were subjected to a PPAR γ receptor molecular docking study. The known PPAR γ agonist, rosiglitazone, was docked into the active site of the ligand binding domain (LBD) of the receptor to calculate the binding affinities of the test compounds in comparison to this positive control. The results are shown in Table 1. Rosiglitazone had a binding affinity of -8.8 kcal·mol $^{-1}$. The test compounds had binding affinities ranging from -8.1 to -10.5 kcal·mol $^{-1}$. The docking program identified three compounds from *P. tomentosa* (3, 8, 11) and five from *M. alba* (23, 32–35) for further testing. The main criterion for the selection of the compounds from *P. tomentosa* was the binding energy (<-9.5 kcal·mol $^{-1}$), since several other *Paulownia* compounds were able to fit into the active site of the ligand-binding domain (LBD). However, compounds 15 and 16 could not be isolated in sufficient quantities for *in vitro* biological assays. Only the five selected compounds from *M. alba* fit into the active site,

Table 1. Binding Energy and Binding Location of the Test Compounds^a

test compound	binding energy [kcal·mol $^{-1}$]	ligand-binding domain
1	-8.3	yes
2	-8.3	yes
3	-9.5	yes
4	-9.2	yes
5	-8.5	yes
6	-8.4	yes
7	-9.3	yes
8	-9.6	yes
9	-9.3	yes
10	-9.3	yes
11	-10.1	yes
12	-8.7	yes
13	-9.8	no
14	-8.5	no
15	-9.9	yes
16	-9.7	yes
17	-9.3	no
18	-8.4	yes
19	-8.1	no
20	-8.9	no
21	-8.5	yes
22	-9.3	no
23	-9.6	yes
24	-9.1	no
25	-9.6	no
26	-9.2	no
27	-8.5	no
28	-9.1	no
29	-9.7	no
30	-9.5	no
31	-8.8	no
32	-8.1	yes
33	-8.3	yes
34	-9.0	yes
35	-9.2	yes
36	-10.5	no
rosiglitazone	-8.8	yes

^aCompounds selected for subsequent *in vitro* experiments are shown in bold.

and therefore, these were further analyzed regardless of the value of the binding energy.

PPAR γ Luciferase Reporter Gene Transactivation. *In silico* hits were isolated from the respective natural sources and subjected to PPAR γ -driven luciferase reporter gene assays. First, they were tested in HEK293 cells transiently transfected with the full-length receptor at a concentration of 1 μ M. As shown in Figure 2, the most promising test compounds were compounds 3 and 8 isolated from *P. tomentosa*. In addition, test compounds 32 and 35 were selected for further experiments due to low (although not significant) activity among compounds isolated from *M. alba* and their different structural skeletons (i.e., benzofurans). All selected compounds were less active than rosiglitazone, which was chosen as a positive control.

Concentration–response curves were then performed with the selected compounds (3, 8, 32, and 35). The test compounds were incubated with the same cell line at concentrations of 5, 3, 1, 0.3, and 0.1 μ M. The most active

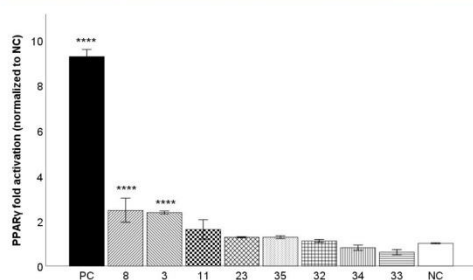


Figure 2. PPAR γ agonistic activity of the test compounds from *P. tomentosa* (3, 8, 11) and *M. alba* (23, 32–35) and rosiglitazone (PC) at a concentration of 1 μ M after a 16 h incubation with the transiently transfected HEK293 cell line. The results are expressed as the mean \pm SEM for three independent experiments measured in quadruplicate and are statistically compared to NC using a Kruskal–Wallis test followed by a pairwise comparison with a Bonferroni correction (**** $p \leq 0.0001$).

compound was compound 3, as shown in Figure 3. Compound 3 showed a statistically significant 3.4-fold activation of PPAR γ at a concentration of 3 μ M ($p \leq 0.0001$; $d = 7.431$ (large)), whereas the positive control, rosiglitazone, activated PPAR γ 7-fold ($d = 6.612$ (large)). Therefore, we hypothesized that compound 3 might be a partial agonist of PPAR γ . Compound 8 showed a similar activity, although slightly lower, with 2.4-fold activation of the PPAR γ receptor at a concentration of 3 μ M ($p \leq 0.0001$; $d = 3.110$ (large)). Compounds 32 and 35 activated PPAR γ approximately 2-fold at concentrations of 3 and 5 μ M.

To further confirm PPAR γ agonism, we employed a one-hybrid luciferase reporter system, in which the PPAR γ ligand binding domain (PPAR γ -LBD) is coupled to the DNA-binding

domain of the yeast transcription factor Gal4, which then binds to its response element in the promoter of a luciferase reporter gene. The results for the same test compounds and concentrations are shown in Figure 4. Again, the highest activity was shown by compound 3 at a concentration of 5 μ M (3.2-fold; $p \leq 0.0001$; $d = 8.345$ (large)), followed by compound 8 (2.9-fold; $p \leq 0.0001$; $d = 2.820$ (large)). Compound 35 also showed a small but significant activation of PPAR γ at concentrations of 3 and 5 μ M.

Figures 5 and 6 visualize the docking of the two most promising compounds (3 and 8, respectively) into the active site of the LBD. Both compounds are shown in red and compared to rosiglitazone (blue). The results show that compound 3 fits into the pocket of the active site slightly better than compound 8, which is consistent with the results shown in Figures 3 and 4.

PPAR γ Protein Expression. The next step in our experiments was to determine whether the selected compounds (3, 8, 32, and 35) were able to increase the level of PPAR γ protein expression. The selected compounds were incubated with HepG2 cells at a concentration of 1 μ M for 24 h and Western blot analyses were performed. None of the compounds showed a positive effect on PPAR γ expression (data not shown) except compound 32. As shown in Figure 7, compound 32 showed a tendency to increase the expression of PPAR γ protein level, but without statistical significance.

Quantification of GLUT4 Translocation. The selected compounds 3, 8, 32, and 35 at a concentration of 10 μ M were then tested for their ability to enhance GLUT4 translocation in HeLa GLUT4-myc-GFP cells using TIRF microscopy (Figure 8).⁴⁶ The most active compound was compound 8. After 10 min of incubation, the GFP signal in the cells increased by 3.62% in a statistically significant manner ($p \leq 0.0001$; $d = 4.545$ (large)), which is approximately one-third of the activation of the positive control insulin at a concentration

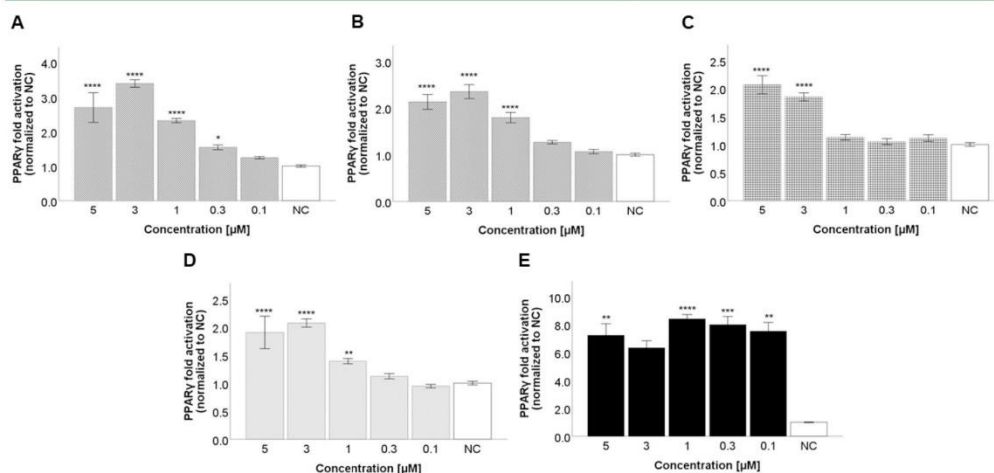


Figure 3. PPAR γ agonistic activity of the test compounds 3 (A), 8 (B), 32 (C), 35 (D), and rosiglitazone (E). The test compounds were incubated with the transiently transfected HEK293 cell line at concentrations of 5, 3, 1, 0.3, and 0.1 μ M. The results are expressed as the mean \pm SEM for two independent experiments measured in quadruplicate and are statistically compared to NC using a Kruskal–Wallis test followed by a pairwise comparison with a Bonferroni correction (* $p \leq 0.05$, ** $p \leq 0.01$, *** $p \leq 0.001$, and **** $p \leq 0.0001$).

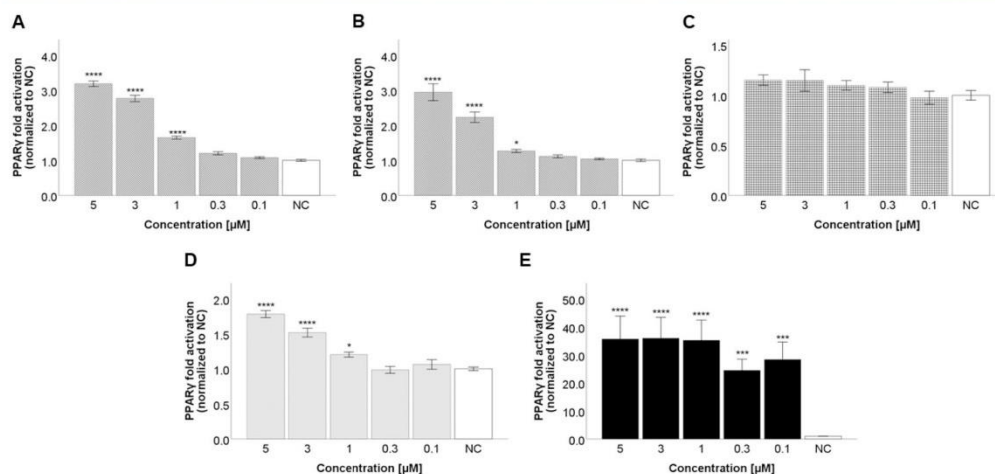


Figure 4. PPAR γ -LBD agonistic activity (one-hybrid reporter assay) of the test compounds **3** (A), **8** (B), **32** (C), **35** (D), and rosiglitazone (E). The test compounds were incubated with the same cell line at concentrations of 5, 3, 1, 0.3, and 0.1 μ M. The results are expressed as the mean \pm SEM for three independent experiments measured in quadruplicate and are statistically compared to NC using a Kruskal–Wallis test followed by a pairwise comparison with a Bonferroni correction (** $p \leq 0.01$, *** $p \leq 0.001$, and **** $p \leq 0.0001$).

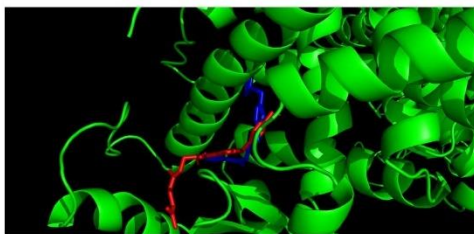


Figure 5. Visualization of molecular docking of compound **3** (red) into the active site of LBD compared to rosiglitazone (blue).

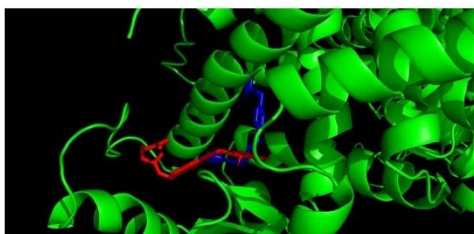


Figure 6. Visualization of molecular docking of compound **8** (red) into the active site of LBD compared to rosiglitazone (blue).

of 100 nM. Compound **3** was less active; in this case, the signal increased by 3.00% ($p \leq 0.0001$). On the other hand, the remaining compounds **32** and **35** slightly increased the signal after 10 min ($p \leq 0.0001$), but their GLUT4-GFP signal change values were below the 3% threshold for positive results.^{41,42,47}

Hen's Egg Test-Chorioallantoic Membrane (HET-CAM). Finally, the selected compounds (**3**, **8**, **32**, and **35**)

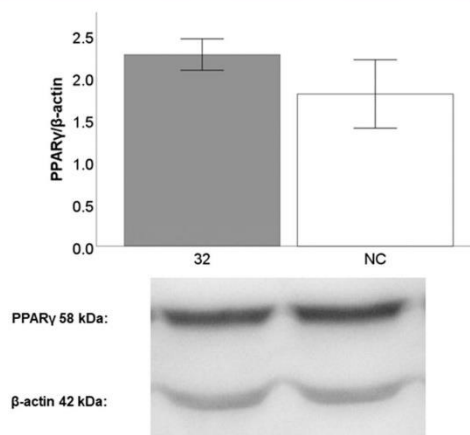


Figure 7. PPAR γ protein expression after a 24-h incubation with compound **32** at a concentration of 1 μ M, compared to DMSO used as solvent (NC). The results are expressed as the mean \pm SEM for one experiment measured in triplicate.

were evaluated for their efficacy in lowering blood glucose levels in chicken embryos using the HET-CAM assay. The selected compounds (at a concentration of 40 μ M) were incubated for 60 and 120 min to observe possible glucose-lowering effects. An insulin analog (3 U/mL) was used as a positive control. The data for the change in blood glucose levels normalized to the solvent (0.4% DMSO) are shown in Figure 9. Compound **32** proved to be the most potent with a statistically significant 7.33% reduction in blood glucose after 120 min ($p \leq 0.01$; $d = 0.931$ (large)). Two other compounds, **8** and **35**, were able to statistically significantly reduce blood

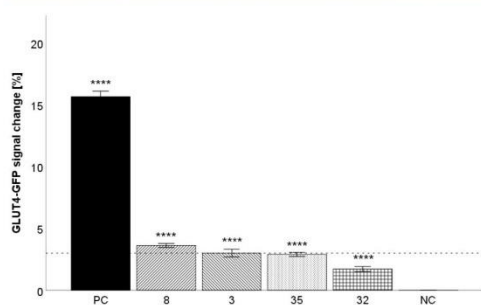


Figure 8. Quantification of GLUT4 translocation in HeLa GLUT4-myc-GFP cells after incubation with the test compounds 3, 8, 32, and 35 at a concentration of 10 μ M. Insulin (100 nM) was used as a positive control (PC). KRPH was used as a negative control (NC). The GLUT4-myc-GFP signal change was analyzed, and a threshold of 3% was defined for positive hits (dashed line).^{41,42,47} Data are shown as the mean \pm SEM ($n > 42$) and are statistically compared to NC using a Kruskal–Wallis test followed by a pairwise comparison with a Bonferroni correction (** $p \leq 0.01$, and **** $p \leq 0.0001$).

glucose levels by 3.69 and 3.84% after 120 min ($p \leq 0.01$; $d = 0.741$ (medium/large) and $p \leq 0.001$; $d = 0.836$ (large)), respectively, while compound 3 showed a negligible effect.

DISCUSSION

Based on the data obtained from our experiments, mimulone (3) can be described as a partial PPAR γ agonist. It did not influence PPAR γ expression, slightly affected the translocation of GLUT4 transporters and insignificantly decreased glucose levels during *in ovo* experiments. Dipsacone (8) showed a similar profile of activity, with the exception of a greater effect on GLUT4 translocation and a significant decrease in glycemia *in ovo*. Both compounds are geranylated flavanones with proven antioxidant and anti-inflammatory activity.^{48,49}

Consistent with our observations, Zhang et al. described how compound 1 (structurally similar to dipsacone (8), but without the geranyl moiety) increased insulin-stimulated glucose uptake in both HepG2 and differentiated 3T3-L1 adipocytes under high-glucose conditions. This compound was also able to upregulate PPAR γ 2 expression at both the mRNA and protein levels. Furthermore, compound 1 was able to reactivate an important kinase, protein kinase B (Akt), in the insulin signaling pathway in HepG2 cells with high-glucose-induced insulin resistance.⁵⁰

Another step in reinforcing the insulin pathway may be the inhibition of protein tyrosine phosphatase 1B (PTP1B). Song et al. demonstrated on isolated enzyme that mimulone (3) was the most active with IC₅₀ 1.9 μ M.⁵¹ Dipsacone (8) was not among the compounds tested in their experiment, but from the results, we can deduce that the most preferred arrangement of ring B of the flavonoid is with the hydroxyl at C-4'. Other hydroxy or methoxy groups at C-3' or C-5' decreased the activity.

Zima et al. performed *in vivo* experiments on alloxan-induced diabetes in mice to demonstrate the antidiabetic activity of compounds 3 and 8.⁵² Their results do not fully agree with the results of our experiments. Compounds 3 and 8 were not able to reduce blood glucose levels in their model, with the only exception that compound 8 showed a significant reduction on day 1 ($p \leq 0.05$). On the other hand, Zima et al. found a cytoprotective effect of compound 8 on pancreatic cells, which may be explained by its antioxidant activity, since alloxan induces diabetes via oxidative damage to the pancreas.⁵²

Moracin M (32) and mulberrofuran Y (35) showed very low agonism to PPAR γ compared to the two previous compounds. In GLUT4 translocation experiments, both compounds significantly induced translocation, but their GLUT4-GFP signal change values are below the 3% threshold for positive results. Both 32 and 35 were active in the *in ovo* blood glucose assays, with 32 being the most active among the compounds tested, significantly lowering blood glucose levels, especially after 60 min of incubation. The efficacy obtained was

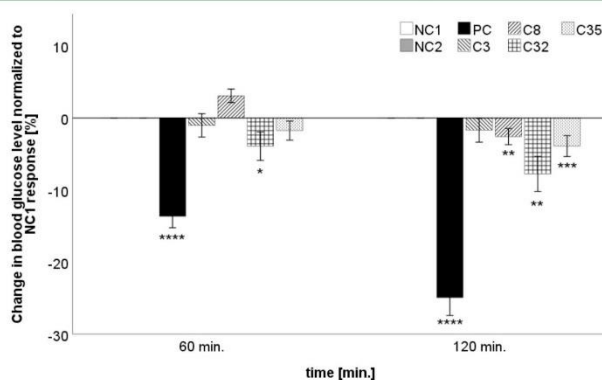


Figure 9. Quantification of lowering blood glucose efficacy in chicken embryos using HET-CAM assay. The test compounds (3, 8, 32, and 35) at a concentration of 40 μ M were incubated for 60 and 120 min to observe possible glucose-lowering effects. The insulin analog NovoRapid (3U/ml) was used as a positive control (PC). The data for the change in blood glucose levels were normalized to the solvent (0.4% DMSO; NC2), are shown as the mean \pm SEM ($n = 23$ –28), and are statistically compared to ultrapure water using a Mann–Whitney U test (NC1; * $p \leq 0.05$, ** $p \leq 0.01$, *** $p \leq 0.001$, and **** $p \leq 0.0001$).

comparable to that of various plant extracts tested in several previous studies.^{47,53,54}

Moracin M (32) is not described as a PPAR γ agonist in the scientific literature, but a similar compound, moracin D, is. Compared to compound 32, the structure of moracin D contains an additional prenyl moiety that is condensed with the hydroxyl group on the aryl segment of the structure. Moracin D was able to activate PPAR γ /PKC- δ and inhibit PKC- α , thereby inducing apoptosis in prostate cancer DU145 cells.⁵⁵

Kwon et al. reported PTP1B inhibitory activity for compound 32, but this activity was very low, with an IC₅₀ of 333.1 \pm 20.53 μ M.⁵⁶ Consistent with our results, Zhang et al. reported a decreasing trend in fasting blood glucose levels in alloxan-diabetic mice after administration of compound 32. The effect was dose-dependent, and the fasting blood glucose level was 18.52 \pm 6.61 mmol/L at the dose of 100 mg/kg, which was not significantly different from that of the model group (23.58 \pm 5.61 mmol/L).⁵⁷ The possible mechanism of the hypoglycemic effect of moracin M (32) was described by Kwak et al.⁵⁸ Moracin M (32) incubated with C2C12 cells (at concentrations of 5 and 25 μ M) induced phosphorylation of phosphatidylinositol 3-kinase (PI3K) and Akt, two key regulators in the insulin transduction pathway.⁵⁸

Also, mulberrofuran Y (35) has not been previously reported as a PPAR γ agonist or as a hypoglycemic agent. However, another compound from the group of 2-arylbenzofurans, mulberrofuran G, has been reported as an inhibitor of PTP1B, with an IC₅₀ of 0.57 \pm 0.04 μ M.⁵⁹ Ha et al. also reported the same compound as an inhibitor of PTP1B, but with a different IC₅₀ value of 4.56 \pm 0.88 μ M. In the same work, other compounds of our study (27, 32, 34, and 36) were screened for PTP1B inhibition, but their effect was negligible.⁶⁰

The bioavailability and intestinal absorption of the tested compounds are not known. However, Erlund et al. studied the plasma kinetics of the flavanones naringenin (2) and hesperetin (both similar to compound 8) in humans. After ingestion of orange or grapefruit juice (8 mL/kg), the peak plasma concentration reached 6.0 \pm 5.4 μ M for naringenin (2) and 2.2 \pm 1.6 μ M for hesperetin.⁶¹ In addition, You et al. administered moracin C (similar to compounds 32 and 35) orally to mice (100 mg/kg) and the peak plasma concentration was 5.8 \pm 4.0 μ M.⁶² These results are quite variable, but the concentrations we used in our experiments are achievable.

The three main tissues in the human body involved in the regulation of glycemia are adipose tissue, liver, and skeletal muscle. The HeLa cell line used in our GLUT4 translocation experiment is derived from human cervical carcinoma cells but is also insulin responsive (Figure 8). The HET-CAM experiments take advantage of the use of chicken embryos at day 11 of development. This avoids the need for animal experiments, which require approval, and the model has the advantage of mimicking *in vivo* conditions.⁴⁵

In summary, the selected compounds showed a diverse profile of action as hypoglycemic agents. Our hypothesis of selecting compounds based on PPAR γ agonism and subsequent investigation of their effect on GLUT4 translocation and glycemia *in ovo* appeared not to be generally useful. Moracin M (32) and mulberrofuran Y (35) reduced glycemia *in ovo* without convincing agonism on PPAR γ , whereas mimulone (3) was shown to be a partial PPAR γ agonist

without affecting glycemia *in ovo*. Only diplacone (8) showed activity in all these aspects.

■ ASSOCIATED CONTENT

Supporting Information

The Supporting Information is available free of charge at <https://pubs.acs.org/doi/10.1021/acs.jafc.4c11398>.

HPLC analysis of test compounds; HPLC chromatogram of mimulone (3) (Figure S1); HPLC chromatogram of diplacone (8) (Figure S2); HPLC chromatogram of tomentone II (11) (Figure S3); HPLC chromatogram of kuwanon U (23) (Figure S4); HPLC chromatogram of moracin M (32) (Figure S5); HPLC chromatogram of mulberrofuran Y (33) (Figure S6); HPLC chromatogram of moracin O (34) (Figure S7); HPLC chromatogram of moracin C (35) (Figure S8) (PDF)

■ AUTHOR INFORMATION

Corresponding Author

Jakub Trembl – Department of Molecular Pharmacy, Masaryk University, 612 00 Brno, Czech Republic; orcid.org/0000-0002-8690-9981; Email: tremblj@pharm.muni.cz

Authors

Jiří Václavík – Department of Natural Drugs, Masaryk University, 612 00 Brno, Czech Republic
Lenka Molčanová – Department of Natural Drugs, Masaryk University, 612 00 Brno, Czech Republic
Marie Culenová – Department of Natural Drugs, Masaryk University, 612 00 Brno, Czech Republic
Scarlet Hummelbrunner – Department of Pharmaceutical Sciences, University of Vienna, A-1090 Vienna, Austria
Catharina Neuhauser – Center of Excellence Food Technology and Nutrition, University of Applied Sciences Upper Austria, 4600 Wels, Austria
Verena M. Dirsch – Department of Pharmaceutical Sciences, University of Vienna, A-1090 Vienna, Austria; orcid.org/0000-0002-9261-5293
Julian Weghuber – Center of Excellence Food Technology and Nutrition, University of Applied Sciences Upper Austria, 4600 Wels, Austria; FFoQSI GmbH-Austrian Competence Centre for Feed and Food Quality, Safety and Innovation, 3430 Tulln, Austria; orcid.org/0000-0001-6312-4666
Karel Šmejkal – Department of Natural Drugs, Masaryk University, 612 00 Brno, Czech Republic

Complete contact information is available at: <https://pubs.acs.org/doi/10.1021/acs.jafc.4c11398>

Notes

The authors declare no competing financial interest.

■ ACKNOWLEDGMENTS

The authors thank Michaela Jahodová for her help with the experiments. This work was supported by Masaryk University project [MUNI/A/1654/2020] and the Czech Science Foundation Role of prenylation and glycosylation patterns in anti-inflammatory activity and metabolism of natural phenolic compounds [GA23-04655S]. This research was also funded by the Christian Doppler Forschungsgesellschaft (Josef Ressel Center for Phytogetic Drug Research, Wels, Austria). In addition, this work was created within a research project of the

Austrian Competence Centre for Feed and Food Quality, Safety and Innovation (FFoQSI). The COMET-K1 Competence Centre FFoQSI is funded by the Austrian ministries BMVIT, BMDW, and the Austrian provinces Lower Austria, Upper Austria, and Vienna within the scope of COMET Competence Centers for Excellent Technologies. The program COMET is handled by the Austrian Research Promotion Agency, FFG.

■ ABBREVIATIONS

ATCC, American Type Culture Collection; DM, diabetes mellitus; DMEM, Dulbecco's modified Eagle's medium; DMSO, dimethyl sulfoxide; DNA, deoxyribonucleic acid; EGFP, enhanced green fluorescent protein; FBS, fetal bovine serum; FDA, Food and Drug Administration; GLUT4, glucose transporter type 4; HBSS, Hanks' Balanced Salt solution; HEK, human embryonic kidney; HET-CAM, hens egg test-chorioallantoic membrane; LBD, ligand-binding domain; PBS, phosphate saline buffer; PDB, Protein Data Bank; PKC, protein kinase C; PPAR γ , peroxisome proliferator-activated receptor γ ; PTP1B, protein tyrosine phosphatase 1B; SDS-PAGE, sodium dodecyl sulfate–polyacrylamide gel electrophoresis; T2DM, type 2 diabetes mellitus; TIRF, total internal reflection fluorescence; TZD, thiazolidinediones

■ REFERENCES

- (1) IDF. *Facts & Figures*, International Diabetes Federation. <https://idf.org/about-diabetes/diabetes-facts-figures/> (accessed Jan 20, 2024).
- (2) Stolar, M. Glycemic Control and Complications in Type 2 Diabetes Mellitus. *Am. J. Med.* **2010**, *123* (S3), S3–S11.
- (3) Davies, M. J.; Aroda, V. R.; Collins, B. S.; Gabbay, R. A.; Green, J.; Maruthur, N. M.; Rosas, S. E.; Del Prato, S.; Mathieu, C.; Mingrone, G.; Rossing, P.; Tankova, T.; Tsapas, A.; Buse, J. B. Management of Hyperglycemia in Type 2 Diabetes, 2022. A Consensus Report by the American Diabetes Association (ADA) and the European Association for the Study of Diabetes (EASD). *Diabetes Care* **2022**, *45* (11), 2753–2786.
- (4) Wang, L.; Waltenberger, B.; Pferschy-Wenzig, E.-M.; Blunder, M.; Liu, X.; Malainer, C.; Blazevic, T.; Schwaiger, S.; Rollinger, J. M.; Heiss, E. H.; Schuster, D.; Kopp, B.; Bauer, R.; Stuppner, H.; Dirsch, V. M.; Atanasov, A. G. Natural Product Agonists of Peroxisome Proliferator-Activated Receptor Gamma (PPAR γ): A Review. *Biochem. Pharmacol.* **2014**, *92* (1), 73–89.
- (5) Ahmadian, M.; Suh, J. M.; Hah, N.; Liddle, C.; Atkins, A. R.; Downes, M.; Evans, R. M. PPAR γ Signaling and Metabolism: The Good, the Bad and the Future. *Nat. Med.* **2013**, *19* (5), 557–566.
- (6) Soccio, R. E.; Chen, E. R.; Lazar, M. A. Thiazolidinediones and the Promise of Insulin Sensitization in Type 2 Diabetes. *Cell Metab.* **2014**, *20* (4), 573–591.
- (7) Kaur, S.; Wong, H. K.; Southall, M. D.; Mahmood, K.; Kaur, S.; Wong, H. K.; Southall, M. D.; Mahmood, K. *Paulownia Tomentosa* (Princess Tree) Extract Reduces DNA Damage and Induces DNA Repair Processes in Skin Cells. In *Advances in DNA Repair*; IntechOpen, 2015 DOI: 10.5772/60005.
- (8) Molčanová, L.; Tremblé, J.; Brezání, V.; Maršik, P.; Kurhan, S.; Trávníček, Z.; Uhrin, P.; Šmejkal, K. C-Geranylated Flavonoids from *Paulownia Tomentosa* Steud. Fruit as Potential Anti-Inflammatory Agents. *J. Ethnopharmacol.* **2022**, *296*, No. 115509.
- (9) Donath, M. Y.; Shoelson, S. E. Type 2 Diabetes as an Inflammatory Disease. *Nat. Rev. Immunol.* **2011**, *11* (2), 98–107.
- (10) Zhu, Z.-H.; Chao, C.-J.; Lu, X.-Y.; Xiong, Y. G. *Paulownia in China: Cultivation and Utilization*; Asian Network for Biological Science and International Development Research Centre, 1986.
- (11) Wei, H. *Morus Alba* L. (Sang, White Mulberry). In *Dietary Chinese Herbs: Chemistry, Pharmacology and Clinical Evidence*; Liu, Y., Wang, Z., Zhang, J., Eds.; Springer: Vienna, 2015; pp 721–730 DOI: 10.1007/978-3-211-99448-1_81.
- (12) Liu, C.-H.; Liu, F.; Xiong, L. Medicinal Parts of Mulberry (Leaf, Twig, Root Bark, and Fruit) and Compounds Thereof Are Excellent Traditional Chinese Medicines and Foods for Diabetes Mellitus. *J. Funct. Foods* **2023**, *106*, No. 105619.
- (13) Yuan, Q.; Zhao, L. The Mulberry (*Morus Alba* L.) Fruit—A Review of Characteristic Components and Health Benefits. *J. Agric. Food Chem.* **2017**, *65* (48), 10383–10394.
- (14) Polumackanycz, M.; Sledzinski, T.; Goyke, E.; Wesolowski, M.; Viapiana, A. A Comparative Study on the Phenolic Composition and Biological Activities of *Morus Alba* L. Commercial Samples. *Molecules* **2019**, *24* (17), No. 3082.
- (15) Schneiderová, K.; Šmejkal, K. Phytochemical Profile of *Paulownia Tomentosa* (Thunb). *Stud. Phytochem. Rev.* **2015**, *14* (5), 799–833.
- (16) de Paulo Farias, D.; de Araújo, F. F.; Neri-Numa, I. A.; Pastore, G. M. Antidiabetic Potential of Dietary Polyphenols: A Mechanistic Review. *Food Res. Int.* **2021**, *145*, No. 110383.
- (17) Sarkar, D.; Christopher, A.; Shetty, K. Phenolic Bioactives From Plant-Based Foods for Glycemic Control. *Front. Endocrinol.* **2022**, *12*, No. 727503.
- (18) Babu, P. V. A.; Liu, D.; Gilbert, E. R. Recent Advances in Understanding the Anti-Diabetic Actions of Dietary Flavonoids. *J. Nutr. Biochem.* **2013**, *24* (11), 1777–1789.
- (19) Šmejkal, K.; Grycová, L.; Marek, R.; Lemiére, F.; Jankovská, D.; Forejtníková, H.; Vančo, J.; Suchý, V. C-Geranyl Compounds from *Paulownia Tomentosa* Fruits. *J. Nat. Prod.* **2007**, *70* (8), 1244–1248.
- (20) Hanáková, Z.; Hošek, J.; Babula, P.; Dall'Acqua, S.; Václavík, J.; Šmejkal, K. C-Geranylated Flavonones from *Paulownia Tomentosa* Fruits as Potential Anti-Inflammatory Compounds Acting via Inhibition of TNF- α Production. *J. Nat. Prod.* **2015**, *78* (4), 850–863.
- (21) Šmejkal, K.; Chudík, S.; Klouček, P.; Marek, R.; Cvačka, J.; Urbanová, M.; Julínek, O.; Kokoška, L.; Šlapetová, T.; Holubová, P.; Zima, A.; Dvorská, M. Antibacterial C-Geranylflavonoids from *Paulownia Tomentosa* Fruits. *J. Nat. Prod.* **2008**, *71* (4), 706–709.
- (22) Molčanová, L.; Kauerová, T.; Dall'Acqua, S.; Maršik, P.; Kollár, P.; Šmejkal, K. Antiproliferative and Cytotoxic Activities of C-Geranylated Flavonoids from *Paulownia Tomentosa* Steud. Fruit. *Bioorg. Chem.* **2021**, *111*, No. 104797.
- (23) Navrátilová, A.; Schneiderová, K.; Veselá, D.; Hanáková, Z.; Fontana, A.; Dall'Acqua, S.; Cvačka, J.; Innocenti, G.; Novotná, J.; Urbanová, M.; Pelletier, J.; Čížek, A.; Žemličková, H.; Šmejkal, K. Minor C-Geranylated Flavonones from *Paulownia Tomentosa* Fruits with MRSA Antibacterial Activity. *Phytochemistry* **2013**, *89*, 104–113.
- (24) Hanáková, Z.; Hošek, J.; Kutil, Z.; Temml, V.; Landa, P.; Vaněk, T.; Schuster, D.; Dall'Acqua, S.; Cvačka, J.; Polanský, O.; Šmejkal, K. Anti-Inflammatory Activity of Natural Geranylated Flavonoids: Cyclooxygenase and Lipoxygenase Inhibitory Properties and Proteomic Analysis. *J. Nat. Prod.* **2017**, *80* (4), 999–1006.
- (25) Šmejkal, K.; Holubová, P.; Zima, A.; Muselík, J.; Dvorská, M. Antiradical Activity of *Paulownia Tomentosa* (Scrophulariaceae) Extracts. *Molecules* **2007**, *12* (6), 1210–1219.
- (26) Šmejkal, K.; Babula, P.; Šlapetová, T.; Brognara, E.; Dall'Acqua, S.; Žemlička, M.; Innocenti, G.; Cvačka, J. Cytotoxic Activity of C-Geranyl Compounds from *Paulownia Tomentosa* Fruits. *Planta Med.* **2008**, *74* (12), 1488–1491.
- (27) Šmejkal, K.; Svačinová, J.; Šlapetová, T.; Schneiderová, K.; Dall'Acqua, S.; Innocenti, G.; Závalová, V.; Kollár, P.; Chudík, S.; Marek, R.; Julínek, O.; Urbanová, M.; Kartal, M.; Csöllei, M.; Doležal, K. Cytotoxic Activities of Several Geranyl-Substituted Flavonones. *J. Nat. Prod.* **2010**, *73* (4), 568–572.
- (28) Zelová, H.; Hanáková, Z.; Čermáková, Z.; Šmejkal, K.; Dall'Acqua, S.; Babula, P.; Cvačka, J.; Hošek, J. Evaluation of Anti-Inflammatory Activity of Prenylated Substances Isolated from *Morus Alba* and *Morus Nigra*. *J. Nat. Prod.* **2014**, *77* (6), 1297–1303.
- (29) Vočhyánová, Z.; Pokorná, M.; Rotrekl, D.; Šmélal, V.; Fictum, P.; Suchý, P.; Gajdziok, J.; Šmejkal, K.; Hošek, J. Prenylated Flavonoid

Morusin Protects against TNBS-Induced Colitis in Rats. *PLoS One* **2017**, *12* (8), No. e0182464.

(30) Čulenová, M.; Sychrová, A.; Hassan, S. T. S.; Berchová-Bimová, K.; Svobodová, P.; Helclová, A.; Michnová, H.; Hošek, J.; Vasilev, H.; Suchý, P.; Kuzminová, G.; Švajdlenka, E.; Gajdziok, J.; Čížek, A.; Suchý, V.; Šmejkal, K. Multiple In Vitro Biological Effects of Phenolic Compounds from *Morus Alba* Root Bark. *J. Ethnopharmacol.* **2020**, *248*, No. 112296.

(31) Khazneh, E.; Hříbová, P.; Hošek, J.; Suchý, P.; Kollár, P.; Pražanová, G.; Muselík, J.; Hanáková, Z.; Václavík, J.; Mílek, M.; Legáth, J.; Šmejkal, K. The Chemical Composition of *Achillea Wilhelmsii* C. Koch and Its Desirable Effects on Hyperglycemia, Inflammatory Mediators and Hypercholesterolemia as Risk Factors for Cardiometabolic Disease. *Molecules* **2016**, *21* (4), No. 404.

(32) PDB. RCSB PDB: Homepage Protein Data Bank, <https://www.rcsb.org/> (accessed Jan 27, 2024).

(33) Klierer, S. A.; Umeson, K.; Noonan, D. J.; Heyman, R. A.; Evans, R. M. Convergence of 9-Cis Retinoic Acid and Peroxisome Proliferator Signalling Pathways through Heterodimer Formation of Their Receptors. *Nature* **1992**, *358* (6389), 771–774.

(34) Peyrin-Biroulet, L.; Beisner, J.; Wang, G.; Nuding, S.; Oommen, S. T.; Kelly, D.; Parmentier-Decrucq, E.; Dessein, R.; Merour, E.; Chavatte, P.; Grandjean, T.; Bressenot, A.; Desreumaux, P.; Colombel, J.-F.; Desvergne, B.; Stange, E. F.; Wehkamp, J.; Chamailard, M. Peroxisome Proliferator-Activated Receptor Gamma Activation Is Required for Maintenance of Innate Antimicrobial Immunity in the Colon. *Proc. Natl. Acad. Sci. U.S.A.* **2010**, *107* (19), 8772–8777.

(35) Atanasov, A. G.; Wang, J. N.; Gu, S. P.; Bu, J.; Kramer, M. P.; Baumgartner, L.; Fakhrudin, N.; Ladurner, A.; Malainer, C.; Vuorinen, A.; Noha, S. M.; Schwaiger, S.; Rollinger, J. M.; Schuster, D.; Stuppner, H.; Dirsch, V. M.; Heiss, E. H. Honokiol: A Non-Adipogenic PPAR γ Agonist from Nature. *Biochim. Biophys. Acta, Gen. Subj.* **2013**, *1830* (10), 4813–4819.

(36) Dreier, D.; Resetar, M.; Temml, V.; Ryciek, L.; Kratena, N.; Schnürch, M.; Schuster, D.; M. Dirsch, V.; D. Mihovilovic, M. Magnolol Dimer-Derived Fragments as PPAR γ -Selective Probes. *Org. Biomol. Chem.* **2018**, *16* (38), 7019–7028.

(37) Kucerova-Chlupacova, M.; Halakova, D.; Majekova, M.; Tremel, J.; Stefek, M.; Soltesova Prnova, M. (4-Oxo-2-Thioxothiazolidin-3-yl)acetic Acids as Potent and Selective Aldose Reductase Inhibitors. *Chem. Biol. Interact.* **2020**, *332*, No. 109286.

(38) Lima, K. G.; Schneider Levorse, V. G.; Rosa Garcia, M. C.; de Souza Basso, B.; Pasqualotto Costa, B.; Antunes, G. L.; Luft, C.; Haute, G. V.; Leal Xavier, L.; Donadio, M. V. F.; Rodrigues de Oliveira, J. Octyl Gallate Induces Hepatic Steatosis in HepG2 Cells through the Regulation of SREBP-1c and PPAR-Gamma Gene Expression. *EXCLI J.* **2020**, *19*, 962–971.

(39) Tremel, J.; Leláková, V.; Šmejkal, K.; Paulíčková, T.; Labuda, Š.; Granica, S.; Havlík, J.; Jankovská, D.; Padrtová, T.; Hošek, J. Antioxidant Activity of Selected Stilbenoid Derivatives in a Cellular Model System. *Biomolecules* **2019**, *9* (9), No. 468.

(40) Tremel, J.; Šalamúnová, P.; Hanuš, J.; Hošek, J. The Effect of Curcumin Encapsulation into Yeast Glucan Particles on Antioxidant Enzyme Expression in Vitro. *Food Funct.* **2021**, *12*, 1954.

(41) Stadlbauer, V.; Lanzerstorfer, P.; Neuhauser, C.; Weber, F.; Stübl, F.; Weber, P.; Wagner, M.; Plochberger, B.; Wieser, S.; Schneckenburger, H.; Weghuber, J. Fluorescence Microscopy-Based Quantitation of GLUT4 Translocation: High Throughput or High Content? *Int. J. Mol. Sci.* **2020**, *21* (21), No. 7964.

(42) Stadlbauer, V.; Haselgrübler, R.; Lanzerstorfer, P.; Plochberger, B.; Borgmann, D.; Jacak, J.; Winkler, S. M.; Schröder, K.; Höglinger, O.; Weghuber, J. Biomolecular Characterization of Putative Antidiabetic Herbal Extracts. *PLoS One* **2016**, *11* (1), No. e0148109.

(43) Lanzerstorfer, P.; Stadlbauer, V.; Chitchevoglva, L. A.; Haselgrübler, R.; Borgmann, D.; Wruss, J.; Hinterdorfer, P.; Schröder, K.; Winkler, S. M.; Höglinger, O.; Weghuber, J. Identification of Novel Insulin Mimetic Drugs by Quantitative

Total Internal Reflection Fluorescence (TIRF) Microscopy. *Br. J. Pharmacol.* **2014**, *171* (23), 5237–5251.

(44) Haselgrübler, R.; Stübl, F.; Stadlbauer, V.; Lanzerstorfer, P.; Weghuber, J. An In Ovo Model for Testing Insulin-Mimetic Compounds. *J. Visualized Exp.* **2018**, *134*, No. 57237, DOI: 10.3791/57237.

(45) Haselgrübler, R.; Stübl, F.; Essl, K.; Iken, M.; Schröder, K.; Weghuber, J. Gluc-HET, a Complementary Chick Embryo Model for the Characterization of Antidiabetic Compounds. *PLoS One* **2017**, *12* (8), No. e0182788.

(46) Heckmann, M.; Klanert, G.; Sandner, G.; Lanzerstorfer, P.; Auer, M.; Weghuber, J. Fluorescence Microscopy-Based Quantitation of GLUT4 Translocation. *Methods Appl. Fluoresc.* **2022**, *10* (2), No. 022001.

(47) Haselgrübler, R.; Stadlbauer, V.; Stübl, F.; Schwarzing, B.; Rudzionyte, I.; Himmelsbach, M.; Iken, M.; Weghuber, J. Insulin Mimetic Properties of Extracts Prepared from *Bellis Perennis*. *Molecules* **2018**, *23* (10), No. 2605.

(48) Tremel, J.; Vecerova, P.; Herczogova, P.; Šmejkal, K. Direct and Indirect Antioxidant Effects of Selected Plant Phenolics in Cell-Based Assays. *Molecules* **2021**, *26* (9), 2534.

(49) Vochýánová, Z.; Bartošová, L.; Bujdaková, V.; Fictum, P.; Husník, R.; Suchý, P.; Šmejkal, K.; Hošek, J. Dipalacone and Mimulone Ameliorate Dextran Sulfate Sodium-Induced Colitis in Rats. *Fitoterapia* **2015**, *101*, 201–207.

(50) Zhang, W.-Y.; Lee, J.-J.; Kim, Y.; Kim, I.-S.; Han, J.-H.; Lee, S.-G.; Ahn, M.-J.; Jung, S.-H.; Myung, C.-S. Effect of Eriodictyol on Glucose Uptake and Insulin Resistance in Vitro. *J. Agric. Food Chem.* **2012**, *60* (31), 7652–7658.

(51) Song, Y. H.; Uddin, Z.; Jin, Y. M.; Li, Z.; Curtis-Long, M. J.; Kim, K. D.; Cho, J. K.; Park, K. H. Inhibition of Protein Tyrosine Phosphatase (PTPase) and α -Glucosidase by Geranylated Flavonoids from *Paulownia tomentosa*. *J. Enzyme Inhib. Med. Chem.* **2017**, *32* (1), 1195–1202.

(52) Zima, A.; Hošek, J.; Tremel, J.; Muselík, J.; Suchý, P.; Pražanová, G.; Lopes, A.; Žemlička, M. Antiradical and Cytoprotective Activities of Several C-Geranyl-Substituted Flavanones from *Paulownia tomentosa* Fruit. *Molecules* **2010**, *15* (9), 6035–6049.

(53) Günther, I.; Rimbach, G.; Nevermann, S.; Neuhauser, C.; Stadlbauer, V.; Schwarzing, B.; Schwarzing, C.; Iparraguerre, I. R.; Weghuber, J.; Lüersen, K. Avena Root (*Geum Urbanum* L.) Extract Discovered by Target-Based Screening Exhibits Antidiabetic Activity in the Hen's Egg Test Model and *Drosophila melanogaster*. *Front. Pharmacol.* **2021**, *12*, No. 794404.

(54) Ollinger, N.; Neuhauser, C.; Schwarzing, B.; Wallner, M.; Schwarzing, C.; Blank-Landeshammer, B.; Hager, R.; Sadova, N.; Drotarova, I.; Mathmann, K.; Karamouz, E.; Panopoulos, P.; Rimbach, G.; Lüersen, K.; Weghuber, J.; Röhl, C. Anti-Hyperglycemic Effects of Oils and Extracts Derived from Sea Buckthorn - A Comprehensive Analysis Utilizing In Vitro and In Vivo Models. *Mol. Nutr. Food Res.* **2022**, *66* (12), No. e2101133.

(55) Yoon, J. S.; Lee, H.-J.; Sim, D. Y.; Im, E.; Park, J. E.; Park, W. Y.; Koo, J. I.; Shim, B. S.; Kim, S.-H. Moracin D Induces Apoptosis in Prostate Cancer Cells via Activation of PPAR Gamma/PKC Delta and Inhibition of PKC Alpha. *Phytother. Res.* **2021**, *35* (12), 6944–6953.

(56) Kwon, R.-H.; Thaku, N.; Timalina, B.; Park, S.-E.; Choi, J.-S.; Jung, H.-A. Inhibition Mechanism of Components Isolated from *Morus Alba* Branches on Diabetes and Diabetic Complications via Experimental and Molecular Docking Analyses. *Antioxidants* **2022**, *11* (2), No. 383.

(57) Zhang, M.; Chen, M.; Zhang, H.-Q.; Sun, S.; Xia, B.; Wu, F.-H. In Vivo Hypoglycemic Effects of Phenolics from the Root Bark of *Morus Alba*. *Fitoterapia* **2009**, *80* (8), 475–477.

(58) Kwak, H. J.; Kim, J.; Kim, S.-Y.; Park, S.; Choi, J.; Kim, S. H. Moracin E and M Isolated from *Morus Alba* Linné Induced the Skeletal Muscle Cell Proliferation via PI3K-Akt-mTOR Signaling Pathway. *Sci. Rep.* **2023**, *13* (1), No. 20570.

(59) Paudel, P.; Yu, T.; Seong, S. H.; Kuk, E. B.; Jung, H. A.; Choi, J. S. Protein Tyrosine Phosphatase 1B Inhibition and Glucose Uptake Potentials of Mulberrofuran G, Albanol B, and Kuwanon G from Root Bark of *Morus Alba* L. in Insulin-Resistant HepG2 Cells: An In Vitro and In Silico Study. *Int. J. Mol. Sci.* **2018**, *19* (5), No. 1542.

(60) Ha, M. T.; Seong, S. H.; Nguyen, T. D.; Cho, W.-K.; Ah, K. J.; Ma, J. Y.; Woo, M. H.; Choi, J. S.; Min, B. S. Chalcone Derivatives from the Root Bark of *Morus Alba* L. Act as Inhibitors of PTP1B and α -Glucosidase. *Phytochemistry* **2018**, *155*, 114–125.

(61) Erlund, L.; Meririnne, E.; Alfthan, G.; Aro, A. Plasma Kinetics and Urinary Excretion of the Flavanones Naringenin and Hesperetin in Humans after Ingestion of Orange Juice and Grapefruit Juice. *J. Nutr.* **2001**, *131* (2), 235–241.

(62) You, B. H.; BasavanaGowda, M. K.; Lee, J. U.; Chin, Y.-W.; Choi, W. J.; Choi, Y. H. Pharmacokinetic Properties of Moracin C in Mice. *Planta Med.* **2021**, *87*, 642–651.

The advertisement features a vertical strip on the left showing a 3D molecular model with atoms represented by colored spheres (white, red, blue, green) and bonds as grey rods. The background is a gradient of blue and green. The text is white and yellow on a dark blue background.

CAS BIOFINDER DISCOVERY PLATFORM™

ELIMINATE DATA SILOS. FIND WHAT YOU NEED, WHEN YOU NEED IT.

A single platform for relevant, high-quality biological and toxicology research

Streamline your R&D

CAS
A Division of the American Chemical Society

13972

<https://doi.org/10.1021/acs.jafc.4c11398>
J. Agric. Food Chem. **2025**, *73*, 13960–13972

6.10. ARTICLE 10

Treml, J.; Salamunova, P.; Hanus, J.; Hosek, J. Food & Function 2021, 12, 1954-1957 (IF=6.317).

Cite this: *Food Funct.*, 2021, **12**, 1954

Received 10th December 2020,

Accepted 18th January 2021

DOI: 10.1039/d0fo03237a

rsc.li/food-function

The effect of curcumin encapsulation into yeast glucan particles on antioxidant enzyme expression *in vitro*

Jakub Tremel,^a Petra Šalamúnová,^b Jaroslav Hanuš^b and Jan Hošek^{b,c}

Glucan particles (GPs) from *Saccharomyces cerevisiae* consist mainly of β -1,3-D-glucan. Curcumin is a phenolic compound of plant origin. A 24 h incubation with a mixture of GPs and curcumin increased the expression of the Nrf2 protein and increased the activation of the Nrf2–ARE system significantly.

1. Introduction

Oxidative stress is a common pathophysiological predisposition of many illnesses, including cancer, diabetes mellitus and various inflammatory and neurodegenerative diseases. The stress can be explained as an imbalance between reactive oxygen species (ROS) production and the antioxidant defence system of cells.¹

Compounds of natural origin play an important role in the discovery of new drugs, as well as new lead structures for drug design.² An example of these compounds is curcumin, which was isolated from the rhizomes of *Curcuma longa* L. (Zingiberaceae). Curcumin exhibits a direct antioxidant effect, by free radical scavenging, as well as an indirect modulation of the cellular antioxidant defence system via the nuclear factor (erythroid-derived 2)-like 2 (Nrf2) pathway.^{3,4} Taken together with the observation of anti-inflammatory and antibacterial activities, it makes curcumin a promising molecule. However, curcumin has one downside, which is its poor bioavailability.⁵

One of the strategies to improve this disadvantage is the utilization of a drug carrier, such as yeast purified glucan particles (GPs). GPs are homopolymers of β -(1,3)-D-glucose with or without β -(1,6)-D-glucose in side chains with a diameter of

2–5 μ m. After ingestion, GPs are phagocytosed by M cells in the small intestine and transported via the lymphatic system to various parts of the body.⁶ Because glucan is not digested in the human gastrointestinal tract (GIT) due to the absence of β -amylase,⁷ the loaded cargo is protected during the passage through the GIT. Its biodegradation takes place only by oxidative cleavage in polymorphonuclear leukocytes and monocytes/macrophages after uptake in the gut⁸, and the cargo could be released there. β -Glucans on the surface of GPs are recognized mainly by the dectin-1 receptor and complement receptor 3 and thus possess immunomodulatory and anti-inflammatory effects.^{9,10} This ability enables GPs to serve as drug vehicles targeting macrophages.¹¹

In our previous study⁹ we have studied the direct antioxidant activities of pure curcumin, empty GPs, their mixture and composite suspensions in pyocyanin-stimulated THP-1-XBlue™-MD2-CD14 cells. This study is a continuation of the previous experiments. The aim is to elucidate whether the loading of curcumin into GPs achieves stronger indirect antioxidant activity compared to GPs or curcumin independently. To study the indirect antioxidant activity, we screened the expression of several antioxidant enzymes, such as catalase (CAT), glutathione peroxidase (GPx), heme oxygenase 1 (HO-1), superoxide dismutase 1 (SOD-1) and superoxide dismutase 2 (SOD-2), and the Nrf2 protein in a cell-based *in vitro* model. Furthermore, the activation of the antioxidant responsive element (ARE) by Nrf2 was studied.

2. Materials and methods

2.1 Preparation of glucan particles and composites with curcumin

GPs were prepared from baker's yeast *Saccharomyces cerevisiae* Meyen ex E.C. Hansen (Saccharomycetaceae) (Pakmaya, Ankara, Turkey). The preparation involved a washing process to principally remove the internal content using a method as described previously.¹²

^aDepartment of Molecular Pharmacy, Faculty of Pharmacy, Masaryk University, Palackého 1946/1, 612 00 Brno, Czech Republic. E-mail: tremelj@pharm.muni.cz; Tel: +420 541 562 850

^bDepartment of Chemical Engineering, University of Chemistry and Technology, Prague, Technická 5, 166 28 Prague, Czech Republic

^cDepartment of Pharmacology and Toxicology, Veterinary Research Institute, Hudcova 296/70, 621 00 Brno, Czech Republic

The incorporation of curcumin into GPs was performed by the slurry evaporation method as reported previously.⁹ From all the composites prepared in the previous study, we have chosen GP composites (at a final concentration of 670 $\mu\text{g mL}^{-1}$) with 0.55% (w/w) content of curcumin (corresponding to a concentration of 10 μM). Apart from the composites, GPs and curcumin as a mixture, GPs alone and crude curcumin were tested (in the corresponding concentrations). All the suspensions were prepared freshly and properly mixed with Ultra-Turrax T10 (IKA).

2.2 Cell culture

THP-1 and HepG2 cell lines (European Collection of Cell Cultures, Salisbury, UK) were cultured in RPMI 1640 and DMEM low glucose media (Biosera, France), respectively, as reported previously.¹³ The cells were kept in an incubator at 37 °C under a water-saturated atmosphere of air containing 5% CO_2 . The stabilized cells (12–35th passage) were split into microtitration plates and used for further experiments. Each experiment was performed three times in independent triplicate.

2.3 Protein expression of antioxidant proteins

The effect on the protein expression of antioxidant enzymes and Nrf2 was observed in the THP-1 cell line as reported previously.¹³ The cells were incubated in the form of floating monocytes (1×10^6 cells per mL). After 24 h of incubation with the composites, mixture, GPs alone and crude curcumin, the cells were collected, and protein lysates were prepared. Then the lysates were separated using SDS-PAGE and the proteins were transferred to polyvinylidene fluoride membranes using western blotting and a chemiluminescent kit (Bio-Rad). Specific primary antibodies were applied: mouse anti-CAT 1 : 1000 (Sigma-Aldrich; product no. C0979), rabbit anti-SOD-1 1 : 1000 (Sigma-Aldrich; product no. HPA001401), rabbit anti-SOD-2 1 : 1000 (Abcam, Cambridge, UK; product no. ab16956), rabbit anti-Nrf2 1 : 1000 (Abcam; product no. ab137550), rabbit anti-GPx1 (Abcam; product no. ab22604), mouse anti-HO-1 (Abcam; product no. ab13248) and mouse anti- β -actin 1 : 5000 (Abcam; product no. ab8226). After washing, the secondary antibodies were applied: anti-mouse IgG (Sigma-Aldrich; product no. A0168) or anti-rabbit IgG (Sigma-Aldrich; product no. A0545) at a dilution of 1 : 2000.

2.4 Activation of the Nrf2–antioxidant response element system

The influence on the activity of Nrf2 was estimated using an antioxidant response element (ARE) reporter kit (BPS Bioscience, San Diego, CA, USA) on HepG2 cells as reported previously.¹³ After transient transfection with the ARE reporter kit and serum recovery, the cells were treated for 24 h with the composites, mixture, GPs alone and curcumin alone. As a positive control for this experiment, we have used DL-sulforaphane (Sigma-Aldrich) at a concentration of 10 μM dissolved in DMSO.

2.5 Statistical analysis

Statistical analyses were carried out using the GraphPad Prism 6.01 software (San Diego, CA, USA). The data were graphed as means \pm SEM (standard error of mean). The outlying values were identified using the ROUT algorithm ($Q = 5\%$) and removed from the analysis. Comparisons between groups were made using the Kruskal–Wallis test followed by Dunn's multiple comparison test.

3. Results and discussion

After 24 h of incubation with the composites, mixture, GPs alone and crude curcumin, the expression of selected proteins was measured and normalized to the expression of β -actin and expressed as a ratio of the negative control (NC). The results are shown in Fig. 1. The data for the expression of GPx and SOD-2 are not shown, since there was no observable change compared to the NC.

The expression of the Nrf2 protein was increased significantly ($p < 0.05$) after incubation of cells with the mixture of GPs (670 $\mu\text{g mL}^{-1}$) and curcumin (10 μM). Apart from the mixture, curcumin alone and GPs alone were also able to increase the expression, whereas the composites had no observable effect.

Moreover, the differences in the expression of other proteins were not statistically significant. But there was an observable trend; specifically, the mixture of GPs with curcumin increased the expression of SOD-1, crude curcumin increased the expression of CAT and the composites increased the expression of HO-1.

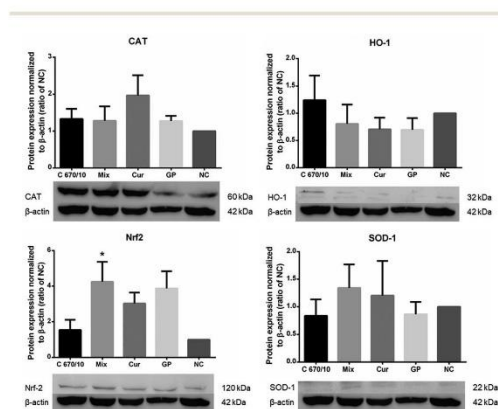


Fig. 1 Change in the protein expression normalized to β -actin (ratio of the NC). C 670/10 denotes the GP composites (670 $\mu\text{g mL}^{-1}$) with encapsulated curcumin (10 μM), Mix represents the mixture of the two components, Cur is crude curcumin, GP means glucan particles alone and NC means the negative control; * denotes $p < 0.05$ compared to the NC.

The results on the activation of the Nrf2-ARE cellular system are shown in Fig. 2 as a ratio of the luminescence signal for reporter and control luciferase (firefly/*Renilla*). There is a significant increase in the case of 24 h incubation with DL-sulforaphane serving as the positive control (PC; $p < 0.0001$).

Additionally, incubation with the mixture of GPs ($670 \mu\text{g mL}^{-1}$) and curcumin ($10 \mu\text{M}$) increased the activation of the Nrf2-ARE system significantly ($p < 0.01$). Other experimental settings had less effect on Nrf2-ARE activation. We can speculate that the different effects of the physical mixture and composites of GPs and curcumin on the expression and activity of Nrf2 could be caused by different dissolution kinetics of curcumin. Curcumin is slightly soluble in water¹⁴ and its incorporation into GPs could affect its solubility. The changed dissolution kinetics then could influence the expression and activity of Nrf2, which is time dependent.¹⁵

The results presented in this short communication follow up on previous studies, mainly on the results of Plavcová *et al.*,⁹ where the composites of GPs and curcumin ($670 \mu\text{g mL}^{-1}$ and $10 \mu\text{M}$) exhibited direct antioxidant and ROS scavenging activities in a cell-based model with pyocyanin stimulation ($5 \mu\text{g mL}^{-1}$). The composites significantly decreased ROS production after 1 h of incubation. After 24 h, significant results were observable for both the composites and mixture.

These results are in accordance with ours, where the mixture of GPs and curcumin was able to increase the expression of the Nrf2 protein and activate the Nrf2-ARE system. Unfortunately, no significant effect was observed on the level of antioxidant enzymes responsible for antioxidant defence. Maybe with different incubation times, the increase of SOD-1 expression would be significant. Or, maybe different antioxidant enzymes are involved.

On the other hand, the results of Ishida *et al.*¹⁵ have shown different results for β -glucans from *Candida albicans*. β -Glucans were applied to oral keratinocytes and they induced HO-1 upregulation via ROS/p38 MAPK/Nrf2 pathway activation, which may have important roles in host defence against the stress caused by *Candida* infection in the oral epithelium.

In our results we have observed only slightly increased expression of HO-1 and only after incubation with composites. For GPs alone, there was no change from the NC. This may be explained by the different cell lines used in our experiments and the different compositions of β -glucans used; it is also problematic to compare the dosage, since Ishida *et al.* used heat-killed *Candida albicans* in the amount of 10^8 cells per mL.¹⁵ Furthermore, Youn *et al.* showed the effect of curcumin alone on the expression of HO-1 via Nrf2 activation after incubation with the HaCaT cell line.¹⁶

4. Conclusions

Although the presented results did not show the effect of composites to be superior to that of the mixture or GPs alone or crude curcumin, we have proven the positive effect of the mixture on Nrf2/ARE activation. Also, there was an observable increase of the expression of superoxide dismutase 1 (by the mixture of GPs and curcumin), catalase (by crude curcumin) and heme oxygenase 1 (by the composites).

Eventually, the mixture of GPs and curcumin showed positive results and should be further examined.

Conflicts of interest

There are no conflicts to declare.

Acknowledgements

This work was supported by grant no. 16-27522A from the Ministry of Health of the Czech Republic (<http://www.azvcr.cz>), by the Ministry of Education, Youth and Sports of the Czech Republic under the project "FIT" CZ.02.1.01/0.0/0.0/15_003/0000495, and Czech Ministry of Agriculture grant no. RO0518.

References

- 1 J. Tremblé and K. Šmejkal, *Compr. Rev. Food Sci. Food Saf.*, 2016, **15**, 720–738.
- 2 A. G. Atanasov, B. Waltenberger, E.-M. Pferschy-Wenzig, T. Linder, C. Wawrosch, P. Uhrin, V. Temml, L. Wang, S. Schwaiger, E. H. Heiss, J. M. Rollinger, D. Schuster, J. M. Breuss, V. Bochkov, M. D. Mihovilovic, B. Kopp, R. Bauer, V. M. Dirsch and H. Stuppner, *Biotechnol. Adv.*, 2015, **33**, 1582–1614.

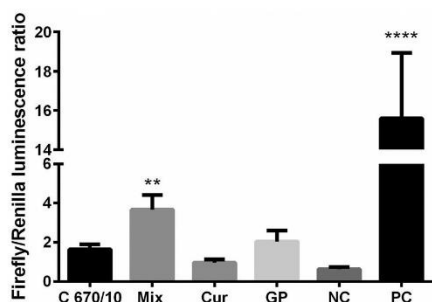


Fig. 2 Change in the firefly/*Renilla* luminescence expressing Nrf2-ARE activation. C 670/10 denotes the GP composites ($670 \mu\text{g mL}^{-1}$) with encapsulated curcumin ($10 \mu\text{M}$), Mix represents the mixture of the two components, Cur is crude curcumin, GP means glucan particles alone, NC means the negative control and PC means the positive control, DL-sulforaphane; ** denotes $p < 0.01$, **** denotes $p < 0.0001$ compared to the NC.

- 3 R. Ahsan, M. Arshad, M. Khushtar, M. A. Ahmad, M. Muazzam, M. S. Akhter, G. Gupta and M. Muzahid, *Drug Res.*, 2020, **70**, 441–447.
- 4 I. Muhammad, H. Wang, X. Sun, X. Wang, M. Han, Z. Lu, P. Cheng, M. A. Hussain and X. Zhang, *Front. Pharmacol.*, 2018, **9**, 554.
- 5 T. Esatbeyoglu, P. Huebbe, I. M. A. Ernst, D. Chin, A. E. Wagner and G. Rimbach, *Angew. Chem., Int. Ed.*, 2012, **51**, 5308–5332.
- 6 Y. Xie, X. Hu, H. He, F. Xia, Y. Ma, J. Qi, X. Dong, W. Zhao, Y. Lu and W. Wu, *J. Mater. Chem. B*, 2016, **4**, 2864–2873.
- 7 V. Castranova, *Toxicology of 1-3-Beta-Glucans: Glucans as a Marker for Fungal Exposure*, 1st edn, 2007..
- 8 I. Nono, N. Ohno, A. Masuda, S. Oikawa and T. Yadomae, *J. Pharmacobiodyn.*, 1991, **14**, 9–19.
- 9 Z. Plavcová, P. Šalamúnová, I. Saloň, F. Štěpánek, J. Hanuš and J. Hošek, *Int. J. Pharm.*, 2019, **568**, 118532.
- 10 T. Ren, J. Gou, W. Sun, X. Tao, X. Tan, P. Wang, Y. Zhang, H. He, T. Yin and X. Tang, *Mol. Pharm.*, 2018, **15**, 2870–2882.
- 11 C. Sabu, P. Mufeedha and K. Pramod, *Expert Opin. Drug Delivery*, 2019, **16**, 27–41.
- 12 I. Saloň, J. Hanuš, P. Ulbrich and F. Štěpánek, *Food Bioprod. Process.*, 2016, **99**, 128–135.
- 13 J. Treml, V. Leláková, K. Šmejkal, T. Paulíčková, Š. Labuda, S. Granica, J. Havlík, D. Jankovská, T. Padrtová and J. Hošek, *Biomolecules*, 2019, **9**, 468.
- 14 D. de, M. Carvalho, K. P. Takeuchi, R. M. Geraldine, C. J. de Moura, M. C. L. Torres, D. de, M. Carvalho, K. P. Takeuchi, R. M. Geraldine, C. J. de Moura and M. C. L. Torres, *Food Sci. Technol.*, 2015, **35**, 115–119.
- 15 Y. Ishida, K. Ohta, T. Naruse, H. Kato, A. Fukui, H. Shigeishi, H. Nishi, K. Tobiume and M. Takechi, *Infect. Immun.*, 2018, **86**, e00575–17.
- 16 G. S. Youn, D.-J. Kwon, S. M. Ju, S. Y. Choi and J. Park, *BMB Rep.*, 2013, **46**, 410–415.

6.11. ARTICLE 11

Salamunova, P.; Cupalova, L.; Majerska, M.; **Treml, J.**; Ruphuy, G.; Smejkal, K.; Stepanek, F.; Hanus, J.; Hosek, J. International Journal of Biological Macromolecules 2021, 169, 443-451 (IF=8.025).



Incorporating natural anti-inflammatory compounds into yeast glucan particles increases their bioactivity *in vitro*

Petra Šalamúnová^{a,1}, Lucie Čupalová^{b,c,1}, Monika Majerská^a, Jakub Tremel^c, Gabriela Ruphuy^a, Karel Šmejkal^d, František Štěpánek^a, Jaroslav Hanuš^a, Jan Hošek^{b,e,*}

^a Department of Chemical Engineering, University of Chemistry and Technology Prague, Technická 5, 166 28 Prague, Czech Republic

^b Division of Biologically Active Complexes and Molecular Magnets, Regional Centre of Advanced Technologies and Materials, Faculty of Science, Palacký University Olomouc, Šlechtitelů 27, 783 71 Olomouc, Czech Republic

^c Department of Molecular Pharmacy, Masaryk University, Palackého tř. 1946/1, 612 00 Brno, Czech Republic

^d Department of Natural Drugs, Faculty of Pharmacy, Masaryk University, Palackého tř. 1946/1, 612 00 Brno, Czech Republic

^e Department of Pharmacology and Toxicology, Veterinary Research Institute, Hudcova 296/70, 621 00 Brno, Czech Republic

ARTICLE INFO

Article history:

Received 8 July 2020

Received in revised form 30 October 2020

Accepted 14 December 2020

Available online 16 December 2020

Keywords:

β-glucan microparticles
Drug carrier
Inflammation
Monocytes
Natural compounds
Pharmaceutical composite

ABSTRACT

Yeast glucan particles (GPs) are promising agents for the delivery of biologically active compounds as drugs. GPs possess their own biological activities and can act synergistically with their cargo. This study aimed to determine how incorporating artemisinin, ellagic acid, (–)-epigallocatechin gallate, morusin, or *trans*-resveratrol into GPs affects their anti-inflammatory and antioxidant potential *in vitro*. Two different methods – slurry evaporation and spray drying – were used to prepare composites (GPs + bioactive compound) and the anti-inflammatory and antioxidant properties of the resultant products were compared. Several of the natural compounds showed the beneficial effects of being combined with GPs. The materials prepared by spray drying showed greater activity than those made using a rotary evaporator. Natural compounds incorporated into yeast GPs showed greater anti-inflammatory potential *in vitro* than simple suspensions of these compounds as demonstrated by their inhibition of the activity of transcription factors NF-κB/AP-1 and the secretion of the pro-inflammatory cytokine TNF-α.

© 2020 Elsevier B.V. All rights reserved.

1. Introduction

Nature is a rich source of bioactive compounds that have served to inspire many drugs currently in use [1]. Many natural compounds possess significant antioxidant, anti-inflammatory, anticancer, antimicrobial, and other activities as shown by *in vitro*, *in vivo*, or clinical trials. The use of herbal remedies to treat different inflammatory diseases in traditional medicines has been well described [2]. However, although

many natural compounds have shown promising effects in different studies, their clinical use has been limited by their often low bioavailability, rapid metabolism, or both [3,4].

Different delivery systems have been developed to modify the pharmacokinetic profiles of natural compounds. Micro- or nanoemulsions, liposomes and their modified forms, and micro- or nanoparticles have been studied the most [5]. Glucan particles (GPs) prepared from yeasts (*Saccharomyces cerevisiae*) are an interesting group of natural microparticles. They are spheroidal or ellipsoidal particles with a central cavity and porous walls. The walls consist mainly of β-(1–3)-D-glucan with or without β-(1–6)-D-glucose in side chains (> 85%), chitin (~2%), proteins, and lipids [6,7]. As natural materials, they are ideally suited to become biocompatible drug carriers that can be recognized and actively captured from the gut lumen by microfold cells (M-cells) [8–10]. Immune cells associated with these M-cells can then use the lymphatic system to distribute the cargo of the GPs to various organs of the reticulo-endothelial system, such as the liver, the lung, the spleen, and the kidney [9–11], or into inflamed sites and tumors [8,12,13]. These features make GPs suitable candidates for the oral delivery of diagnostic or therapeutic compounds.

In addition to their ability to serve as drug carriers, GPs possess their own immunomodulatory activities, which can affect immune cells and

Abbreviations: AC, active compound; AP-1, activator protein 1; DMSO, dimethyl sulfoxide; EGCG, (–)-epigallocatechin gallate; GPs, yeast glucan particles; H₂DCF-DA, 2',7'-dichlorodihydrofluorescein diacetate; HPLC, high performance liquid chromatography; HRMS, high-resolution mass spectrometry; LPS, lipopolysaccharide; NF-κB, nuclear factor κB; PMA, phorbol myristate acetate; RE, rotary evaporation; ROS, reactive oxygen species; SD, spray drying; SE, standard error of the mean; SPM, serum-free medium; THF, tetrahydrofuran; TNF-α, tumor necrosis factor α; XRD, X-ray diffraction.

* Corresponding author at: Division of Biologically Active Complexes and Molecular Magnets, Regional Centre of Advanced Technologies and Materials, Faculty of Science, Palacký University Olomouc, Šlechtitelů 27, 783 71 Olomouc, Czech Republic.

E-mail addresses: petra.salamunova@vscht.cz (P. Šalamúnová), tremelj@pharm.muni.cz (J. Tremel), ruphuyg@vscht.cz (G. Ruphuy), frantisek.stepanek@vscht.cz (F. Štěpánek), jaroslav.hanus@vscht.cz (J. Hanuš), jan.hosek@upol.cz (J. Hošek).

¹ P. Šalamúnová and L. Černá contributed equally to this work.

thereby contribute to the general anti-inflammatory, antioxidant, and anti-tumor arsenals of organisms [14–16]. Their immunostimulating effect can also be used to develop carriers for vaccines [17,18]. We hypothesize that loading GPs with bioactive compounds could produce composites with synergic effects of these two components.

In this research, we have focused on five chemically different natural compounds – the sesquiterpene lactone artemisinin (1), the ellagitannin ellagic acid (2), the catechin (–)-epigallocatechin gallate (EGCG; 3), the prenylated flavonoid morusin (4), and the stilbene *trans*-resveratrol (5) (Fig. 1). All of these compounds possess significant anti-inflammatory effects as demonstrated using different *in vitro* or *in vivo* models; some have also been tested in clinical trials [19–23]. They can serve as study compounds for proof-of-concept and were selected because, as they represent different chemical groups, incorporating them into GPs could result in composites with significantly different characteristics.

This study aimed to determine how incorporating compounds 1–5 into GPs affects their anti-inflammatory and antioxidant potentials *in vitro*. The prepared composites were compared with physical mixtures of the corresponding pure GPs and test compounds. Two different methods, slurry evaporation (using rotary evaporator) and spray drying method, were used to prepare composites (GPs + test compound) and the anti-inflammatory potential and antioxidant effect of the resultant products were compared. According to our best knowledge, this is the first reported comparison of the biological effects resulting from two different ways of preparing glucan composites.

2. Materials and methods

2.1. Preparation of glucan particles

The glucan particles were prepared from instant yeast (*Saccharomyces cerevisiae*) (Pakmaya, Ankara, Turkey) using a protocol based on the procedure of Saloň et al. [6]. Briefly, 150 g of dried yeast was dispersed in 600 mL of 1 M NaOH solution and heated to 90 °C for

60 min. The suspension was centrifuged (6000 ×g) for 3 min and the supernatant was discarded. This alkali extraction was repeated twice (3-times in total). The mixture was adjusted to pH ≈ 4.5 with concentrated HCl and heated at 75 °C for 2 h. The suspension was centrifuged (3 min, 6000 ×g) and the supernatant was removed. The resultant sludge was washed with deionized water (3×), isopropanol (4×) and acetone (2×), with each and every wash followed by centrifuging for 3 min at 6000 ×g and all of the supernatant liquid was discarded. The final sludge was lyophilized for 48 h, protected against moisture and stored in a refrigerator. Approximately 15 g of GPs were obtained from starting 150 g of yeasts. The pure GPs used to prepare physical mixtures with the active compounds for comparison with spray-dried composites were then resuspended in 96% ethanol and spray dried in the same way as the composites.

Hydrochloric acid, acetone, and isopropanol were purchased from Lach-Ner, Czech Republic. Sodium hydroxide, methanol, and ethanol were purchased from Penta, Czech Republic.

2.2. Preparation of composites

Composites of glucan particles with artemisinin (1), ellagic acid (2), (–)-epigallocatechin gallate (EGCG; 3), morusin (4), and *trans*-resveratrol (5) were prepared by two different methods: slurry evaporation and spray drying (Table 2). Artemisinin (1) and EGCG (3) were purchased from SantaCruz Biotechnology (USA), ellagic acid (2) and *trans*-resveratrol (5) from Sigma-Aldrich, Germany. Morusin (4) was kindly provided by Assoc. Prof. PharmDr. Karel Šmejkal of the Department of Natural Drugs, Masaryk University.

2.2.1. Slurry rotary evaporation (RE)

A stock solution of each of the five test compounds was prepared by dissolving a weighed amount of the compound in ethanol (the amounts used for each compound are shown in Table 1). A defined volume of the stock solution of the tested compound (see Table 1), together with additional 50 mL of ethanol, was added to 500 mg of glucan particles in

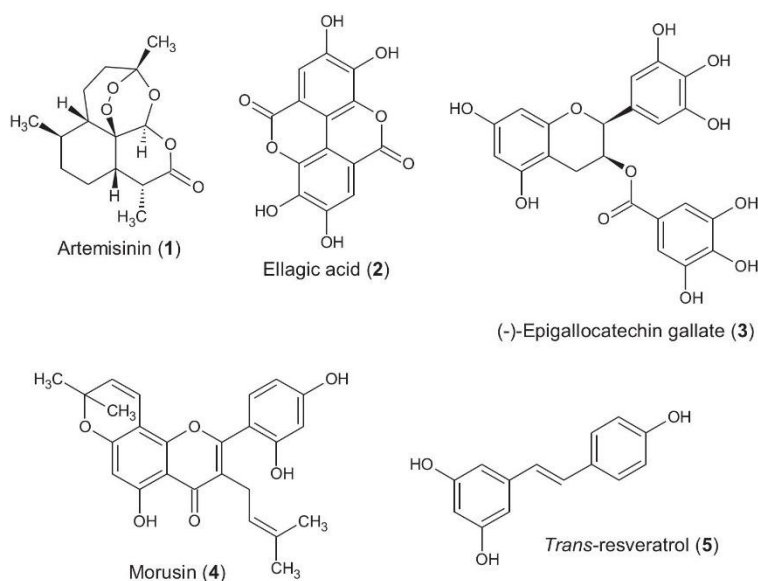


Fig. 1. Structures of the test compounds.

Table 1

The amounts of active compounds (AC) and the masses of glucan particles used for the preparation of the composites by the slurry evaporation method (RE) and the spray-drying method (SD). The final suspension of each composite used for the *in vitro* experiments contained an amount of the active compound corresponding to a concentration of 1 μM .

	Concentration of AC in stock solution	Volume of stock solution used for RE/SD	Mass of GPs [mg] used for RE/SD	Mass fraction of AC in GPs [w/w]
Artemisinin (1) composites	0.5 mg/mL	422 μL /843 μL	500/1000	0.042%
Ellagic acid (2) composites	0.14 mg/mL	1611 μL /3222 μL	500/1000	0.045%
EGCG (3) composites	0.5 mg/mL	684 μL /1368 μL	500/1000	0.068%
Morusin (4) composites	0.5 mg/mL	628 μL /1255 μL	500/1000	0.063%
<i>Trans</i> -resveratrol (5) composites	0.5 mg/mL	341 μL /681 μL	500/1000	0.034%

a round bottom flask. The resulting suspension was homogenized using a T10 basic Ultra-Turrax (IKA, Germany). The suspension was then placed into a rotary evaporator to slowly eliminate the solvent, according to the method described by Plavcová et al. [24]. Concisely, the rotary evaporator was set to 175 RPM, the water bath was heated to 60 °C, and the pressure was slowly reduced from atmospheric to 300 mbar. The ethanol was evaporated at 300 mbar and the composites were then dried fully at 80 mbar. The product, a dry powder, was lyophilized for 48 h to remove any remaining moisture. Composites prepared by this way are called “RE composites” in this study. The loaded glucan particles were protected against light and moisture and stored in a refrigerator.

2.2.2. Spray drying (SD)

Suspensions of each test compound were prepared by adding 1000 mg of glucan particles to a mixture containing 50 mL of ethanol and the volume of stock solution of that particular active compound specified in Table 1. Before spray drying, the suspension was homogenized for 5 min using a T10 basic Ultra-Turrax (IKA).

The samples were spray dried using a Mini Spray Dryer B-290 (Büchi) equipped with an ultrasonic nozzle and operated in inert loop with an atmosphere of nitrogen. The following conditions were applied: inlet temperature 120 °C, feed rate 5.0 mL/min, nitrogen flow rate 246 L/h, flow meter 20 mm, and power output at the nozzle 2.4 W. The outlet temperature ranged between 70 and 75 °C. Composites prepared by this way are called “SD composites” in this study.

2.3. Characterization of the prepared composites

The amount of each active compound contained in its composite was determined by high-resolution mass spectrometry (HRMS) LTQ Orbitrap Velos - hybrid ion-trap-orbitrap instrument (Thermo Scientific), high performance liquid chromatography (HPLC) Agilent 1100, employing an Ascentis Express RP-Amide 100 \times 2.1 mm, 2.7 μm column, or UV-Vis spectrophotometry on a Specord 205 BU UV-Vis spectrophotometer, using a Hellma QX semi-micro cuvette. Artemisinin (1) and ellagic acid (2) were extracted into methanol. Two milliliters of methanol was added to 10–13 mg of composites and this mixture was placed in an ultrasonic bath for 10 min to extract the compounds from the GPs matrix. The supernatant liquid was separated from the solid particles by centrifugation (3 min, 6000 $\times g$), the supernatant was filtered through a 0.2 μm filter, and the content of the active compound was then measured using HRMS. Flow injection analysis combined with high-resolution mass spectral detection was used. Extracts were further diluted with methanol and injected using a 5 μL loop (Rheodyne). The standard addition method was used for quantification, because a screening effect of the glucan matrix had been observed. EGCG (3) was extracted from the composites using an ethanol-water mixture (20% v/v). Two milliliters of the solvent was added to 10–11 mg of EGCG (3) composites. The procedure of sonication, centrifugation, and filtration was the same as that used to extract 1 and 2. The UV-Vis absorbance was then measured using methanolic extract of untreated GPs as a blank and the content of EGCG was determined from the absorbance at 273 nm. A standard calibration curve was prepared beforehand ($R^2 = 0.9994$). HPLC was used to determine the contents of morusin (4)

and *trans*-resveratrol (5) in the prepared composites. For each, ten milligrams of composites was weighed into a glass vial and 1 mL of methanol was added. The vial was placed in an ultrasonic bath for 15 min. The suspension was then centrifuged (6000 $\times g$, 3 min) and the supernatant was carefully collected. The extract of morusin (4) composite was injected (1 μL) into a mobile phase of acetonitrile and 0.2% (v/v) HCOOH. The gradient was started with a composition of 40:60 (v/v) and increased linearly to 80:20 (v/v) over the 20 min run. The column was an Ascentis Express RP-Amide (100 \times 2.1 mm, 2.7 μm ; Supelco, USA), the flow rate 0.3 mL/min, and the column block temperature was 40 °C. The content of morusin (4) was calculated using a standard calibration curve ($R^2 = 0.9388$). The detection wavelength was 290 nm and the retention time 17.5 min.

The methanolic extract of *trans*-resveratrol (5) obtained from the composites (1 μL) was injected into a mobile phase composed of acetonitrile and 0.2% (v/v) HCOOH. The composition changed linearly from 10:90 (v/v) at time zero to 50:50 (v/v) after 15 min. An Ascentis Express RP-Amide (100 \times 2.1 mm, 2.7 μm) column was used with a flow rate of 0.3 mL/min and a column block temperature of 40 °C. *Trans*-resveratrol (5) was detected at 280 nm, with a retention time of 12.5 min. The *trans*-resveratrol (5) content was calculated using a standard calibration curve ($R^2 = 0.9775$) constructed by making serial injections of 5 (Sigma-Aldrich). All of the samples were measured in triplicate.

The prepared composites were visualized using optical and fluorescence microscopy (Olympus IX81, WU fluorescence cube with excitation in the 330–385 nm range and detection at wavelengths greater than 420 nm). An Olympus UPLSAPO Objective 40 \times was employed. The crystallinity of the samples was checked by X-ray powder diffraction analysis (PANalytical X'Pert Pro with High Score Plus diffractometer; 5° to 50° 2 θ angle). FTIR spectra of pure SD and RE GPs were measured using FTIR spectrometer Nicolet 6700 (Thermo-Nicolet, USA) with GladiATR crystal (PIKE, USA), DTGS KBr detector, and Happ-Genzel apodization.

2.4. Preparation and maintenance of monocytes and macrophages

The THP-1-XBlue™-MD2-CD14 cell line was purchased from Invivogen (San Diego, CA, USA). The cell line was cultured in RPMI 1640 medium containing stabilized 2 mM L-glutamine (Biosera, Nuaille, France) containing antibiotics [100 U/mL penicillin and 100 mg/mL streptomycin (Biosera)] and 10% fetal bovine serum (HyClone, Logan, UT, USA), hereinafter referred to as the complete medium. The cell culture was passaged once a week and fresh complete medium was added twice a week. Cells were maintained in an incubator at 37 °C under a humidified atmosphere, containing 5% CO₂.

THP-1-XBlue™-MD2-CD14 monocytes were differentiated to macrophages using phorbol myristate acetate (PMA) at a final concentration of 50 ng/mL, as described previously [25]. Briefly, monocytes were seeded into 96-well plates at a concentration of 50,000 cells/well and stimulated with PMA. After 24 h of differentiation, the medium was replaced, and the cells were incubated for 24 h in complete medium without PMA. Then the cells were washed with phosphate buffered saline and serum-free medium (SFM) was added 2 h before treatment.

The viability of the cell lines used (5th – 18th passage) was greater than 95% for each experiment. At the concentrations tested, the samples did not show cytotoxic effects on the viability of the cells.

2.5. Determination of the relative cell viability

The non-differentiated floating THP-1-XBlue™-MD2-CD14 monocytes (555,555 cells/mL for the suspensions of composites and GPs and 500,000 cells/mL for solutions or suspension of the pure compounds **1–5**) were transferred into SFM and seeded into 96-well plates, 90 µL/well for the composites and 100 µL/well for the crude active compounds, i.e., 50,000 cells per well, in triplicate. In order to compensate for subsequent dilutions, test suspensions and solutions were prepared as a concentrated stock suspensions and solutions – a factor of ten for the composites and a thousand for the concentrated stock solution of each active compounds. Each prepared suspension was homogenized for 1 min using a T10 basic Ultra-Turrax (IKA) at approximately 20,000 RPM. After 2 h, 10 µL of the stock suspension of one of the test composites with encapsulated active compounds **1–5**, or 2 µL of the stock suspension or solution of one of the pure active compounds **1–5** suspended in SFM or dimethyl sulfoxide (DMSO; Sigma-Aldrich) was added to the cells. The final concentrations of compounds **1–5** in SFM or DMSO were 20, 10, 5, 2.5, and 1.25 µM. Measurements were taken after 24 h of incubation with the test substances. The relative viability of the cells was measured using a Cell Proliferation Reagent kit WST-1 (Roche Diagnostics, Basel, Switzerland) according to the manufacturer's manual. The control cells, which were treated with SFM or DMSO only, were assigned as 100%. IC₅₀ values were calculated from the resultant viability curves by four-parameter logistic (4PL) analysis.

The viability of THP-1-XBlue™-MD2-CD14 monocytes incubated for 24 h with pure glucan particles was calculated manually using a hemocytometer. Trypan blue (Sigma-Aldrich, Germany) dye was used to distinguish the dead from the vital cells. The viability of cells was calculated as the number of living cells divided by the total number of live and dead cells and was performed three times. The cell viability was relativized to the control cells, which were treated with SFM only and assigned as 100%.

2.6. Determination of NF-κB/AP-1 activity

The activity of NF-κB/AP-1 was evaluated as described previously [24]. Briefly, the THP-1-XBlue™-MD2-CD14 cell line was used in SFM. All samples were suspended in SFM and added to the cell culture 2 h after the cell seeding and the start of incubation. Lipopolysaccharide (LPS) isolated from *E. coli* O111:B4 (Sigma-Aldrich) at a final concentration of 1 µg/mL was then added 1 h later to trigger an inflammation-like response. After 24 h of incubation, the activity of the NF-κB/AP-1 transcription factors was determined as the activity of secreted embryonic alkaline phosphatase (SEAP), the expression of which is controlled by an artificial NF-κB/AP-1 promoter, using Quanti-Blue™ reagent (Invivogen) according to the manufacturer's instructions.

2.7. Determination of TNF-α secretion

The differentiated macrophages THP-1-XBlue™-MD2-CD14 were used to determine the secretion of TNF-α as described previously [25]. Cells were treated with samples and after 1 h LPS was added to activate the inflammatory response. After 24 h, the supernatant liquid was collected and the concentration of TNF-α was measured using a Human TNF-α ELISA Kit (Dialone, Besançon, France) according to the manufacturer's manual.

2.8. Detection of the intracellular production of reactive oxygen species (ROS)

A method based on 2',7'-dichlorodihydrofluorescein diacetate (H₂DCF-DA) was used to determine evaluation of antioxidant and pro-oxidant action of the test materials as described previously [24]. Briefly, THP-1-XBlue™-MD2-CD14 cells in SFM were used. The cells were seeded and incubated 2 h. After they were treated with the test materials. After a further hour, pyocyanin (Sigma-Aldrich) at a concentration of 100 µM was added to the cells used for antioxidant assays and controls. After continued periods of 1, 4, or 24 h, 5 µg/mL of H₂DCF-DA was added to determine the formation of ROS. The intracellular fluorescence of the dichlorofluorescein created was measured by FLUOstar Omega Microplate Reader (BMG Labtech) using 480 nm as the excitation wavelength and 530 nm to measure the emission.

2.9. Statistical evaluation

Statistical analyses were carried out using GraphPad Prism 8.01 software (San Diego, CA, USA). The data were graphed as the mean ± the standard error of the mean (SE). Outlying values were identified by ROUT algorithms (parameter Q = 5%) and removed from the analysis. Comparisons between groups were made using a one-way ANOVA test followed by an uncorrected Fisher's LSD *post-hoc* test for multiple comparison.

3. Results and discussion

3.1. Characterization of glucan particles and composites

The glucan microparticles were prepared from dried yeast (*S. cerevisiae*) as described previously [24]. Two different methods of loading were used for the encapsulation: slurry rotary evaporation (RE) and a spray-drying (SD) method. In total, 10 samples were prepared, 5 by each method.

Representative micrographs obtained by optical microscopy for each prepared composite and for the pure GPs are presented in the Supplementary material (Figs. S1–S12). In contrast to the fluorescence micrographs of curcumin composites presented in Plavcová et al. [24] and Ruphuy et al. [26], the composites prepared in this study showed only slightly increased fluorescence when compared with pure GPs. This is because the test compounds used in this study do not fluoresce as strongly as curcumin and the amounts of the substances that were used correspond to only the lowest concentration used in the previous study [24]. Micrographs of the RE and SD composites show no signs of the active compound existing outside the GPs, as was the case for some of the preparations in Ruphuy et al. [26]. This suggests that the encapsulation was fully successful. XRD spectra (see the Supplementary material Fig. S13) of all the composites do not differ from the spectra of the pure GPs. This can be interpreted as a sign that the composites do not contain much of the crystalline form of the active compound, however, the total amount in all forms was relatively small.

3.2. Determination of the content of active compounds encapsulated in GPs

The content of the active compounds morusin (**4**) *trans*-resveratrol (**5**) and in their composites was determined by HPLC, but for artemisinin (**1**), ellagic acid (**2**), and EGCG (**3**), HPLC was not sufficiently sensitive (Table 2). Artemisinin (**1**) possesses a weak chromophore (absorbing only at 205–215 nm) and HPLC-UV-Vis analysis could not reliably determine low concentrations, such as those used in the study of Lapkin et al. [27]. Ellagic acid (**2**) and EGCG (**3**) were difficult to determine probably because they have great affinity for GPs when methanol is used as the extraction solvent. Therefore, an ethanol-water 20:80 (v/v) mixture was eventually used to extract EGCG (**3**) from composites, with simple UV-Vis spectrophotometry (characteristic detection

Table 2

Summary of the planned contents of active compounds (AC) in GPs and the actual AC contents measured using HPLC-UV, UV-Vis spectrophotometry, or HRMS; the planned content of each AC was assigned as 100% loading effectiveness.

	Planned content of AC in GPs (w/w)	Composites – RE (w/w)	Composites – SD (w/w)	Method of determination
Artemisinin (1) composites	0.042%	0.043 ± 0.005% (102.4%)	0.041 ± 0.004% (97.6%)	HRMS
Ellagic acid (2) composites	0.045%	0.020 ± 0.002% (44.4%)	0.028 ± 0.003% (62.2%)	HRMS
EGCG (3) composites	0.068%	0.035 ± 0.003% (51.5%)	0.042 ± 0.005% (61.8%)	UV-Vis spectrophotometry
Morusin (4) composites	0.063%	0.036 ± 0.002% (57.1%)	0.040 ± 0.001% (63.5%)	HPLC-UV
Trans-resveratrol (5) composites	0.034%	0.039 ± 0.001% (114.7%)	0.047 ± 0.001% (138.2%)	HPLC-UV

wavelength at approx. 280 nm [28]) then used to determine the EGCG (3) contents of both the RE and SD composites. Artemisinin (1) and ellagic acid (2) were determined using high-resolution mass spectrometry (HRMS).

3.3. Evaluation of the cytotoxicity of the test materials

The cytotoxic effects of compounds 1–5 dissolved in SFM or DMSO were tested on THP-1-XBlue™-MD2-CD14 cells (Table 3). We first tested the effects of the test compounds dissolved in DMSO. Artemisinin (1) did not show any cytotoxic effect on THP-1-XBlue™-MD2-CD14 cells at any of the concentrations tested and the relative viability of the cells was approx. 100% in every case. Ellagic acid (2) affected the viability of the cells only slightly, with the relative viability decreasing only for 20 µM, the highest concentration tested. EGCG (3) affected the cells at 5, 10, and 20 µM, which reduced the relative viability of the cells to approx. 80%. At lower concentrations (1.25 and 2.5 µM), EGCG (3) did not affect the relative viability of the cells significantly (reduced to 95%). In contrast, trans-resveratrol (5) affected the cells at 10 and 20 µM, which reduced the relative viability of the cells to 50–60%. Concentration of 5 in DMSO lower than 5 µM reduced the relative cell viability to 80%. Morusin (4) showed the greatest cytotoxic effect with IC₅₀ at 10 µM. Morusin (4) tested at concentrations of 1.25 and 2.5 µM reduced the relative cell viability to 80–85%.

Artemisinin (1), ellagic acid (2), EGCG (3), morusin (4), and trans-resveratrol (5) were further tested as the suspension in SFM. As it had in DMSO, artemisinin (1) showed almost no cytotoxic activity at the concentrations tested, with relative cell viability around 90%. With the exception of 4, all of the compounds tested showed cytotoxic effects that were comparable for both solvents DMSO and SFM (Table 3). Morusin (4) significantly reduced the cell viability when it was dissolved in DMSO, but in the aqueous medium SFM, this effect vanished completely.

Table 3

IC₅₀ values of materials dissolved in DMSO or resuspended in SFM tested on THP-1-XBlue™-MD2-CD14 cells. The results are expressed as the mean ± SE. N/A – not analyzed.

Material tested	IC ₅₀ in DMSO	IC ₅₀ in SFM
Artemisinin (1)	IC ₅₀ > 10 µM	IC ₅₀ > 20 µM
Ellagic acid (2)	IC ₅₀ > 10 µM	IC ₅₀ > 20 µM
EGCG (3)	IC ₅₀ > 10 µM	IC ₅₀ > 20 µM
Morusin (4)	9.4 ± 1.7 µM	IC ₅₀ > 20 µM
Trans-resveratrol (5)	IC ₅₀ > 10 µM	IC ₅₀ > 20 µM
Composite GP/1	N/A	IC ₅₀ > 670 µg/mL
Composite GP/2	N/A	IC ₅₀ > 670 µg/mL
Composite GP/3	N/A	IC ₅₀ > 670 µg/mL
Composite GP/4	N/A	IC ₅₀ > 670 µg/mL
Composite GP/5	N/A	IC ₅₀ > 670 µg/mL
Empty GPs	N/A	IC ₅₀ > 670 µg/mL

Based on these results and previous experiments, the 1 µM concentration of used compounds was selected for further analysis as non-toxic and pharmacologically relevant.

After a 24 h incubation with the glucan particles (lyophilized and spray dried), THP-1-XBlue™-MD2-CD14 cells showed viability similar to that of the untreated controls (Table 3). The composites were tested on the cells at a concentration of 670 µg/mL in SFM, what corresponds to the 1 µM concentration of used compounds 1–5. Such composites did not affect the cell viability significantly, as it was proved by WST-1 assay (Table 3) and lactate dehydrogenase release assay (Sigma-Aldrich; data not shown).

3.4. Analysis of the anti-inflammatory potential

3.4.1. Determination of the activity of NF-κB/AP-1

The influence of incorporating compounds 1–5 into GPs on their potential to affect an inflammation-like state was evaluated using a model of the LPS activation of transcription factors NF-κB/AP-1. Composites prepared by rotary evaporation (RE) and spray drying (SD) were compared (Fig. 2). Pure GPs (without loaded compounds) at a concentration of 670 µg/mL demonstrated significant effects on NF-κB/AP-1, as previously observed [24]. Interestingly, empty GPs prepared by SD showed four times higher anti-inflammatory activity than empty particles prepared by RE. Apparently, the drying process critically affects the properties of prepared composites. Fast drying in a spray dryer preserves the original microstructure of the GPs, whereas slower drying distorts and compress their surface microstructure [29,30] and decreases their wettability [26]. The different drying processes therefore affect the microstructure of GPs, including the organization of the OH groups on their surfaces. The subtle differences in the hydrogen bonding between SD and RE glucan particles can be tracked in their FTIR spectra – see Supplementary material (Fig. S14). According to Hromádková et al. [29], the difference between bound and free hydroxyl groups can be observed in the hydroxyl stretching region between 3000 and 3600 cm⁻¹ with the main band located around 3300 cm⁻¹. Briefly, hydrogen-bonding of hydroxyl groups can cause shifting of the band maximum position to lower frequencies, increase of intensity and/or broadening of the band as well as its symmetry distortion. In our case, we can observe that the maximum of this band is shifted from 3321 cm⁻¹ (spray dried GPs) to 3299 cm⁻¹ (GPs from rotary evaporator) and the FWHM increases from 420 cm⁻¹ (SD GPs) – to 460 cm⁻¹ (RE GPs). IR spectra therefore suggest that the SD GPs possess more free OH groups (that are ready to be hydrated and/or interact with other compounds) than RE GPs – and this effect can lead to the observed difference in biological activity.

The tested compounds suspended in water showed very low anti-inflammatory activity, and when they were mixed with GPs (simple physical mixture), the resultant effects were the same as for empty GPs. When these test compounds were incorporated into GPs using a rotary evaporator, their effects were significantly increased, with the

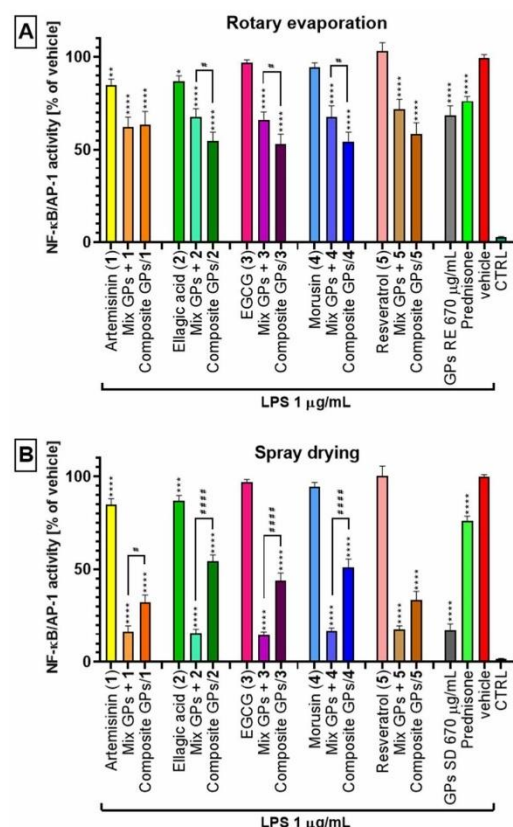


Fig. 2. Effects of pure compounds 1–5, empty glucan particles (GPs), their mixtures (Mix) and composites prepared either by rotary evaporation (RE, A) or by spray drying (SD, B) on NF- κ B/AP-1 activity. THP-1-XBlue™-MD2-CD14 cells were pre-treated for 1 h with the test compounds 1–5 (1 μ M resuspended in RPMI 1640 medium), empty GPs (670 μ g/mL), a mixture of GPs and suspensions of the pure compounds (670 μ g/mL of GPs and 1 μ M of pure compound), composites (670 μ g/mL), prednisone (1 μ M resuspended in RPMI 1640 medium), or with the vehicle (RPMI 1640 medium) only (vehicle and CTRL). Subsequently, LPS (1 μ g/mL) was added [except for the control cells (CTRL)] to trigger the activation of NF- κ B/AP-1. After 24 h, the activity of NF- κ B/AP-1 was measured spectrophotometrically. The results are expressed as the mean \pm SE for five independent experiments measured in triplicate. * Indicates a significant difference in comparison with the vehicle-treated cells $p < 0.05$, ** indicates $p < 0.01$, *** indicates $p < 0.001$, and **** corresponds to $p < 0.0001$; # indicates a significant difference between particular groups $p < 0.05$, ### indicates $p < 0.001$.

exception of artemisinin (1) ($p = 0.883$) and resveratrol (5) ($p = 0.082$). Incorporating the test compounds by the RE technique increased their anti-NF- κ B/AP-1 effects by ~20% as compared with physical mixtures. In the case of SD composites, the results were the opposite – the composites were less efficient than the corresponding physical mixtures and empty pure GPs. However, when the anti-NF- κ B/AP-1 activities of the RE and SD composites prepared with the same compound were compared, the effects of the SD composites were greater.

To exclude the influence of the presence of GPs on the LPS cell binding or SEAP activity, their mutual interaction was evaluated (see the Supplementary material Figs. S15–S16). The experiments performed showed that GPs did not diminish the action of LPS. The attenuation of

the SEAP activity was 8.9% for GPs prepared by rotary evaporation and 5.6% for spray-dried GPs. The direct interaction of the yeast's glucan with NF- κ B/AP-1 signaling pathways is in agreement with previous studies [31–33].

3.4.2. Determination of TNF- α secretion

Based on the promising results of the inhibition of NF- κ B/AP-1, composites of artemisinin (1) and *trans*-resveratrol (5) were selected for further analysis of their ability to modulate the secretion of the pro-inflammatory cytokine TNF- α . Both these compounds have shown their ability to reduce the production of TNF- α in many *in vitro* and *in vivo* studies [34,35]. All of the prepared composites of 1 and 5 attenuated the secretion of TNF- α , which is under the transcription control of NF- κ B/AP-1 (Fig. 3). With the exception of 5 loaded into GPs by the RE technique, all of the prepared composites were more active than their corresponding physical mixtures by 20–30%. As with the anti-NF- κ B/AP-1 activity, materials prepared by SD showed greater effects than those made using RE. Moreover, the prepared GPs composites significantly increased the activity of the test compounds, if they were applied in the form of water suspension without any organic solvent. The strongest effect was observed for *trans*-resveratrol (5) composites. Interestingly, composites with 5 prepared by spray drying more effectively inhibited the release of TNF- α than empty GPs, but empty GPs were more effective in the case of anti-NF- κ B/AP-1 activity. It can be hypothesized that the expression of TNF- α is affected not only by the inhibition of its transcription, but also by its translation and post-translational processing. Thus, the general effect is significantly anti-inflammatory.

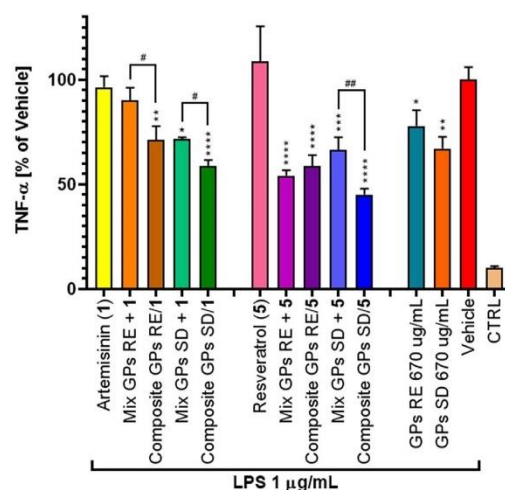
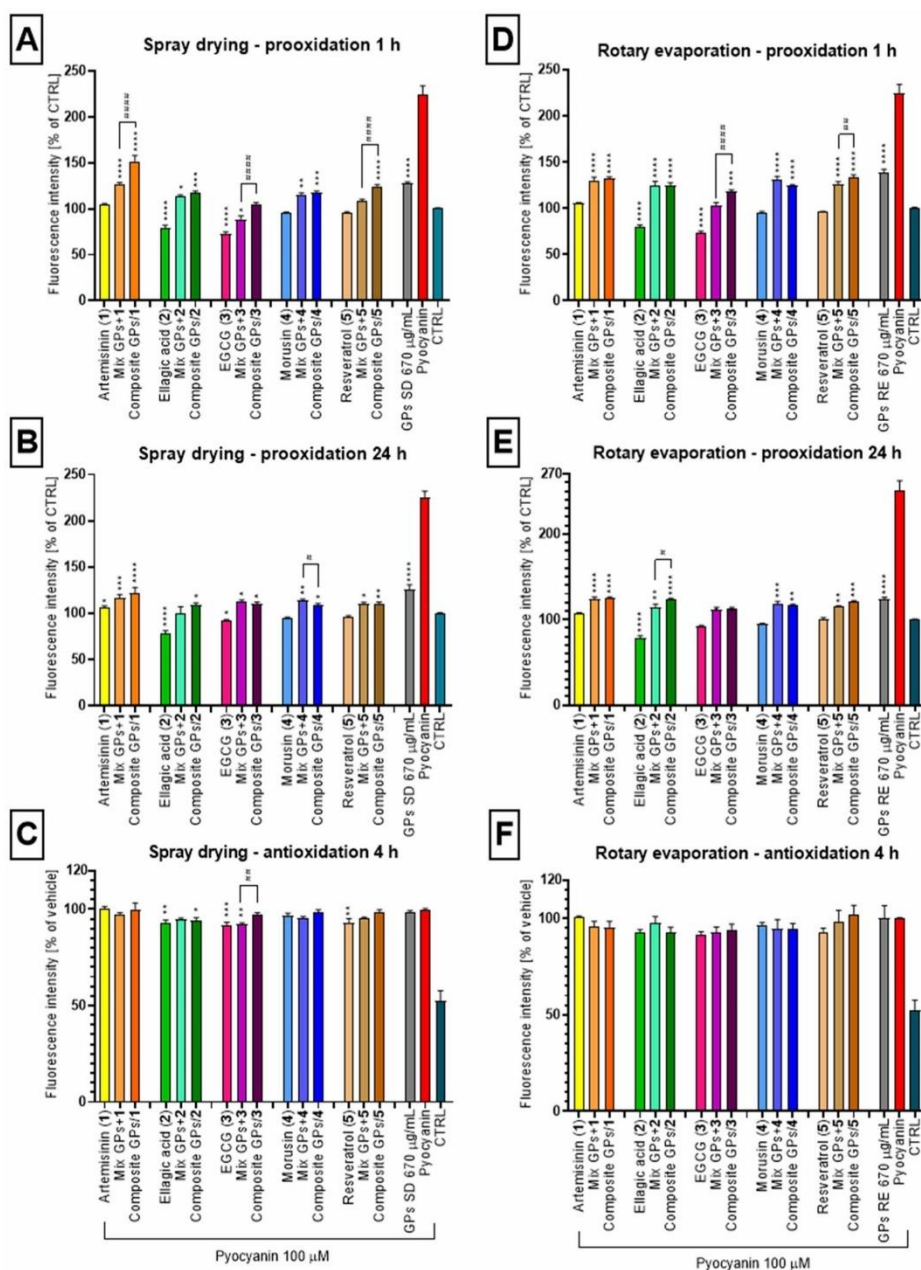


Fig. 3. Effects of pure compounds 1 and 5, empty glucan particles (GPs), their mixtures (Mix), and composites prepared either by rotary evaporation (RE) or spray drying (SD) on the secretion of TNF- α . THP-1-XBlue™-MD2-CD14 cells were pre-treated for 1 h with the test compounds (1 μ M resuspended in RPMI 1640 medium), empty GPs (670 μ g/mL), a mixture of GPs and suspensions of the pure compound (670 μ g/mL of GPs and 1 μ M of pure compound), composites (670 μ g/mL), prednisone (1 μ M resuspended in RPMI 1640 medium), or with the vehicle (RPMI 1640 medium) only (vehicle and CTRL). Subsequently, LPS (1 μ g/mL) was added [except for the control cells (CTRL)] to trigger the expression of TNF- α . After 24 h, the amount of TNF- α produced was measured by ELISA. The results are expressed as the mean \pm SE for five independent experiments measured in triplicate. * Indicates a significant difference in comparison with the vehicle-treated cells $p < 0.05$, ** indicates $p < 0.01$, *** indicates $p < 0.001$, and **** corresponds to $p < 0.0001$; # indicates a significant difference between particular groups $p < 0.05$, ## indicates $p < 0.01$.

Tested GPs and composites prepared by the spray-drying technique showed greater effects compared with rotary evaporation for both the NF- κ B/AP-1 and TNF- α assays. This effect could be caused by improved homogeneity of the suspension. The improved features of homogeneous

dispersions of GPs composites formed with poorly water soluble drugs brought about by spray drying has been described previously [26]. Greater solubility, stability, and activity has been previously found for *trans*-resveratrol (5) encapsulated into yeast glucan particles [36,37].



In previous studies, *trans*-resveratrol (**5**) has been tested at concentrations greater than 10 μM [38,39], but such supraphysiological doses could lead to undesirable cell behavior, e.g., greater expression of cyclooxygenase 2 or interleukin 1 β [40]. Clinical trials on healthy volunteers showed that the maximum plasma concentration of *trans*-resveratrol (**5**) after single or repeated administration was below 0.5 μM [41,42]. Slightly greater plasma concentrations have been found for artemisinin (**1**) [43,44]. In our study, the 1 μM concentration of artemisinin (**1**) and *trans*-resveratrol (**5**) was sufficient to obtain a desirable effect when the drug was incorporated into GPs.

3.4.3. Determination of the intracellular production of ROS

Natural compounds, including those used in this study, often possess antioxidant activity. However, none of the compounds tested showed cellular antioxidant activity after pyocyanin stimulation when applied in the form of a suspension (Fig. 4C and F). Surprisingly, incorporating the compounds into GPs composites did not increase this activity.

On the other hand, yeast GPs are known for their pro-oxidant action [24,45], as has been confirmed in this study (Fig. 4A, B, D, and E). Suspensions of the pure test compounds showed an observable reduction of the basal production of ROS, but this effect was diminished when they were applied together with GPs in both forms – as physical mixtures or composites.

The beneficial effects of incorporating bioactive compounds into yeast glucan particles on different models of diseases have been previously confirmed by other research groups. GPs loaded with the synthetic drugs methotrexate [46] or NK007 [13], ameliorated dextran sodium sulfate induced colitis in mice. GPs with cisplatin-derived nanoprecursors or paclitaxel were successfully targeted into tumors *in vivo* and reduced the negative side effects of parental compounds [12,47]. And GPs with indomethacin and rapamycin were effective in the treatment of atherosclerosis in ApoE^{−/−} mice [48]. All of the above-mentioned loaded GPs showed superior effects to those of the pure compounds or empty GPs, although the enhancement of activity was usually less than 2-fold. The only exception was the *in vitro* application of NK007, for which at several concentrations the drug was more active in its pure form than when loaded into glucan particles. It should be noted that in this case, the glucan-mannan particles were sealed by alginate. However, a physical mixture of the drug and GPs has not been tested in any study, so the effect of incorporation could not be completely evaluated. These results showed and confirmed that the main benefits of using GPs as drug carriers are the elimination of organic solvents during application, the targeting to macrophages, and the improved possibility of using oral administration.

4. Conclusions

The results obtained demonstrate modest beneficial effects of yeast glucan particles (GPs) as carriers of several bioactive natural compounds. GPs are not only a passive vehiculum. They have their own activity and contribute significantly to the overall biological effect. The method of processing and preparing of GPs and composites influences the effects observed. Materials prepared by spray drying showed greater activity than that prepared on a rotary evaporator. The incorporation of natural compounds into yeast GPs increased their anti-inflammatory potential *in vitro*. The GPs composites inhibited the NF- κ B/AP-1 pathway and their antioxidant or pro-oxidant effects were

negligible. Importantly, the desired biological effect of test natural compounds was achieved without using organic solvents for *in vitro* analysis.

CRediT authorship contribution statement

Petra Šalamúnová: investigation, writing original draft, visualization; **Lucie Čupalová**: investigation, writing original draft; **Monika Majerská**: investigation; **Jakub Tremil**: investigation; **Gabriela Ruphuy**: investigation; **Karel Šmejkal**: investigation, writing revision; **František Štěpánek**: conceptualization; **Jaroslav Hanuš**: conceptualization, visualization, supervision, funding acquisition, writing revision; **Jan Hošek**: conceptualization, supervision, project administration, funding acquisition, writing original draft, writing revision.

Declaration of competing interest

The authors declare no competing interest.

Acknowledgement

This work was supported by grant no. 16-27522A from the Ministry of Health of the Czech Republic (<http://www.azvcr.cz>), by the Ministry of Education, Youth and Sports of the Czech Republic under the project "FIT" CZ.02.1.01/0.0/0.0/15_003/0000495, and Czech Ministry of Agriculture grant no. RO0518.

Appendix A. Supplementary material

Supplementary material to this article can be found online at <https://doi.org/10.1016/j.ijbiomac.2020.12.107>.

References

- [1] D.J. Newman, G.M. Cragg, Natural products as sources of new drugs from 1981 to 2014, *J. Nat. Prod.* 79 (3) (2016) 629–661, <https://doi.org/10.1021/acs.jnatprod.5b01055>.
- [2] L. Rubio, M.J. Motilva, M.P. Romero, Recent advances in biologically active compounds in herbs and spices: a review of the most effective antioxidant and anti-inflammatory active principles, *Crit. Rev. Food Sci. Nutr.* 53 (9) (2013) 943–953, <https://doi.org/10.1080/10408398.2011.574802>.
- [3] A.G. Muller, S.D. Sarker, I.Y. Saleem, G.A. Hutcheon, Delivery of natural phenolic compounds for the potential treatment of lung cancer, *Daru* 27 (1) (2019) 433–449, <https://doi.org/10.1007/s40199-019-00267-2>.
- [4] H. Teng, L. Chen, Polyphenols and bioavailability: an update, *Crit. Rev. Food Sci. Nutr.* 59 (13) (2019) 2040–2051, <https://doi.org/10.1080/10408398.2018.1437023>.
- [5] C. Puglia, M.R. Lauro, G.G. Tirendi, G.E. Fassari, C. Carbone, F. Bonina, G. Puglisi, Modern drug delivery strategies applied to natural active compounds, *Expert Opin Drug Deliv.* 14 (6) (2017) 755–768, <https://doi.org/10.1080/17425247.2017.1234452>.
- [6] I. Saloň, J. Hanuš, P. Ulbrich, F. Štěpánek, Suspension stability and diffusion properties of yeast glucan microparticles, *Food Bioprod. Process.* 99 (Supplement C) (2016) 128–135, <https://doi.org/10.1016/j.fbp.2016.04.010>.
- [7] T.H. Nguyen, G.H. Fleet, P.L. Rogers, Composition of the cell walls of several yeast species, *Appl. Microbiol. Biot.* 50 (2) (1998) 206–212, <https://doi.org/10.1007/s002530051278>.
- [8] C. Sabu, P. Mufeedha, K. Pramod, Yeast-inspired drug delivery: biotechnology meets bioengineering and synthetic biology, *Expert Opin Drug Deliv.* 16 (1) (2019) 27–41, <https://doi.org/10.1080/17425247.2019.1551874>.
- [9] Y. Xie, X. Hu, H. He, F. Xia, Y. Ma, J. Qi, X. Dong, W. Zhao, Y. Lu, W. Wu, Tracking translocation of glucan microparticles targeting M cells: implications for oral drug delivery, *J. Mater. Chem. B* 4 (17) (2016) 2864–2873, <https://doi.org/10.1039/C5TB02706C>.

Fig. 4. Effects of pure compounds 1–5, empty glucan particles (GPs), their mixtures (Mix), and composites prepared by spray drying (A–C) or rotary evaporation (D–F) on the production of ROS. THP-1-XBlue™-MD2-CD14 cells were pre-treated for 1 h with the test compounds (1 μM resuspended in RPMI 1640 medium), empty GPs (670 $\mu\text{g}/\text{mL}$), a mixture of GPs and suspensions of the pure compound (670 $\mu\text{g}/\text{mL}$ of GPs and 1 μM of pure compound), composites (670 $\mu\text{g}/\text{mL}$), or with the vehicle (RPMI 1640 medium) only (vehicle and CTRL). After 1 h (A, D) and 24 h (B, E), the amount of ROS produced was determined by a test with H₂DCF-DA. The antioxidant activity was measured after 1 h of pre-treatment with the test material followed by a 4 h incubation with pyocyanin (C, F). The results are expressed as the mean \pm SE for five independent experiments measured in triplicate. * Indicates a significant difference in comparison with the vehicle-treated cells $p < 0.05$, ** indicates $p < 0.01$, *** indicates $p < 0.001$, **** corresponds to $p < 0.0001$; # indicates a significant difference between particular groups $p < 0.05$, ## indicates $p < 0.01$, ### indicates $p < 0.001$.

- [10] M.R. Neutra, E. Pringault, J.P. Kraehenbuhl, Antigen sampling across epithelial barriers and induction of mucosal immune responses, *Annu. Rev. Immunol.* 14 (1996) 275–300, <https://doi.org/10.1146/annurev.immunol.14.1.275>.
- [11] M. Aouadi, G.J. Tesz, S.M. Nicoloso, M. Wang, M. Chouinard, E. Soto, G.R. Ostroff, M.P. Czech, Orally delivered siRNA targeting macrophage Map4k4 suppresses systemic inflammation, *Nature* 458 (7242) (2009) 1180–1184, <https://doi.org/10.1038/nature07774>.
- [12] X. Zhou, X.J. Zhang, S.L. Han, Y. Dou, M.Y. Liu, L. Zhang, J.W. Guo, Q. Shi, G.H. Gong, R.B. Wang, J. Hu, X.H. Li, J.X. Zhang, Yeast microcapsule-mediated targeted delivery of diverse nanoparticles for imaging and therapy via the oral route, *Nano Lett.* 17 (2) (2017) 1056–1064, <https://doi.org/10.1021/acs.nanolett.6b04523>.
- [13] S.M. Chen, J. Wang, H. Cheng, W.J. Guo, M. Yu, Q. Zhao, Z.Z. Wu, L.Q. Zhao, Z.N. Yin, Z.Y. Hong, Targeted delivery of NK007 to macrophages to treat colitis, *J. Pharm. Sci.-US* 104 (7) (2015) 2276–2284, <https://doi.org/10.1002/jps.24473>.
- [14] B. Du, C. Lin, Z. Bian, B. Xu, An insight into anti-inflammatory effects of fungal beta-glucans, *Trends Food Sci. Technol.* 41 (1) (2015) 49–59, <https://doi.org/10.1016/j.tifs.2014.09.002>.
- [15] D.L. Williams, Overview of (1 → 3)-beta-D-glucan immunobiology, *Mediat. Inflamm.* 6 (4) (1997) 247–250, <https://doi.org/10.1080/09629359791550>.
- [16] M. Divya, N. Gopi, A. Iswarya, M. Govindarajan, N.S. Alharbi, S. Kadaikunnan, J.M. Khaled, T.N. Almana, B. Vaseeharan, β -glucan extracted from eukaryotic single-celled microorganism *Saccharomyces cerevisiae*: dietary supplementation and enhanced ammonia stress tolerance on *Oreochromis mossambicus*, *Microb. Pathog.* 139 (2020), 103917, <https://doi.org/10.1016/j.micpath.2019.103917>.
- [17] R. De Smet, L. Allais, C.A. Cuvelier, Recent advances in oral vaccine development: yeast-derived beta-glucan particles, *Human vaccines & immunotherapeutics* 10 (5) (2014) 1309–1318, <https://doi.org/10.4161/hv.28166>.
- [18] V.K. Berner, M.E. Sura, K.W. Hunter, Conjugation of protein antigen to microcapsulate beta-glucan from *Saccharomyces cerevisiae*: a new adjuvant for intradermal and oral immunizations, *Appl. Microbiol. Biot.* 80 (6) (2008) 1053–1061, <https://doi.org/10.1007/s00253-008-1618-8>.
- [19] Y.K. Wang, Y.T. Wang, F.M. You, J.X. Xue, Novel use for old drugs: the emerging role of artemisinin and its derivatives in fibrosis, *Pharmacol. Res.* 157 (2020), 104829, <https://doi.org/10.1016/j.phrs.2020.104829>.
- [20] Z. Lin, C. Lin, C.C. Fu, H.W. Lu, H.D. Jin, Q. Chen, J. Pan, The protective effect of Ellagic acid (EA) in osteoarthritis: An in vitro and in vivo study, *Biomed. Pharmacother.* 125 (2020), 109845, <https://doi.org/10.1016/j.biopha.2020.109845>.
- [21] D. Mereles, W. Hunstein, Epigallocatechin-3-gallate (EGCG) for clinical trials: more pitfalls than promises? *Int. J. Mol. Sci.* 12 (9) (2011) 5592–5603, <https://doi.org/10.3390/ijms12095592>.
- [22] Z. Vochyanova, M. Pokorna, D. Rotrekl, V. Smekal, P. Fictum, P. Suchy, J. Gajdzio, K. Smejkal, J. Hosek, Prenylated flavonoid morusin protects against TNBS-induced colitis in rats, *PLoS One* 12 (8) (2017), e0182464, <https://doi.org/10.1371/journal.pone.0182464>.
- [23] E.J. Park, J.M. Pezzuto, The pharmacology of resveratrol in animals and humans, *Biochimica Et Biophysica Acta-Molecular Basis of Disease* 1852 (6) (2015) 1071–1113, <https://doi.org/10.1016/j.bbadis.2015.01.014>.
- [24] Z. Plavcova, P. Salamonova, I. Salon, F. Stepanek, J. Hanus, J. Hosek, Curcumin encapsulation in yeast glucan particles promotes its anti-inflammatory potential in vitro, *Int. J. Pharm.* 568 (2019), 118532, <https://doi.org/10.1016/j.ijpharm.2019.118532>.
- [25] V. Brezani, V. Lelakova, S.T.S. Hassan, K. Berchova-Bimova, P. Novy, P. Kloucek, P. Marsik, S. Dall'Acqua, J. Hosek, K. Smejkal, Anti-infectivity against herpes simplex virus and selected microbes and anti-inflammatory activities of compounds isolated from *Eucalyptus globulus* Labill, *Viruses* 10 (7) (2018) <https://doi.org/10.3390/v10070360>.
- [26] G. Ruphuy, I. Salon, J. Tomas, P. Salamonova, J. Hanus, F. Stepanek, Encapsulation of poorly soluble drugs in yeast glucan particles by spray drying improves dispersion and dissolution properties, *Int. J. Pharm.* 576 (2020), 118990, <https://doi.org/10.1016/j.ijpharm.2019.118990>.
- [27] A.A. Lapkin, A. Walker, N. Sullivan, B. Khambay, B. Mlambo, S. Chemat, Development of HPLC analytical protocols for quantification of artemisinin in biomass and extracts, *J. Pharm. Biomed. Anal.* 49 (4) (2009) 908–915, <https://doi.org/10.1016/j.jpba.2009.01.025>.
- [28] S.T. Saito, A. Welzel, E.S. Suyenaga, F. Bueno, A method for fast determination of epigallocatechin gallate (EGCG), epicatechin (EC), catechin (C) and caffeine (CAF) in green tea using HPLC, *Food Science and Technology* 26 (2006) 394–400, <https://doi.org/10.1590/s0101-20612006000200023>.
- [29] Z. Hromadkova, A. Ebringerova, V. Sasinkova, J. Sandula, V. Hribalova, J. Omelkova, Influence of the drying method on the physical properties and immunomodulatory activity of the particulate (1 → 3)-beta-D-glucan from *Saccharomyces cerevisiae*, *Carbohydr. Polym.* 51 (1) (2003) 9–15, [https://doi.org/10.1016/S0144-8617\(02\)00110-8](https://doi.org/10.1016/S0144-8617(02)00110-8).
- [30] V. Zechner-Krpan, V. Petrávič-Tominac, P. Galović, V. Galović, J. Filipović-Grčić, S. Srećec, Application of different drying methods on β -glucan isolated from spent brewer's yeast using alkaline procedure, *Agric. Conspec. Sci.* 75 (1) (2014) 45–50 (doi).
- [31] Y. Sun, X.D. Shi, X. Zheng, S.P. Nie, X.J. Xu, Inhibition of dextran sodium sulfate-induced colitis in mice by baker's yeast polysaccharides, *Carbohydr. Polym.* 207 (2019) 371–381, <https://doi.org/10.1016/j.carbpol.2018.11.087>.
- [32] M. Zhang, X. Jin, Y.F. Yang, beta-Glucan from *Saccharomyces cerevisiae* induces SBD-1 production in ovine ruminal epithelial cells via the Dectin-1-Syk-NF-kappa B signaling pathway, *Cell. Signal.* 53 (2019) 304–315, <https://doi.org/10.1016/j.cellsig.2018.10.018>.
- [33] J. Battle, T.Z. Ha, C.F. Li, V. Della Beffa, P. Rice, J. Kalbfleisch, W. Browder, D. Williams, Ligand binding to the (1 → 3)-beta-D-glucan receptor stimulates NF kappa B activation, but not apoptosis in U937 cells, *Biochem. Biophys. Res. Commun.* 249 (2) (1998) 499–504, <https://doi.org/10.1006/bbrc.1998.9175>.
- [34] W.B. Yao, F. Wang, H. Wang, Immunomodulation of artemisinin and its derivatives, *Sci. Bull.* 61 (18) (2016) 1399–1406, <https://doi.org/10.1007/s11434-016-1105-z>.
- [35] S.C. Gupta, A.K. Tyagi, P. Deshmukh-Taskar, M. Hinojosa, S. Prasad, B.B. Aggarwal, Downregulation of tumor necrosis factor and other proinflammatory biomarkers by polyphenols, *Arch. Biochem. Biophys.* 559 (2014) 91–99, <https://doi.org/10.1016/j.abb.2014.06.006>.
- [36] G.R. Shi, L.Q. Rao, H.Z. Yu, H. Xiang, H. Yang, R. Ji, Stabilization and encapsulation of photosensitive resveratrol within yeast cell, *Int. J. Pharm.* 349 (1–2) (2008) 83–93, <https://doi.org/10.1016/j.ijpharm.2007.07.044>.
- [37] V. Vetrivcka, T. Volny, S. Saraswat-Ohri, A. Vashista, Z. Vancikova, J. Vetrivcka, Glucan and resveratrol complex—possible synergistic effects on immune system, *Biomed. Pap. Med. Fac. Univ. Palacky Olomouc Czech Repub.* 151 (1) (2007) 41–46, <https://doi.org/10.5507/bp.2007.007>.
- [38] H.M. Li, G.C. Ou, Y.L. He, L. Ren, X.H. Yang, M. Zeng, Resveratrol attenuates the MSU crystal-induced inflammatory response through the inhibition of TAK1 activity, *Int. Immunopharmacol.* 67 (2019) 62–68, <https://doi.org/10.1016/j.intimp.2018.12.004>.
- [39] S.N. Sun, M.J. Zhang, Q.B. Yang, Z.Y. Shen, J.H. Chen, B. Yu, H. Wang, J.L. Qu, D.X. Pang, W.Z. Ren, H.S. Ouyang, X.C. Tang, Resveratrol suppresses lipoprotein-associated phospholipase A(2) expression by reducing oxidative stress in macrophages and animal models, *Mol. Nutr. Food Res.* 61 (10) (2017), 1601112, <https://doi.org/10.1002/mnfr.201601112>.
- [40] L. Feng, R. Yasmeen, N.W. Schoene, K.Y. Lei, T.T.Y. Wang, Resveratrol differentially modulates immune responses in human THP-1 monocytes updates and macrophages, *Nutr. Res.* 72 (2019) 57–69, <https://doi.org/10.1016/j.nutres.2019.10.003>.
- [41] H. Tani, S. Hikami, S. Iizuna, M. Yoshimatsu, T. Asama, H. Ota, Y. Kimura, T. Tatefuji, K. Hashimoto, K. Higaki, Pharmacokinetics and safety of resveratrol derivatives in humans after oral administration of melinjo (*Gnetum gnemon* L.) seed extract powder, *J. Agr. Food Chem.* 62 (8) (2014) 1999–2007, <https://doi.org/10.1021/jf4048435>.
- [42] L. Almeida, M. Vaz-da-Silva, A. Falcao, E. Soares, R. Costa, A.I. Loureiro, C. Fernandes-Lopes, J.F. Rocha, T. Nunes, L. Wright, P. Soares-da-Silva, Pharmacokinetic and safety profile of trans-resveratrol in a rising multiple-dose study in healthy volunteers, *Mol. Nutr. Food Res.* 53 (2009) S7–S15, <https://doi.org/10.1002/mnfr.200800177>.
- [43] K. R  th, K. Taxis, G. Walz, C.H. Gleiter, S.-M. Li, L. Heide, Pharmacokinetic study of artemisinin after oral intake of a traditional preparation of *Artemisia annua* L. (annual wormwood), *The American Journal of Tropical Medicine and Hygiene* 70 (2) (2004) 128–132, <https://doi.org/10.4269/ajtmh.2004.70.128>.
- [44] M. Ashton, T. Gordi, T.N. Hai, N. Van Huong, N.D. Sy, N.T. Nieu, D.X. Huong, M. Johansson, L.D. C  ng, Artemisinin pharmacokinetics in healthy adults after 250, 500 and 1000 mg single oral doses, *Biopharm. Drug Dispos.* 19 (4) (1998) 245–250, [https://doi.org/10.1002/\(sici\)1099-081x\(199805\)19:4<245::aid-bdd99>3.0.co;2-z](https://doi.org/10.1002/(sici)1099-081x(199805)19:4<245::aid-bdd99>3.0.co;2-z).
- [45] D. Rotrekl, B. Devriendt, E. Cox, L. Kavanova, M. Faldyna, P. Salamonova, Z. Bad  , V. Prokopec, F. Stepanek, J. Hanus, J. Hosek, Glucan particles as suitable carriers for the natural anti-inflammatory compounds curcumin and diaplacene – evaluation in an ex vivo model, *Int. J. Pharm.* 582 (2020), 119318, <https://doi.org/10.1016/j.ijpharm.2020.119318>.
- [46] Y. Sun, B.C. Duan, H.H. Chen, X.J. Xu, A novel strategy for treating inflammatory bowel disease by targeting delivery of methotrexate through glucan particles, *Adv. Healthc. Mater.* 9 (6) (2020), 1901805, <https://doi.org/10.1002/adhm.201901805>.
- [47] X. Zhou, K.J. Ling, M.Y. Liu, X.J. Zhang, J. Ding, Y. Dong, Z.Q. Liang, J.J. Li, J.X. Zhang, Targeted delivery of cisplatin-derived nanoprecursors via a biomimetic yeast microcapsule for tumor therapy by the oral route, *Theranostics* 9 (22) (2019) 6568–6586, <https://doi.org/10.7155/thno.35353>.
- [48] X. Zhang, X. Xu, Y. Chen, Y. Dou, X. Zhou, L. Li, C. Li, H. An, H. Tao, H. Hu, X. Li, J. Zhang, Bioinspired yeast microcapsules loaded with self-assembled nanotherapies for targeted treatment of cardiovascular disease, *Mater. Today* 20 (6) (2017) 301–313, <https://doi.org/10.1016/j.mattod.2017.05.006>.

6.12. ARTICLE 12

Nykodýmová, D.; Molčanová, L.; Kotouček, J.; Mašek, J.; **Treml, J.** ChemistryOpen 2025, doi: 10.1002/open.202500209 (IF=3.100).

PPAR γ Agonistic Activity of Mimulone and Diplacone Encapsulated in Liposomes and Cyclodextrin Complexes

Daniela Nykodýmová,* Lenka Molčanová, Jan Kotouček, Josef Mašek, and Jakub Tremel

The therapeutic application of flavonoids is limited by their low solubility, bioavailability, and metabolic stability. This study evaluates the peroxisome proliferator-activated receptor gamma (PPAR γ) agonistic activity of two geranylated flavonoids from *Paulownia tomentosa*, mimulone and diplacone, and compares the efficacy of different nanoparticle delivery systems, including liposomes and cyclodextrins, in preserving their biological activity. Using the PPAR γ CALUX reporter gene assay, it is shown that mimulone dissolved in DMSO and incubated with cell culture activates the PPAR γ pathway, resulting in 2.97-fold and 3.9-fold increases in luciferase activity at concentrations of 5 and 2.5 μ M, respectively. Diplacone, however, shows significant cytotoxicity, with an average

cell viability of about 10% at 10 μ M. Encapsulation in anionic, cationic, and neutral liposomes results in a significant reduction of biological activity of both flavonoids, with the best formulation (anionic liposomes) preserving only 54% of mimulone's activity. In contrast, hydroxypropyl- β -cyclodextrins (HP- β -CDs) retain up to 91.5% of mimulone's biological activity and significantly improve the viability profile of diplacone, maintaining cell viability at \approx 100%. The performance of the HP- β -CDs can be attributed to their ability to form stable inclusion complexes with hydrophobic molecules. These results suggest that cyclodextrin-based delivery systems might effectively address solubility and stability challenges associated with flavonoid therapy.

1. Introduction

Flavonoids are polyphenolic natural compounds with diverse biological activities and their therapeutic potential is well-documented, including evidence of benefits in metabolic and inflammatory disorders. However, wide clinical application has been limited by some of their properties, such as low solubility, bioavailability, and metabolic stability. The low water solubility and rapid metabolic elimination of flavonoids necessitate the development of novel delivery systems to improve their therapeutic efficacy.^[1] Many flavonoids have shown a potential to influence glucose metabolism by modulating the peroxisome proliferator-activated receptor gamma (PPAR γ).^[2] Previous studies

have demonstrated that geranylated flavonoids from *Paulownia tomentosa* Steud. (Paulowniaceae), such as mimulone and diplacone, exhibit potent biological activities, including the inhibition of protein tyrosine phosphatase 1B and α -glucosidase.^[3] Based on these results, we investigated whether these compounds can also modulate glucose metabolism via activation of the PPAR γ pathway.

PPARs are ligand-inducible transcription factors that play crucial roles in glucose and lipid metabolism, adipogenesis, and anti-inflammatory responses.^[4] There are three isoforms of PPARs: PPAR α , PPAR β/δ , and PPAR γ .^[5,6] As nonsteroidal nuclear receptors, PPARs are located predominantly in the nucleus, where they form heterodimers with the retinoid X receptor (RXR).^[7] In their ligand-free state, PPAR-RXR heterodimers are bound to corepressor proteins and remain inactive. Upon binding a ligand, a conformational change releases the corepressors, switching the complex to its active state, where it binds to specific DNA sequences called peroxisome proliferator response elements and regulates gene transcription.^[6, 8] Activation of PPAR γ isoform by specific ligands leads to changes in gene expression that improve insulin sensitivity, fatty acid storage, and glucose homeostasis, making it an important therapeutic target for type 2 diabetes and related metabolic syndromes. While synthetic PPAR γ agonists, such as rosiglitazone (a member of the thiazolidinedione (TZD) class), are effective in enhancing insulin sensitivity, TZDs are associated with notable side effects, including cardiovascular risks and weight gain, which have limited their use in long-term therapy.^[2,9,10] The need for safer alternatives has increased interest in identifying natural product agonists and partial agonists that may offer similar benefits with reduced adverse effects. Some flavonoids have shown potential as selective PPAR γ modulators

D. Nykodýmová, J. Tremel
Department of Molecular Pharmacy
Faculty of Pharmacy
Masaryk University
Palackého tř. 1946/1, 612 00 Brno, Czech Republic
E-mail: nykodymovad@pharm.muni.cz

L. Molčanová
Department of Natural Drugs
Faculty of Pharmacy
Masaryk University
Palackého tř. 1946/1, 612 00 Brno, Czech Republic

J. Kotouček, J. Mašek
Department of Pharmacology and Toxicology
Veterinary Research Institute
Hudcova 296/70, 621 00 Brno, Czech Republic

Supporting information for this article is available on the WWW under <https://doi.org/10.1002/open.202500209>

© 2025 The Author(s). ChemistryOpen published by Wiley-VCH GmbH. This is an open access article under the terms of the Creative Commons Attribution License, which permits use, distribution and reproduction in any medium, provided the original work is properly cited.

(SPPARMS), which may activate PPAR γ pathways with partial agonist activity, thereby reducing unwanted side effects seen with full agonists like rosiglitazone.^[2]

Liposomes are highly effective drug delivery systems for flavonoids, capable of improving their solubility, stability, and bioavailability. Recent research has made significant progress in this field, providing innovative solutions for efficiently delivering these bioactive compounds in various applications.^[11–13] The interaction and encapsulation of the flavonoids and liposomal particles involve hydrophobic interactions within the lipid bilayer and hydrophilic interactions through hydrogen bonding with the polar head groups of the lipids at the membrane interface.^[14] These interactions significantly influence the encapsulation efficiency (EE) and release rates of flavonoids from the liposomes. However, overly strong interactions between flavonoids and the liposomal structure can present a limitation, potentially reducing therapeutic efficacy. To address this limitation, we explored cyclodextrins as an alternative drug delivery system. In addition to liposomes, cyclodextrins have emerged as another promising platform for encapsulating flavonoids to address their inherent challenges of poor solubility, stability, and bioavailability. Recent studies have focused on the interactions between flavonoids and cyclodextrins, leveraging the unique molecular structure of cyclodextrins to form inclusion complexes with these bioactive compounds.^[15–19]

The aim of this study was to evaluate the PPAR γ -agonistic activity of mimulone and diplacone *in vitro* and to compare the efficacy of different nanoparticle delivery systems in maintaining their biological activity. In particular, the main objective was to identify the most effective nanoparticle system—among anionic, cationic, and neutral liposomes and cyclodextrins—for encapsulating these geranylated flavonoids and enhancing their bioavailability and stability.

2. Results and Discussion

2.1. Nanoparticle Analysis

The characterization of the nanoparticles, as determined by dynamic light scattering (DLS) and ultraviolet-visible (UV–VIS) spectroscopy, is summarized in Table 1. UV–VIS spectroscopy further confirmed the encapsulation of the active compound in the nanoparticles, with the corresponding absorbance peaks used to calculate the EE values. The methodology took advantage of the poor water solubility of the active compound, as mimulone does not exhibit UV–VIS absorbance when unsolubilized. This inherent property ensured that only the solubilized fraction of the compound contributed to the UV–VIS measurements, enabling accurate determination of EE. Furthermore, any unsolubilized aggregates were removed by filtration to eliminate potential interference. The DLS characterization of the liposomes revealed that the average hydrodynamic radius for all liposomal samples, except for the blank neutral liposomes, was ≈ 154 nm. The blank neutral liposomes exhibited a relatively higher hydrodynamic radius of 194 ± 2 nm. All liposomal samples demonstrated low polydispersity index (PDI) values below 0.15, indicating a narrow size distribution. The distribution analysis, intensity, and number exhibit the narrow profiles of the particle size distribution (the data are available in Appendix A, Figure S1–S5, Supporting Information). The detailed distribution data show that the liposomal samples maintained a consistent and uniform size range, further confirming the reliability and stability of the formulations under the test conditions. The ζ -potential for neutral liposomes remained consistent regardless of the presence or absence of mimulone. In contrast, anionic liposomes (AL) with high mimulone concentration showed a slight increase in ζ -potential from -26.1 ± 2.0 mV for empty liposomes to -23.3 ± 1.8 mV for high mimulone concentrations. For cationic liposomes, the ζ -potential

Table 1. Characterization of nanoparticles by DLS including hydrodynamic radius (Z-average), PDI, concentration (particles mL⁻¹), and ζ (zeta potential) measured in mV. The concentration refers to the final concentration of mimulone, with 51 and 204 $\mu\text{g mL}^{-1}$ representing low and high concentrations, respectively, in the case of liposomes. In the case of cyclodextrins (HP- β -CDs), the low concentration represents 51 $\mu\text{g mL}^{-1}$ and high (*) 510 $\mu\text{g mL}^{-1}$ of mimulone and diplacone, respectively. The encapsulation efficiency (EE%) was determined from the UV–VIS data.

Sample	Concentration	Z-Average [d nm]	Polydispersity index (PI)	Concentration [particles mL ⁻¹]	ζ [mV]	EE [%]
Neutral liposomes	Low	156 \pm 3	0.085 \pm 0.029	9.12 \pm 1.48 $\cdot 10^{10}$	2.1 \pm 0.2	27
	High	168 \pm 1	0.079 \pm 0.019	3.01 \pm 0.06 $\cdot 10^{11}$	1.4 \pm 0.8	77
	Blank	194 \pm 2	0.104 \pm 0.018	3.64 \pm 0.18 $\cdot 10^{10}$	1.3 \pm 0.3	–
Anionic liposomes	Low	153 \pm 1	0.127 \pm 0.003	2.89 \pm 0.39 $\cdot 10^{11}$	-26.6 \pm 0.6	42
	High	145 \pm 1	0.138 \pm 0.013	4.06 \pm 0.48 $\cdot 10^{11}$	-23.3 \pm 1.8	60
	Blank	152 \pm 1	0.123 \pm 0.006	3.33 \pm 0.08 $\cdot 10^{11}$	-26.1 \pm 2.0	–
Cationic liposomes	Low	166 \pm 1	0.105 \pm 0.013	2.44 \pm 0.05 $\cdot 10^{11}$	18.0 \pm 1.2	82
	High	161 \pm 1	0.112 \pm 0.007	3.55 \pm 0.13 $\cdot 10^{11}$	14.9 \pm 1.3	51
	Blank	167 \pm 1	0.098 \pm 0.016	2.32 \pm 0.17 $\cdot 10^{11}$	18.5 \pm 0.9	–
HP- β -CD-mimulone	Low	3 \pm 0	0.242 \pm 0.005	5.71 \pm 3.17 $\cdot 10^{17}$	–	101
	High*	3 \pm 0	0.237 \pm 0.003	4.98 \pm 1.35 $\cdot 10^{17}$	–	52
	Blank	2 \pm 0	0.166 \pm 0.015	1.40 \pm 0.31 $\cdot 10^{18}$	–	–
HP- β -CD-diplacone	Low	2 \pm 0	0.203 \pm 0.003	2.05 \pm 2.20 $\cdot 10^{18}$	–	91
	High*	12 \pm 8	0.323 \pm 0.026	1.07 \pm 0.89 $\cdot 10^{18}$	–	33

values were 18.0 ± 1.2 mV at low mimulone concentrations and 14.9 ± 1.3 mV at high mimulone concentration, indicating a decrease in the surface charge compared to the empty liposomes, where the ζ -potential value was 18.5 ± 0.9 mV. This suggests that a portion of the active compound could be bound to the surface of the particles.

In the case of hydroxypropyl- β -cyclodextrins (HP- β -CDs), the particle size was consistently uniform at ≈ 3 nm in diameter across all measured samples. However, the PDI was relatively higher, around 0.2, indicating the presence of some larger entities. The higher PDI in the samples containing mimulone or diplacone indicates that the presence of an active compound contributes to the formation of these aggregates. The blank samples had a lower PDI of 0.166 ± 0.015 . The distribution analysis (the data are available in Appendix A, Figure S4–S5, Supporting Information) shows that while larger particles were present, the majority of the particles remained uniformly small. This suggests that HP- β -CD forms primarily small particles with a minor population of larger aggregates.

To visualize the uptake of neutral and cationic liposomes, the fluorescent probe Liss Rhodamine was incorporated into

the membranes of empty liposomes (without mimulone). From images A and C in Figure 1, it is evident that after 8 h of incubation, a strong fluorescent signal was observed for liposomes with a zeta potential close to 0 mV. This indicates significant cellular uptake for these neutral liposomes. In contrast, for the test cationic liposomes shown in Figure 1B,D, with a zeta potential of ≈ 18 mV, the uptake by cells was noticeably lower compared to the PEGylated liposomes. Despite the positive surface charge, which generally promotes interaction with negatively charged cell membranes, the cationic liposomes did not exhibit the same level of cellular uptake as the PEGylated counterparts. Although AL were not visualized in this study, the primary purpose of the visualization tests was to confirm that the reduced biological activity of mimulone was not due to a lack of liposome entry into the cells. The results demonstrated that, even with cationic and PEGylated liposomes, which showed low biological activity for mimulone, there was significant particle uptake by the cells following incubation. This indicates that the liposomes were indeed internalized, suggesting that the reduced biological activity of mimulone is not due to insufficient cellular uptake.

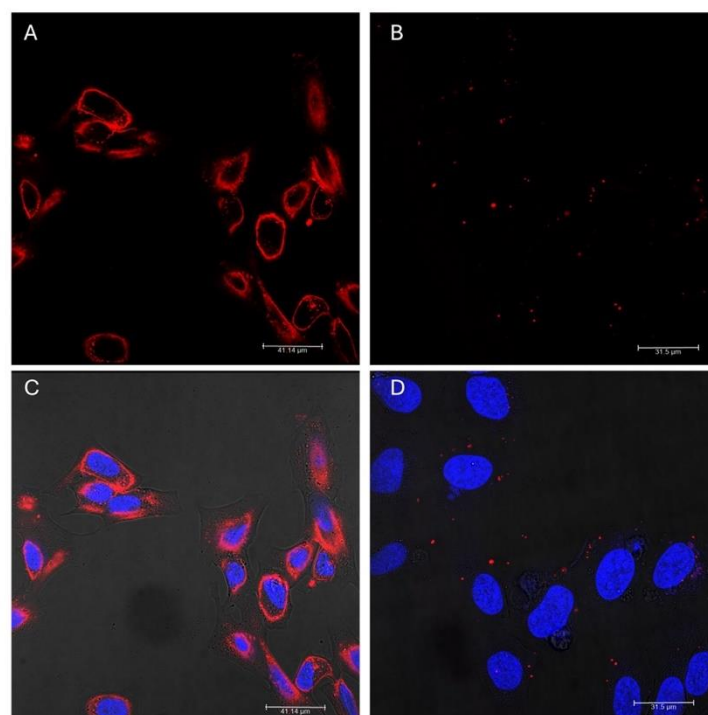


Figure 1. Confocal fluorescence microscopy images of PPAR- γ 2 CALUX cells after 8 h of incubation with neutral and cationic liposomes containing 0.1 mol% of the fluorescent probe 18:1 Liss Rhod PE. A,C) Neutral liposomes consisted of EPC/Chol./DC-Chol./DSPE-PEG-2000 (55/40/25/5); B,D) cationic liposomes were composed of EPC/DC-Chol (80/20) : (A,B) Liposomes within the cells, showing the distribution and localization of the fluorescently labeled liposomes; (C,D) merged images combining liposome (red) and nuclei (blue) fluorescence signals.

2.2. Cytotoxicity Assay

The ability of the test compounds (TC) to affect cell viability (cytotoxic effect) was assessed using the water-soluble tetrazolium salt (WST-1) method, and the results were compared between the compounds alone and the compounds incorporated into nanoparticles. The aim was to determine whether the encapsulation process of the TC could influence (or potentially reduce) their cytotoxic effect. The WST-1 assay results on PPAR- γ 2 CALUX cells indicate significant differences in cell viability between the TC and their encapsulated forms. As shown in Figure 2A, mimulone dissolved in DMSO maintained cell viability at $\approx 100\%$ across all concentrations tested, similar to the control, and indicating no significant cytotoxic effects. In contrast, diplacone exhibited greater cytotoxicity, with an average cell viability of about 10% at $10\text{ }\mu\text{M}$. Rosiglitazone also demonstrated a decrease in cell viability but still preserved its high biological activity as a full PPAR γ agonist in subsequent experiments. Figure 2B shows that AL caused the greatest reduction in cell viability among all of the liposome formulations tested. Nevertheless, the biological effect of encapsulated mimulone on activation of the PPAR γ pathway was the highest with AL. In Figure 2C, all cyclodextrin formulations, including their combinations with the TC, maintained cell

viability around 100%. This improvement in viability profile was observed for all concentrations of diplacone when it was analyzed as cyclodextrin-encapsulated diplacone versus pure diplacone. The cyclodextrin-encapsulated mimulone combination (CD-M, $10\text{ }\mu\text{M}$) was an exception, showing a lower average viability and a higher standard deviation compared to other combinations, with no clear explanation for this variability. These observations emphasize the varying impacts of nanoparticle systems on cell viability and their potential to influence the biological activity of the TC.

2.3. PPAR γ Agonistic Activity of the TC (without Encapsulation)

First, we evaluated the ability of the compounds to activate the PPAR γ pathway independently at two concentrations: 2.5 and $5\text{ }\mu\text{M}$. Rosiglitazone was used as a positive control at the same concentrations as the TC. The results of these experiments are summarized in Figure 3, with the luciferase activity expressed as a fold change relative to the negative control (DMSO).

Our findings indicate that mimulone exhibited PPAR γ agonistic activity at both concentrations: $5\text{ }\mu\text{M}$ (2.97-fold) and $2.5\text{ }\mu\text{M}$

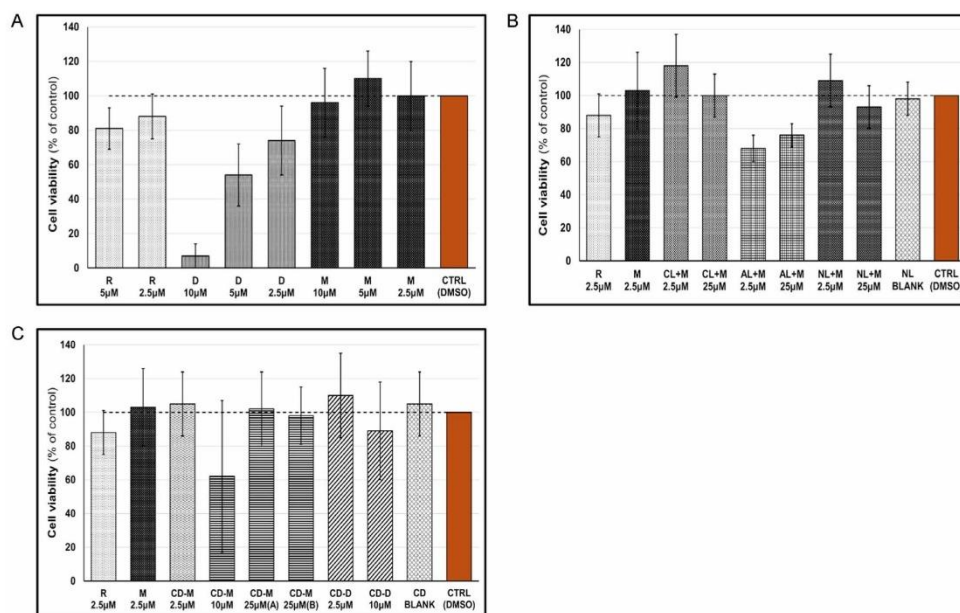


Figure 2. The effect of the TC on the viability of PPAR- γ 2 CALUX cells. The cell viability was measured using the WST method and assessed for free compounds and nanoparticle combinations. A) TC dissolved in DMSO. B) TC encapsulated into liposomes. C) TC encapsulated into HP- β -cyclodextrins. R = rosiglitazone; M = mimulone; D = diplacone. Liposomes: cationic (CL), anionic (AL), and neutral (NL); CD refers to HP- β -cyclodextrins. The letters (M, D) indicate specific combinations with the test compound; the values are the exact concentrations of the test compound used. Two CD-M $25\text{ }\mu\text{M}$ combinations differ in CD composition: 10 mg mL^{-1} (sample A) and 100 mg mL^{-1} (sample B). The results are expressed as the mean \pm SEM ($n = 3$), measured at least in tetraplicate and compared to the negative control group (DMSO; set as 100%).

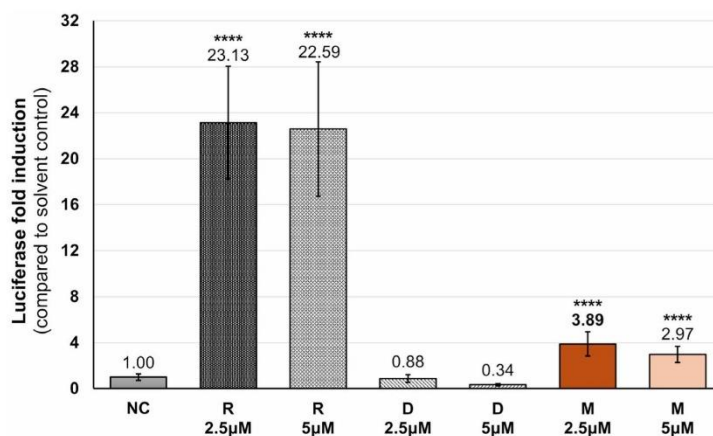


Figure 3. Effect of mimulone (M) and diplacone (D) on activation of the PPAR γ pathway. The luciferase activity was measured by the CALUX reporter gene assay in the PPAR γ 2 CALUX cell line and expressed as fold induction compared to the negative control (i.e., the solvent). Rosiglitazone (R) was used as the standard, DMSO served as the negative control (NC). Values refer to the exact compound concentrations used. The results are expressed as the mean \pm SEM ($n = 3$), measured in tetraplicate. Statistical analysis is based on the Kruskal Wallis test followed by the Bonferroni correction for multiple tests. Asterisks indicate a significant difference from the solvent control: * $p < 0.05$; ** $p < 0.01$; *** $p < 0.001$; and **** $p < 0.0001$.

(3.9-fold), both with statistical significance ($p \leq 0.0001$). Given that the maximum response compared to rosiglitazone at a concentration of 2.5 μ M was only 16.8%, we suspect that mimulone acts as a partial agonist in the observed cellular pathway or that activation occurs through other ligand-independent mechanisms. In contrast, diplacone showed no statistically significant effect at either concentration.

The chemical structure of mimulone, in particular the presence of a hydroxyl group at the C-4 position on the B-ring, likely accounts for its observed biological activity (Figure 4). This feature distinguishes mimulone from diplacone, which has two hydroxyl groups at the ring B. Liang et al. emphasized the importance of hydroxyl groups at positions A-5, A-7, and B-4

for PPAR γ activation. This matches the mimulone substitution pattern, and they also suggested that an additional hydroxyl group at B-3 could reduce PPAR γ activation. This is consistent with our results and the inactivity observed for quercetin and diplacone, both of which contain a B-3 hydroxyl group.^[20] In contrast, another study reported that myricetin, which has additional hydroxyl groups at B-3 and B-5, is a more effective PPAR γ ligand than kaempferol, which has only a B-4 hydroxyl group.^[21] That prenyl group at C-6 may also have an effect on the mimulone activity is supported by a study of sanggenon-type flavanones that found the presence of a prenyl group at C-6 is crucial for PPAR γ agonistic effects.^[22]

The structure of mimulone resembles other prenylated flavanones, such as bavachinin, which also showed substantial PPAR γ agonistic activity.^[23] This study aligned with previous findings in that it confirmed that the prenyl group position C-6 of the A-ring is crucial for PPAR γ agonistic activity. But it also indicated that a methoxyl group at C-7 increases PPAR γ agonist activity, whereas hydroxyl groups, such as these in mimulone, reduce it. However, our results do not support this finding. Mimulone achieved a 3.9-fold activation at a concentration of 2.5 μ M (equivalent to 16.8% of the maximal response of 2.5 μ M rosiglitazone), compared to bavachinin's 13.12-fold activation at 25 μ M (19.1% of the maximal response of 5 μ M rosiglitazone), whereas the concentration of the test compound was five times as higher as that of the positive control.

There is evidence that PPAR γ can be activated through both ligand-dependent and independent mechanisms. The compounds that stimulate PPAR γ in the desired manner, that is, less effect than synthetic agonists and greater effect than weak agonists, are referred to as partial agonists.^[24] Moreover, structural differences among PPAR γ modulators significantly impact their

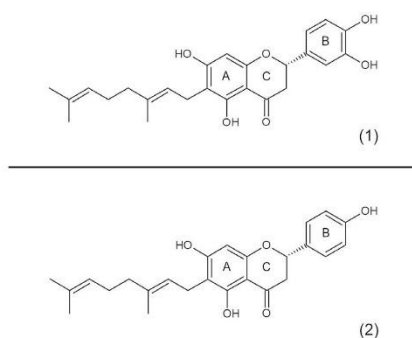


Figure 4. Structures of the TC 1) diplacone and 2) mimulone. The letters A, B, and C denote aromatic and heterocyclic rings according to the conventional nomenclature used for flavonoid scaffolds.

agonistic behavior. Fisetin, for example, acts as a full agonist probably because of its specific structural features.^[25] Fang et al. demonstrated that kaempferol and quercetin act as partial PPAR γ agonists, with maximal responses of less than 45% and 20%, respectively, compared to rosiglitazone.^[26] This aligns with our findings, where the maximal response of mimulone is less than that of rosiglitazone, suggesting a similar partial agonistic mechanism. Similarly, it has been reported that flavonoids extracted from *Melissa officinalis* and *Matricaria chamomilla*/*Matricaria recutita* flowers behave as partial agonists for PPAR γ by activating it with a half-maximal effective concentration (EC₅₀) of 86 mg mL⁻¹ and had 26% of maximal potency as compared to rosiglitazone.^[24,27,28] On the contrary, the competitive binding assays conducted by Beekmann et al. showed that quercetin and kaempferol, despite increasing PPAR γ -mediated gene expression, are not direct agonists of the receptor.^[29] Their action likely involves receptor activation by endogenous agonists and an increase in PPAR γ receptor levels. Additionally, the activation mechanisms of hesperidin and morin provide parallels to mimulone's activity. Hesperidin involves both PPAR γ -dependent and independent mechanisms to exert its effects,^[30] while morin binds to PPAR γ and acts as a moderate ligand.^[31] These findings suggest that the partial agonistic behavior of mimulone might involve a combination of direct receptor interaction and modulation through other pathways or coregulators.

An interesting observation is that the lower of the two concentrations tested (2.5 μ M) achieved more activation of the PPAR γ signaling pathway than the higher concentration (5 μ M). A similar effect was observed for diplacone. A study by Barthel et al. showed the concentration-dependent influence of troglitazone on the insulin-induced expression of fatty acid synthase and the activity of protein kinase B in 3T3-L1 adipocytes. It found increased activity at low concentrations (250 nM) and inhibitory effects at higher concentrations ($\geq 1 \mu$ M). This biphasic response suggests that low concentrations of the compound enhance the activation of the pathway, whereas higher concentrations may inhibit it. The mechanism likely involves the optimal activation of signaling pathways at lower doses and the inhibition of potential feedback or off-target interactions at higher doses.^[32] These findings are comparable to our observations with mimulone and diplacone, where the lower concentration (2.5 μ M) exhibited superior PPAR γ activation compared to the higher concentration (5 μ M).

2.4. PPAR γ Reporter Assay with Mimulone Incorporated into Liposomes

The main limitations of the wider use of flavonoids in therapy include limited solubility, bioavailability, and metabolic stability.^[33] Encapsulation into nanoparticles represents a promising option to improve these characteristics of flavonoids. Following the identification of mimulone efficacy in activating the PPAR γ pathway, our next step was to encapsulate the test substances into various nanoparticle systems. One of the most versatile carriers are liposomes. In a previous study by Brezani et al., various types of

nanocarriers, including cationic, anionic, and pegylated liposomes meant to improve the solubility and bioavailability of poorly soluble lipophilic compounds of macasiamenene F were tested. The formulation of neutral liposomes composed of DC-CHOL/CHOL/EPC/DSPE-PEG 2000 showed high cellular uptake and other desirable properties on various cell lines including THP-1 and THP-1-XBlue-MD2-CD14 monocytes and BV-2 microglia while keeping the anti-inflammatory properties of macasiamenene F.^[34]

In this study, we tested anionic, cationic, and neutral liposomes and two concentrations of the encapsulated compound: one was identical to the active concentration of the pure substance (i.e., 2.5 μ M), the other was ten times as high (25 μ M). AL showed a 2.10-fold induction of PPAR γ activation (AL + 25 μ M mimulone, $p \leq 0.01$ compared to the negative control), indicating effective delivery but with a significant reduction in maximal response compared to free mimulone. The experiments aimed to find the composition of the nanoparticle system that would preserve the maximum biological activity of mimulone, that is, the luciferase activity should not differ significantly from free mimulone. The results with all groups of liposomes are summarized in Figure 5, with luciferase activity expressed as a percentage of the fold change relative to the maximal response of mimulone. The best anionic liposome formulation retained 54% of the biological activity of mimulone. Cationic and neutral liposomes also activated PPAR γ , but their efficacy was lower than that of AL and free mimulone.

One plausible explanation for the reduced efficacy of liposome-encapsulated mimulone is the strong binding of mimulone within the liposome membrane. Due to its smaller and more linear structure (chalcone backbone), mimulone can intercalate easily into the lipid bilayer. The hydroxyl groups present can form hydrogen bonds with the polar head groups of lipids. Similar findings are presented in the work of Wesołowska et al., where prenylated chalcones and flavanones from the common hop were shown to intercalate into DPPC bilayers, decreasing the melting temperature and demonstrating strong interactions with the lipid bilayer. The magnitude of the induced effect correlated with the lipophilicity and structure of the compounds, supporting the idea that smaller and more linear structures can intercalate more easily into lipid bilayers.^[35] Furthermore, the research by Johnston et al. highlights how the structural characteristics of liposomal constituents, including the presence of cholesterol, can modulate the fluidity and stability of the membrane, impacting the encapsulated bioavailability of the drug.^[36] Experimental studies performed by Kerdudo et al. studied the encapsulation of naringenin and rutin in liposomes. In the case of naringenin, a nonprenylated flavonoid, a significant portion was absorbed on the surface of the liposomes rather than encapsulated. This study also indicated that small flavonoids interact through hydrogen bonding with the head groups on the upper part of the phosphatidylcholine membrane.^[37] Sadžak et al. published a study on the interaction of flavonoids with lipid bilayers, showing that the hydroxyl groups of flavonoids can form hydrogen bonds with the polar head groups of lipids.^[38] This interaction was primarily via hydrogen bonds, which is consistent with the proposed mechanism for mimulone. We investigated this

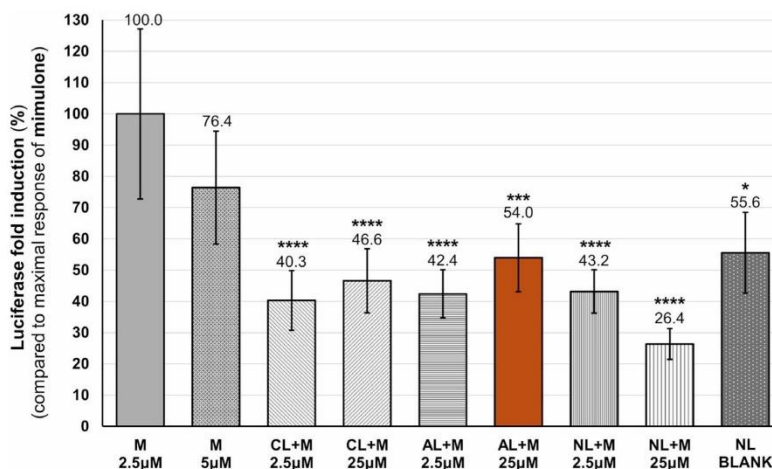


Figure 5. PPAR γ pathway activation of mimulone (M) encapsulated within liposomes. Luciferase activity was measured by the CALUX reporter gene assay, calculated as the fold induction compared to the solvent control (DMSO), and expressed as a percentage of the maximal response of mimulone. The liposomes were divided into groups according to their different zeta potentials: cationic (CL), anionic (AL), and neutral (NL). Values refer to the specific concentrations of the encapsulated mimulone; the BLANK samples were prepared without mimulone. The results are expressed as the mean \pm SEM for three independent experiments measured in tetraplicate. Statistical analysis is based on the Kruskal Wallis test followed by the Bonferroni correction for multiple tests. Asterisks indicate a significant difference from the maximal response of mimulone: * $p < 0.05$; ** $p < 0.01$; *** $p < 0.001$; and **** $p < 0.0001$.

hypothesis using DSPC as the model lipid bilayer to investigate the effect of the mimulone behavior of the phospholipid membrane. The results indicate strong interactions between mimulone and the lipid bilayer. Specifically, the incorporation of mimulone into DSPC liposomes led to significant shifts in the transition temperature of the lipid bilayer. For instance, the T_m of the pure DSPC bilayer was $54.4 \pm 0.3^\circ\text{C}$, whereas the presence of mimulone at various concentrations caused a decrease in T_m , with the most pronounced effect observed at the highest concentration of $510 \mu\text{g mL}^{-1}$, where T_m decreased to $50.8 \pm 0.1^\circ\text{C}$. This decrease in T_m suggests that mimulone strongly interacts with the lipid bilayer, disrupting its structure and reducing thermal stability. (For more information about differential scanning calorimetry (DSC) thermograms, please see Appendix A, Figure S6, Supporting Information). These interactions likely involve the intercalation of mimulone within the lipid bilayer, facilitated by its chalcone backbone and the ability to form hydrogen bonds with the lipid head groups. Such interactions can immobilize mimulone within the membrane, limiting its release and reducing its bioavailability and efficacy. To further investigate this aspect, we employed confocal microscopy to examine the entry of fluorescently labeled liposomes into cells. After 8 h of incubation, we observed a pronounced fluorescence signal from the labeled particles within the cells, indicating successful cellular uptake of the liposomes (Figure 1). Interestingly, there was no significant difference in cellular uptake among the test liposomes with varying surface charges. We used cationic liposomes as a positive control, given that the positively charged surface is expected to interact more readily with the negatively charged cell membrane theoretically

facilitating a higher rate of uptake. Kang et al. found that liposomes with different surface charges (cationic, neutral, and anionic) showed time-dependent uptake via specific endocytic pathways. In glioblastoma cells, cationic and AL were primarily taken up via macropinocytosis, whereas neutral liposomes used caveolae-mediated endocytosis. In fibroblast cells, all liposomes entered via clathrin-mediated endocytosis. Despite this, the uptake of cationic liposomes was comparable to that of neutral and AL.^[39] This uniformity in the rates of uptake further supports the notion that the strong interaction between the liposomal lipids and mimulone hinders its release, irrespective of the surface charge of the liposome, thereby reducing its efficacy.

Villegas et al. successfully incorporated four prenylated flavonoids into polymeric lipophilic nanoparticles, whose negative zeta potential values ensured good stability of the nanoparticles. It has been previously reported that compared to liposomes, polymers have a lower loading capacity but are more stable and allow for more controlled properties of release.^[40] One of the test substances, 5,7-dihydroxy-6-prenylflavanone, which differs from mimulone only by the absence of the C-4' hydroxyl group, demonstrated the best results among the TC in release and skin permeation studies and showed anti-inflammatory activity. Our findings are consistent with these results, indicating a higher efficacy of nanoparticles with negative zeta potential. Additionally, the study reported a smaller drug release rate (50%) from nanoparticles for the compound discussed. This finding could correlate with our results concerning reducing the maximal response of mimulone incorporated into liposomes to about half the efficacy of the free compound.^[41]

2.5. PPAR γ Reporter Assay with Mimulone Incorporated into HP- β -Cyclodextrins

Considering the significant loss of biological efficacy of mimulone in liposomes, the next step was transition to another nanoparticle system with different parameters expected to encapsulate the lipophilic substance in the nanoparticle cavity. HP- β -CDs were selected for further testing. Previous findings confirmed that lipophilic compounds are entrapped in the hydrophobic cavity of CDs, which increases their solubility and stability. However, CDs have a limited ability to accommodate compounds due to the fixed size of their cavity.^[42] In our experiments, HP- β -CDs proved to be a more effective nanoparticle system for maintaining the biological efficacy of mimulone than liposomes. The most effective combination (HP- β -CD + 2.5 μ M mimulone) demonstrated only a 10.5% loss in the maximal mimulone response (the fold induction of the PPAR γ activation measured was not statistically different from that of mimulone dissolved in DMSO) and notably showed a significantly different response compared to “empty” cyclodextrins (the CD blank, without an active substance incorporated). This combination also significantly improved the activation of the test pathway compared to the negative control—DMSO ($p < 0.05$). A summary of the experiments to determine the activation of the PPAR γ pathway of the TC incorporated into cyclodextrins is shown in Figure 6. The luciferase

activity is expressed as percentages of the fold change relative to the maximum response of mimulone.

Cyclodextrins are known for their ability to form inclusion complexes with various compounds, including flavonoids, which enhances their solubility, stability, and bioavailability. Some studies have shown that cyclodextrin complexes can provide controlled release and better protection for encapsulated substances.^[43,44] Several studies have indicated that cyclodextrins might be more effective than liposomes for certain applications. For example, in the study by Azzi et al., the flavonoid quercetin encapsulated in cyclodextrins showed greater stability and solubility than liposomal formulations.^[45] In addition, a study by Yao et al. on the flavonoid glycoside didymin demonstrated that its inclusion complex with β -cyclodextrin and hydroxypropyl- β -cyclodextrin significantly improved its water solubility and bioavailability.^[46] A study by Costescu et al. provided a comparative analysis of the cavity characteristics of cyclodextrins and small unilamellar liposomes using molecular modeling techniques. The results suggest that cyclodextrins provide a more stable and efficient encapsulation environment for small, hydrophobic molecules, such as flavonoids, compared to liposomes.^[47] An interesting comparison to our results is provided by a study that evaluated the bioavailability of hesperetin in various nanoparticles, including coated nanoliposomes and cyclodextrins.^[42] Hesperetin ((S)-5,7-dihydroxy-2-(3-hydroxy-4-methoxyphenyl)chroman-4-one) is also a flavanone,

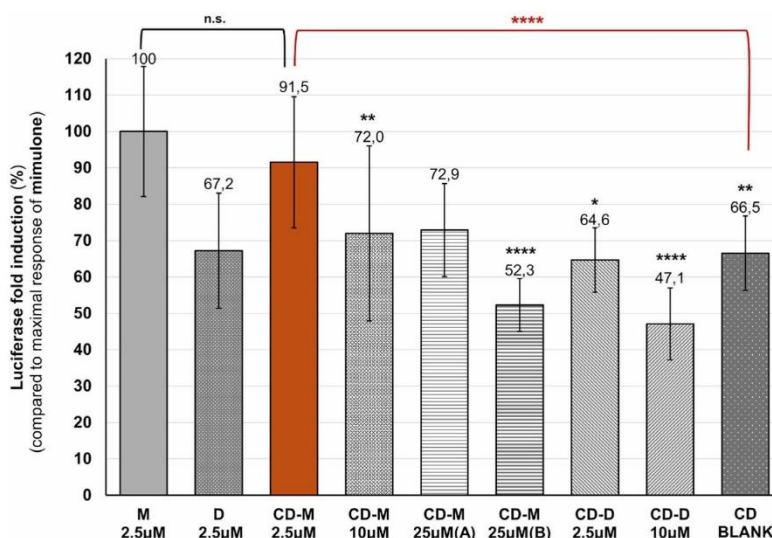


Figure 6. Activation of the PPAR γ pathway of mimulone (M) and diplacone (D) encapsulated into HP- β -cyclodextrins. The luciferase activity was measured by the CALUX reporter gene assay and expressed as percentages of the fold change relative to the maximal response of mimulone. CD refers to HP- β -cyclodextrins, the letters (M, D) indicate specific combinations with the test compound. Values refer to the exact concentrations of mimulone used; the BLANK samples were prepared without mimulone. Two CD-M 2.5 μ M combinations differ in CD composition: Sample A contained a CD concentration of 10 mg mL⁻¹, which was insufficient to encapsulate the active compound at 25 μ M. To address this problem, the CD concentration was increased to 100 mg mL⁻¹ in sample B. The results are expressed as the mean \pm SEM for three independent experiments measured in tetraplicate. Statistical analysis is based on the Mann-Whitney U test and the Kruskal Wallis test, followed by the Bonferroni correction for multiple tests. Asterisks indicate a significant difference from the maximal response of mimulone: * $p < 0.05$; ** $p < 0.01$; *** $p < 0.001$; and **** $p < 0.0001$.

differing from mimulone in the substitution pattern on the B-ring (3'-hydroxy-4'-methoxy) and the absence of a prenyl group at the C-6 position. The study noted that CDs retained 66% of hesperetin after intestinal digestion, suggesting moderate protective efficiency compared to maltodextrin (MD), but less than the coated nanoliposomes, which retained 76% of hesperetin postdigestion and exhibited the highest hesperetin transfer rate through the intestinal epithelium. Cyclodextrins, although effective in enhancing solubility, were reported to be less protective under gastrointestinal conditions compared to robust double-coated liposomes.^[42] The difference with our findings may be attributed to the lower lipophilicity of hesperetin compared to mimulone, which likely results in hesperetin being less prone to hydrophobic interactions and binding within the phospholipid bilayer of the nanoparticle, and thus, more easily released from the structure.^[42]

3. Conclusion

This study evaluates the PPAR γ agonistic potential of mimulone and diplacone, two geranylated flavanones from *P. tomentosa*, and their encapsulation in various nanoparticle systems to enhance bioavailability and stability. Our results demonstrate that mimulone dissolved in DMSO activates the PPAR γ signaling pathway, showing a 2.97-fold and 3.9-fold increase in luciferase activity at concentrations of 5 and 2.5 μ M, respectively. Diplacone, however, exhibited significant cytotoxicity, with an average cell viability of about 10% at 10 μ M.

Encapsulation into anionic, cationic, and neutral liposomes resulted in a significant reduction in the biological activity of the active compound. The most effective liposomal formulation, AL, preserved only 54% of the activity of mimulone.

In contrast, HP- β -CDs emerged as a superior nanoparticle system for maintaining the biological activity of both flavonoids. The most effective combination (HP- β -CD + 2.5 μ M mimulone) showed only a 10.5% loss of maximal mimulone response, with PPAR γ activation comparable to that of DMSO-dissolved mimulone. Cyclodextrin encapsulation also significantly improved the viability profile of diplacone, maintaining cell viability at around 100%, in stark contrast to the free form of the compound. The enhanced performance of HP- β -CDs could be attributed to their ability to form stable inclusion complexes with hydrophobic molecules, thereby improving solubility, stability, and controlled release. These findings suggest that cyclodextrin-based delivery systems effectively address the solubility and stability challenges associated with flavonoid therapy and offer a promising approach to improving the bioavailability and therapeutic efficacy of these compounds.

4. Experimental Section

Chemicals

Rosiglitazone (CAS no: 122,320-73-4), Dimethyl sulfoxide (CAS no: 67-68-5, DMSO, 99.9%), Phosphate buffered saline (PBS), Dulbecco's

Modified Eagle Medium with Ham's Nutrient Mixture F-12 (1:1) (DMEM/F12) without phenol red, Nonessential amino acids (NEAA), Fetal Bovine Serum (FBS), and Charcoal Stripped Fetal Bovine Serum (CS-FBS) were purchased from Merck (KGaA, Darmstadt, Germany); Penicillin-Streptomycin Solution 100X and trypsin was obtained from Biosera (Cholet, France); DMEM/F-12 with GlutaMAX supplement was supplied by Thermo Fisher Scientific (Waltham, USA); and chloroform (p.a. 99.8%) by Sigma Aldrich, CZ. Lipids L- α -phosphatidylcholine (EPC), 3 β -[N-(N',N'-dimethylaminoethane)-carbamoyl] cholesterol (DC-cholesterol), POPG (1-palmitoyl-2-oleoyl-sn-glycero-3-phospho-(1-rac-glycerol)), DSPC (1,2-distearoyl-sn-glycero-3-phosphocholine), and cholesterol were purchased from Avanti Polar Lipids (Alabaster, U.S.). 1,2-distearoyl-sn-glycero-3-phosphoethanolamine-N-[amino (polyethylene glycol)-2000] (DSPE-PEG 2000) was obtained from Nof Corporation (Japan). 2-Hydroxypropyl- β -cyclodextrin (HP- β -CD) was purchased from Sigma-Aldrich (CZ; product number H107, CAS: 128446-35-5). The average molecular weight was 1396 Da, with a degree of substitution around 0.6 and a purity \geq 98%. The compound was provided as a white powder.

TC

The TC were isolated from unripe fruits of *P. tomentosa* Steud. (Paulowniaceae) and characterized at the Faculty of Pharmacy, Masaryk University Brno, Brno, Czech Republic.^[48,49] high-performance liquid chromatography analysis verified that the purity of each test compound exceeded 95%. All of the TC were dissolved in DMSO, with the final DMSO concentration in the cellular assays set at 0.1% (v/v).

Preparation of Nanoparticles

Nanoliposomes were prepared using the film hydration method with the following lipids: L- α -phosphatidylcholine (EPC), DC-cholesterol, POPG, DSPE-PEG 2000, and cholesterol. The liposomal formulations used in this study were based on a previously optimized composition reported by Brezani et al.^[34] The required amounts of lipids based on Table 2, with or without the active compound (mimulone, at final concentrations of 51 and 204 μ g mL⁻¹), were dissolved in chloroform in a round-bottom flask (the total lipid concentration was 5 mg mL⁻¹). The solvent was removed using a rotary vacuum evaporator at 55 $^{\circ}$ C, which is above the highest transition temperature of the lipid mixture. After the removal of the solvent, the resulting thin film was rehydrated with an aqueous solvent (PBS buffer, pH 7.4). Liposomes were homogenized by membrane extrusion through a 200 nm polycarbonate filter (Whatman Nuclepore, Sigma Aldrich, CZ) using a manual extruder (LiposoFast, Avestin, Canada).

Cyclodextrin nanoparticles loaded with mimulone were prepared using the following method. An appropriate amount of HP- β -CD was dissolved in phosphate-buffered saline (PBS, pH 7.4) at a concentration of 10 mg mL⁻¹ and/or 100 mg mL⁻¹. Separately, mimulone was dissolved in ethanol (EtOH). Under constant stirring, the mimulone solution was added dropwise into the heated (45 $^{\circ}$ C) HP- β -CD

Table 2. Summary of individual liposomal compositions and corresponding mol%.

Liposomes	Compositions (mol%)
Neutral/PEG	EPC/Chol/DC-Chol/DSPE-PEG-2000 (55/25/15/5)
Anionic	EPC/POPG (70/30)
Cationic	EPC/DC-Chol (80/20)

solution. The final concentrations of mimulone were 51 and 204 $\mu\text{g mL}^{-1}$, with a volume ratio of 1:1. Based on the molecular weights of HP- β -CD and mimulone the resulting guest/host molar ratios were ≈ 0.007 , 0.028, and 0.007, respectively with strong molar excess of the carrier. The mixture was stirred for an additional 2 h to ensure the complete formation of nanoparticles and the encapsulation of mimulone. After this reaction, EtOH was evaporated under reduced pressure (400 PSI, 45 $^{\circ}\text{C}$), using a rotary vacuum evaporator, and the solution was filtered through a 0.22 μm filter.

Characterization of Nanoparticles

The size, polydispersity, and concentration of the nanoparticles were determined using multiangle DLS (MADLS) (Zetasizer Nano ZSP, Malvern, Great Britain). Approximately 50 μL of the sample was placed in a low-volume quartz batch cuvette ZEN2112 (Malvern Panalytical Ltd, Malvern, UK) and measured using the MADLS technique with a Zetasizer Ultra (Malvern Panalytical Ltd, UK) at a constant temperature of 25 $^{\circ}\text{C}$. The device was equipped with a HeNe Laser (633 nm) and three detectors set at the angles: 173 $^{\circ}$ (backscatter), 90 $^{\circ}$ (side scatter), and 13 $^{\circ}$ (forward scatter). The zeta (ζ) potential of the nanoliposomes was determined using the electrophoretic light scattering method (Zetasizer Nano ZSP, UK). Approximately 800 μL of the sample was placed in a folded capillary zeta cell DTS1070 (Malvern Panalytical Ltd, Malvern, UK). Analysis was performed using the monomodal mode at a constant temperature of 25 $^{\circ}\text{C}$. The data were evaluated using ZS Xplorer software, version 3.50 (Malvern Panalytical Ltd, UK). The measured values are reported as the mean value ($n = 3$) \pm the standard deviation (Table 1).

In Vitro Cellular Uptake

To evaluate the uptake of the liposomes by PPAR- γ 2 CALUX cells, liposomes were labeled with a fluorescent probe. The fluorescently labeled liposomes were prepared as described previously, with the addition of the fluorescent dye 1,2-dioleoyl-sn-glycero-3-phosphoethanolamine-N-(lissamine rhodamine B sulfonyl) (Lis-Rhodamin-PE) at a final concentration 0.1 mol%. The wavelengths for the excitation and emission maximum for this probe were 560 and 583 nm, respectively. The fluorescently labeled liposomes (50 $\mu\text{g mL}^{-1}$) were incubated with the target cells under standard culture conditions. The cells were seeded to achieve $\approx 50\%$ confluence before proceeding with further experimental steps. After incubation (8 h) in μ -Slide 8 Well (IBIDI), the cells were washed using PBS buffer to remove any unbound liposomes and fixed for confocal microscopic analysis. The uptake of the fluorescent liposomes by the cells was visualized using a Leica TCS SP8 MP confocal fluorescence microscope (Leica Microsystems, DE).

EE

The EE was calculated from the UV-VIS data obtained using a DAD spectrometer (Specord S600, Analytik Jena, DE). For the construction of the calibration curve, the required amount of mimulone was dissolved in absolute ethanol (EtOH) and diluted to concentrations ranging from 1 to 0.003 mg mL^{-1} . Approximately 400 μL of each sample was placed into a UV Quartz SUPRASIL Semi-Micro Cell with a 10 mm path length and measured in the range from 200 to 380 nm at a constant temperature of 25 $^{\circ}\text{C}$. The concentration of mimulone in the nanoparticles was determined using the established calibration curve. All samples were measured against blank samples, which consisted of either liposomes or cyclodextrins without the active

compound. The spectrum of the blank was subtracted from the sample spectra to ensure accurate analysis. The EE was calculated using the following formula

$$\text{EE}(\%) = \frac{\text{Concentration of encapsulated mimulone}}{\text{Theoretical concentration of mimulone}} \times 100 \quad (1)$$

DSC Analysis

The lipid transition temperature (T_m) and the influence of the active compound, mimulone, on the model of lipid membrane were analyzed using a MicroCal PEAQ-DSC Automated system (Malvern Panalytical Ltd, Malvern, UK). A sample volume of 350 μL was used for the analysis, and PBS buffer at pH 7.4 served as the reference. DSPC liposomes were prepared using the hydration of lipid film method with a total lipid concentration of 5 mg mL^{-1} and various concentrations of mimulone: 0 $\mu\text{g mL}^{-1}$ (blank), 51, 204, and 510 $\mu\text{g mL}^{-1}$. Each sample was measured in duplicate. The samples were loaded into the DSC cell, and the reference cell was filled with PBS buffer. The DSC scans were conducted from 5 to 120 $^{\circ}\text{C}$ at a rate of 120 $^{\circ}\text{C}$ per hour. Data collection and analysis were performed using MicroCal PEAQ-DSC software, version 2.21, to determine the transition temperatures.

Cell Culture

The PPAR- γ 2 CALUX cells, obtained from BioDetection Systems BV (Amsterdam, the Netherlands), were derived from human osteosarcoma U2OS cells and had been stably transfected with a PPAR- γ 2 expression vector along with a firefly luciferase reporter construct controlled by the peroxisome proliferator responsive element.^[50] These cells were cultured in DMEM/F12 GlutaMAX medium enriched with 7.5% fetal bovine serum, 1% nonessential amino acids, 100 U mL^{-1} penicillin, and 100 mg mL^{-1} streptomycin. To ensure the selection pressure, G418 (Roche, Mannheim, Germany) at a final concentration of 200 $\mu\text{g mL}^{-1}$ was added once a week. The cells were incubated at 37 $^{\circ}\text{C}$ in a humidified environment with 5% CO_2 .

Cell Viability Testing (Cytotoxicity Assay)

The viability of PPAR- γ 2 CALUX cells was measured using the cell proliferation reagent WST-1 (Roche, Basel, Switzerland) according to the manufacturer's manual, as reported previously.^[51]

Reporter Gene Assays

The ability of flavanones to stimulate PPAR- γ 2-driven luciferase expression was evaluated by measuring the luciferase activity in PPAR- γ 2 CALUX reporter cells. PPAR- γ 2 CALUX cells were seeded into 96-well tissue culture-treated microtiter plates (TPP, Switzerland) at a density of 10,000 cells per well in 100 μL of assay medium (DMEM/F12 without phenol red, supplemented with 5% charcoal-stripped FBS and 1% NEAA, all from Merck KGaA, Darmstadt, Germany). After a 24-h incubation period to allow cell adherence and the formation of a confluent monolayer, the central 60 wells were treated with the TC at specified concentrations in an assay medium for an additional 24 h. Each concentration was tested in a tetraplicate. The final DMSO concentration in the medium was maintained at 0.1%. Following this exposure, the cells were examined microscopically

for cytotoxic effects. The medium was then removed, the plates were frozen at -80°C for 15 min, and the cells were lysed with 30 μL of a lysis buffer containing 25 mM Tris buffer (pH 7.8), 2 mM dithiothreitol, 2 mM 1,2-diaminocyclohexane-tetraacetic acid, 10% glycerol, and 1% Triton X-100, procured from BDS (Amsterdam, Netherlands). The luciferase activity was quantified using a luminometer (FLUOstar Omega microplate reader, BMG Labtech, Germany) after adding 100 μL of flash mix (20 mM tricine, 1.07 mM $(\text{MgCO}_3)_4$ Mg $(\text{OH})_2$, 2.67 mM MgSO_4 , 0.1 mM EDTA, 2.0 mM dithiothreitol, 470 μM luciferin, 5.0 mM ATP) per well. The flash mix was also obtained from BDS (Amsterdam, Netherlands). Luciferase activity was reported as relative light units per well.

Statistical Analysis

The experimental data were processed in Excel (Microsoft). Statistical analyses were carried out using IBM SPSS Statistics for Windows, software version 26.0 (Armonk, NY, USA). The data were graphed as the mean \pm SEM. Comparisons between groups were made using the Mann–Whitney U test and/or a Kruskal–Wallis test followed by the Bonferroni correction for multiple tests.

AI Statement

During the preparation of this work the author(s) used ChatGPT 4 in order to improve the readability and language of the research paper. After using this tool, the authors reviewed and edited the content as needed and take full responsibility for the content of the publication.

Acknowledgements

Special thanks to Frank Thomas Campbell for the language correction and manuscript editing. This work was supported by Masaryk University under the Specific Research Programme – Support for Student Projects, Grant No. MUNI/A/1280/2021: Determination of PPAR Gamma Agonism of Selected Natural Products in Nanoparticle Systems, and by the Czech Science Foundation (GAČR), Grant No. 22-03187S: Rational Design of Polysaccharide Particle Systems for Drug Delivery with Broad-Spectrum Biological Activity for Mucosal Therapy.

Conflict of Interest

The authors declare no conflict of interest.

Data Availability Statement

The data that support the findings of this study are available from the corresponding author upon reasonable request.

Keywords: cyclodextrins · geranylated flavanones · liposomes · nanoparticles · peroxisome proliferator-activated receptor gamma

- [1] S. Ranjbar, A. Emamjomeh, F. Sharifi, A. Zarepour, K. Aghababasi, A. Dehshahri, A. M. Sepahvand, A. Zarrabi, H. Beyzaei, M. M. Zahedi, R. Mohammadinejad, *Pharmaceutics* **2023**, *15*, 1944.
- [2] L. Wang, B. Waltenberger, E.-M. Pferschy-Wenzig, M. Blunder, X. Liu, C. Malainer, T. Blazevic, S. Schwaiger, J. M. Rollinger, E. H. Heiss, D. Schuster, B. Kopp, R. Bauer, H. Stuppner, V. M. Dirsch, A. G. Atanasov, *Biochem. Pharmacol.* **2014**, *92*, 73.
- [3] Y. H. Song, Z. Uddin, Y. M. Jin, Z. Li, M. J. Curtis-Long, K. D. Kim, J. K. Cho, K. H. Park, *J. Enzyme Inhib. Med. Chem.* **2017**, *32*, 1195.
- [4] E. Rigamonti, G. Chinetti-Gbaguidi, B. Staels, *Arterioscler., Thromb., Vasc. Biol.* **2008**, *28*, 1050.
- [5] B. Grygiel-Gorniak, *Nutr. J.* **2014**, *13*, 17.
- [6] Y. Xi, Y. Zhang, S. Zhu, Y. Luo, P. Xu, Z. Huang, *Cells* **2020**, *9*, 352.
- [7] N. R. de Almeida, M. Conda-Sheridan, *Med. Res. Rev.* **2019**, *39*, 1372.
- [8] O. Amber-Vitos, N. Chaturvedi, E. Nachliel, M. Gutman, Y. Tsfadia, *Biochim. Biophys. Acta, Mol. Cell Biol. Lipids* **2016**, *1861*, 1852.
- [9] M. Hamblin, L. Chang, Y. Fan, J. Zhang, Y. E. Chen, *Antioxid. Redox Signaling* **2009**, *11*, 1415.
- [10] A. Z. Mirza, I. I. Althagafi, H. Shamshad, *Eur. J. Med. Chem.* **2019**, *166*, 502.
- [11] M. Huang, E. Su, F. Zheng, C. Tan, *Food Funct.* **2017**, *8*, 3198.
- [12] N. Mignet, J. Seguin, M. R. Romano, L. Brullé, Y. S. Touil, D. Scherman, M. Bessodes, G. G. Chabot, *Int. J. Pharm.* **2012**, *423*, 69.
- [13] S.-S. Ang, Y. Y. Thoo, L. F. Siow, *Food Bioprocess Technol.* **2024**, *17*, 424.
- [14] N. Mignet, J. Seguin, G. G. Chabot, *Pharmaceutics* **2013**, *5*, 457.
- [15] A. Cesari, G. U. Barretta, K. N. Kirschner, M. Pappalardo, L. Basile, S. Guccone, C. Russotto, M. R. Lauro, F. Cavaliere, F. Balzano, *New J. Chem.* **2020**, *44*, 16431.
- [16] B. dos Santos Lima, S. Shanmugam, J. de Souza Siqueira Quintans, L. J. Quintans-Júnior, A. A. de Souza Araújo, *Phytochem. Rev.* **2019**, *18*, 1337.
- [17] V. Pittol, K. S. Veras, E. Doneda, A. D. Silva, M. G. Delagustin, L. S. Koester, V. L. Bassani, *Pharm. Dev. Technol.* **2022**, *27*, 625.
- [18] K. Wdowiak, N. Rosiak, E. Tykarska, M. Zarowski, A. Plazińska, W. Plaziński, J. Cielecka-Piontek, *Int. J. Mol. Sci.* **2022**, *23*, 4000.
- [19] J.-S. Kim, *Prev. Nutr. Food Sci.* **2020**, *25*, 449.
- [20] Y. C. Liang, S. H. Tsai, D. C. Tsai, S. Y. Lin-Shiau, J. K. Lin, *FEBS Lett.* **2001**, *496*, 12.
- [21] A. Zoehling, F. Liebner, A. Jungbauer, *Food Funct.* **2011**, *2*, 28.
- [22] L.-J. Xu, M.-H. Yu, C.-Y. Huang, L.-X. Niu, Y.-F. Wang, C.-Z. Wu, P.-M. Yang, X. Hu, *Fitoterapia* **2018**, *127*, 109.
- [23] S. Ma, Y. Huang, Y. Zhao, G. Du, L. Feng, C. Huang, Y. Li, F. Guo, *Phytochem. Lett.* **2016**, *16*, 213.
- [24] S. Ballav, B. Biswas, V. K. Sahu, A. Ranjan, S. Basu, *Cells* **2022**, *11*, 3215.
- [25] S. Garg, S. L. Khan, R. K. Malhotra, M. K. Sharma, M. Kumar, P. Kaur, T. C. Nag, J. B. RumaRay, D. S. Arya, *Arch. Biochem. Biophys.* **2020**, *694*, 108572.
- [26] X.-K. Fang, J. Gao, D.-N. Zhu, *Life Sci.* **2008**, *82*, 615.
- [27] C. Weidner, S. J. Wowro, A. Freiwald, V. Kodelja, H. Abdel-Aziz, O. Kelber, S. Sauer, *Mol. Nutr. Food Res.* **2014**, *58*, 903.
- [28] S. Afzal, M. A. Sattar, E. J. Johns, O. A. Eseyin, A. Attiq, *PPAR Res.* **2021**, *2021*, 6661181.
- [29] K. Beekmann, L. Rubió, L. H. J. de Haan, L. Actis-Goretta, B. van der Burg, P. J. van Bladeren, I. M. C. M. Rietjens, *Food Funct.* **2015**, *6*, 1098.
- [30] A. Ghorbani, M. Nazari, M. Jeddi-Tehrani, H. Zand, *Eur. J. Nutr.* **2012**, *51*, 39.
- [31] M. Yue, N. Zeng, Y. Xia, Z. Wei, Y. Dai, *Mol. Nutr. Food Res.* **2018**, *62*, 1800202.
- [32] A. Barthel, K.-D. Krüger, R. A. Roth, H.-G. Joost, *Naunyn-Schmiedeberg's Arch. Pharmacol.* **2002**, *365*, 290.
- [33] S. Liga, C. Paul, F. Péter, *Plants* **2023**, *12*, 2732.
- [34] V. Brezani, N. Blondeau, J. Kotouček, E. Klásková, K. Šmejkal, J. Hošek, E. Mašková, P. Kulich, V. Prachyawarakorn, C. Heurteaux, J. Mašek, *ACS Omega* **2024**, *9*, 9027.
- [35] O. Wesolowska, J. Gąsiorowska, J. Petrus, B. Czarnik-Matusiewicz, K. Michalak, *Biochim. Biophys. Acta, Biomembr.* **2014**, *1838*, 173.
- [36] M. J. W. Johnston, S. C. Semple, S. K. Klimuk, S. Ansell, N. Maurer, P. R. Cullis, *Biochim. Biophys. Acta* **2007**, *1768*, 1121.
- [37] A. Kerdudo, A. Dingas, X. Fernandez, C. Faure, *Food Chem.* **2014**, *159*, 12.
- [38] A. Sadžak, Z. Brkljača, M. Eraković, M. Kriechbaum, N. Maltar-Strečeki, J. Přibyl, S. Šegota, *J. Lipid Res.* **2023**, *64*, 100430.
- [39] J. H. Kang, W. Y. Jang, Y. T. Ko, *Pharm. Res.* **2017**, *34*, 704.
- [40] H. Lu, S. Zhang, J. Wang, Q. Chen, *Front. Nutr.* **2021**, *8*, <https://doi.org/10.3389/fnut.2021.783831>.
- [41] V. Domínguez-Villegas, B. Clares-Naveros, M. L. García-López, A. C. Calpena-Campmany, P. Bustos-Zagal, M. L. Garduño-Ramírez, *Colloids Surf., B* **2014**, *116*, 183.

- [42] X. Meng, C. Fryganas, V. Fogliano, T. Hoppenbrouwers, *Food Hydrocolloids* **2024**, 151, 109872.
- [43] A. Horablagă, A. Şibu, C. I. Megyesi, D. Gligor, G. S. Bujancă, A. B. Velcirov, F. E. Morariu, D. I. Hădăruşă, C. D. Mişcă, N. G. Hădăruşă, *Plants* **2023**, 12, 2352.
- [44] J. Ghitman, S. I. Voicu, *Carbohydr. Polym. Technol. Appl.* **2023**, 5, 100266.
- [45] J. Azzî, A. Jraij, L. Auezova, S. Fourmentin, H. Greige-Gerges, *Food Hydrocolloids* **2018**, 81, 328.
- [46] Q. Yao, M.-T. Lin, Q.-H. Lan, Z.-W. Huang, Y.-W. Zheng, X. Jiang, Y.-D. Zhu, L. Kou, H.-L. Xu, Y.-Z. Zhao, *Drug Delivery* **2020**, 27, 54.
- [47] C. Costescu, L. Corpas, N. Hădăruşă, D. I. Hădăruşă, Z. Gărbău, *Stud. Univ. Babeş-Bolyai Chem.* **2011**, 56, 83.
- [48] L. Molčanová, T. Kauerová, S. Dall'Acqua, P. Maršik, P. Kollár, K. Šmejkal, *Bioorg. Chem.* **2021**, 111, 104797.
- [49] K. Šmejkal, L. Grycová, R. Marek, F. Lemièrre, D. Jankovská, H. Forejtníková, J. Vančo, V. Suchý, *J. Nat. Prod.* **2007**, 70, 1244.
- [50] L. Gijssbers, H. D. L. M. van Eekelen, L. H. J. de Haan, J. M. Swier, N. L. Heijink, S. K. Kloet, H.-Y. Man, A. G. Bovy, J. Keijer, J. M. M. J. G. Aarts, B. van der Burg, I. M. C. M. Rietjens, *J. Agric. Food Chem.* **2013**, 61, 3419.
- [51] Z. Hanáková, J. Hošek, P. Babula, S. Dall'Acqua, J. Václavík, K. Šmejkal, *J. Nat. Prod.* **2015**, 78, 850.

Manuscript received: March 31, 2025
Revised manuscript received: July 18, 2025
Version of record online: